Epigenetic coregulators of androgen signalling in prostate cancer

Veronika Metzler, MSc

Thesis submitted to the University of Nottingham for the degree of Doctor of Philosophy

September 2019

Abstract

Prostate cancer (PCa) is initially an androgen dependent disease and is treated by androgen deprivation therapies (ADTs). However, within ~18 months of ADT use, PCa becomes androgen independent and resistant to ADTs, which is called castrate resistant prostate cancer (CRPC) and remains incurable. It is therefore crucial to find alternative therapeutic approaches. One novel therapeutic approach is to target the epigenetic coregulators of the androgen receptor (AR), which are crucial for androgen signalling. The discovery of the histone lysine demethylase (KDM) families and their implications in cancer suggest their potential as drug targets for the treatment of PCa. A recent study discovered that the tumour suppressive microRNA *miR137* inhibits the expression of an extended network of AR coregulators, including the well-studied KDM1A, but also other coregulators, such as KDM5B and KDM7A. The aim of this study therefore was to investigate the role of KDM5B and KDM7A in androgen signalling and cell proliferation in PCa. In addition, combination therapies harbour the potential of being more effective than single KDM targeting, and therefore the effect of combined targeting of KDM1A and KDM7A was tested. Bioinformatic analysis of the TCGA PRAD dataset revealed that *KDM1A*, *KDM5B* and *KDM7A* respectively were altered in ~one third of PCa patients. Immunohistochemical staining in PCa tissue specimens showed that KDM1A expression was higher in tumour compared to normal tissue, whereas KDM5B expression was lower and KDM7A expression did not differ. KDM1A, KDM5B and KDM7A expression respectively was higher in PCa cells compared to normal epithelial prostate cells. To investigate the function of the KDMs in AR-regulated gene transcription, siRNA-mediate knockdown experiments were performed and pharmaco-selective inhibitors targeting KDM1A, KDM5B and KDM7A respectively were applied. Overall, the results suggested that the knockdown and inhibition of KDMs attenuated androgen-induced gene expression. RNASeq analysis further confirmed that pharmaco-selective inhibition of KDMs affected the expression of genes involved in PCa progression and cancer pathways, suggesting an oncogenic function of KDMs in PCa. In addition, pharmaco-selective inhibitors blocked PCa cell proliferation and combined inhibition of KDMs had an additive inhibitory effect, indicating combined KDM inhibition may be more effective than single KDM targeting. These results suggest an important role of KDM5B and KDM7A in androgen signalling and cell proliferation in PCa. Pharmaco-selective inhibitors targeting KDMs represent a promising therapeutic approach to treat both localised and advanced PCa.

Acknowledgements

First of all, I would like to thank my supervisors Prof Nigel Mongan, Prof David Heery, Dr Catrin Rutland and Dr Jennie Jeyapalan for their unwavering support and guidance during these four years. I would like to especially thank Nigel for being such a great mentor and supporting my professional development and career beyond. I could not have asked for a better supervision team.

I would like to thank all our collaborators, including Prof Lorraine Gudas, Dr Brian Robinson and Dr Jenny Persson. I would like to thank Prof Emad Rakha at City Hospital, Nottingham for the collaboration to construct the prostate cancer tissue microarray (TMA) in this study. A huge thanks goes to Michael Shawky Toss without whom the construction of the TMA would not have been possible. Thank you for your generous and unwavering help.

A very special thanks goes to Jennie, Daisy, Corinne, Jenny and Nataliya for being such great colleagues and friends. I greatly enjoyed working with you all and I will never forget all the laughters we had. I know you will miss my singing, especially U2, but I think I can finally say "I have found what I'm looking for". Someone who has been most inspirational in many ways and incredibely supportive is PostDoc Jennie Jeyapalan, my "KDM buddy". I could not have done this PhD without your scientific and mental support. Also, thank you, Corinne and Daisy, for making the Hopper bus journeys an enjoyable part of the day. I will miss you all loads.

I also would like to thank all my other friends in the VetSchool, Ahmad, Emma, Aouatif, Ramzi, Lola, Lamiya, Abril and the lovely rest of the lunch group. The lunch breaks with you all were definitely the most fun and insightful ones I have ever had.

I would like to thank the administrative and technical team in the VetSchool and everyone else indirectly involved in this study. I would also like to thank the BBSRC and Univeresity of Nottingham for providing me with a scholarship which enabled me to conduct this study.

A big thank you goes to my plant science friends for many fun evenings and weekends in Nottingham, the Peak District or elsewhere in England. A special thanks goes to George for having been there during my PhD, you kept me going.

I would especially like to thank Eliana, the best climbing and squash partner. Meeting you after a busy lab day to do a bit of sports and a lot of chatting, was most relaxing. I also would like to thank the other girls from Gateway for absolutely fun girls' evenings.

Thank you, Tom, for always making me laugh and forget about stressful PhD times. You are my best advisor. Thank you for being there. Never will I forget the Lion King (alias King of Lions) evening.

I would like to say DANKE to the best family in the world. Mum, dad, I could have never done this without your ongoing support. Thank you for supporting me with going abroad. I greatly enjoyed our countless skype calls, where you always lend me an open ear and which allowed me to peak into the living room. Thank you for all your encouraging words along this PhD journey. I loved every single home holiday, where you would spoil me with the best Austrian dishes (thanks mum) and the best airport transfer service (thanks dad). I would like to thank my lovely sister and friend Anna for always being there for me (and sorry for all the sneaky screenshots during skyping). I will also never forget our amazing meet-ups in the UK. Thanks a million.

(Ein großes DANKE geht an die beste Familie der Welt. Mama, Papa, ich hätte das nie ohne eure andauernde Unterstützung geschafft. Danke, dass ihr mich darin bestärkt und unterstützt habt, ins Ausland zu gehen. Ich habe unsere zahllosen Skype-Gespräche, in denen ihr mir immer ein offenes Ohr geliehen habt und ich einen Blick ins Wohnzimmer erhaschen konnte, sehr genossen. Danke für all die ermutigenden Worte während dieser PhD Zeit. Ich liebte jeden einzelnen Heimaturlaub, in dem ihr mich mit den besten österreichischen Gerichten (danke Mami) und dem besten Flughafen-Taxi Service (danke Papi) verwoehnt habt. Ich möchte mich auch bei meiner allerliebsten Schwester und Freundin Anna bedanken, die immer für mich da ist (und sorry für die heimtückischen Screenshots während des Skypens). Auch werde ich nie unsere wunderschönen Treffen in GB vergessen. Tausend Dank.)

And of course, I would also like to thank my best friends in Austria. Mimi, Märi, Julia, Sara, Isi and Chrischi, thank you for always being there. You were the highlight of my home visits. I will also never forget how you all surprised me and stood at the train station at the 24th of December to welcome me back with prosecco and a poster from my internship in Australia. Thank you to all the Austrian and Erasmus friends who came to Nottingham to visit me, this really meant a lot to me. And, Julia, I will never forget that you stepped into the plane to come to Nottingham when I most needed it.

Contents

Abbreviations and Acronyms

aa	Amino acid
ACSS1	Acyl-CoA synthetase short chain family member 1
ACTH	Adrenocorticotropic hormone
ADP	Adenosine diphosphate
ADT	Androgen deprivation therapy
AED	Androstenedione
AF	Activation function
AIS	Androgen insensitivity syndrome
Akt	AKT serine/threonine kinase
ANGPT1	Angiopoietin 1
ANOVA	Analysis of variance
AO	Amino oxidase
AOL	Amino oxidase-like domain
APS	Ammonium persulfate
AQP7	Aquaporin 7
AR	Androgen receptor
ARE	Androgen response element
AR-FL	Androgen receptor full length
ARID	AT-rich interaction domain
ARKO	Androgen receptor knockout
ARL14EP	ADP ribosylation factor like GTPase 14 effector protein
AR-V	Androgen receptor splice variant
ATP	Adenosine triphosphate
AURKA	Aurora kinase A
AZ	Anterior zone
B3GAT3	Beta-1,3-glucuronyltransferase 3
BAK	BCL2 antagonist/killer 1
BAX	BCL2 associated X, apoptosis regulator
BBS9	Bardet-Biedl syndrome 9
BCR	Biochemical recurrence
BER	Base excision repair
BET	Bromodomain and extra-terminal motif

bp	Base pair
BPH	Benign prostatic hyperplasia
BRCA	Breast cancer gene
CAIS	Complete androgen insensitivity syndrome
CBP	CREB-binding protein
CDK	Cyclin-dependent kinase
cDNA	Complementary DNA
CHD1	Chromodomain helicase DNA binding protein 1
CITED2	Cbp/P300 interacting transactivator with Glu/Asp rich carboxy-terminal domain 2
CNS	Central nervous system
CNTNAP2	Contactin associated protein like 2
CoREST	RE1 silencing transcription factor corepressor
CREB	cAMP response element-binding protein
CRPC	Castration resistant prostate cancer
CT	Computed tomography
CYP17A	Cytochrome P450 17 α-hydroxysteroid dehydrogenase
CZ	Central zone
DAB	3,3'-diaminobenzidine tetrahydrochloride
DBDs	DNA binding domain
DBG	Corticosteroid-binding globulin
ddH2O	Double-distilled water
DDIT4	DNA damage inducible transcript 4
DHCR24	24-dehydrocholesterol reductase
DHEA	Dehydroepiandrostenedione
DMSO	Dimethyl sulfoxide
DNA	Desoxyribonucleic acid
DNMT	DNA methyltransferase
ECL	Enhanced chemiluminescence
EMT	Epithelial to mesenchymal transition
EPB41L4B	Erythrocyte membrane protein band 4.1 like 4b
ER	Endoplasmic reticulum
ERG	Epidermal growth factor
ERG	ETS-related gene
ERK	Extracellular signal–regulated kinase

Erα	Estrogen receptor alpha
ETS	E twenty-six
ETS Variant 1	Transmembrane serine protease 2
ETV1	ETS Variant 1
FAD	Flavin adenine dinucleotide
FBS	Fetal bovine serum
FDR	False discovery rate
FFPE	Formalin fixed paraffin embedded
FOXA1	Forkhead box A1
FOXK1	Forkhead box K1
FOXN3	Forkhead box N3
FS del	Frame shift deletion
FSH	Follicle-stimulating hormone
GABAA	γ-aminobutyric acid
GAPDH	Glyceraldehyde 3-phosphate dehydrogenase
GDF15	Growth differentiation factor 15
GISTIC	Genomic identification of significant targets in cancer
GNA12	Guanine nucleotide binding protein (G protein) alpha 12
GnRH	Gonadotropin-releasing hormone
GR	Glucocorticoid receptor
GRB1	Growth factor receptor bound protein 2-associated protein 1
GST	Glutathione S-transferase
GUCY1A3	Guanylate cyclase 1 soluble subunit alpha 1
H&E	Haemotoxylin & eosin
H2AFJ	H2A histone family member J
HAT	Histone acetyltransferases
HCl	Hydrochloric acid
HDAC	Histone deacetylase
HIF1α	Hypoxia-inducible factor 1-alpha
HP1	Heterochromatin protein 1
HRP	Horse radish peroxidase
HSP	Heat shock protein
IgG	Immunoglobulin G
IHC	Immunohistochemistry
IL	Interleucin

JHDM	Jumonji C domain-containing histone demethylase
Jmj	Jumonji
KAT	Lysine acetyltransferase
KCNMA1	Potassium calcium-activated channel subfamily M alpha 1
KCNN2	Potassium calcium-activated channel subfamily N member 2
kDa	Kilodalton
KDM	Lysine demethylase
KEGG	Kyoto encyclopedia of genes and genomes
KLK3	Kallikrein-3
KMT	Lysine methyltransferase
LBD	Ligand binding domain
LH	Luteinizing hormone
LHRH	Luteinizing hormone-releasing hormone
LHX6	LIM/homeobox protein Lhx6
LiAc	Lithium-acetate
lncRNA	Long non-coding RNA
LRR	Leucine-rich repeat
LRRC8A	Leucine rich repeat containing 8 family member A
LSD1	Lysine-specific demethylase 1
MAGI2	Membrane-associated guanylate kinase inverted 2
MAIS	Mild androgen insensitivity syndrome
MAPK	Mitogen-activated protein kinase
MBOAT2	Membrane bound O-acyltransferase domain containing 2
MED	Mediator complex subunit 1
MEK	MAPK/ERK kinase
miRNA	MicroRNA
MR	Mineralocorticoid receptor
MRI	Magnetic resonance imaging
mRNA	Messenger RNA
MRP4	Multi-drug resistance protein 4
mTOR	Mammalian target of rapamycin
MTT	Di-methyl thiazol diphenyl tetrazolium bromide
MVB	Multivesicular body
NaCl	Sodium chloride
NAD	Nicotinamide adenine dinucleotide

NBL1	Neuroblastoma suppressor of tumorigenicity 1
NCL1	Neuronal ceroid-lipofuscinosis type 1
NCOA	Nuclear receptor coactivator
ncRNA	Non-coding RNA
NDUFA4L2	NADH dehydrogenase [ubiquinone] 1 alpha subcomplex subunit 4-like 2
NePC	Neuroendocrine prostate cancer
NES	Nuclear export signal
NGS	Next generation sequencing
NHS	National Health Service
NID	Nuclear interaction domain
NKX3.1	NK3 homeobox 1
NLS	Nuclear localisation signal
NTD	N-terminal domain
NUH	Nottingham University Hospitals
OD	Optical density
ONPG	O-nitrophenyl-beta-D-galactopyranoside
P2RY1	Purinergic receptor P2Y, G-protein coupled, 1
p53	Tumour protein 53
PAcP	Prostate acid phosphatase
PAGE	Polyacrylamide gel electrophoresis
PAIS	Partial androgen insensitivity syndrome
PBX1	Pre-B-cell leukemia homeobox 1
PCR	Polymerase chain reaction
PDP1	Pyruvate dehyrogenase phosphatase catalytic subunit 1
PEG	Polyethylene glycol
PHD	Plant homeodomain
PI3K	Phosphoinositide 3-kinase
PIN	Prostatic intraepithelial neoplasia
piRNA	Piwi-interacting RNA
PLZF	Promyelocytic leukaemia zinc finger
PNI	Perineural invasion
PR	Progesterone receptor
PREC	Prostate epithelial cells
PRK1	Protein kinase C-related kinase 1
PRKAR2B	Protein kinase CAMP-dependent type II regulatory subunit beta

PRR15L	Proline-rich protein 15-like protein
PSA	Prostate-specific antigen
PTEN	Phosphatase and tensin homolog
PVDF	Polyvinylidene difluoride
PXDN	Peroxidasin
PYGB	Glycogen Phosphorylase B
PZ	Peripheral zone
RASSF5	Ras association domain family member 5
Rb	Retinoblastoma
RGP1	Retrograde golgi transport protein 1
RNA	Ribonucleic acid
RNASeq	RNA sequencing
RNF144A	Ring finger protein 144A
qRT-PCR	Real-time quantitative polymerase chain reaction
SAH	S-adenosyl-homocysteine
SAM	S-adenosyl-methionine
SDS	Sodium dodecyl sulfate
SEER	Surveillance, Epidemiology and End Results
SEMA3C	Semaphorin 3C
SGEF	Src homology 3 domain-containing guanine nucleotide exchange factor
SHBG	Sex hormone-binding globulin
SHOC2	SHOC2 leucine rich repeat scaffold protein
siRNA	Small-interfering RNA
snRNA	Small nuclear RNA
SPOCK1	SPARC (osteonectin), cwcv and kazal like domains proteoglycan 1
SPON2	Spondin 2
SPOP	Speckle type BTB/POZ protein
SPSB1	SplA/ryanodine receptor domain and SOCS box containing 1
SPSS	Statistical Package for Social Sciences
SRC-1	Steroid receptor coactivator-1
ST6GAL1	ST6 beta-galactoside alpha-2,6-sialyltransferase 1
STEAP2	Six transmembrane epithelial antigen of the prostate 2
STON2	Stonin 2
STXBP5L	Syntaxin binding protein 5 like
SU2C/PCF	Stand Up To Cancer-Prostate Cancer Foundation

SUZ12	Suppressor of zeste 12 protein homolog
SWIRM	Swi3p, Rsc8p and Moira
TAU	Transcription activation unit
TBS	Tris-buffered saline
TEMED	Tetramethylethylenediamine
TET	Ten-eleven translocation
TGM2	Transglutaminase 2
THDOC	Tetrahydrodeoxy-corticosterone
TMA	Tissue microarray
TMPRSS2	Transmembrane serine protease 2
TMPRSS2	Transmembrane serine protease 2
TNM	Tumour-node-metastasis
TP53INP1	Tumor protein p53-inducible nuclear protein 1
TR4	Testicular orphan nuclear receptor 4
TRIM2	Tripartite motif-containing protein 2
TRO	Trophinin
TRUS	Transrectal ultrasound
TSS	Transcription start site
TUT1	Terminal uridylyl transferase 1
TZ	Transition zone
UPR	Unfolded protein response
VEGFA	Vascular endothelial growth factor A
VGLL4	Vestigial like family member 4
Y2H	Yeast-2-hybrid
YPD	Yeast extract peptone dextrose
YSM	Yeast selective medium
ZBTB12	Zinc finger and BTB domain containing 16
ZF	Zinc finger
ZNF704	Zinc finger protein 704
α-DHT	Alpha-dihydrotestosterone
α-KG	Alpha-ketoglutarate
β-gal	Beta-galactosidase

List of Tables

List of Figures

Chapter 1: General introduction

Chapter 1 General introduction

1.1 Androgen signalling

1.1.1 Steroid hormones

Androgen is a steroid hormone. Steroid hormones are lipophilic molecules and their chemical structure contains a characteristic four ring system: three six-membered rings (A-C) and one five-membered ring (D) (**Figure 1.1**) (Nagorny and Cichowicz, 2016, Roos and Roos, 2014)

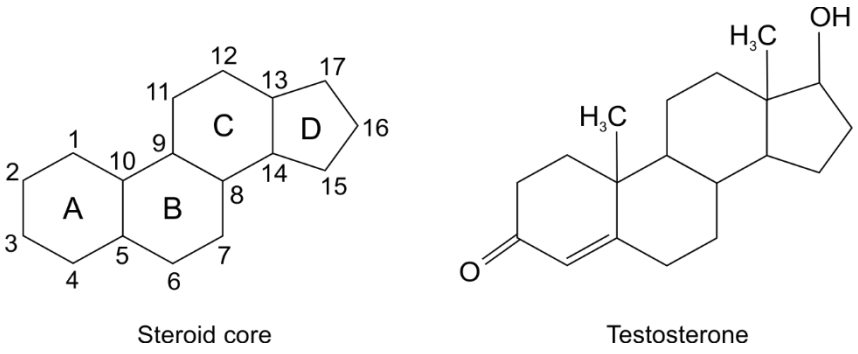

Figure 1.1: Chemical structure of the steroid core.
The steroid core is composed of 17 carbon molecules that form three six-membered rings (A, B, C) and one five-membered ring (D). The steroid hormone testosterone is given as an example.

Steroid hormones can be physiologically divided into three main groups: 1) glucocorticoids, 2) mineralocorticoids, and 3) gonadal steroids. They are synthesised from the precursor molecule cholesterol, and their synthesis pathways are depicted in **Figure 1.2**. Glucocorticoids, such as cortisol, regulate cardiac processes, blood pressure, energy, glucose metabolism, and inflammatory and immune response. (Busada and Cidlowski, 2017). The mineralcorticoids, such as aldosterone, act on the distal tube of the kidney where they act to increase resorption of sodium and consequently water (via osmosis), and renal excretion of potassium, thereby regulating kidney function (Waller and Sampson, 2017). Cortisol, which is more abundant than aldosterone, is known to have weak mineralcorticoid activity (Ferrari and Bonny, 2003). Both cortisol and aldosterone are produced in the cortex of the adrenal gland. The gonadal steroids, also known as sex steroids, include estrogen, progesterone and androgen, and are important for sexual development and reproduction. Estrogen is responsible for menstruation, maintainance of pregnancy and the development of the secondary sexual characteristics in women, whilst

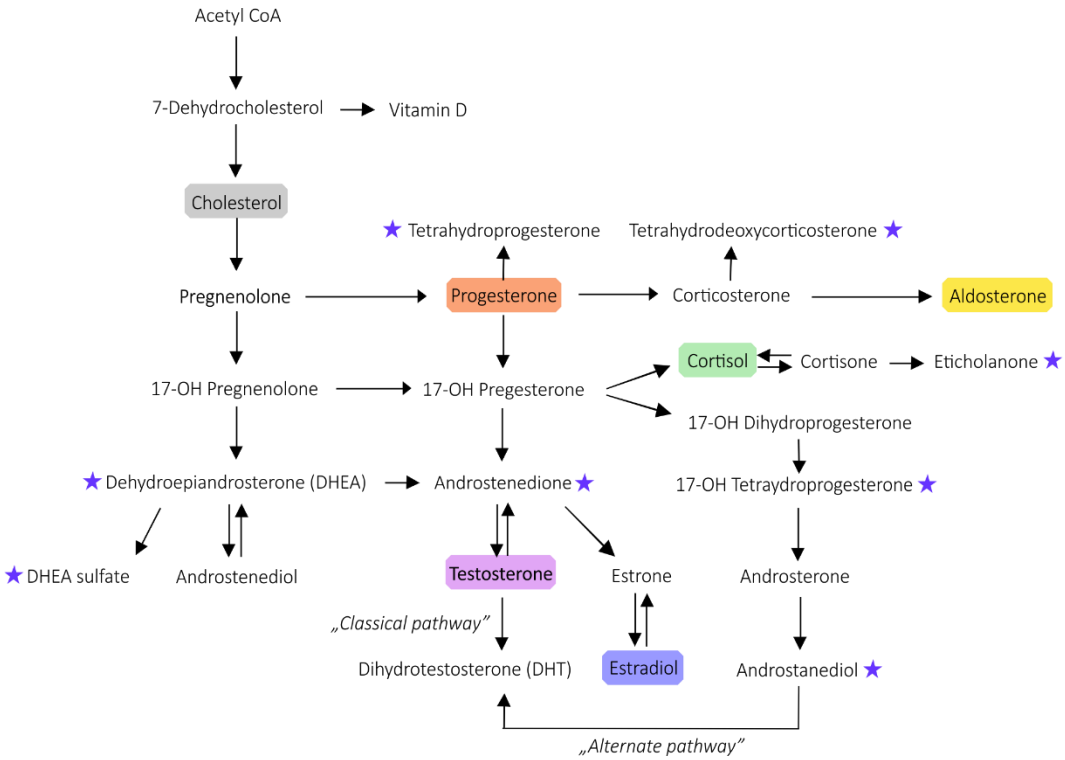

Figure 1.2: Synthesis pathways of steroid hormones from Acetyl-CoA.
Acetyl CoA is converted to Cholesterol which can then be converted to steroid hormones through various steps of chemical reactions. Steroid hormones with neuronal activity are marked with a blue star. Dihydrotestosterone (DHT) can be produced by the "*classical pathway*" or the "*alternate pathway*".

progesterone is important for menstruation and pregnancy such as preparation of the uterus and lactation (Csapo et al., 1973, Miller et al., 2004, Stillwell, 2016). Both estrogens and progesterones are mainly produced in the ovaries, but also the cortex of the adrenal gland, breast and, in the case of pregnancy, the placenta (Holst et al., 2004). The most abundant androgen in men is testosterone and plays a crucial role in the normal embryonic development, pubertal maturation and the normal function of the prostate gland in men (Chang et al., 1995, Wilson, 2011). Testosterone is primarily produced in the testes, more precisely in the cells adjacent to the seminiferous tubulus, called Leydig cells (Gao et al., 2005). Most of the secondary androgens, like androstenedione (AED) and dehydroepiandrostenedione (DHEA) are synthesised by the adrenal glands (Nussey and Whitehead, 2013). In women, testosterone is also produced in the ovaries, as well as liver and adrenal gland (Gao et al., 2005). Some steroid hormones are so-called neurosteroids because they can modulate neuron excitability and gene expression in the brain (Paul and Purdy, 1992, Rose et al., 1997, Tuem and Atey, 2017) (**Figure 1.2**). In this study the focus will be on gonadal steroids, in particular testosterone.

The production of gonadal steroids is regulated by and in the hypothalamus where the luteinizing hormone-releasing hormone (LHRH) triggers the release of the luteinizing hormone (LH) and adrenocorticotropic hormone (ACTH) from the pituitary gland (**Figure 1.3**) (Nussey and Whitehead, 2013). The LH in turn acts on the gonads (ovaries and testis) where most of the estrogen, progesterone and testosterone is made. On the other hand, ACTH acts on the adrenal gland which mainly stimulates the release of glucocorticoids, such as cortisol, from the zona fasciculata in the adrenal cortex, usually as a response to stress, which is referred to as the hypothalamic-pituitary-adrenal-achsis (**Figure 1.3**) (Smith and Vale, 2006). Glucocorticoids in turn reduce the secretion of LHRH and ACTH, thereby providing a negative feedback mechanism (Handa and Weiser, 2014). However, the adrenal gland also stimulates the biosynthesis and release of a small proportion of gonadal steroids (Turcu et al., 2011).

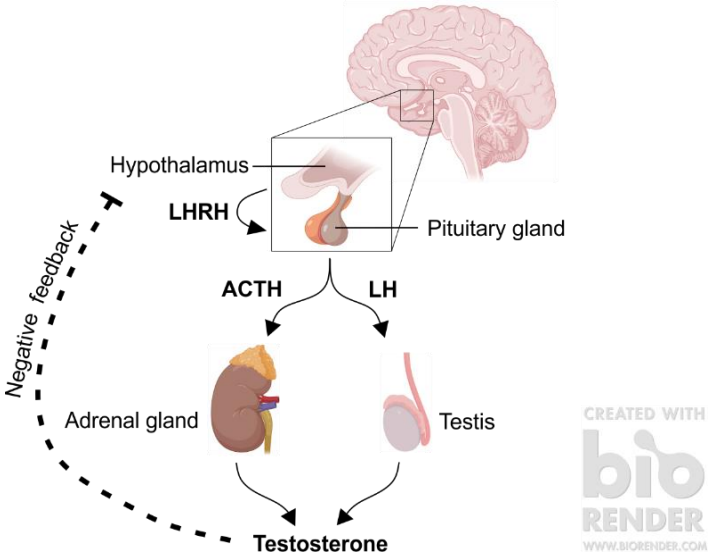

Figure 1.3: Schematic of hypothalamic-pituitary-adrenal axis.
The hypothalamus stimulates the release of ACTH and LH from the pituitary gland through LHRH secretion. This in turn activates the release of gonadal steroids, such as testosterone, from the adrenal gland and testes. A negative feedback mechanism regulates the release of hormones by the hypothalamic–pituitary–adrenal axis. LHRH = luteinizing hormone-releasing hormone; ACTH = adrenocorticotropic hormone; LH = luteinizing hormone.

Gonadal steroids move through the blood bound to plasma proteins. They are bound to either albumin or the sex hormone-binding globulin (SHBG) (estrogen and testosterone) and corticosteroid-binding globulin (CBG), also called transportin, (progesterone) respectively, whilst only about ~2-3% of hormone is circulating free and unbound (Baker, 2001, Becker, 2001, Rosner et al., 1991). When steroid hormones reach their target cells, they can easily pass the cell membrane due to their lipophilic nature. Inside the cell they bind to steroid receptors which are a subfamily of the nuclear receptor superfamily

(Weikum et al., 2018). Unlike membrane bound receptors, nuclear receptors are intracellular and regulate the transcription of genes directly, i.e. they act as transcription factors (Whirledge and Cidlowski, 2019). Nuclear receptors are ligand dependent which means they are only activated when an endogenous ligand is binding. The ligand can be a steroid or non-steroid hormone. Non-steroid hormones include vitamin D, thyroid hormones and retinoids (Ji et al., 2012). In addition, phospholipids, like phosphatidylcholine or phosphoinositide, have been shown to be able to bind and activate certain nuclear receptors (Crowder et al., 2017, Irvine, 2003). For some nuclear receptors, called orphan receptors, no physiological ligand has been identified yet (Lala and Heyman, 2000). Regarding their ligands, nuclear receptors can be divided into 1) Steroid hormone receptors, 2) Non-steroid receptors and 3) Orphan receptors (Table 1.1) (Shiota et al., 2019). The focus of this study is the androgen receptor, its ligands and signalling pathway.

1.1.2 Androgen signalling in normal physiology

The androgen receptor (AR) is expressed in many different tissues and organs with the highest expression level in the prostate, adrenal gland and epididymis (Keller et al., 1996). The generation of androgen receptor knockout (ARKO) mice and phenotypic analysis helped elucidate the role of androgen signalling in normal physiology (Chang et al., 2013, Rana et al., 2014, Zhou, 2010). Several studies showed that ARKO mice have smaller testes that were situated within the abdomen and blocked spermatogenesis (Notini et al., 2005, Yeh et al., 2002). Sato et al (2004) reported atypical sexual behaviour in male ARKO mice and that the AR is important for the masculinisation of the brain in the time immediately before and after birth (Sato et al., 2004). The AR is also highly important for the formation of bones (Venken et al., 2006, Yeh et al., 2002). The AR has been shown to be crucial for the inhibition of osteoclasts which are responsible for bone resorption. In ARKO mice this inhibition is lost, leading to an imbalance between bone resorption by osteoclasts and bone formation by osteoblasts and thereby resulting in reduced bone volume and size (Kawano et al., 2003, Tanaka et al., 2005). Studies on the effect of ARKO mice on muscle development have proven that the AR receptor is an important regulator of muscle mass development (MacLean et al., 2008, Ophoff et al., 2009). It was also shown that the AR regulates specific proteins and cell types in muscles, for example the AR signalling pathway supports so-called slow-twitch fibres which are crucial for long- endurance exercises (Altuwaijri et al., 2004). AR has also been reported to be expressed in
muscle cells of the heart (cardiomyocytes) and is directly involved in the physiological

Table 1.1: The members of the nuclear receptor superfamily.
Nuclear receptors can be classified into 1) Steroid hormone receptors, 2) Non-steroid receptors and 3) Orphan receptors. The members of each class are given and their site of expression, involvement in biological processes and role in prostate cancer is stated. CNS = Central nervous system, PCa = prostate cancer.

Classification	Member	Site of expression	Involved in regulation of	Role in PCa
1) Steroid hormone receptor	**Estrogen receptor (ER)**	Uterus, ovary, mammary gland, bladder, lung, testis, prostate, brain, and bone	Female reproductive system and other organs	Oncogenic
	Progesterone receptor (PR)	Uterus, ovary, mammary gland, prostate, cardiovascular system, brain, and bone	Female reproductive system and other organs	Oncogenic
	Androgen receptor (AR)	Testis, cardiovascular system, brain, muscle and bone	Male reproductive system and other organs	Oncogenic
	Glucocorticoid receptor (GR)	Various organs and tissues	Energy metabolism, reproduction, immune and cardiovascular system	Oncogenic
	Mineralocorticoid receptor (MR)	Various organs and tissues	Kidney, CNS, and cardiovascular system	Antioncogenic
2) Non-steroid receptors	**Retinoic acid receptor (RAR)**	Various organs and tissues	Cell growth and differentiation	Antioncogenic
	Peroxisome proliferator-activated receptor (PPAR)	Adipose and intestine tissue,	Adipogenesis, lipid metabolism, and adipocyte differentiation	Controversial, complex
	Farnesoid X receptor (FXR)	Liver, gut	Bile acid, lipid and carbohydrate metabolism	Antioncogenic
	Liver X receptor (LXR)	Liver, kidney, intestine, adipose tissue, adrenal gland, hematopoietic cells	Cholesterol and lipid metabolism	Antioncogenic
	Vitamin D receptor (VDR)	Various organs and tissues	Cell proliferation, calcium & phosphate homeostasis, and immune system	Antioncogenic
	Retinoid X receptors (RXR)	Adipose and intestine tissue	Adipogenesis and adipocyte differentiation	Antioncogenic
3) Orphan receptors	**Estrogen-related receptor (ERR)**	Various organs and tissues	Energy metabolism, obesity, insulin, and bone	Antioncogenic
	Retinoic acid receptor-related orphan receptors (ROR)	Various organs and tissues	Development of lymphoid thymocytes & lymph nodes	Controversial, complex
	Testicular orphan nuclear receptors (TR)	Testis, bone, muscle, liver and other organs and tissues	Fetility, bone and muscle, energy metabolism. immune system	Controversial, complex
	Chicken ovalbumin upstream promoter-transcription actors (COUP-TF)	Nervous system, lung, kidney, pancreas, testis and prostate	Neuronal development and organogenesis	Controversial, complex
	Dosage-sensitive sex reversal-adrenal hypoplasia congenital critical region on the X chromosome, gene 1 (DAX1)	Testis, prostate, ovary, adrenal gland	Steroidogenesis, development, reproduction	Antioncogenic
	Short heterodimeric partner (SHP)	Liver, intestine	Bile acid synthesis, cholesterol homeostasis	Antioncogenic

enlargement and thickening (hypertrophy) of the walls of the heart, in response to high blood pressure for example (Marsh et al., 1998). Another study reported that AR signalling is important in the normal growth of the heart and to inhibit cardiac fibrosis, which is the abnormal accumulation of extracellular matrix responsible for wall thickening and reduced contractility (Ikeda et al., 2005). The AR also plays an important role in inhibiting the development of adipocytes (fat cells) and the differentiation of pre-adipocytes into terminal adipocytes (Dieudonne et al., 1998, Yeh et al., 2002). A study by Holland *et al* (2016) revealed that testosterone impairs the expression of lipogenic genes in abdominal fat through an estrogen-dependent mechanism (Holland et al., 2016). Another study revealed that ARKO mice develop late-onset obesity through increased secretion of adiponectin, a adipocyte-specific hormone that regulates lipid and glucose metabolism (Fan et al., 2005, Nasr et al., 1982, Scherer et al., 1995). These data is supported by another study who reported obesity in ARKO mice was due to increased levels of the adipocyte specific hormones leptin and adiponectin and reduced voluntary activity in mice (Rana et al., 2011). In addition, AR plays an important role in the immune system by regulating the function and development of neutrophils and the recruitment of macrophages involved in wound healing (Lai et al., 2012). Huang *et al* (2013) has proven a role of AR in blood cells by showing that ARKO mice exhibit an enhanced ability of mesenchymal stem cells to re-new themselves in the bone marrow (Huang et al., 2013). These knockout studies studies provide evidence that the androgen signalling pathway is important for many processes in normal physiology including reproduction, muscles, bones, the brain, the heart, fat metabolism, and the immune and haemopoietic system (Rana et al., 2014). The AR acts on the cells in those organs and tissues either through genomic or non-genomic androgen signalling pathway both of which will be described in the following sections (Bennett et al., 2010, Freedman, 1998).

1.1.2.1 Genomic androgen signalling

The genomic AR signalling pathway, also called “classical” or “canonical” pathway, involves the binding of AR to DNA (**Figure 1.4**). When testosterone enters a prostate cell, it can be converted to the more active metabolite 5α-dihydrotestosterone (5α-DHT) by the steroid-5α-reductase (Randall, 1994). 5α-DHT has a higher binding affinity for the AR than testosterone, but testosterone compensates this defect by mass action (95% abundant) (Gao et al., 2005, Grino et al., 1990). The AR is bound to a complex of heat shock proteins (Hsps) which dissociates from the receptor upon agonist binding (**Figure 1.4**) (Pratt and Toft, 1997, Veldscholte et al., 1992b). Agonist binding to the AR also induces

conformational changes and AR dimerization. AR usually forms homodimers, but the formation of heterdimers with TR4 and ERα have been reported. However, those heterodimers decreased the transcriptional activity of AR in both studies (Lee et al., 1999, Panet-Raymond et al., 2000). Similar to other steroid receptors, the AR homodimer usually is a "head-to-head" formation (Shaffer et al., 2004). AR is then translocated to the nucleus where it binds to the androgen response element (ARE) on the DNA (**Figure 1.4**) (Bennett et al., 2010, Nelson et al., 2002). The consensus sequence for ARE is an inverted or direct repeat of 5′-AGAACA-3′ and 5′-TCTTGT-3′ respectively, separated by three random basepairs, for example 5′-AGGTCA | NNN | TGACCT-3′. In the last decades, research groups found AREs which do not contain this consensus sequence (Bolton et al., 2007, Denayer et al., 2010, Ham et al., 1988). In 1996, Claessens et al. identified a consensus sequence which is specific for the androgen receptor, namely 5'-GGTTCT-3' (Claessens et al., 1996). Since the androgen and glucocorticoid receptor have a highly conserved LBD domain, single point mutations in this sequence have been reported to shift the binding specificity from the androgen to the glucocorticoid receptor (Claessens et al., 1996, Mangelsdorf et al., 1995). To date it is not fully understood how the steroid receptors with their highly conserved DBDs achieve receptor specific binding of DNA response elements. Some crystallographic studies suggest the structure and stability of receptor dimerisation plays a role (Shaffer et al., 2004). AR contains an additional interface that supports the AR-dimer binding to ARE, whereas dimers of other steroid receptors do not exhibit the same stability and therefore are unable to bind ARE (Claessens et al., 2008). The transcriptional activity of AR requires the recruitment of transcription factors and so-called epigenetic co-regulator proteins (**Figure 1.4**) (Heinlein and Chang, 2002). Epigenetic co-regulator proteins covalently modify histone residues which results in chromatin remodelling giving way to the transcription initiation complex (Heinlein and Chang, 2002).

1.1.2.2 Non-genomic androgen signalling

The non-genomic androgen signalling pathway, also referred to as the "non-classical" or "non-canonical" pathway differs from the genomic pathway regarding speed (Lucas-Herald et al., 2017). Whilst the genomic pathway usually takes hours for gene transcription to occur after androgen exposure, the non-genomic pathway can show an effect within seconds to minutes (Cato et al., 1988). In the non-genomic pathway, androgens, bound to the SHBG, do not enter the target cell. Instead they act through membrane-associated

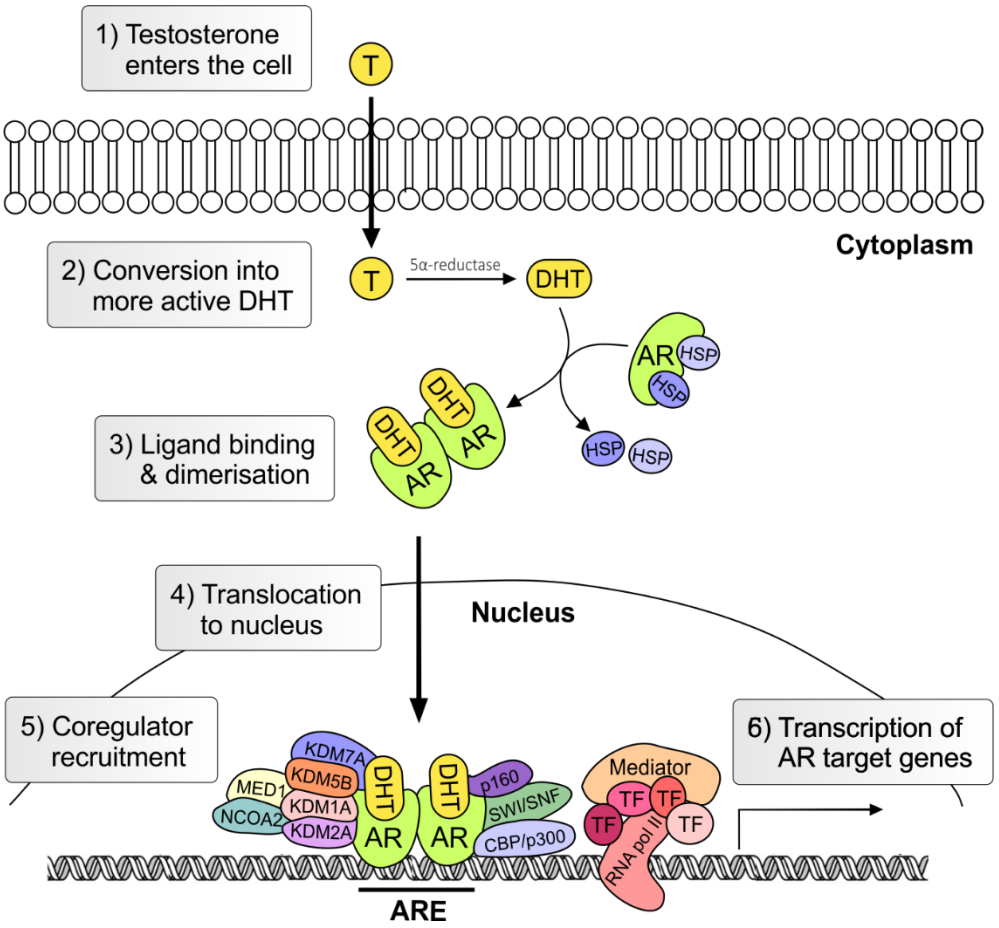

Figure 1.4: Genomic androgen receptor signalling pathway.
Androgens, such as testosterone and dihydrotestosterone, enter the cell and are converted in the more active metabolite (5α-DHT) by the steroid-5α-reductase. Upon ligand binding heat stress protein (HSP) chaperones are released and AR undergoes conformational change and dimerization. In the nucleus the AR together with co-regulators activates the transcription of androgen regulated genes. T, testosterone; AR, androgen receptor; DHT, 5α-dihydrotestosterone; HSP, heat shock protein; KDM, lysine demethylase; MED1, Mediator Complex Subunit 1; NCO2, Nuclear Receptor Coactivator 2.

proteins or channels and 2nd messenger pathways (**Figure 1.5**) (Estrada et al., 2006, Lieberherr and Grosse, 1994, Liu et al., 2005, Wunderlich et al., 2002). It was suggested that non-genomic pathway induced phosphorylations regulate the AR transactivation of the genomic pathway by phosphorylating AR or coregulator proteins (Chmelar et al., 2007, Lamont and Tindall, 2011, Ueda et al., 2002b).

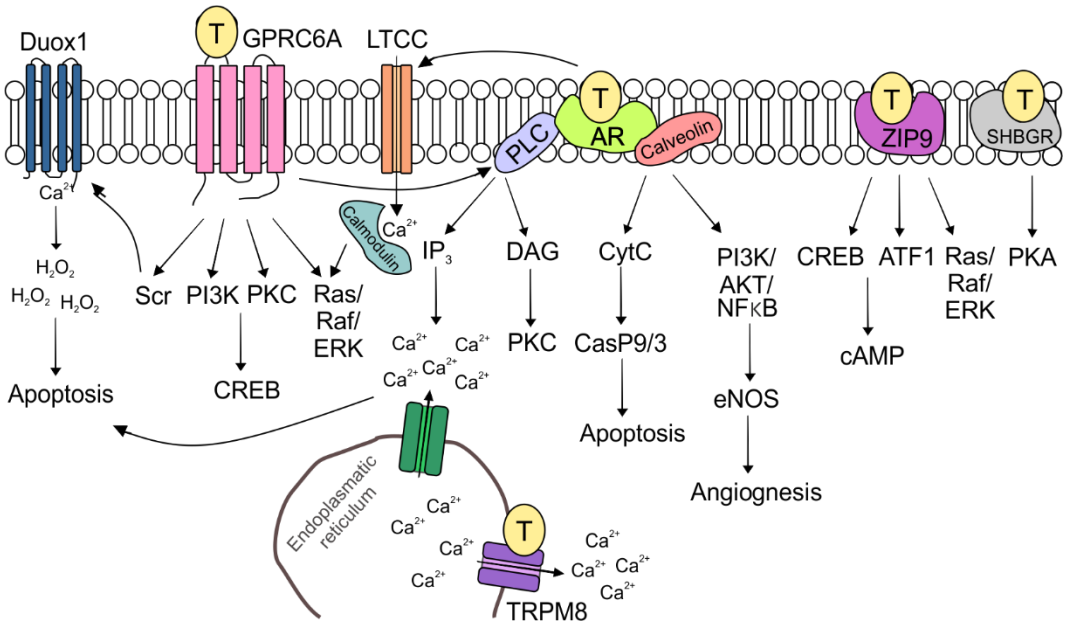

Figure 1.5: Non-genomic androgen receptor signalling pathway.
Extracellular testosterone can bind to transient membrane-androgen receptors, G-protein coupled receptors and other membrane-bound proteins which switches on various signalling pathways crucial in normal physiology. T = testosterone; AR = androgen receptor; Duox1 = dual oxidase 1; GPRC6A = G protein-coupled receptor family C group 6 member A; LTCC = L-type Ca^{2+} channel; PLC = phospholipase C; SHBGR = steroid hormone binding globulin receptor; Zip9 = zinc transporter 9; Src = tyrosine kinase; PI3K = phosphatidylinositol 3-kinase; PKC = protein kinase C; CREB = cAMP response element-binding protein; cAMP = cyclic adenosine monophosphate; IP_3 = inositol trisphosphate; DAG = diacylglycerol; ERK = extracellular Signal-regulated Kinase-1; CytC = cytochrome C; casp9/3 = caspase9/3; Akt = serine/threonine kinase, NFκB = nuclear factor κB; ATF1 = activating transcription factor 1; TRPM8 = transient receptor potential cation channel subfamily M member 8.

1.1.3 Structure of the androgen receptor

The *androgen receptor (AR)* gene is located on chromosome X and spans 186,587 base pairs (bp) (**Figure 1.6**) (Migeon et al., 1981). The protein coding region is ~2757 nucleotides long and the protein is comprised of 920 amino acids (NM_000044.3). The 110 kDa AR protein is encoded by eight exons and contains four domains: The N-terminal domain (NTD), the DNA-binding domain (DBD), the hinge region and the ligand binding domain (LBD) (**Figure 1.6**) (Simental et al., 1991). The NTD is the most variable region of nuclear receptors in both sequence and size. In AR, it harbours a polyglutamine (CAG) repeat, ranging between ~11-37 repeats, and a polyglycine (GGC) repeat, ranging between ~12-29 repeats (Choong and Wilson, 1998). The number of repeats varies within human populations, for example Japanese have shorter GGC repeats than Caucasians (Sasaki et al., 2003). The length of the repeats influences the folding and conformation of AR, giving it high plasticity and allowing it to interact with distinct co-regulator proteins or

transcription factors (Bevan et al., 1999). Moreover, long polyglutamine repeats have been associated with reduced expression of the androgen receptor gene and it is therefore not surprising that variations in repeats have been implicated in various diseases which will be discussed in the next chapter (Callewaert et al., 2003, Choong et al., 1996). In contrast to the NTD, the DBD is highly conserved between the steroid hormone receptors and is situated in the centre of the polypeptide (Cutress et al., 2008). It is composed of two zinc fingers, each of which contains four cystine residues coordinating a zinc ion (Shaffer et al., 2004). The N-terminal zinc finger is responsible for the recognition of the androgen response element (ARE) in enhancer and promoter regions of AR target genes (Luisi and Sigler, 1991, Luisi et al., 1991). The highly conserved DBD ensures that the ARE of a gene is only recognised by AR and not any other steroid hormone receptors, allowing highly selective binding. The other zinc finger is, together with the NTD and LBD, involved in the AR dimerisation (Shaffer et al., 2004). The DBD and LBD are separated through a variable hinge region which is important for AR transactivation, nuclear translocation and binding of the DNA minor groove (Clinckemalie et al., 2012, Haelens et al., 2007, Rastinejad, 2001) (Figure 1.6). Within the COOH-terminus of the DBD and hinge region there is a so-called nuclear localisation signal (NLS) which is responsible for the transport of the AR into the nucleus (Zhou et al., 1994). In detail, AR is bound to a protein called importin 7 which inhibits AR import in the absence of a ligand. If a ligand binds to AR, importin 7 is released, which then allows NLS to bind to a protein called karyopherin α (KPNA) / importin-α resulting in AR nuclear translocation (Ni et al., 2013). On the other hand, the signal responsible for the export of AR from the nucleus to the cytoplasm is located in the LBD. It is called the nuclear export signal (NES) and in the absence of ligand, NES is dominant over NLS (Saporita et al., 2003). The LBD is composed of eleven α-helices and four β strands, forming a three-layered α-helical sandwich. In contrast to other nuclear receptors, AR lacks the α-helix H2 and harbours a flexible linker instead (Tan et al., 2015). The LBD is the site where both ligands and coregulatory proteins bind. In addition, the LBD is the site where heat shock proteins bind to the AR, preventing the AR to bind to the DNA (Nemoto et al., 1992). The AR also harbours two activation functions (Figure 1.6). The activation function-1 (AF-1) is located in the NTD, whereas the activation function-2 (AF-2) is situated in the LBD. The function of AF-1 and AF-2 have been determined by mutational deletion studies. AF-1 has been shown to be constitutively active and the truncation of the LBD did not affect the activity of the receptor, suggesting AF1 is ligand-independent (Jenster et al., 1991, Rundlett et al., 1990, Simental et al., 1991, Zhou et al., 1994). Bevan et al. (1999) reported that AF-1 is composed of two overlapping transcription activation units (TAUs) called TAU-

1 (aa 100-370) and TAU-5 (aa 360-529) and that their function is context dependent (**Figure 1.6**). In full-length AR, TAU-1 is responsible for activation, whereas in AR with deleted LBD, TAU-5 fulfils the activation function (Callewaert et al., 2006, Jenster et al., 1991). AF-2, on the other hand, is ligand dependent and crucial for the interaction of the N-terminal and C-terminal domains. If a ligand is binding, the most COOH-terminal α-helix (H12) "flips over" and creates a hydrophobic binding pocket composed of α-helices 3, 4 and 12. This hydrophobic binding surface is the AF-2. The AR NH2-terminus then binds to the AF-2 through its FQNLF motif (Bevan et al., 1999, He et al., 1999, He et al., 2000, Parker and White, 1996). Subsequently, a second motif, WXXLF, in the NH2-terminus becomes available and binds to the LBD too, but outside of AF-2 (He et al., 2000) (**Figure 1.6**). The conformational change is important to stabilise ligand binding (H12 acts like a lid to close the ligand binding pocket), reduce the ligand dissociation rate and to create a new surface area for other co-regulator proteins to bind.

Co-regulator proteins bind to the hydrophobic pocket of AF-2 through their LxxLL (L = leucine, x = any amino acid) motif (Alen et al., 1999, Darimont et al., 1998, Heery et al., 1997, McInerney et al., 1998) . This motif is highly conserved between nuclear receptor interacting proteins such as the steroid receptor coactivator-1 (SRC-1) and was shown to be necessary and sufficient to mediate coregulator binding to the LBD of the nuclear receptor (Heery et al., 1997). He et al. (2002) found a second motif, namly F*XX*LF, which is also present in the NTD of the AR (FQNLF). This motif is therefore important for both interactions within AR itself and AR interaction with coregulator proteins (He et al., 2002). The latter interaction is stabilised by further conformational changes and the so-called "charge clamp" which is hydrogen bonds between the coregulator and two highly conserved residues, a lysine (K720) in H3 and a glutamate (E897) in H12 (He et al., 2004, Hodgson et al., 2008, Hur et al., 2004). Coregulator proteins often share the same binding motif, however, the way the binding pocket of AR can bind coregulator proteins specifically is by electrostatical interactions with positively or negatively charged amino acids flanking the motif (Darimont et al., 1998, McInerney et al., 1998). For example, nuclear receptor coactivators 2 and 3 (NCoA2/NCoA3) harbour negatively charged sides beside the motif which enables them to strongly interact with positively charged residues in the binding pocket (Estébanez-Perpiñá et al., 2005). Since the helical structure and the "charge clamp" of the ligand binding domain is similar between the steroid receptors this can lead to cross activation often seen with synthetic steroids (Gao et al., 2005).

The androgen receptor can be post-transcriptionally modified by phosphorylation, acetylation, methylation, ubiquitination, and sumoylation (Coffey and Robson, 2012) (Figure 1.6). Modifications can occur in all four domains of the androgen receptor with phosphorylation being the most common modification. Phosphorylation sites often are serine residues, but also threonine and tyrosine residues (Chen et al., 2006a, Kuiper et al., 1993, Yeh et al., 1999, Zhou et al., 1995). Post-translational modifications play an important role in AR stability, transport, transcriptional activity, recruitment of other binding partners, and regulation of AR expression and degradation (Daniels et al., 2013, Gioeli and Paschal, 2012, Ward and Weigel, 2009).

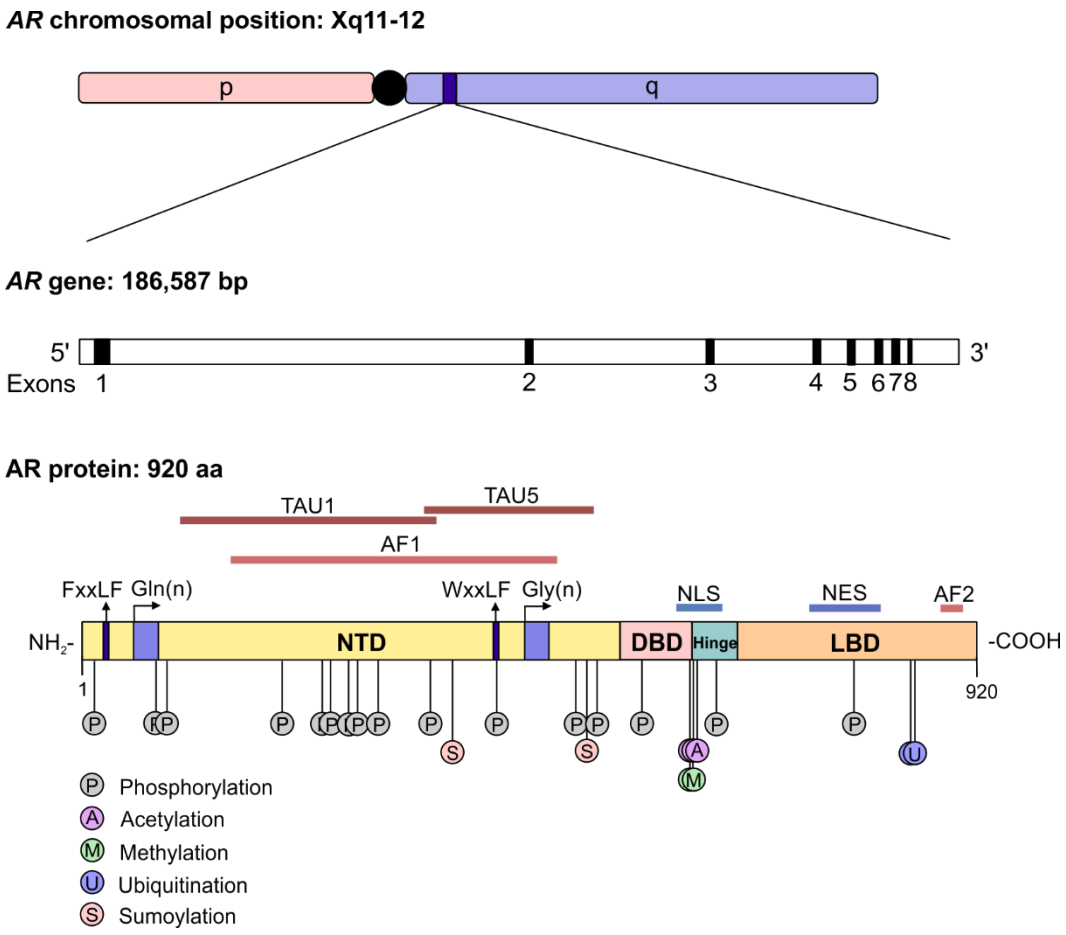

Figure 1.6: The structure of the androgen receptor gene and protein.
The AR gene is situated on position q11-12 of chromosome X and contains 8 exons. The protein reference sequence NM_000044.3 is comprised of 920 amino acids and is composed of different domains which are depicted. In addition, posttranslational modifications are shown. AR = androgen receptor; bp = base pair; NTD = N-terminal domain; DBD = DNA binding domain; LBD = ligand binding domain; AF = activation function; TAU = transcription activation unit; NLS = nuclear localisation signal; NES = nuclear export signal.

1.1.4 Androgen signalling in disease

As described above, androgen signalling is important in many processes of normal physiology, however, defective androgen signalling can lead to disorders like the androgen insensitivity syndrome (AIS), Kennedy's disease, hypogonadism, insulin resistance and obesity, benign prostatic hyperplasia (BPH) and cancer (Matsumoto et al., 2013, Shukla et al., 2016). The defects are usually due to mutations in the AR or due to abnormalities in the androgen signalling pathway. In 2012, Gottlieb et al described the androgen receptor gene (AR) mutations database which is available online at http://androgendb.mcgill.ca (Gottlieb et al., 2012). The total number of identified AR mutations is ~1029 which are predominantly located in the DBD and LBD domain of the AR. Four types of mutations have been characterised: (1) single point mutations causing substitutions or premature stop codons, (2) nucleotide insertions and deletions resulting in frameshifts, (3) complete or partial gene deletion, and (4) intronic mutations interfering with RNA splicing (Gottlieb et al., 2012). The Kennedy's disease, also called spinal bulbar muscular atrophy, is the progressive degeneration of motor neurons and is caused by extended CAG repeats in the NTD of the androgen receptor, ranging between 40 and 62 (Amato et al., 1993). Individuals with a large numbers of CAG repeats exhibit an early onset and a faster progression of the disease (Doyu et al., 1992, Igarashi et al., 1992). Extended CAG repeats cause a misfolded AR protein and the accumulation of misfolded AR in the nucleus of motor neurons causes transcriptional dysregulation and ultimate cell death (Li et al., 1998, Orafidiya and McEwan, 2015). Hypogonadism, also referred to as testosterone deficiency, describes the inability of the testicles to produce normal levels of testosterone and therefore symptoms include delayed puberty, smaller testes and prostate, decreased muscle mass, decreased body hair growth, osteoporosis, loss of libido and impotence, reduced or absent sperm production (Abadilla and Dobs, 2012). The cause of hypogonadism is either due to a dysfunction in the hypothalamic-pituitary axis or a disorder of the testicles (Abadilla and Dobs, 2012, Heidelbaugh, 2016, Wu et al., 2008).

1.1.4.1 Androgen-insensitivity syndrome

In 1953, Morris *et al* first reported about hormone resistance in patients and later in 1974, Wilson *et al* described the androgen insensitivity syndrome (AIS) (Morris, 1953, Wilson et al., 1974). The AIS is a developmental disorder characterised by the inability of cells to respond to androgen (Mongan et al., 2015). The syndrome can occur in complete, incomplete or mild forms. The complete form of AIS (CAIS) is characterised by a female

phenotype and a XY karyotype. In early childhood, CAIS often presents as a bump or swelling in the inguinal canal or labia, caused by testes. CAIS patients have female external genitalia, but their vagina is shortened and their uterus, cervix and ovaries are absent because of the anti-Muellerian hormones secreted by the testes (Brown, 1995, Josso et al., 2013, Klein et al., 2011, Quigley et al., 1995). The testes produce normal levels of testosterone in the blood which can be converted to estrogen by the enzyme aromatase. The level of testosterone and the luteinising hormone (LH) is normal or elevated, whilst the follicle-stimulating hormone (FSH) is not increased (Doehnert et al., 2015, Melo et al., 2003). The estrogen, synthesised from the testosterone or the LH, elicits breast development in puberty of CAIS patients but menses and sexual hair growth are absent (Hughes et al., 2012, Mongan et al., 2015). Currently it is therefore recommended not to remove gonads in early childhood but rather to wait until after puberty is completed (Mongan et al., 2015). In contrast, in the partial form of AIS (PAIS) the androgen receptor is partially able to respond to androgen. Patients with PAIS have a XY karyotype, but the phenotype can vary from a mainly female appearance, over ambiguous genitalia, to a mostly male appearance (Boehmer et al., 2001, Quigley et al., 1995). PAIS patients with a female appearance have external female genitalia and pubic hair but can have a mildly enlarged clitoris and partly fused labia. In contrast, patients with a male appearance have a micropenis, enlargement of breast tissue (gynecomastia) in puberty, their urethral opening is often positioned in the area between the anus and the scrotum (perineal hypospadias), and their testes may fail to descend from the abdomen to the scrotum (cryptorchidism) (Batch et al., 1993, Evans et al., 1997, Imasaki et al., 1994). In PAIS normal levels of hormones are produced by the testes and during puberty testosterone, LH and estrogen levels are increased (Brown, 1995). In contrast to CAIS, it can be a complex clinical challenge to determine which sex to assign to a child (Mongan et al., 2015). In most of the cases, parents decide for a male phenotype and hypospadiasa, cryptorchidism, micropenis and later gynecomastia are corrected via surgery (Kolesinska et al., 2014). Androgen supplementation is common too (Mongan et al., 2015).

In the mild androgen insensitivity syndrome (MAIS) patients usually have normal or only very mildly abnormal genitalia, however, when they enter puberty they exhibit gynecomastia and infertility (Zuccarello et al., 2008). The most common cause of MAIS are mutated AR and, as reported above, the AR is crucial for spermatogenesis (Wang et al., 2009b). MAIS also occurs in bulbar and spinal muscular atrophy (Kennedy's disease), whose cause is a hyperexpansion of the CAG repeat in the N-terminal domain of the androgen receptor as described before.

The best studied cause of AIS are mutations in the androgen receptor. About 90-95% of all CAIS cases show mutations in the AR causing hormone resistance, whereas in PAIS AR mutations are identified in less than a third of cases (Hiort, 2013, Jääskeläinen, 2012, Mongan et al., 2015). This raises the potential that other components of the AR signaling pathway, including epigenetic coregulator proteins of AR, are involved in PAIS (Audi et al., 2010, Mongan et al., 2015). Indeed AR mutations which impair coregulator recruitment have been identified in AIS patients (Li et al., 2005, Umar et al., 2005). Numerous mutations, which impair the recruitment of coactivators in prostate cancer, seem to be involved in CAIS (Adachi et al., 2000, Lagarde et al., 2012, Li et al., 2005, Nazareth et al., 1999). In patients with PAIS two mutations, one in the N-terminal domain and one in the ligand binding domain of the androgen receptor, have been shown to interfere with interactions between the AR and the coactivators NCoA2/TIF2 (nuclear receptor coactivator 2/transcriptional mediators/intermediary factor 2) and MAGE11 (Melanoma Antigen Gene Protein 11) (Cheikhelard et al., 2008, Duff and McEwan, 2005). Although there is clinical evidence suggesting a coregulator role in AIS (Adachi et al., 2000), to date no coregulator mutations have been identified in AIS, despite intense efforts (Lim et al., 2001, Mongan et al., 2001, Mongan et al., 2003, Adachi et al., 2000). Another mutation was discovered in a patient with PAIS that blocked the interaction between the NTD and the LBD crucial for AR activation (Quigley et al., 2004). Overall, AIS has provided valuable insights into the structure and function of the AR and highlights the significance of AR mutations in PCa.

1.1.4.2 Prostate benign hyperplasia and cancer

The risk for benign prostatic hyperplasia (BPH) increases with age and about ~50% of over 50-year-old men have BPH (Berry et al., 1984, Verhamme et al., 2002). BPH is the enlargement of both epithelial and stromal tissue of the prostate which mainly influences the transition zone (**Figure 1.7**) (McNeal, 1988). This enlargement can compress the urethra, leading to lower urinary tract symptoms (LUTS) including difficulties urinating like hesitancy, incomplete emptying and urgency, and incontinence (Kim et al., 2016). Potential causes for the development of BPH include age, genetics and associated metabolic and hormonal factors, however, the exact mechanisms are yet to be described (Chen et al., 2012a, Ho and Habib, 2011, Montie and Pienta, 1994). Dysfunctional androgen signalling can also lead to prostate cancer which is the focus of this study and will be described in detail in the next sections.

1.2 Prostate cancer

In this section the function and structure of the prostate gland and the role of AR signalling in PCa will be described. The incidence and mortality rates of prostate cancer will be covered, as well as risk factors including race and genetics. Then the diagnosis and treatment options of prostate cancer patients will be discussed, followed by an in-depth description of first and second generation androgen deprivation therapies. The last section is designated to the molecular mechanisms of hormone refractory prostate cancer.

1.2.1 Physiology of the prostate

The prostate is a male reproductive gland which generally has the size of a walnut and is situated beneath the bladder, surrounding the urethra (**Figure 1.7**). The prostate gland is composed of four different zones, the central zone (CZ), transition zone (TZ), peripheral zone (PZ) and anterior zone (AZ) (McNeal, 1988) (**Figure 1.7**). The prostate can also be divided into the base (upper third of the gland, just below the bladder), the mid-prostate (middle third) containing the verumontanum, also called seminal colliculus, which is the marking point where the ejaculatory duct enters the urethra, and the apex (lower third) (Bhavsar and Verma, 2014). The PZ makes up ~70% of the prostate (**Figure 1.7**). Diseases like chronic prostatitis, post-inflammatory atrophy and cancer most commonly arise in the peripheral zone (De Marzo et al., 1999, McNeal, 1988). The PZ is comprised of many ducts, acini and some smooth muscle tissue (Bhavsar and Verma, 2014). The CZ is situated between the PZ and TZ and accounts for ~25% of the gland (**Figure 1.7**). It is cone-shaped, surrounds the ejaculatory ducts and gets thinner at the verumontanum. The TZ makes up only 5% of the gland, surrounds the urethra and is enlarged in patients with benign prostatic hyperplasia. The AZ does not contain any glandular structures but fibrous and smooth muscular tissue (**Figure 1.7**). It is the connection point to the pelvic diaphragm and also covers part of the prostate as a thin fibrous capsule (Bhavsar and Verma, 2014). The prostate plays an important role during ejaculation. When the sperm travels from the testes through the *vas deferens* to the prostate, the prostate contracts to close the connection between the bladder and the urethra. Its main function though is to secrete a fluid which accounts for one third of the total volume of the semen. The slightly acidic fluid contains various enzymes and zinc which is crucial for semen liquefaction and motility (Huggins and Neal, 1942, Sørensen et al., 1999, Yoshida et al., 2008). The other two thirds of the semen is produced by the seminal vesicle and is slightly alkaline which is important for the sperm to survive in the acidic environment of the vagina (McKay and Sharma, 2019).

The fluid contains proteins, enzymes, vitamin C and fructose which is a crucial energy source for sperm cells (Druart and de Graaf, 2018). For example the protein semenogelin is important to form a gel-like matrix, called seminal coagulum, which holds the sperm cells encased to avoid immediate functional maturation (capacitation). The enzyme prostate-specific antigen (PSA) and its proteolytic activity is crucial to degrade the seminal coagulum and to liquefy the sperm (Wang and Wang, 2018). The muscular tissue of the prostate also helps to push the seminal fluid into the urethra.

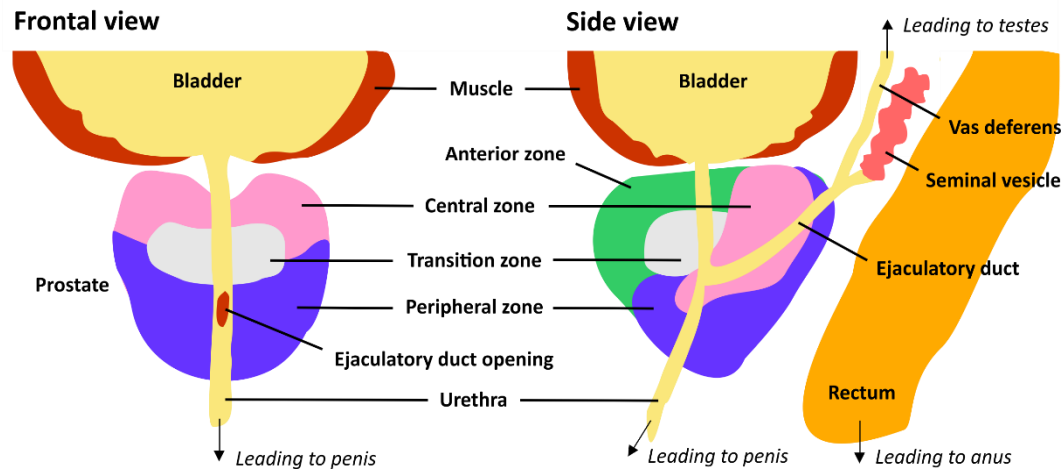

Figure 1.7: Anatomy of the prostate gland and surrounding organs.
The prostate is a gland situated between the bladder and the penis, in front of the rectum, and surrounds the urethra. It is divided into the anterior, central, transition and peripheral zone.

The glandular structure of the prostate is, like other glands, comprised of ducts which have a branching function, and acini which are responsible for secretion (**Figure 1.8**). Acinar adenocarcinoma is the most common type of all prostate cancers and makes up around 95%, whereas ductal adenocarcinoma accounts for only 0.4-0.8% (Orihuela and Green, 2008). Ductal adenocarinoma usually arises in periurethral ducts and extends towards the urethra (Bock and Bostwick, 1999). The epithelium of the ducts and acini is mainly composed of luminal and basal cells, but also intermediate, neuroendocrine and stem cells (**Figure 1.8**) (Shen and Abate-Shen, 2010). Luminal cells are terminally differentiated secretory cells of the prostate gland that are responsible for the exocrine activity of the prostate. They express high levels of AR and secrete proteins including the prostate specific antigen (PSA/KLK3) and prostate acid phosphatase (PAcP) into the lumina of the gland (Shen and Abate-Shen, 2010). The PAcP is thought to be important for fertility and sperm motility (Coffey and Pienta, 1987, Veeramani et al., 2005). Interestingly, even though PAcP has been shown to be elevated in the serum of PCa patients, it is a known tumour suppressor, exhibiting lower expression in tumour cells compared to non-tumour cells

(Ortlund et al., 2003, Yam, 1974). Luminal cells are thought to be the main cell of origin for PCa and primary PCa almost always has a luminal cell-like phenotype with atypical glands, enhanced AR signalling and absence of basal cells (Wang et al., 2014, Zhang et al., 2018a). A study by Wang et al (2009) has described a rare luminal population of castrastion-resistant NKX3.1-expressing cells (CARNs) that exhibit stem cell-like properties (Wang et al., 2009c). Basal cells have been characterised as undifferentiated precursors of luminal cells (Figure 1.8) (Bonkhoff and Remberger, 1996). They express very little or no AR, are in direct contact with luminal cells via gap junctions and form a barrier between the luminal cells and the blood (El-Alfy et al., 2000). Like luminal cells, basal cells can give rise to tumours, however, bioinformatic analysis suggests that luminal-cell derived tumours are more aggressive (Wang et al., 2013). High-grade prostatic intraepithelial neoplasia (PIN) is defined by increase in luminal cells, decrease of basal cells and cells generally have atypical and enlarged nuclei and nucleoli (Bostwick and Brawer, 1987). It is regarded as the most common precursor for PCa and its incidence and volume increase with age in men (Brawer, 2005, McNeal and Bostwick, 1986). Intermediate cells make up an only small proportion of the epithelium and are situated within the basal layer (Figure 1.8). They co-express basal and luminal cytokeratin markers, however, it remains controversial if intermediate cells represent a distinct cell type within the prostate gland epithelium (Toivanen and Shen, 2017, Verhagen et al., 1992, Xue et al., 1998).

During development and puberty, prostate stem cells and progenitor cells are responsible for the formation of the prostate, and several studies suggest that these cells also exist in the prostate epithelium of adults (Figure 1.8) (Bonkhoff and Remberger, 1996, Wang et al., 2001). Stem cells make up ~0.1-3% of the epithelial cell population and reside within "niches" near the basement membrane. The third most common cell type, besides luminal and basal cells, are neuroendocrine cells which have neuronal characteristics (Figure 1.8) (Abrahamsson, 1999, Aprikian et al., 1993, Bonkhoff and Remberger, 1996). There are two morphologically different types of neuroendocrine cells. The "closed type" which resides on the basal lamina and connects adjacent cells but does not reach the lumen, and the "open type" which are exposed to the lumen (Churukian and Agarwal, 1985). Neuroendocrine cells originate from either neural crest progenitors or urogenital epithelial progenitors which also give rise to basal, luminal and intermediate cells (Toivanen and Shen, 2017). Only about ~0.5-2% of prostate cancer patients have neuroendocrine prostate cancer (NePC) at the initial diagnosis (Humphrey, 2012, Mucci et al., 2000). NePC frequently emerges after patients have received androgen deprivation therapies (ADTs) and accounts for about ~25% of all metastatic prostate cancers (Humphrey, 2012, Mucci

et al., 2000). Histological characteristics of NePC, also called small-cell NePC, are poorly differentiated, atypical, small cells that lack glandular structures (Helpap and Köllermann, 1999). NePC cells do not express detectable levels of PSA and AR and instead are positive for neuroendocrine differentiation specific markers like chromogranin A and synaptophysin, which are most sensitive, but also the neural cell adhesion molecule and neuron-specific enolase (Gould et al., 1987, Helpap et al., 1999). In recent years, the loss of the tumour suppressor proteins retinoblastoma (Rb), p53 and Pten (Phosphatase and tensin homolog) have been reported in NePC cases (Krausch et al., 2011, Tan et al., 2014). A study showed that mutated p53 results in highly increased levels of Aurora kinase A (AURKA) in NePC (Li et al., 2015b). AURKA is a serine/threonine kinases responsible for spindle assembly and chromosome segregation during mitosis and causes aneuploidy and cell transformation if aberrantly expressed, thus acting as an oncogene (Kivinummi et al., 2017, Willems et al., 2018). Immunohistochemical analysis of NePC patients revealed that AURKA and N-myc, a well-known proto-oncogene, are amplified in prostatic adenocarcinomas that are likely to progress to NePC after hormone deprivation therapy and therefore could serve as prognostic and predictive biomarkers (Mosquera et al., 2013, Ramsay et al., 1986). In addition, almost half of all neuroendocrine prostate cancer cases harbour the TMPRSS2-ERG fusion gene expression (John et al., 2012, Lotan et al., 2011).

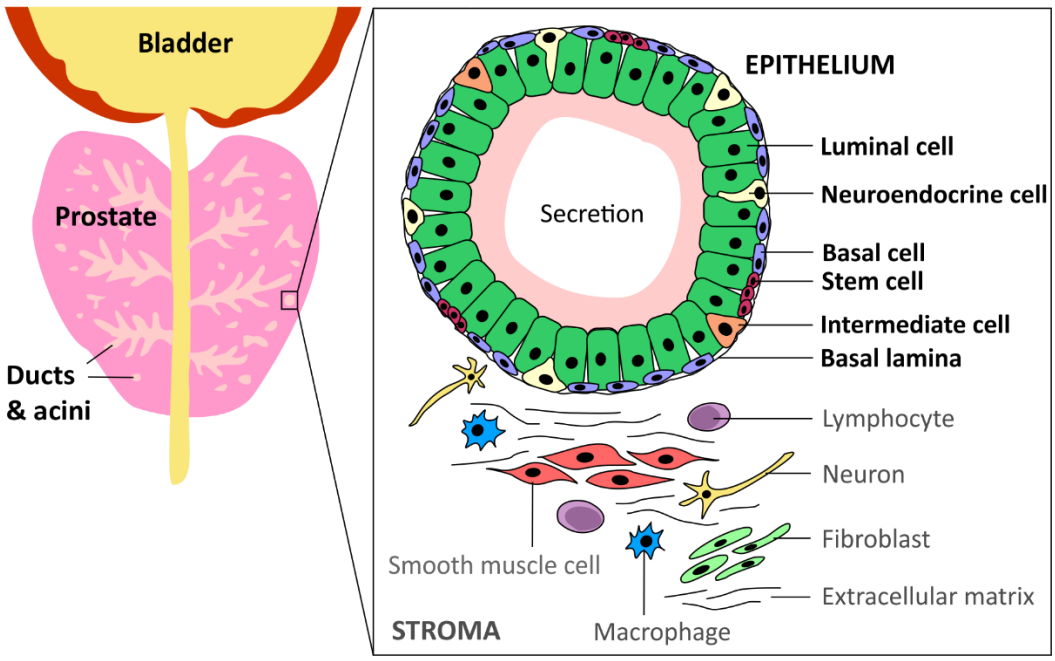

Figure 1.8: Histology of the prostate epithelium and stroma.
The glandular structure of the prostate is made up of ducts and acini. The epithelium contains luminal, basal, intermediate, neuroendocrine and stem cells which reside on the basal lamina. The stroma is made up of extracellular matrix, immune cells (lymphocytes, macrophages), fibroblasts, neurons and smooth muscle cells.

There are two theories of how NePC can arise, one of which is that NePC originates from the same cell as normal neuroendocrine cells (Beltran et al., 2014, Bonkhoff et al., 1995). The other explanation is that NePC trans-differentiates from adenocarcinoma cells (Yuan et al., 2007). A study by Burchardt *et al* (1999) confirmed the trans-differentiation theory *in vitro* and *in vivo* by proofing that LNCaP cells trans-differentiate into neuroendocrine cells when exposed to hormone-deficient medium and castrated mice harbour more chromogranin A-positive neuroendocrine cells compared to non-castrated mice (Burchardt et al., 1999). NePC is highly proliferative and aggressive in most cases and since it is negative for AR it represents a major therapeutic challenge (Beltran et al., 2014, Hu et al., 2002).

1.2.2 Incidence and risk factors

PCa is one of the four most common malignancies in the world with breast, colorectal and lung cancer (Ferlay et al., 2013, Ferlay et al., 2015). According to recent cancer statistics in the United States (US), PCa is the most common cancer affecting men and lead to 31,620 deaths and 174,650 new cases in the US alone in 2019 (Siegel et al., 2019). Incidence rates have been increasing by ~40% since the 1990s, however, it is important to consider that the incidence rates reflect the availability of early detection tests (Jemal et al., 2006a, Jemal et al., 2006b). Indeed the widespread availability of the prostate-specific antigen (PSA) test starting in the 1990s has enabled the early diagnosis of asymptomatic PCa through screening programs. This has resulted in an increase in numbers of PCa cases diagnosed (Potosky et al., 1995). Incidence and mortality strongly vary between different countries and races (Jemal et al., 2010). Prostate cancer is also the most common cancer in men in Western and Northern Europe, North and South America and Australia. The lowest incidence rates are recorded in Asia and North Africa, however, it needs to be considered that accurate reporting may not be in place in certain areas (Ferlay et al., 2010). Mortality rates have been declining in the majority of western countries, including the USA, Canada, Portugal, France, Italy, the Netherlands, Norway, Sweden, Finland, Israel and Australia, which may be due to early detection and improved treatments (Baade et al., 2009, Collin et al., 2008, Etzioni et al., 2008). On the other hand, incidence and mortality rates are rising in some Asian and Eastern European countries (Baade et al., 2009). The reason for this may lie in the recent westernisation of diet and lifestyle in these countries, involving factors like animal fat consumption and obesity (Jemal et al., 2010). Men of African descent have an almost 50% greater incidence rate of prostate cancer than white men (Koulibaly et al.,

1997, Marwick, 1998, Powell et al., 1999). Another study showed that the risk for prostate cancer is even three-fold higher in black men compared to men of Asian-Indian descent (Bunker et al., 2002). A large sample size study revealed that African-American men with advanced disease are at a significantly higher risk to die after receiving hormonal therapy, suggesting ethnic differences in the biology of prostate cancer (Thompson et al., 2001). More research is needed to elucidate why men of African descent are more likely to develop prostate cancer and why their prostate cancer is more aggressive and lethal. This aspect in prostate cancer now starts to be investigated by many research groups (Huang et al., 2017, Khani et al., 2014).

Risk factors for prostate cancer are age, race, family history and diet and prostate cancer is thought to be the result of a combination of factors (Pienta and Esper, 1993). The Surveillance, Epidemiology and End Results (SEER) program of the National Cancer Institute in the US reported that the incidence rate for men aged 40-44 years is 9.2/100,000 and after that the rate increases with a peak at 70-74-year-old men (984.8/100,000). The incidence rate for men older than 74 years slightly declines (Surveillance Research Program, 2016). Several studies on families and particularly on twins have shown that men with a family history of prostate cancer are more likely to develop prostate cancer too (Carter et al., 1992, Ghadirian et al., 1997, Grönberg et al., 1994, Lichtenstein et al., 2000). Many studies on the relationship between diet and prostate cancer risk have been performed and reviewed and suggest that a highly caloric and fatty diet correlates with increased prostate cancer progression (Marshall, 2012). On the other hand, some dietary components have been shown to prevent prostate cancer, like lycopene (antioxidant in tomatoes), selenium, vitamin E, calcium, soy proteins and green tea (Sonn et al., 2005).

1.2.3 Diagnosis and treatment of prostate cancer

Patients are generally diagnosed either as a consequence of routine screening or following clinical investigation of urinary dysfunction. The first step of diagnosis of prostate cancer is often a digital rectal exam (DRE) and prostate specific antigen (PSA) test which is performed with a patient's blood sample. PSA is an enzyme which is expressed by both normal and cancerous prostate cells, however, in benign prostatic hyperplasia (BPH) and prostate cancer (PCa) serum PSA levels are elevated (Raaijmakers et al., 2004). Even though early detection of cancer is generally considered as beneficial, PSA screening has led to over-diagnosis and over-treatment (Caram et al., 2016, Srivastava et al., 2016). Thus the benefits of PSA screening regarding patients' well-being and survival remain controversial (Cuzick

et al., 2014). While a European study revealed a lower risk for death in patients that received PSA screening (Schröder et al., 2012), a study in the US found no significant changes in mortality rate (Andriole et al., 2012). If the PSA is > 4 ng/ml, a transrectal ultrasound guided (TRUS) prostate biopsy is usually taken, and the tissue analysed by a histopathologist to determine if malignant cells are present. There are various details about the PCa a histopathologist can report about from such needle biopsy, and even more from a radical prostatectomy (Montironi et al., 2006). As discussed later, a histopathological report includes parameters like the type of cancer, percentage of prostatic tissue and tumour size if available, Gleason score, pathological staging (pTNM), high grade PIN, extraprostatic extension, surgical margins and perineural invasion (Montironi et al., 2003). The Gleason grading system is a prognostic tool introduced in the 1970s (Gleason and Mellinger, 1974). A Gleason grade can range from 1 to 5, with 1 representing prostate tissue with a normal-glandular appearance and 5 describing very abnormal cell proliferation and loss of glandular structures (Humphrey, 2004). An overall Gleason score is calculated by adding together the most common grade and the highest grade of the cells in the sample. Since grade 1 and 2 describe normal tissue the Gleason score of a PCa patient can only lie between 6 (3+3) and 10 (5+5). One challenge for histopathologists is to distinguish between Gleason 3+4 and 4+3 (Chan et al., 2000). A study showed that patients with Gleason 4+3 are at a three-fold higher risk to die of PCa than patients with Gleason 3+4 (Stark et al., 2009).

The pTNM, tumour-node-metastasis, staging system was first applied in 1974 and has been updated and revised by the International Union Against Cancer (UICC) and the American Joint Committee on Cancer (AJCC) since then (**Figure 1.9**) (Sobin, 2009, Sobin et al., 2011). Within the T-stage, TX means the tumour cannot be assessed, and T0 describes no evidence of tumour. T1 means that there is tumour but it is clinically unapparent, i.e. the cancer is too small to be seen on a scan (**Figure 1.9**). T2 describes a tumour that is confined within the prostate gland, which is also called **localised PCa**. The T2-stage is further divided into T2a (one half of one lobe or less involved), and T2b (more than half of one lobe, but not both lobes involved) and T2c (both lobes involved). Prostate cancer is staged T3 if the tumour has grown outside the prostate gland into nearby tissue, also called **locally advanced PCa** (**Figure 1.9**). A tumour stated at least T3 equals extraprostatic extension. T3 is further divided into T3a (unilateral or bilateral extracapsular extension) and T3b (tumour invades seminal vesicle) (**Figure 1.9**). If the tumour invades adjacent tissues other than the seminal vesicles, including the bladder, rectum and pelvic wall, the tumour is staged as T4 (**Figure 1.9**). The N-stage determines if the cancer is present in regional lymph nodes, called

local metastasis (Christofori, 2006, Steeg and Theodorescu, 2008). It is divided into NX (regional lymph nodes cannot be assessed), N0 (no metastasis in regional lymph nodes) and N1 (metastasis in regional lymph nodes). The M-stage is defined by **distant metastasis**. This is the most advanced stage where the cancer cells have entered the lymphatic system or blood stream and can be carried to distant organs where the tumour then expands at a secondary site which in many cases is the bone (Sturge et al., 2011). M0 stands for no distant metastasis and M1 for distant metastasis. M1 is further divided into M1a (non-regional lymph nodes), M1b (bones) and M1c (other metastatic sites). Metastasis are identified by diagnostic imaging such as magnetic resonance imaging (MRI) and computed tomography (CT) bone scans (Lecouvet et al., 2007, Soloway et al., 1988).

A positive surgical margin means that the prostate cancer cells extend to the inked surface of the tissue specimen, suggesting that not all of the tumour has been removed by the surgeon. The surgical margin can be described as negative if the cancer cells are close to (<0.1 mm) but not in contact with the inked surface (Emerson et al., 2005). The assessment of surgical margins can be challenging depending on the processing of the tissue specimen and can lead to variability in reports between histopathologists (Evans et al., 2008).

Perineural invasion (PNI) is present if the cancer cells invade and grow along nerve fibers within the prostate (Pennington et al., 1967). PNI is found in about ~20% of all prostate cancer patients and is associated with potentially aggressive and metastatic PCa and a poorer clinical outcome (Lu et al., 2015a).

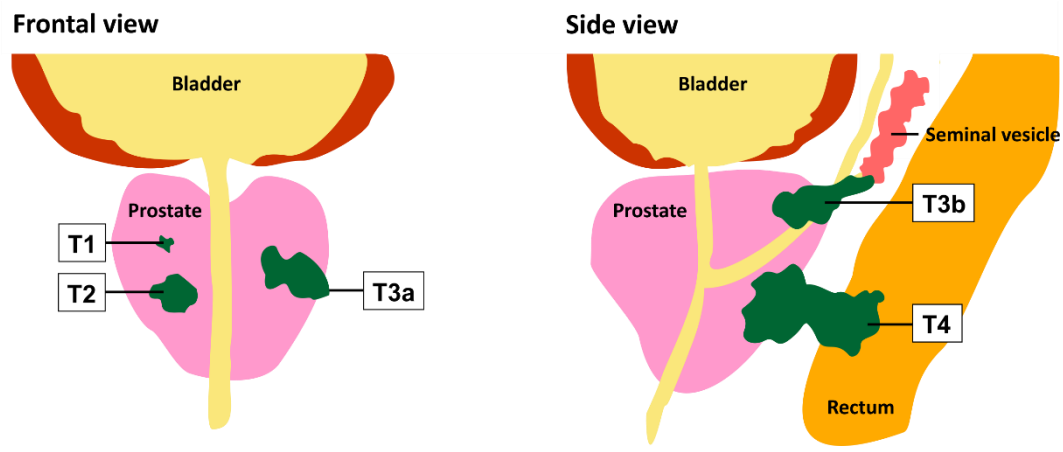

Figure 1.9: Localised and locally advanced prostate cancer.
Localised prostate cancer can be present but clinically not detectable by imaging or rectal exam (T1). If the tumour is clinically detectable but confined to the prostate gland it is staged T2. Locally advanced prostate cancer extends through the prostate capsule (T3a) and may grow into the seminal vesicle (T3b). If the cancer grows into nearby tissue, such as the rectum, it is staged T4.

There are various treatment options for PCa and the choice depends on different factors like age and general health of the patient, and the stage and grade of the cancer. The stage specifies how far the cancer has spread, whereas the grade describes the cell differentiation status (Cooper and Hausman, 2000). As described above, these parameters can be defined by looking at the tissue pattern and cell morphology in a core biopsy or following complete surgical resection of the prostate gland. Decision making on the appropriate therapeutic approach is complex and a very sensitive issue as these therapies can be associated with impaired quality of life. Some treatments, including surgery and radiotherapy can cause side effects such as urinary incontinence and erectile dysfunction (de Brot et al., 2015, Isbarn et al., 2009, Taylor et al., 2009).

For patients with localised PCa or older patients "active surveillance" may be an option to avoid unnecessary treatment (Klotz, 2010). Active surveillance involves regular tests like PSA screening, biopsies and MRI and aims to cure the cancer if treatment is given. In contrast, "watchful waiting" is suggested for men with either localised or advanced PCa who have other health problems (Coen et al., 2011). These patients may not be able to receive certain treatments due to co-morbidities and treatment usually serves to control the cancer rather than to cure it.

Therapies will generally be suggested on the basis of the aggressiveness of the cancer that is characterized by the pathologic stage and grade of the tumour. In general, localised PCa (stage 1) is treated by surgical removal of the prostate gland (prostatectomy), external radiotherapy or brachytherapy (D'Amico et al., 1998). Brachytherapy is a form of internal radiation thearpy where small radioactive seeds are implanted near or in the tumour (Bertermann and Brix, 1990). The advantage of this method is that a high dose of radiation can be delivered to the tumour without damaging the surrounding tissue. About 40% of patients undergoing radical prostatectomy experience recurrence and for patients using brachotherapy it is about ~25% (Boorjian et al., 2012, Heidenreich et al., 2014a, Heidenreich et al., 2014b). If the cancer starts to spread, then local treatment alone will not be sufficient. Locally advanced and metastatic PCas are treated by systemic approaches like hormonal therapy, immunotherapy and chemotherapy. Hormone refractory prostate cancer (HRPC) patients often receive chemotherapy, primarily docetaxel, a semisynthetic taxane that stabilises microtubules thereby interfering with the mitotic spindle apparatus which induces cytotoxicity and apoptosis (Fauzee et al., 2011, Petrylak et al., 2004). The most common treatment for PCa patients with advanced disease are androgen-deprivation therapies (ADTs) which aim to diminish testosterone levels and will be discussed further in the next chapter.

1.2.4 Androgen deprivation therapies

Since PCa is an androgen-dependent disease it is not surprising that for more than 70 years PCa has been treated by 'depriving' prostate cells from androgen. Huggins et al. (1941) first demonstrated that the castration of PCa patients leads to reduced levels of androgenic hormones and subsequently to a significant improvement of the disease (Huggins et al., 1941). Until today, the inhibition of androgen production or blocking the action of the AR is the mainstay of so-called androgen deprivation therapies (ADT) (Sharifi et al., 2005). Nowadays patients with a localised tumour usually undergo surgical castration through laparoscopic and robot-assisted radical prostatectomy (Ilic et al., 2018b). About 80% of all cases remain tumour-free after radical prostatectomy or radiotherapy (Boorjian et al., 2012). If the tumour has spread though, chemical castration will be administered to reduce circulating levels of the androgen in the body (Gomella, 2009). The first chemical castration therapy was estrogen that was shown to inhibit tumour growth in 1972 (Huggins and Hodges, 1972). However, estrogen therapy has several side effects affecting the cardiovascular and thrombotic system (Klotz et al., 1999, Christoforou et al., 2014). Nowadays, chemical castration is achieved through various pharmaceuticals that can be divided into two classes: 1) androgen synthesis blockers and 2) androgen receptor antagonists. These classes are further grouped into first generation and second generation drugs, the latter representing more effective and recently developed pharmaceuticals. Second generation drugs are commonly applied in patients castration resistant prostate cancer (CRPC) who no longer respond to standard hormonal therapies.

1.2.4.1 Androgen synthesis blockers

Luteinising hormone releasing hormone (LHRH) agonists, were first introduced as an alternative to estrogen therapy in the 1980s (Denmeade and Isaacs, 2002). LHRH agonists are androgen synthesis blockers (**first generation drugs**) which suppress androgen production by acting on the hypothalamus–pituitary–gonadal axis (**Figure 1.10**) (Crawford and Hou, 2009). In the initial phase of the therapy LHRH agonists stimulate the production of LH, resulting in increased serum testosterone levels which temporarily worsens the disease and causes clinical flare in some patients (Thompson, 2001). After 7-10 days, LHRH eventually down-regulates the gonadotropin-releasing hormone (GnRH) receptor in the pituitary gland that controls LH secretion. As a result, testosterone production is decreased. The exact mechanism through which LHRH agonists act on the GnRH receptors is not fully understood. The gene expression of the pituitary GnRH receptor may be

inhibited by counteracting the stimulatory effect of LHRH (Kovacs and Schally, 2001). To overcome the side effects of LHRH agonists, GnRH antagonists have been developed (Figure 1.10). GnRH antagonists bind directly to the GnRH receptor and thus act faster and without causing testosterone surge (Cook and Sheridan, 2000a, Cook and Sheridan, 2000b, Stricker, 2001). However, in LHRH agonists and antagonist treatments, androgen precursors released from the adrenal glands remain unaffected and can be metabolised into 5α-DHT (Labrie et al., 1993).

Thus, ketoconazole and abiraterone (second generation drugs) have been introduced which irreversibly inhibit the Cytochrome P450 17 α-hydroxysteroid dehydrogenase (CYP17A) enzyme (Figure 1.10) (Rowlands et al., 1995). CYP17A harbours a hydroxylase activity which is responsible for the conversion of pregnenolone to 17-OH Pregnenolone and a lyase activity to further convert 17-OH Pregnenolone into dehydroepiandrosterone. These are precursor molecules required for androgen biosynthesis in both testes and adrenal gland (Rowlands et al., 1995). Ketoconazole was developed first, however, it has been shown not to be tolerated well and not to prolong patient survival (Trump, 2004). Therefore, the more potent and selective inhibitor abiraterone was introduced which has been proven to be more effective than ketoconazole in a study with metastatic castration resistant prostate cancer (CRPC) patients (Peer et al., 2014). Several studies reported that the survival among patients with metastatic castraction resistant PCa (CRPC) treated with abiraterone was improved (Fizazi et al., 2012, Ryan et al., 2013) and older patients or patients who have received chemotherapy seem to tolerate abiraterone well (Smith et al., 2015). However, abiraterone is associated with hypertension, hypokalemia and edema as a result of an excess of mineralocorticoids due to the repression of CYP17A (Mostaghel, 2014). Nevertheless, Abiraterone is currently used as a standard treatment for patients with metastatic CRPC (Ramaekers et al., 2017).

1.2.4.2 Androgen receptor antagonists

Androgen synthesis blockers are often combined with androgen receptor antagonists, also called anti-androgens, which compete with androgen for AR binding sites, consequently blocking the action of both androgens of adrenal and testicular origins (Figure 1.10) (Chen et al., 2009, Gillatt, 2006). Anti-androgens can be divided into two groups: steroidal and non-steroidal anti-androgens (Chen et al., 2009). Steroidal anti-androgens have partial agonist activity and interact with AR and also other nuclear receptors. Therefore mostly pure non-steroidal anti-androgens are used that all bind the AR which includes flutamide,

bicalutamide and nilutamide (First generation drugs) (Figure 1.10) (Rathkopf and Scher, 2013). Flutamide was one of the first anti-androgens and came to market as Euflex® in 1984 (Canada). It has been shown to have positive effects on therapy response and PCa patient survival when combined with surgical or chemical castration (Labrie et al., 1985). In a long-term study from 1986-1993 it was shown that the progression-free survival was significantly better when patients received orchiectomy combined with nilutamide than orchiectomy alone (Janknegt et al., 1993). Nilutamide has a unique side effect that is the visual difficulty to adapt light-to-dark, affecting 20% of patients (Nakabayashi et al., 2005). Bicalutamide is thought to have a more favorable tolerability profile relative to flutamide and nilutamide (Gillatt, 2006). In 2000 bicalutamide was proven to be an attractive alternative to surgical castrations in patients with locally advanced tumours (Iversen et al., 2000). Later studies with advanced prostate cancer patients have shown that bicalutamide combined with an LHRH agonist resulted in improved PSA levels and overall survival compared to LHRH agonist treatment alone (Akaza et al., 2009, Akaza et al., 2004).

In contrast, enzalutamide, apalutamide, and darolutamide (Second generation drugs) are AR antagonists too, but have a greater affinity for the AR than first generation drugs, and additionally block nuclear translocation of the AR, co-activator recruitment and DNA binding (Figure 1.10) (Rathkopf and Scher, 2013, Semenas et al., 2013, Tran et al., 2009). Since second generation drugs block AR transcription through multiple mechanisms, they are considered more effective. In a study with castration-resistant LNCaP human PCa cells enzalutamide bound the AR with a 5-8 fold higher affinity than bicalutamide (Tran et al., 2009). Enzalutamide has been shown to prolong the survival in patients with CRPC that have been treated with docetaxel before (Heck et al., 2013). Another study on 396 CRPC patients (STRIVE trial, phase II) revealed a better PSA decline and progression-free survival after enzalutamide treatment compared to bicalutamide treatment (Penson et al., 2016). Furthermore, enzalutamide does not have agonist activity like the first generation antagonists. However, another study demonstrated that enzalutamide activity was very low in docetaxel and abiraterone pre-treated patients (Bianchini et al., 2014). In addition, enzalutamide has been shown to promote NePC trans-differentiation (Dang et al., 2015).

Apalutamide was recently approved as a new drug to treat men with CRPC (Figure 1.10). A recent study by Chi *et al* (2019) (TITAN study, phase III) tested whether the addition of apalutamide to ADT will improve survival of metastatic CRPC patients (Chi et al., 2019). The study involved 525 patients who received apalutamide treatment and 527 patients who received placebo treatment in addition to ADT. The trial revealed that metastatic CRPC patients had a better overall and progression-free survival after apalutamide and ADT

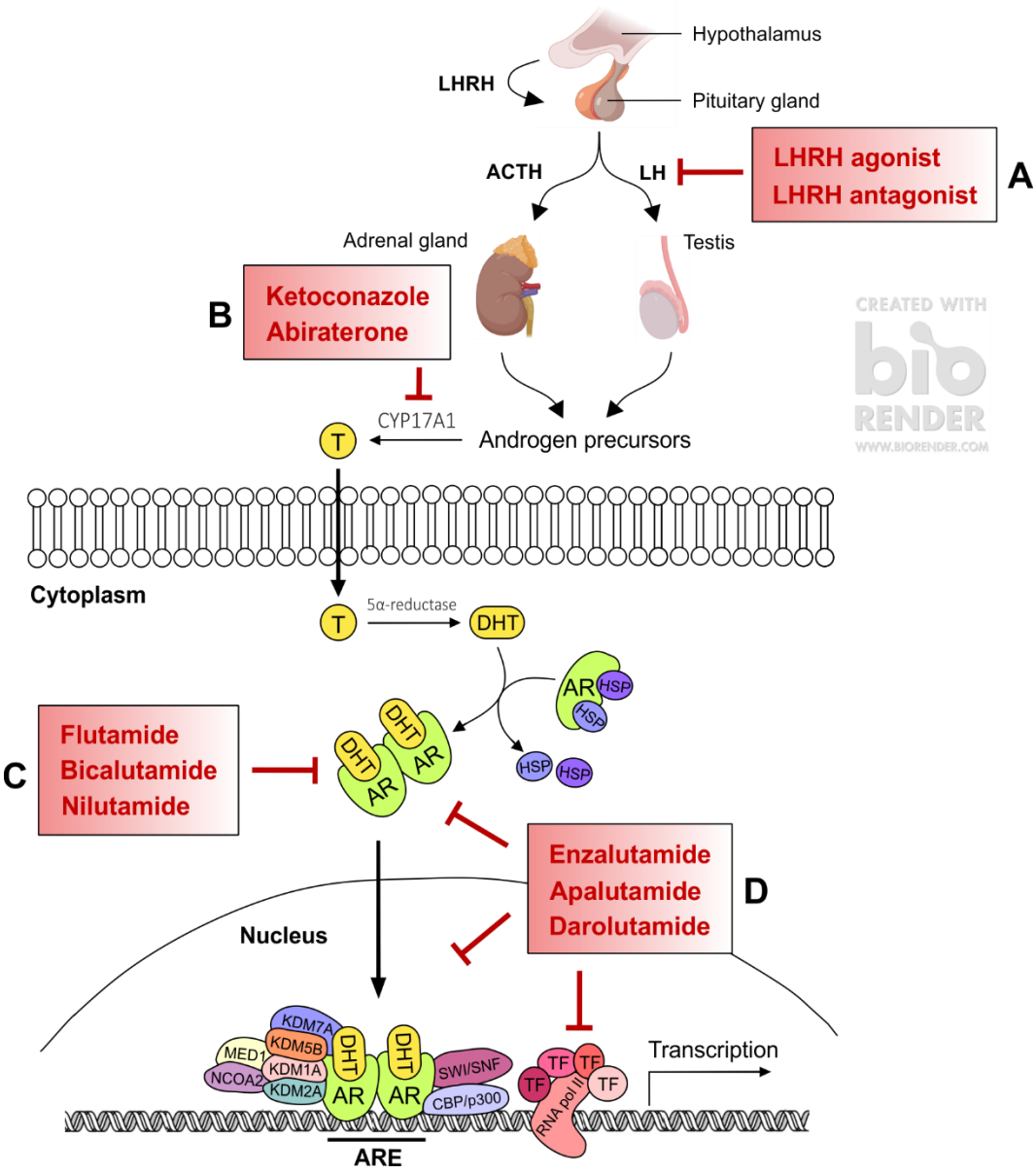

Figure 1.10: Schematic of first and second generation androgen deprivation therapies.
(**A**) LHRH agonists and LHRH antagonists are first generation ADTs that block the production of androgen precursors released from the testes. (**B**) On the other hand, ketokonazole and abiraterone rank among second generation ADTs and inhibit CYP17A1, an enzyme responsible for testosterone production from precursors released from both the adrenal gland and testes. (**C**) Flutamide, bicalutamide and nilutamide are first generation anti-androgens which block ligand binding of the AR. (**D**) In contrast, enzalutamide, apalutamide and darolutamide are second generation anti-androgens which block ligand binding and additionally block nuclear translocation, coregulator recruitment and DNA binding. ADT = androgen deprivation therapy; CYP17A1 = Cytochrome P450 17 α1-hydroxysteroid dehydrogenase; LHRH = luteinising hormone releasing hormone; ACTH = adrenocorticotropic hormone; LH = luteinising hormone; DHT = 5α-dihydrotestosterone; HSP = heat shock protein; KDM = lysine (K) demethylase; MED1 = Mediator Complex Subunit 1; NCO2 = Nuclear Receptor Coactivator 2; CBP = CREB-binding protein;

treatment than after placebo and ADT. In addition, the side effects between the apalutamide and placebo treatment were the same (Chi et al., 2019). Tagawa and colleagues (2019) suggest a triple therapy comprised of apalutamide, abiraterone and

docetaxel which targets various points in the androgen signalling pathway and thereby should increase treatment efficiency. In their study all men experienced major PSA declines, tumour regression and good drug tolerability. To sum up, apalutamide represents a promising drug to treat metastatic CRPC patients. Another promising drug that has recently been studied is Darolutamide which is a structurally unique androgen receptor antagonist (**Figure 1.10**) (Fizazi et al., 2019). A study by Fizazi *et al* (2019) in men with nonmetastatic CRPC (ARAMIS trial, phase III) showed a significant improvement of metastasis-free survival in patients who received darolutamide (n = 955) compared to patients who received placebo (n = 554) (Fizazi et al., 2019). In April 2019, the Food and Drug Administration (FDA) granted a priority review for darolutamide as a treatment for patients with nonmetastatic CRPC (Burnett, 2019).

1.2.5 Castration resistant prostate cancer

1.2.5.1 Mechanisms of CRPC

Despite recent success in developing more specific and effective ADTs, current ADTs are still only effective for 12-18 months (Seruga et al., 2011). After that patients commonly progress to a lethal and incurable form of PCa, called castrate-resistant prostate cancer (CRPC) (Chandrasekar et al., 2015). Previously CRPC has also been referred to as hormone-refractory or androgen-independent PCa, but it has become clear that most CRPC cases remain influenced by androgen receptor signaling (Coutinho et al., 2016). CRPC requires its resistance to ADT through the ability to abberantly activate the AR signaling pathway. The mechanisms behind persistent AR signaling with concomitant ADT-resistance are the topic of many recent reviews and include AR overexpression, hypersensitivy to low androgen, increased androgen levels, *AR* gene mutations, drug antagonist-to-agonist switching, ligand promiscuity, bypassing the AR signaling pathway, AR splice variants, *AR* genomic structural rearrangements (*AR*-GSRs), and alterations in transcription factors and AR co-regulators (Chandrasekar et al., 2015, Ferraldeschi et al., 2015, Seruga et al., 2011). These mechanisms are thought to be the result of selective pressure of ADTs and to provide the tumour with a selective advantage in the absence of androgen (Kumari et al., 2017).

AR overexpression is one of the most common alterations in CRPC and is often mediated through AR copy number gain (Coutinho et al., 2016). Several studies confirm that half of the CRPC cases harbour AR gene amplification (Beltran et al., 2013, Grasso et al., 2012, Robinson et al., 2014), whereas the analysis of 333 primary PCa samples revealed almost

no *AR* gene amplification or AR mutation (Beltran et al., 2013, Grasso et al., 2012, Cancer Genome Atlas Research Network, 2015). These findings confirm that AR copy number gain is an adaptive response to ADT. It has to be pointed out that AR amplification is not always due to copy number gain but can also occur through transcriptional upregulation (Coutinho et al., 2016, Taylor et al., 2010). This is best illustrated by the means of the AR autoregulation mechanism through recruitment of ligand-bound AR and lysine-specific histone demethylase 1A (KDM1A) to an enhancer in intron 2 (Cai et al., 2011). As discussed later, KDM1A can demethylate K4me1 and K4me2 on histone H3, thereby suppressing the AR enhancer activity and inhibiting AR gene transcription via chromatin looping back to the promoter. This negative feedback mechanism is lost at low androgen levels in the case of ADT (Cai et al., 2011).

AR mutations are not common and only 159 of the known pathogenic 1029 AR mutations were identified in PCa (Gottlieb et al., 2012). However, they mainly arise in advanced prostate cancers after ADT (Tilley et al., 1996, Zong and Goldstein, 2013). Most mutations occur in the ligand-binding domain (LBD) of the AR which facilitates ligand promiscuity and antagonist-agonist switching. In 1992, Veldscholte and colleagues (Veldscholte et al., 1992a) first showed in the human prostate cancer cell line LNCaP that a single point mutation (T868A) in the AR ligand binding domain enables progestagens, estrogens and diverse anti-androgens to act as AR agonists. Another interesting phenomenon that has been observed is the “flutamide withdrawal syndrome” in which patients initially do not respond well to flutamide but improve again as soon as flutamide is withdrawn (Scher and Kelly, 1993). The reason for that is that the treatment with flutamide may elicit a selective pressure leading to AR mutations. In a study in PCa bone marrow metastases, patients mutations in the *AR* codon T877A have been described to be responsible for the change of flutamide from an antagonist to an agonist (Taplin et al., 1999). Another mutation, L701H, promotes the binding of glucocorticoids whose affinities are especially increased when both mutations in codon T877A and L701H are present (Zhao et al., 2000). The mutations F876L and W741L/C enable enzalutamide and bicalutamide respectively to bind to the AR as agonists rather than an antagonists (Bohl et al., 2005, Korpal et al., 2013). The H874Y mutation allows the binding of a broader range or steroids and nonsteroid ligands, and interestingly, H874Y induces enhanced interactions with members of the p160 coactivator family, leading to increased AR transactivation activity (Duff and McEwan, 2005). In addition to mutations, variation in repeat lengths of CAG and GGN in the NTD of the AR have been linked with a higher risk to develop PCa (Hsing et al., 2000, Schleutker, 2012).

Ligand independency in PCa can also be acquired by bypassing the AR pathway and instead activating other signalling pathways, such as the PI3K–Akt or Ras-Raf-ERK/MAPK cascade (Feldman and Feldman, 2001). These signalling pathways are important to regulate cell proliferation, differentiation and apoptosis independent of AR (Jason and Cui, 2016, Zhang and Liu, 2002), however they have also been shown to phosphorylate and activate the AR (Gioeli et al., 2006, Van Laar et al., 1990). Several studies confirmed *in vivo* and *in vitro* that the Ras-Raf-ERK/MAPK pathway is associated with the development of CRPC. Bakin et al. (2003) reported that constitutively active MAPK signalling in LNCaP cells sensitises the AR to low androgen levels and makes LNCaP less dependent on androgen regarding its growth and AR regulated gene expression (Bakin et al., 2003). Other studies reported that increased rate and degree of MAPK activation correlates with advanced PCa stage and grade, i.e. activated MAPK induces to cancer progression (Gioeli et al., 1999, Weber and Gioeli, 2004). It was also shown that Ras signalling is sufficient and necessary for cancer progression (Weber and Gioeli, 2004). Another study by Edwards et al (2003) revealed that downstream signalling pathways of MAPK and PI3K were amplified in CRPC samples (Edwards et al., 2003). Immunohistochemical staining revealed that phosphorylated Akt was higher expressed in Gleason 8-10 patients (92% of speciemens strongly stained) compared to lower Gleason score and prostatic intraepithelial neoplasia patients (10% of speciemens strongly stained) (Malik et al., 2002). Another study on human PCa specimens confirmed that phosphorylated Akt and phosphorylated AR correlated with poor survival in patients (McCall et al., 2008). In addition, the PI3K-Akt pathway has been shown to activate the expression of AR mRNA and protein, suggesting a mechanism to escape hormone dependency (Yang et al., 2005). To summarise, these results provide evidence that activated Ras-Raf-ERK/MAPK and PI3K–Akt pathways contribute to the development of CRPC.

Another consequence of ADT induced selective pressure is the expression of truncated AR variants (AR-V) which emerge through alternative splicing or *AR* gene rearrangements (Schweizer and Plymate, 2016). In the full length AR (AR-FL) the N-terminal domain is encoded by exon 1, the DNA-binding domain by exon 2 and 3, the hinge region by the 5' portion of exon 4 and the ligand binding domain by the rest of exon 4 and exon 5-8 (**Figure 1.11**). In contrast, AR-Vs contain the NTD and full or part of the DBD, but lack all or part of the LBD (**Figure 1.11**). Instead they harbour different 3'terminal ends with distinct lengths and sequences which are the result of the incorporation of cryptic exons and/or exon skipping (Antonarakis et al., 2016). In 2010 Hu *et al.* discovered seven AR variants, numerically numbered from AR-V1 to AR-V7, lacking the ligand binding domain due to

alternative splicing of the upstream reading frame of exon 3 (or exon 2 in the case of AR-V3 (Figure 1.11). Alternative splicing is caused by in-frame stop codons and thereby leading to 'intronic' exons (Hu et al., 2010). They also demonstrated that AR-V1 and AR-V7 mRNA are expressed 20-fold higher in PCa patients that failed ADT (n = 25) than in hormone naïve PCa (n = 82) (Hu et al., 2010). Subsequently several other studies have identified additional AR-Vs harbouring cryptic exons (Dehm et al., 2008, Guo et al., 2009, Marcias et al., 2010). Sun *et al.* identified an AR variant in which exons 5, 6 and 7 are deleted and therefore called it ARv567es (Figure 1.11) (Sun et al., 2010). They further showed that ARv567es is constitutively active and can form a heterodimer with AR-FL, the first time an interaction between an AR variant and the full length AR has been shown. In addition, ARV567es enhances PCa growth following ADT *in vivo* suggesting ARV567es contributes to CRPC (Sun et al., 2010). After seven years of extensive AR-Vs research and a better appreciation of their heterogeneity, it is believed that ADTs induce the formation of AR-Vs and that AR-Vs play a significant role in CRPC progression (Coutinho et al., 2016, Hu et al., 2010). Much research has gone into the splice variant AR-V7 and confirmed that AR-V7 is present and increased in metastatic CRPC patients and that it is associated with ADT resistance, progression to CRPC and short overall survival (Antonarakis et al., 2017, Hörnberg et al., 2011, Qu et al., 2015, Robinson et al., 2015, Scher et al., 2016, Umar et al., 2005, Welti et al., 2016). AR-V7, and other splice variants, hold the potential as promising therapeutic

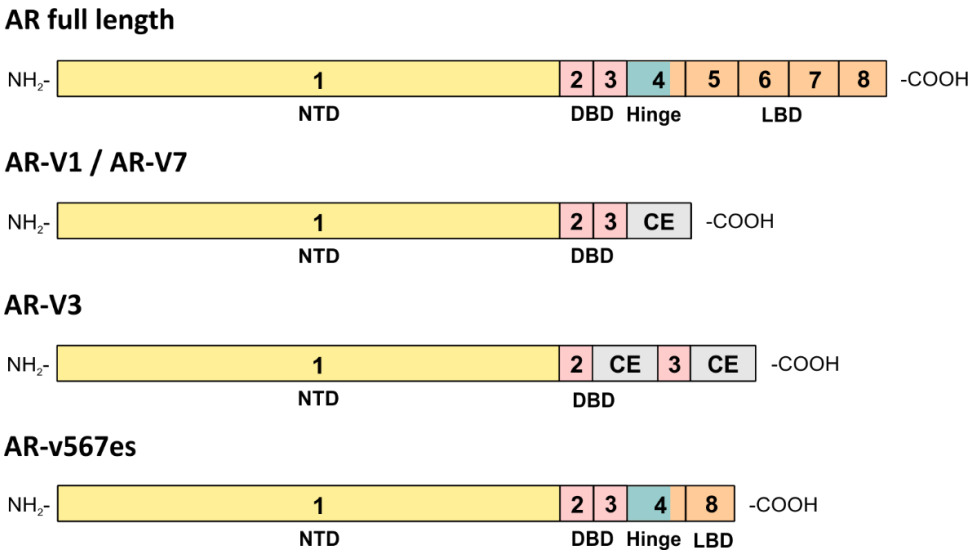

Figure 1.11: Structure of full length androgen receptor and splice variants.
The AR-FL is composed of eight exons whereas exon 1 encodes the NTD, exon 2 and 3 the DBD and exon 4-8 the hinge region and LBD. AR-V1 and AR-V7 also contain the NTD and DBD but comprise a cryptic exon at the C-terminal end. AR-V3 harbours a cryptic exon between exon 2 and 3 and another cryptic exon after exon 3. AR-v567es is an AR variant that lacks exons 5-7. AR-FL = androgen receptor full length; AR-V = androgen receptor variant; NTD = N-terminal domain; DBD = DNA-binding domain; LBD = ligand-binding domain.

targets and CRPC biomarkers, however, their functional implication in PCa still has to be further clarified. A recent study by Cato and colleagues (2019) revealed that AR-V7 heterodimerises with AR-FL and inhibits the transcription of tumour suppressor genes, suggesting a mechanism by which AR-V7 contributes to the CRPC progression (Cato et al., 2019).

In addition to the above mentioned mechanisms, alterations in other transcription factors and AR coregulators, crucial players for the activation of androgen receptor target gene expression, are also thought to be implicated in CRPC (Chandrasekar et al., 2015, Takayama and Inoue, 2013). For example the transcription factor NANOG has been shown to promote CRPC and resistance to ADT (Jeter et al., 2009, Jeter et al., 2011). Another transcription factor, c-Jun, which is a subunit of the activator protein 1 (AP1) complex, can induce AR transactivation by binding to the N-terminal domain of the AR and has been shown to be implicated in prostate cancer progression and recurrence (Ouyang et al., 2008, Wise et al., 1998). However, it is controversial whether c-Jun activates or represses transcription of AR target genes (Hsu and Hu, 2013). Coregulator proteins influence transcription by interacting with transcription factors and/or covalently modifying histones and other proteins (McKenna et al., 1999). They are thought to play a role in the development of CRPC by supporting AR transcriptional activity at low androgen levels and/or by influencing ligand specificity (Edwards and Bartlett, 2005). In a study by Miyamoto *et al.* (1998), it was demonstrated that the interaction between AR and the coactivator ARA70, also called nuclear receptor coactivator 4 (NCOA4), enhanced agonist activity of known androgen receptor antagonists such as (hydroxy)flutamide and bicalutamide (Miyamoto et al., 1998). Another study by Halkidou et al. (2003) demonstrated that the histone acetylase TIP60, also called K(Lysine) Acetyltransferase 5 (KAT5), was upregulated when androgen was withdrawn from the PCa cell lines CWR22 and LNCaP, suggesting a role for TIP60 in the development of androgen independency (Halkidou et al., 2003). Jose et al. (2002) revealed an interesting mechanism involving the histone acetylase p300, a functional homologue of the CREB-binding protein (CBP), which are crucial coactivators in hormone-dependent AR transactivation (Chakravarti et al., 1996, Debes et al., 2002). The activity of p300 was shown to be induced by IL-6 through the MAPK pathway and p300 can then switch on AR gene transcription even in the absence of a ligand (Debes et al., 2002, Ueda et al., 2002a). Further studies confirmed the role of p300/CBP in the development of androgen independency and suggest to target p300/CBP in order to treat CRPC (Debes et al., 2005, Jin et al., 2017).

To sum up, several mechanisms for the development of androgen independency and CRPC have been determined. This came concomitantly with the need to develop new strategies to treat CRPC some of which will be described in the following.

1.2.5.2 Therapies to treat CRPC

As mentioned above, second generation drugs like ketoconazole and abiraterone (androgen synthesis blockers) and enzalutamide, apalutamide, and darolutamide (androgen receptor antagonists) have been developed to treat CRPC (Tran et al., 2009). These drugs are more efficient than first generation drugs, though not curative (Nelson and Yegnasubramanian, 2013). Other approaches such as AR-V degraders (niclosamide and galeterone), AR NTD binding blockers (EPI-001 and niphatenones) and coregulator inhibitors have been introduced and studied in the context of treating CRPR. Niclosamide is an anti-helminthic drug which has been proven to inhibit tumour growth *in vitro* by degrading androgen receptor splice variants and/or inhibiting signalling pathways that are relevant in CRPC, such as the PI3K/AKT/mTOR and Wnt signalling pathway (Balgi et al., 2009, Circu et al., 2016, Liu et al., 2014). Galeterone was originally designed to inhibit the CYP17A enzyme, but it also inhibits AR nuclear translocation and degrades AR splice variants (Yu et al., 2014). EPI-001 and niphatenones both are compounds that target the AR N-terminal domain (NTD) and thereby prevent the binding of AR to the DNA (Lallous et al., 2013).

Another potential way of inhibiting androgen receptor signalling in PCa is to target the epigenetic coregulator proteins, and this is the focus of this dissertation. Bromodomain-containing proteins are chromatin-binding and exhibit an important role in scaffolding transcription factors and regulating transcription (Devaiah et al., 2016, Dey et al., 2000). Several studies have proven that AR signalling is inhibited by BET inhibitors and a study by Asagani *et al* (2016) has indicated that BET inhibitors inhibit growth of enzalutamide-resistant CRPC cells (Asangani et al., 2014, Chan et al., 2015). In addition, BET inhibitors are more efficient if combined with antiandrogens (Asangani et al., 2014).

Even though the above mentioned therapies have survival benefits, they are no curative treatments for HRPC patients. There is therefore an urgent need to find novel targets and develop new drugs to treat HRPC.

1.2.6 Precision medicine

Precision medicine, also called personalised medicine, describes the approach to treat patients based on their individual genes, environment and lifestyle (Ashley, 2015, Jameson and Longo, 2015). This allows a more accurate prediction of disease treatment and prevention for each individual patient. Prostate cancer has been considered a clinically heterogenous disease (Barbieri et al., 2012b). However, through Next Generation Sequencing (NGS) and RNA sequencing, frequent changes in the genome of PCa patients have been discovered and homogenous disease subtypes identified (Barbieri et al., 2012b, Berger et al., 2011). Genetic alterations which are common and have been detected early on include alterations in *p53*, *NKX3.1* and *PTEN*. In 1994, Massenkeil et al. discovered p53 mutations and deletions in advanced prostate cancer samples, suggesting a role in prostate cancer progression (Massenkeil et al., 1994). P53 is a well-known tumour suppressor which is mutated in almost half of all cancers (Strano et al., 2007). The homeobox-containing transcription factor NKX3.1 is mainly expressed in the prostate epithelium and plays a pivotal role in the normal development of prostatic ducts and production of secretory proteins (Bhatia-Gaur et al., 1999). Heterozygous loss of *NKX3.1* has been linked to pre-stages of PCa like prostatic epithelial hyperplasia and PIN (Abdulkadir et al., 2002, Kim et al., 2002), and more importantly to PCa progression (Abate-Shen et al., 2003, Bowen et al., 2000, Cai et al., 2011). *PTEN* is a gene that encodes the phosphatidylinositol-3,4,5-trisphosphate 3-phosphatase which inhibits the PI3K/AKT pathway and thereby is a key tumour suppressor in prostate cancer (Trotman et al., 2003).

In 2005, Tomlins et al. (2005) found that the fusion of *TMPRSS2* with *ERG* and *ETV1*, which are members of the erythroblast transformation-specific (ETS) transcription factor family, occurs in prostate cancer patients at a high frequency (Tomlins et al., 2005). *ERG* and *ETV1* have been shown to be highly overexpressed in prostate cancer which is likely to cause the fusion with TMPRSS2 according to Tomlins et al. (2005) (Petrovics et al., 2005, Tomlins et al., 2005). Subsequently, a total of 17 different hybrid transcripts of combined *TMPRSS2* and *ERG* gene sequences were identified, nine of which are predicted to encode either a TMPRSS2-ERG fusion or truncated ERG protein (Clark et al., 2007, Soller et al., 2006). The most common hybrid transcripts were a fusion between *TMPRSS2* exon 1 and *ERG* exon 4, and *TMPRSS2* exon 1 and *ERG* exon 5. They were usually harboured by the same patient, suggesting that they may be the result of an alternatively spliced *TMPRSS2-EGR* gene fusion (Clark et al., 2007). The *TMPRSS2:ERG* gene fusion has then been discovered to be a predictor for high-grade PIN, a precursor for prostate cancer (Park et al., 2014). Kashyap and colleagues (2013) found that the *TMPRSS2* locus is positively regulated by the

androgen receptor co-regulator lysine-specific histone demethylase 1 (LSD1), also known as KDM1A, which has been shown to be implicated in PCa recurrence and upregulated in CRPC patients (Kahl et al., 2006, Kashyap et al., 2013, Sehrawat et al., 2018). Another study showed that the histone methyltransferase EHMT2 dimethylates KDM1A at the amino acid K114 in an androgen dependent manner and that this mark is read by the chromodomain Helicase DNA Binding Protein 1 (CHD1), a chromatin modifier which has been reported to be required for *TMPRSS2-ERG fusions* in PCa (Burkhardt et al., 2013, Metzger et al., 2016). Indeed, the interaction between KDM1A K114me2 and CHD1 is pivotal for androgen-dependent gene expression and chromosomal rearrangements including the *TMPRSS2-ERG* fusion (Metzger et al., 2016).

In 2012, an exome sequencing study including 112 prostate adenocarcinoma samples revealed novel frequent mutations in various genes, such as *MED12, FOXA1* and *SPOP*, with mutated *SPOP* being the most frequent one (Barbieri et al., 2012a). *SPOP* (speckle type BTB/POZ protein) encodes the substrate-binding subunit of the cullin-RING-based BCR (BTB-CUL3-RBX1) E3 ubiquitin-protein ligase complex and acts as a tumour suppressor in PCa by directly binding to the hinge region of AR and thereby inducing AR degradation (Geng et al., 2014, Nagai et al., 1997). In addition, SPOP ubiquitinates the oncogene ATF2 (Activating Transcription Factor 2), a member of the ATF/CREB basic region-leucine zipper family of transcription factors which in turn inhibits PCa disease (Ma et al., 2018). If *SPOP* is mutated, both the degradation of AR and ATF2 is lost, leading to prostate cancer progression. Interestingly, prostate cancer samples with mutated *SPOP* did not harbour *ETS* rearrangements, suggesting SPOP mutations may describe a new subtype of PCa (Barbieri et al., 2012a). Another interesting finding was that *PTEN* deletion seems to contribute to the development of *SPOP* mutant PCa (Blattner et al., 2017).

The above mentioned genetic alterations in PCa patients, and many more, represent useful genetic markers to facilitate the diagnosis of PCa subtypes, the choice of treatment and prognosis of patients (McCrea et al., 2018). RNA profiling tests have been developed to predict disease prognosis. Decipher™, for example, predicts metastasis and mortality after patients have received radical prostatectomy (Karnes et al., 2013). PCa initiation and progression is not only driven by genomic but also epigenetic alterations.

The fact that advanced prostate cancer remains incurable emphasises the need to develop new therapeutical approaches and agents. In the next chapter the epigenetic metchanisms in prostate cancer will be discussed, as well as epigenetic coregulators of the androgen receptor.

1.3 Epigenetic coregulators

1.3.1 Epigenetics

The term “epigenetics” was introduced by Waddington in the early 1940s and nowadays is defined as heritable changes in chromatin, without altering the underlying DNA sequence, that affect gene expression (Waddington, 1940, Waddington, 2011). Epigenetics involve DNA methylation, histone variants, posttranslational modifications of histones, chromatin remodelling and non-coding RNAs (Liao and Xu, 2019).

1.3.1.1 DNA methylation

DNA modifications were first described in 1948 and were later linked with regulation of gene expression (Griffith and Mahler, 1969, Hotchkiss, 1948). The modification is a methylation reaction in which a methyl (-CH_3) group is covalently attached to a cytosine or adenine of the DNA (Robertson, 2005). This reaction is mainly catalysed by enzymatic members of the DNA methyltransferase (DNMT) family (Kumar et al., 1994). The removal of methyl groups is preliminarily conducted by enzymatic members of the ten-eleven translocation (TET) family of dioxygenases and base excision repair (BER) (Kohli and Zhang, 2013). Demethylation can also occur passively by inhibition of DNMTs during *de novo* DNA synthesis in replication (Kohli and Zhang, 2013). DNA methylation regulates gene expression in various ways. In 1986, Bird described unmethylated CpG-rich islands which are situated in the promotor region of many genes and the methylation of these islands lead to gene silencing (Bird, 1986, Chomet, 1991). In addition, DNA methylation also occurs outside of promotor regions, such as enhancers, and even within genes which might play a role in transcriptional elongation and alternative splicing (Jones, 2012). On the other hand, Jones (1999) described the “DNA methylation paradox” in which DNA methylation in transcribed genes correlates with high gene expression. Today DNA methylation is recognised as a dynamic process (Jones, 2012). Baubec et al. (2015) found an interesting link between the DNMT3B and the lysine 36 on histone H3 (H3K36) . Methylated H3K36 is associated with transcriptional activation and has been shown to support DNA methylation by recruiting the DNMT3B in transcribed genes (Baubec et al., 2015, Huang and Zhu, 2018, Morselli et al., 2015). This describes a mechanism of how epigenetic marks on histones and DNA modifying enzymes work together to regulate gene expression. Dysregulation of DNA methylation is implicated in many diseases. In prostate cancer, global hypomethylation correlates with disease progression and is most dominant in metastatic PCa (Bedford and

Van Helden, 1987, Santourlidis et al., 1999, Schulz et al., 2002). DNA hypomethylation, which mainly occurs in introns and between genes, is thought to increase mutations and instability in the genome and thereby leads to cancer progression (Liao and Xu, 2019). DNA hypermethylation of promotor region is seen in many genes in PCa, for example the glutathione S-transferase pi (GSTP1) (Henrique and Jerónimo, 2004). As a consequence of the hypermethylation, the expression of these genes is decreased. Henrique and Jerónimo (2004) have shown that GSTP1, which is important in detoxification during redox stress, is hypermethylated in ~90% of PCa patients (Henrique and Jerónimo, 2004). On the basis of that, the first epigenetics-based diagnostic assay was developed (Stewart et al., 2013). The assay includes GSTP1, as well as Adenomatous polyposis coli (APC), which is an inhibitor of the Wnt signalling pathway, and the Ras association domain family member 1 (RASSF1), a tumour suppressor (Partin et al., 2014, Van Neste et al., 2017). This epigenetics-based diagnostic assay should help detect cancer in patients that has been missed in biopsy, but also to avoid unnecessary biopsies.

1.3.1.2 Non-coding RNAs

Non-coding RNAs (ncRNAs) are evolutionarily conserved and are transcribed from DNA without being subsequently translated into proteins (Zaratiegui et al., 2007). They are involved in many biologically important processes like DNA replication, transcription, translation and RNA splicing and can be divided into two groups regarding their size: short non-coding RNAs (sncRNAs) and long non-coding RNAs (lncRNAs) (Ponting et al., 2009). Short non-coding RNAs include microRNAs (miRNAs), small-interfering RNAs (siRNAs), small nuclear RNAs (snRNAs) and piwi-interacting RNAs (piRNAs). The best studied class is the miRNAs which are around ~21-25 nucleotides long and are important in posttranscriptional regulation of genes by targeting specific mRNAs for degradation or translational inhibition (Bartel, 2004, Wahid et al., 2010). In prostate cancer, miRNAs with both oncogenic and tumour suppressor function have been discovered (Ambs et al., 2008). A tumour suppressor in PCa, *miR137*, was discovered by Nilsson et al. (2015) whose gene locus has been proven to be slightly methylated in LNCaP and LnCaP:C4-2 cells and highly methylated in PC3 cells (Nilsson et al., 2015). Increased DNA methylation is correlated with high Gleason score (Nilsson et al., 2015). They found a mechanism by which androgen treatment induces *miR137* expression in LNCaP cells which in turn suppresses a network of epigenetic coregulators involved in disease progression. Interestingly, this negative feedback loop is lost in the androgen independent PCa cell lines LnCaP:C4-2 and PC3,

thereby relieving the inhibition of coregulator expression, resulting in enhanced AR-coregulator complex activity (Nilsson et al., 2015). This study was the basis of the current project.

In the recent years, exosomes have gained much interest in research. Exosomes are extracellular vesicles which carry cell-type specific cargo including lipids, proteins, DNA, mRNA and ncRNAs. Exosomes are small (<150 nm in diameter) and are formed as intraluminal vesicles in an endosomal compartment within the cell, called multivesicular body (MVB) (Hessvik and Llorente, 2018). When the MVB fuses with the plasma membrane of the cell, exosomes are released into the extracellular space (Hessvik and Llorente, 2018). Exosomes are important in various processes including detoxification by discharging waste products and cell-cell communication (Dragomir et al., 2018, Harischandra et al., 2017, Maia et al., 2018). Not only in normal physiology, but also in the tumour microenvironment exosomes have been shown to be implicated and represent potential therapeutic targets (Chulpanova et al., 2018, Samanta et al., 2018). A study in docetaxel-resistant Du145 and 22Rv1 cells has shown that exosomes are capable of transferring the docetaxel-resistance to resistance-naïve Du145, 22Rv1 and LNCaP cells and thereby promote tumour invasion and proliferation (Corcoran et al., 2012). Another study has proven that exosomes derived from LNCaP and PC3 cells, which have been exposed to hypoxia, carry certain proteins which induce increased invasiveness and motility in hypoxia-naïve LNCaP and PC3 cells, thus leading to enhanced cancer aggressiveness (Ramteke et al., 2015). In 2018, Probert et al. found a mechanism by which prostate cancer cells communicate with osteoblasts through RNA-cargo in extracellular vesicles and thereby mediate bone metastasis (Probert et al., 2019). Specific miRNAs in extracellular vesicles have been shown to be enriched in the serum of metastatic PCa patients (Bryant et al., 2012). Exosomal miRNA can also be used as a biomarker to detect treatment success after radiotherapy in PCa patients (Malla et al., 2018). In contrast to tissue biopsies, so-called “liquid biopsies” are non-invasive and allow the detection of circulating cell-free DNA, RNA, proteins and exosomes in the patient’s body fluids and represent an important tool to identify biomarkers in precision medicine (Di Meo et al., 2017).

1.3.1.3 Histone modifications

Eukaryotic DNA is tightly packed around a core of histone proteins to form a nucleosome (**Figure 1.12**) (Kornberg, 1974). The histone core consists of an octamer composed of a

tetramer of two H3 and H4 subunits and two copies each of H2A and H2B. Around 1.75 superhelical turns of DNA (~146 bp) are wrapped around the histone core (**Figure 1.12**) (Luger et al., 1997). Histone proteins are highly conserved and rich in basic amino acids such as arginine and lysine. They are positively charged and therefore tightly bind to the negatively charged DNA, primarily through electrostatic interactions (salt bridges and hydrogen bonds (Campos and Reinberg, 2009, Liao and Xu, 2019). The nucleosomes are separated by ~20-30 bp of DNA, called linker, which gives the DNA the classic beads-on-a-string structure (**Figure 1.12**) (Olins and Olins, 1974, Olins and Olins, 2003, Woodcock, 1973). A fifth histone, histone H1, is responsible for stabilising and protecting the linker DNA and binds to the sites where the DNA enters and exits the nucleosomes (**Figure 1.12**) (Boulikas et al., 1980, Brockers and Schneider, 2019). Even though nucleosomes represent a highly compact unit, their composition, structure and location at the DNA is highly dynamic (Kamakaka, 2003). The dynamic is achieved through histone variants, ATPase-dependent chromatin remodelling complexes, and posttranslational modifications. Histone variants are non-allelic and have different sequences to the major histones, ranging from a change in only a few amino acids to very divergent changes (Kamakaka and Biggins, 2005). They are tissue-specific and during development major histones can be replaced by histone variants, contributing to differentiation (Franklin and Zweidler, 1977, Malik and Henikoff, 2003). ATP-dependent chromatin remodelling complexes, such as SWI/SNF, are large and consist between 4 and 17 subunits, including an ATPase subunit (Tang et al., 2010). They recognise histone marks and can mobilise, replace and remove nucleosomes through the hydrolysis of ATP (Vignali et al., 2000). Post-translational histone modifications usually occur on the N-terminal tails of histones (and C-terminus of H2A) which project outward (Dutnall and Ramakrishnan, 1997, Kouzarides, 2007). The amino acids on these tails can be enzymatically modified, including acetylation, methylation, phosphorylation, ubiquitylation, SUMOylation, *O*-glycosylation, ADP ribosylation, proline isomerization and tail clipping (Bannister and Kouzarides, 2011, Liao and Xu, 2019). These covalent modifications alter the electrostatic and chemical properties of histones, which as a consequence 1) loosens or tightens the chromosomal structure and 2) recruits other proteins or disrupts interactions between the DNA and proteins (Liao and Xu, 2019). In 2000, the term “histone code” was introduced, in analogy to genetic code, to describe histone modifications as another language and layer of complexity (Liao and Xu, 2019, Strahl and Allis, 2000). The histone code is a certain combination or sequence of histone modifications which is read by other proteins to activate downstream events (Strahl and Allis, 2000). Histone marks can also “cross-talk” which means that the modification of one

histone induces or prevents another histone modification, either in the same histone (*cis*) or in a different histone (*trans*) (Fingerman et al., 2008).

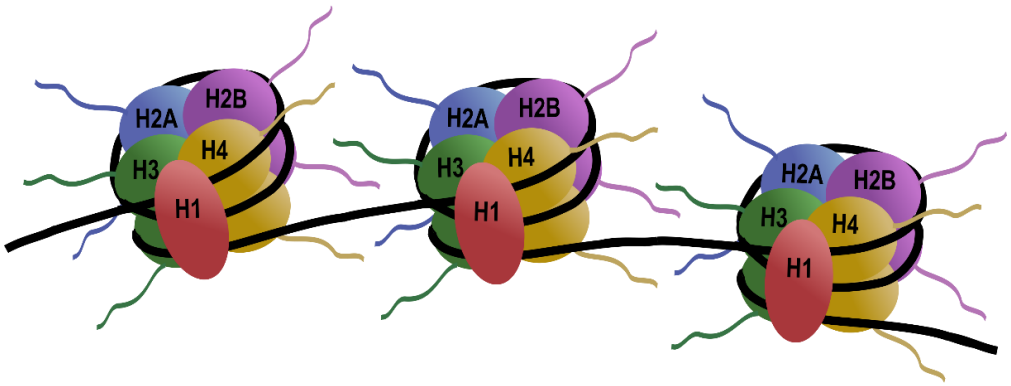

Figure 1.12: Schematic of nucleosomes and DNA in beads-on-a-string structure.
The DNA (black) is wrapped around a histone octamer, composed of two copies of H2A, H2B, H3 and H4 each, called nucleosome. Histone H1 binds to the nucleosome at the sites where the linker DNA enters and exits the histone core. The N-terminal tails of the histones project outward of the nucleosome and are target of post-translational modifications.

In the following sections, the main modifications relevant to this dissertation, acetylation, phosphorylation and methylation, will be discussed in further detail.

1.3.1.3.1 Histone acetylation

In 1964, Allfrey and colleagues first discovered the acetylation and methylation of histones and their implication in transcription (Allfrey et al., 1964). Around 31 years later, research groups identified the first histone acetyltransferases (HATs), which are enzymes responsible for the acetylation of lysines in histone proteins (Brownell et al., 1996, Parthun et al., 1996). KATs catalyse the transfer of an acetyl group, derived from the coenzyme acetyl-CoA, to the ε-amino group ($-NH_2$) of histone lysine residues, leading to acetylated lysine (**Figure 1.13**) (Marmorstein and Zhou, 2014). This acetylation neutralises the positively charged histone and therefore loosens the interaction between DNA and histone leading to less compacted chromatin (Jenuwein and Allis, 2001). However, it is worth mentioning that the main mechanism by which histone marks alter the chromatin is not by themselves but by recruiting non-histone effector proteins, such as bromodomains and chromodomains (Grewal and Moazed, 2003, Iizuka and Smith, 2003, Peterson and Laniel, 2004). The reverse reaction, the removal of acetyl groups from histone lysine residues, is catalysed by histone deacetylases (HDACs) and returns the chromatin into its compacted state (**Figure 1.13**) (Seto and Yoshida, 2014). Acetylation and deacetylation are a highly dynamic process and the general paradigm is that KAT activity increases DNA accessibility, thus activating gene transcription, whereas HDACs are associated with transcriptional

repression (Bannister and Kouzarides, 2011, Eberharter and Becker, 2002). However, it is important to note that coregulators exhibit transcriptional activation and repression properties in a cell, signal and epigenomic context dependent manner (An and Roeder, 2003, Bannister and Kouzarides, 2011, Paz et al., 2014).

HATs and HDACs usually act in a site and histone-specific manner important for distinct physiological processes and most of the HATs and HDACs identified are part of a complex widening their specificity (Chrun et al., 2017, Peterson and Laniel, 2004). The specificity is also determined by different families within the KATs, which differ regarding amino-acid sequence and protein conformation, including the p300/CBP family which has been shown to be implicated in the progression of PCa (Heemers et al., 2008). The acetylation marks on histones are recognised ("read") by other proteins, such as bromodomains and PHD-fingers (Marmorstein and Zhou, 2014). Bromodomains are well characterised and known to bind acetylated lysine residues on histones (Bannister and Kouzarides, 2011, Dhalluin et al., 1999). They are often associated with HATs and chromatin-remodelling complexes (Hassan et al., 2002). Acetlyation cross-talks with other histone modifications such as phosphorylation and methylation (Eberharter and Becker, 2002). A study by Vandel and Trouchea (2001) has shown that p300/CBP, a transcriptional activator, physically interacts with a methyl transferase (HMT) that can methylate H3K4 and H3K9, suggesting this interaction is needed for transcriptional activation (Vandel and Trouche, 2001). These examples highlight the synergism of post-translational modifications and complexity in chromatin remodelling and transcriptional regulation.

Alterations in acetylation status in histones can cause diseases, such as cancer, usually by increased HDAC activity and/or decreased HAT activity. In PCa, several studies have shown that HDACs are overexpressed in patients and that this HDAC increase causes disease recurrence and progression (Halkidou et al., 2004, Patra et al., 2001, Weichert et al., 2008). Thus, research group have put intensive efforts into the development of HDAC inhibitors and indeed, HDAC inhibitors have been shown to inhibit PCa growth and metastasis (Butler et al., 2000, Makarević et al., 2018, Roy et al., 2005). HDAC inhibitors have been suggested to be used as combination therapies and for various types of cancer they have entered clinical trials. However, in PCa current HDAC inhibitors are not effective, especially for the treatment of CRPC (Suraweera et al., 2018). A very recent study by Wen-Yang *et al.* (2019) reports about the design of a hybrid between Enzalutamide and HDAC inhibitor and that this hybrid drug is a better antagonist of full length AR and AR-V7 than Enzalutamide alone (Hu et al., 2019). More research needs to go into the optimisation of HDAC inhibitors, however, they still represent promising therapeutical agents to treat PCa.

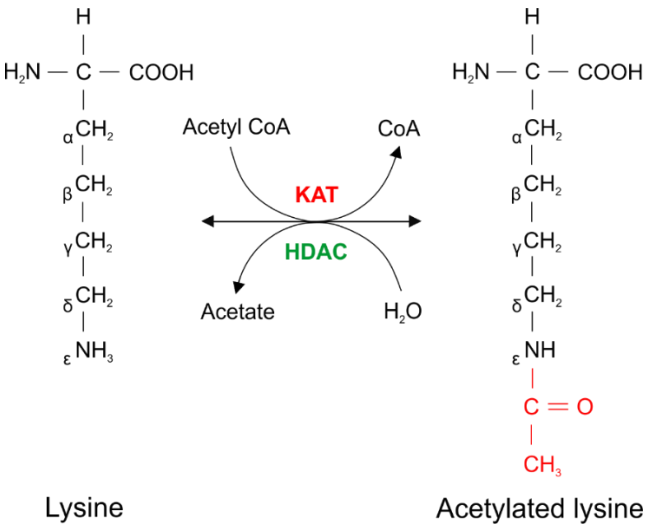

Figure 1.13: Histone acetylation.
Lysine acetyl transferases (KAT) catalyse the addition of an acetyl group to the ε-amino group of lysine by using Acetyl CoA as a co-substrate, creating acetylated lysine. The histone deacteylases (HDAC) reverses this reaction by deacetylation, leading back to lysine.

Recently identified histone modifications at lysine residues, which are structurally similar to acetylation, include malonylation, succinylation, formylation, propionylation, butyrylation, crotonylation and glutarylation (**Figure 1.14**) (Arnaudo and Garcia, 2013, Chen et al., 2007, Jiang et al., 2007, Rothbart and Strahl, 2014, Wiśniewski et al., 2007, Xie et al., 2012). They all require a donor acyl-coA as a metabolic source and have partly been shown to be catalysed by HATs and HDACs (Chen et al., 2007, Kebede et al., 2015).

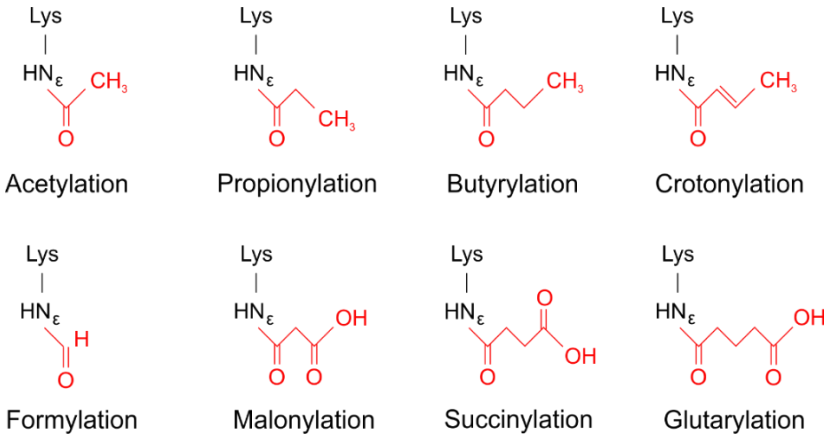

Figure 1.14: Histone lysine modifications.
The structure of the lysine modifications propionylation, butyrylation, crotonylation, formylation, malonylation, succinylation and glutarylation are similar to acetylation and use acyl-CoA as a co-enzyme.

1.3.1.3.2 Histone phosphorylation

Like acetylation, the phosphorylation of histones is a highly dynamic process and occurs on serine, threonine and tyrosine residues, and like acetylation, mainly in the N-terminal tails of histones (**Figure 1.15**) (Bannister and Kouzarides, 2011, Oki et al., 2007). The transfer of a phosphate group to the OH-group of a target amino acid is catalysed by kinases using adenosine triphosphate (ATP), leading to phosphorylated serine, threonine or tyrosine and adenosine diphosphate (**Figure 1.15**) (Mersfelder and Parthun, 2006). In contrast, the removal of the phosphate group is catalysed by phosphatases (**Figure 1.15**) (Mersfelder and Parthun, 2006). Phosphorylation of histone proteins is crucial in various biological processes including transcription, meiosis and mitosis, DNA repair, apoptosis and various signalling pathways in response to growth factors, stress and immune stimulation (Sawicka and Seiser, 2014). Another very important function of phosphorylation is to cross-talk and regulate other histone modifications, such as acetylation and methylation (Suganuma and Workman, 2008). One such example is the combinatorial phosphorylation and acetylation on histone H3 which is a crucial recognition site for the "14-3-3" family (Macdonald et al., 2005, Walter et al., 2008). The 14-3-3- family is pivotal for cell signalling and can interact with various proteins, including TATA-binding protein, p53 and HDACs (Sawicka and Seiser, 2014). It was the first selective protein discovered to interact with phosphorylated serine 10 at histone 3 (Macdonald et al., 2005). Several studies showed that the phosphorylation of H3S10 induces the acetylation of H3K9 and H3K14 which has been shown to switch on GCN5 (KAT2A) regulated gene expression (Cheung et al., 2000, Lo et al., 2000). Interestingly, the binding affinity of 14-3-3 to phosphorylated H3S10 is higher when the adjacent lysine residues, H3K9 and/or H3K14, are acetylated (Walter et al., 2008, Winter et al., 2008). In addition, the phosphorylation of H3S10 by the kinase Aurora B elicits the release of heterochromatin protein 1 (HP1) which recognises and binds the methylation mark on H3K9 (Hirota et al., 2005, Lachner et al., 2001). HP1 is known as a repressor and to interact with polycomb/trithorax groups of proteins which are involved in chromatin remodelling (Bannister et al., 2001, Fischle et al., 2005). Ultimately, these epigenetic events lead to transcriptional activation and the histone mark H3S10phK14ac has been shown to be situated at many activated promoters (Macdonald et al., 2005, Winter et al., 2008). Examples for the correlation between phosphorylation and methylation marks include a study which has described a mechanism in which H3K28 is phosphorylated by stress-activated kinases (Lau and Cheung, 2011). H3K28ph, together with the adjacent H3K27me3 mark, induces the displacement of the repressive polycomb group and thereby activates the transcription of target genes (Gehani et al., 2010). Metzger and colleagues (2008)

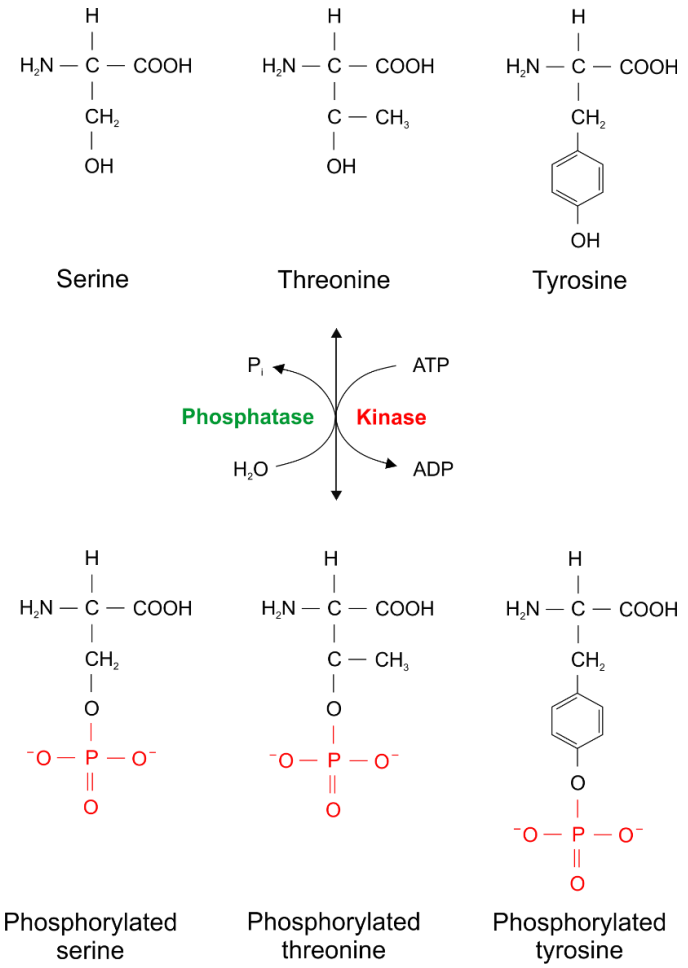

Figure 1.15: Histone phosphorylation.
The addition of phosphate groups is catalysed by kinases using adenosine triphosphate (ATP) and the removal by phosphatases. In histone proteins serine, threonine and tyrosine residues can be mono-, di- and tri-phosphorylated, whereas in this figure mono-phosphorylation is depicted.

identified a mechanism in which the phosphorylation of H3T11 by the protein kinase C-related kinase 1 (PRK1) is necessary for the demethylation of H3K9me3 by the JMJD2C (KDM4C) which in turn activates AR-dependent transcription (Metzger et al., 2008). In addition, they showed that high PRK1 and H3T11ph levels in PCa specimens correlate with high Gleason score and the inhibition of PRK1 reduced LNCaP cell growth, suggesting PRK1 may represent a promising target in PCa (Metzger et al., 2008). Metzger and colleagues also describe a new chromatin mark, namely H3T6ph, which is phosphorylated by the protein kinase C beta I (PKCβ_I) and which in turn prevents the lysine-specific demethylase 1 (LSD1) from demethylating mono- and demethylated H3K4, a known mark for active transcription (Metzger et al., 2010). This finding provides more insight into the mechanisms of the dual function of LSD1, which represses transcription by demethylating H3K4, but activates transcription by demethylating H3K9 (Metzger et al., 2010).

1.3.1.3.3 Histone methylation

Histone methylation mainly occurs on lysine and arginine residues at the N-terminal tail of histones (Black et al., 2012, Musselman et al., 2014). It is the transfer of a methyl group (-CH_3) to the nitrogen of the ε-amino group of lysine or the δ-guanidino group of arginine, leading to methyl-lysine and methyl-arginine respectively (**Figure 1.16**) (Black et al., 2012, Musselman et al., 2014). The enzymes catalysing this reaction are methyltransferase and use S-adenosyl-methionine (SAM or AdoMet) as a donor, releasing in S-adenosyl-homocysteine (SAH or AdoHcy) (**Figure 1.16**) (Black et al., 2012, Chiang et al., 1996). Protein arginine methyltransferases (PRMTs) are capable of mono- or di-methylating histone arginine residues (Di Lorenzo and Bedford, 2011). The PRMT family is composed of several members which are well studies and known to be transcriptional coregulators (Chen et al., 1999, Di Lorenzo and Bedford, 2011). In contrast, little is known about arginine demethylation and therefore arginine methylation is currently considered a very stable mark (Di Lorenzo and Bedford, 2011).

The methylation of histone lysine residues was long believed to be a static epigenetic modification too. In 1964, the methylation of histone lysines and its role in RNA synthesis was discovered (Allfrey et al., 1964, Allfrey and Mirsky, 1964, Murray, 1964). In 2000, Rea and colleagues discovered the first enzyme that catalyses histone methylation, namely the lysine methyltransferase (KMT) SUV39H1, also referred to as KMT1A, which contains the for many KMTs characteristic SET (Su(Var)3-9, Enhancer of zeste, Trithorax) domain (Rea et al., 2000). Subsequently, many more KMTs were discovered which mono-, di- and tri-methylate lysine residues in histones (Dillon et al., 2005, Nimura et al., 2010). In 2004, Shi et al. discovered the first histone lysine demethylase (KDM), called LSD-1 (Lysine-Specific Histone Demethylase 1A), also referred to as KDM1A, opening a completely new view on histone methylation being a dynamic and reversible process rather than a static epigenetic mark (Shi et al., 2004). Thereafter, many more KDMs where found, which are divided into two subgroups according to their enzymatic mechanism (Anand and Marmorstein, 2007, Hou and Yu, 2010). The KDM1 family are FAD-dependent amine oxidase enzymes that require protonated lysine residues for di- and mono-demethylating histones (Hou and Yu, 2010, Shi et al., 2004).

In 2006, Tsukada and colleagues discovered JHDM1, later referred to as KDM2A, which is the first member of the second subgroup of KDMs, namely the family of Jumonji C domain-containing histone demethylases (JHDMs) (Tsukada et al., 2006). JHDMs are Fe(II) and α-ketoglutarate dependent oxygenases which act on methyl groups by radical attack, and therefore are also capable of mono-, di- and tri-demethylate lysine residues (Hou and Yu,

2010, Tsukada, 2012). The two subclasses will be described in more detail in the next section. The capability of mono-, di- and tri-demethylating lysine residues makes methylation a more complex modification than acetylation and phosphorylation (Bannister and Kouzarides, 2011). Interestingly, in contrast to acetylation and phosphorylation, methylation does not seem to alter the electrostatic charge of histones though (Bannister and Kouzarides, 2011, Hyun et al., 2017). Instead, methyl marks are considered as sites for "reader" proteins and indeed, many proteins which contain a methyl-lysine binding motif have been identified, including PHD, tudor, zf-CW, PWWP, chromo and bromo domain proteins (Musselman et al., 2014). Those reader proteins bind methyl-lysine in a selective manner depending on the site and state of methylation (Hyun et al., 2017).

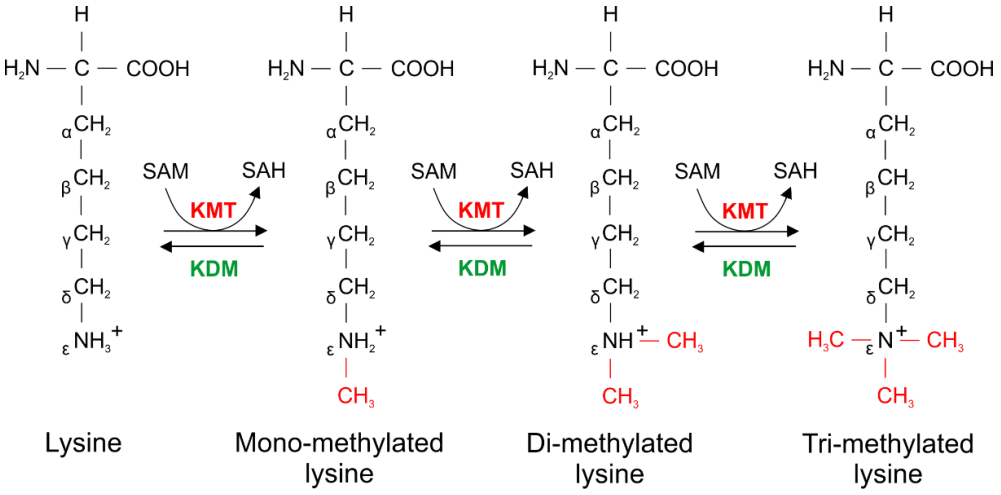

Figure 1.16: Histone methylation at lysine.
The lysine methyl transferases (KMT) catalyses the transfer of one to three methyl groups to lysine, by using the co-substrate SAM, leading to mono-, di- or tri-methylated lysine. The reaction is reversed by the lysine demethylase (KDM). SAM = S-adenosyl methionine; SAH = S-adenosyl homocysteine.

The methylation of lysine and arginine residues occurs throughout all five histone proteins (Greer and Shi, 2012, Tan et al., 2011). The best studied lysine methylation sites include H3K4, H3K9, H3K27, H3K36, H3K79 and H4K20. The consensus is that methylated H3K4, H3K36 and H3K79 is associated with transcriptionally active sites, whereas methylated H3K9, H3K27 and H4K20 is related to silenced genes (Black et al., 2012). The focus of this study are the histone marks H3K4, H3K9 and H3K27 and the enzymes demethylating these marks, which will be described in the next section.

To sum up, histones can be altered through various chemical modifications, altering the chromatin structure and accessibility for the replication and transcription machinery. A schematic of the most intensively studied modifications in core histones is presented in Figure 1.17 (Kimura, 2013, Tessarz and Kouzarides, 2014, Zhao and Garcia, 2015). The cross-talk between those modifications appears to be complex and context-dependent and more research is needed to further elucidate the roles of histone modifications and how they influence each other.

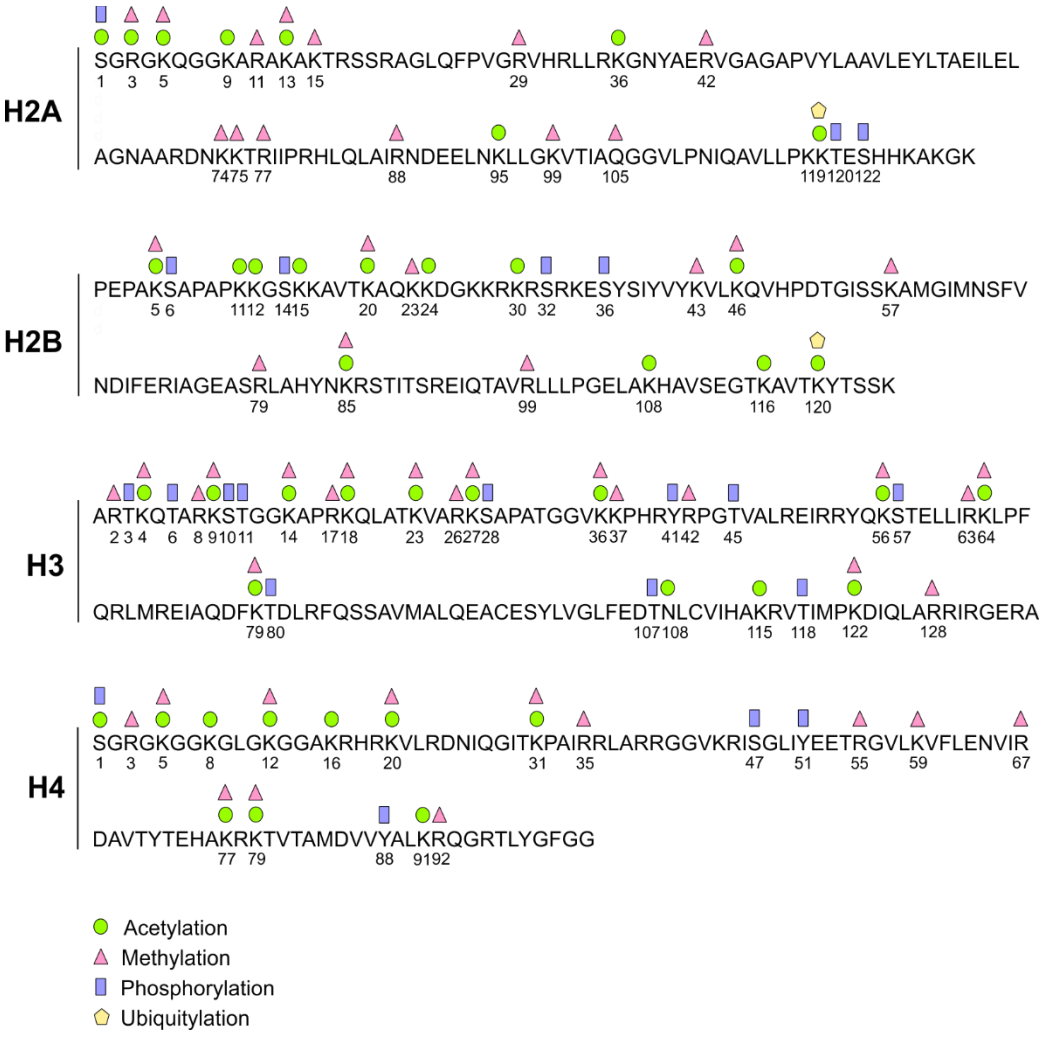

Figure 1.17: Histone modifications in core histone proteins.
The location of the common histone modifications acetylation, methylation, phosphorylation and ubiquitylation in the core histones H2A (AAN59974.1; 130aa), H2B (CAA41051.1; 126aa), H3 (AAN39284.1; 136aa) and H4 (NP_003533.1; 103aa) is depicted.

1.3.2 Histone demethylases

As described in the previous section, histone demethylases can be divided into two subgroups: (1) The FAD-dependent amine oxidase enzymes, which includes the KDM1 family; and (2) the Fe(II) and α-ketoglutarate dependent oxygenase enzymes, which comprise the Jumonji family (Anand and Marmorstain, 2007, Hou and Yu, 2010, Tsukada et al., 2006). In **Table 1.2** the members of the subgroups are listed, including their name, synonyms, protein domains and histone demethylation targets (Bian et al., 2017, Hoffmann et al., 2012, Labbé et al., 2014, Shmakova et al., 2014). A schematic of the demethylation targets is presented in **Figure 1.18**. In 2004, the very first KDM discovered was KDM1A, which was originally named lysine-specific histone demethylase 1 (LSD1) (Shi et al., 2004) (**Table 1.2**). A systematic nomenclature has been applied and LSD1A is now referred to as KDM1A and serves as the KDM prototype (Pajtler et al., 2013). KDM1A will be described in detail in the next section. Five years after the discovery of KDM1A, a second flavin-dependent histone demethylase was identified and termed LSD2/KDM1B (Karytinos et al., 2009). In contrast to KDM1A, which targets H3K4me2/me1 and H3K9me2/me1, KDM1B is strictly specific for H3K4me2/me1 and contains a zinc finger motif (Karytinos et al., 2009) (**Table 1.2**). Since KDM1A is not capable to demethylate trimethyl-lysine residues, additional KDMs with a tri-methyl lysine substrate specificity are required. Indeed, over the last years an extended family of demethylases were characterized whose members contain a so-called Jumonji domain (**Table 1.2**). Jumonji literally means cruciform in Japanese and refers to a mutation observed in the jumonji mouse gene involved in the neural groove development (Takeuchi et al., 1995). Shortly after that, the jumonji gene was characterized in humans and is 90% homologous to the jumonji mouse gene (Bergé-Lefranc et al., 1996).

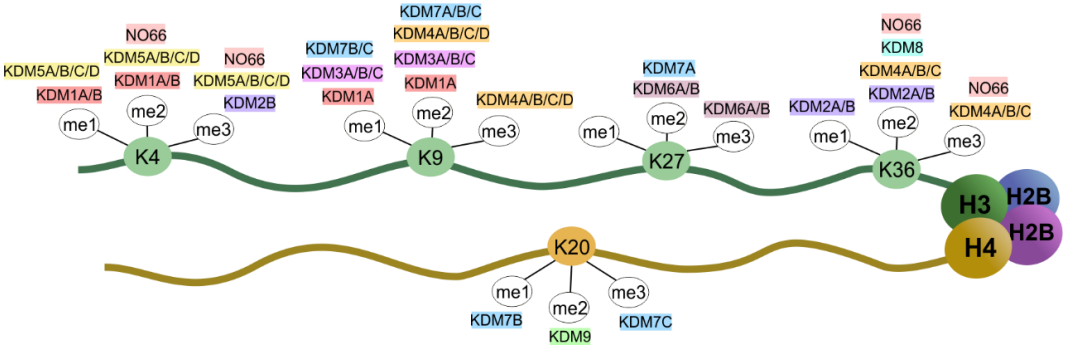

Figure 1.18: KDM histone marks.
Histone lysine demethylases (KDMs) target mono-, di- and tri-methylated lysine residues at histone H3 (K4, K9, K27, K36) and H4 (K20). The specificity of the members of the subclasses KDM1 to KDM9 and NO66 are given.

Table 1.2: Histone demethylase families and their implications in prostate cancer.
For each histone demethylase, the name, synonyms, protein domains and histone demethylation targets are stated. In addition, their implications and function as a tumour suppressor or oncogene in PCa are given. SWIRM = Swi3p, Rsc8p and Moira; AO = amino oxidase; Jmj = Jumonji; ZF = zinc finger, PHD = plant homeodomain; LRR = leucine-rich repeat; ARID = AT-rich interaction domain; TPR = tetratrico peptide repeat; PCa = prostate cancer; EMT = epithelial-mesenchymal transition; CRPC = castrate resistant prostate cancer.

Name	Synonyms	Domains	Histone targets	Implications in PCa	References
KDM1A	LSD1, AOF2	SWIRM AO Tower	H3K4me2/me1 H3K9me2/me1	Increased expression AR-coactivator PCa initiation, progression, recurrence, angiogenesis, migration, invasion, EMT	(Kahl et al., 2006, Kashyap et al., 2013, Metzger et al., 2005, Wang et al., 2015)
KDM1B	LSD2, AOF1	SWIRM AO, ZF	H3K4me2/me1	-	
KDM2A	JHDM1A FBXL11A, KIAA1004	JmjC ZF, PHD F-box, LRR	H3K36me2/me1	Downregulated Centromeric rearrangements and mitotic aberrations	(Frescas et al., 2008)
KDM2B	JHDM1B FBXL10B	JmjC ZF, PHD F-box, LRR	H3K4me3 H3K36me2/me1	Cell-cell adhesion, actin cytoskeleton organisation PCa cell migration	(Zacharopoulou et al., 2018)
KDM3A	JHDM2A JMJD1A KIAA0742	JmjC	H3K9me2/me1	Overexpressed AR-coactivator PCa growth and survival	(Fan et al., 2016, Wilson et al., 2017, Yamane et al., 2006)
KDM3B	JHDM2B JMJD1B KIAA1082	JmjC	H3K9me2/me1	Overexpressed	(Björkman et al., 2012)
KDM3C	JHDM2C KIAA1380 TRIP8	JmjC	H3K9me2/me1	-	-
KDM4A	JHDM3A JMJD2A KIAA0677	JmjC, JmjN PHD Tudor	H3K9me3/me2 H3K36me3/me2	Overexpressed AR-coactivator	(Berry and Janknecht, 2013, Shin and Janknecht, 2007)
KDM4B	JHDM3B JMJD2B KIAA0876	JmjC, JmjN PHD Tudor	H3K9me3/me2 H3K36me3/me2	Overexpressed AR-coactivator Responsible for AR stability	(Coffey et al., 2013, Berry and Janknecht, 2013)
KDM4C	JHDM3C JMJD2C KIAA0780	JmjC, JmjN PHD Tudor	H3K9me3/me2 H3K36me3/me2	Overexpressed AR-coactivator Cooperates with KDM1A	(Wissmann et al., 2007, Berry and Janknecht, 2013)
KDM4D	JHDM3D JMJD2D	JmjC, JmjN	H3K9me3/me2	Maybe AR-coactivator	(Shin and Janknecht, 2007)
KDM5A	JARID1A RBP2	JmjC, JmjN PHD, PLU-1 ZF, ARID	H3K4me3/me2/me1	Overexpressed May contribute to drug resistance	(Sharma et al., 2010)

Name	Synonyms	Domains	Histone targets	Implications in PCa	Function
KDM5B	JARID1B PLU-1 RBP2-H1	JmjC, JmjN PHD, PLU-1 ZF, ARID	H3K4me3/me2/me1	Overexpressed AR-coactivator	(Li et al., 2015a, Lu et al., 2015b, Xiang et al., 2007b)
KDM5C	JARID1C XE169 SMCX	JmjC, JmjN PHD, PLU-1 ZF, ARID	H3K4me3/me2/me1	Overexpressed Marker for relapse after radioactive therapy	(Stein et al., 2014)
KDM5D	JARID1D SMCY KIAA0234	JmjC, JmjN PHD, PLU-1 ZF, ARID	H3K4me3/me2/me1	Downregulated (CRPC) Docetaxel resistance Marker for invasion & metastasis	(Komura et al., 2016, Li et al., 2016)
KDM6A	UTX KABUK2	JmjC TPR	H3K27me3/me2	Overexpressed	(Morozov et al., 2017)
KDM6B	JMJD3 KIAA0346	JmjC	H3K27me3/me2	Overexpressed PCa progression	(Morozov et al., 2017, Xiang et al., 2007a)
KDM7A	JHDM1D KIAA1718	JmjC PHD	H3K9m2 H3K27me2	Overexpressed AR-coactivator, PCa growth	(Lee et al., 2018)
KDM7B	JHDM1F KIAA1111 PHF8	JmjC PHD	H3K9me2/me1 H4K20me1	Overexpressed PCa growth, migration, invasion	(Björkman et al., 2012)
KDM7C	JHDM1E KIAA0662 PHF2, GRC5	JmjC PHD	H3K9me2/me1 H4K20me3	Potentially deleted	(Lee et al., 2015, Zhang et al., 2018b)
KDM8	JMJD5	JmjC	H3K36me2	Overxpressed AR co-activator PCa growth & CRPC	(Wang et al., 2019)
KDM9	ROSBIN DPY-21	JmjC	H4K20me2	-	-
NO66	JMJD9 RIOX1	JmjC	H3K4me3/me2 H3K36me3/me2	Overexpressed Survival, invasion, metastasis, CRPC, PCa growth in bone	(Sinha et al., 2019)
MINA	JMJD10 RIOX2	JmjC	Potentially H3K9me3	-	-

The jumonji family now comprises more than 100 members from bacteria, fungi, plants and animals, and share two conserved motives, the jmjC domain and the more N-terminally situated jmjN domain, whereat the jmjN domain is not present in all members (Balciunas and Ronne, 2000, Takeuchi et al., 1995). Thereafter, Tsukada and colleagues characterised the first JmjC domain-containing histone demethylase that specifically demethylates H3K36 in the presence of Fe(II) and α-ketoglutarate (Tsukada et al., 2006). They named it JmjC domain-containing histone demethylase 1 (JHDM1, later referred to as KDM2A) (Tsukada et al., 2006). In the following years, more JHDMs were identified and are classified into the KDM-nomenclature according to their structure and domains (**Table 1.2**). The

Jumonji domain is important for the catalytic activity, whereas the other domains, including the PHD, SWIRM, ARID, zinc finger and tudor domain, fulfil different crucial functions, such as DNA binding, protein binding and reading and binding histone marks (Hoffmann et al., 2012). Many KDMs have been shown to be implicated in various types of cancer (Black et al., 2012, Hoffmann et al., 2012, Hyun et al., 2017). Their implications in prostate cancer are listed in (Table 1.2). KDM2A (Frescas et al., 2008), KDM5D and potentially KDM7C (Lee et al., 2015, Zhang et al., 2018b) are considered to function as tumour suppressors in prostate cancer. In contrast, most KDMs fulfil an oncogenic role in prostate cancer, including KDM1A, KDM2B, KDM3A, KDM3B, KDM4A-C, KDM4A, KDM4B, KDM4C, potentially KDM4D, KDM5A, KDM5C, KDM6A, KDM6B, KDM7A, KDM8, NO66 (Table 1.2). Even though KDM5B has been reported to be overexpressed in PCa and described as an oncogene, its exact role remains controversial (Li et al., 2015a, Lu et al., 2015b, Xiang et al., 2007). This highlights the potential of developing drugs and therapies targeting KDMs to treat prostate cancer (D'Oto et al., 2016, Hoffmann et al., 2012).

This study will focus on the methylation marks at H3K4, H3K9 and H3K27 and thus the role of these marks will be described. The methylation of H3K4 is a known mark for active transcription, whereas methylated H3K9 and H3K27 are generally considered repressive marks (Black et al., 2012). The methylation level of H3K4 has been reported to exhibit a "5' to 3' gradient" at actively transcribed genes, with high levels of H3K4m3 at the transcription start site (TSS), H3K4me2 further downstream and H3K4me1 most distal (Barski et al., 2007, Soares et al., 2017). This gradient is important to guide transcription factors and coregulators, for example H3K4me3 mainly attracts transcriptional co-activators, whereas H3K4me2 is read by HDACs which suppress transcription to avoid cryptic gene expression (Buratowski and Kim, 2010, Pinskaya and Morillon, 2009). Ernst and Kelly (2010) performed a large-scale characterisation of chromatin states through ChIP-seq analysis and revealed that H3K4me3 is highly frequent at the promoter sites, together with evolutionarily conserved motifs, CpG islands and bound transcription factors (Ernst and Kellis, 2010). H3K4me1 is frequently found at the enhancer (Ernst and Kellis, 2010). At the TSS, H3K4me2/1 and H3K9me1 are present at higher levels (Ernst and Kellis, 2010). In silent genes, higher H3K9me3/me2 levels are present around the TSS, which is associated with heterochromatin and gene silencing (Barski et al., 2007). Higher H3K9me1 levels are found around the TSS, when the promoter is active, suggesting H3K9me1 may be implicated in transcriptional activation (Barski et al., 2007). Interestingly, H3K9me3/me2 levels are found to be high in internal exons and have been shown to contribute to exon

inclusion, whereas H3K9 demethylation leads to exon skipping, suggesting a role for H3K9 methylation in alternative splicing (Bieberstein et al., 2016). Similarly, H3K27me3/me2 is higher at silent promoters compared to active promoters (Barski et al., 2007). Surprisingly, H3K27me1 is found to be enriched at active promoters which highlights the complexity of histone modifications in transcriptional regulation (Barski et al., 2007). Active histone marks, such as H3K4me3, have been shown to antagonise H3K27me3 and are rarely present at the same histone H3 (Wiles and Selker, 2017). However, promoters can be "bivalent", if they harbour both H3K4me3 and H3K27me3 (Bernstein et al., 2006, Ke et al., 2009). A study in PCa has revealed that both non-malignant epithelial prostate cells and malignant PC3 cells harbour the same proportion of bivalent H3K4me3 and H3K27me3 promoters, however, which genes harbour these bivalent combinations differs greatly, leading to differential gene expression between normal and prostate cancer cells (Ke et al., 2009). A study on global histone H3K4 and H3K9 modifications in PCa tissue revealed that H3K4me1, H3K9me2, H3K9me3 levels are decreased in PCa tissue compared to normal prostate tissue (Ellinger et al., 2010). They further showed that H3K9me2 correlates with advanced TNM stage and H3K9me2/me1 with Gleason score (Ellinger et al., 2010). H3K9me3/me2 and H3K4me2 correlates with high PSA (Ellinger et al., 2010). H3K4me3/me2/me1 correlates with lymph node involvement, Gleason score and is higher expressed in patients with HRPC compared to localised PCa, i.e. it could be an indicator for PCa progression (Ellinger et al., 2010).

The lysine residues at H3K4, H3K9 and H3K27 can be demethylated by KDM1A, KDM5B and KDM7A (**Figure 1.18**), which will be described in more detail in the next sections.

1.3.2.1 KDM1A

KDM1A was the very first human KDM discovered by Shi and colleagues (2004). It is a nuclear amine oxidase homologue and has the unique feature to oxidise the amino groups of histones through a flavin-dependent amine oxidation reaction (Shi et al., 2004). KDM1A is capable of demethylating mono- and di-methylated H3K4 and H3K9 and therefore can act as both a transcriptional corepressor and coactivator (Metzger et al., 2005, Shi et al., 2004). KDM1A can interact with protein complexes, receptors, non-coding RNAs, other epigenetic coregulators and transcription factors (Ismail et al., 2018). Interestingly, the substrate specificity of KDM1A depends on which partner is bound. Lee *et al*. (2005) found that the demethylation of H3K4 requires KDM1A to be in complex with the histone deacetylase HDAC1/2 and the REST (RE1 silencing transcription factor) corepressor 1 (co-REST) (Hakimi et al., 2002, Lee et al., 2005, You et al., 2001). The SANT domain in coREST

allows interaction with KDM1A and links KDM1A with the chromatin structure (Boyer et al., 2002, Shi et al., 2005). KDM1A has also been found to be bound to other co-repressor complexes such as the nucleosome remodeling deacetylase (NuRD) complex, an interaction implicated in breast cancer metastasis (Wang et al., 2009d). On the other hand, Metzger and colleagues (2005) performed a study in LnCaP cells and aimed to investigate the regulation of the AR by KDM1A involved in prostate cancer. They found that KDM1A demethylates the histone marks mono- and dimethyl H3K9 in an androgen-dependent manner, thereby activating gene expression (Metzger et al., 2005). This finding further highlights that KDM1A acts in a complex-dependent manner, either as a gene repressor or activator. KDM1A not only demethylates histone proteins but also non-histone proteins (Nicholson and Chen, 2009). For example, a study by Huang and colleagues (2007) has shown that demethylation of p53 by KDM1A inactivates p53 and thereby inhibits apoptosis (Huang et al., 2007).

Many studies revealed KDM1A is crucial for mammalian development and various biological processes (Amente et al., 2013, Burg et al., 2015). In 2007, Wang *et al.* demonstrated that KDM1A is essential in cell-lineage determination and differentiation during pituitary organogenesis, by recruiting co-activator and co-repressor complexes to target genes (Wang et al., 2007). However, KDM1A is also involved in many types of cancer, including head and neck (Yuan et al., 2015), ovarian (Chen et al., 2015), (Liu et al., 2017), lung (Lv et al., 2012), liver (Zhao et al., 2012) and colon (Ding et al., 2013). As already mentioned above, KDM1A is also implicated in PCa by co-localising with the AR and acting as an AR co-activator (Metzger et al., 2005). Cai and colleagues (2011) reported about an interesting AR feedback mechanism. At low androgen levels, such as in CRPC, AR can bind to an enhancer, positioned in the second intron of *AR*, to induce *AR* gene expression (Cai et al., 2011). At high AR levels, AR recruits KDM1A to the enhancer and thereby inhibits *AR* gene expression (Cai et al., 2011). Another study revealed that in high-risk prostate tumours, KDM1A mRNA and protein levels are significantly up-regulated and high levels of KDM1A correlates with PCa recurrence (Kahl et al., 2006). These findings were confirmed and extended by Kashyap and colleagues (Kashyap et al., 2013) who reported that siRNA-mediated inhibition of KDM1A function blocks androgen induction of pro-metastatic gene networks. Furthermore, pharmacological inhibition of KDM1A decreased proliferation of androgen dependent and independent cell lines (Kashyap et al., 2013). Moreover, they suggest a direct role for KDM1A in regulating VEGF-A expression, providing first evidence for a link between KDM1A and pro-angiogenic pathways (Kashyap et al., 2013). Not surprisingly, in the recent years, inhibitors targeting KDM1A have been developed (Niwa

and Umehara, 2017). Wang *et al.* (2015) reported that the inhibition of up-regulated KDM1A through the KDM1A inhibitor pargyline reduced prostate cancer cell migration, invasion and epithelial-to-mesenchymal transition (EMT) *in vitro* and *in vivo (Wang et al., 2015)*. They propose the repression of KDM1A as a complementary therapy to ADT in advanced PCa (Wang et al., 2015). Another study in docetaxel-resistant prostate cancer cells revealed that the KMD1A antagonist HCI-2509 increases H3K9me2 in a dose-dependent manner, inhibits *c-myc* expression and reduces tumour growth in mice (Gupta et al., 2016). Very recently, a research group identified the compound NCL1 as a highly selective KDM1A inhibitor which inhibits CRPC cell growth, including 22Rv1 and PC3 cells, by inducing apoptosis and autophagy (Etani et al., 2015). KDM1A thus is a promising therapeutic target and biomarker and KDM1A inhibitors for different cancer types, such as acute myeloid leukemia and small cell lung cancer, have entered into cancer clinical trials (Magliulo et al., 2018, Niwa and Umehara, 2017, Yang et al., 2018).

KDM1A is a 90kDa protein and contains three domains: the AOL domain, the SWIRM domain and the Tower domain (Figure 1.19) (Hayward and Cole, 2016). Similar to other FAD-dependent amino oxidases, it contains an amine oxidase-like domain (AOL) (Figure 1.19) (Laurent and Shi, 2016). The AOL domain is responsible for the catalytic activity and provides binding sites for its substrates and the cofactor flavin adenine dinucleotide (FAD) (Chen et al., 2006b). Whilst the FAD-binding sites are similar to other amino oxidases, KDM1A has a more expansive substrate binding pocket which is responsible for its ability to bind a broad spectrum of substrates, including histone and non-histone proteins (Burg et al., 2016, Ismail et al., 2018). The acidic binding pocket of KDM1A needs at least 21 amino acids of its substrate for efficient catalysis, for example, the first 21 amino acids of the basic N-terminal tail of histone H3 (Forneris et al., 2005, Stavropoulos et al., 2006). The AOL also harbours two LxxLL motifs which are known to facilitate the interaction with nuclear receptors such as the androgen receptor (Figure 1.19) (Heery et al., 1997). Within the catalytic core of KDM1A, there is a protruding "Tower" domain which contains two antiparallel α-helices that create a coiled coil structure (Figure 1.19). The Tower domain is the site for interaction with CoREST and other proteins (Chen et al., 2006b, Laurent and Shi, 2016). The SWIRM (Swi3p, Rsc8p and Moira) domain, which is not present in other FAD-dependent amino oxidases and therefore is unique for KDM1A, is important for protein-protein interactions and interactions with the AOL, but is not involved in DNA binding (Aravind and Iyer, 2002, Chen et al., 2006b, Stavropoulos et al., 2006). The interaction between SWIRM/AOL forms a surface groove which is crucial to recognise and bind the substrate (Burg et al., 2016, Stavropoulos et al., 2006).

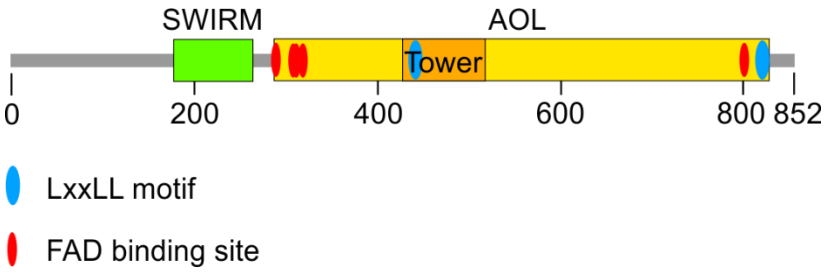

Figure 1.19: KDM1A protein domains.
The KDM1A protein (NP_055828) is composed of 852 amino acids and harbours a SWIRM, amino oxidase and "tower" domain. The sites of LxxLL motifs and FAD binding sites are depicted. SWIRM = Swi3p, Rsc8p and Moira; AOL = amine oxidase-like domain; aa = amino acid.

1.3.2.2 KDM5B

In contrast to KDM1A, KDM5B is capable of demethylating mono-, di- and tri-methylated H3K4 and is also referred to as JARID1B or PLU-1 because of its domains (Iwase et al., 2007, Scibetta et al., 2007, Yamane et al., 2007). KDM5B is a 180 kDa protein which contains 1,544-amino-acid and is composed of multiple domains (**Figure 1.20**) (Dorosz et al., 2019, Scibetta et al., 2007). The catalytic activity of KDM5B is dependent on the JmjC, JmjN and C5HC2 (C = cysteine, H = histidine) zinc finger domain (**Figure 1.20**) (Horton et al., 2016). The JmjC domain harbours substrate and iron binding sites and links with the JmjN which is important for engagement with the substrate and iron (Horton et al., 2016). The exact role of the C5HC2 zinc finger domain is still not clear, however, it is thought to be involved in the catalytic activity of KDM5B and potentially bind DNA through one or several of its eight zinc ligand-binding residues (Horton et al., 2016, Laity et al., 2001, Rujirabanjerd et al., 2010). KDM5B harbours three PHD domains which are thought to have different substrate specificities (**Figure 1.20**) (Klein et al., 2014). Interestingly, PHD1 has been shown to have a very strong affinity to H3K4me0, but also binds H3K4m1. In contrast, PHD2 does not seem to bind histones, and PHD3 preferably binds H3K4me3, but also H3K4me1/2 (Klein et al., 2014, Zhang et al., 2014c). The AT-rich interactive domain (ARID), originally also referred to as BRIGHT domain, is responsible for DNA binding and has been shown to bind to the consensus DNA sequence GCACA/C (**Figure 1.20**) (Scibetta et al., 2007, Tu et al., 2008). The PLU-1 domain has not been fully characterised yet but may be implicated in DNA binding and also shows to harbour several LxxLL binding motifs which is needed for nuclear receptor binding (**Figure 1.20**) (Heery et al., 1997, Horton et al., 2016, Lu et al., 1999). In electron microscopy KDM5B has a dumbbell shape, similar to the structure of the KDM1A/CoREST complex, suggesting KDM1A and KDM5B share a similar mechanism of demethylation (Dorosz et al., 2019).

Since KDM5B demethylates H3K4me3, which is a mark for active transcription, at transcription start sites, it is generally thought to be a transcriptional repressor (Han et al., 2017). KDM5B has been implicated in various processes during development, especially neuronal development, including mitosis, cell cycle, embryonic stem cells and differentiation (Albert et al., 2013, Huang et al., 2015, Madsen et al., 2003, Schmitz et al., 2011, Xie et al., 2011a). During development, KDM5B is crucial for fine-tuning H3K4me3 levels and thereby balances the activation and repression of regulator genes, which in turn controls proliferation and differentiation processes (Fueyo et al., 2015). KDM5B can also fulfill a demethylase-independent function as a linker protein and has been shown to directly interact with transcription factors and histone deacetylases (HDACs) (Barrett et al., 2007, Han et al., 2017, Tan et al., 2003). It has been indicated to interact with HDACs through its PHD domains (Barrett et al., 2007). Another study revealed that KDM5B can also act as a coactivator by directly interacting with the retinoic acid receptor alpha (RARα) and binding to the DNA element of retinoic acid (RA) responsive genes (Zhang et al., 2014b). In the presence of RA, KDM5B releases the polycomb repressive complex 2 (PRC2) it associates with in the absence of RA, and instead recruits co-activators which in turn switch on RA signalling (Zhang et al., 2014b). KDM5B has also been shown to bind KDM1A, in association with the nucleosome remodeling and deacetylase (NuRD) complex, and this interaction is important to inhibit angiogenesis and metastasis in breast cancer, describing KDM5B as a tumour suppressor (Klein et al., 2014, Li et al., 2011).

KDM5B is implicated in various types of cancer (Han et al., 2017). When KDM5B was first discovered it was reported to be up-regulated in breast cancer (Barrett et al., 2007). Multiple studies on the oncogenic role of KDM5B in breast cancer followed and revealed that KDM5B is involved in breast cancer cell proliferation, mammary gland development, lineage-driving of luminal cells and invasive ductal carcinoma (Zhao and Liu, 2015, Zou et al., 2014). KDM5B has also been shown to be up-regulated in prostate cancer and to directly interact with the androgen receptor, thus regulating AR-transcriptional activity (Xiang et al., 2007). Another study on a microarray dataset showed that *KDM5B* was expressed higher in tumour samples compared to normal prostate samples (Li et al., 2015a). The expression of *KDM5B* is targeted by the tumour suppressor *miR-29a* which in turn inhibits PCa cell proliferation and induces apoptosis and this tumour suppressive function is lost in PCa tissues where *miR-29a* expression levels are low (Li et al., 2015a). Aberrant methylation levels at H3K4 are associated with PCa progression and development of HRPC (Ellinger et al., 2010, Lu et al., 2015b). Lu and colleagues (2015) found that the S-phase kinase-associated protein 2 (SKP2), which is an E3 ubiquitin ligase involved in protein

degradation, is highly expressed in PCa and targets KDM5B, leading to aberrant H3K4me3 levels in PCa (Lu et al., 2015b). They showed that SKP2 inactivation increases KDM5B protein levels which in turn leads to a reduction of H3K4me3 levels (Lu et al., 2015b). It therefore remains controversial, whether KDM5B fulfils a tumour suppressive or oncogenic role in PCa and further investigation is needed to explain how high levels of both H3K4me3 and KDM5B can be present and contribute to PCa progression. During the last years, KDM5B selective inhibitors have been developed. For example, the inhibitor PBIT selectively inhibits KDM5B (IC_{50} = 3 µM) over other members of the KDM5-family and has been shown to inhibit proliferation of UACC-812 breast cancer cells at a concentration of 10 µM PBIT (Sayegh et al., 2013). More recently, a more selective, competitive inhibitor of KDM5B, named CPI-455, was developed with an IC_{50} of 0.003 µM and was also shown to inhibit proliferation of drug-tolerant cancer cells (Vinogradova et al., 2016).

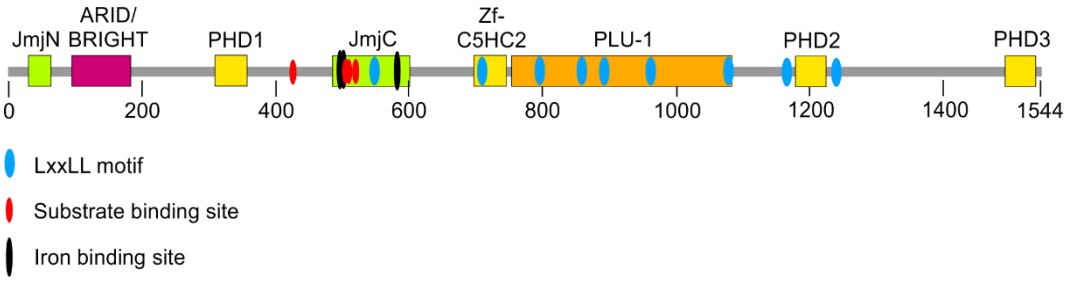

Figure 1.20: KDM5B protein domains.
The KDM5B protein (NP_006609) has 1544 amino acids and contains a JmjN, JmjC, ARID/BRIGHT, PHD1, PHD2, PHD3, Zf-C5HC2 and PLU-1 domain. The sites for the LxxLL motif, substrate binding and iron binding sites are shown. JmjN/C = Jumonji N/C; ARID = AT-rich interaction; PHD = plant homeodomain; Zf = Zinc finger.

1.3.2.3 KDM7A

While KDM1A and KDM5B have been extensively studied in gene regulation, development and various diseases, little is known about KDM7A. However more and more research groups focus on the role of KDM7A in normal physiology and disease. In 2010, Huang et al. identified KIAA1718 as a member of the KDM7 family and thus it was assigned KDM7A (Huang et al., 2010). KDM7A is capable of demethylating H3K9me2 and H3K27me2 (Huang et al., 2010). KDM7A harbours a plant homeodomain (PHD)-type zinc finger motif and a Jumonji C (JmjC) domain (**Figure 1.21**). As mentioned before, the JmjC domain is responsible for the enzymatic activity and harbours Fe^{2+} and α-oxoglutarate binding sites (**Figure 1.21**) (Klose et al., 2006). The PHD domain is a highly conserved, around ~30 amino acids short domain which contains a zinc-binding motif and is important for "reading" histone modification marks which will be described later (Sanchez and Zhou, 2011). KDM7A

has a unique dual-specificity for the repressive methyl marks on H3K9 and H3K27, acting as a transcriptional activator by demethylating repressive methyl marks (Huang et al., 2010, Yokoyama et al., 2010). Chromatin immunoprecipitation (ChIP)-sequence analysis of KDM7A from *Caenorhabditis elegans* (ceKDM7A) revealed that the PHD domain of ceKDM7A binds H3K4me3, which is a known transcriptionally activating mark, and that this binding is crucial for ceKDM7A's demethylase activity in the promotor region of genes (Lin et al., 2010). Crystallisation studies further suggested that the PHD domain can bind H3K4me3 at one histone molecule, whilst the JmjC domain binds H3K9me2 at a different histone molecule, describing a *trans*-histone binding mechanism and providing a novel mechanism of histone methylation regulation (Yang et al., 2010). Horton and colleagues (2010) confirmed that both KDM7A and KDM7B bind H3K4m3 via their PHD domain, however, they found that the presence of H3K4m3 on the same histone peptide makes KDM7A demethylate H3K27 but not H3K9, and vice versa, makes KDM7B favour H3K9 over H3K27 (Horton et al., 2010). The reason for this relates to the linker region between the PHD domain and the JmjC domain (Chaturvedi et al., 2019, Horton et al., 2010). The linker region of KDM7A is slightly longer and more rigid than the linker region of KDM7B, which means that if KDM7A binds to H3K4, demethylation of H3K9 is hindered. In contrast, in KDM7B the linker region is more flexible, allowing its JmjC domain to reach H3K9 for demethylation (Chaturvedi et al., 2019, Horton et al., 2010).

KDM7A is evolutionarily conserved in mammals and seems to be crucial in development, including cell lineage specification in embryos, neuronal development and cardiac, adipogenic and osteogenic cell differentiation (Rissi et al., 2019, Son et al., 2016, Tang et al., 2014, Yang et al., 2019). KDM7A has also been implicated in various diseases, including the auto-immune disease systemic lupus erythematosus (SLE) and the DiGeorge syndrome, also referred to as 22q11 deletion syndrome causing heart defects and learning difficulties (Guo et al., 2015, Nawrocki et al., 2015). KDM7A has also been linked to different cancer types, including pancreatic (Kondo et al., 2017, Pan et al., 2015), leukemia (Chen et al., 2012b), breast (Kondo et al., 2017, Meng et al., 2019, Pan et al., 2015, Xie et al., 2017), cervical cancer and melanoma (Osawa et al., 2011). A recent study in breast cancer cells elegantly demonstrated that KDM7A regulates the transcription of estrogen receptor (ER) target genes together in a protein complex with KDM6A and the acetyltransferase CBP (cAMP response element - binding protein) (Xie et al., 2017). The KDM7A/KDM6A/CBP complex does this by regulating the transition of the repressive mark H3K27me3 to the activating mark H3K27ac. While KDM6A (H3K27me3>me2) and KDM7A (H3K27me2>H3K27me1) regulate the demethylation of trimethylated H3K27 (Xie et al.,

2017), CBP is responsible for H3K27 acetylation, a modification known to increase chromatin accessibility for transcriptional activation (Raisner et al., 2018). Besides its epigenetic function, KDM7A has recently been shown to regulate the stability of the intercellular adhesion molecule1 (ICAM1) via a lysosome-dependent pathway (Choi and Jo, 2016).

Only one study indicated that KDM7A may play a role in prostate cancer, by suggesting that KDM7A is part of a transcriptional coregulator network of AR in PCa (Nilsson et al., 2015). Very recently, a study by Lee and colleagues confirmed that KDM7A induces androgen receptor activity and prostate cancer growth (Lee et al., 2018). During the last years, researchers have tried to develop selective inhibitors for KDM7A. The compound BIX-01294, which mimics the structure of the histone substrate H3K9, inhibits the demethylation of H3K9 by KDM7A (IC_{50} = 16.5 µM), but also the H3K9 methylation activity of the methyltransferase G9a, at an even lower IC_{50} of 0.25 µM (Upadhyay et al., 2012). Rose and colleagues (2012) then described Daminozide, which has been used as a plant growth regulator but was then stopped due to toxicity concerns, as a selective inhibitor of both the KDM2 and KDM7 family (Rose et al., 2012). However, KDM7B (0.55 µM) and KDM2A (1.5 µM) have a lower IC_{50} than KDM7A (2.1 µM) for this inhibitor and therefore Daminozide may not be very selective for KDM7A (Rose et al., 2012). Thus, Suzuki *et al.* (2013) developed a competitive inhibitor, which mimics the structure of the co-substrate α-OG named TC-E 5002, which is more selective for KDM7A (0.2 µM) over KDM7B (1.2 µM) and KDM2A (6.8 µM) (Suzuki et al., 2013). They also showed that TC-E 5002 inhibits the proliferation of mouse neuroblastoma N2a (Gi_{50} = 86 µM), cervical cancer HeLa (Gi_{50} = 40 µM) and esophageal squamous cell carcinoma KYSE-150 cells (Gi50 = 16 µM) *in vitro* (Suzuki et al., 2013). TC-E 5002 was also applied in the study by Lee *et al.* (2018) in LNCaP PCa cells where it decreased cell growth and the expression of AR-target genes and if applied together with Enzalutamide, apoptosis was induced (Lee et al., 2018). Gerken et al. (2017) emphasise the importance of developing even more selective inhibitors for KDM7A and since the KDM2 and KDM7 family is structurally similar, they developed and tested inhibitors which mimic the histone substrate rather than the α-KG (Gerken et al., 2017). They found a compound which is 75-fold more selective for KDM2A and KDM7A than other JmjC lysine demethylases and which reduces both H3K9 and H3K36 demethylation in cells, however, more research still needs to go into the development of KDM7A-selective inhibitors (Gerken et al., 2017).

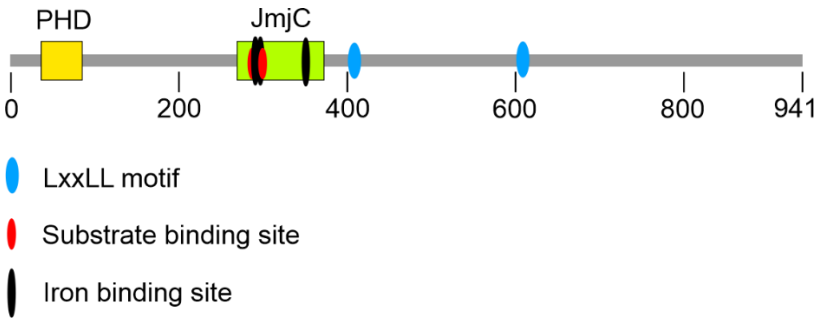

Figure 1.21: KDM7A protein domains.
The KDM7A protein (NP_085150) is made up of 941 amino acids and contains a PHD and JmjC domain. LxxLL motifs, substrate binding sites and iron binding sites are indicated. PHD = plant homeodomain; JmjC = Jumonji C.

1.4 Aim of study

A recent study in PCa cells, reported by Nilsson and colleagues (2015), revealed a novel negative feedback mechanism of androgen coregulators through the microRNA *miR137*, a tumour suppressor which has previously been shown to regulate *KDM1A* in other cancers (Althoff et al., 2013, Balaguer et al., 2010). In androgen responsive LNCaP cells, androgen treatment leads to an induction of *miR137* expression (Nilsson et al., 2015). In turn, *miR137* suppresses the expression of essential AR coregulators, including *KDM1A, KDM2A, KDM4A, KDM5B, KDM7A, MED1,* and *SUZ12*. This negative feedback mechanism is lost in LNCaP:C4-2 (androgen-independent) and PC3 (AR-negative) cells, thereby relieving the inhibition of coregulator expression, resulting in enhanced AR-coregulator complex activity (Nilsson et al., 2015). KDM1A is the most extensively studied KDM and inhibitors for KDM1A in cancer treatment have entered into cancer clinical trials (Magliulo et al., 2018, Niwa and Umehara, 2017, Yang et al., 2018). The study by Nilsson et al. (2015) reveals the potential of not only KDM1A representing a possible target for PCa treatments but also other coregulator proteins, such as KDM5B and KDM7A, which are part of the *miR137* regulated network. The aim of this study therefore was to further elucidate the role of KDM5B and KDM7A in androgen signalling in the context of PCa. The hypothesis was that KDM5B and KDM7A, like KDM1A, are required for AR signalling in PCa. To test this hypothesis the following experiments were completed. (**1**) The expression of KDM5B and KDM7A in PCa specimens and cell lines was investigated. (**2**) KDM5B and KDM7A respectively were functionally deleted by siRNA-mediated knockdown to determine the effect on AR signalling. (**3**) The effect of KDM5B and KDM7A selective pharmaco-inhibitors was tested on AR signalling and PCa cell proliferation. Collectively these aims will determine a complex role for KDMs in AR signalling in PCa.

Chapter 2: Material and methods

Chapter 2 Material and methods

2.1 Bioinformatics

The cBioPortal for Cancer Genomics was used to study genetic alterations in *KDM1A*, *KDM5B* and *KDM7A* respectively in PCa patients (https://www.cbioportal.org/, accessed 12.08.2019) (Cerami et al., 2012). The genetic alterations included missense mutation, amplification, deep deletion, mRNA upregulation and mRNA downregulation. The frequencies of alterations in prostate adenocarcinoma, metastatic adenocarcinoma and neuroendocrine carcinoma were compared. KDM mutations and their location in the genome were determined. The overall survival and the disease/progression-free survival regarding alterations were calculated by Kaplan-Meier estimate using the cBioPortal. Three studies were included in the analysis: (1) The TCGA Provisional Prostate Adenocarcinoma study (n = 499), (2) the SU2C/PCF Dream Team Metastatic Prostate Adenocarcinoma study (n = 444) and (3) the Trento/Cornell/Broad Neuroendocrine Prostate Cancer study (n = 114).

2.2 Tissue micro array (TMA)

In collaboration with the Nottingham University Hospitals (NUH) NHS Trust a tissue microarray (TMA) was constructed on a well characterised prostate cancer (PCa) cohort at Nottingham City Hospital, Nottingham. The study was ethically approved by the NUH Biobank (ACP0000184) and the University of Nottingham (UoN) (1533 150901). The ethics approval number for the TMA was 1861 161006. I applied for and received an honorary contract with NUH NHS Trust as a Research Assistant, which allowed me to work with patient data at Nottingham City Hospital. For the construction of the TMA, specialist support was given by Michael Shawky Toss, a histopathologist and PhD student at City Hospital, who was a crucial contributor in the process of TMA construction and is the histopathologist (MST) mentioned in the following sections. A flowchart of the different steps of the TMA construction is depicted in **Figure 2.1**.

2.2.1 Prostate cancer database

First, patients in the NHS database at City Hospital, Nottingham were filtered for patients diagnosed with prostate cancer (PCa) between 2003-2007 using the Winpas Software (**Figure 2.1, step 1**). These PCa patients were further filtered for patients who were treated

surgically with prostatectomy (n = 165) (**Figure 2.1, step 2**). Needle biopsies could not be used for TMA construction as the tissue area is too small to core, hence it was important to filter for prostatectomy only. Of these 165 PCa patients, a database was then generated using the NHS NOTTIS Software (**Figure 2.1, step 3**). The database included demographic, clinical and pathological data (**Appendix 1**).

Figure 2.1: Flow chart of the tissue microarray (TMA) construction.
The construction of the TMA can be divided into 18 steps, each of which is stated with the required equipment (machine or software) and location. The steps are colour coded regarding their corresponding section (Patient database, Collection of patient blocks, TMA construction & evaluation, IHC and H-Score). The people contributing to the different steps are given with their initials. VM, Veronika Metzler; MT, Michael Toss; CW, Corinne Woodcock; JJ, Jennie Jeyapalan; JL, Jennifer Lothion-Roy.

2.2.2 Collection of patient blocks

The diagnostic slides (~10-40 slides per patient) of the 165 PCa patients were collected in the Biobank archive at City Hospital, Nottingham (**Figure 2.1, step 4**). The slides were reviewed by a histopathologist to confirm the diagnosis and identify the best representative formalin fixed paraffin embedded (FFPE) block for the TMA construction (**Figure 2.1, step 5**). If the tumour area was considered too small to be suitable for the TMA construction, the patient was excluded from the study. The best block per patient was defined as the one with the largest area of tumour burden and Gleason score. As a positive control, non-malignant prostate tissue was used. If the main tumour block did not contain any normal tissue for positive control, an extra FFPE block with adjacent normal tissue was selected. The selected FFPE blocks suitable for the TMA construction were retrieved from the Biobank archive at City Hospital, Nottingham (**Figure 2.1, step 6**). To facilitate the TMA construction and because the Haemotoxylin & Eosin (H&E) staining of some slides had faded and therefore could not be reviewed properly, fresh sections (4 µM) of the FFPE blocks were cut and newly stained with H&E at Queens Medical Centre, Nottingham (**Figure 2.1, step 7**). The slides were scanned using the NanoZoomer scanner (Hamamatsu Photonics, UK) at Queens Medical Centre, Nottingham. The H&E stained sections were re-evaluated to confirm the presence of tumour and/or adjacent normal tissue (**Figure 2.1, step 8**).

2.2.3 Construction of the tissue micro array

Before the tissue micro array (TMA) was constructed, the digitally scanned H&E stained slides were marked for 0.6 mm TMA cores (**Figure 2.1, step 9**), i.e. it was determined where the cores should be taken from the FFPE blocks during TMA construction. The programme used was the Panoramic Viewer Software, version 1.15.4. A maximum number of suitable cores in both tumour and adjacent normal tissue for each image was marked. For the TMA construction, the slides were digitally scanned using a high-resolution slide scanner (Pannoramic 250 Flash III, 3DHISTECH Ltd.) at 20x magnification (**Figure 2.1, step 10**) and viewed using the Xplore Viewer software (Xplore &TMA Pathology Research Suite, Philips, UK). The TMA was constructed with a TMA GRAND MASTER 2.4-UG-EN MACHINE, using 0.6 mm punch sets (**Figure 2.1, step 11**).The recipient block was an standard paraffin wax based block (3 x 2.5 x 0.4 cm). The layout of the TMA was 160 recipient cores: 104 tumour tissue cores in the upper half and 56 normal tissue cores in the lower half. Three cores of liver and three cores of tonsil were used as orientation points in the first and last rows

respectively. The gap between each 0.6 mm core was 0.8 mm. The layout of the TMA can be found in the **Appendix 2**. The automated TMA arrayer was loaded with a maximum of 60 FFPE blocks and 4 recipient blocks. The FFPE blocks were labelled with an anonymised identification number, while the four recipient blocks were labelled VM1, VM2, VM3 and VM4 respectively. The marked and scanned images were matched with the related FFPE blocks to know where to take the cores from. Then the cores from the donor blocks were automatically sampled and embedded into the recipient blocks. A photograph of the TMA block is shown in **Figure 2.2, A**.

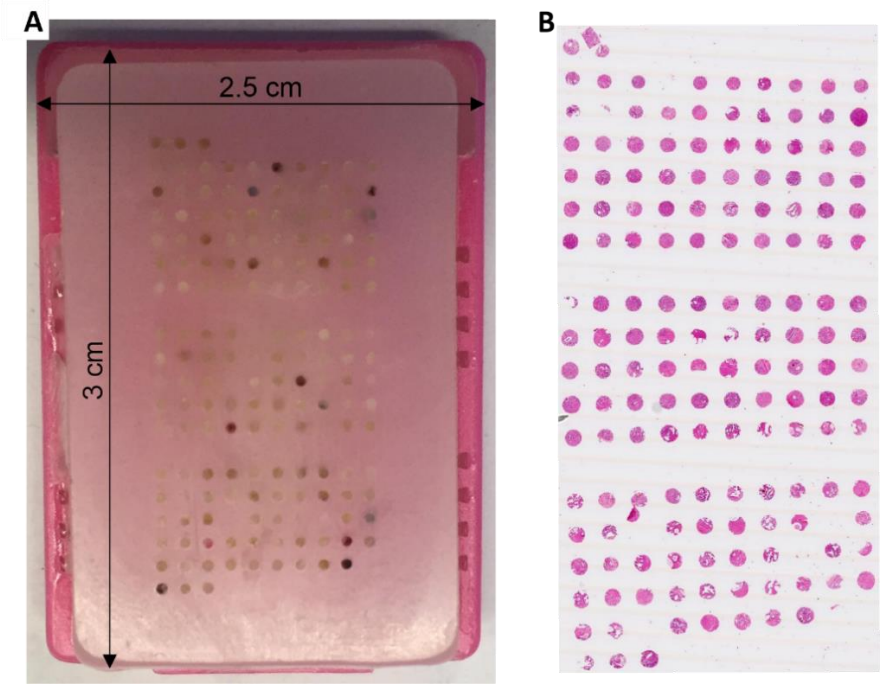

Figure 2.2: Tissue micro array block.
(**A**) Photograph of the recipient FFPE block with cores. (**B**) H&E staining of TMA cores.

After the TMA was constructed, the tissue cores were annealed to the recipient blocks (**Figure 2.1, step 12**). This is important for the cores not to fall out and to level the TMA in order to maximise the number of sections containing all cores. To do so, the TMA recipient blocks were placed facing upward in an oven at 37°C for 3 hours. A clean glass microscope slide was placed on the top of the blocks and gently pushed down to ensure an even surface and all cores were at the same level. The blocks were left to cool at room temperature for 3 hours. The TMA blocks were stored at 4°C for subsequent sectioning. The TMA blocks were sectioned at 4 µm thickness with the tissue microtome and stained with hematoxylin and eosin (H&E) to assess the quality of the constructed TMAs (**Figure 2.2, B**), and to evaluate potential missing cores and picked cores without tumour or normal tissue via Microsoft Excel (**Figure 2.1, step 13-14**). The evaluation can be viewed in **Appendix 2**.

2.2.4 Immunohistochemistry

To stain the proteins of interest, sections (4 µM) were cut from the TMA block VM4 which showed the highest number of tumour tissue (89.4%) amongst all TMA blocks (**Figure 2.1, step 15**). The IHC staining was performed by Corinne Woodcock (CW), Jennie Jeyapalan (JJ), and Jenny Lothion-Roy (JL). The slides were labelled with a pencil and placed on the 60°C hotplate for 10 minutes. Then the slides were allowed to cool and placed in the Leica autostainer rack. The rack was loaded into the autostainer and 'Programme 1' was run to dewax and rehydrate the sections: Xylene 2x 5min, Industrial Methylated Spirit (IMS) 3x 2min, H_2O 5min. Then the rack was placed in a water bath. Antigen retrieval was performed with 1X Citrate buffer, pH 6.0 (adjusted with 1M sodium hydroxide solution) for 20 minutes in the Whirlpool 'Sixth Sense' microwave oven. After antigen retrieval, the slides were washed for 5 minutes with tap water. For IHC staining the Novolink™ Max Polymer Detection System (# RE7280-K, Leica Biosystems) was used. For antibody optimisation Sequenza plates and racks were applied, whereas for the actual staining of the proteins of interest a humidity chamber was used. The Leica Biosystems' protocol was followed. For Sequenza plates 100 µL of solution was used in each step, whereas in the humidity chamber 300 µL solution was applied. All washing steps were performed with TBS-Tween (Tris Buffered Saline containing 0.1% Tween 20®) three times for 5 minutes. Here it had to be taken care to hold slides vertically to flood with TBS-Tween and not to wash cores directly. First, slides were washed and 300 µl Peroxidase Block was applied for 5 minutes. The slides were washed and 300 µl Protein Block was added for 5 minutes. Another washing step followed. The primary antibody for KDM1A (#NB100-1762, Novus Biologicals; 1:1000 dilution), KDM5B (#H00010765-M02, Abnova; 1:20 dilution) and KDM7A (#NBP1-81382, Novus Biologicals; 1:100 dilution) was added and incubated for 1 hour at room temperature. The dilutions were made up with Leica antibody diluent. The slides were washed and 300 µl Post Primary solution was added for 30 minutes. Another washing step followed and then the slides were incubated with 300µl Polymer for 30 minutes. The slides were washed, whilst the DAB working solution was freshly made up of 1:20 DAB chromogen in DAB substrate buffer. The DAB working solution was applied to the slides for 5 minutes followed by a washing step. Then 300 µl Novolink haematoxylin was applied for 6 minutes. After, the slides were dehydrated and cleared using the Leica austostainer 'Programme 2': IMS 3x 2 min, Xylene 2x 5 min. In the end, the sections were mounted with DPX and covered with coverslips. The slides were incubated on room temperature for 24 hours and were then scanned with the NanoZoomer scanner (Hamamatsu Photonics, UK) at Queens Medical Centre, Nottingham (**Figure 2.1, step 16**).

2.2.5 Scoring staining intensity

The staining intensity of KDM1A, KDM5B and KMD7A respectively was assessed in the X-plore Viewer software using the H-score method (Goulding et al., 1995) (**Figure 2.1, step 17**). The H-score ranged between 0-300 and was calculated by adding up the percentage of cells at a certain staining intensity level. The staining intensity levels were determined as 3 = strong staining, 2 = moderate staining, 1 = weak staining, 0 = no staining, i.e. the following formula was used:

3 x % of strongly stained cells + 2 x % of moderately stained cells + 1 x % of weakly stained cells = 0 - 300.

For both nucleus and cytoplasm H-scores were determined and noted down in Microsoft Excel. To ensure patient confidentiality it was necessary that an independent assessor was used to score the TMA. For this reason, the scoring process was performed by Jenny Lothion-Roy (JL), Corinne Woodcock (CW) and Jennie Jeyapalan (JJ). Each marker (10%) was scored by a second scorer to control for internal consistency. The H-scores were then correlated with the clinical data of the patient database and statistical analysis was performed using the Statistical Package for Social Sciences (IBM® SPSS® Statistics, Version 24) software (**Figure 2.1, step 18**).

2.3 Cell culture

2.3.1 Cell lines

In this study, one normal prostate cell line and three prostatic carcinoma (PCa) cell lines were used (**Table 2.1**). The human prostate epithelial cell line PNT1A was provided by Dr. Jenny Persson (Lund University). The PCa cell lines LNCaP (#89110211, Health protection agency, Public Health England), LNCaP-C4-2 (#CRL-3314), 22Rv1 (#CRL-2502), PC3 (#CRL-1435) and Du145 (#HTB-81) PCa cells were a generous gift from Dr. Doug Scherr, Department of Urology, Weill Cornell Medical College. They were purchased from the American Type Culture Collection (ATCC, Manassas, VA). PNT1A served as a benign prostate epithelial cell line in this study. Five different PCa cell lines were used to reflect the different stages in PCa progression (**Figure 2.3**). LNCaP cells reflect an early stage of PCa which is androgen-dependent and androgen-sensitive. LNCaP:C4-2, 22Rv1, PC3 and Du145 cells are models to study recurrent, hormone refractory PCa and resistance to ADT. While LNCaP:C4-2 and 22Rv1 are androgen sensitive, PC3 and Du145 are androgen-insensitive and reflect highly metastatic PCa.

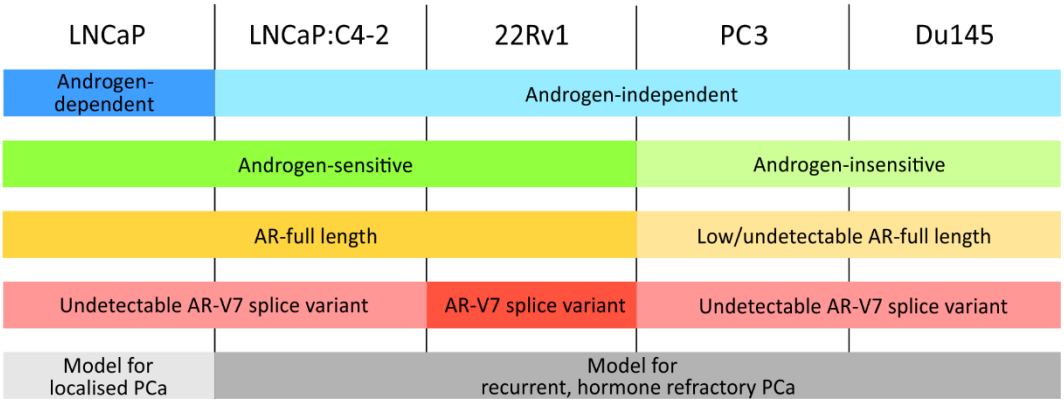

Figure 2.3: Characteristics of the prostate cancer cell lines.
The androgen-dependency, androgen-sensitivity, androgen receptor (AR) presence, AR splice variants and model characteristics were given.

2.3.2 Culture conditions

Cell culture solutions were purchased from Gibco® by Thermo Fisher Scientific, UK unless otherwise indicated. All cell lines were maintained in 5% CO_2 in phenol red containing RPMI-1640 medium supplemented with 10% fetal bovine serum (FBS) (Sigma-Aldrich®, UK), 1% penicillin-streptomycin-glutamine, 2 mM L-Glutamine and 1 mM sodium pyruvate. Experiments that involved the use of R1881 (synthetic androgen) required the removal of all hormones from the medium. To do so we used either commercial dialysed or charcoal stripped FBS. FBS was charcoal stripped by adding activated charcoal (Sigma-Aldrich®, UK) to a final concentration of 1 % and adding Dextran T-70 (Sigma-Aldrich®) to a final concentration of 0.1 %. An incubation for 1 hour at room temperature whilst stirring and a centrifugation at 12,000 x g for 15 min followed. The supernatant was vacuum-filtered through a 110 diameter qualitative filter paper (Whatman®) and then filter-sterilised via Millex-GP Syringe Filter Units, 0.22 µm (Merck). The medium used for cell treatments involving R1881 therefore contained phenol red-free RPMI-1640 medium supplemented with charcoal-stripped 10% fetal bovine serum (FBS) (Sigma-Aldrich®, UK) or 10% HyClone® dialysed fetal bovine serum (Thermo Scientific, USA), 1% penicillin-streptomycin-glutamine, 2 mM L-Glutamine and 1 mM sodium pyruvate.

2.4 Growing cells for investigating basal expression levels

PNT1A, LNCaP, LNCaP:C4-2, 22Rv1, PC3 and Du145 cells were grown in 6-well plates (Greiner Bio-one) with 2 mL medium per well and cultured to 90-95% confluency. Cells were then collected for RNA and protein extraction.

Table 2.1: Description of normal prostate and prostatic cancer cell lines.
The tissue origin, cell morphology, culture properties, androgen receptor expression and disease are stated.

	PNT1A	*LNCaP*	*LNCaP:C4-2*	*22Rv1*	*PC3*	*Du145*
Disease	None	Prostatic carcinoma	Prostatic carcinoma	Prostatic carcinoma	Prostatic carcinoma	Prostatic carcinoma
Tissue derived from	Normal adult prostatic epithelium representing differen-tiated luminal prostatic cells (Cussenot et al., 1991)	Metastatic site: left supraclavicular lymph node	A castrated mouse was co-inocu-lated with LNCaP and bone stromal fibroblasts leading to a chimeric tumor (Thalmann et al., 1994)	CWR22 xenograft regresses after castration and relapses leading to CWR22R. CWR22R has been serially transplanted in mice leading to 22Rv1 (Sramkoski et al., 1999)	Metastatic site: bone	Metastatic site: brain
Morphology	Epithelial	Epithelial	Epithelial	Epithelia	Epithelial	Epithelial
Culture properties	Adherent	Adherent	Adherent	Adherent	Adherent	Adherent
Cell growth doubling time	~30 hrs	~42 hrs	~30 hrs	~35 hrs	~30 hrs	~25 hrs
Karyotype	~44 chromo-somes	~76-91 chromo-somes	~85-87 chromo-somes	~50 chromo-somes	~55-62 chromo-somes	~61-64 chromo-somes
Androgen-dependent	No	Yes	No	No	No	No
AR expression	Androgen receptor negative	Androgen receptor positive	Androgen receptor positive, but lower steady-state levels of AR protein and mRNA transcript (Wu et al. 1994)	Androgen receptor positive, but lower AR protein levels than in LNCaP (Sramkoski et al., 1999)	Reported to be androgen receptor negative but sometimes very low AR levels detected (Sramkoski et al., 1999, Brolin et al, 1992)	Reported to be androgen receptor negative but sometimes very low AR levels detected (Sramkoski et al., 1999, Brolin et al, 1992)
PSA expression	No	Yes	Yes	Yes	No	No

2.5 Androgen (R1881) treatment

PNT1A, LNCaP, LNCaP:C4-2, 22Rv1, PC3 and Du145 cells were grown in 6-well plates (Greiner Bio-one) with 2 mL medium per well and cultured to 30-40% confluency. Medium was removed and replaced by 2 mL charcoal-stripped medium per well containing 1 nM R1881 (#R0908, Sigma-Aldrich) (synthetic androgen dissolved in 100% ethanol) and 0.1%

ethanol as vehicle control (R1881 is dissolved in ethanol). Cells were incubated for three days and cells were then harvested for RNA extraction.

2.6 siRNA treatment

Functional depletion of *KDM1A*, *KDM5B* and *KDM7A* was performed via siRNA technique (Dharmacon™, Lafayette, CO) using ON-TARGETplus siRNA – SMART pools for Human KDM1A (#L-009223-00-0005), KDM5B (#L-009899-00-0005) and KDM7A (#L-025357-01-0005) (GE Dharmacon™) (Table 2.2). ON-TARGETplus non-targeting control siRNAs (#D-001810-10-05, GE Dharmacon™) were employed as negative controls. Cells were transfected using DharmaFECT 2 Transfection Reagent (GE Dharmacon™) and transfection was performed after manufacturer's instructions with small adjustments.

For RNA extraction, LNCaP, LNCaP:C4-2, 22Rv1 and PC3 were plated in 12-well plates (Falcon®) with 2 mL medium per well and cultured to 30% confluency. LNCaP cells were grown until 40% confluency because their doubling time is higher than in the other cell lines and they do not grow well if plated sparsely. Androgen treatment and siRNA treatment were started at the same time and performed over a period of 3 days. Medium was removed from the cells and replaced with 2mL charcoal-stripped medium per well containing 1 nM R1881 (synthetic androgen) and 0.1% ethanol as control. The siRNA and DharmaFECT transfection reagent were prepared in separate tubes; the following is an example for the preparation of one well:

Tube	Components	Volume (µL)
Tube 1	Charcoal-stripped medium	41.5
	siRNA (20 µM stock)	1
Tube 2	Charcoal-stripped medium	41.5
	DharmaFECT transfection reagent	1
	Total volume	85

In the case of combinatorial experiments, the following was pipetted:

Tube	Components	Volume (µL)
Tube 1	Charcoal-stripped medium	40.5
	siRNA A (20 µM stock)	1
	siRNA B (20 µM stock)	1
Tube 2	Charcoal-stripped medium	41.5
	DharmaFECT transfection reagent	1
	Total volume	85

The contents in the tubes were gently mixed by carefully pipetting up and down once. They were then incubated for 5 minutes at room temperature. After that, the content of tube 1 was added to tube 2 and gently mixed by pipetting up and down once. An incubation of 15-20 minutes at room temperature followed. Then 85 µL of mixed content was added to each well by pipetting dropwise, leading to an end concentration of 10 nM siRNA per well and per siRNA. The plate was very gently shaken by hand and placed in the incubator for 3 days. Cells were then collected for RNA extraction.

For protein extraction, LNCaP and LNCaP:C4-2 cells were plated in 6-well plate with 2 mL medium per well. The same procedure as described above was followed, however, no androgen was added in this experiment as we just wanted to confirm the siRNA knockdown of KDM1A / KDM5B / KDM7A on the protein level in this experiment.

Table 2.2: ON-Target plus human KDM1A/KDM5B/KDM7A smart pools.
The catalogue numbers and target sequences are stated.

Target	No	Sequence
KDM1A	J-009223-05	GGAAGUUGUCAUUCAGUUA
	J-009223-06	CCACCGAGUUCACAGUUAU
	J-009223-07	CAUAAGUGACGAUGUGAUU
	J-009223-08	CUAUAAAGCUCCAAUACUG
KDM5B	J-009899-05	GGAGAUGCACUUCGAUAUA
	J-009899-06	UAAGUUAGUUGCAGAAGAA
	J-009899-07	UCGAAGAGAUCCCUGCAUA
	J-009899-08	GGAAGAUCUUGGACUUAUU
KDM7A	J-025357-09	CUAUAAACAACCCGUGUAA
	J-025357-10	UGAUGGAUGUGGAACGUUA
	J-025357-11	GUACCUGAAUGGAGAGCGA
	J-025357-12	CCUAGUACAGGGAGUGAAA

2.7 KDM Inhibitor treatment

For RNA extractions, LNCaP, LNCaP:C4-2, 22Rv1, PC3 and Du145 cells were plated in 6-well plates (Greiner Bio-one) with 2 mL medium per well and grown until 60-70% confluent before treatment. At the day of inhibitor treatment, the medium was removed and replaced by 2 mL charcoal stripped medium per well containing R1881 and inhibitor. The inhibitors we used selectively target KDM1A, KDM5B and KDM7A respectively; details about their selectivity and action of inhibition can be found in Table 2.3. The inhibitors were

commercially purchased and their manufacturers and catalog numbers are given in Table 2.3. For gene expression analysis the cells were treated with the following inhibitor concentrations: 50 µM, Namoline; 25 µM PBIT; 25 µM, 50 µM CPI-455; 10 µM, 50 µM, 75 µM, 100 µM TC-E 5002. All inhibitor stock solutions were dissolved in 100% Dimethyl sulfoxide (DMSO) and therefore cells were incubated with DMSO concentrations of 0.05-0.09% in the control wells. The DMSO concentrations varied depending on the experiment but were kept under 0.1%, as this is the maximal DMSO concentration cells can tolerate. R1881 treatment was performed as described above with 1 nM R1881 (synthetic androgen) and 0.1% ethanol in the control respectively. Treatment with inhibitors and R1881 was performed for three days and cells were then harvested for RNA extraction. The cells were carefully scraped off the bottom of the well into the medium and centrifuged down at 1,500 rpm (Eppendorf® Centrifuge 5417R). The cell pellet was used for subsequent RNA isolation.

For proliferation assays, PNT1A, LNCaP, LNCaP:C4-2, 22Rv1, PC3 and Du145 cells were plated in 96-well plates (Corning®) with 150 µL medium per well and grown until 10% confluent for PNT1A, LNCaP:C4-2, PC3 and Du145, 20% confluent for 22Rv1 and 30% confluent for LNCaP cells (Figure 2.4). Cells were then treated with the following inhibitor concentrations: 25 µM, 50 µM, 75 µM Namoline; 25 µM PBIT; 50 µM CPI-455; 20 µM, 200 µM, 400 µM Daminozide; 35 µM, 100 µM, 175 µM TC-E 5002. Inhibitor treatment was performed for three and six days respectively. After three days the plate for the 3-days treatment was used to perform the proliferation assay. In the plate for the 6-days treatment the medium was removed and cells were treated with the same inhibitor concentrations again. After three days of further incubation the proliferation assay was performed on the plate for the 6-days treatment.

Table 2.3: Pharmaco-selective KDM5B and KDM7A inhibitors.
The drug selectivity and half maximal inhibitory concentrations (IC_{50}) for inhibition of corresponding lysine demethylases (KDMs) are given. Furthermore, the inhibitory action of the drug and its effect on cell proliferation are stated where available. The drugs were commercially purchased and their catalog numbers and manufacturers are stated.

Inhibitor	Selectivity (IC_{50})	Action of inhibition	Effect on cell growth	References	Catalog no., manufacturer
Namoline	KDM1A (51 µM)	Competitive inhibition	*In vitro*: Inhibits proliferation of LNCaP cells (50 µM). *In vivo*: Growth of subcutaneously implanted LNCaP cells in nude mice was restricted upon Namoline treatment	(Willmann et al., 2012)	# ab144666, Abcam
PBIT	KDM5B (3 µM) KDM5C (4.9 µM) KDM5A (6 µM) KDM5D (28 µM)	Undefined; unlikely to be an iron chelator	Inhibits proliferation of most UACC-812 breast cancer cells at 10 µM PBIT, but only minimally toxic to MCF7 and MCF10A cells. UACC-812 cells express higher level of KDM5B.	(Sayegh et al., 2013)	# ABE7658, Source BioScience LifeSciences
CPI-455	KDM5B: 0.003 µM KDM5A: 0.01 µM KDM5C: 0.014 µM	Competitive inhibition	Inhibits proliferation of drug-tolerant persister cancer cells in a dose-dependent manner (6.25 – 25 µM)	(Vinogradova et al., 2016)	# 2573, Axon
Daminozide	KDM7B (0.55 µM) KDM2A (1.5 µM) KDM7A (2.1 µM)	Competitive inhibition	N/A	(Rose et al., 2012)	# 12033, Cayman Chemical Company
TC-E 5002	KDM7A (0.2 µM) KDM7B (1.2 µM) KDM2A (6.8 µM)	Competitive inhibition	Inhibits proliferation of mouse neuroblastoma N2a cells (Gi50 = 86 µM) and cancer cells HeLa (Gi50 = 40 µM) and KYSE-150 (Gi50 = 16 µM) *in vitro.*	(Suzuki et al., 2013)	# 5089, Tocris Bioscience

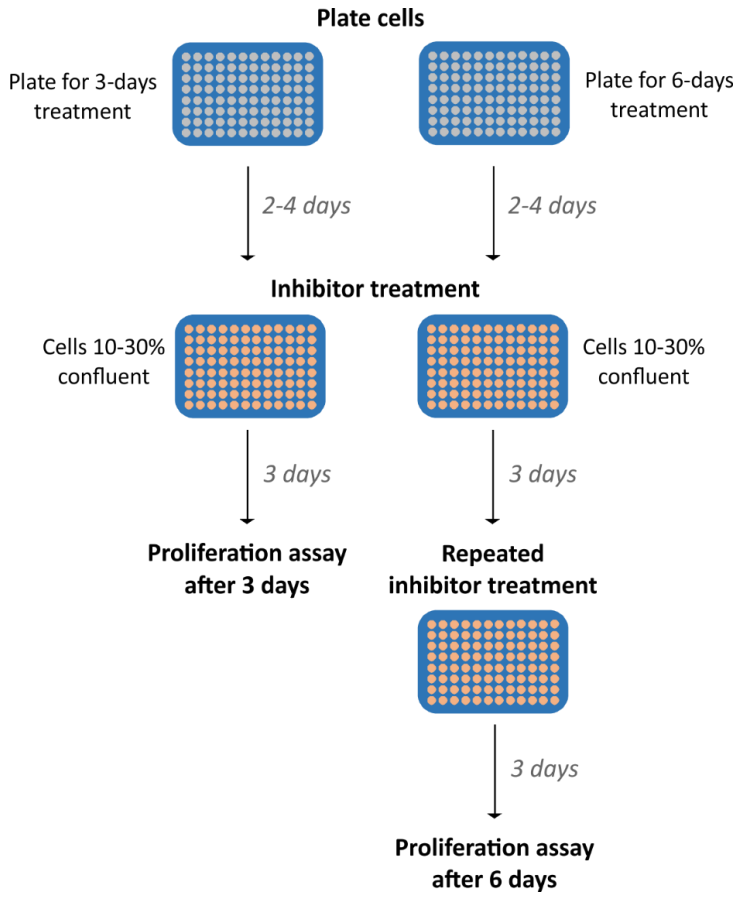

Figure 2.4: Steps of inhibitor treatment for subsequent proliferation assay.
Cells were plated in 96-well plates and treated with the corresponding inhibitor for a period of either 3 or 6 days before the proliferation assay was performed.

2.8 Proliferation assay

After three and six days of inhibitor treatment respectively (Figure 2.4), the cell proliferation of PNT1A, LNCaP, LNCaP:C4-2, 22Rv1, PC3 and Du145 was assessed via the CyQUANT® NF Cell Proliferation Assay Kit (Invitrogen™). This assay is based on the measurement of cellular DNA content, compared to colorimetric assays which measure the metabolic activity in a cell, like the MTT (Di-Methyl Thiazol Diphenyl Tetrazolium Bromide) assay. The advantage of the CyQUANT® over the MTT assay is that it is not dependent on physiological activity which may be variable independent of cell numbers. In the CyQUANT® assay a plasma membrane permeabilisation reagent allows the fluorescent dye to enter the cell and bind to the DNA. The DNA content is proportional to cell number.

In these experiments the manufacturer's protocol was followed. After inhibitor treatment the medium was carefully removed from the cells and 80 µL dye binding solution (containing the fluorescent dye) per well was pipetted on the cells. The cells were then incubated for 1.5 hours for equilibration of the dye binding to the DNA. This ensures a stable fluorescence intensity endpoint. Fluorescence measurement was performed with

excitation at ~485 nm and emission detection at ~530 nm in the Varioskan® Flash (Thermo Fisher Scientific™).

2.9 RNA extraction

2.9.1 Phenol-chloroform isolation

Total cellular RNA was extracted using the TRIzol® reagent (Ambion® by life technologies™) following manufacturer's instructions. To lyse the cells, medium was removed and 500 µL of TRIzol® reagent added per well of a 12-well plate and transferred into a 1.5 mL microcentrifuge tube. In the case of 6-well plates and high cell confluence, a higher volume of 750 µL TRIzol® reagent was used. The tubes were incubated for 5 minutes at room temperature to allow complete homogenisation. Then 100 µL of chloroform was added to the 500 µL TRIzol® reagent and tubes were inverted vigorously 15 times to mix the TRIzol® reagent and chloroform well. The samples were incubated for 2-3 minutes at room temperature and then centrifuged for 10 minutes at 13,000 x g at 4°C (Eppendorf® Centrifuge 5417R). After centrifugation three separate phases are visible: (1) lower red phenol-chloroform (containing proteins and cellular debris), (2) interphase (containing the DNA), (3) and a colourless upper aqueous phase (containing the RNA). The aqueous phase was transferred into a new tube and 250 µL isopropanol was added to precipitate the RNA. The samples were incubated for 10 minutes at room temperature and centrifuged for 10 minutes at 13,000 x g at 4°C. The supernatant was discarded by carefully pipetting it off and 500 µL of 75% Ethanol added to the pellet to wash the RNA. The pellet often is invisible at that stage. The tubes were given a quick vortex before they were centrifuged for 5 minutes at 9,000 x g at 4°C. The supernatant was removed completely by pipetting and tubes incubated at room temperature for 3-5 minutes with the lids open to allow remaining Ethanol to evaporate. In the end RNA was dissolved in 30-50 µL RNase-free H_2O and RNA concentrations and purities (260/280 ratio) were assessed via NanoDrop™ 8000 Spectrophotometer (Thermo Fisher Scientific™). The RNA was stored at -80°C.

2.9.2 RNA isolation via column

When cells were treated with pharmaco-selective inhibitors, the Phenol-Chloroform method was not used, but instead the RNA was extracted with the GenElute™ Mammalian Total RNA Miniprep Kit (Sigma-Aldrich™). The kit allowed extraction of pure RNA from very low cell numbers which was needed in some of the inhibitor treatments that reduced cell proliferation. Cells were thawed from the -80°C and the pellet vortexed to loosen the cells. An appropriate amount of Lysis Solution/2-ME Mixture was prepared by adding 10 µL 2-mercaptoethanol per 1 mL of Lysis Solution. I added 250 µL of Lysis Solution/2-ME Mixture to the pellet and vortexed for around 20 seconds until all clumps disappeared. To remove the cellular debris and shear the DNA, the lysed cells were passed through a GenElute Filtration Column, that was placed into a 2 mL collection tube, by centrifuging at 13,000 x g for 2 minutes. The filtration column was thrown away. To bind the lysate to the silica membrane, 250 µL 70% ethanol was added to the filtered lysate. The samples were then loaded onto the GenElute Binding Column that was placed into a 2 mL collection tube and centrifuged at 13,000 x g for 15 seconds. The flow-through liquid was discarded and the binding column place into a fresh 2 mL collection tube. The RNA was washed by pipetting 250 µL of Wash Solution 1 onto the filter in the binding column and centrifuging at 13,000 x g for 15 seconds. If the samples were sent off for sequencing, an On-column DNase I Digestion was performed by pipetting 80 µL (10 µL of DNase with 70 µL of DNase Digest Buffer) onto the filter. An incubation of 15 minutes at room temperature followed. After that the RNA was washed a second time with 250 µL of Wash Solution 1 and centrifuged at 13,000 x g for 15 seconds. Then the binding column was transferred into a fresh 2 mL collection tube. For pure RNA, the filter was washed by adding 500 µL onto the column and centrifuging at 13,000 x g for 15 seconds. The flow-through liquid was thrown away and the RNA washed a second time with 500 µL of Wash solution 2 and centrifuged at 13,000 x g for 2 minutes. The flow-through was discarded and the column was centrifuged for another minute at 13,000 x g to remove any residual wash solution. To elute the RNA, the binding column was transferred to a 1.5 mL microcentrifuge tube and 30 µL of the Elution Solution was added onto the filter of the binding column. Columns were incubated for 2-3 minutes at room temperature, followed by a centrifugation at 13,000 x g for 1 minute. RNA concentration was measured by nanodrop as described above and the RNA stored at -80°C

2.10 cDNA synthesis

Complementary DNA (cDNA) was synthesized from ~1 µg of total RNA by reverse transcription with the qScript™ cDNA Synthesis Kit (Quanta Biosciences™) following the manufacturer's guidelines.

The reaction mix was made up of the following:

Component	Volume
RNA (1 µg) dissolved in nuclease-free water	7.5 µL
5x concentrated master mix (containing oligo DT(20), random hexamer, dNTP, magnesium)	2.0 µL
20x concentrated qScript reverse transcriptase	0.5 µL
Total volume	**10 µL**

After pipetting the components into a 1.5 microcentrifuge tube, tubes were centrifuged down and incubated at 42°C for 1 hour in the waterbath (Grant SUB Aqua Pro, Grant Instruments). Then 190 µL deionised ddH_2O was added, leading to an end volume of 200 µL with an end DNA concentration of 5 ng/µL. The DNA was stored at -20°C.

2.11 qPCR analysis

For mRNA expression analysis, hydrolysis probe based real-time quantitative polymerase chain reaction (RT qPCR) was performed with the following TaqmanTM probes (Thermo ScientificTM):

Gene	Catalog no
GAPDH	Hs03929097_g1
PSA/KLK3	Hs02576345_m1
TMPRSS2	Hs01122322_m1
VEGFA	Hs00900055_m1
HIF1α	Hs00153153_m1
NDUFA4L2	Hs00220041_m1
AR	Hs00171172_m1
FOXA1	Hs04187555_m1
NKX3.1	Hs00171834_m1
KDM1A	Hs01002741_m1
KDM5B	Hs00981910_m1
KDM7A	Hs01398501_m1

GAPDH was used as a house keeping gene. The qRT-PCR reactions were performed in a LightCycler 480 II (Roche) instrument and one qRT-PCR reaction was made up of the following:

Component	Volume
LightCycler® 480 Probes Master	7.50 µL
Probe	0.65 µL
PCR-grade H_2O	5.85 µL
DNA	1.00 µL
Total volume	**15 µL**

The mastermix (MM) containing LightCycler® 480 Probes Master (Roche), probe and H_2O was distributed in a LightCycler480 Multiwell Plate 96 (Roche) by pipetting 14 µL MM per well with a Eppendorf Multipipette® M4 using Combitips advanced 0.2 mL (Eppendorf). The DNA was added by pipetting 1 µL per well. Before the plate was run, the plate was centrifuged down in the Heraeus Labofuge 400 Centrifuge (Thermo Fisher Scientific). The qRT-PCR programme was as followed:

Step	Temperature (°C)	Time	Cycles
1) Hot start	95	10 min	x1
2) Denaturation	95	10 sec	x45
Annealing	60	30 sec	
Amplification	72	1 sec	
3) Cooling	4	30 sec	x1

Relative gene expression analysis was carried out using the Pfaffl method which does not afford any calibration curve (Pfaffl, 2001). Relative expression was calculated with the following formula:

$$\text{ratio} = \frac{(E_{target})^{\Delta Ct\ target\ (control\text{-}treated)}}{(E_{ref})^{\Delta Ct\ ref\ (control\text{-}treated)}}$$

2.12 Protein extraction from human cells

The cells for protein extraction were collected by removing the growth medium from the plates, washing the cells with 1X phosphate-buffered saline (PBS) and pipetting 100-300 µL SDS-denaturing buffer (100 mM Tris-HCl pH 6.8, 4% SDS, 20% glycerol) (volume depended on the cell numbers) on the cells. The cells were scraped off and the lysate was transferred into a 1.5 mL microcentrifuge tube. To maximise lysis of the cells, the tubes were rattled along the tube rack 20 times for sonication, boiled at 95°C for 5 min, and 2-3 freezing-

thawing cycles were conducted. Proteins were stored at -80°C. Protein concentration was measured using the DC™ (detergent compatible) Protein Assay (BIO-RAD) which is a colorimetric assay based on the reaction of copper ions with Folin–Ciocalteu leading to a blue colour. The Microplate Assay Protocol provided by the manufacturer was used and a bovine serum albumin (BSA) standard curve with the following concentrations employed: 0 µg/mL, 125 µg/mL, 250 µg/mL, 500 µg/mL, 1000 µg/mL, 2000 µg/mL BSA. The BSA dilutions were made up freshly with FSB, the same buffer the proteins were stored in. First, the working Reagent A' was prepared by adding 20 µl of Reagent S to each mL of Reagent A that was needed in the assay. Reagent A is an alkaline copper tartrate solution and Reagent S helps reduce surface tension. The assay was performed in a 96-well plate with flat bottom and 5 µl of BSA standards and protein samples respectively were pipetted per well. Then 25 µl of Reagent A' was added to each well. At this step, the copper ions in Reagent A bind to the peptide bonds. Subsequently, 200 µl Reagent B was added into each well. Reagent B contains a dilute Folin reagent which reacts with the copper ions turning the solution into a blue colour. The intensity of the blue colour reflects the amount of proteins. Before incubating the plate for at least 15 minutes at room temperature, the plate was gently agitated to mix the reagents. The absorbance of the blue colour was measured at 750 nm with the Varioskan® Flash (Thermo Fisher Scientific™). Proteins were diluted to around 800-1500 µg/µL stock solutions for western blot analysis and stored at -80°C.

2.13 Western blot analysis in human cells

2.13.1 Sample loading and protein separation

For western blot analysis, protein samples were diluted accordingly from the 800-1500 µg/µL stock solutions stored at -80°C, in order to load 10-20 µg protein on the gel. Western blot analysis of KDM5B acquired loading of 20 µg, whereas for KDM1A and KDM7A 10 µg protein loading was sufficient. Before loading, protein samples were combined with 5X Laemmli loading buffer and boiled at 95°C for 5 minutes. The protein sample volume loaded on the gel was 25 µL and as a ladder I used 8 µL of the Thermo Scientific Spectra Multicolor Broad Range Protein Ladder (Appendix 3). For KDM1A and KDM7A protein analysis, proteins were separated on a 10% self-made acrylamide gel which were composed of a resolving gel and a stacking gel. The resolving gel contained the following components:

Resolving gel components	Volume
30% acrylamide and bis-acrylamide solution, 29:1 (BIO-RAD)	3.33 mL
ddH_2O	4.67 mL
1.878 M Tris HCL, pH 8.8	2 mL
10 % SDS	100 µl
TEMED (added shortly before casting)	5 µL
10% APS (added shortly before casting)	50 µL
Total volume	~ 10 mL

The resolving gel was poured first in the Mini-PROTEAN® Spacer Plates with 1.0 mm Integrated Spacers (BIO-RAD) and covered with a layer of isopropanol to allow even setting of the gel. After 40 minutes the resolving gel was set, the isopropanol removed and the space above the resolving gel washed with ddH_2O to get rid of any isopropanol residues. Then the stacking gel was pipetted on top of the resolving gel. The stacking gel contained the following components:

Stacking gel components	Volume
30% acrylamide and bis-acrylamide solution, 29:1 (BIO-RAD)	675 µl
ddH_2O	3.8 mL
1.25 M Tris HCL, pH 6.8	500 µl
10 % SDS	500 µl
TEMED (added shortly before casting)	5 µL
10% APS (added shortly before casting)	30 µL
Total volume	~ 5.5 mL

After pouring the stacking gel, a Mini-PROTEAN® Comb, 10-well, 1 mm (BIO-RAD) was inserted and the gel set for another 30 minutes. Before loading the comb was removed. In contrast, for KDM5B 4–20% Mini-PROTEAN® TGX™ precast polyacrylamide gels with 10 wells (BIO-RAD) were used because KDM5B is a big protein with the size of 180 kDa. Proteins on both self-made and pre-casted gelds were separated in 1X gel electrophoresis buffer in the Mini-PROTEAN® Tetra System (BIO-RAD) at 140-180 Volt for 40-60 minutes, using the PowerPac™ Basic (BIO-RAD). Per sample 15-25 µL was loaded and 8 µL of the ladder (Thermo Scientific Spectra Multicolor Broad Range Protein Ladder, Appendix 4).

2.13.2 Protein transfer and blocking

The proteins were transferred from the gel onto a polyvinylidene difluoride (PVDF) membrane (Immobilon-P Membrane, 0.45 µm, Merck) via semi-dry blotting. The blotting sandwich was constructed with the following from the bottom to the top: four Whatman®

papers, membrane, gel, four Whatman® papers. Before the construction of the sandwich, the PVDF membrane was activated in 100% methanol for 10 seconds and the Whatman® papers, gel and membrane were incubated in Blotting buffer for 10 minutes. Potential air bubbles were removed with a roller and the blotting sandwich was placed in the cassette of the Trans-Blot® Turbo™ Transfer System (BIO-RAD). The transfer was performed for 10-30 minutes at 25 Volt. The length of the transfer depended on the size of the protein and the thickness of the gel; for example transferring KDM5B (180 kDa) from a pre-casted gel onto the membrane required 30 minutes at 25 Volt, whereas the house keeping protein β-actin (42 kDa) was transferred after 10 minutes. For self-made gels the transfer was generally conducted for 30 minutes for proteins sized between 30-120 kDa. After the transfer, the membrane was blocked to reduce the background. The membrane was blocked in the same solution the primary antibody was diluted in (Table 2.4). Blocking was performed for 1 hour at room temperature on a rocker.

2.13.3 Antibody incubation

After blocking, the membrane was incubated with primary antibody at 4°C overnight on a rocker. Details to the antibody concentration and what the primary antibody was diluted in are given in Table 2.4.

Table 2.4: Primary antibodies used for western blots.
The size of the protein the antibody is targeting was given. The clonality, host, antibody dilution, catalog number and company were stated.

Target	Target size	Clonality	Host	Dilution	Diluted in	Catalog no	Company
GAPDH	~36 kDa	Mono	Mouse	1:5,000	5% BSA	ab9484	Abcam
β-actin	~42 kDa	Mono	Mouse	1:10,000	5% BSA	MA515739	Invitrogen
KDM1A	~120 kDa	Mono	Mouse	1:1,000	3% Milk	NB100-1762	Novus Biologicals
KDM5B	~180 kDa	Polyc	Rabbit	1:1,000	5% BSA	3273	Cell signalling
KDM7A	~106 kDa	Polyc	Rabbit	1:1,000	3% Milk	STJ110565	St. John's lab

The next day, the primary antibody was removed and the membrane washed three times in 1X TBST on room temperature on a rocker. Then the membrane was incubated with the horse radish peroxidase (HRP) conjugated secondary antibody at room temperature for 1 hour. Depending on the host of the primary antibody, Goat Anti-Mouse IgG (ab97023, Abcam) or Goat Anti-Rabbit IgG (ab6721, Abcam) was used. The secondary antibody was diluted in the same solution as the primary antibody and the dilution of the secondary

antibody depended on the protein target: 1:50,000 for GAPDH and β-actin; 1:10,000 for KDM1A and KDM7A; 1:5,000 for KDM5B. After 1 hour of incubation, the secondary antibody was removed and the membrane washed again three times in 1X TBST at room temperature on a rocker. Then the membrane was incubated with 1 mL (500 µL of solution A plus 500 µL of solution B) Amersham™ ECL™ Prime Western Blotting Detection Reagent (GE Healthcare) for 3-5 minutes. The signal was detected using the ChemiDoc™ MP Imaging System (BIO-RAD) and the signal intensity quantified with ImageJ.

2.13.4 Buffers used in western blot analysis

5X Laemmli loading buffer
250 mM Tris HCl pH 6.8
10% SDS
30% Glycerol
5% β-Mercaptoethanol
0.02% Bromophenol Blue

10X Electrophoresis buffer
1.92 M Glycin
0.25 M Tris

1X Electrophorese buffer
10% 10x Elektrophoresis buffer
1% 10x SDS
89% ddH2O

Blotting buffer
10% 100% Methanol
10% 10x Electrophoresis buffer
80% ddH2O

10X TBST
200 mM Tris
1.5 M NaCl
pH 7.5 (HCl)

1X TBST
10% 10x TBST
0.1 % Tween®20
90% ddH2O

2.14 Yeast Two-hybrid assay

2.14.1 Vectors and constructs

To test direct interaction between KMD7A and nuclear receptors, a yeast-2-hybrid (Y2H) assay was performed in the School of Pharmacy, University of Nottingham. Yeast cells were co-transfected with two vectors harbouring the following (**Figure 2.5**): (i) Vector pBTM116mod containing the DNA - binding domain (DBD) employed by the bacterial repressor protein LexA. (ii) Vector pASV3mod containing the activation domain (AD) that derived from the herpes virus protein VP16. These transcriptional activator domains can only be active when non-covalently joined via protein-protein interactions. If the two proteins interact, transcription of the reporter gene (*LacZ*) containing a DBD site will be enhanced.

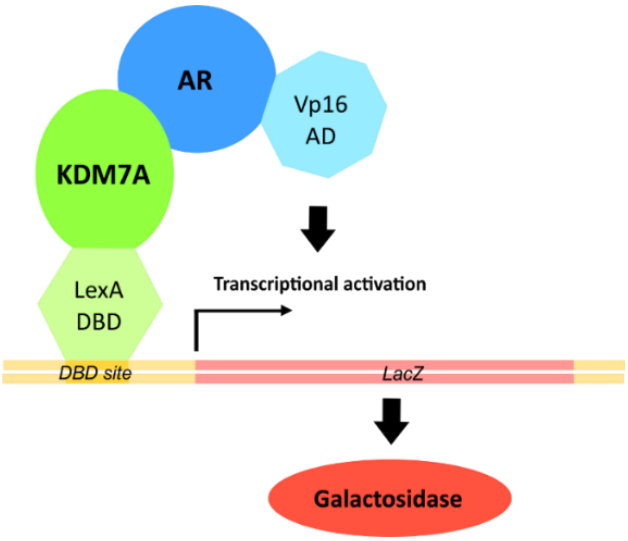

Figure 2.5: Schematic overview of the Yeast 2-hybrid (Y2H) assay.
KDM7A was fused to a DNA-binding domain (called bait) and the AR was fused to an activation domain (called prey). In the case of interaction, the activation domain was recruited and activated the transcription of the reporter gene LacZ encoding the enzyme beta-galactosidase.

Jonathan Whitchurch, a PhD student at the School of Pharmacy, constructed the plasmids containing VP16-AR, LexA-KDM7A and LexA-SRC1 NID (Steroid Receptor Coactivator 1 Nuclear Interaction Domain; positive control) by cloning. For KDM7A, the pcDNA3.1-KDM7A-FLAG-Myc-His plasmid was used as a PCR template. The locations of the primers designed for KDM7A amplification are depicted in Figure 2.6. The amplification of most of the desired fragments failed due to GC-rich regions, however, KDM7A AA 401-606 and AA 565-606 were successfully cloned into the pBTM116mod vector backbone by Jonathan Whitchurch. Construct 401-606 contains both the LLETL and LRLLL nuclear receptor sequence motif, whereas construct 565-606 harbours the LRLLL motif only (Figure 2.6).

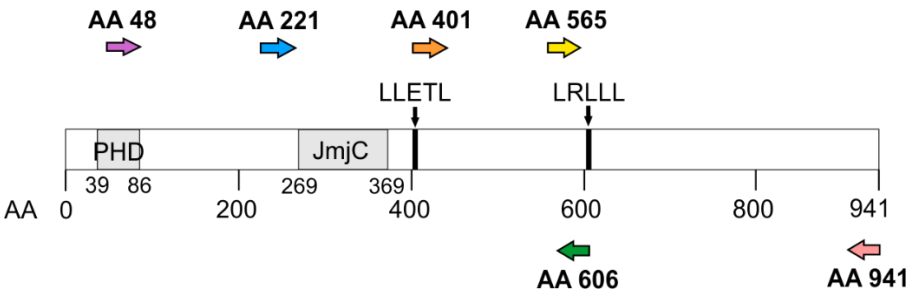

Figure 2.6: Schematic of primer locations.
The primers (shown as arrows, coloured) were used to amplify different fragments of the KDM7A protein (Jonathan Whitchurch). The boundaries of the forward and reverse primers are given in AA. The primers enclose different domains and motifs. Two nuclear receptor binding motifs, LLETL and LRLLL, were found in the AA sequence of KDM7A. PHD = plant homeodomain; JmjC = jumonji C-terminal; AA = amino acid.

2.14.2 Transformation of yeast cells

Yeast cells (strain L40) were grown by inoculating 25 mL volume of Yeast extract peptone dextrose (YPD) medium in a 50 mL Falcon tube and incubating at 30°C overnight on a shaker. The next day, the OD_{600} (optical density) was measured and diluted down to an OD_{600} of approximately 0.5-0.6. Yeast cells were incubated for another hour at 30°C until the exponential growth phase was reached (ideally OD_{600} of 0.8). Then the cells were pelleted by centrifugation at 3,000 x g for 5 minutes at room temperature and the supernatant was discarded. The pellet was resuspended in 10 mL sterile diH_2O and again centrifuged at 3,000 x g for 5 minutes at room temperature. The supernatant was discarded and the pellet resuspended in 250 µL 100 mM LiAc (Lithium-Acetate) to permeabilise the yeast cell wall. An incubation at 30°C for 15 minutes on a rocker followed. In the meanwhile Herring sperm was boiled for 10 minutes for DNA denaturation. Herring sperm was needed because yeast cells harbour nucleases and adding Herring sperm as a DNA carrier decreases the likelihood of the plasmid of interest being degraded. Herring sperm therefore increases transformation efficiency. After the 15 minutes incubation, the transformation mix was pipetted in a 1.5 mL microcentrifuge tube, containing 120 µL 50% PEG (w/v) (Polyethylene glycol), 18 µL 1 M LiAc, 25 µL Herring sperm (2 mg/mL stock solution), 100 µL sterile diH_2O and 500 ng of each plasmid (for example 500 ng of VP16-AR and 500 ng of LexA-SRC1). A negative control was prepared without adding plasmid DNA. The tube with the transformation mix was vortexed. Next, 25 µL of vortexed yeast suspension was added to each tube. The yeast/plasmid/transformation mix was vortexed and incubated at 30°C for 30 minutes whilst shaking. Then the cells were heat shocked at 42°C for 20 minutes.

2.14.3 Selection of yeast cells

After transformation, 100 µL was plated on to yeast selective agar plates and the plates incubated at 30°C for 3 days. The yeast selective agar plates were made with yeast selective medium (YSM) medium (400 mL YSM contained 1.67 Yeast nutrition broth, 0.8 g Glucose and 0.256 g Amino acid drop-out mix) which lacks Leucine (selective for yeast cells containing the pASV3 vector) and Tryptophan (selective for yeast cells containing the pBTM116 vector). After three days, 3 colonies per sample were picked and plated on to YSM agar plates. The plates were incubated at 30°C for another 3 days. Next, the yeast cells, which had grown from a single colony, needed to be grown overnight for the Y2H-assay. To do so, 2X 50 mL Falcon tubes were prepared per sample with one tube containing

30 mL YSM and the other tube being empty. The 30 mL YSM were inoculated with a loop full of yeast and vortexed. Then 15 mL of that were decanted into the empty tube. Mibolerone (synthetic androgen dissolved in 100% Ethanol; 10 mM Stock solution) was added to a final concentration of 1 µM to one of the tubes, and 1.5 µL 100% Ethanol was added as vehicle to the other tube. The tubes were covered in foil to protect from light and incubated on a shaker at 30^{o}C overnight.

2.14.4 Protein extraction from yeast cells

The next day, proteins were extracted by centrifuging down the cells at 4,000 x g for 5 minutes at 4°C. The supernatant was discarded, the pellet resuspended in 1 mL sterile diH_2O and transferred to 2 mL microcentrifuge tubes. A brief centrifugation for 15 seconds followed. The supernatant was removed and the pellet was resuspended in 150 µL Z-buffer (60 mM $Na_2HPO_4.7H_2O$, 40 mM $NaH_2PO_4.H_2O$, 10 mM KCl, 1 mM $MgSO_4.7H_2O$ and 50 mM β-mercaptoethanol (added freshly), pH 7.0, stored at 4°C). To lyse the cells, a single scoop of glass beads was added to each sample and lysis was performed in a disruptor using a cycle of 1 minute disrupting, and 1 minute on ice, repeated three times. The 1 minute on ice was necessary because the samples heated up during disruption. The samples were then centrifuged at 14,000 x g for 30 minutes at 4°C. After that, the supernatant containing the extracted proteins was transferred to a 500 µL Eppendorf tube. The protein concentration was measured using the Bradford assay which is a colorimetric assay based on the dye Coomassie Brilliant Blue G-250 (Bradford, 1976). When proteins bind to Coomassie Blue under acidic conditions, the colour changes from brown to blue which is measured spectroscopically. A standard curve was made with the following BSA (bovine serum albumin) concentrations in diH_2O to a final volume of 800 µL: 0 mg/mL, 2 mg/mL, 4 mg/mL, 6 mg/mL, 8 mg/mL, 10 mg/mL. For the protein extracts of the yeast, 2 µL was added to 800 µL diH_2O. To the 800 µL standard curve dilutions 2 µL Z-buffer was added. In the end, 200 µL Bradford reagent (Sigma-Aldrich®) was added per sample and the absorbance of the samples measured in cuvettes at 595nm in a spectrophotometer.

2.14.5 Beta (β)-Galactosidase assay

For the β-Galactosidase assay, 480 µl of Z-buffer was transferred to a cuvette and 20 µl of protein extract was added. The samples were briefly vortexed to ensure even distribution of the proteins. To begin the β-galactosidase reaction, 100 µl of 4 mg/ml o-nitrophenyl-beta-D-galactopyranoside (ONPG; freshly dissolved in Z-buffer and kept on ice; stock

powder stored at -20°C) was added to each cuvette at a time interval of 30 seconds whilst recording the time of ONPG addition. ONPG is an analog of lactose in which glucose has been replaced by orthonitrophenyl. Upon hydrolysis by β-galactosidase, ONPG is cleaved into galactose and o-nitrophenol which is yellow in colour. Each reaction was allowed to proceed until a pale yellow colour began to appear, upon which time 250 µl of 1 M Na_2CO_3 (sodium carbonate) was added to the relevant cuvette to stop the reaction. The time of addition was noted down. Any sample which had not produced a colour change after 30 minutes was complemented with sodium carbonate regardless. The absorbance of o-nitrophenol in each sample was measured at 420nm in a spectrophotometer. The activity of the β-galactosidase was calculated with the following formula:

$$\text{β-galactose activity (nmoles)} = \frac{OD_{420} * 0.850\ mL}{0.0045 * \text{protein conc (mg/mL)} * 20\ \mu L * \text{time (min)}}$$

In this formula, factor 0.0045 is the optical density of a 1 nmole/mL o-nitrophenol solution, i.e. OD_{450}/0.0045 are the nmoles formed per mL. 0.850 mL is the volume of the whole reaction. The protein concentration was obtained by Bradford assay and expressed as mg/mL. 20 µL is the volume of the protein extract assayed. The time between adding ONPG and stopping the reaction with sodium carbonate was given in minutes.

2.14.6 WB analysis with yeast cell proteins

To control if both the VP16 and the LexA constructs were present in the yeast cells, we performed western blot analysis with the protein extracts used in the β-galactosidase assay. Protein separation was performed with self-made 12% polyacrylamide gels. The recipes of the resolving and stacking gel were as followed:

Resolving gel components	Volume
30% acrylamide and bis-acrylamide solution, 29:1 (BIO-RAD)	8 mL
ddH_2O	6.6 mL
1.5 M Tris HCL, pH 8.8	5 mL
10 % SDS	200 µl
TEMED (added shortly before casting)	8 µL
10% APS (added shortly before casting)	200 µL
Total volume	~ 20 mL

Stacking gel components	Volume
30% acrylamide and bis-acrylamide solution, 29:1 (BIO-RAD)	1 mL
ddH_2O	4.1 mL
1 M Tris HCL, pH 6.8	750 µl
10 % SDS	60 µl
TEMED (added shortly before casting)	6 µL
10% APS (added shortly before casting)	60 µL
Total volume	~ 6 mL

For polyacrylamide gel electrophoresis (PAGE) 10 µg sample and 3 µL ladder (Color Protein Standard Broad Range, **Appendix 3**) was loaded and ran at 200 Volt for ~1 hour and 10 min. Blotting was performed overnight at 4°C in a fully wet tank at 30 Volt. The next day, the membrane was blocked with 5% Milk in 1X PBS for 1 hour. The primary antibodies used were Anti-LexA (#06-716, Merck; Rabbit polyclonal IgG, 1:500 in 5% Milk in PBS) and Anti-VP16 (# sc-7546, Santa Cruz Biotechnology; Mouse monoclonal IgG, 1:500 in 5% Milk in PBS). The membrane was incubated with the primary antibody at 4°C overnight. The next day, the membrane was washed with 1XPBST (1% Tween®20) three times for 5 minutes at room temperature on a shaker. Then the membrane was incubated with the secondary antibody for 1 hour at room temperature. The secondary antibodies used were Chicken anti-mouse IgG HRP (#sc-2954, Santa Cruz Biotechnology; 1:5000 in 5% in 1X PBS) and Goat anti-rabbit IgG HRP (#sc-2004, Santa Cruz Biotechnology; 1:5000 in 5% in 1X PBS). Next, the membrane was washed again with 1XPBST (1% Tween®20) three times for 5 minutes and then incubated with 1 mL (500 µL of solution A plus 500 µL of solution B) Pierce™ ECL Western Blotting Substrate (Thermo Fisher Scientific™). The signal was detected using the Las-4000 Luminescent Image Analyzer, UK.

2.15 Statistical analysis

P-values lower than 0.05 were considered statistically significant with a confidence interval of 95%.

2.15.1 Clinical correlations of TMA

Statistical *p*-values were determined by χ^2-test (asymptotic significance, 2-sided) using IBM® SPSS® Statistics, Version 24 and the VassarStats Website for Statistical Computation (©Richard Lowry). Statistical significances of Kaplan-Meier estimates were calculated using the log-rank (Mantel-Cox) test. Scoring reliability between two independent scorers was analysed by both Cronbach's alpha in SPSS and Spearman's rank-order correlation in Microsoft Excel.

2.15.2 Cell culture experiments

All experiments were performed on a minimum of two independent repeats analysed in triplicates, unless stated differently. Statistical analysis was carried out using GraphPad Prism 7. For multiple comparisons one-way ANOVA was used by comparing the mean of each column with the mean of every other column. The one-way ANOVA was performed with no matching or pairing and corrected by Bonferroni statistical hypothesis testing. For comparison of two means, parametric t-test was carried out. If different cell lines were compared to each other, unpaired t-test was used. For comparisons within the same cell line paired t-test was performed. In general 2-fold difference in gene or protein expression was considered biologically important.

2.16 RNASeq analysis

RNASeq analysis was performed in duplicates with the RNA of LNCaP and LNCaP:C4-2 cells treated with the following pharmaco-selective inhibitors: (1) Androgen (R1881, 1 nM) and DMSO treated control LNCaP cells, (2) androgen and CPI-455 (50 μM) treated LNCaP cells, (3) androgen and Namoline (50 μM) + TC-E 5002 (50 μM) (combined) treated LNCaP cells, (4) androgen and DMSO treated control LNCaP:C4-2 cells, and (5) androgen and Namoline (50 μM) + TC-E 5002 (50 μM) (combined) treated LNCaP:C4-2 cells. RNASeq analysis was performed by Nigel Mongan. Fastq files were quality processed (phred score >30 retained) and adapters trimmed using the Trim Galore wrapper for FastQC and Cutadapt. The QC-processed reads were aligned to the human Ensembl annotated reference genome (GRCh38) using the STAR aligner using a gene annotation set including all mRNA and lncRNAs. Differential gene expression were calculated using FeatureCounts (Liao et al., 2013) and EdegR (Robinson et al., 2010) as described (Minton et al., 2016). Heatmaps were created by Nigel Mongan using the Cluster 3.0 software and edited with the Java TreeView software. For the heatmaps, the gene counts (+1, to avoid 0) were log2 transformed, mean centred and average linkage clustering performed. The RNASeq was validated using qRT-PCR analysis. Venn diagrams were created to compare differentially expressed genes between cell lines. Pathway analysis was performed using the Kyoto Encyclopedia of Genes and Genomes (KEGG) pathway database (https://www.genome.jp/kegg/pathway.html, accessed 12.08.2019). For the Venn diagrams and the pathway analysis the RNASeq data was filtered according to logFC ≥1 and ≥-1 respectively.

Chapter 3: KDM5B in androgen signalling

Chapter 3 KDM5B in androgen signalling

3.1 Introduction

To date, there are no curative treatment options for metastatic castration resistant prostate cancer (CRPC) and PCa recurrence and drug resistance remains a big issue (Chandrasekar et al., 2015, Semenas et al., 2012, Seruga et al., 2011, Yuan et al., 2014). It is therefore important to find new drug targets and develop novel therapies. In recent years, epigenetic co-regulators of the androgen receptor have gained more interest as potential targets for PCa treatments (Biron and Bédard, 2016, Ferraldeschi et al., 2015, Foley and Mitsiades, 2016, Heemers et al., 2010, Heemers and Tindall, 2005). One such coregulator is the histone lysine demethylase KDM1A which has been extensively studied and shown to be a potential target to treat PCa (Civenni et al., 2018, Magliulo et al., 2018, Niwa and Umehara, 2017, Sehrawat et al., 2018, Yang et al., 2018).

A recent study by Nilsson and colleagues (2015) found that the tumour suppressor *miR137* inhibits the expression of an essential network of AR coregulators, including *KDM1A, KDM2A, KDM4A, KDM5B, KDM7A, MED1,* and *SUZ12*, upon androgen, and that this negative feedback mechanism by *miR137* is lost in CRPC cell models (Nilsson et al., 2015). This study reveals the potential that not only KDM1A, but also other co-regulators, such as KDM5B, represent promising targets to treat PCa. KDM1A can demethylate only mono- and di-methylated H3K4, whereas KDM5B is additionally able to demethylate tri-methylated H3K4 (Scibetta et al., 2007, Shi et al., 2004). Methylated H3K4 is a known histone mark for active transcription and dysregulated H3K4 methylation levels have been implicated in PCa progression and development of CRPC (Black et al., 2012, Ellinger et al., 2010, Seligson et al., 2005). Given that all methylation levels (H3K4me3/me2/me1) can be modified by KDM5B, it represents an interesting potential target and it is therefore important to understand its implications in PCa.

The hypothesis of this study is that KDM5B, like KDM1A, is required for AR signalling in PCa. To test this hypothesis, the expression of KDM5B was determined in PCa specimens and cell lines. KDM5B knockdown and inhibition experiments were performed to further elucidate the function of KDM5B in AR-regulated gene expression and PCa cell proliferation. These experiments aimed to give more insight into the role of KDM5B in AR signalling in PCa.

3.2 Results

3.2.1 Bioinformatic analysis of *KDM5B*

Bioinformatic analysis was performed using the cBioPortal for Cancer Genomics to investigate *KDM5B* gene alterations in prostate cancer patients (**Figure 3.1**). Three studies were used in the analysis: (1) The TCGA Provisional Prostate Adenocarcinoma study (n = 499), (2) the SU2C/PCF Dream Team Metastatic Prostate Adenocarcinoma study (n = 444) and (3) the Trento/Cornell/Broad Neuroendocrine Prostate Cancer study (n = 114). The analysis of the TCGA Provisional Prostate Adenocarcinoma study revealed that 29.7% of prostate cancer patients harboured alterations in the *KDM5B* (**Figure 3.1, A**). A comparative analysis was performed to determine which cancer type (Prostatic adenocarcinoma vs Metastatic prostate adenocarcinoma vs Neuroendocrine carcinoma) harboured most *KDM5B* alterations. Both mutations and putative copy number alterations from GISTIC were included. The GISTIC software allows the detection of gene amplification and deletions (Beroukhim et al., 2010, Mermel et al., 2011). This analysis revealed that the *KDM5B* gene was altered most frequently in neuroendocrine prostate cancer (**Figure 3.1, B**). In neuroendocrine carcinoma *KDM5B* was altered in 28.07%, including gene amplifications in 33/114 cases (27.19%) and a mutation in 1/114 cases (0.88%). The second highest alteration frequency was observed in metastatic prostate adenocarcinoma with 8.56% of which 35/444 cases (7.88%) exhibited *KDM5B* amplification and 3/444 cases (0.68%) mutations (**Figure 3.1, B**). In the TCGA Provisional prostate adenocarcinoma study, *KDM5B* was altered in only 0.4% (2/499 cases) (**Figure 3.1, B**). When the TCGA Provisional prostate adenocarcinoma study was analysed individually and the mRNA Expression z-Score (RNA Seq V2 RSEM) was included (z = 1), KDM5B was altered in ~29.7% (147/499 cases) of patients of which 16.8% patients had mRNA High (84/499 cases) and 12.4% mRNA Low (62/499 cases) (**Figure 3.1, C**). None of the cases had any amplification, deep deletion or multiple alterations and only 2 cases had a mutation (0.4%).

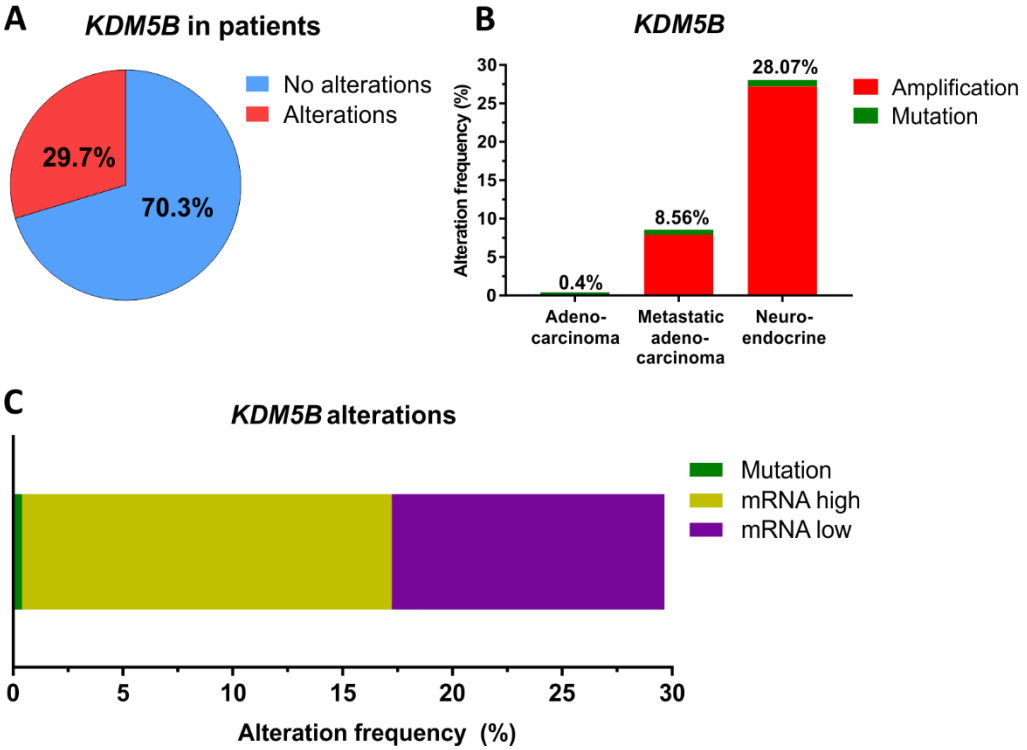

Figure 3.1: *KDM5B* alteration frequencies in prostate cancer patients.
Bioinformatic analysis was performed using the cBioPortal for Cancer Genomics. (**A**) *KDM5B* was altered in 29.7% of prostate cancer patients. (**B**) The *KDM5B* alteration frequency was higher in metastatic adenocarcinoma (~8.6%) compared to primary adenocarcinoma (0.4%), and was highest (~28%) in neuroendocrine carcinoma. (**C**) The TCGA Provisional Prostate Adenocarcinoma study (mRNA expression z-score=1) revealed that the most frequent *KDM5B* alterations were mRNA high (~16.8% of cases) or mRNA low (~12.4%).

In total, six patients within the three studies (1057 patients) harboured a *KDM5B* mutation (**Table 3.1**), four of which had a missense mutation. The location of the mutations are shown in **Figure 3.2**. Two patients, one with neuroendocrine prostate cancer and one with metastatic adenocarcinoma, harbouered the same mutation (K158R, **No. 4**) which was located in the ARID/BRIGHT domain which is responsible for DNA binding (Herrscher et al., 1995). The other missense mutations (R1534H and D972G) were found in prostate adenocarcinoma cases. The R1534H (**No. 1**) mutation is situated in the PHD3 finger domain which is needed to bind H3K4 and was shown to preferably bind to trimethylated H3K4me3 (Klein et al., 2014). The D972G (**No. 2**) mutation lies in the putative DNA and chromatin binding domain PLU-1. In metastatic adenocarcinoma cases there was a frame shift deletion (S1119Afs*4) and a splice mutation (S1028). The frame shift deletion (**No. 3**) is located between the PLU-1 and PHD2 finger domain, whereas the splice mutation (**No. 5**) is in the PLU-1 domain. All six patients harboured a high number of mutations, ranging from ~750-6500.

Table 3.1: *KDM5B* mutations in prostate cancer patients.
The study, protein change, mutation type, copy number, allele frequency and number of mutations in the sample were stated. The mutations were given a number from 1 - 5 which correspond to the numbers in **Figure 3.2**.

No.	Study	Protein Change	Mutation Type	Copy #	Allele Freq (T)	# Mut in Sample
1	Prostate Adenocarcinoma	R1534H	Missense	Diploid	0.29	860
2	Prostate Adenocarcinoma	D972G	Missense	Diploid	0.33	6525
3	Metastatic P Adenocarcinoma	S1119Afs*4	FS del	Diploid	N/A	1150
4	Metastatic P Adenocarcinoma	K158R	Missense	Diploid	0.05	950
5	Metastatic P Adenocarcinoma	X1028_splice	Splice	Diploid	0.19	924
4	Neuroendocrine carcinoma	K158R	Missense	Diploid	0.05	751

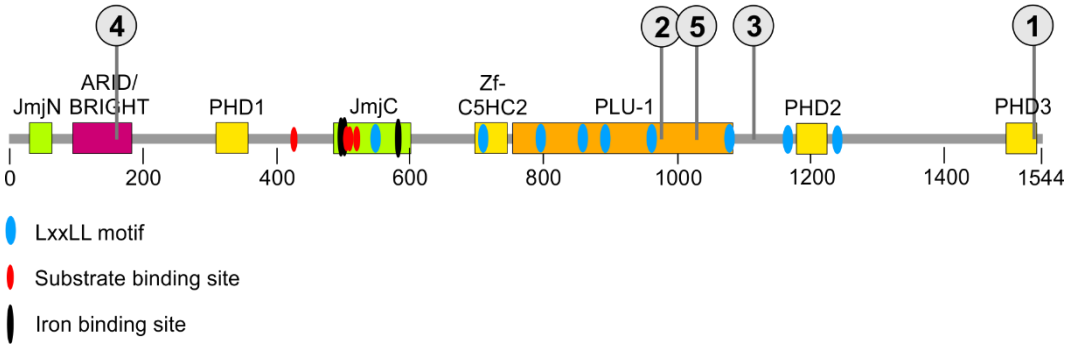

Figure 3.2: Location of KDM5B mutations.
The KDM5B protein is 1544 amino acids long and contains several domains, including the JmjN, JmjC, ARID/BRIGHT, PLU-1 and four zinc finger domains. The mutations were numbered from 1 – 5 and correspond to the mutations in **Table 3.1**. Jmj = Jumonji; ARID = AT-rich interaction domain; Zf = zinc finger; PHD = plant homeodomain.

The TCGA Provisional Prostate Adenocarcinoma study was used to analyse putative copy number alterations from GISTIC (**Figure 3.3**). The majority of cases (466/499) were diploid for the *KDM5B* gene. The two patients with the missense mutation were within the diploid cases. In 29 patients a low level copy number amplification (gain) was found and only four patients exhibited a heterozygous deletion (shallow deletion).

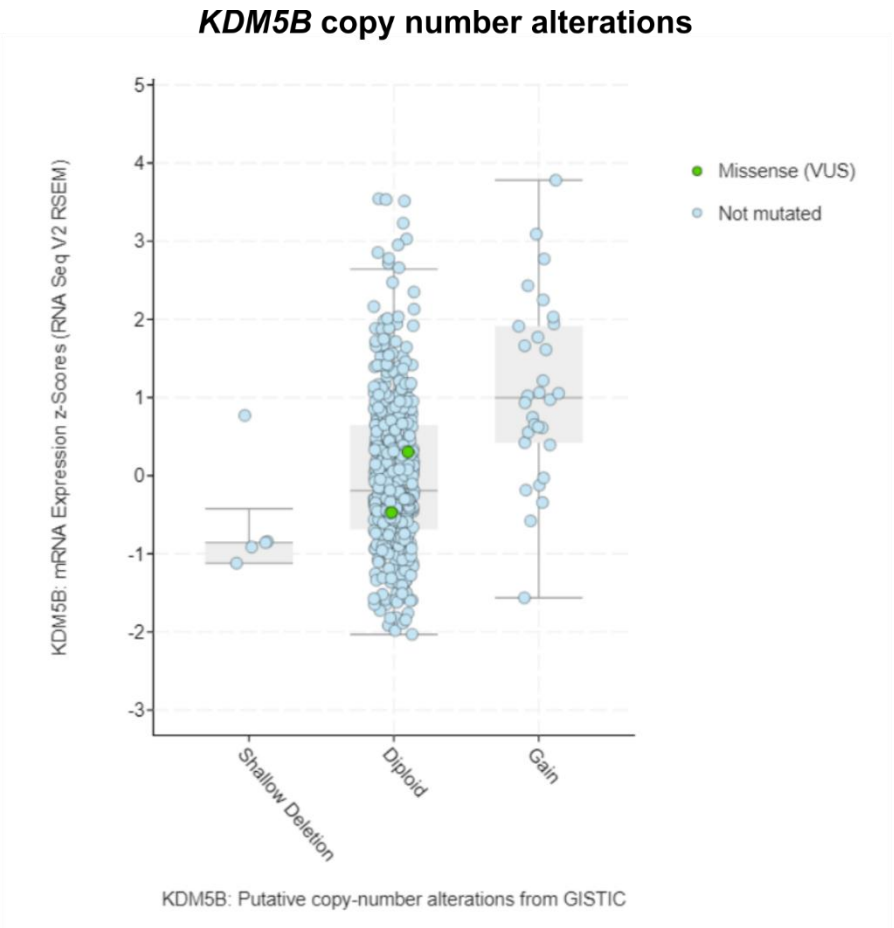

Figure 3.3: *KDM5B* copy number alterations in prostate cancer patients.
The cBioPortal for Cancer Genomics was used for bioinformatic analysis (https://www.cbioportal.org/, accessed 12.06.2019). In most patients the *KDM5B* gene was not altered. Four patients had a shallow deletion and 29 patients a copy number gain.

3.2.2 KDM5B staining in human tissue specimens

To validate the TMA patient database, clinical relevant parameters like Gleason score and TNM (tumour, node, metastasis) stage were correlated with each other using the Statistical Package for Social Sciences (SPSS) (**Figure 3.4, Appendix 4**). As expected, high Gleason score correlated with high TNM stage (T3, ≙ extraprostatic extension) (**A**), extraprostatic extension (**B**), perineural invasion (**C**), biochemical recurrence (BCR) (**D**) and older patients (**E**) ($p \leq 0.05$) (**Figure 3.4**). Similarly, high TNM stage correlated with perineural invasion (**F**), high pre-OP PSA (**G**) and BCR (**H**) ($p \leq 0.05$) (**Figure 3.4**). These results confirmed the validity of the TMA patient database.

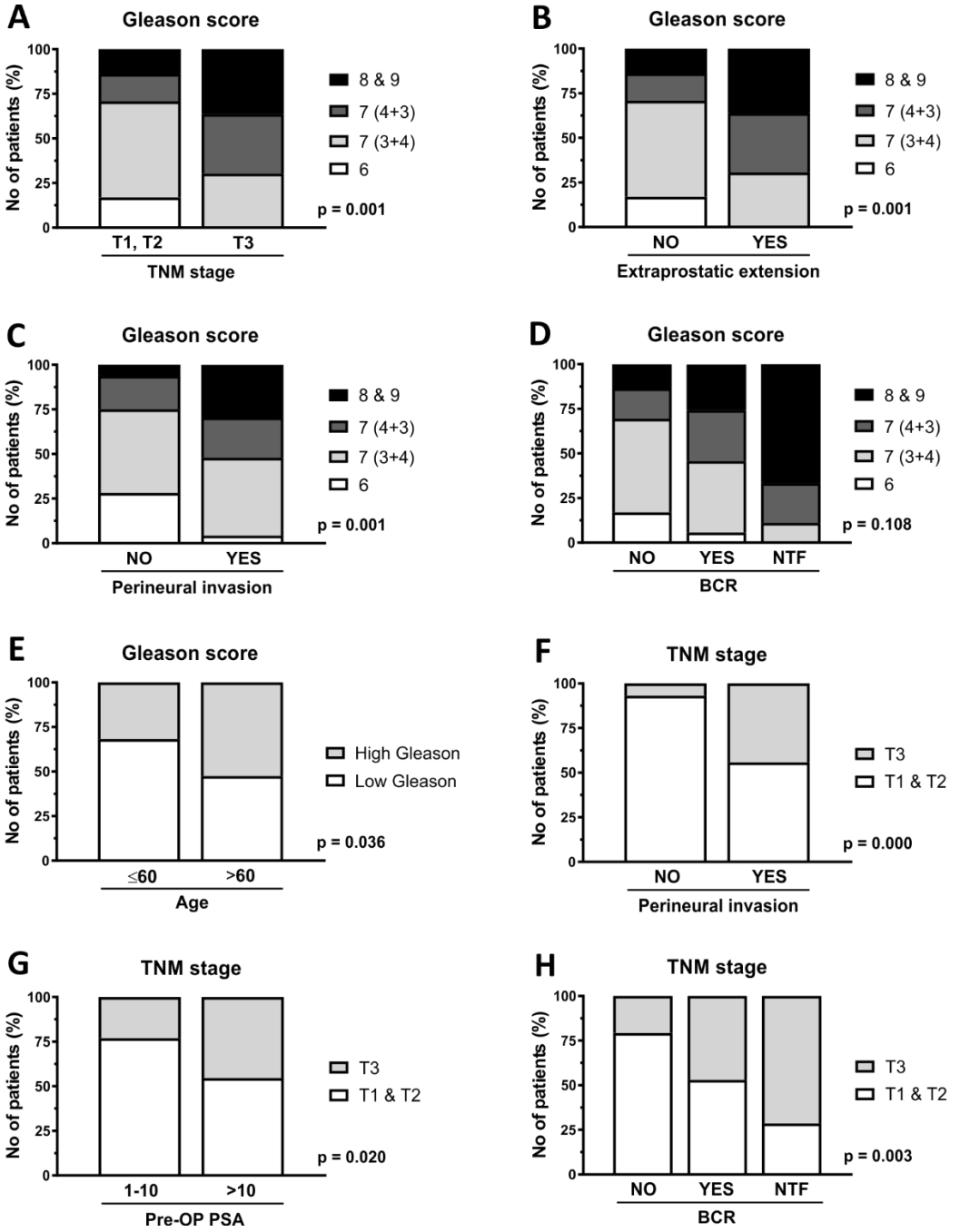

Figure 3.4: Validation of clinical relevant data in the TMA patient database.

To validate the clinical patient database correlations were performed between clinical relevant outcomes using SPSS (n = 104). High Gleason score correlated with TNM stage T3 (**A**), extraprostatic extension (**B**), perineural invasion (**C**), biochemical recurrence (**D**) and age (**E**). TNM stage T3 correlated with perineural invasion (**F**), pre-OP PSA >10 (**G**) and biochemical recurrence (**H**). TNM = tumour, node, metastasis; BCR = biochemical recurrence. Statistical analysis was performed by using $\chi 2$-test.

To investigate KDM5B expression in prostate cancer patients, a tissue microarray (TMA) was constructed and the KDM5B protein expression examined by using immunohistochemical (IHC) staining (**Figure 3.5**). Representative pictures of human specimen with normal prostate tissue (**A, B**), tumour tissue (**C, D**) and less differentiated tumour tissue (**E, F**) are shown when stained with KDM5B antibody (**Figure 3.5**). KDM5B staining was quantified using H-score and 10% of the cores was scored by a second scorer to ensure scoring reliability. To estimate scoring reliability, Spearman's rank-order correlation and the Cronbach's alpha test were performed in Excel and SPSS respectively. The Spearman correlation coefficient (R^2) was between ~0.7 - 0.8 for both nuclear and cytoplasmic H-scores which is considered a "good" association between the two scorers (1 is considered "perfect"). The Cronbach's alpha test revealed an even better reliability between ~0.8 - 1. Both tests confirm the reliability of the H-scores. The distribution curve for the evaluated H-scores across all patients can be found in **Appendix 5**. H-scores were equally divided into three groups (low, medium, high) and revealed that KDM5B nuclear staining was lower ($p \leq 0.05$) in tumour tissue compared to normal tissue (**Figure 3.5, G**). Regarding cytoplasmic staining, there was no statistically significant difference in KDM5B expression between normal and tumour tissue (**Figure 3.5, H**).

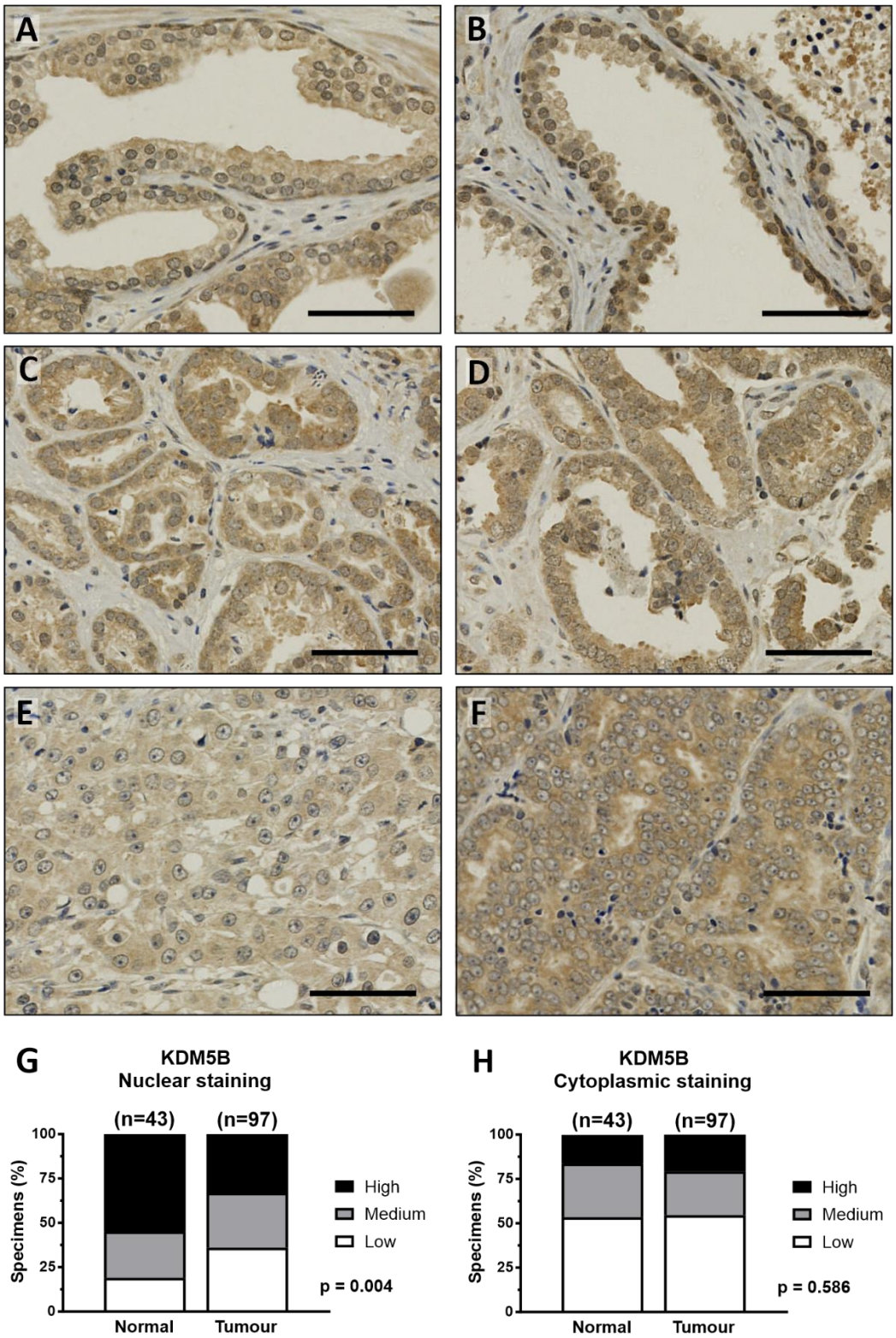

Figure 3.5: Immunohistochemical staining of KDM5B in PCa specimens.

To evaluate expression of KDM5B protein immunohistochemistry was used in non-malignant (n = 43) and prostate cancer (n = 97) specimens. Representative KDM5B staining of normal tissue (**A, B**), tumour tissue (**C, D**) and less differentiated tumour tissue (**E, F**) (Scale bars: 50 µM). (**G**) H-score evaluation of KDM5B staining reveiled lower (p = 0.004) KDM5B nuclear staining in tumour compared to normal specimens. (**H**) Cytoplasmic staining did not differ in normal and tumour specimens. Nuclear H-score: low = 0-20, medium = 25-40, high = 45-155; Cytoplasmic H-score: low = 25-50, medium = 55-75, high = 80-150; BCR = Biochemical recurrence. Statistical p-values were determined by χ^2-test (VassarStats).

To determine whether KDM5B expression in human prostate cancer tissue specimens correlates with BCR, a Kaplan-Meier estimate was conducted via the GraphPad Prism 7 software (Figure 3.6). There was no difference in biochemical recurrence free status in patients with low versus high KDM5B expression both in the nucleus (A) and cytoplasm (B) (Figure 3.6,).

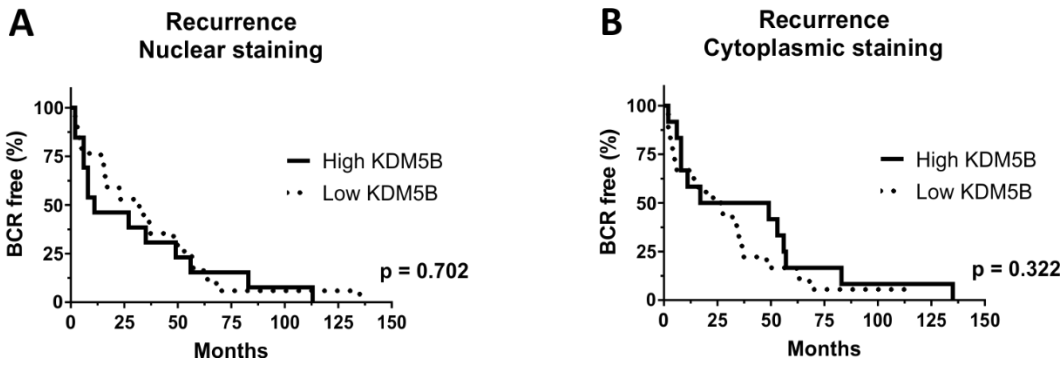

Figure 3.6: Correlation of KDM5B staining with biochemical recurrence.
KDM5B staining was correlated with BCR free time by using the Kaplan Meier estimate (n = 30). Both KDM5B nuclear (A) and cytoplasmic (B) staining did not correlate with biochemical recurrence free status in patients. BCR = Biochemical recurrence; Nuclear H-score, low = 0-30, high = 35-155; cytoplasmic H-score, low = 30-50, high = 60-150. Statistical analysis was performed with log-rank test.

To investigate if there is a relationship between KDM5B expression and other patient parameters, KDM5B nuclear and cytoplasmic staining was correlated with clinical patient data using SPSS (Appendix 6). KDM5B staining was not statistically significantly correlated with age, Gleason score, high grade PIN, perineural invasion, pre-OP PSA and BCR (Appendix 6). However, high KDM5B staining correlated ($p \leq 0.05$) with absence of extraprostatic extension and a low TNM stage (T1, T2; ≙ no extraprostatic extension).

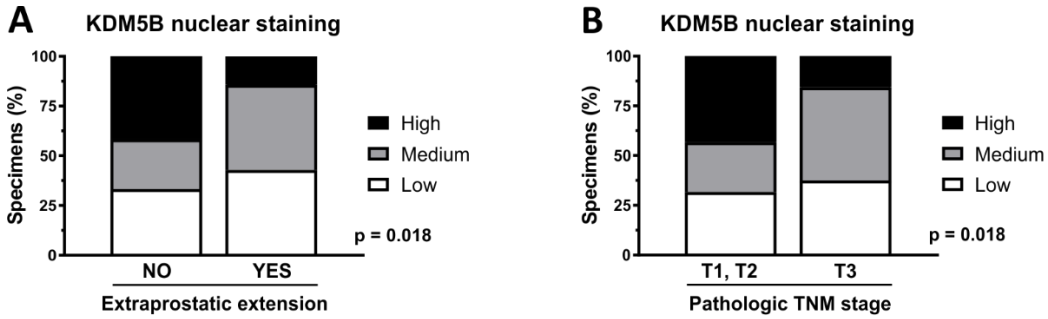

Figure 3.7: Correlation of KDM5B staining with clinical patient data.
KDM5B staining intensities were determined by H-score and correlated with clinical data by SPSS analysis (n = 97). Low KDM5B nuclear staining correlated with extraprostatic extension (A) and TNM stage T3 (B). TNM = tumour, node, metastasis; Nuclear H-score 3 groups, Low = 0-20, Medium = 25-40, High = 45-155. Statistical significances were determined by $\chi 2$-test.

3.2.3 *KDM5B* is overexpressed in LNCaP cells compared to normal prostate cells

Basal expression levels of KDM5B were first investigated in non-malignant prostate PNT1A cells and in the prostate cancer cell lines LNCaP, LNCaP:C4-2, 22Rv1, PC3 and Du145 (Figure 3.8). KDM5B expression was examined at both the mRNA and protein level using qRT-PCR (Figure 3.8, A) and western blots respectively (Figure 3.8, B-C). LNCaP cells showed the highest KDM5B expression with a 11-fold higher ($p \leq 0.05$) on the mRNA level and a 2.7-fold ($p \leq 0.05$) higher protein level as compared to non-malignant prostate PNT1A cells. In LNCaP:C42 cells *KDM5B* mRNA was 4.5-fold ($p \leq 0.05$) higher compared to PNT1A but KDM5B protein was not differentially expressed in comparison to the PNT1A control. Both 22Rv1 and PC3 cells showed elevated *KDM5B* mRNA levels (2.3-fold and 2-fold, $p \leq 0.05$) but exhibited 0.3-fold decreased KDM5B protein levels ($p \leq 0.05$) when compared to PNT1A control cells. In Du145 cells KDM5B expression is moderately lower than in normal PNT1A cells with a 0.6-fold ($p \leq 0.05$) decrease in *KDM5B* mRNA and a 0.4-fold ($p \leq 0.05$) decrease in KDM5B protein compared to PNT1A. In general, 2-fold difference in expression is considered biologically important.

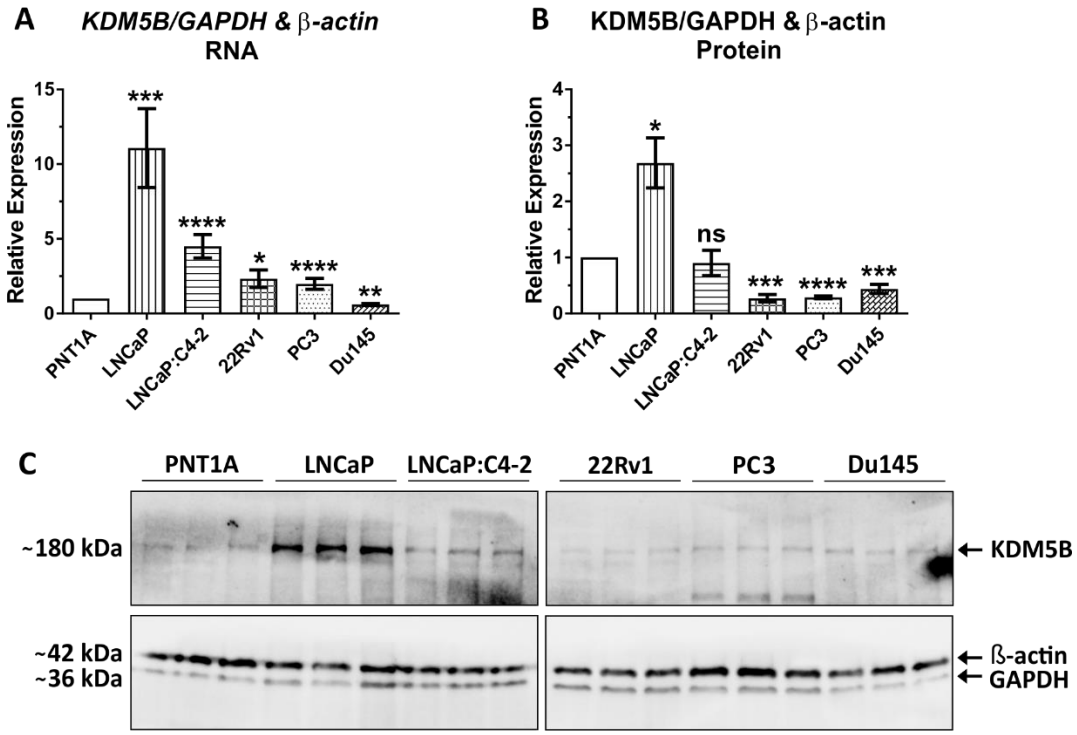

Figure 3.8: KDM5B mRNA and protein expression in PCa cell lines compared to normal cells.
KDM5B basal expression levels were analysed via qRT-PCR and western blots. The intensity of the band in the western blots (C) were quantified by ImageJ (B). Statistical significances were calculated by comparing each cell line to the non-malignant PNT1A cell line (white column). (A) *KDM5B* mRNA is higher in LNCaP, LNCaP:C4-2, 22Rv1 and PC3 cells, and lower in Du145 compared to normal prostate PNT1A cells (n = 9). (B-C) KDM5B protein is higher in LNCaP cells and lower in 22Rv1, PC3 and Du145 compared to PNT1A (n = 3). * = $p \leq 0.05$; ** $p \leq 0.005$; *** = $p \leq 0.001$; **** = $p \leq 0.0001$ by unpaired t-test.

3.2.4 *KDM5B* expression is not androgen regulated

As a positive control, the effect of 1 nM R1881 on the mRNA expression of *kallikrein related peptidase 3/prostate specific antigen (KLK3/PSA)* (Figure 3.9), a prototypical androgen-regulated gene, was investigated in PNT1A, LNCaP, LNCaP:C4-2, 22Rv1, PC3 and Du145 using RT-qPCR analysis. The androgen treatment was performed for three days. Basal *PSA* expression was highest in LNCaP cells, second highest in 22Rv1 cells and lowest in LNCaP:C4-2 cells. Upon R1881 treatment, LNCaP cells exhibited a 8.3-fold ($p \leq 0.05$) higher *PSA* mRNA expression than in the vehicle control (Figure 3.9, A). In LNCaP:C4-2 cells R1881 induced a 96-fold increase ($p \leq 0.05$) in *PSA* mRNA expression (Figure 3.9, B). The lowest R1881-induced *PSA* expression was observed in 22Rv1 with a 2.6-fold ($p \leq 0.05$) increase in *PSA* compared to the vehicle control cells (Figure 3.9, B). As expected, *PSA* was not detected in PNT1A, PC3 and Du145 (data not shown).

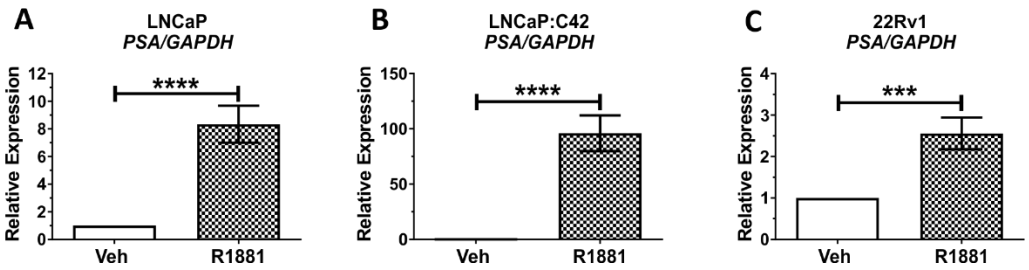

Figure 3.9: Effect of androgen on *PSA* expression in androgen-sensitive PCa cell lines.
PSA mRNA expression of 1 nM R1881 treated androgen-sensitive prostate cancer cells was measured by qRT-PCR. (A-C) In all cell lines *PSA* expression is significantly induced upon R1881 treatment (n = 9). * = $p \leq 0.05$; **$p \leq 0.005$; *** = $p \leq 0.001$; **** = $p \leq 0.0001$ by paired t-test.

The effect of androgen (R1881, 1 nM) on expression of the androgen-regulated *vascular endothelial growth factor A (VEGFA)* gene was next examined as a further positive control (Figure 3.10) (Kashyap et al., 2013). Upon R1881 treatment, LNCaP cells exhibited a 5.3-fold ($p \leq 0.05$) *VEGFA* mRNA increase compared to vehicle control (Figure 3.10, B). In contrast, R1881 did not have any effect on *VEGFA* expression in LNCaP:C4-2 (Figure 3.10, C) and 22Rv1 (Figure 3.10, D). As expected, in the negative control cell line PNT1A *VEGFA* expression did not change upon R1881 (Figure 3.10, A). Surprisingly, in PC3 cells R1881 increased *VEGFA* expression by 1.6-fold, though this did not reach statistical significance (Figure 3.10, E). Similarly, *VEGFA* was expressed significantly higher ($p \leq 0.05$) in Du145 upon R1881 treatment compared to vehicle control, however only 1.3-fold (Figure 3.10, F).

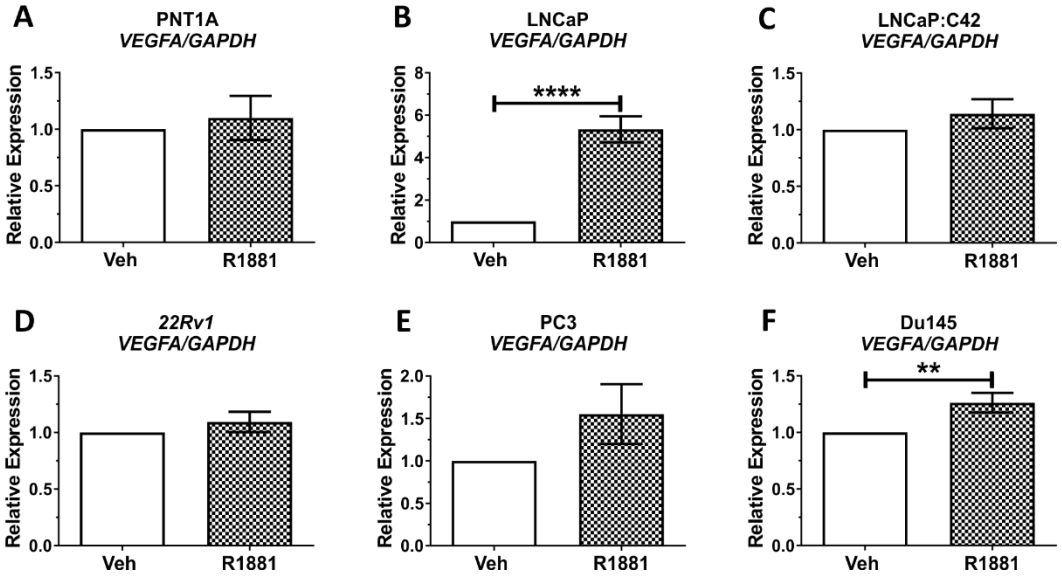

Figure 3.10: Effect of androgen on *VEGFA* expression in normal prostate and PCa cell lines.
qRT-PCR was used to measure *VEGFA* mRNA expression. LNCaP (**B**) was the only androgen-sensitive cell line amongst LNCaP:C4-2 (**C**) and 22Rv1 (**D**) that showed increased *VEGFA* expression upon R1881 treatment (**B**) (n = 9). The negative control cell lines PNT1A (**A**), PC3 (**E**) and Du145 (**F**) did not exhibit any biologically significant changes in *VEGFA* expression (n = 6). * = $p \leq 0.05$; ** $p \leq 0.005$; *** = $p \leq 0.001$; **** = $p \leq 0.0001$ by paired t-test.

To determine whether *KDM5B* mRNA expression is androgen dependent, the effect of the synthetic androgen (R1881, 1 nM) on *KDM5B* expression after three days of treatment was examined using qRT-PCR (**Figure 3.11**). The effect of androgen on *KDM5B* expression was tested in non-malignant prostate cell line PNT1A and the prostate cancer cell lines LNCaP, LNCaP:C4-2, 22Rv1, PC3 and Du145. The androgen-insensitive cell lines PNT1A, PC3 and Du145 which express little or no AR served as negative controls. Interestingly, *KDM5B* expression did not change upon R1881 treatment in either of the androgen-sensitive cell lines LNCaP, LNCaP:C4-2 and 22Rv1 (**Figure 3.11, B-D**) compared to the vehicle control. As expected, R1881 did not have any effect on *KDM5B* expression in PNT1A, PC3 and Du145 which lack AR expression (**Figure 3.11, A, E-F**).

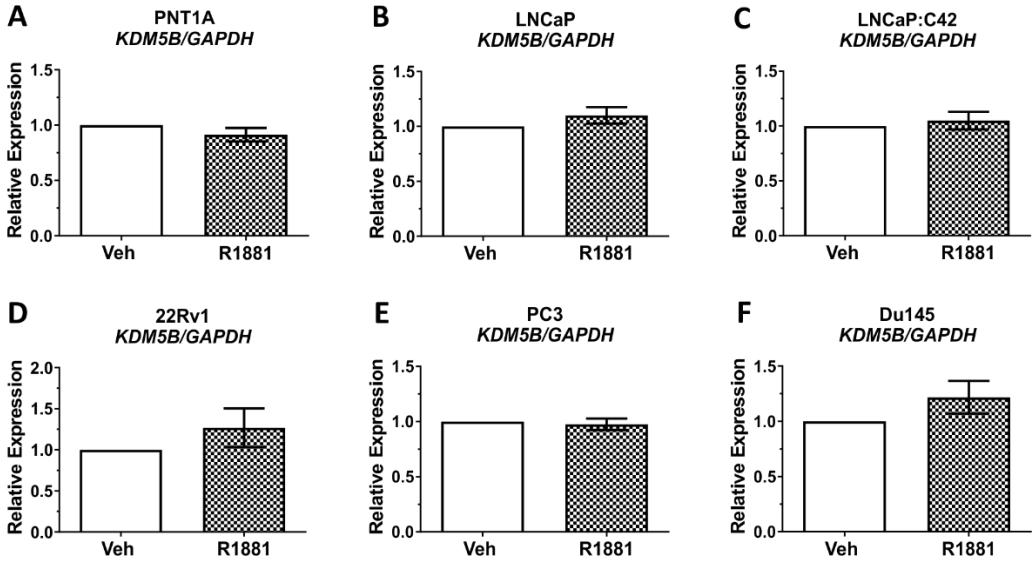

Figure 3.11: Effect of androgen on *KDM5B* expression in normal prostate and PCa cell lines.
Normal and prostate cancer cell lines were treated with 1 nM R1881 and *KDM5B* mRNA expression was measured using qRT-PCR. *KDM5B* expression did not change upon R1881 in LNCaP (**B**), LNCaP:C4-2 (**C**) and 22Rv1 (**D**) compared to vehicle control (n = 9). The negative control cell lines PNT1A (**A**), PC3 (**E**) and Du145 (**F**) did not show any effect (n = 6). * = $p \leq 0.05$; **$p \leq 0.005$; *** = $p \leq 0.001$; **** = $p \leq 0.0001$ by paired t-test.

3.2.5 Functional depletion of KDM5B via siRNA modestly attenuates R1881-induced *PSA* expression

To further elucidate the function of KDM5B in androgen signalling in prostate cancer, siRNAs were used to functionally deplete KDM5B in LNCaP and LNCaP:C4-2. Knockdown was performed for three days and the knockdown efficiency was confirmed in LNCaP and LNCaP:C4-2 cells by qRT-PCR (n = min 9) and western blot analysis (n = 3, **Appendix 7**) (**Figure 3.12**). At the RNA level, siRNA targeting KDM5B resulted in ~60-70% ($p \leq 0.05$) knockdown of *KDM5B* mRNA in LNCaP (**Figure 3.12, A**) and LNCaP:C4-2 (**Figure 3.12, B**) respectively. The knockdown was confirmed on the protein level where both LNCaP (**Figure 3.12, C**) and LNCaP:C4-2 (**Figure 3.12, D**) showed a weaker band in siKDM5B compared to the siScramble control.

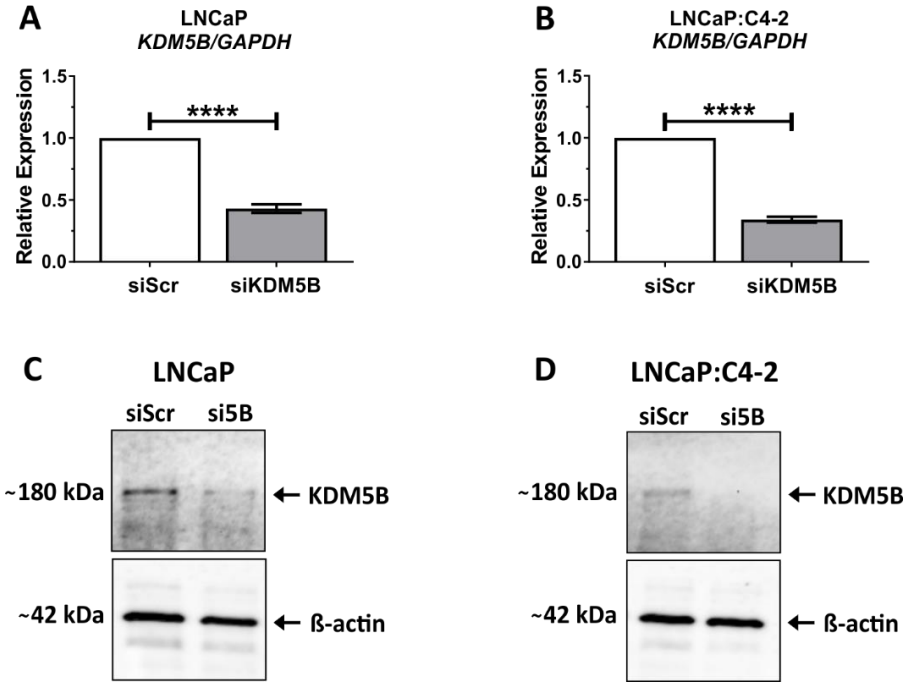

Figure 3.12: Confirmation of siRNA-mediated knockdown of KDM5B on the RNA and protein level in LNCaP and LNCaP:C4-2.
qRT-PCR analysis (n = min. 9) and western blot (n = 3 in Appendix 7) analysis was used to confirm KDM5B knockdown. Both LNCaP (**A, C**) and LNCaP:C4-2 (**B, D**) cells exhibited strongly reduced mRNA and protein KDM5B levels through siKDM5B mediated silencing. siScr = siScramble, si5B = siKDM5B, * = $p \leq 0.05$; **$p \leq 0.005$; *** = $p \leq 0.001$; **** = $p \leq 0.0001$ by paired t-test.

To determine if the addition of androgen (R1881, 1 nM) influenced *KDM5B* mRNA expression of siKDM5B treated LNCaP and LNCaP:C4-2 cells, qRT-PCR analysis was performed (**Figure 3.13**). Both the siKDM5B treatment and the androgen treatment were performed simultaneously for a period of three days. Both in LNCaP and LNCaP:C4-2, siRNA targeting KDM5B achieved ~60-70% ($p \leq 0.05$) knockdown in R1881 treated samples (**Figure 3.13, A** and **Figure 3.13, B** respectively).

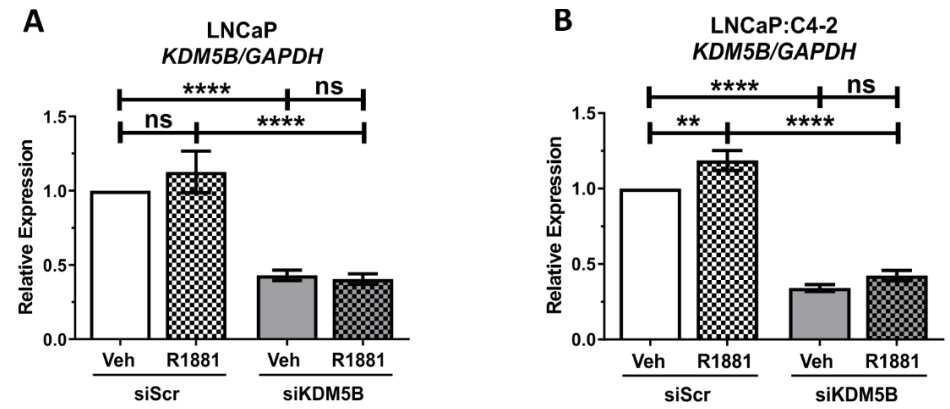

Figure 3.13: Effect of R1881 on siRNA-mediated *KDM5B* knockdown in LNCaP and LNCaP:C4-2.
KDM5B mRNA expression was analysed by qRT-PCR (n = 12). In both LNCaP (**A**) and LNCaP:C4-2 (**B**), *KDM5B* was significantly knocked down also in R1881 treated samples. * = $p \leq 0.05$; **$p \leq 0.005$; *** = $p \leq 0.001$; **** = $p \leq 0.0001$ by ANOVA with Bonferroni's post hoc test.

To investigate if the siRNA-mediated KDM5B knockdown had an effect on the expression of androgen regulated genes, qRT-PCR analysis was conducted on *PSA* and *transmembrane serine protease 2 (TMPRSS2)* mRNA expression (Figure 3.14). As shown previously, R1881 induced *PSA* 4.6-fold ($p \leq 0.05$) in LNCaP. SiRNA depletion resulted in a modest (20%) though statistically significant ($p \leq 0.05$) reduction in androgen induction of PSA in LNCaP (Figure 3.14, A) but not in LNCaP:C4-2 (Figure 3.14, B). Expression of *TMPRSS2* was unchanged by KDM5B depletion (Figure 3.14, C-D).

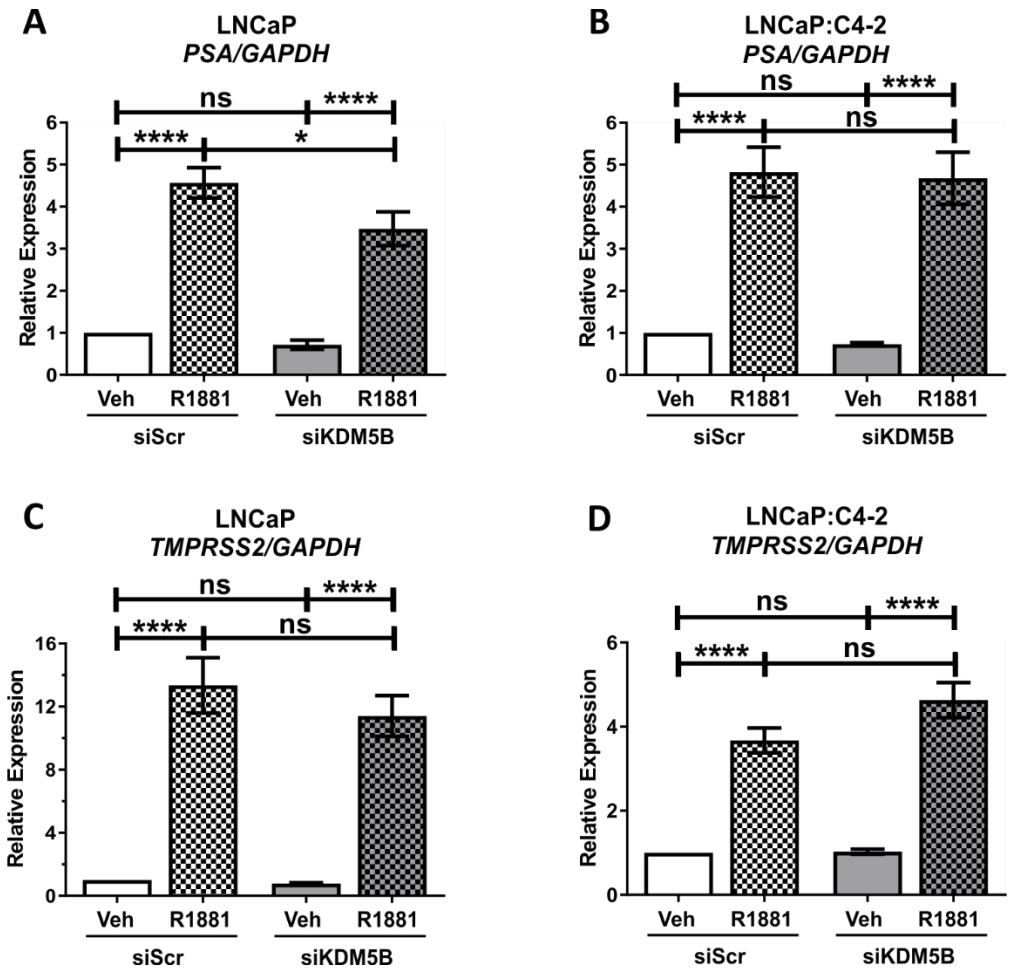

Figure 3.14: Effect of KDM5B knockdown on *PSA* and *TMPRSS2* expression in LNCaP and LNCaP:C4-2. qRT-PCR analysis was used to measure *PSA* and *TMPRSS2* mRNA. KDM5B knockdown slightly but significantly attenuated R1881-induced *PSA* expression in LNCaP cells (A), whereas in LNCaP:C42 cells siKDM5B had no effect on PSA (B) (n = 11). R1881-induced *TMPRSS2* expression was affected by siKDM5B neither in LNCaP (C) nor in LNCaP:C4-2 (D) (n = 12). * = $p \leq 0.05$; **$p \leq 0.005$; *** = $p \leq 0.001$; **** = $p \leq 0.0001$ by ANOVA with Bonferroni's post hoc test.

The effect of siRNA-mediated KDM5B knockdown was tested on two androgen-regulated genes, *VEGFA* and *NADH dehydrogenase ubiquinone 1 alpha subcomplex subunit 4-like 2 (NDUFA4L2)* which are involved in angiogenesis (**Figure 3.15**). R1881-induced 3.4-fold induction of *VEGFA* mRNA was modestly (20%) but significantly ($p \leq 0.05$) attenuated by KDM5B knockdown in LNCaP cells (**Figure 3.15, A**), whereas in LNCaP:C4-2 cells *VEGFA* was unchanged (**Figure 3.15, B**). In LNCaP cells, *NDUFA4L2* mRNA expression was 2.6-fold increased ($p \leq 0.05$, t-test) upon R1881 and was further elevated (1.5-fold) by siKDM5B, however not statistically significantly (**Figure 3.15, C**). In contrast, *NDUFA4L2* did not change in LNCaP:C4-2 (**Figure 3.15, D**).

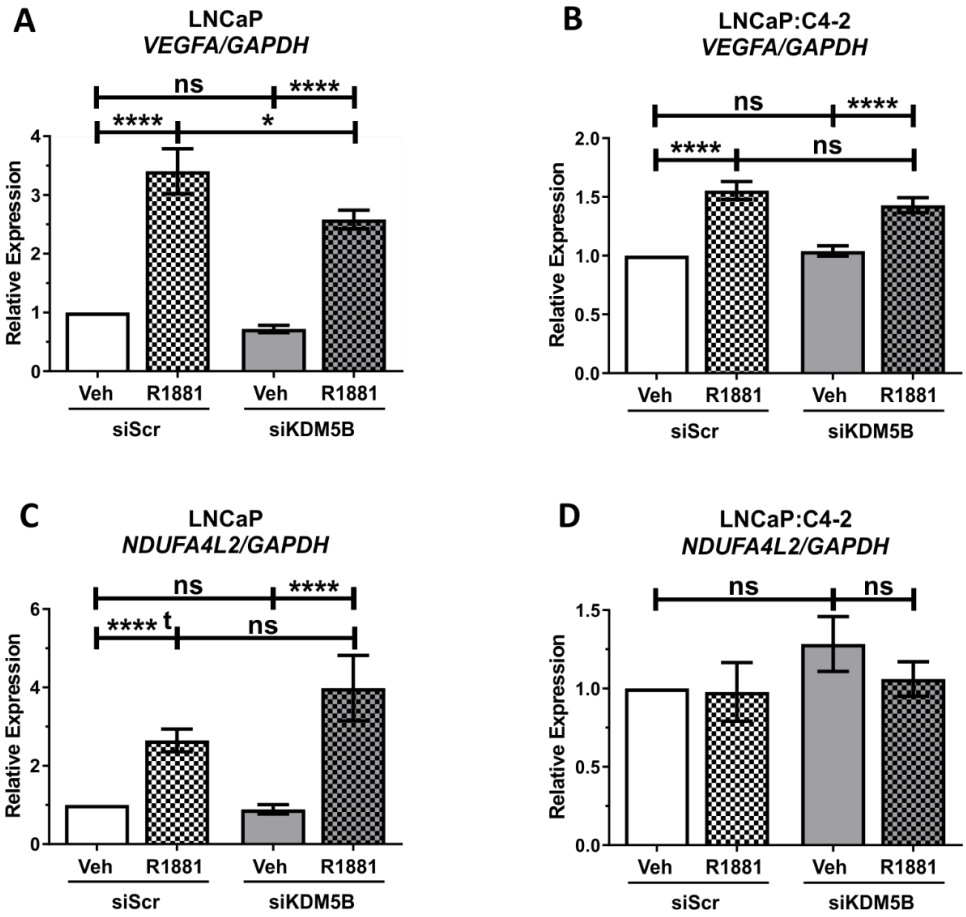

Figure 3.15: Effect of KDM5B knockdown on *VEGFA* and *NDUFA4L2* expression in LNCaP and LNCaP:C4-2.

VEGFA and *NDUFA4L2* mRNA expression were measured by qRT-PCR. KDM5B knockdown slightly but significantly attenuated R1881-induced *VEGFA* expression in LNCaP cells (**A**), whereas in LNCaP:C42 cells siKDM5B had no effect on *VEGFA* (**B**) (n = 12). R1881-induced *NDUFA4L2* expression was not significantly affected by siKDM5B either in LNCaP (**C**) or in LNCaP:C4-2 (**D**) (n = min 8). * = $p \leq 0.05$; **$p \leq 0.005$; *** = $p \leq 0.001$; **** = $p \leq 0.0001$ by ANOVA with Bonferroni's post hoc test.

In addition to LNCaP and LNCaP:C4-2 cells, the effect of functional depletion of KDM5B was tested in an androgen-independent prostate cancer cell line, PC3 which expresses little or no AR (Figure 3.16). Gene expression changes of *VEGFA*, *Hypoxia-inducible factor 1-alpha (HIF-1α)* and *NDUFA4L2*, which are involved in angiogenesis, were examined (Minton et al., 2016). SiRNA-mediated depletion of KDM5B resulted in ~60% ($p \leq 0.05$) knockdown of *KDM5B* mRNA in PC3 cells (Figure 3.16, A). KDM7A depletion resulted in a modest (30%) though statistically significant ($p \leq 0.05$) reduction of *VEGFA* (Figure 3.16, B). In contrast, *HIF-1α* and *NDUFA4L2* did not change (Figure 3.16, C-D). Because the aim of this study was to elucidate the role of KDM5B in androgen signalling, further experiments were focused on the androgen-sensitive cell lines LNCaP and LNCaP:C4-2.

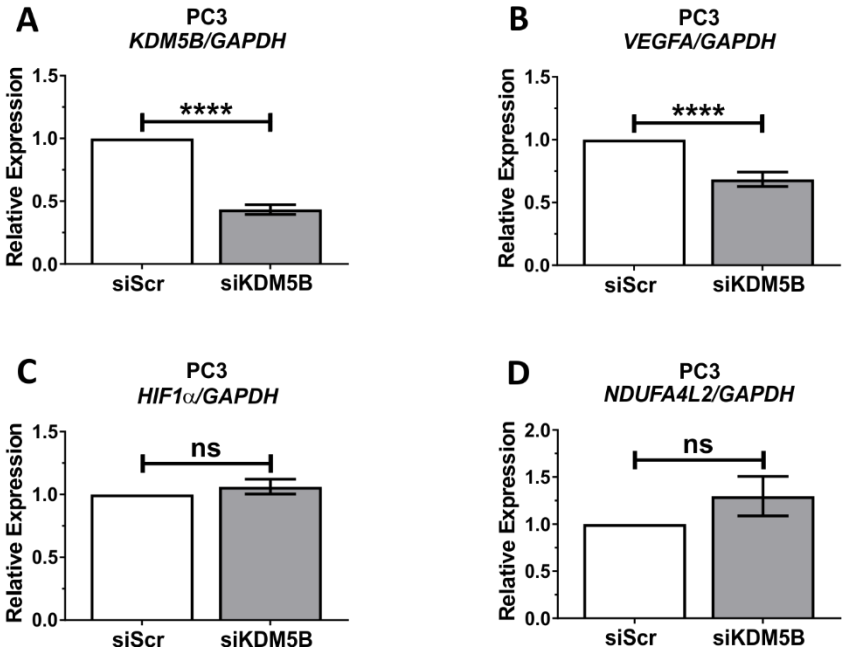

Figure 3.16: Effect of KDM5B knockdown on the expression of angiogenesis-related genes in PC3. Gene expression changes were examined using qRT-PCR. (**A**) Knockdown efficiency of *KDM5B* via siRNA was 60% (n = 12). (**B**) *VEGFA* mRNA expression (**B**) was significantly decreased through KDM5B knockdown (n = 12), (**C-D**) whereas no effect was observed on *HIF1α* (n = 9) and *NDUFA4L2* (n = 6) expression. * = $p \leq 0.05$; **$p \leq 0.005$; *** = $p \leq 0.001$; **** = $p \leq 0.0001$ by paired t-test.

3.2.6 KDM5B-selective pharmaco-inhibitors attenuate R1881-induced *PSA* expression

The role of KDM5B in androgen signalling was not only examined by siRNA-mediated KDM5B depletion but also by applying KDM5B-selective pharmacological inhibitors (Sayegh et al., 2013, Vinogradova et al., 2016). To do this, LNCaP and LNCaP:C4-2 cells were simultaneously treated with androgen (R1881, 1 nM) and the KDM5B-selective inhibitors PBIT (25 µM) and CPI-455 (25 µM) respectively for 3 days (Figure 3.17). PBIT selectively

inhibits KDM5B (IC_{50} 3 µM) over other members of the KDM5-family (KDM5A IC_{50} 6 µM, KDM5C IC_{50} 4.9 µM, KDM5D IC_{50} 28 µM). Compared to PBIT, CPI-455 inhibits KDM5B with an even higher selectivity for KDM5B (IC_{50} 0.003 µM) over other KDM5 family members (KDM5A IC_{50} 0.01 µM, KDM5C IC_{50} 0.014 µM). The effect of the KDM5B inhibitors on R1881-induced *PSA* expression was analysed using qRT-PCR analysis. Treating LNCaP cells PBIT (25 µM) lead to 30% reduction ($p \leq 0.05$) of R1881-induced *PSA* (Figure 3.17, A). In contrast, PBIT did not have any effect in LNCaP:C4-2 (Figure 3.17, B). These results were consistent with the siRNA experiments where *PSA* expression was affected in LNCaP but not LNCaP:C4-2 (Figure 3.14Figure 3.17, A-B). Interestingly, R1881-induced *PSA* was unchanged in LNCaP cells after CPI-455 (25 µM) treatment (Figure 3.17, C), whereas in LNCaP:C4-2, CPI-455 reduced R1881-induced *PSA* expression by 35% ($p \leq 0.05$) (Figure 3.17, C).

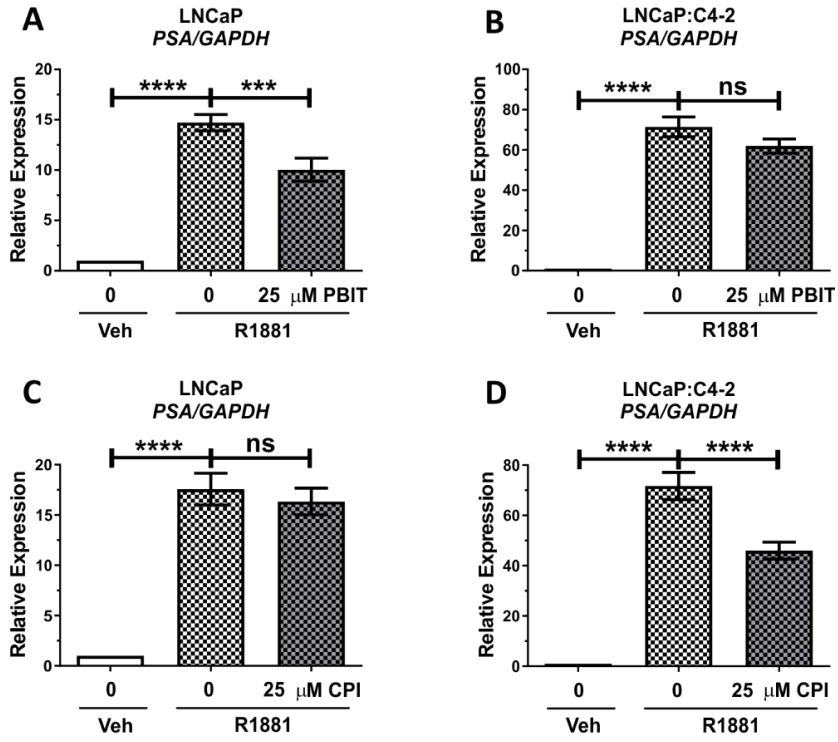

Figure 3.17: Effect of KDM5B-selective inhibitors on *PSA* expression in LNCaP and LNCaP:C4-2.
Gene expression changes were measured by qRT-PCR. (**A**) In LNCaP cells, 25 µL PBIT significantly reduced *PSA* expression 0.7-fold (n = 6), whereas (**B**) in LNCaP:C4-2 cells no change in *PSA* was observed (n = 12). * = $p \leq 0.05$; **$p \leq 0.005$; *** = $p \leq 0.001$; **** = $p \leq 0.0001$ by paired t-test.

To test if a higher inhibitor concentration could inhibit *PSA* in both LNCaP and LNCaP:C4-2, cells were treated with a higher concentration of the highly selective KDM5B inhibitor CPI-455 (50 µM). Androgen-sensitive cell lines LNCaP, LNCaP:C4-2 and 22Rv1 were simultaneously treated with androgen (R1881) and CPI-455 (50 µM) and the effect on *PSA* and *VEGFA* expression was analysed by qRT-PCR (Figure 3.18: Effect of KDM5B-selective inhibitor CPI-455 on androgen-induced *PSA* and *VEGFA* expression in androgen-sensitive PCa cell lines., A-F). In both LNCaP and LNCaP:C42, CPI-455 decreased R1881-induced *PSA* by 80-90% ($p \leq 0.05$) (Figure 3.18, A-B). In contrast, CPI-455 did not have any effect on *PSA* in 22Rv1 (Figure 3.18, C). Interestingly, CPI-455 increased (2.6-fold and 1.7-fold respectively, $p \leq 0.05$) *VEGFA* expression in LNCaP and LNCaP:C4-2 (Figure 3.18, D-E). On the other hand, *VEGFA* was not affected by CPI-455 in 22Rv1 cells (Figure 3.18, F).

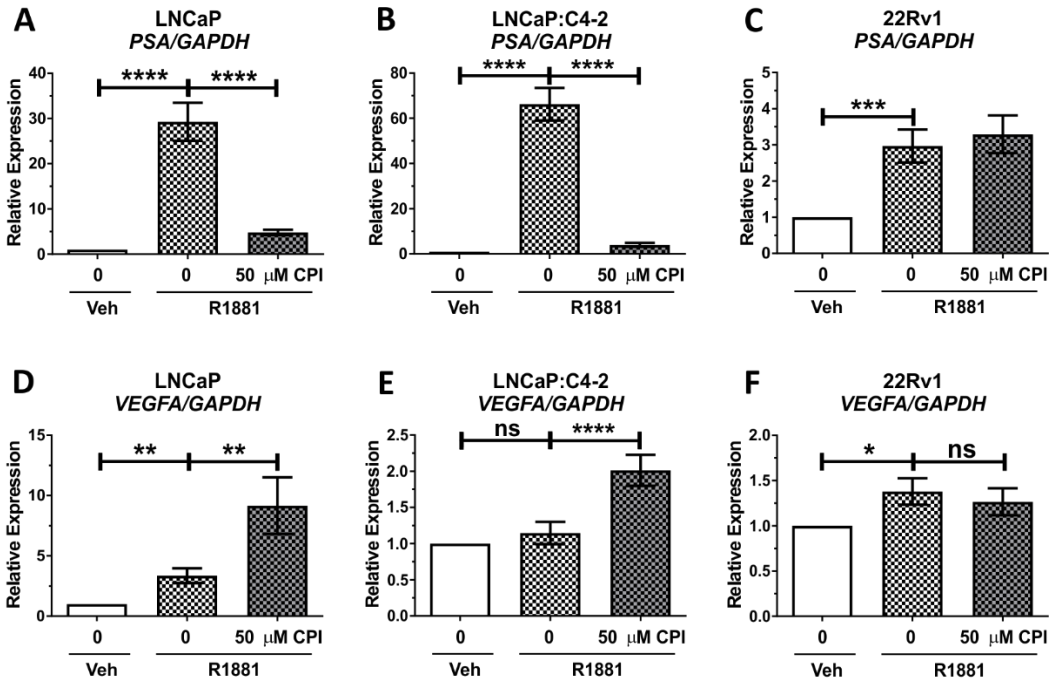

Figure 3.18: Effect of KDM5B-selective inhibitor CPI-455 on androgen-induced *PSA* and *VEGFA* expression in androgen-sensitive PCa cell lines.

The mRNA expression levels of *PSA* and *VEGFA* were analysed via qRT-PCR. CPI-455 (50 µM) inhibited *PSA* expression in LNCaP (n = 6) (**A**) and LNCaP:C4-2 (n = 9) (**B**) but not in 22Rv1 (n = 6) (**C**). *VEGFA* was elevated in LNCaP (n = 6) (**D**) and LNCaP:C4-2 (n = 12) (**E**) but stayed the same in 22Rv1 (n = 6) (**F**) upon CPI-455 treatment. * = $p \leq 0.05$; **$p \leq 0.005$; *** = $p \leq 0.001$; **** = $p \leq 0.0001$ by paired t-test.

3.2.7 CPI-455 attenuates R1881-induced expression of various androgen-responsive genes

To further examine the effect of KDM5B-selective inhibitor CPI-455 on the transcriptome of LNCaP cells, RNA sequencing (RNA-Seq) analysis was performed. The RNA-Seq was conducted in duplicates with androgen (R1881, 1 nm) and DMSO treated control samples and androgen and CPI-455 (50 µM) treated samples in **Figure 3.18 A, D**. Heatmap analysis was used to present differentially expressed genes (**Figure 3.19** and **Figure 3.20**). For the heatmaps a selected list of AR-regulated genes (1359 genes in total) was used (Sharma et al., 2013). The gene counts of the RNASeq analysis were log2 converted and unsupervised hierarchical gene clustering was applied by Nigel Mongan. The treatment of androgen and CPI-455 induced a lower gene expression in most AR-regulated genes compared to the androgen and DMSO control (**Figure 3.19**). Only a small subset of genes was upregulated. In addition, the sample "CPI-455_2" exhibited lower gene expression than "CPI-455_1" overall. To investigate the genes that are in the same hierarchical cluster as *KLK3/PSA*, the *KLK/PSA* containing cluster was analysed in more detail (**Figure 3.20**). Genes with oncogenic (yellow), tumour suppressive (blue) and dual (orange) functions in PCa are highlighted.

To validate RNASeq data, qRT-PCR analysis was performed. The log fold change (logFC) of the genes tested is given in **Table 3.2.** In addition, the logFC of *KDM1A* and *KDM5B* is depicted, however, these were not confirmed by qRT-PCR. As already described, CPI-455 (50 µM) induced a decreased *PSA* (**Figure 3.18, A**) and increased *VEGFA* gene expression (**Figure 3.18, D**) according to qRT-PCR analysis, which is conform with the RNASeq logFC for those genes (**Table 3.2**). In addition, the logFC of *TMPRSS2*, *FOXA1*, *NKX3.1* and *AR* was confirmed by qRT-PCR analysis (**Figure 3.21**). The effect of CPI-455 on these genes was additionally examined in LNCaP:C4-2 cells, as a comparison to LNCaP cells (**Figure 3.21**). R1881-induced *TMPRSS2* expression was reduced by ~50% ($p \leq 0.05$) in LNCaP (**A**) and by ~30% in LNCaP:C4-2 (**B**) though not statistically significantly (**Figure 3.21**). *FOXA1* was moderately (~15%) but not statistically significantly attenuated in LNCaP (**C**), whereas in LNCaP:C42 *FOXA1* was decreased by 45% ($p \leq 0.05$) (**D**). CPI-455 treatment reduced androgen induction of NKX3.1 by ~80% ($p \leq 0.05$) and ~45% ($p \leq 0.05$) in LNCaP and LNCaP:C-42 respectively (**Figure 3.21, E-F**). In both LNCaP and LNCaP:C4-2, *AR* expression was not induced by R1881 but was significantly decreased by ~80% ($p \leq 0.05$) upon CPI-455 treatment in LNCaP cells (**G**). In contrast, CPI-455 had no effect on *AR* expression in LNCaP:C4-2 (**Figure 3.21, H**). To sum up, RNASeq logFC could be validated for the genes

PSA, *TMPRSS2*, *NKX3.1* and *AR* by qRT-PCR and thus confirmed CPI-455 attenuation of androgen-induced expression in these genes in LNCaP cells.

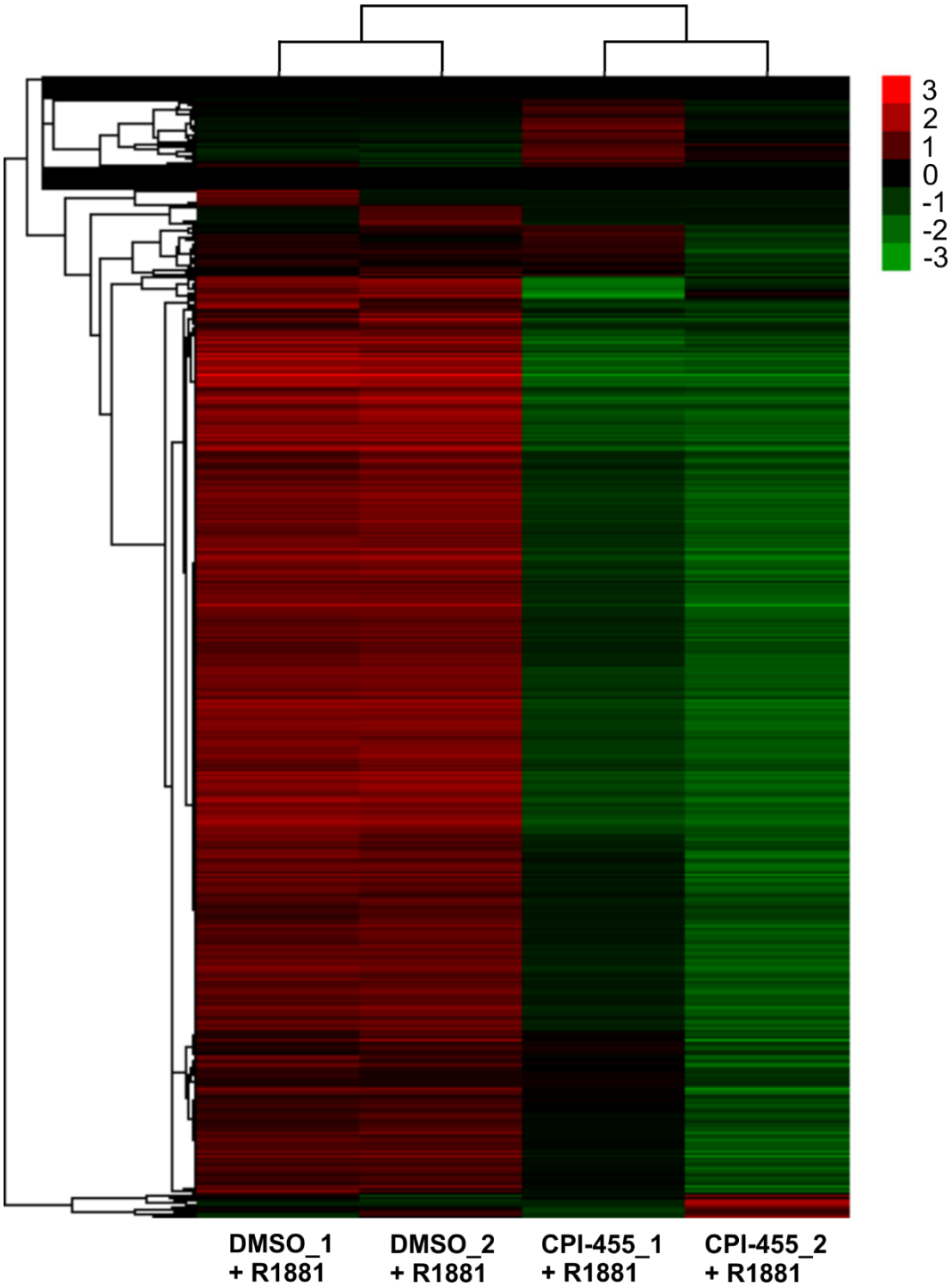

Figure 3.19: Heat map analysis of AR-regulated genes in CPI-455 treated LNCaP cells.
Androgen (R1881, 1 nM) and Namoline + TC-E 5002 treated samples were compared with androgen (R1881, 1 nM) and DMSO control samples and the differentially expressed genes (as log2) are depicted. High gene expression is coloured as red, whereas low gene expression is depicted in green. The majority of genes is down-regulated upon CPI-455 treatment in LNCaP cells compared to the DMSO control, and only a small subset of genes is up-regulated. (Heatmap created by Nigel Mongan)

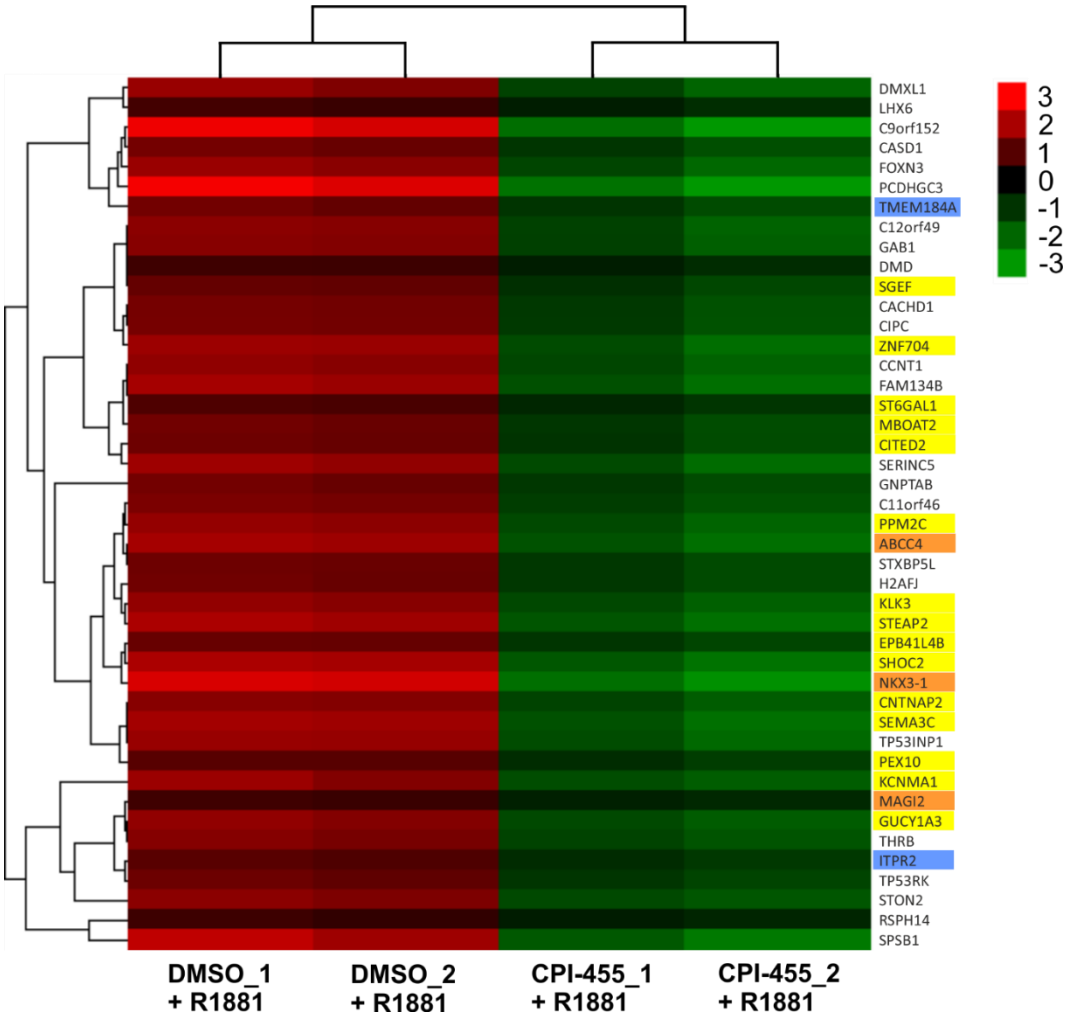

Figure 3.20: Detailed KLK3/PSA hierarchical cluster in LNCaP.
The cluster, which contains *KLK3/PSA*, of the heatmap in Figure 3.19 is shown in more detail. Genes with oncogenic functions in PCa are highlighted in yellow, tumour suppressors in blue, and genes with dual role in PCa are highlighted in orange.

Table 3.2: RNASeq gene expression logFC in CPI-455 treated LNCaP cells.
The logFC was determined by comparing androgen (R1881, 1 nM) and CPI-455 (50 µM) treated samples with androgen and DMSO treated control samples. Negative values represent down-regulated genes, whereas positive values represent up-regulated genes. For example, *KLK3/PSA* is decreased by 1.768-log fold in CPI-455 treated samples compared to the DMSO control. The FDR is depicted for each gene and coloured in red if statistically significant. FC = fold change; FDR = false discovery rate

Gene	ID	logFC	FDR
KLK3/PSA	ENSG00000142515	-1.768	≤ 0.05
VEGFA	ENSG00000112715	0.338	0.188
TMPRSS2	ENSG00000184012	-0.775	≤ 0.05
FOXA1	ENSG00000129514	-2.808	≤ 0.05
NKX3.1	ENSG00000167034	-3.503	≤ 0.05
AR	ENSG00000169083	-2.476	≤ 0.05
KDM1A	ENSG00000004487	0.430	0.066
KDM5B	ENSG00000117139	-1.193	≤ 0.05

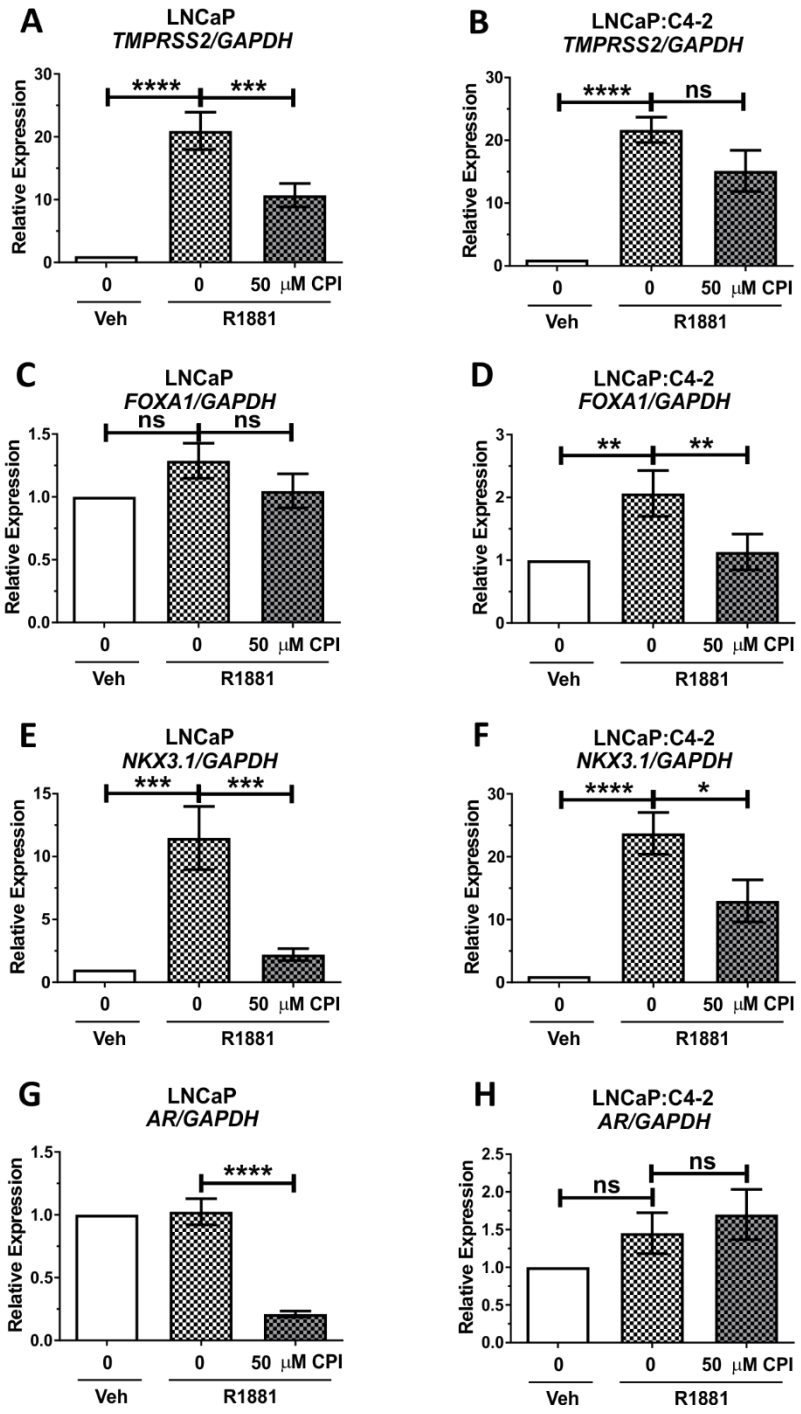

Figure 3.21: Validation of RNASeq gene counts by qPCR analysis in LNCaP and comparison to LNCaP:C4-2.

LNCaP and LNCaP:C4-2 cells were treated with androgen (R1881, 1 nM) and 50 μM CPI-455 for 3 days and gene expression changes were analysed by qRT-PCR (n = min 6). R1881-induced *TMPRSS2* expression was attenuated by CPI-455 in both LNCaP (**A**) and LNCaP:C4-2 (**B**). *FOXA1* was decreased in LNCaP:C4-2 (**D**) but not in LNCaP (**C**). In both cell lines CPI-455 attenuated R1881-induced *NKX3.1* expression (**E-F**). *AR* was reduced by CPI-455 in LNCaP (**G**) but not LNCaP:C4-2 cells (**H**). * = $p \leq 0.05$; **$p \leq 0.005$; *** = $p \leq 0.001$; **** = $p \leq 0.0001$ by ANOVA with Bonferroni's post hoc test.

To elucidate the effect of CPI-455 (50 µM) on the gene regulation in cancer related pathways in LNCaP cells, pathway analysis was performed using the Kyoto Encyclopedia of Genes and Genomes (KEGG) pathway database (**Figure 3.22**) (https://www.genome.jp/kegg/pathway.html, accessed 17.07.2019) (Kanehisa, 2019, Kanehisa and Goto, 2000, Kanehisa et al., 2019). For this analysis, only genes that exhibited a logFC ≥1 (up-regulated genes) and ≥-1 (down-regulated genes) were included. Within these filtration criteria, 6626 genes were up-regulated and 5416 genes down-regulated after CPI-455 treatment in LNCaP cells. The KEGG pathway database analysis revealed that many of the down-regulated genes are involved in various cancer pathways (**Figure 3.22, coloured green**), including the mTOR signalling pathway, PI3K-Akt signalling pathway, cAMP signalling pathway, VEGF and HIF-1 signalling pathway, TGF-β signalling pathway, cytokine-cytokine receptor interactions and adherens junctions (**Figure 3.22, coloured yellow**). In contrast, some genes involved in the cancer related pathways were up-regulated (**Figure 3.22, coloured red**) and other genes showed to be both up- and down-regulated (**Figure 3.22, coloured blue**). The reason for this is because some protein families, such as Wnt, comprise several members. For example, Wnt10 and Wnt16 were up-regulated, whereas Wnt4, Wnt5, Wnt7 and Wnt8 were down-regulated through CPI-455 treatment. Overall, the KEGG cancer pathway analysis revealed that the treatment of CPI-455 in LNCaP cells dysregulated several important cancer pathways.

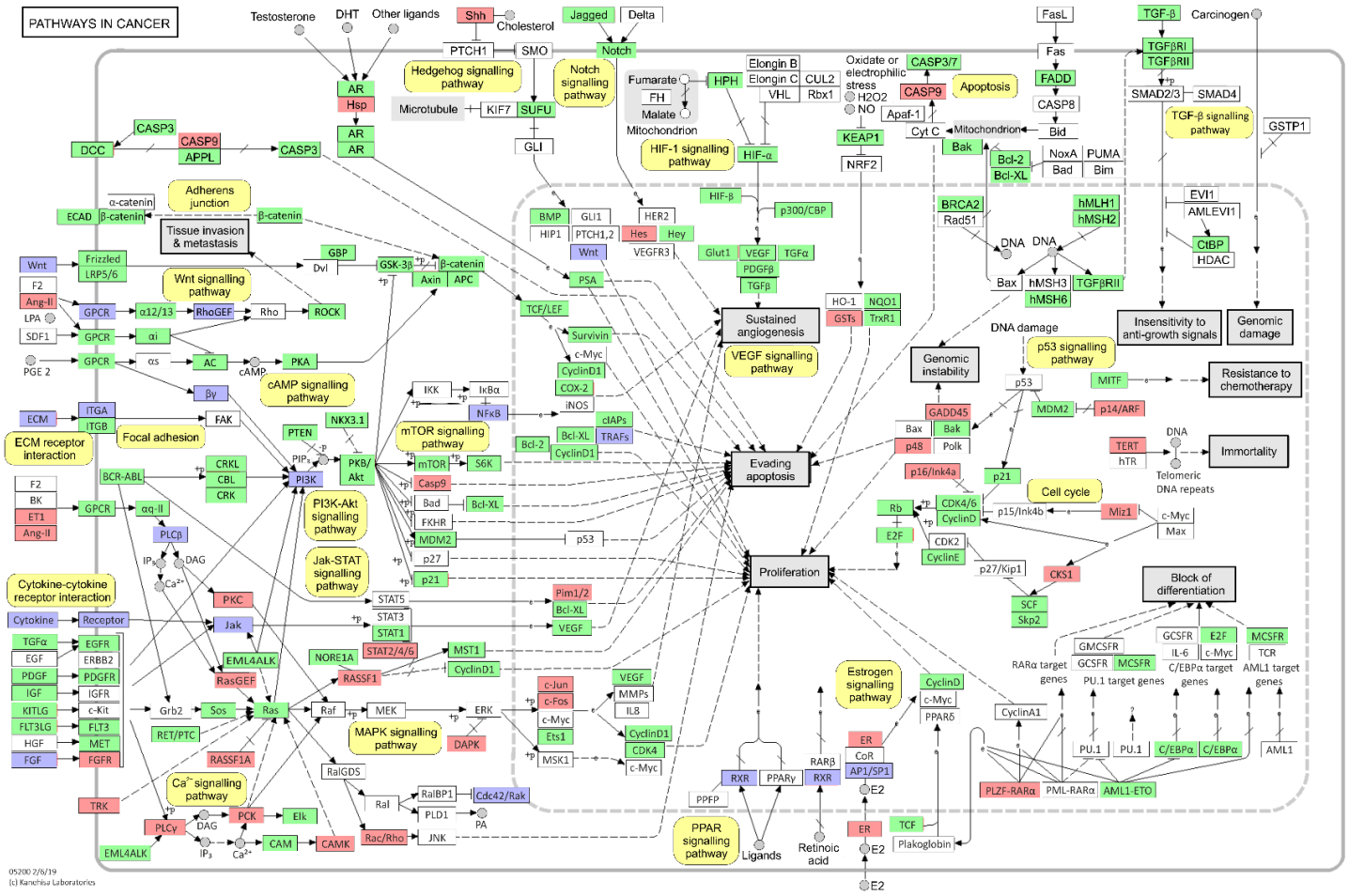

Figure 3.22: Gene regulation of cancer pathways in CPI-455 treated LNCaP cells.
Up-regulated genes are indicated in red, down-regulated genes are green and blue stands for both up- and down-regulation (https://www.genome.jp/kegg/pathway.html, accessed 17.07.2019).

3.2.8 KDM5B-selective inhibitors reduce cell proliferation of prostate cancer cells

The effect of KDM5B-selective inhibitors, PBIT and CPI-455, on malignant and non-malignant prostate cell proliferation was tested using the CyQUANT™ Cell Proliferation Assay which quantifies cells by measuring the DNA content (**Figure 3.23**). DNA content was measured after 3 and 6 days of treatment with 10 μM PBIT and 50 μM CPI-455 respectively. Statistical significances were calculated in comparison to untreated control cells using t-test (**Figure 3.23**). In non-malignant PNT1A, cell proliferation was not affected by PBIT and modestly (20%, $p \leq 0.05$) increased by CPI-455 after 3 days (**Figure 3.23, A**). After 6 days though, PNT1A proliferation was 50-60% decreased by both PBIT and CPI-455. LNCaP cell proliferation decreased from 20-40% to 60-70% ($p \leq 0.05$) by KDM5B-selective inhibitors (**Figure 3.23, B**). In LNCaP:C4-2 and 22Rv1, cell proliferation was reduced ~40-60% after 3 days but did not further decrease after 6 days (**Figure 3.23, C-D**). PC3 cell proliferation was not affected by KDM5B-selective inhibitors after 3 days but was 20% and 50% ($p \leq 0.05$) reduced by PBIT and CPI-455 respectively after 6 days (**Figure 3.23, E**). In Du145, PBIT decreased cell proliferation by 50-60% ($p \leq 0.05$) after 3 and 6 days (**Figure 3.23, F**). Like in PC3, in Du145 CPI-455 seemed to exhibit a stronger effect than PBIT with a 50% ($p \leq 0.05$) reduction in proliferation after 3 days and 80% ($p \leq 0.05$) reduction after 6 days.

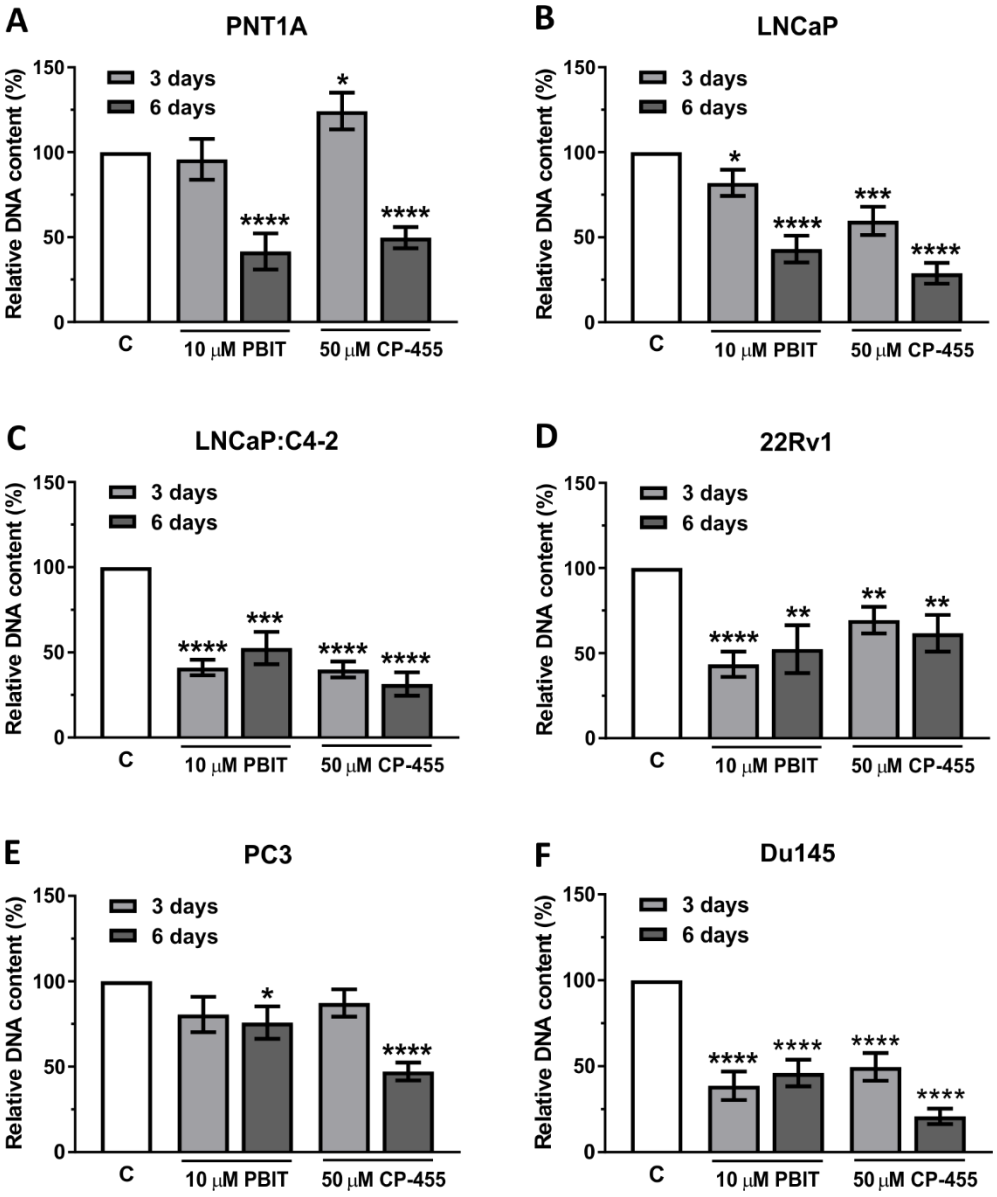

Figure 3.23: Effect of KDM5B-selective inhibitors on cell proliferation of normal prostate and PCa cell lines.

The CyQUANT™ assay was performed to assess cell proliferation after 3 days and after 6 days of inhibitor treatment. Statistical significances were calculated in comparison to the untreated control cells (white column) (n = 18). (**A-F**) All cell lines showed reduced proliferation upon PBIT and CPI-455 treatment. PNT1A (**A**) and PC3 (**E**) proliferation was reduced after 6 days only, whereas LNCaP (**B**), LNCaP:C4-2 (**C**), 22Rv1 (**D**) and Du145 (**F**) cell numbers were already affected after 3 days. * = $p \leq 0.05$; **$p \leq 0.005$; *** = $p \leq 0.001$; **** = $p \leq 0.0001$ by paired t-test.

3.3 Discussion

Currently, the exact role of KDM5B in androgen signalling is not clear. KDM5B has been shown to directly interact with the androgen receptor and even though it has been reported to be up-regulated in PCa, indicating an oncogenic function (Xiang et al., 2007,. Li et al., 2015a), KDM5B also seems to have a tumour suppressive role in PCa (Lu et al., 2015b). The aim of this study was to further elucidate the role of KDM5B in androgen signalling in PCa.

Bioinformatic analysis using the cBioPortal for Cancer Genomics revealed that *KDM5B* gene expression is altered in about a third of PCa patients, whereas half of these patients exhibit low *KDM5B* mRNA levels and the other half high *KDM5B* mRNA levels. Interestingly, the *KDM5B* gene was amplified more frequently in patients with metastatic prostate adenocarcinoma, suggesting an oncogenic function in CRPC (Cerami et al., 2012). KDM5B was highly amplified in neuroendocrine PCa (NePC) patients (~ almost one third of patients), however, since the focus of this study was the role of KDM5B in androgen signalling and the AR is absent in NePC cells (Bonkhoff, 2001), KDM5B in NePC was not further investigated in this study, however, would be interesting to do in future studies.

According to the cBioPortal, KDM5B is not as heavily mutated in PCa as other cancer types, such as breast, bladder, colorectal, lung, skin and head and neck (https://www.cbioportal.org/, accessed 13.08.2019) (Cerami et al., 2012). KDM5B mutations in these cancer types mainly occur in the ARID, PLU-1, JmjC, and PHD2 domain, as well as between the domains. Only five different mutations were found in PCa patients (**Figure 3.2**). In contrast to lung and breast cancer, where most mutations cause a gain or amplification in copy number, none of the mutations found in PCa change the diploid copy number. Two PCa patients, one with metastatic and one with neuroendocrine PCa, exhibited the same mutation, namely Lys158Arg, in the ARID domain of KDM5B (**Table 3.1**). This mutation can be caused by a single point mutation (AAA→AGA or AAG→AGG). Since the mutation is in the ARID domain, this could influence the DNA binding properties of KDM5B (Scibetta et al., 2007, Tu et al., 2008). Both lysine and arginine are basic amino acids, which are positively charged, and play a crucial role in protein stability, being mainly found at the surface of proteins forming electrostatic interactions, such as salt-bridges and hydrogen bonds (Yokota et al., 2006). However, the guanidinium group of arginine enables it to form more electrostatic interactions than lysine, which could influence the protein

stability of KDM5B and give KDM5B an advantage during PCA progression (Sokalingam et al., 2012).

Interestingly, whilst the PHD2 domain in KDM5B seems to be heavily mutated in cancer, PHD3 harbours only few mutations and PHD1 almost none (https://www.cbioportal.org/, accessed 13.08.2019) (Cerami et al., 2012). PHD1 preferably binds H3K4me0, but also H3K4m1, and PHD3 preferably binds H3K4me3, but also H3K4me2/me1, whereas PHD2 has not been shown to bind histones (Klein et al., 2014, Zhang et al., 2014c). In prostate cancer, one mutation was found in the PHD3 domain (Arg1534His) which is likely to be the result of a single point mutation (CGU→CAU or CGC→CAC) (**Figure 3.2** and **Table 3.1**). The mutation Arg→His is common in cancer and is suggested to be an adaptive response to an increased intracellular pH (Szpiech et al., 2017, White et al., 2017). Both arginine and histidine are basic amino acids, however, the pKa of arginine is higher than that of histidine, i.e. whilst arginine is positively charged, histidine is titratable and therefore a better pH sensor (Szpiech et al., 2017). Cancer cells have a higher pH than non-malignant cells which facilitates metabolic adaptation, cancer cell proliferation, migration and invasion (Webb et al., 2011). The amino acid switch Arg→His therefore provides cancer cells with a selective advantage in a higher pH environment. Interestingly, in bladder urothelial carcinoma, a mutation in the same location (1534aa) was found, however, the amino acid change was arginine to isoleucine, potentially through a single point mutation (AGA→AUA), which lead to a gain of copy number (Gao et al., 2018b, Hoadley et al., 2018, Taylor et al., 2018). Mutations in the PHD3 domain could also change KDM5B's selectivity to target specific methylation levels of H3K4, since PHD3 was shown to preferably bind H3K4me3 (Klein et al., 2014, Zhang et al., 2014b). Mutations in the PHD3 domain have been shown to disrupt or decrease the interaction of KDM5B with H3K4me3 before (Klein et al., 2014).

Two mutations, one missense, Asp972Gly (most probably caused through a single point mutation, GAC→GGC), and one splice site mutation (X1028), were found in the PLU-1 domain (**Figure 3.2** and **Table 3.1**). Aspartate has a negatively charged side chain, whereas glycine is uncharged and the smallest amino acid. KDM5B mutations in the PLU-1 domain may influence DNA binding and/or interactions with nucelar receptors, such as the androgen receptor, since it harbours several LxxLL motifs (Heery et al., 1997, Horton et al., 2016, Lu et al., 1999). Interestingly, mutations at the position 1028 have been found in stomach and esophageal cancer where glutamine (CAA or CAG) was mutated into a stop

codon (UAA or UAG), leading to a nonsense mutation (Liu et al., 2018, Network, 2017, Sanchez-Vega et al., 2018, Taylor et al., 2018).

The fifth mutation, found in a metastatic prostate cancer patient, was a frame shift deletion of four amino acids (Ser1119Ala*4) between the PLU-1 and PHD2 domain (**Figure 3.2** and **Table 3.1**). This frame shift deletion in KDM5B was found in five patients with other types of cancers (two patients with stomach, two patients with esophageal and one patient with Pancoast lung cancer), indicating Ser1119Ala*4 is a common KDM5B mutation in cancer (Campbell et al., 2016, Liu et al., 2018, Network, 2017, Sanchez-Vega et al., 2018, Taylor et al., 2018). In stomach and lung cancer, KDM5B is responsible for cancer cell proliferation and invasion (Bao et al., 2016, Shen et al., 2015). Similarly, in esophageal cancer, KDM5B facilitates cancer cell growth and the maintenance of cancer stem cells (Kano et al., 2013). Interestingly, this frame shift deletion does not necessarily have to affect the enzymatic function of KDM5B, as it still harbours the ARID, JMjC, PLU-1 domain. However, the shortened amino acid sequence is likely to affect the structure of KDM5B and may affect its PHD2 and PHD3 domain. A study, which compared mutations in PHD1 and PHD3, showed that KDM5B suppressed cell migration in the human breast cancer cell line MDA-MB 231 and that the recognition of H3K4me0 by PHD1 is crucial for that, whereas the recognition of H3K4me3 was not needed (Klein et al., 2014). This study provides an example of how KDM5B uses its PHD domains for different functions.

If KDM5B is an oncogene, it does not exert its oncogenic function through copy number gain, because the *KDM5B* copy number is not altered in the majority of PCa patients. Around ~5-6% of PCa patients exhibited a low copy number amplification and not even ~1% of patients had a heterozygous *KDM5B* deletion. This raises the question whether *KDM5B* expression is up-regulated on a transcriptional and/or translational level in PCa. We therefore investigated *KDM5B* mRNA expression in PCa cell lines and KDM5B protein expression in both PCa cell lines and human PCa tissue specimens. Both androgen dependent (LNCaP) and androgen-independent (LNCaP:C4-2, 22Rv1, PC3) cell lines had higher *KDM5B* mRNA levels than the human non-malignant prostate cell line PNT1A, with LNCaP exhibiting the highest *KDM5B* expression and LNCaP:C4-2 the second highest, followed by 22Rv1 and PC3 (**Figure 3.8, A**). The same trend was observed by Nilsson and colleagues (2013) where *KDM5B* mRNA levels gradually decreased from LNCaP, over LNCaP:C4-2, to PC3 cells, however, they used primary prostate epithelial cells (PRECs) as a non-malignant prostate control cell line and PRECs exhibited the same KDM5B mRNA

expression level as LNCaP cells. In contrast, PNT1A is an immortalised cell line which expresses AR but not PSA, as a result of growing PNT1, which used to express both AR and PSA, for more than 75 passages (Cussenot et al., 1991, Degeorges et al., 1995). It is interesting that PSA expression is absent in PNT1A, which is concomitant with an apparently lower *KDM5B* expression level than in PREC. Similar to the results of this study, another study found that *KDM5B* mRNA expression is elevated in the prostate cancer cell lines LNCaP, 22Rv1, PC3 and Du145, with 22Rv1 exhibiting the highest expression, compared to the control cell line WPMY-1, which is a non-malignant myofibroblast stromal cell line derived from the prostate (Li et al., 2015a). The overexpression of *KDM5B* mRNA in PCa is consistent with two studies that examined *KDM5B* expression using microarray analysis and confirmed *KDM5B* up-regulation in PCa (Li et al., 2015a, Xiang et al., 2007). Additionally, it was found that *KDM5B* is expressed at even higher levels in metastatic PCa (Xiang et al., 2007). In contrast to the *mRNA* expression levels, KDM5B protein expression was only up-regulated in LNCaP cells compared to non-malignant PNT1A cells, and was even down-regulated in the CRPC cell lines 22Rv1, PC3 and Du145 (**Figure 3.8, A**). The possibility, that KDM5B may mainly be regulated at the translational level rather than the transcriptional level in PCa, has already been suggested by Li and colleagues (2015) and could be an explanation for the discrepancy between mRNA and protein KDM5B levels.

A tissue microarray (TMA) was constructed to investigate KDM5B protein levels in PCa specimens and revealed that nuclear KDM5B protein was expressed at a lower level in PCa tissue specimens (n = 97) compared to normal, non-malignant PCa specimens (n = 43) (**Figure 3.5, G**). This contradicts a study where KDM5B protein expression was detected at high levels in frozen prostate cancer tissue samples (n = 10) by western blot analysis, whereas KDM5B was not detectable in benign prostate hyperplasia tissue samples (n = 4) (Xiang et al., 2007). In that western blot analysis, the same antibody was used as was used in the TMA of this study, however, the sample size of the western blot analysis was very small and the nuclear fraction was not analysed separately from the cytoplasmic fraction in the western blot, i.e. the differences in nuclear KDM5B may be influenced by the presence of cytoplasmic KDM5B. In addition, the bands for KDM5B in the western blot analysis seem to vary in intensity between the PCa samples (Xiang et al., 2007), indicating KDM5B protein expression differs from patient to patient. However, in our study, KDM5B staining did not correlate with age, Gleason score, perineural invasion or biochemical recurrence (**Appendix 6**). Surprisingly, low KDM5B expression correlated with extraprostatic extension which equals TNM stage T3 (**Figure 3.7**). Unlike the study by Xiang

et al. (2007), our results suggests a tumour suppressive role of KDM5B. Even though KDM5B is described to be an oncogene in many types of cancer, it was shown to have a tumour suppressive function in the migration of breast cancer cells before (Han et al., 2017, Klein et al., 2014). Cell migration and invasion assays, such as the scratch assay and Boyden chamber assay, will have to be performed to investigate if KDM5B has a tumour suppressive role in PCa cell migration and invasion (Justus et al., 2014).

Androgen signalling has long been recognised to elicit and promote PCa (Banerjee et al., 2018, Cunha et al., 1987, Heinlein and Chang, 2004). The androgen used in this study was Methyltrienolone (R1881) which is a synthetic androgen. R1881 and another synthetic androgen, called Mibolerone, have the advantage over 5α-dihydrotestosterone (5aDHT) that they cannot be metabolised and only very weakly bind the sex hormone binding protein (Bonne and Raynaud, 1975, Bonne and Raynaud, 1976, Liao et al., 1973, Schilling and Liao, 1984). All androgen treatments in this study were performed with 1 nM R1881 for 72 hours, which has shown to be effective on androgen signalling (Kashyap et al., 2013, Metzger et al., 2005, Nilsson et al., 2015). The androgen-responsiveness in androgen-sensitive PCa cell lines (LNCaP, LNCaP:C4-2 and 22v1) was confirmed by determining *PSA* mRNA expression after R1881 treatment and as expected, all androgen-sensitive cell lines exhibited an increased *PSA* expression upon R1881 (**Figure 3.9**). The lowest R1881-induced *PSA* expression (~2.5-fold) was seen in 22Rv1, whereas *PSA* was increased almost ~100-fold in LNCaP:C4-2.The reason for the high induction of *PSA* during qRT-PCR analysis is due to low *PSA* basal expression levels in the vehicle control of LNCaP:C4-2 (**Figure 3.9, B**). To exactly determine and compare the basal *PSA* expression levels in LNCaP, LNCaP:C4-2 and 22Rv1, qualitative RT-PCR analysis would have to be performed.

The effect of R1881 in the prostate cancer cell lines was further tested on another androgen-regulated gene, namely *VEGFA* (Eisermann and Fraizer, 2017) (**Figure 3.10**). As shown before, R1881 (1 nM) induces increased *VEGFA* mRNA expression in LNCaP (Kashyap et al., 2013), which is concomitant with the qRT-PCR experiment in this study (**Figure 10, B**). Interestingly, R1881 did not have any effect on *VEGFA* in the androgen-sensitive but independent cell lines LNCaP:C4-2 and 22Rv1 (**Figure, C-D**), indicating *VEGFA* gene expression may be regulated in an androgen independent manner in these cell lines. In a study, where 22Rv1 was treated with a higher R1881 concentration (5 nM), *VEGFA* mRNA was up-regulated (Eisermann et al., 2013), suggesting *VEGFA* regulation may depend on how high androgen levels are.

Since prostate cancer is an AR-regulated disease, it is important to understand the role of KDM5B in androgen signalling. Xiang et al. (2007) have shown by co-immunoprecipitation that KDM5B directly interacts with the AR, and that KDM5B promotes the transcription of the AR-regulated genes in a dose-dependent manner by using luciferase assay. These results suggest that androgen-dependent activation of AR-regulated genes need KDM5B as a co-activator. It was of interest if there is an AR-KDM5B feedback mechanism, i.e. if *KDM5B* mRNA expression is regulated by the androgen signalling pathway. However, the addition of R1881 (1 nM) to normal and prostate cancer cell lines did not have any effect on *KDM5B* mRNA expression (**Figure 3.11**), suggesting AR does not regulate *KDM5B* gene expression.

As already mentioned, Xiang et al. (2007) showed that the enzymatic activity of KDM5B is important for androgen induced and AR-regulated *PSA* expression by performing luciferase assays with KDM5B mutants that lack the JmjC domain. These luciferase assays were performed in LNCaP cells (Xiang et al., 2007). To further elucidate the role of KDM5B in androgen signalling at different stages in PCa progression, knockout experiments were performed in LNCaP (androgen-dependent) and LNCaP:C4-2 (androgen-independent) cells, and the effect on androgen-regulated genes examined. The *KDM5B* mRNA and protein were successfully knocked-down by siRNA-mediated depletion after 72 hours in both LNCaP and LNCaP:C4-2 cells (**Figure 3.12**), however, the effect on R1881-induced *PSA* and *VEGFA* expression was surprisingly modest in LNCaP cells (**Figure 3.14, A** and **Figure 3.15, A**). In LNCaP:C4-2 cells, the knockdown of KDM5B did not have any effect on R1881-induced *PSA* or *VEGFA* gene expression, suggesting KDM5B may only play an important role in androgen signalling in early stage, androgen-dependent PCa, or a more effective inhibition of KDM5B is necessary to achieve an effect on AR-regulated gene expression in LNCaP:C4-2. Similarly, the siRNA-mediated knockdown of *KDM5B* in the AR-negative cell line PC3 affected *VEGFA* expression only very modestly (**Figure 3.16, B**).

In contrast to siRNA-mediated KDM5B depletion, functional inhibition through KDM5B-selective pharmaco-inhibitors, such as PBIT and CPI-455, attenuated R1881-induced *PSA* expression in an inhibitor dose-dependent manner in LNCaP and LNCaP:C4-2 cells (**Figure 3.17**). Interestingly, these two cell lines seemed to have a different susceptibility towards PBIT and CPI-455, with 25 μM PBIT modestly inhibiting R1881-induced PSA in LNCaP but not in LNCaP:C4-2, and vice versa, 25 μM CPI-455 having a modest effect on LNCaP:C4-2

but not LNCaP (**Figure 3.17**). However, at 50 µM CPI-455, R1881-induced *PSA* expression was dramatically attenuated (~80-90%) in both LNCaP and LNCaP:C4-2 (**Figure 3.18, A-B**). The siRNA and inhibitor results suggest, that the inhibition of KDM5B is dependent on the concentration and duration of inhibition. For example, siRNA-mediated depletion takes longer to have an effect on KDM5B protein compared to pharmaco-selective inhibition, which could be a potential explanation why the attenuating effect on R1881-induced *PSA* expression was stronger with CPI-455 than with siRNA-mediated knockdown. Non-selective inhibition of other KDM5 family members by CPI-455 can be largely excluded due to CPI-455's selectivity for KDM5B, with an IC_{50} of 0.003 µM, compared to an IC_{50} of at least 0.01 µM for KDM5A and KDM5C. However, to definitely confirm selective binding of the small molecule CPI-455 to KDM5B, techniques such as mass spectrometry, small molecule microarray and subsequent western blot analysis with antibodies targeting diverse KDM5B family members, would have to be used (Vegas et al., 2008, Vilenchik et al., 2011).

Surprisingly, R1881-induced *VEGFA* expression was further up-regulated by KDM5B pharmaco-selective inhibition in both LNCaP and LNCaP:C4-2 cells (**Figure 3.18, D-E**). An explanation for this could be that KDM5B regulates AR-regulated gene transcription in different ways, either acting as a co-activator or co-repressor, or the up-regulation of *VEGFA* could also be an androgen-independent response to cellular stress, such as the unfolded protein response (UPR) in the endoplasmic reticulum (ER) which is associated with *VEGFA* up-regulation (Ghosh et al., 2010, Lin et al., 2008a, Miyagi et al., 2013, Pereira et al., 2013). Interestingly, the KDM5B-selective inhibitor CPI-455 (50 µM) did not have any effect on *PSA* and *VEGFA* expression in 22Rv1, an androgen-independent cell line which is known to harbour the AR splice variant AR-V7 implicated in CRPC (Dehm et al., 2008, Guo et al., 2009, Henzler et al., 2016). This indicates that KDM5B may not play an important coregulatory role in androgen signalling in prostate cancer cells harbouring ARV7.

To further understand the role of KDM5B in AR-regulated gene transcription in PCa, RNASeq analysis was performed. The transcriptome of LNCaP, which was treated with the KDM5B-selective inhibitor CPI-455 (50 µM) and androgen (R1881, 1 nM) for three days, was analysed and compared to R1881-treated LNCaP control cells. Unsupervised hierarchical clustering was performed with a list of AR-regulated genes identified by a study by Sharma et al. (2013), who performed AR ChIP-seq analysis with the tissue of ten PCa patients (three untreated patients, two ADT responsive patients, five CRPC patients) and two patients with BPH. The majority of the AR-regulated genes in LNCaP was down-

regulated through pharmaco-selective inhibition of KDM5B (**Figure 3.19**). In addition, *AR* was found to be significantly down-regulated by CPI-455 (**Table 3.2**) which was confirmed by qRT-PCR analysis (**Figure 3.21, G**), and which explains the downregulation of AR-regulated genes (**Figure 3.19**). This suggests that KDM5B is involved in *AR* gene regulation in LNCaP. Not surprisingly, *PSA* was significantly down-regulated by CPI-455 treatment (**Table 3.2**).

A further investigation was undertaken to determine the genes which clustered with *PSA* in the hierarchical clustering (**Figure 3.20**). PSA has long been recognised as a marker for PCa diagnosis and the detection of biochemical recurrence and is still widely used (Ilic et al., 2018a, Paul et al., 1995), even though the benefits of PSA screening have been in debate in the last years (Lin et al., 2008b, Vickers, 2017). In a hierarchically clustered heatmap, genes in the same cluster share similar gene expression patterns. Clustering therefore is a useful tool to identify co-expressed genes which may have similar gene regulation and pathways in common (D'haeseleer et al., 2000). *PSA* was clustered with the *six transmembrane epithelial antigen of the prostate 2 (STEAP2)* which is known to drive PCa progression by enhancing proliferation, migration and invasion (Burnell et al., 2018, Whiteland et al., 2014). *PSA* and *STEAP2* in turn were clustered with the histone variant gene H2AFJ, which is altered in other cancer types, such as breast cancer and melanoma, however, to our knowledge, no link to PCa has been discovered yet (Monteiro et al., 2014). The next proximal cluster is comprised of *CC11orf46*, *PPM2C*, *ABCC4* and *STXBP5L*. The *pyruvate dehyrogenase phosphatase catalytic subunit 1* (*PDP1*, also referred to as *PPM2C*) was shown to be amplified and overexpressed in PCa and suggested as a potential target (Chen et al., 2018). The exact role of the multi-drug resistance protein 4 (MRP4, also referred to as ABCC4) in PCa is unclear. A study suggests MRP4 could be a potential target to delay or reverse docetaxel resistance in PCa cells (Li et al., 2017), whereas MRP4 immunohistochemical staining revealed that MRP4 protein gradually decreases over PCa progression (Montani et al., 2013). For the other two genes, the *ADP ribosylation factor like GTPase 14 effector protein* (ARL14EP, also referred to as C11orf46) and *syntaxin binding protein 5 like* (*STXBP5L*), no link to PCa has been reported so far.

The next proximal cluster is compromised of *EPB14L4B*, *SHOC2* and *NKX3.1*. The erythrocyte membrane protein band 4.1 like 4b (EPB41L4B) is involved in cytoskeletal protein binding, influencing cell adhesion and migration, and has been shown to be upregulated in PCa (Schulz et al., 2010). EPB41L4B overexpression is associated with ERG

(ETS-related gene) overexpression, which is a well known oncogene in PCa (Adamo and Ladomery, 2016, Schulz et al., 2010). The leucine rich repeat scaffold protein SHOC2 has very recently been reported to be implicated in the MAPK/ERK signalling pathway and suggested to be an interesting cancer target to selectively inhibit this signalling pathway, opposed to inhibiting core components of the RAF/MAPK/ERK signalling cascade (del Río et al., 2019, Jones et al., 2019). Since the MAPK/ERK signalling pathway is highly implicated in PCa, the inhibition of SHOC2 could be beneficial in PCa patients too (Gan et al., 2010, Rodríguez-Berriguete et al., 2012). The dysregulation of NKX3.1 has long been recognised in PCa, however, its exact role as a tumour suppressor or oncogene remains unclear (Bhatia-Gaur et al., 1999, Bowen et al., 2000, He et al., 1997, Korkmaz et al., 2000). A study by Tan et al. (2011) showed that NKX3.1 is a direct transcriptional target of AR and in turn co-localises with AR and FOXA1 to regulate AR-regulated gene transcription in advanced and recurrent PCa, suggesting a role in PCa progression (Tan et al., 2012). FOXA1 is a pioneer transcription factor, which means that it can directly bind to DNA and is the first to engage at the chromatin of AR target sites (Gao et al., 2003, Lupien et al., 2008, Sekiya et al., 2009). It binds nucleosomes, is a histone code reader and, interestingly, has been shown to be dependent on the distribution of H3K4me2, acting as a coregulator of AR (Lupien et al., 2008, Taslim et al., 2012). It has a dual role in prostate cancer as it acts cell context-dependent and it can either activate or repress AR transcriptional activity (Sahu et al., 2011, Wang et al., 2011). Studies have shown that FOXA1 is highly expressed in localised PCa where it promotes cell cycle and PCa cell growth in an AR-dependent manner (Sahu et al., 2011). On the other hand, it represses cell motility independent of AR and therefore, as PCa progresses, FOXA1 is expressed at low levels to allow for PCa cell motility and epithelial to mesenchymal transition (EMT) to occur, leading to metastasis (Jin et al., 2013). Interestingly, *FOXA1* was significantly downregulated by CPI-455 too, according to the RNASeq analysis (**Table 3.2**), however, this could not be confirmed by qRT-PCR (**Figure 3.21, C**), whilst the downregulation of *NKX3.1* was confirmed by qRT-PCR (**Figure 3.21, E**). The reason for the discrepancy between the RNASeq and qRT-PCR result for *FOXA1* is that in the RNASeq analysis only two samples were analysed (n = 2), whereas in the qRT-PCR analysis six samples were tested (n =6). When only the two samples of the RNASeq were analysed by qRT-PCR, *FOXA1* was down-regulated (**data not shown**), however, for biological conclusions the qRT-PCR result of n = 6 (and ideally more) needs to be considered (Fang and Cui, 2011). Interestingly, in LNCaP:C4-2 cells, qRT-PCR analysis revealed that *AR* was unchanged upon pharmaco-selective inhibition of KDM5B by CPI-455 (**Figure 3.21, H**), however, both *FOXA1* and *NKX3.1* were significantly decreased (**Figure 3.21, D, F**). This

suggests that *AR* gene expression may be dependent on KDM5B in LNCaP cells, but not in LNCaP:C4-2. The mechanisms, through which *NKX3.1* is downregulated in LNCaP and LNCaP:C4-2 cells, appear to be different, but in both cell lines, the *NKX3.1* downregulation is linked to the enzymatic inhibition of KDM5B by CPI-455. For further comparisons, it would be crucial to investigate the transcriptome of LNCaP:C4-2 cells after CPI-455 treatment by RNASeq analysis too.

Another gene, that is closely clustered with *PSA* and *NKX3.,1* is the well-known PCa oncogene semaphorin *SEMA3C*, which is associated with PTEN positive tumours and promotes CRPC and drug resistance (Herman and Meadows, 2007, Li et al., 2013, Peacock et al., 2018, Tam et al., 2017). Many other genes are in neighbouring clusters, which have been shown to be overexpressed in PCa, such as *SGEF* (Wang et al., 2012), *ST6GAL1* (Wei et al., 2016), *CITED2* (Shin et al., 2018), *KCNMA1* (Bloch et al., 2007, Bloch et al., 2004), *GUCY1A3* (Kelly et al., 2016, Zhang et al., 2005), *CNTNAP2* (Love et al., 2009), and *TP53INP1* (Giusiano et al., 2012), and other genes involved in metastatic PCa, such as *ZNF704* (Rubicz et al., 2017), *MBOAT2* (Han et al., 2018, Yan et al., 2017), and *FOXN3* (Tepper and Tsubota, 2013). In addition, some genes closely clustered to PSA have been implicated in other types of cancers, such as *GAB1* (Sang et al., 2013, Wang et al., 2019c), *STON2* (Xu et al., 2018), and *SPSB1* (Feng et al., 2014), but their function in PCa has not been described yet. More research is needed to investigate the genes, whose expression is affected by KDM5B-selective inhibition, however, many genes involved in cancer pathways seem to be downregulated by CPI-455 in LNCaP cells (**Figure 3.22**). Overall, these results indicate an important role of KDM5B in AR-regulated gene expression in LNCaP and confirm its potential as a target in PCa (Xiang et al., 2007).

In addition to AR-regulated gene expression, KDM5B also plays an important role in PCa cell proliferation. Pharmaco-selective inhibition of KDM5B by PBIT and CPI-455 significantly decreased LNCaP and LNCaP:C4-2 cell proliferation (**Figure 3.23, B, C**). After three days of inhibition, cell numbers in LNCaP cells were not as affected as in LNCaP:C4-2 cells, which is likely because LNCaP cells have a longer doubling time than LNCaP:C4-2 (**Table 2.1**). Interestingly, CPI-455 also strongly inhibited cell proliferation of the metastatic CRPC cell line Du145 (**Figure 3.23, F**) (Gilloteaux et al., 2013). On the other hand, PC3, another metastatic CRPC cell line, was most resistant for KDM5B-selective pharmaco-selective inhibitors among the PCa cell lines tested (**Figure 3.23, E**). Both PC3 and Du145 express very low or undetectable levels of AR (Alimirah et al., 2006, Brolin et al., 1992, Culig et al., 1993,

EDELSTEIN et al., 1994, Sramkoski et al., 1999), however, they differ in that PC3 metastasises in the bone whereas Du145 metastasises to the brain (Kaighn et al., 1979, Stone et al., 1978). Interestingly, even though KDM5B-selective inhibition did not have any influence on *VEGFA* and *PSA* gene expression in 22Rv1, cell proliferation was reduced by KDM5B-selective inhibitors (**Figure 3.23, D**), i.e. KDM5B might be relevant in ARv7 positive patients as KDM5B likely has AR independent functions. More research is needed to further elucidate the androgen-independent role of KDM5B in the CRPC cell lines 22Rv1, PC3 and Du145. Interestingly, both KDM5B-selective inhibitors PBIT and CPI-455 did not have any effect on cell proliferation in non-malignant epithelial prostate cells PNT1A after three days of treatment, whilst having an effect on LNCaP, LNCaP:C4-2, 22Rv1 and Du145, representing KDM5B as a promising therapeutic target to treat PCa, whilst having less effect on normal prostate cells (**Figure 3.23, A**). Future experiments will aim to determine the mechanism through which KDM5B-selective inhibitors reduce PCa cell proliferation (Kepp et al., 20011, Vandenabeele et al., 2010).

In summary, the role of KDM5B in androgen signalling appears to be dependent on the stage of PCa, reflected by androgen-dependent and independent cell lines in this study. KDM5B seems to be crucial for *AR* gene regulation, AR-regulated gene expression, such as *PSA*, and PCa cell proliferation in LNCaP cells. On the other hand, KDM5B does not regulate *AR* expression in LNCaP:C4-2 cells, but seems to be involved in AR-regulated gene expression. The qRT-PCR results of this study suggest, that the AR genes, which are regulated by KDM5B, differ between LNCaP and LNCaP:C4-2 cells, indicating KDM5B may change its function as PCa progresses. In metastatic CRPC, KDM5B may exert its oncogenic function through androgen-independent mechanisms, as KDM5B pharmaco-selective inhibition did not have any effect on androgen-regulated genes in 22Rv1, but inhibited 22Rv1 cell proliferation. On the other hand, KDM5B was expressed lower in PCa specimens compared to normal prostate specimens and low KDM5B expression correlated with extraprostatic extension, which indicates a tumour suppressive role of KDM5B. Whilst the function of KDM5B in androgen-dependent PCa could be clarified further by this study, more research needs to go into the role of KDM5B in metastatic CRPC.

Chapter 4: KDM7A in androgen signalling

Chapter 4 KDM7A in androgen signalling

4.1 Introduction

KDM7A has been shown to be implicated in cancer (Osawa et al., 2011, Pan et al., 2015, Kondo et al., 2017, Meng et al., 2019, Xie et al., 2017). However, very little is known about its role in PCa. Nilsson et al. (2015) suggested that KDM7A is part of a coregulator network of the AR in PCa, suggesting a role in androgen signalling. KDM7A is a unique histone demethylase as it demethylates H3K9me2 and H3K27me2 residues. Methylated H3K9 and H3K27 are considered repressive histone marks and therefore KDM7A is generally thought of a transcriptional activator (Black et al., 2012). The methyl mark H3K9 is also demethylated by the extensively studied and well known PCa oncogene KDM1A (Metzger et al., 2005, Wissmann et al., 2007), further emphasising the importance of studying the role of KDM7A in PCa. In addition, in contrast to KDM5B and KDM1A which have been shown to directly interact with the AR (Metzger et al., 2005, Xiang et al., 2007), the interaction between KDM7A and AR remains unclear.

Thus, the hypothesis for this chapter is that KDM7A is required for AR signalling in PCa. To test this hypothesis, the expression of KDM7A was investigated in PCa patients and cell lines. KDM7A knockdown and inhibition experiments aimed to give further insight into its role in AR-regulated gene expression and PCa growth. In addition, the interaction between KDM7A and nuclear receptors was investigated. Collectively, this study aimed to provide more information about the role of KDM7A in AR signalling in PCa. During the course of this study, Lee et al. (2018) provided evidence for a role of KDM7A in AR signalling in PCa, which will be discussed later.

4.2 Results

4.2.1 Bioinformatic analysis of *KDM7A*

To assess *KDM7A* alterations and mutations in prostate cancer patients, bioinformatic analysis was performed (**Figure 4.1**). Using the cBioPortal for Cancer Genomics three studies were analysed as in the previous chapter (**Chapter 4**): (1) The TCGA Provisional Prostate Adenocarcinoma study (n = 499), (2) the SU2C/PCF Dream Team Metastatic Prostate Adenocarcinoma study (n = 444) and (3) the Trento/Cornell/Broad

Neuroendocrine Prostate Cancer study (n = 114). According to the TCGA Provisional Prostate Adenocarcinoma study 33.5% of prostate cancer cases had altered *KDM7A* (**Figure 4.1, A**). To investigate patients with which cancer type (Prostatic adenocarcinoma vs Metastatic prostate adenocarcinoma vs Neuroendocrine carcinoma) harboured most *KDM7A* alterations, a comparative analysis was performed and revealed that the alteration frequency is higher in metastatic prostate adenocarcinoma compared to prostate adenocarcinoma (**Figure 4.1, B**). In prostate adenocarcinoma *KDM7A* was altered in 2.2% of all 499 cases with 6 amplification cases (1.2%), 3 mutation cases (0.6%) and 2 deep deletion cases (0.4%). In metastatic prostate adenocarcinoma *KDM7A* was altered in 4.5% with the majority of cases harbouring amplifications (19 cases, 2.28%) and 1 case a mutation. In neuroendocrine prostate cancer patients *KDM7A* was not altered. When including mRNA expression in the TCGA Provisional prostate adenocarcinoma study (z-score = 1), *KDM7A* was altered in ~33.5% of all 499 prostate cancer patients which was made up of ~19% (96/499) mRNA high, ~12% (60/499) mRNA low, 9 cases with multiple alterations, 1 case with a mutation and 1 case with an amplification (**Figure 4.1, C**).

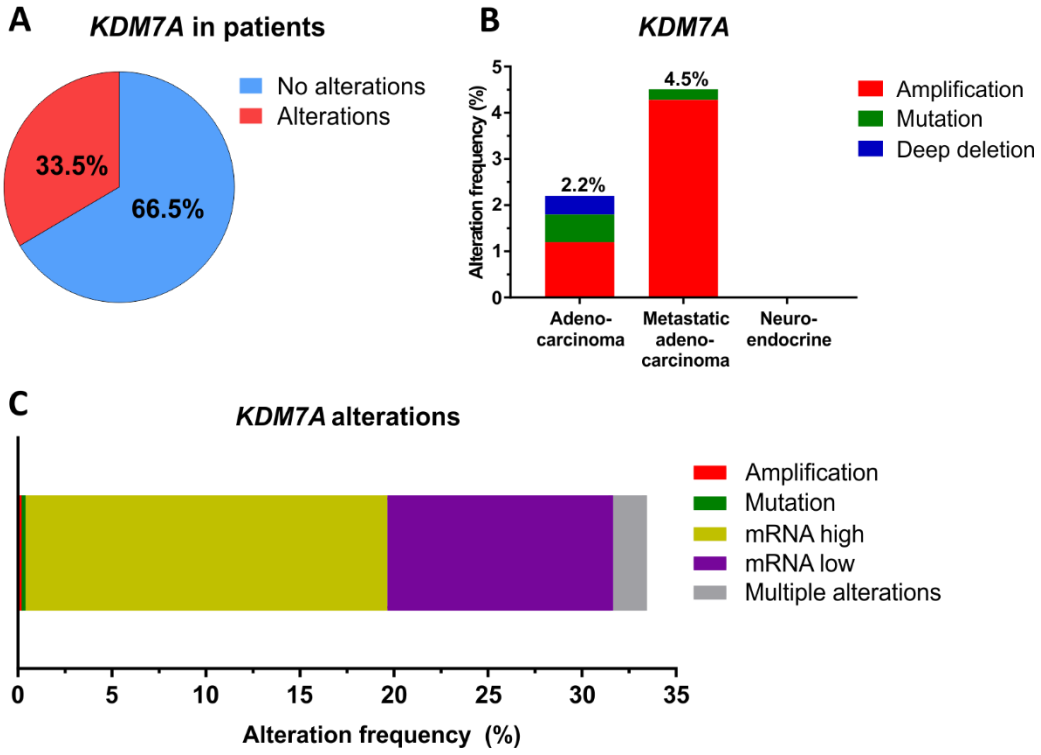

Figure 4.1: *KDM7A* alteration frequencies in prostate cancer patients.
The cBioPortal for Cancer Genomics was used for bioinformatic analysis. (**A**) In 33.5% of prostate cancer patients *KDM7A* was altered. (**B**) The *KDM7A* alteration frequency was highest in metastatic adenocarcinoma (~4.5%) and second highest in prostate adenocarcinoma (2.2%). In neuroendocrine carcinoma cases *KDM7A* was not altered. (**C**) The analysis of the TCGA Provisional Prostate Adenocarcinoma study (mRNA expression z-score=1) resulted in 19.2% mRNA high cases, 12.0% mRNA low cases, 0.2% mutation, 0.2% amplification and 1.8% with multiple alterations.

Regarding mutations, four patients within the three studies (1057 patients) had a mutation in *KDM7A* (**Table 4.1**Table 3.1), three of which had a missense mutation. Two missense mutations were found in prostate adenocarcinoma patients (R913H, **No. 1** and I472M, **No. 2**), which are not located in any functional domains (**Figure 4.2**). One missense mutation was harboured by a metastatic prostate adenocarcinoma patient (E54Q, **No. 4**) which lies in the PHD-finger domain (**Figure 4.2**). The PHD-finger domain in KDM7A is important to recognise and read, but not demethylate, H3K4me3 (Aasland et al., 1995, Li et al., 2006, Sanchez and Zhou, 2011). The mutations I472M and E54Q were also associated with gain of copy number. One prostate adenocarcinoma patient had a frame shift deletion mutation (E70Kfs*24, **No. 3**) in the PHD-finger domain (**Figure 4.2**).

Table 4.1: *KDM7A* mutations in prostate cancer patients.
Information about the study, protein change, mutation type, copy number, allele frequency and number of mutations in the sample were included. The mutations were given a number from 1 - 4 which correspond to the numbers in **Figure 4.2**.

No.	Study	Protein Change	Mutation Type	Copy #	Allele Freq (T)	# Mut in Sample
1	Prostate Adenocarcinoma	R913H	Missense	Diploid	0.42	20
2	Prostate Adenocarcinoma	I472M	Missense	Gain	0.05	18
3	Prostate Adenocarcinoma	E70Kfs*24	FS del	Diploid	0.31	6650
4	Metastatic Adenocarcinoma	E54Q	Missense	Gain	0.11	119

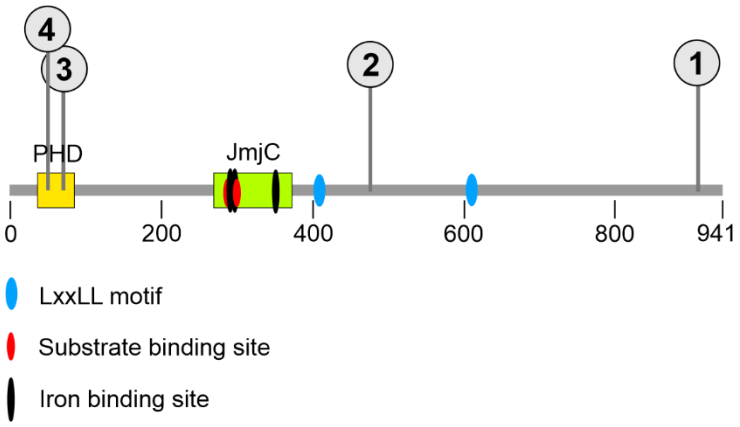

Figure 4.2: Location of KDM7A mutations.
The KDM7A protein spans 941 amino acids and harbours a PHD and a JmjC domain. The mutations were numbered from 1 – 4 and correspond to the mutations in **Table 4.1**. Jmj = Jumonji; PHD = plant homeodomain.

To determine putative *KDM7A* copy number alterations from GISTIC, the TCGA Provisional Prostate Adenocarcinoma study was used (**Figure 4.3**). Most patients were diploid for the *KDM7A* gene. In ~14% of cases *KDM7A* was amplified on a low level (gain) and in 6 cases *KDM7A* was amplified on a high level (amplification). In contrast, only 6 patients harboured

a shallow *KDM7A* deletion (heterozygous deletion) and 2 patients a deep deletion (homozygous). The truncating mutation was in a diploid patient and two missense mutations in a diploid and copy number gain case, respectively.

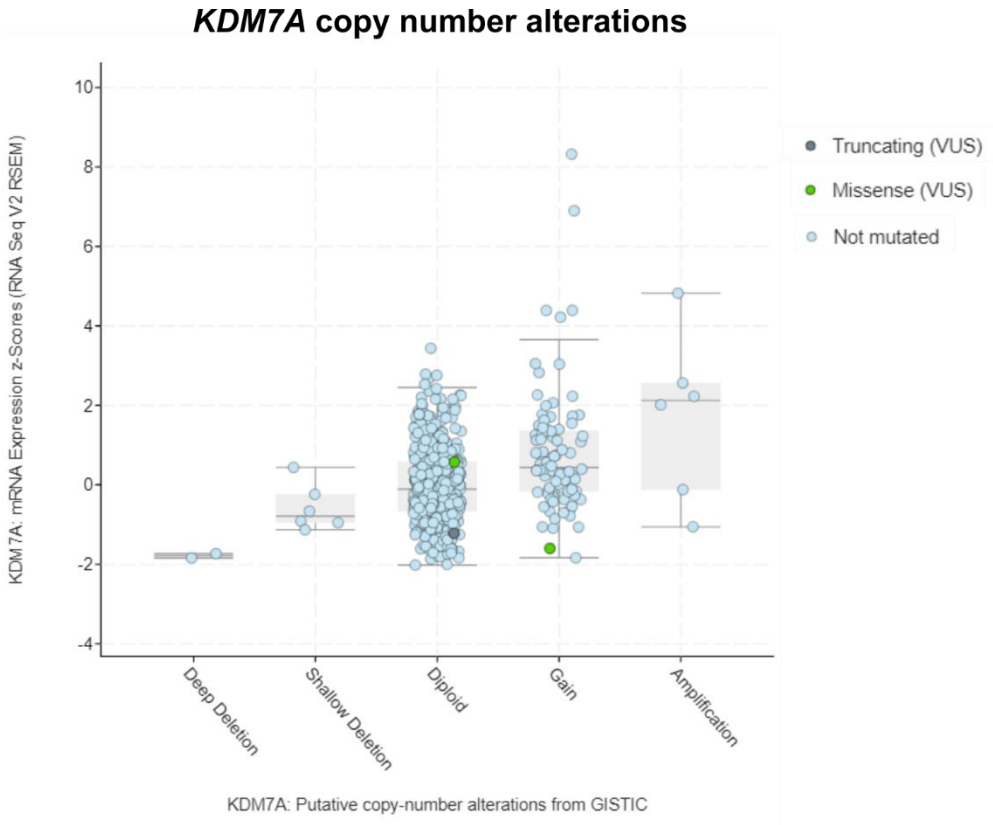

Figure 4.3: *KDM7A* copy number alterations in prostate cancer patients.
Bioinformatic analysis was performed using the cBioPortal for Cancer Genomics (https://www.cbioportal.org/, accessed 12.06.2019). Most prostate cancer patients harboured a diploid *KDM7A* copy number. Around 14% of patients had a low level *KDM7A* amplification (gain) and only a few patients had a deletion or high level amplification.

To investigate if *KDM7A* alterations influenced patient survival, Kaplan-Meier estimates were conducted using the TCGA Provisional Prostate Adenocarcinoma study (z-Score=2). Two parameters were determined, the overall survival and the progression/disease-free survival. The overall survival provides information about how long people lived after treatment, whereas the progression/disease-free survival describes the time between the treatment and clinical evidence of cancer recurrence, specifically, an increase in PSA. Overall survival did not differ between cases with *KDM7A* alterations and without alterations (**Figure 4.4, A**). However, patients with KDM7A alterations had a significantly ($p \leq 0.05$) poorer disease/progression-free survival rate (**Figure 4.4, B**).

A **Overall survival Kaplan-Meier Estimate (z=2)**

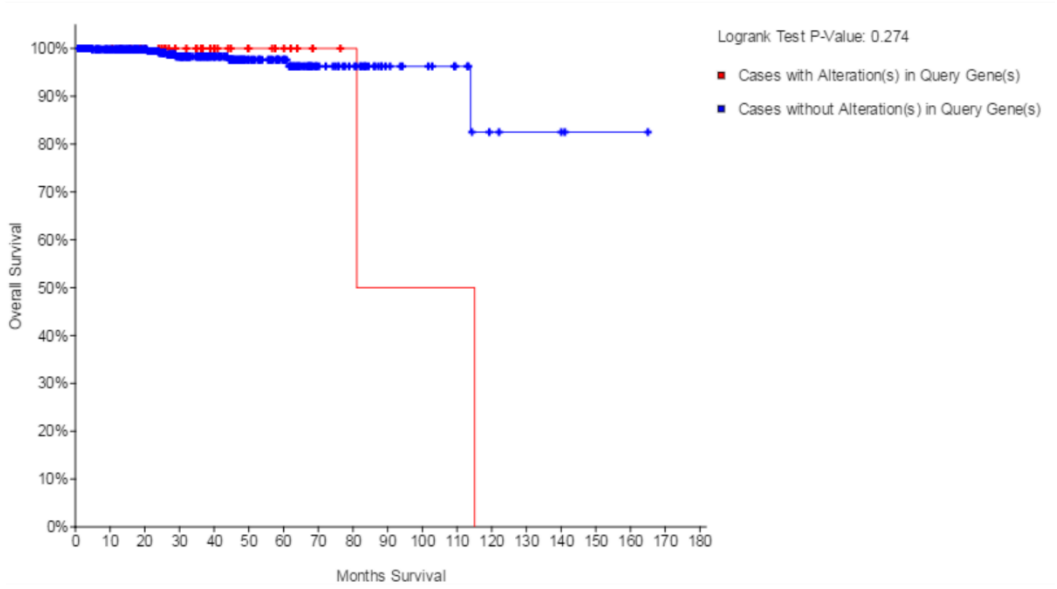

	Number of cases, Total	Number of cases, Deceased
Cases with Alteration(s) in Query Gene(s)	**39**	**2**
Cases without Alteration(s) in Query Gene(s)	**459**	**8**

B **Disease/Progression-free survival Kaplan-Meier Estimate (z=2)**

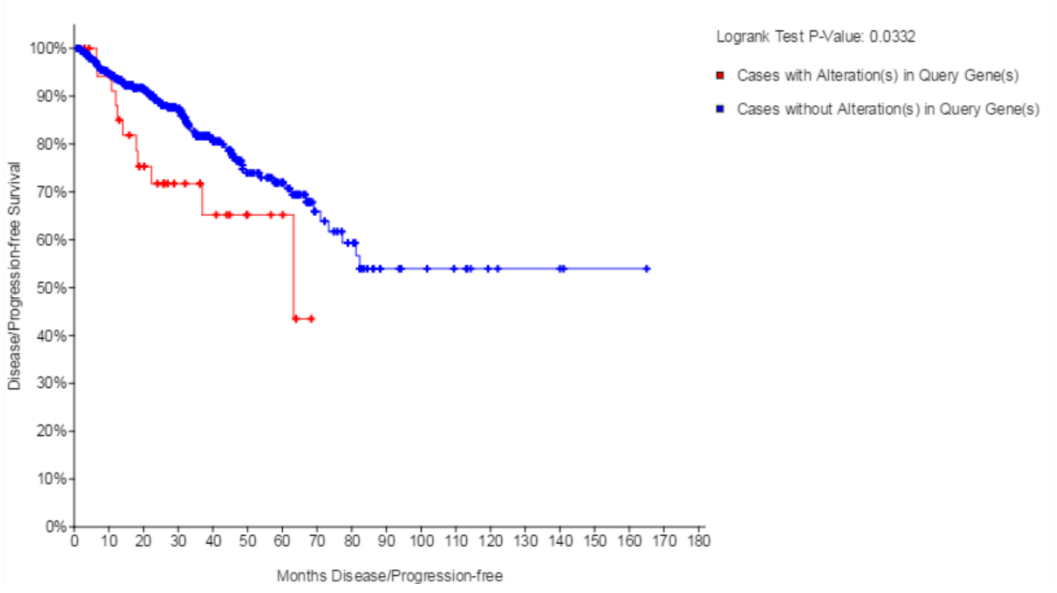

	Number of cases, Total	Number of cases, Relapsed/Progressed
Cases with Alteration(s) in Query Gene(s)	**38**	**11**
Cases without Alteration(s) in Query Gene(s)	**454**	**80**

Figure 4.4: Kaplan-Meier survival estimates regarding *KDM7A* alterations (z-score=2).
The analysis was performed using the cBioPortal for cancer genomics with the TCGA Provisional Prostate Adenocarcinoma study. (**A**) The overall survival of cases with *KDM7A* alterations did not differ from cases without alterations. (**B**) Regarding disease/progression-free survival, there was a significant ($p \leq 0.05$) difference between cases with and without *KDM7A* alterations.

4.2.2 KDM7A staining in human tissue specimens

To determine KDM7A expression in prostate cancer specimens, a tissue microarray (TMA) was constructed and KDM7A protein stained by immunohistochemical (IHC) (**Figure 4.5**). Representative pictures of KDM7A staining in normal prostate tissue (**A, B**), tumour tissue (**C, D**) and less differentiated tumour tissue (**E, F**) are depicted (**Figure 4.5**). As described before, KDM7A staining was scored by H-score and to ensure reliability 10% of the cores was scored by an independent scorer. The Spearman correlation coefficient (R^2) was between ~0.6 – 1 (between "good" and "perfect") and the Cronbach's alpha coefficient was above 0.9, confirming scoring reliability. The distribution curve for the evaluated H-scores across all patients can be found in **Appendix 8**. As before, H-scores were equally divided into three groups (low, medium, high). In both KDM7A nuclear (**G**) and cytoplasmic (**H**) staining there was no significant difference in KDM7A expression between normal and tumour tissue (**Figure 4.5**).

To investigate if KDM7A expression correlates with BCR, a Kaplan-Meier estimate was performed using GraphPad Prism (**Figure 4.6**). Regarding both the nuclear (**A**) and cytoplasmic (**B**) staining, there was no difference in biochemical recurrence free status in patients with low versus high KDM7A expression (**Figure 4.6**).

To examine if there is a relationship between KDM7A expression and clinical patient parameters SPSS analysis was used. KDM7A expression did not correlate with age, TNM, high grade PIN, extraprostatic extension, perineural invasion, pre-OP PSA and BCR (**Appendix 9**). However, high KDM7A nuclear staining correlated ($p \leq 0.05$) with high Gleason scores (Gleason 4+3, 8 and 9) if H-scores were divided into four equal groups (low, medium low, medium high and high staining) (**Figure 4.7, A**). Similarly, cytoplasmic staining correlated ($p \leq 0.05$) with high Gleason scores (**B**). KDM7A nuclear staining correlated ($p \leq 0.05$) with KDM7A cytoplasmic staining (**Figure 4.7, C**).

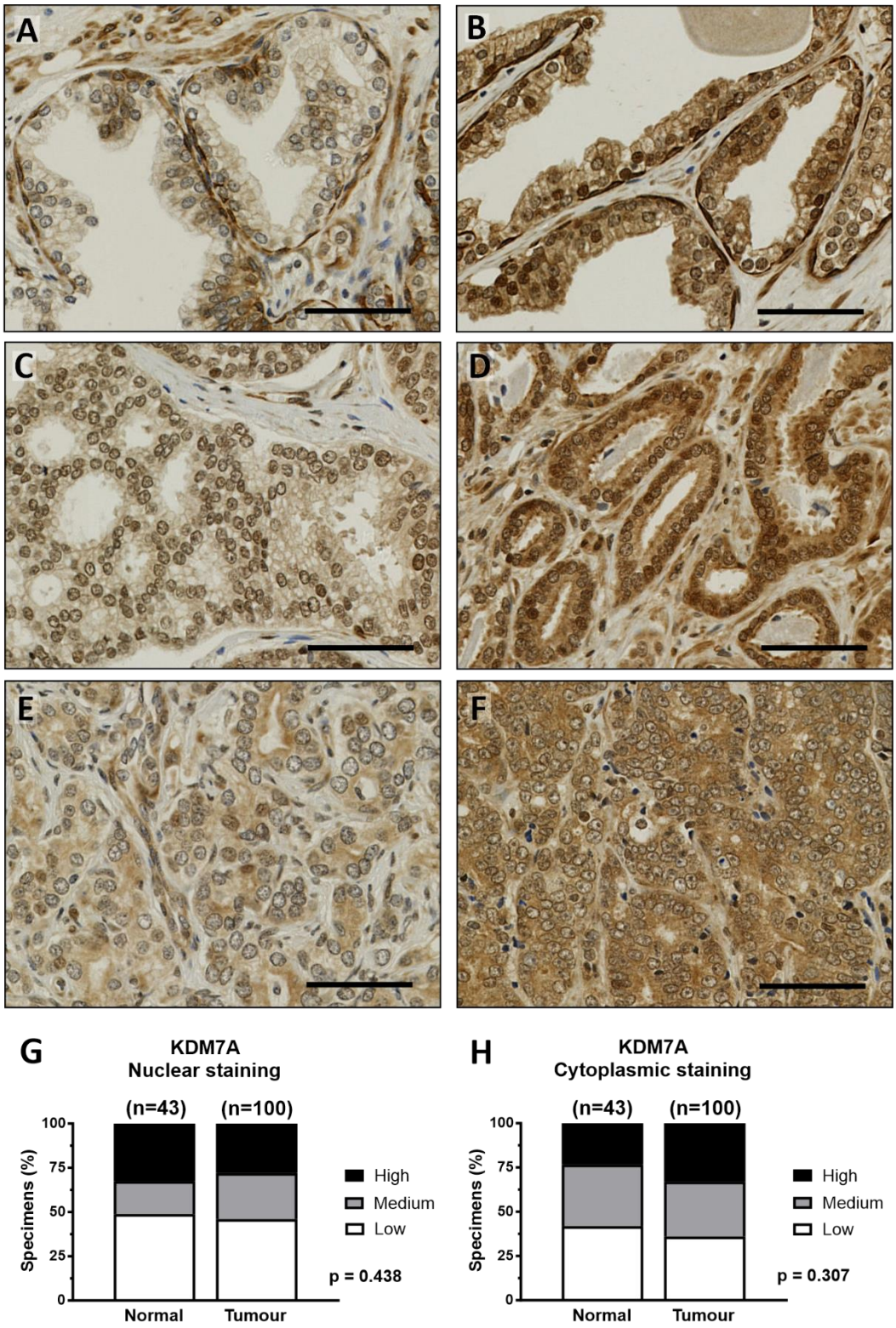

Figure 4.5: Immunochistochemical staining of KDM7A in PCa specimens.
Immunohistochemistry was used to determine KDM7A staining in non-malignant (n = 43) and malignant (n = 100) PCa specimens. Representative KDM7A staining of normal tissue (**A, B**), tumour tissue (**C, D**) and less differentiated tumour tissue (**E, F**) with low (**A, C, E**) and high (**B, D, F**) staining intensity (Scale bars: 50 µM). There was no difference in nuclear (**G**) and cytoplasmic (**H**) KDM7A staining between normal and tumour specimens. Nuclear H-score: low = 25-100, medium = 110-125, high = 130-220; Cytoplasmic H-score: low = 40-100, medium = 110-140, high = 145-270; BCR = Biochemical recurrence. Statistical p-values were determined by χ^2-test (VassarStats).

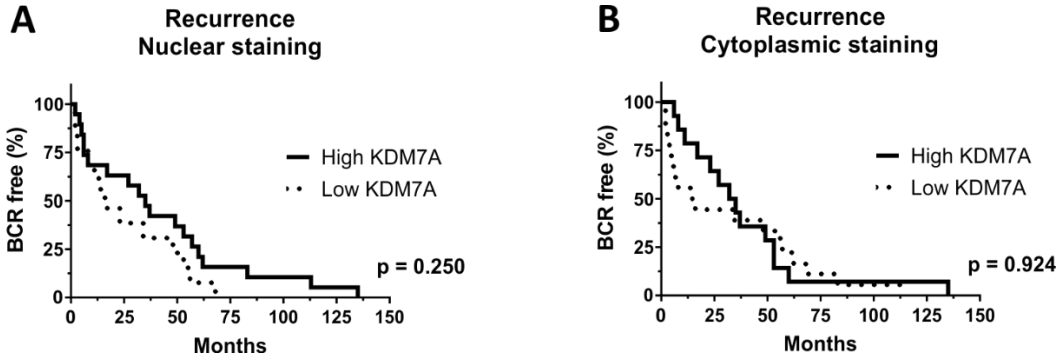

Figure 4.6: Correlation of KDM7A staining with biochemical recurrence.

Kaplan Meier estimate was used to correlate KDM7A staining with BCR free time in PCa patients (n = 32). (**A-B**) KDM7A staining did not correlate with biochemical recurrence free status in patients. BCR = Biochemical recurrence; Nuclear H-score, low = 25-100, high = 110-220; cytoplasmic H-score, low = 40-110, high = 120-270. Statistical analysis was performed with log-rank test.

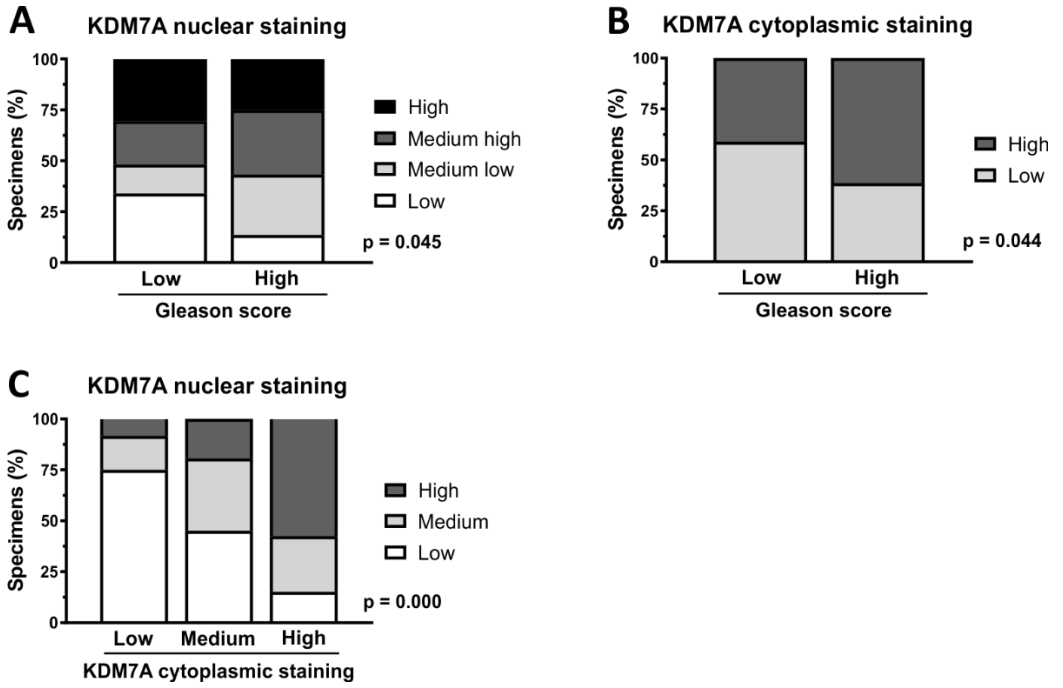

Figure 4.7: Correlation of KDM7A staining with clinical patient data.

H-score was used to determine KDM7A nuclear and cytoplasmic staining intensities and correlated with clinical data using SPSS (n = 100). High KDM7A nuclear (**A**) and cytoplasmic (**B**) staining correlated with Gleason score ($p \leq 0.05$). (**C**) High nuclear and high cytoplasmic staining correlated ($p \leq 0.05$). Gleason score, Low = 3+3=6 and 3+4=7, High = 4+3=7 and Gleason 8, 9; Nuclear H-score 3 groups, Low = 25-100, Medium = 110-125, High = 130-220; Cytoplasmic H-score 3 groups, Low = 40-100, Medium = 110-140, High = 145-270; Cytoplasmic H-score, 2 groups Low = 40-110, High = 120-270. Statistical significances were determined by $\chi 2$-test.

4.2.3 *KDM7A* is overexpressed in LNCaP and LNCaP:C4-2 cells

Basal expression levels of KDM7A were investigated in non-malignant PNT1A cells and in prostate cancer cells LNCaP, LNCaP:C4-2, 22Rv1, PC3 and Du145 (**Figure 4.8**). *KDM7A* mRNA expression was determined by qRT-PCR (**Figure 4.8, A**) and KDM7A protein by western blots (**Figure 4.8, B-C**). LNCaP and LNCaP:C4-2 cells exhibited higher KDM7A on both the RNA and protein level compared to non-malignant PNT1A cells. In LNCaP, *KDM7A* mRNA was ~22-fold ($p \leq 0.05$) higher and protein was ~2-fold ($p \leq 0.05$) higher. In LNCaP:C4-2 cells, *KDM7A* mRNA was ~50-fold ($p \leq 0.05$) higher and protein ~1.8-fold ($p \leq 0.05$) higher. In 22Rv1, *KDM7A* mRNA was as high as in PNT1A but the KDM7A protein was ~0.6-fold ($p \leq 0.05$) lower. PC3 cells exhibited ~5-fold ($p \leq 0.05$) higher *KDM7A* mRNA levels but on the protein level KDM7A expression was similar as compared to PNT1A. Surprisingly, in Du145 *KDM7A* mRNA was ~0.07-fold ($p \leq 0.05$) lower, but KDM7A protein was ~1.5-fold ($p \leq 0.05$) higher than in PNT1A, suggesting potential for translational control of KDM7A.

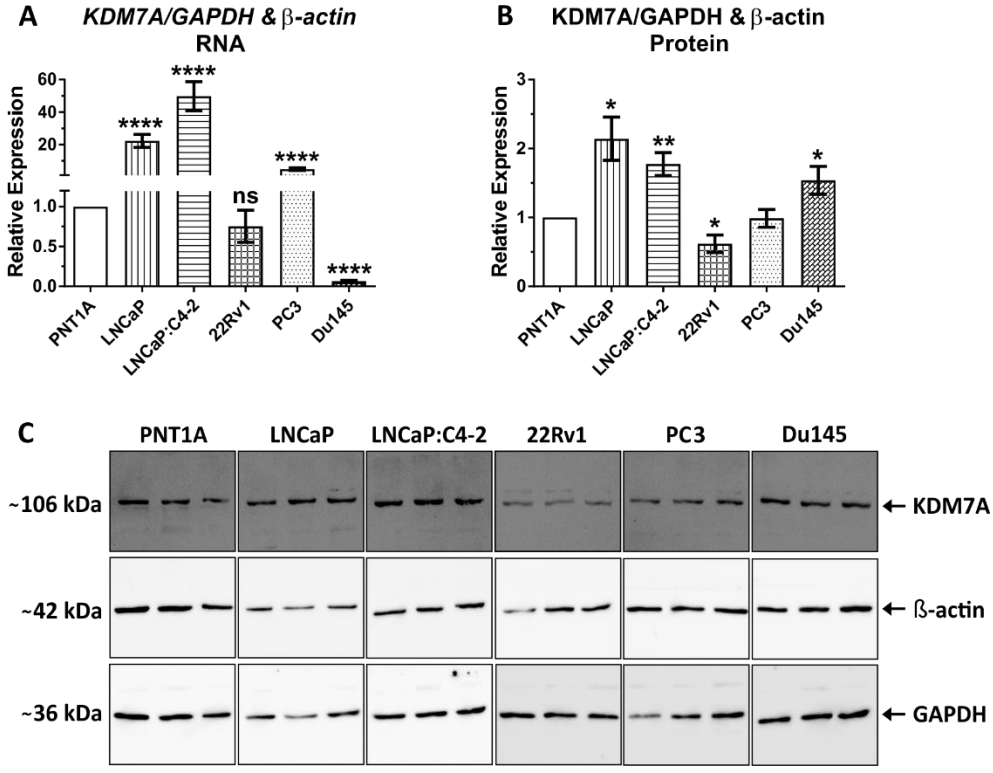

Figure 4.8: KDM7A mRNA and protein expression in PCa cell lines compared to non-malignant cells. KDM7A basal expression was analysed using qRT-PCR and western blots. The western blots band intensities **(C)** were quantified by ImageJ **(B)**. Statistical significances were calculated in comparison to the non-malignant PNT1A cell line (white column). **(A)** *KDM7A* mRNA is higher in LNCaP, LNCaP:C4-2 and PC3 cells, and lower in Du145 compared to non-malignant PNT1A cells (n = 9). **(B-C)** KDM7A protein is higher in LNCaP, LNCaP:C4-2 and Du145 cells and lower in 22Rv1 than in PNT1A (n = 3). * = $p \leq 0.05$; **$p \leq 0.005$; *** = $p \leq 0.001$; **** = $p \leq 0.0001$ by unpaired t-test.

4.2.4 *KDM7A* expression is androgen regulated

To investigate whether *KDM7A* mRNA expression is androgen regulated, the effect of the synthetic androgen (R1881, 1 nM) on *KDM7A* expression was tested in non-malignant PNT1A cells and prostate cancer cells LNCaP, LNCaP:C4-2, 22Rv1, PC3 and Du145 by using qRT-PCR analysis (**Figure 4.9**). As reported previously, the androgen-insensitive cell lines PNT1A, PC3 and Du145 served as negative controls. All androgen-sensitive cell lines showed elevated *KDM7A* upon R1881 treatment (**Figure 4.9, B-D**). *KDM7A* expression was increased 3-fold ($p \leq 0.05$) in LNCaP (**Figure 4.9, B**), 2-fold ($p \leq 0.05$) in LNCaP-C4-2 (**Figure 4.9, C**) and 1.7-fold ($p \leq 0.05$) in 22Rv1 (**Figure 4.9, D**). As expected, R1881 treatment did not have any effect on *KDM7A* in the negative control cell lines PNT1A, PC3 and Du145 which lack AR expression (**Figure 4.9, A, E, F**)

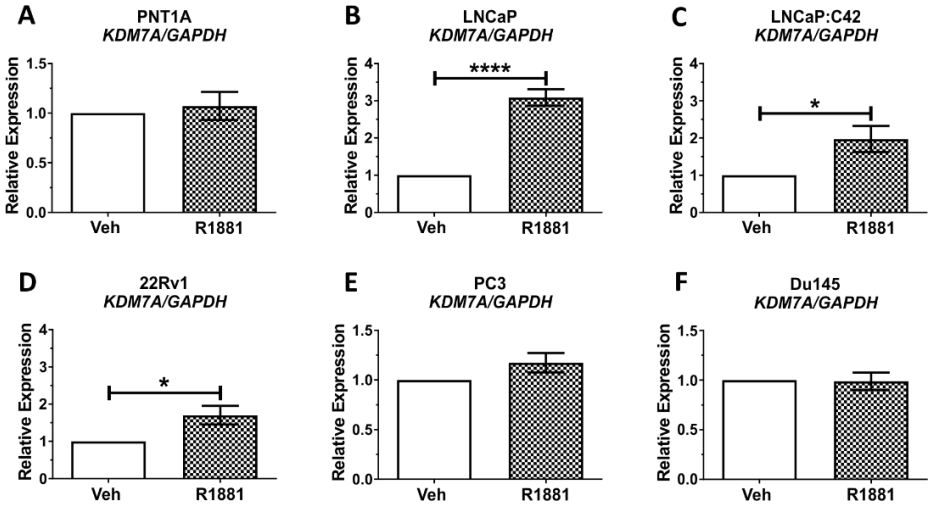

Figure 4.9: Effect of androgen on *KDM7A* expression in normal prostate and PCa cell lines.
The effect of 1 nM R1881 on *KDM7A* mRNA was measured using qRT-PCR. Upon R1881, *KDM7A* expression was increased in all androgen-sensitive cell lines LNCaP (**B**), LNCaP:C4-2 (**C**) and 22Rv1 (**D**) (n = 9). As expected, *KDM7A* was unchanged in the negative control cell lines PNT1A (**A**), PC3 (**E**) and Du145 (**F**) (n = 6). * = $p \leq 0.05$; **$p \leq 0.005$; *** = $p \leq 0.001$; **** = $p \leq 0.0001$ by paired t-test.

4.2.5 Functional depletion of KDM7A via siRNA attenuates R1881-induced *PSA* expression

To further determine KDM7A function in androgen signalling, siRNAs were used to functionally deplete KDM7A in LNCaP, LNCaP:C4-2, 22Rv1 and PC3 cells. Knockdown was performed for three days and the knockdown efficiency was confirmed in LNCaP and LNCaP:C4-2 cells by qRT-PCR (n = min 9) and western blots (n = 3, **Appendix 10**) (**Figure 4.10**). At the RNA level, depletion of KDM7A resulted in ~50% ($p \leq 0.05$) knockdown of *KDM7A* mRNA in LNCaP (**Figure 4.10, A**) and ~80% ($p \leq 0.05$) knockdown of *KDM7A* in LNCaP:C4-2 (**Figure 4.10, B**). In both LNCaP and LNCaP:C4-2 (**Figure 4.10, C-D**) the

knockdown was confirmed on the protein level as evidenced where the siKDM7A band is weaker than the KDM7A band of the siScramble control

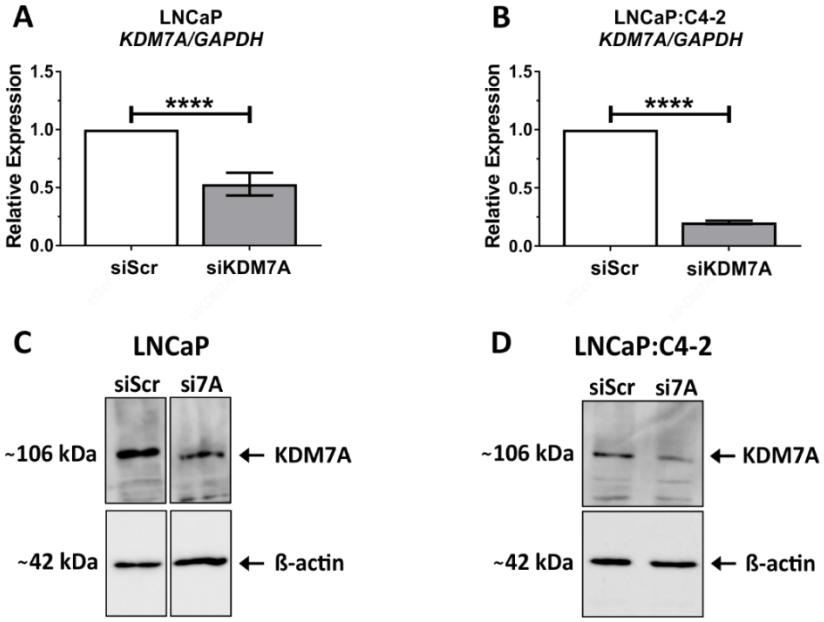

Figure 4.10: Confirmation of siRNA-mediated knockdown of KDM7A on the RNA and protein level in LNCaP and LNCaP:C4-2.
To confirm KDM7A knockdown, qRT-PCR analysis (n = min 9) and western blots (n = 3 in Appendix 10) were used. Both LNCaP (**A, C**) and LNCaP:C4-2 (**B, D**) cells showed decreased mRNA and protein KDM7A levels after KDM7A deletion. siScr = siScramble, si7A = siKDM7A, * = $p \leq 0.05$; **$p \leq 0.005$; *** = $p \leq 0.001$; **** = $p \leq 0.0001$ by paired t-test.

To test if the addition of androgen (R1881, 1 nM) influenced *KDM7A* mRNA expression of siKDM7A treated LNCaP, LNCaP:C4-2 and 22Rv1 cells, qRT-PCR analysis was conducted (**Figure 4.11**). The siKDM7A treatment and the androgen treatment were performed simultaneously for a period of three days. In all three cell lines, siRNA targeting KDM7A achieved ~60-70% ($p \leq 0.05$) knockdown in R1881 treated samples (**Figure 4.7, A-C**).

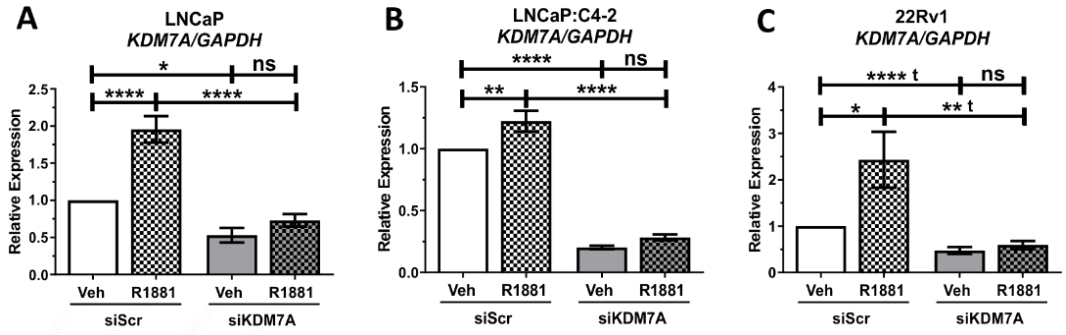

Figure 4.11: Effect of R1881 on siRNA-mediated KDM7A knockdown in LNCaP, LNCaP:C4-2 and 22Rv1.
qRT-PCR was used to determine *KDM7A* mRNA expression upon R1881 treatment (1 nM). In all cell lines LNCaP (n = 11) (**A**), LNCaP:C4-2 (n = 9) (**B**) and 22Rv1 (n = 5) (**C**), *KDM7A* was significantly reduced upon KDM7A depletion independent of R1881 treatment. * = $p \leq 0.05$; **$p \leq 0.005$; *** = $p \leq 0.001$; **** = $p \leq 0.0001$ by ANOVA with Bonferroni's post hoc test and paired t-test.

To determine if the siRNA-mediated KDM7A knockdown had an effect on androgen regulated genes, qRT-PCR analysis was performed on *kallikrein related peptidase 3/prostate specific antigen (KLK3/PSA)* and *transmembrane serine protease 2 (TMPRSS2)* mRNA expression (**Figure 4.12**). In LNCaP, depletion of KDM7A lead to a ~50% ($p \leq 0.05$) reduction in R1881-induced *PSA* mRNA expression (**Figure 4.12, A**). Similarly, KDM7A knockdown resulted in a ~40% ($p \leq 0.05$) reduction of *PSA* in LNCaP:C4-2 (**Figure 4.12, B**). In contrast, KDM7A deletion had no effect on *PSA* expression in 22Rv1 (**Figure 4.12, C**). *TMPRSS2* was modestly (~20%) but not statistically significantly reduced by siKDM7A in LNCaP (**Figure 4.12, C**). In LNCaP:C4-2 and 22Rv1, KDM7A knockdown did not have any effect on *TMPRSS2*.

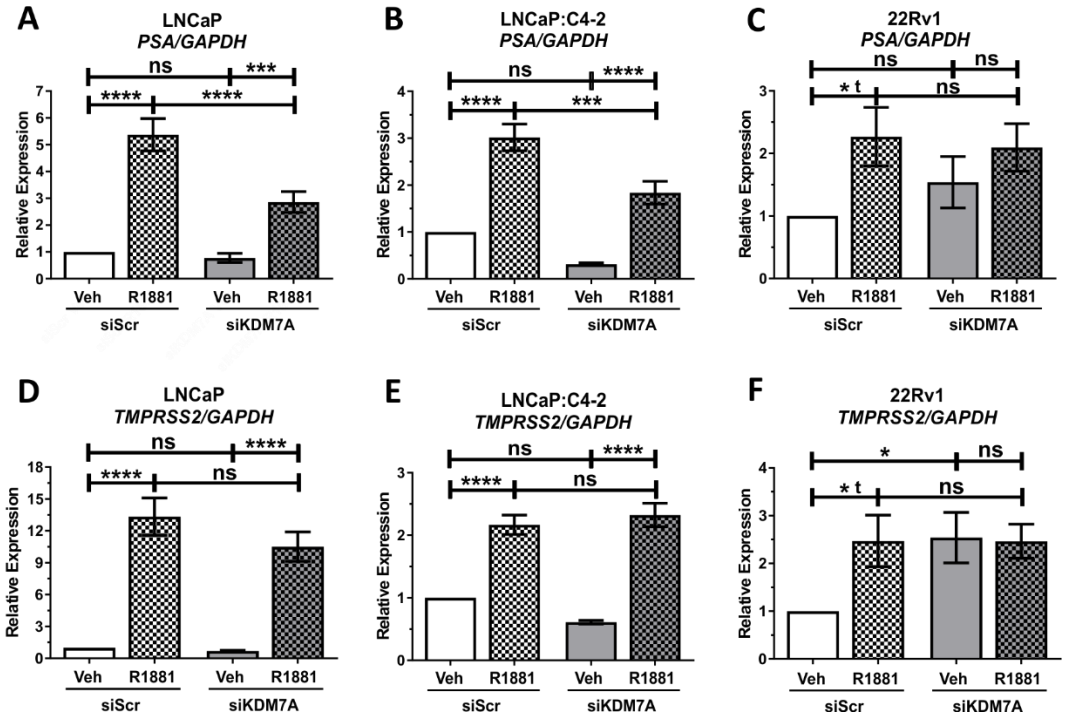

Figure 4.12: Effect of KDM7A knockdown on *PSA* and *TMPRSS2* expression in LNCaP, LNCaP:C4-2 and 22Rv1.

qRT-PCR analysis was used to measure *PSA* and *TMPRSS2* mRNA. In both LNCaP (n = 11) (**A**) and LNCaP:C4-2 (n = 9) (**B**) KDM7A knockdown slightly but significantly attenuated R1881-induced *PSA* expression, however, in 22Rv1 (n = 5) *PSA* was unchanged. (**D-F**) In neither of the cell lines (LNCaP n = 12, LNCaP:C4-2 n = 9, 22Rv1 n = 5) R881-induced *TMPRSS2* expression was affected by siKDM5B. * = $p \leq 0.05$; **$p \leq 0.005$; *** = $p \leq 0.001$; **** = $p \leq 0.0001$ by ANOVA with Bonferroni's post hoc test and paired t-test..

The effect of siRNA-mediated KDM7A knockdown was tested on two androgen-regulated genes, *vascular endothelial growth factor A (VEGFA) and NADH dehydrogenase ubiquinone 1 alpha subcomplex subunit 4-like 2 (NDUFA4L2)* which are involved in angiogenesis (**Figure 4.13**). In LNCaP, R1881-induced *VEGFA* mRNA expression was modestly (30%) but

significantly ($p \leq 0.05$) attenuated through KDM7A depletion (**Figure 4.13, A**). In contrast, *VEGFA* was unaffected in LNCaP:C4-2 and 22Rv1 (**Figure 4.13, B-C**). In both LNCaP and LNCaP:C4-2, the knockdown of KDM7A did not change *NDUFA4L2* mRNA expression. (**Figure 4.13, D-E**).

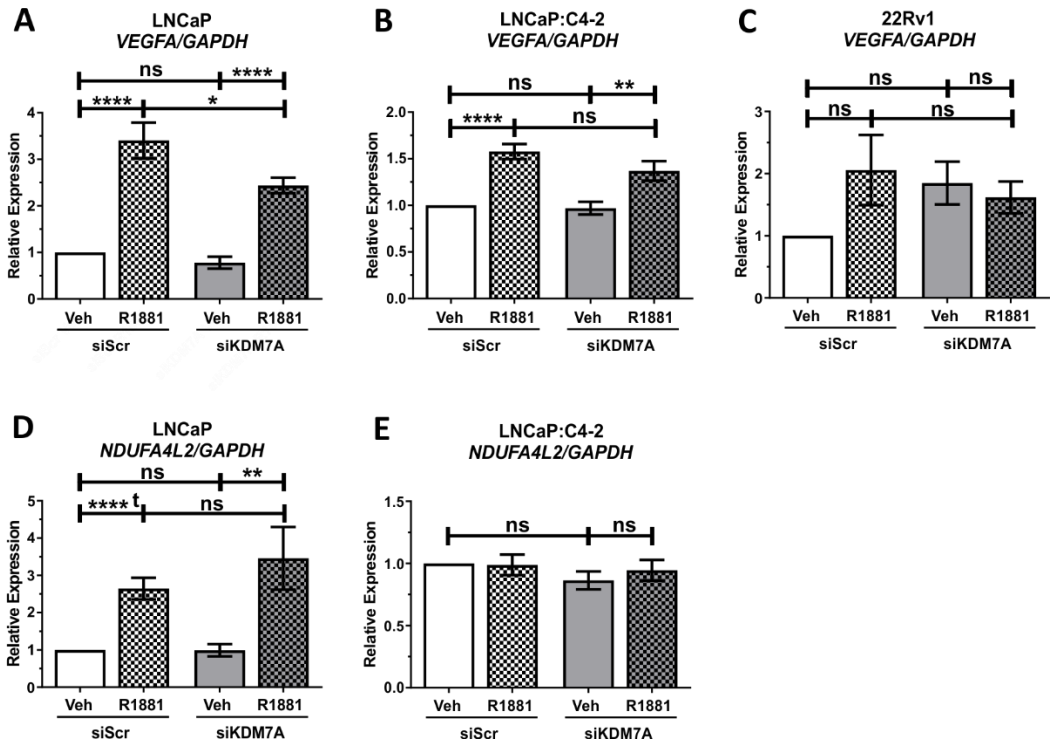

Figure 4.13: Effect of KDM7A knockdown on *VEGFA* and *NDUFA4L2* expression in LNCaP, LNCaP:C4-2 and 22Rv1.

VEGFA and *NDUFA4L2* mRNA expression were measured by qRT-PCR. Depletion of KDM5B slightly but significantly attenuated R1881-induced *VEGFA* expression in LNCaP cells (n = 11) (**A**), whereas in LNCaP:C42 (n = 9) (**B**) and 22Rv1 (n = 5) (**C**) *VEGFA* was not affected. Neither in LNCaP (n = 9) (**D**) nor in LNCaP:C4-2 (n = 9) (**E**) *NDUFA4L2* expression was affected by siKDM5B. * = $p \leq 0.05$; ** $p \leq 0.005$; *** = $p \leq 0.001$; **** = $p \leq 0.0001$ by ANOVA with Bonferroni's post hoc test and paired t-test.

The effect of functional depletion of KDM7A on *VEGFA*, *Hypoxia-inducible factor 1-alpha (HIF-1α)* and *NDUFA4L2*, which are involved in angiogenesis, was also examined in PC3 cells, an androgen-independent prostate cancer cell line (**Figure 4.14**). SiRNA targeting KDM7A resulted in ~60% ($p \leq 0.05$) knockdown of *KDM7A* mRNA in PC3 cells (**Figure 4.14, A**). KDM7A depletion modestly (30%) though statistically significantly ($p \leq 0.05$) reduced *VEGFA* mRNA expression (**Figure 4.14, B**). In contrast, *HIF-1α* and *NDUFA4L2* were unaffected by siKDM7A (**Figure 4.14, C-D**). Because the focus of this study was to study KDM7A in androgen signalling, further experiments were performed with androgen-sensitive cell lines.

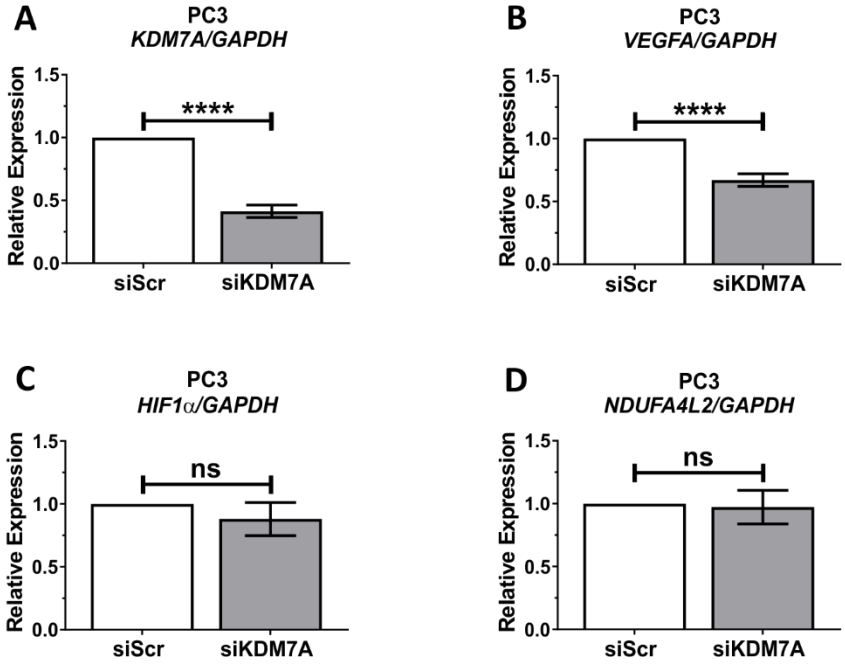

Figure 4.14: Effect of KDM7A knockdown on the expression of angiogenesis-related genes in PC3.
qRT-PCR was used to investigate gene expression changes. (**A**) siRNA-mediated deletion of KDM7A lead to a 60% reduction in *KDM7A* mRNA expression (n = 9). (**B**) KDM7A knockdown moderately but significantly reduced *VEGFA* expression (n = 11). (**C-D**) However, siKDM7A did not have any effect on *HIF1α* (n = 8) and *NDUFA4L2* (n = 6) expression. * = p ≤ 0.05; **p ≤ 0.005; *** = p ≤ 0.001; **** = p ≤ 0.0001 by paired t-test.

4.2.6 KDM7A-selective pharmaco-inhibitor TC-E 5002 attenuates R1881-induced *PSA* expression

KDM7A-selective pharmacological inhibitors were used to further study the role of KDM7A in androgen signalling. The androgen-sensitive cell lines LNCaP, LNCaP:C4-2 and 22Rv1 were simultaneously treated with androgen (R1881, 1 nM) and the KDM7A-selective inhibitor TC-E 5002 for 3 days (**Figure 4.15**) (Suzuki et al 2013). TC-E 5002 selectively inhibits KDM7A (IC_{50} 0.2 µM) over KDM7B (IC_{50} 1.2 µM) and KDM2A (IC_{50} 6.8 µM). The effect of TC-E 5002 on gene expression was analysed by qRT-PCR analysis. In LNCaP cells, 50 µM TC-E 5002 decreased R1881-induced *PSA* expression by 40% (p ≤ 0.05) (**Figure 4.15, A**) which was consistent with the siKDM7A results (**Figure 4.12, A**). Surprisingly, higher concentrations of TC-E 5002 did not inhibit *PSA* as effectively and TC-E 5002 (100 µM) even modestly (20%) but statistically significantly (p ≤ 0.05) increased *PSA* (**Figure 4.15, A**). To confirm these results, LNCaP was treated with a lower TC-E 5002 concentration (10 µM) and confirmed that 10 µM TC-E 5002 inhibited *PSA* more than the 50 µM TC-E 5002 treatment (p ≤ 0.05) (**Figure 4.16, A**). This suggests that lower TC-E 5002 concentrations are more effective at inhibiting *PSA* than high concentrations in LNCaP cells. In contrast, *PSA* mRNA in LNCaP:C4-2 and 22Rv1 was more suppressed the higher the TC-E 5002

concentration (Figure 4.15, B-C). In LNCaP:C4-2, *PSA* mRNA was ~60% ($p \leq 0.05$) reduced by 100 µM TC-E 5002 (Figure 4.15, B) and in 22Rv1 *PSA* was even ~93% ($p \leq 0.05$) decreased (Figure 4.15, C). As expected, reducing the TC-E 5002 concentration to 10 µM in LNCaP:C4-2 did not further decrease *PSA* expression compared to 50 µM TC-E 5002 (Figure 4.16, B), further confirming a inhibitor dose response in LNCaP:C4-2. R1881-induced *VEGFA* expression was ~50-60% ($p \leq 0.05$) decreased by 50 µM TC-E 5002 in both LNCaP and LNCaP:C4-2, however, 100 µM TC-E 5002 increased *VEGFA* by 30% in LNCaP but not statistically significantly (Figure 4.16, D-E). Similarly, in 22Rv1, TC-E 5002 (50 µM) had no effect and TC-E 5002 (100 µM) increased *VEGFA* 2.5-fold ($p \leq 0.05$) (Figure 4.16, F).

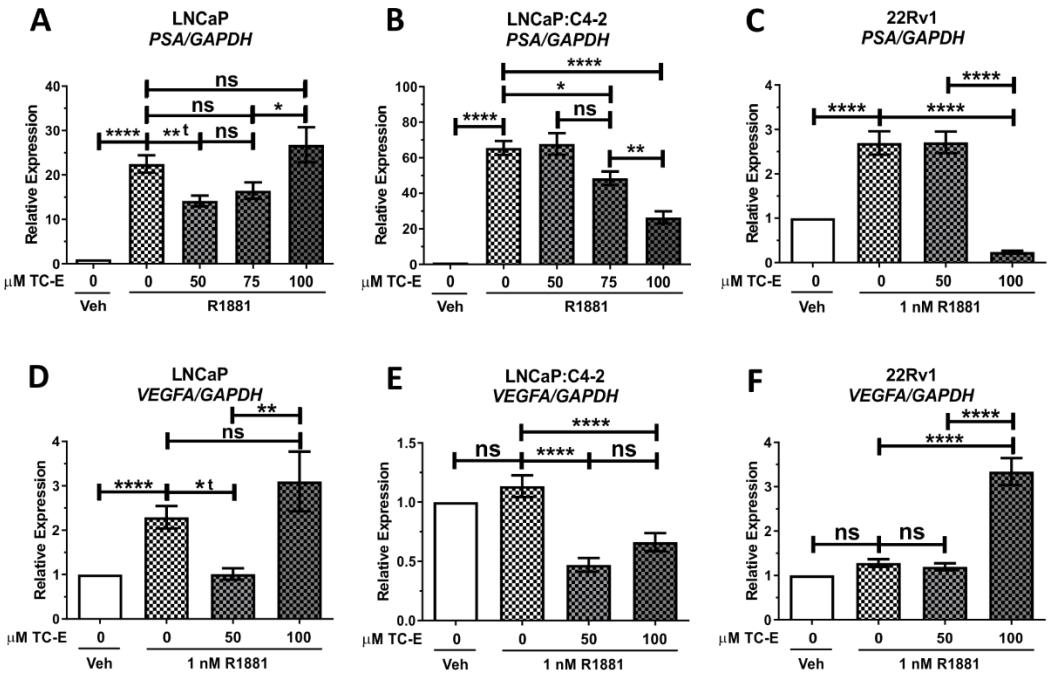

Figure 4.15: Effect of KDM7A-selective inhibitor TC-E 5002 on *PSA* expression in LNCaP, LNCaP:C4-2 and 22Rv1.

Gene expression changes were determined by qRT-PCR (n = min 6). In LNCaP (A) 50 µL TC-E 5002 and in LNCaP:C4-2 (B) and 22Rv1 (C) 100 µL TC-E 5002 attenuated R1881-induced *PSA* expression. Both in LNCaP (D) and LNCaP:C4-2 (E) 50 µL inhibited *VEGFA* expression. In 22Rv1, TC-E 5002 increased *VEGFA* (n = 6) (F). * = $p \leq 0.05$; **$p \leq 0.005$, *** = $p \leq 0.001$, **** = $p \leq 0.0001$ by ANOVA with Bonferroni's post hoc and paired t-test.

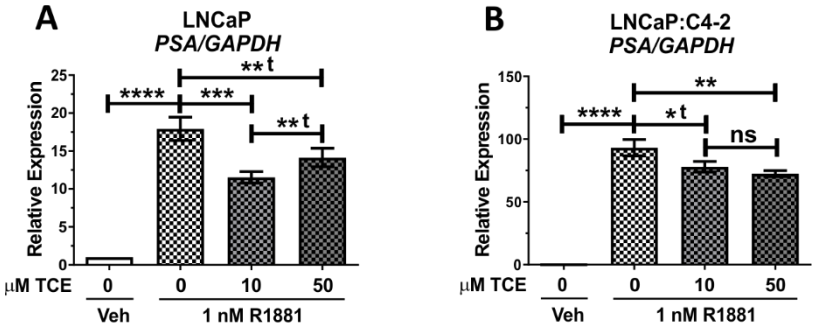

Figure 4.16: Effect of lower TC-E 5002 concentration on PSA expression in LNCaP and LNCaP:C4-2. qRT-PCR was used to examine *PSA* mRNA expression. (**A**) In LNCaP, lowering the TC-E 5002 concentration to 10 μM attenuated R1881-induced PSA expression even more than 50 μM (n = 6). (**B**) As expected, 10 μM and 50 μM TC-E 5002 had a similar effect on LNCaP:C4-2 (n = 3). * = p ≤ 0.05; **p ≤ 0.005; *** = p ≤ 0.001; **** = p ≤ 0.0001 by ANOVA with Bonferroni's post hoc and paired t-test.

4.2.7 KDM7A-selective inhibitor TC-E 5002 decreases proliferation of prostate cancer cells

The CyQUANT™ assay was used to measure the effect of KDM7A-selective inhibitors on cell proliferation of non-malignant PNT1A and the prostate cancer cells LNCaP, LNCaP:C4-2, 22Rv1, PC3 and Du134 (**Figure 3.23**). Proliferation was measured after 3 and 6 days of treatment and statistical significances were calculated in comparison to untreated control cells. A dose curve was performed with two pharmaco-inhibitors that target KDM7A, Daminozide and TC-E 5002 (**Appendix 11** and **Appendix 12** respectively) (Rose et al., 2012). Daminozide inhibits KDM7A at an IC_{50} of 2.1 μM, but also inhibits KDM7B (0.55 μM) and KDM2A (1.5 μM). All Daminozide concentrations tested (20 μM, 200 μM and 400 μM) did not inhibit prostate cancer cell proliferation (with a few exceptions, **Appendix 11**) and modestly increased proliferation of non-malignant PNT1A cells (**Figure 3.23**). TC-E 5002 on the other hand, which is more selective for KDM7A than Daminozide, inhibited proliferation of all cell lines in a dose-responsive manner (**Appendix 12**). After 6 days of treatment, 100 μM TC-E significantly (p≤0-05) reduced cell proliferation of PNT1A by ~25%, LNCaP by ~60%, LNCaP:C4-2 by ~30%, PC3 by ~45% and Du145 by 55% (**Figure 3.23**). 22Rv1 cells were not affected by 100 μM, but 175 μM TC-E decreased proliferation by ~80% (p ≤ 0.05) after 6 days (**Appendix 12**).

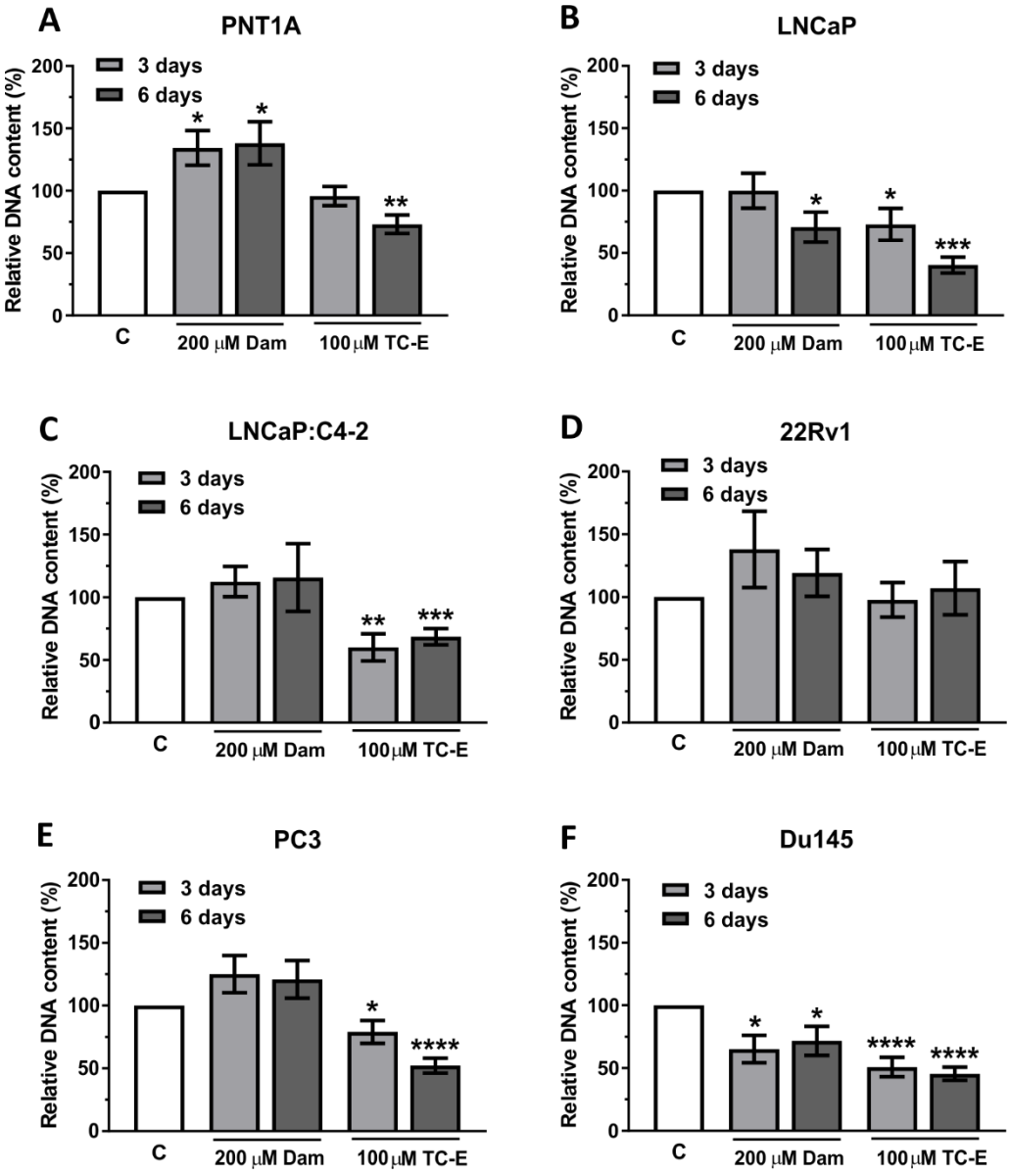

Figure 4.17: Effect of KDM7A-selective inhibitors on cell proliferation of normal prostate and PCa cell lines.

To assess cell proliferation the CyQUANT™ assay was conducted after 3 and 6 days of inhibitor treatment. Statistical significances were calculated compared to the untreated control cells (white column) (n = min 9). Daminozide increased cell proliferation in non-malignant PNT1A (**A**) and had no effect on prostate cancer cells (**C-E**) except for a modest reduction in proliferation in LNCaP (**B**) and Du145 (**F**). In contrast, all cell lines except 22Rv1 showed decreased proliferation upon TC-E 5002 treatment (**A-F**). * = $p \leq 0.05$; **$p \leq 0.005$; *** = $p \leq 0.001$; **** = $p \leq 0.0001$ by paired t-test.

4.2.8 KDM7A may interact with the androgen receptor directly

To investigate if KDM7A directly interacts with the androgen receptor (AR), the KDM7A amino acid (aa) sequence was analysed for nuclear receptor LxxLL binding sequence motifs (Bevan et al., 1999, Heery et al., 1997). Two motifs were found within the 941 aa long KDM7A sequence, namely LLETL and LRLLL (**Figure 4.18**). To determine whether KDM7A binds to AR or other nuclear receptors like the estrogen receptor alpha (ERα) and progesterone receptor (PR) via these motifs, yeast two-hybrid (Y2H) assays were performed. Restriction digestion of the KDM7A construct was performed to create two different constructs (performed by JW on my behalf): 1) KDM7A 401-606 containing both LLETL and LRLLL and 2) KDM7A 565-606 containing the LRLLL motif only (**Figure 4.18**).

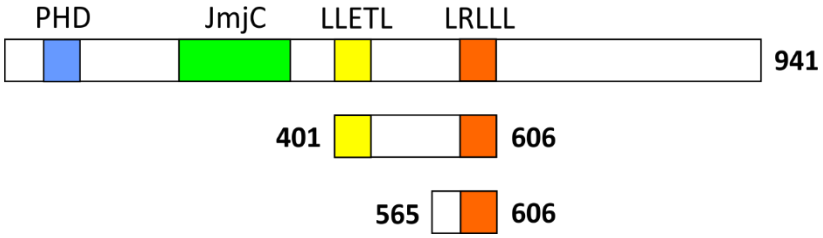

Figure 4.18: KDM7A containing nuclear receptor sequence motifs.
LLETL and LRLLL are two known nuclear receptor binding motifs and were found in the amino acid (AA) sequence of KDM7A. For the Y2H assay, two randomly cut constructs were used, one ranging from AA 401-606 and the other one from 565-606. PHD=plant homeodomain, JmjC=jumonji C-terminal

In the Y2H assay the steroid receptor coactivator-1 (SRC1) nuclear receptor interaction domain (NID) was used as a positive control as it is known to strongly bind to nuclear receptors via its LXXLL binding motifs upon androgen (Heery et al, 1997). In the Y2H assay, direct protein-protein interaction elicited the transcription of the colorimetric reporter gene *LacZ* encoding the beta-galactosidase (β-gal) enzyme. As expected, synthetic androgen (Mibolerone, 1 µM) induced direct interaction between SRC1 NID and the nuclear receptors and lead to a 400-fold ($p \leq 0.05$) increase in β-gal activity with AR, a 35-fold ($p \leq 0.05$) increase with ER and a 480-fold ($p \leq 0.05$) increase with PR (**Figure 4.19, A-C**). When combining the KDM7A constructs with AR, the KDM7A "401 construct" induced a modest ~2.3-fold increase in β-gal activity upon Mibolerone and the KDM7A "565 construct" a ~1.6-fold increase, but not statistically significantly (**Figure 4.19, A**). The KDM7A "401 construct" increased β-gal activity ~1.6-fold when combined with ER (**Figure 4.19, B**) and PR (**Figure 4.19, C**) respectively upon Mibolerone treatment, but not statistically significantly. The KDM7A "565 construct" did not have any effect on ER or PR (**Figure 4.19, B-C**).

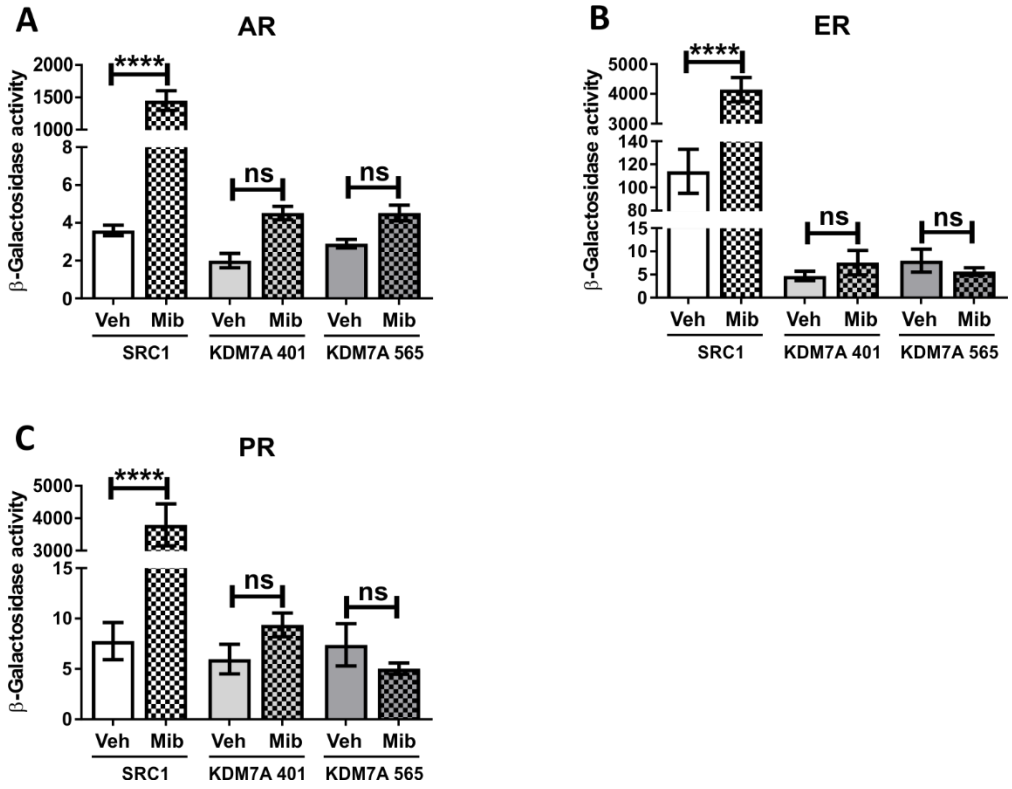

Figure 4.19: Androgen-induced direct interaction between KDM7A and nuclear receptors.
Y2H assay was performed to measure direct interaction through beta-galactosidase (β-gal) activity. (**A-C**) The positive control SRC1 increased β-gal activity by directly interacting with all nuclear receptors. (**A**) The KDM7A "constructs 401 and 565" modestly but not statistically significantly increased β-gal activity when combined with AR (n = 18). No activity was detected with ER (**B**) or PR (**C**) (n = 9). AR, androgen receptor; ER, estrogen receptor; PR, progesterone receptor; Mib, miberolone; SRC1, steroid receptor co-activator 1; * = $p \leq 0.05$; ** $p \leq 0.005$; *** = $p \leq 0.001$; **** = $p \leq 0.0001$ by paired t-test.

To validate that all constructs used in the Y2H assay were present and did not degrade in the yeast cells, western blots were performed detecting VP16-AR, VP16-ER, VP-PR, LexA-SRC1, LexA-KDM7A 401 and LexA-KDM7A 565 via primary antibodies targeting VP16 and LexA (**Figure 4.20**). All VP-16 constructs were present with AR and ER exhibiting a strong band and PR a weaker band (**Figure 4.20, A**). Regarding the LexA constructs, SRC1 and KDM7A 565 were represented by a strong band, however, the band of KDM7A 401, the construct that contained both the LLETL and LRLLL binding motif, was very weak indicating degradation or limited expression in yeast.

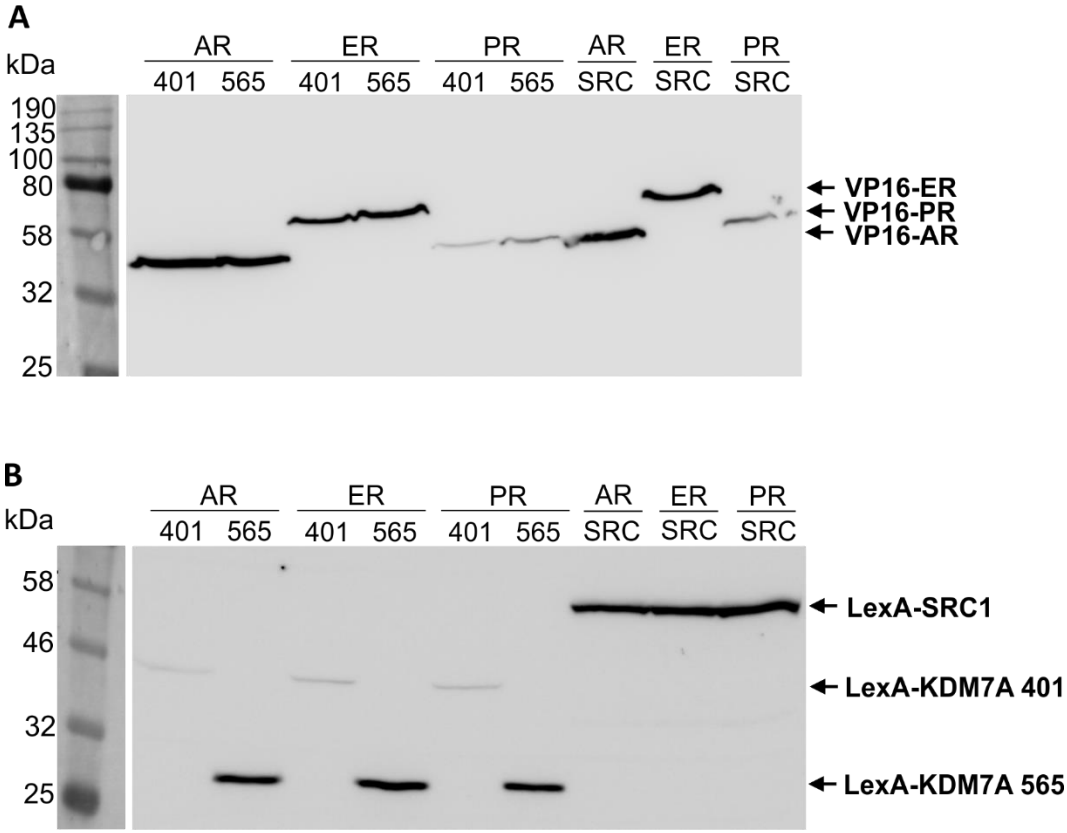

Figure 4.20: Validation of constructs used in the Y2H assay.

The presence of the constructs was validated by western blot analysis using primary antibodies targeting VP16 and LexA. (**A**) VP16-AR and VP-ER were visible by a strong band, whereas VP16-PR exhibited a weaker band. (**B**) LexA-SRC1 and LexA-KDM7A 565 had strong bands, however, the band of the LexA-KDM7A 401 construct was very weak. AR, androgen receptor; ER, estrogen receptor; PR, progesterone receptor; Mib, miberolone; SRC1, steroid receptor co-activator 1.

4.3 Discussion

When this study was commenced, very little was known about the role of KDM7A in prostate cancer. In other cancer types, both tumour suppressive (Osawa et al., 2011, Pan et al., 2015) and oncogenic functions (Kondo et al., 2017, Meng et al., 2019, Xie et al., 2017) of KDM7A have been described. A study by Nilsson et al. (2013) suggested that KDM7A may play a role in prostate cancer as part of a transcriptional coregulator network of AR. Thus, the aim was to investigate the role of KDM7A in androgen signalling in PCa. Simultaneously with this study, another research group investigated and reported about the role of KDM7A in PCa (Lee et al., 2018).

Similar to *KDM5B*, the *KDM7A* gene is altered in about a third of PCa patients, with most patients exhibiting elevated *KDM7A* mRNA levels according to the cBioPortal (https://www.cbioportal.org/, accessed 16.05.2019) (Cerami et al., 2012) (**Figure 4.1**). This is concordant with studies using the cancer microarray database Oncomine, which showed that *KDM7A* mRNA is significantly elevated in PCa samples compared to normal tissue (Lee et al., 2018, Rhodes et al., 2004). In addition, the *KDM7A* amplification frequency was higher in metastatic PCa patients, and no *KDM7A* alterations were detected in neuroendocrine PCa (NePC) patients (**Figure 4.1, B**), suggesting KDM7A is important in AR-related PCa only.

Among several cancer types, including breast, lung, stomach, skin, cervical, and head and neck, *KDM7A* mutations are evenly distributed in the *KDM7A* gene and found both within the PHD and JmjC domain, but also many mutations are located outside of the domains (https://www.cbioportal.org/, accessed 22.08.2019) (Cerami et al., 2012). Around half of these mutations are harboured by patients with a copy number gain, indicating an oncogenic role of KDM7A in cancer. In PCa, only four mutations were found in *KDM7A*. Two patients had a missense mutation outside and C-terminal of the JmjC domain (**Table 4.1** and **Figure 4.2**). One missense mutation was an Arg913His mutation, located at the end of the amino acid sequence, and is likely to be the result of a single point mutation (CGU→CAU or CGC→CAC). Interestingly, this mutation exhibited an allele frequency of 0.42 and, as described earlier, the change from arginine to histidine may provide the cancer cells with a selective advantage for high intracellular pH (Szpiech et al., 2017, White et al., 2017). The other missense mutation was in a patient with a *KDM7A* copy number gain and was Ile472Met, located in the middle of the KDM7A amino acid sequence. Both isoleucine

and methionine have hydrophobic side chains, however, the side chain of methionine is longer. The mutation most likely arose from a single point mutation (AUU/AUC/AUA→AUG). Interestingly, both patients exhibited a very low (~18-20) overall number of mutations in their PCa cells and the mutation in *KDM7A* was one of these mutations. More research is needed to investigate these missense mutations and their effect on the KDM7A protein structure and function.

Two prostate cancer patients had mutations in the KDM7A PHD domain (**Table 4.1** and **Figure 4.2**). The PHD domain is crucial to read and bind the histone marks H3K9me2 and H3K27me2 (Sanchez and Zhou, 2011). One mutation, Glu54Gln, was a missense mutation in a metastatic PCa patient harbouring a copy number gain. This mutation is most likely the result of a single point mutation (GAA→CAA or GAG→CAG) and changes the charge, as glutamic acid is negatively charged and glutamine has an uncharged side chain. Interestingly, this patient did not harbour many mutations in the PCa cells overall (~119) too. Given this mutation occurred in the PHD domain and changes the charge, this may alter the properties of KDM7A to bind and read its histone targets.

The other mutation was a frame shift deletion of 24 amino acids (Glu70Lysfs*24) in the PHD domain of a PCa patient (**Table 4.1** and **Figure 4.2**). Another frame shift deletion of 15 amino acids (L79Rfs*15) in the PHD domain of KDM7A was found in a lung cancer patient (Campbell et al., 2016). A very common frame shift deletion of 41 amino acids (R97Gfs*41), however, situated just outside of the PHD domain, occurred in five patients with stomach cancer and one patient with head and neck cancer (Cancer Genome Atlas Network, 2015, Cancer Genome Atlas Research Network, 2017). These frame shift deletions are likely to affect the protein structure of KDM7A and if the frame shift deletion occurs in the PHD domain, this will likely alter and/or affect the ability of KDM7A to bind and recognise its specific histone targets.

Regarding copy number alterations, most patients were diploid for *KDM7A*, however, around ~15% of patients had a *KDM7A* copy number gain and almost no patients harboured a *KDM7A* deletion (**Figure 4.3**), indicating an oncogenic function of KDM7A. In addition, patients with *KDM7A* alterations exhibited a significantly poorer disease/progression-free survival than patients with unaltered *KDM7A*. To further elucidate the role of KDM7A in PCa, a PCa human tissue microarray was constructed, and KDM7A protein was stained and correlated with clinical patient data (see **Chapter 2: Tissue**

micro array). The expression of KDM7A, both in the nucleus and cytoplasm, did not differ in tumour specimens compared to non-malignant, normal tissue specimens. On the contrary, an immunohistochemical study by Lee et al. (2018) revealed that KDM7A expression is higher in PCa tissue (n = 70) than in normal tissue (n = 7). Lee et al. (2018) uses a different antibody than the antibody used in this TMA and they did not distinguish between nuclear and cytoplasmic staining. However, Lee and colleagues (2018) investigated KDM7A expression by western blot, using the tumour and adjacent normal tissue of 24 PCa patients and confirmed higher expression of KDM7A in tumour than in normal tissue. The Gleason score of these 24 patients correlated with KDM7A expression (Lee et al., 2018), which was concordant with our study, where high KDM7A staining was associated with high Gleason score (Figure 4.7, A-B). KDM7A staining did not correlate with age, perineural invasion or biochemical recurrence (Figure 4.6 and Appendix 9). Interestingly, KDM7A nuclear staining correlated with KDM7A cytoplasmic staining (Figure 4.7, C), indicating that if a patient exhibits high KDM7A expression in the cytoplasm, KDM7A is likely to be transported into the nucleus to a high extent. The reason for the differences between the study of Lee et al. (2018) and our study could be because two different patient cohorts were used. In our study more normal tissue was represented (normal to tumour ratio at 1:1.8), whereas Lee et al. (2018) had a ratio of 1:10. In addition, in our study it was distinguished between nuclear and cytoplasmic staining. For future experiments, ideally, a bigger PCa patient cohort needs to be investigated to determine KDM7A expression in PCa patients.

To investigate the role of KDM7A in androgen signalling, different prostate cancer cell lines were used, including LNCaP, LNCaP:C4-2 and 22Rv1, reflecting various stages of PCa progression. Interestingly, *KDM7A* mRNA was highly expressed in LNCaP:C4-2 and second highest in LNCaP compared to the non-malignant prostate control cell line PNT1A (Figure 4.8, A). This was concordant with a study by Nilsson et al. (2013) who compared *KDM7A* mRNA expression in LNCaP, LNCaP:C4-2 and PC3 to the non-malignant prostate cell line PREC. However, in their study, PC3 cells express the same level of *KDM7A* as PREC cells, whereas in our study *KDM7A* levels were higher in PC3 than in the control cell line PNT1A (Figure 4.8, A), indicating *KDM7A* may be expressed lower in PNT1A than in PREC which may have to do with the differences in PREC and PNT1A described earlier (see Chapter 3: Discussion). Similar to the RNA level, KDM7A protein was highly expressed in both LNCaP and LNCaP:C4-2 too, compared to PNT1A (Figure 4.8, B). Interestingly, the AR-V7 positive cell line 22Rv1 had the lowest KDM7A protein levels of all cell lines tested (Figure 4.8, B-C),

suggesting KDM7A may have different roles in PCa cells depending on if they harbour AR full length or splice variants, and how much the PCa has progressed. Surprisingly, whilst *KDM7A* mRNA levels were lowest in Du145, the KDM7A protein level was increased compared to PNT1A (**Figure 4.8**). Even though the translation rate of a protein is dependent on the abundance of mRNA transcripts, it is also dependent on many other factors, such as the regulation of the translation rate and protein product, and many studies have discussed that mRNA levels are not always proportional to protein levels (Greenbaum et al., 2003, Liu et al., 2016, Maier et al., 2009). An explanation for why KDM7A protein levels are high in Du145 despite apparently low *KDM7A* mRNA expression could be that the KDM7A translation rate is upregulated through regulatory proteins or even non-coding RNAs (Liu et al., 2016, Ye et al., 2012), or the KDM7A protein stability may be enhanced in Du145 (Liu et al., 2016).

To investigate the role of KDM7A in androgen signalling in PCa, it first was of interest if *KDM7A* mRNA expression is regulated by the androgen signalling pathway. Indeed, the treatment of androgen-responsive cell lines LNCaP, LNCaP:C4-2 and 22Rv1 with androgen (R1881, 1 nM) increased *KDM7A* expression (**Figure 4.9**). Interestingly, the R1881-induced *KDM7A* expression is higher in androgen-dependent LNCaP cells than in androgen-independent LNCaP:C4-2 and 22Rv1 cells, indicating *KDM7A* regulation may be dependent on the cell line and therefore PCa stage. To investigate this further, western blot analysis would have to be performed to confirm KDM7A expression on the protein level.

Nilsson and colleagues (2013) have suggested that KDM7A is involved in the androgen signalling pathway in PCa, and to further elucidate this, knockdown and inhibitor experiments were performed. KDM7A was knocked down by siRNA-mediated depletion and the effect on AR-regulated genes (*PSA*, *TMPRSS2*, *VEGFA*) was investigated in LNCaP, LNCaP:C4-2 and 22Rv1 cells. Interestingly, R1881-induced (1 nM) *PSA* expression was attenuated by KDM7A knockdown in LNCaP and LNCaP:C4-2, but not 22Rv1 cells (**Figure 4.12, A, C**). The reason for this most likely is that KDM7A needs to be knocked down more efficiently, either by a higher siRNA concentration or longer duration of depletion, to see an effect on *PSA*, since the study by Lee et al. (2018), who applied lentivirus-mediated stable knock-down of KDM7A, showed an effect on *PSA* and *TMPRSS2* expression in 22Rv1. Similarly, in our study no effect was detected on *TMPRSS2* in LNCaP and LNCaP:C4-2 through KDM7A siRNA-mediated knockdown (**Figure 4.12, D-E**), whilst lentivirus-mediated stable knockdown of KDM7A has an effect on *TMPRSS2* in LNCaP and LNCaP:C4-2B (Lee et

al., 2018). In addition, the effect of KDM7A knockdown was investigated on the angiogenesis-related genes *VEGFA* and *NDUFA4L2*. *VEGFA* is an AR-regulated gene and *VEGFA* expression was shown to be dependent on KDM1A in PCa (Kashyap et al., 2013). *NDUFA4L2* is a target gene of the oncogene HIF1α which is crucial for angiogenesis in cancer (Semenza, 2003, Tello et al., 2011). However, the knockdown of KDM7A had only a modest effect on R1881-induced *VEGFA* expression in LNCaP, and no effect was seen on *NDUFA4L2* (**Figure 4.13, A, D**). In addition, no effect was seen on any of these genes in the androgen-independent cell lines LNCaP:C4-2 and 22Rv1 (**Figure 4.13**). The reason for that may be the same as described above and more effective knockdown techniques will give more insight into the role of KDM7A in AR-regulated angiogenesis in PCa. However, overall, what can be concluded from these results, is that AR-regulated gene expressions seem to be more susceptible to KDM7A knockdown in LNCaP cells than in LNCaP:C4-2 and 22Rv1, which are androgen-sensitive but independent (Sramkoski et al., 1999, Thalmann et al., 1994). If KDM7A is an important coregulator of the AR, it is not surprising that AR-regulated genes in LNCaP cells are more dependent on KDM7A than in LNCaP:C4-2 and 22Rv1, since LNCaP is androgen dependent and harbours higher levels of AR than LNCaP:C4-2 and 22Rv1 (Gleave et al., 1991, Sramkoski et al., 1999, Thalmann et al., 1994). Coimmunoprecipitation experiments by Lee et al. (2018) confirm that KDM7A binds to the promotor region of AR target genes, such as *KLK3* and *KLK2*, in prostate cancer cell lines, including LNCaP, 22Rv1 and VCaP, and even more so upon androgen (DHT, 5 nM) treatment.

To inhibit KDM7A more effectively and determine the effect on AR-regulated gene expression, prostate cells were treated with the pharmaco-selective inhibitor TC-E 5002 (Suzuki et al., 2013). TC-E 5002 selectively inhibits KDM7A with an IC_{50} of 0.2 µM, over KDM7B (IC_{50} = 1.2 µM) and KDM2A (IC_{50} = 6.8 µM). KDM7B and KDM2A are phylogenetically closely related to KDM7A, based on their protein structure and domains (Klose et al., 2006). As expected, the treatment of LNCaP cells with TC-E 5002 (50 µM) attenuated *PSA* and *VEGFA* expression (**Figure 4.15, A, D**). This is concordant with a study by Lee et al. (2018), where TC-E 5002 (10 µM) inhibited DHT-induced (5 nM) *PSA* expression in LNCaP. Surprisingly, treating LNCaP cells with increasing TCE-E 5002 concentrations, reversed the effect and lead to an increased *PSA* expression (**Figure 4.15, A**). An explanation for that could be that in LNCaP, at high TC-E 5002 concentrations, such as 100 µM, KDM7B and KDM2A could be unselectively targeted. KDM7B, which demethylates H3K9me2/me1 and H4K20me1, has been shown to be upregulated in PCa and to play an oncogenic function in an AR-independent manner (Ma et al., 2015). KDM2A, on the other hand, demethylates

H3K36me2/me1 and was shown to be down-regulated in PCa, suggesting a tumour suppressor function (Frescas et al., 2008). Low KDM2A levels lead to an aberrant heterochromatin state at the centromer of chromosomes and therefore causes mitotic abnormalities and chromosomal rearrangements in PCa (Frescas et al., 2008). A study by Nilsson et al. (2013) reported that KDM2A is part of the AR coregulator network and, interestingly, *KDM2A* mRNA is expressed in the same pattern as *KDM7A* mRNA in PCa cell lines, exhibiting the highest expression in LNCaP:C4-2 and the second highest in LNCaP (Nilsson et al., 2013). More experiments are needed to clarify the role of KDM2A and KDM7B in PCa, and to elucidate if the unselective binding of TC-E 5002 to other KDMs could be the reason for the reversed effect of TC-E 5002 on *PSA* expression in LNCaP (**Figure 4.15, A**). On the contrary, in LNCaP:C4-2 and 22Rv1 cells, TC-E 5002 attenuated R1881-induced *PSA* expression in a dose-dependent manner, with no inhibition at 50 μM TC-E 5002 and the highest inhibition at 100 μM TC-E 5002 (**Figure 4.15, B-C**). Interestingly, VEGFA mRNA expression is decreased by TC-E 5002 (100 μM) in LNCaP:C4-2, but increased in 22Rv1 (**Figure 4.15, E-F**), indicating that the role of KDM7A at AR-regulated genes is cell line dependent. The *VEGFA* increase in 22Rv1 could also be due to cellular stress, as mentioned above (Ghosh et al., 2010, Lin et al., 2008a, Miyagi et al., 2013, Pereira et al., 2013). To gain more insight into cell and genome-specific actions of KDM7A and its demethylase activity at different genes, chromatin immunoprecipitation (ChIP) assays with antibodies targeting specific histone modifications would have to be used (Milne et al., 2009). To investigate site-specific binding of KDM7A in the genome, an antibody targeting KDM7A could be used. After ChIP, the isolated DNA fragments are analysed by high-throughput sequencing (seq), together called ChIP-seq analysis (O'Geen et al., 2011). ChIP-seq analysis will be crucial to give more insight into the role of KDM7A in gene regulation and to determine differences between the PCa cell lines and thereby different stages of PCa.

In addition to gene regulation, it was of interest whether KDM7A plays a role in PCa cell proliferation. Suzuki et al. (2013) demonstrated that inhibition of KDM7A by TC-E 5002 blocks the proliferation of different cancer cell types, including neuroblastoma (Gi_{50} = 86 μM), cervical (Gi_{50} = 40 μM) and esophageal (Gi_{50} = 16 μM) cancer cells. We therefore tested the effect of TC-E 5002 on the proliferation of PCa cell lines. In addition, we tested another inhibitor called Daminozide, which is a plant growth regulator and selectively inhibits KDM7B (IC_{50} = 0.55 μM), KDM2A (IC_{50} = 1.5 μM) and KDM7A (IC_{50} = 2.1 μM) (Rose et al., 2012, Suzuki et al., 2013). Daminozide did not inhibit PCa cell proliferation and modestly increased cell proliferation of the non-malignant prostate cell line PNT1A (**Figure**

4.17, Appendix 11). In contrast, the KDM7A-selective inhibitor TC-E 5002 blocked cell proliferation of the PCa cell lines LNCaP, LNCaP:C4-2, 22Rv1, PC3 and Du145, in a dose-dependent manner (Appendix 12), whereby LNCaP cells seemed most sensitive and 22Rv1 cells most resistant to KDM7A inhibition by TC-E 5002 (Figure 4.17), further suggesting KDM7A plays an important role in androgen-dependent prostate cancer, but maybe not as much in PCa patients who harbour the AR splice variant ARv7. Another study by Lee et al. (2018) showed that stable KDM7A knockdown lead to a reduced cell viability and colony formation in LNCaP, LNCaP:C4-2B and 22Rv1. In their experiments, 22Rv1 did not exhibit a higher resistance to KDM7A inhibition regarding cell growth, however, in contrast to the CyQuant assay, which measures DNA content, the cell viability assay Lee et al. (2018) used, measures protein content. Lee et al. (2008) further confirmed that KDM7A is important for tumour growth in mouse xenograft models, by injecting 22Rv1 cells expressing *KMD7A* shRNA, which inhibited tumour growth in contrast to control shRNA. Similar to pharmaco-selective inhibition of KDM5B (see Chapter 2: Discussion), it will be important to determine the mechanisms through which cell growth is inhibited by TC-E 5002 (Evan and Vousden, 2001, Pietenpol and Stewart, 2002, Kepp et al., 2011, Vandenabeele et al., 2010).

Since KDM7A seems to play an important role as a coregulator of the AR to regulate gene expression, the question was whether KDM7A directly interacts with AR or whether it is a functional relationship. The KDM7A amino acid sequence contains two LxxLL sequence motifs, LLETL and LRLLL, which are known to be crucial for nuclear receptor binding (Heery et al., 1997) (Figure 4.18). A yeast two-hybrid assay was used to investigate the direct interaction of KDM7A with the AR, estrogen receptor alpha (ERα) and progesterone receptor (PR) respectively. The steroid receptor coactivator-1 (SRC-1) nuclear receptor interaction domain (NID) was used as a positive control and, as expected, directly interacted with the nuclear receptors upon androgen (Mibolerone, 1 µM) (Figure 4.19). In contrast, KDM7A did not seem to directly interact with AR, ERα and PR respectively (Figure 4.19). However, the KDM7A fragment, ranging from amino acid 401-606 and harbouring both LLETL and LRLLL, seemed to be expressed to a much lesser extent than SRC-1 NID, according to western blot analysis (Figure 4.20, B). An explanation for this is that yeast cells differ from eukaryotic cells and the KDM7A construct may not be stable in yeast cells, thus it was not highly expressed (Brückner et al., 2009, Van Criekinge and Beyaert, 1999). In addition, yeast cells lack posttranslational modifications and the folding of the protein may influence the interaction (Van Criekinge and Beyaert, 1999). Due to GC-rich regions, it was not possible to amplify and clone the full length KDM7A, hence fragments of KDM7A,

containing the LxxLL motif(s), were applied (Jonathan Whitchurch). However, for future experiments, it will be important to carefully choose other KDM7A fragment boundaries, by making protein folding predictions using the programme Protein Homology/Analogy Recognition Engine V 2.0 (Phyre 2.0). Therefore no conclusion can be made yet, whether the KDM7A 401-606 fragment, containing both LLETL and LRLLL, interacts with AR. However, it can be concluded that the KDM7A fragment, ranging from amino acid 565-606 and containing the LRLLL motif, did not interact with steroid receptors (Figure 4.19), given it was expressed at similar levels to SRC-1 NID (Figure 4.20, B). Another technique to investigate direct protein-protein interaction is co-immunoprecipitation (co-IP), and indeed, Lee et al. (2018) revealed a direct interaction between KDM7A and AR by using ectopic expression of AR and Flag-tagged KDM7A in human embryonic kidney (HEK) cells and coimmunoprecipitation experiments.

In summary, KDM7A is an important AR coregulator involved in AR-regulated gene expression and PCa growth. KDM7A appears to play an oncogenic function in PCa, however, the exact role of KDM7A at more advanced PCa stages remains unclear, reflected by the cell lines 22Rv1, PC3 and Du145 in this study. Interestingly, *KDM7A* was more amplified in patients with metastatic PCa, however, *KDM7A* mRNA and protein expression seemed comparatively low in the CRPC cell lines 22Rv1, PC3 and Du145. The cell line 22Rv1, which harbours the Arv7 splice variant (Dehm et al., 2008, Guo et al., 2009, Henzler et al., 2016), seemed to behave somewhat less dependent on KDM7A regarding AR-regulated gene expression and PCa growth. In addition, KDM7A may have an AR-independent function, since the cell proliferation of PC3 and Du145, which are AR negative cell lines (Alimirah et al., 2006, Sramkoski et al., 1999), was reduced by pharmaco-selective inhibition of KDM7A. It is therefore important to further investigate the function of KDM7A in CRPC and PCa patients which harbour AR splice variants, such as ARv7. For future experiments, it will be crucial to investigate the mechanisms by which KDM7A regulates AR-dependent and independent genes and to determine histone methylation marks at the relevant gene loci. It is also necessary to determine the functional interactions of KDM7A and KMD1A given the common substrate preference of these two coregulators.

Chapter 5: Combinatorial analysis of KDMs in androgen signalling

Chapter 5 Combinatorial analysis of KDMs in androgen signalling

5.1 Introduction

Among the KDMs, the role of KDM1A in PCa has been best characterised and many studies support KDM1A as a promising therapeutic target to treat PCa (Cai et al., 2014, Ellis and Loda, 2018, Kahl et al., 2006, Kashyap et al., 2013, Ketscher et al., 2014, Metzger et al., 2005, Sehrawat et al., 2018, Wang et al., 2019d, Wissmann et al., 2007). KDM1A has been described as a transcriptional repressor in association with CoREST and HDAC1/2 when demethylating the active histone mark H3K4me2/me1 (Lee et al., 2005, Shi et al., 2004, Shi et al., 2005, You et al., 2001). In contrast, when bound to AR, KDM1A changes its substrate specificity to H3K9me2/me1 and acts as a transcriptional activator (Metzger et al., 2010, Metzger et al., 2005, Metzger et al., 2008, Wissmann et al., 2007). However, the dual function of KDM1A has been shown to be more complex and that KDM1A also demethylates H3K4me2/me1 at transcriptionally active AR target genes (Cai et al., 2014). In addition, KDM1A can demethylate non-histone proteins, such as p53 (Huang et al., 2007) and E2F1 (Xie et al., 2011b), and is involved in regulating DNA methylation by demethylating the DNA methyltransferase DNMT1 (Wang et al., 2009a). Sahrawat et al. (2018) further suggest that KDM1A plays an important role in PCa progression independent of its demethylase activity.

The aim of this study therefore was to further elucidate the role of KDM1A in AR-regulated gene expression and the proliferation in different PCa cell lines, reflecting progressive stages of PCa. Combination therapy has gained much interest in the recent years and can be more effective and efficient than inhibiting a single target (Mokhtari et al., 2017, Xu and Qiu, 2019). It also holds the potential to overcome drug resistance (Chou, 2006, Miles et al., 2002, Mokhtari et al., 2017, Saputra et al., 2018, Semenas et al., 2012, Xu and Qiu, 2019) and to improve patients' surival (Fizazi et al., 2015, Sweeney et al., 2015). The hypothesis therefore was that combined targeting of KDM1A and KDM7A, which are both part of the coregulator network identified by Nilsson et al. (2015), has an additive effect on the inhibition of AR target gene expression, such as *PSA* and *VEGFA*, and PCa cell growth, compared to targeting single KDMs.

5.2 Results

5.2.1 Bioinformatic analysis of *KDM1A*

Bioinformatics were conducted using the cBioPortal for Cancer Genomics to determine *KDM1A* gene alterations in prostate cancer patients (**Figure 5.1**). As in the previous chapters (**Chapter 3**, **Chapter 4**), three studies were used in the analysis: (1) The TCGA Provisional Prostate Adenocarcinoma study (n = 499), (2) the SU2C/PCF Dream Team Metastatic Prostate Adenocarcinoma study (n = 444) and (3) the Trento/Cornell/Broad Neuroendocrine Prostate Cancer study (n = 114). The TCGA Provisional Prostate Adenocarcinoma study revealed that 29.5% of prostate cancer patients harboured alterations in the *KDM1A* gene (**Figure 5.1, A**). The different cancer types (Prostatic adenocarcinoma vs Metastatic prostate adenocarcinoma vs Neuroendocrine carcinoma) were compared to elucidate in which cancer type *KDM1A* is altered most frequently. *KDM1A* was altered most frequently in neuroendocrine prostate cancer with ~5.3% of patients (6/114) exhibiting *KDM1A* amplification (**Figure 3.1, B**). Second most alterations were found in prostate adenocarcinoma patients (~1.2%) with 0.2% *KDM1A* amplification (1/499 cases), 0.4% mutation (2/499) and 0.6% deep deletion (1/499). In metastatic prostate adenocarcinoma cases, 3 of 444 cases (~0.7%) harboured a mutation in *KDM1A* (**Figure 3.1, B**). The analysis of *KDM1A* mRNA expression (z-score = 1) within the TCGA Provisional prostate adenocarcinoma study revealed that *KDM1A* was altered in ~29.5% (146/499 cases) (**Figure 3.1, C**). Of these 146 patients, 70 (~14%) had high KDM1A mRNA levels, 71 (~14.2) low mRNA levels, 3 had multiple *KDM1A* alterations (0.6%), and 3 patients had a mutation (0.2%), amplification (0.2%) and deep deletion (0.2%) respectively.

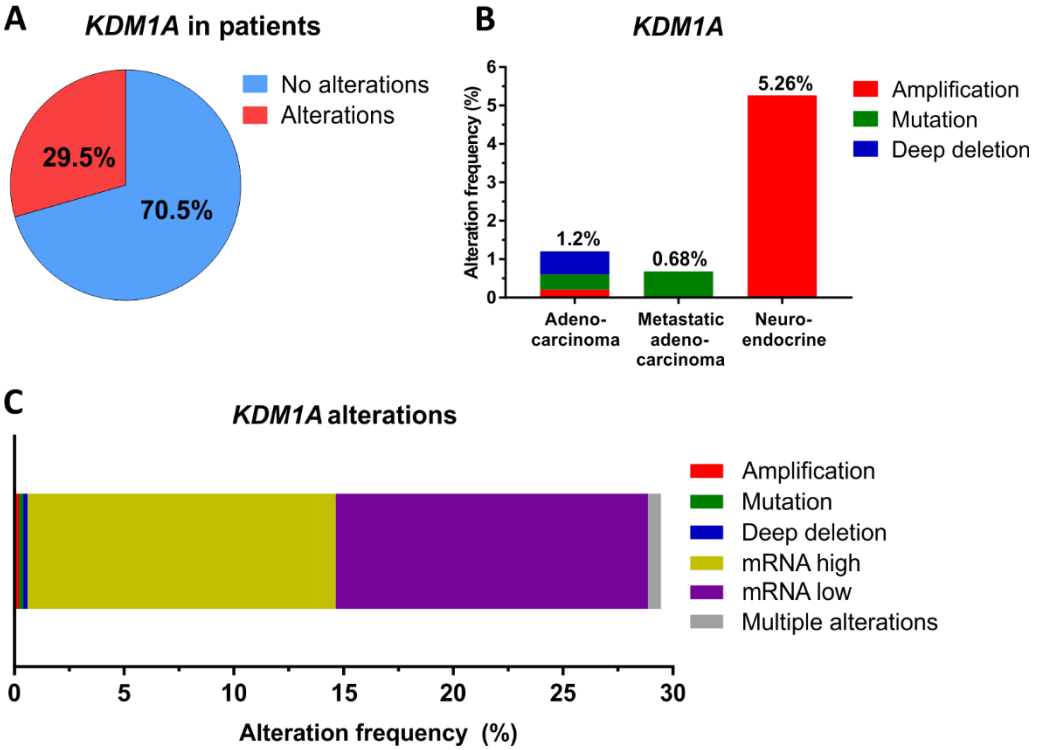

Figure 5.1: *KDM1A* alteration frequencies in prostate cancer patients.
Bioinformatic analysis was performed using the cBioPortal for Cancer Genomics. (**A**) *KDM1A* was altered in 29.5% of prostate cancer patients. (**B**) The *KDM1A* alteration frequency was higher in prostate adenocarcinoma (~1.2%) than in metastatic adenocarcinoma (~0.7%) but was highest (~5.3%) in neuroendocrine carcinoma. (**C**) The TCGA Provisional Prostate Adenocarcinoma study was used for *KDM1A* mRNA expression analysis (z-score=1) and revealed that the most frequent alterations were *KDM1A* mRNA high (~14% of cases) and mRNA low (~14%).

Mutations were found only in prostate adenocarcinoma and metastatic adenocarcinoma patients, but not in neuroendocrine carcinoma cases (**Table 5.1**). Two patients with prostate adenocarcinoma had a missense mutation (I199T, **No. 1** and P471S, **No. 2** respectively). The I199T, **No. 1** mutation is situated in the Swi3p, Rsc8p and Moira (SWIRM) domain which is important for protein-protein interactions in chromatin-associated compelexes (**Figure 5.2**) (Da et al., 2006, Iyer et al., 2002). The P471S, **No. 2** mutation is located in the coiled-coil tower domain which protrudes from the amino oxidase (AO) domain involved in catalysis (Stavropoulos et al., 2006). Two patients with metastatic prostate adenocarcinoma had a missense mutation (L664V, **No. 3** and A309S, **No. 4**). The A309S, **No. 4** mutation is located precisely inbetween two flavin adenine dinucleotide (FAD) binding sites at amino acid 308 and 310 in the AO (**Figure 5.2**) which is crucial for the amine oxidation reaction catalysed by flavin-containing amine oxidases (Shi et al., 2004). The L664V, **No. 3** mutation is located within the AO domain and interestingly another metastatic carcinoma case had a in frame deletion (L664del, **No. 5**) at the exact same amino acid (**Figure 5.2**).

Table 5.1: *KDM1A* mutations in prostate cancer patients.
The study, protein change, mutation type, copy number, allele frequency and number of mutations in the sample were stated. The mutations were given a number from 1 - 5 which correspond to the numbers in **Figure 5.2**.

No.	Study	Protein Change	Mutation Type	Copy #	Allele Freq (T)	# Mut in Sample
1	Prostate Adenocarcinoma	I199T	Missense	Diploid	0.10	27
2	Prostate Adenocarcinoma	P471S	Missense	Diploid	0.49	6625
3	Metastatic Adenocarcinoma	L664V	Missense	Diploid	0.17	44
4	Metastatic Adenocarcinoma	A309S	Missense	Gain	0.06	1093
5	Metastatic Adenocarcinoma	L664del	IF del	Diploid	N/A	58

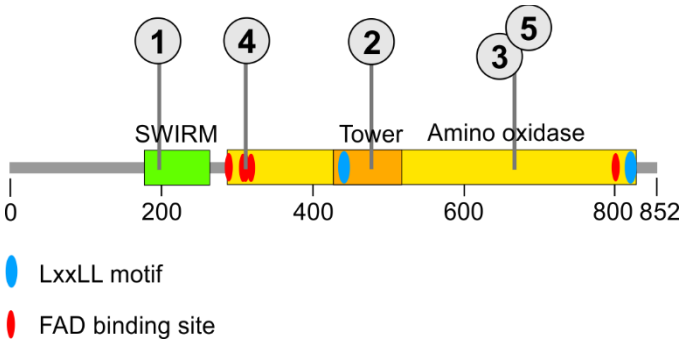

Figure 5.2: Location of KDM1A mutations.
The KDM1A protein is 852 amino acids long and contains a SWIRM and an amino oxidase (AO)-like domain which harbours a helical Tower domain. The mutations were numbered from 1 – 5 and correspond to the mutations in **Table 5.1**. SWIRM = Swi3p, Rsc8p and Moira; FAD = Flavin adenine dinucleotide.

Putative *KDM1A* copy number alterations from GISTIC were analysed using the TCGA Provisional Prostate Adenocarcinoma study (**Figure 5.3**). The majority of cases was diploid for the *KDM1A* gene. About 8% of all 499 cases had a heterozygous (shallow) and 3 cases a homozygous (deep) *KDM1A* deletion. Only 4 patients had a *KDM1A* copy number gain and 1 case a copy number amplification.

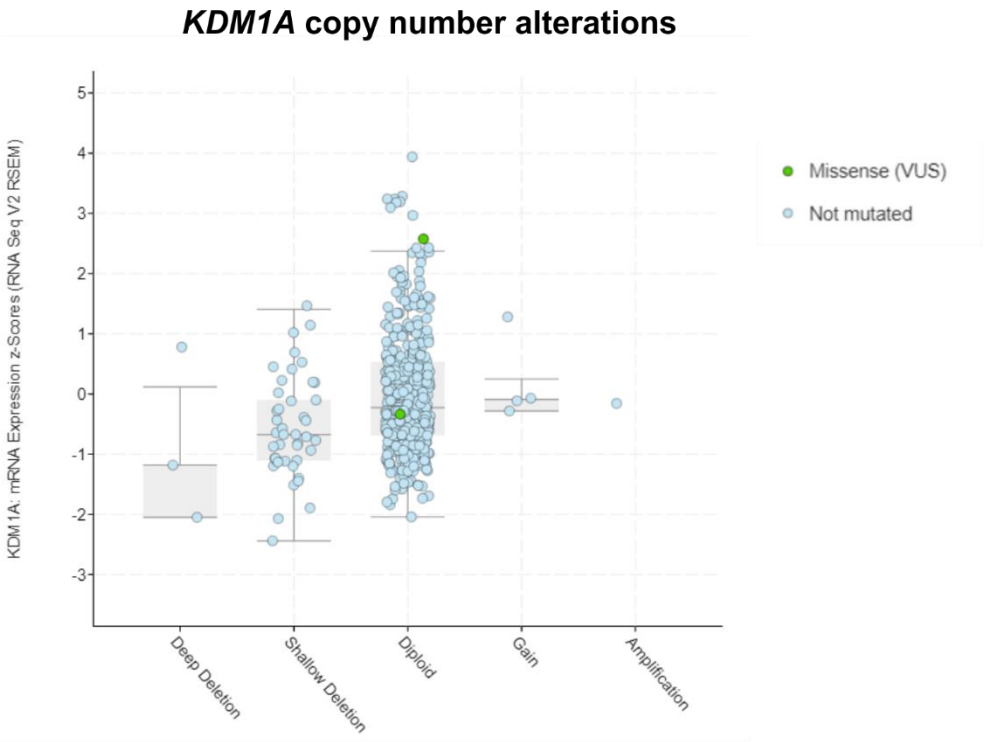

Figure 5.3: *KDM1A* copy number alterations in prostate cancer patients.
The cBioPortal for Cancer Genomics was used for bioinformatic analysis (https://www.cbioportal.org/, accessed 12.06.2019). The majority of patients was diploid for *KDM1A*, however, around 8% had a heterozygous deletion (shallow deletion) and only a few had a *KDM1A* homozygous deletion (deep deletion) or copy number gain.

Kaplan-Meier estimates were performed using the TCGA Provisional Prostate Adenocarcinoma study (z-score=1) to investigate overall survival and progression/disease-free survival. Cases with *KDM1A* alterations had the same overall survival as cases without alterations (**Figure 4.4, A**). However, the disease/progression-free survival was significantly poorer ($p \leq 0.05$) if *KDM1A* was altered (**Figure 4.4, A**).

A **Overall survival Kaplan-Meier Estimate (z=1)**

KDM1A

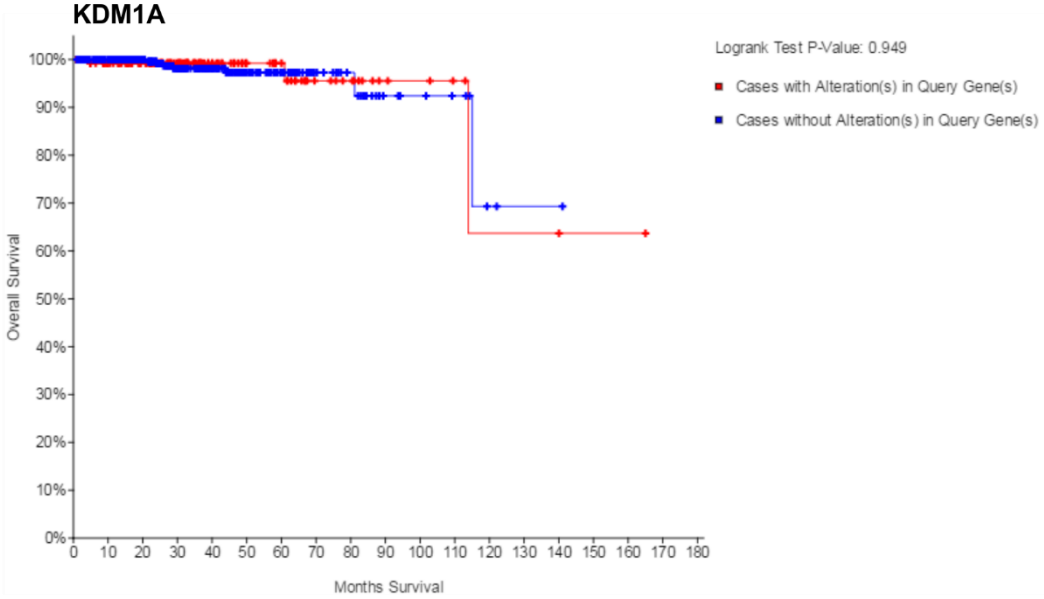

	Number of cases, Total	Number of cases, Deceased
Cases with Alteration(s) in Query Gene(s)	**147**	**3**
Cases without Alteration(s) in Query Gene(s)	**351**	**7**

B **Disease/Progression-free survival Kaplan-Meier Estimate (z=1)**

KDM1A

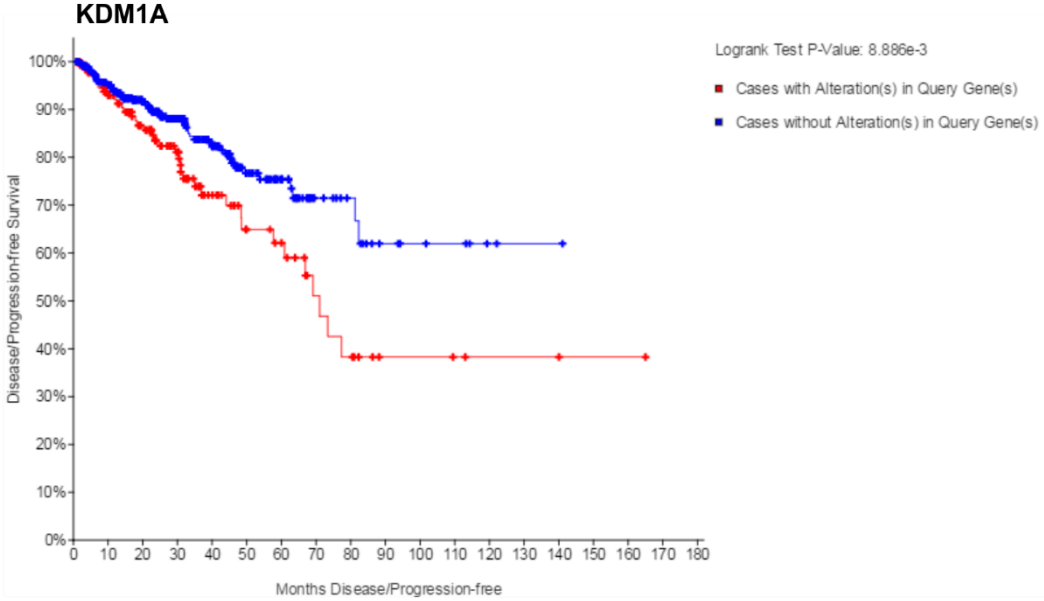

	Number of cases, Total	Number of cases, Relapsed/Progressed
Cases with Alteration(s) in Query Gene(s)	**146**	**37**
Cases without Alteration(s) in Query Gene(s)	**346**	**54**

Figure 5.4: Kaplan-Meier survival estimates regarding KDM1A alterations (z-score=1).
The TCGA Provisional Prostate Adenocarcinoma study was analysed with the cBioPortal for cancer genomics. (**A**) The overall survival did not differ between cases with and without *KDM1A* alterations. (**B**) Cases with *KDM1A* alterations had a significantly lower disease/progression-free survival than cases without alterations.

5.2.2 KDM1A staining in human tissue specimens

A tissue microarray (TMA) was used to investigate KDM1A expression in prostate cancer patients (see **Chapter 2: 2.2 Tissue micro array**). KDM1A protein expression was examined by using immunohistochemical (IHC) staining and H-score evaluation (**Figure 5.5**). Representative pictures of KDM1A staining of normal prostate tissue (**A, B**), tumour tissue (**C, D**) and less differentiated tumour tissue (**E, F**) are depicted (**Figure 5.5**). As described before, KDM1A was scored by a second independent scorer (CW) and scoring reliability tested. The Spearman correlation coefficient (R^2) lied above 0.6 for both nuclear and cytoplasmic H-scores which is considered "good" (1 = "perfect") and the Cronbach's alpha test revealed a value of ~0.9, validating the scoring reliability. The distribution curve for the evaluated H-scores across all patients can be found in **Appendix 13**. H-scores were equally divided into three groups (low, medium, high). As reported before (Battaglia et al., 2017, Kahl et al., 2006, Kashyap et al., 2013, Metzger et al., 2005, Wang et al., 2019d), KDM1A nuclear (**A**) and cytoplasmic (**B**) staining were higher in tumour tissue compared to normal tissue (**Figure 5.5**).

A Kaplan-Meier estimate was performed to confirm the relationship between KDM1A expression and biochemical recurrence in patients, however surprisingly, KDM1A expression did not correlate with biochemical recurrence which contradicts previous findings (Kashyap et al., 2013) (**Figure 5.6**).

KDM1A staining was correlated with other patient parameters like Gleason and TNM stage and revealed that there was no correlation with KDM1A nuclear expression (**Appendix 14**). However, low cytoplasmic staining correlated ($p \leq 0.05$) with high Gleason score (**A**) and high cytoplasmic staining correlated ($p \leq 0.05$) with extraprostatic extension (**B**) (≙ TNM stage T3, **Appendix 14**) (**Figure 5.7**).

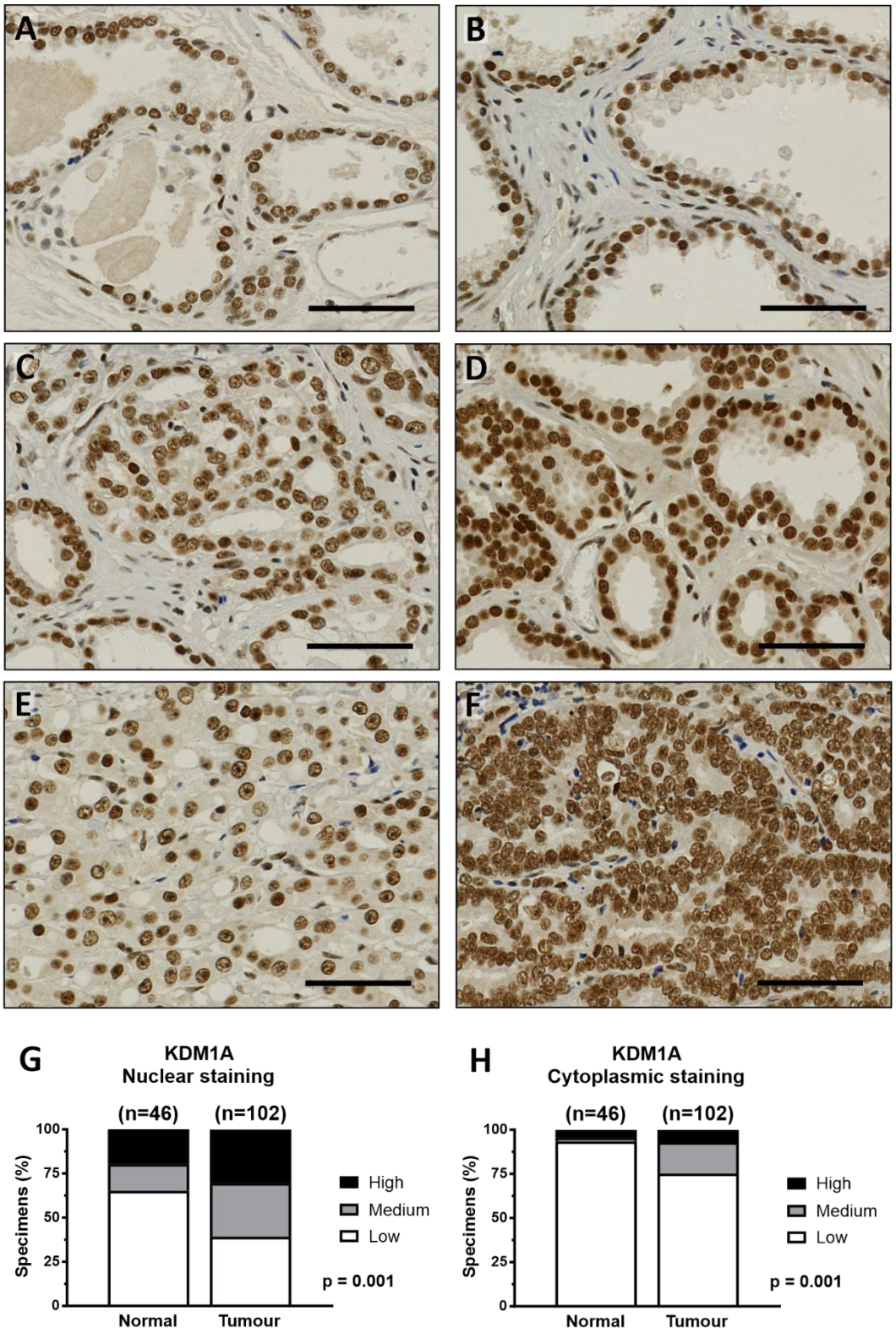

Figure 5.5: Immunohistochemical staining of KDM1A in PCa specimens.
To determine the expression of KDM1A protein, immunohistochemistry was used in normal (n = 46) and tumour (n = 102) specimens. Representative KDM1A staining of normal tissue (**A, B**), tumour tissue (**C, D**) and less differentiated tumour tissue (**E, F**) (Scale bars: 50 µM). KDM1A staining was higher (p = 0.001) in tumour compared to normal specimens in both nucleus (**J**) and cytoplasm (**K**). Nuclear H-score, low = 90-110, medium = 120-140, high = 150-220; Cytoplasmic H-score, low = 0, medium = 10-50, high = 90-100; BCR = Biochemical recurrence. Statistical p-values were determined by χ^2-test (VassarStats).

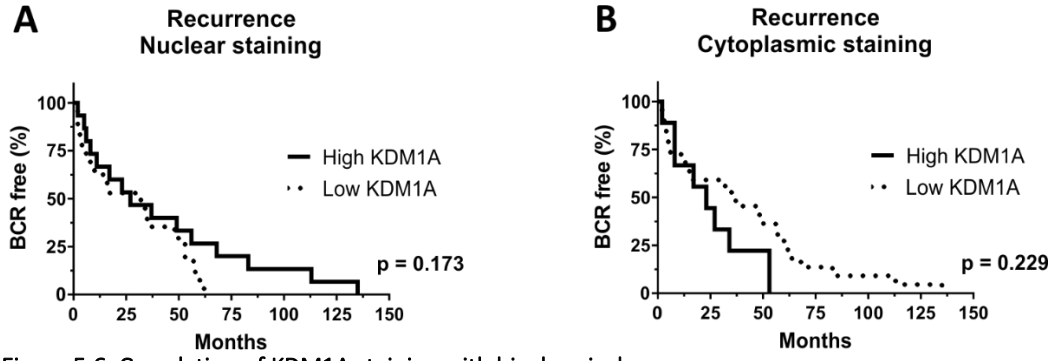

Figure 5.6: Correlation of KDM1A staining with biochemical recurrence.
The Kaplan Meier estimate was used to correlate KDM1A staining with the BCR free time of patients (n = 32). KDM1A nuclear (A) and cytoplasmic (B) staining in tumour tissue did not correlate with BCR free status in patients. BCR = Biochemical recurrence; Nuclear H-score, low = 90-120, high = 130-220; cytoplasmic H-score, low = 0, high = 10-100. Statistical analysis was performed with log-rank test.

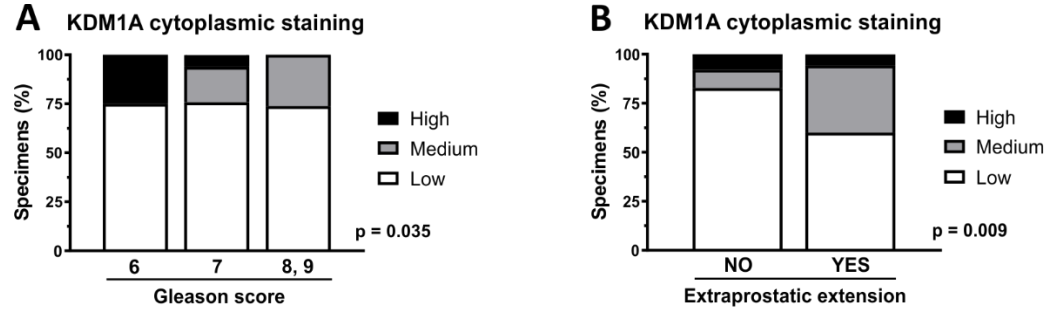

Figure 5.7: Correlation of KDM1A staining with clinical patient data.
KDM1A nuclear and cytoplasmic staining intensities were assessed by H-score and correlated with clinical data by using SPSS analysis (n = 102). Low KDM1A cytoplasmic staining correlated with high Gleason score (A) and extraprostatic extension (B). Cytoplasmic H-score 3 groups, Low = 0, Medium = 10-50, High = 90-100; Statistical analysis was performed by χ2-test.

To determine the relationship between KDM expression in prostate cancer patients, KDM1A, KDM5B and KDM7A staining respectively were correlated with each other (Figure 5.8). Interestingly, high KDM1A nuclear staining correlated with high KDM7A and KDM5B nuclear staining (Figure 5.8, A), and similarly KDM7A nuclear staining correlated with KDM5B nuclear staining (Figure 5.8, B), suggesting a functional relationship between KDM expression (Appendix 15).

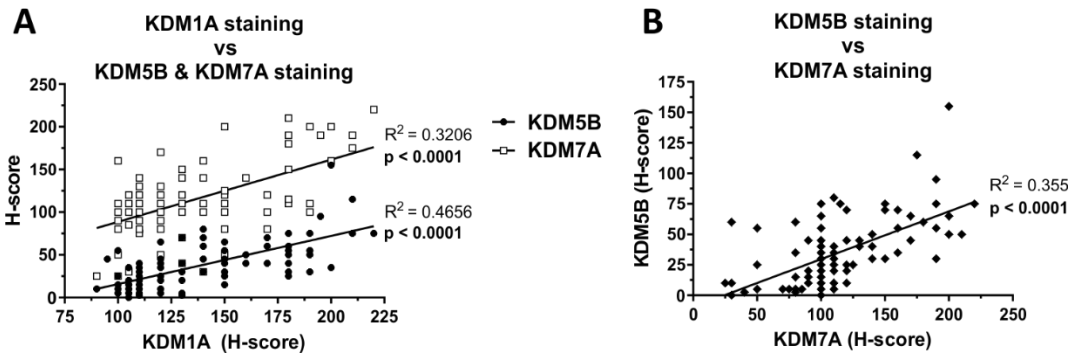

Figure 5.8: Relationship between staining intensities of KDMs.
Linear regression and statistical analysis were performed with GraphPad Prism. (**A**) High KDM1A nuclear staining correlated with high KDM7A nuclear and high KDM5B nuclear staining. (**B**) High KDM5B and KDM7A nuclear stainings correlated too. Goodness of Fit was expressed as R^2 and whether the slope was significantly non-zero was given as p-value.

5.2.3 KDM1A is overexpressed in prostate cancer cell lines

Basal expression levels of KDM1A were investigated in normal prostate PNT1A cells and in the prostate cancer cell lines LNCaP, LNCaP:C4-2, 22Rv1, PC3 and Du145 (**Figure 5.9**). KDM1A expression was examined at both the mRNA and protein level using qRT-PCR (**Figure 5.9, A**) and western blots respectively (**Figure 5.9, B-C**). On the mRNA level, *KDM1A* expression was higher in all prostate cancer cell lines compared to non-malignant PNT1A cells with the highest level in 22RV1 and Du145 (~7-fold higher, $p \leq 0.05$), second highest in LNCaP and LNCaP:C4-2 (~4-fold, $p \leq 0.05$) and 2-fold ($p \leq 0.05$) elevated in PC3 cells (**Figure 5.9, A**). On the protein level, KDM1A expression was highest in LNCaP being ~2.6-fold ($p \leq 0.05$) higher than in PNT1A and second highest in LNCaP:C4-2 (~1.8-fold, $p \leq 0.05$) (**Figure 5.9, B**). In 22Rv1 and Du145 KDM1A was elevated only ~1.5-fold ($p \leq 0.05$) and in PC3 only ~1.3-fold compared to PNT1A, but did not reach statistical significance.

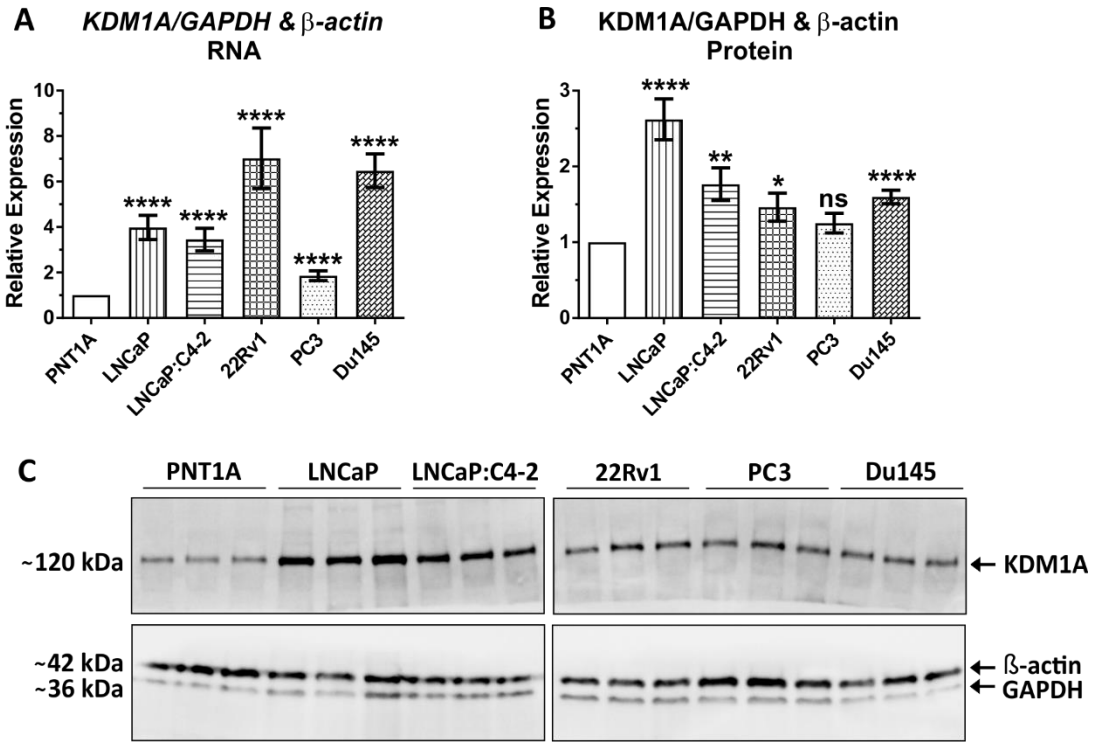

Figure 5.9: *KDM1A* mRNA and protein expression in PCa cell lines compared to normal cells.
KDM1A basal expression levels were determined by using qRT-PCR and western blots. The band intensities in the western blots **(C)** were quantified with ImageJ **(B)**. Statistical significances were calculated by comparing each cell line to the non-malignant PNT1A cell line (white column). (**A-B**) All prostate cancer cell lines express higher levels of KDM1A on both the mRNA (n = 9) and protein

(n = 3) level compared to non-malignant PNT1A. * = p ≤ 0.05; **p ≤ 0.005; *** = p ≤ 0.001; **** = p ≤ 0.0001 by unpaired t-test.

5.2.4 KDM1A expression is not androgen regulated

To investigate whether *KDM1A* mRNA expression is androgen regulated, cells were treated with the synthetic androgen (R1881, 1 nM) for three days and the effects on *KDM1A* expression investigated using qRT-PCR (Figure 5.10). The cell lines tested were non-malignant PNT1A cells and the prostate cancer cell lines LNCaP, LNCaP:C4-2, 22Rv1, PC3 and Du145. PNT1A, PC3 and Du145 served as negative controls as they are androgen-insensitive. In LNCaP, *KDM1A* mRNA expression was modestly (30%, p ≤ 0.05) decreased upon R1881 treatment (Figure 5.10, B). In contrast, *KDM1A* was not affected by R1881 in LNCaP:C4-2 and 22Rv1 (Figure 5.10, C-D). As expected, R1881 did not have any effect on *KDM5B* expression in PNT1A, PC3 and Du145 which lack AR expression (Figure 5.10, A, E-F)

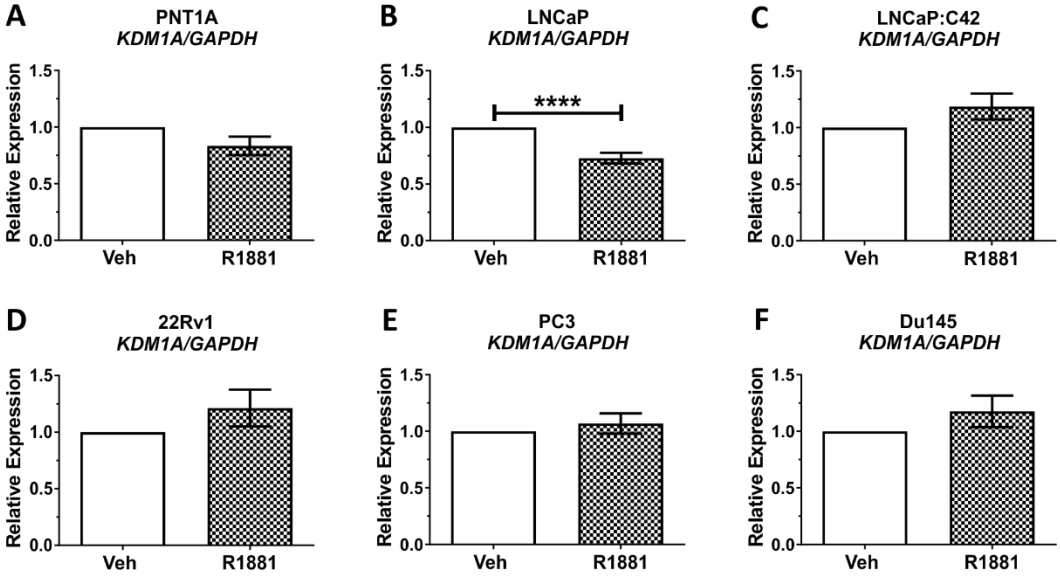

Figure 5.10: Effect of androgen on *KDM1A* expression in normal prostate and PCa cell lines.
Cells were treated with 1 nM R1881 and *KDM1A* mRNA expression was examined by qRT-PCR. (B-D) In the androgen-sensitive cell lines, *KDM1A* did not change upon R1881 treatment except for LNCaP (B) where *KDM1A* was moderately decreased (n = 9). As expected, R1881 did not have any effect in the androgen-insensitive control cell lines PNT1A (A), PC3 (E) and Dua145 (F) (n = 6). * = p ≤ 0.05; **p ≤ 0.005; *** = p ≤ 0.001; **** = p ≤ 0.0001 by paired t-test.

5.2.5 Functional depletion of KDM1A via siRNA attenuates R1881-induced PSA expression in LNCaP but not LNCaP:C4-2 and 22Rv1

To confirm the function of KDM1A in androgen signalling in prostate cancer, siRNAs were used to functionally deplete KDM1A in LNCaP, LNCaP:C4-2 and 22Rv1 cells. Knockdown was performed concomitantly with R1881 treatment for three days and the knockdown efficiency was confirmed by qRT-PCR (Figure 5.11). Knockdown efficiency of *KDM1A* in

LNCaP was around ~40 and ~50% ($p \leq 0.05$) in androgen untreated and treated samples respectively (**Figure 5.11, A**), and around ~90% ($p \leq 0.05$) in LNCaP:C4-2 and 22Rv1 (**Figure 5.11, B-C**). To examine the effect of KDM1A depletion on *PSA* and *VEGFA* mRNA expression, qRT-PCR was used (**Figure 5.11, D-I**). As shown before (Kashyap et al., 2013, Metzger et al., 2005). Knockdown of KDM1A attenuated R1881-induced *PSA* expression in LNCaP cells by 60% ($p \leq 0.05$) (**Figure 3.12, D**). In contrast, R1881-induced *PSA* was ~2-fold further increased in LNCaP:C4-2 and ~1.4-fold further elevated in 22Rv1 by KDM1A depletion (**Figure 5.11, E-F**), however, not statistically significantly. R1881-induced *VEGFA* expression was not statistically significantly, though modestly (~25%) reduced by siKDM1A in LNCaP (**Figure 5.11, G**). In LNCaP:C4-2, *VEGFA* was almost 3-fold ($p \leq 0.05$) increased through KDM1A knockdown, whereas *VEGFA* was unchanged in 22Rv1 (**Figure 5.11, H-I**).

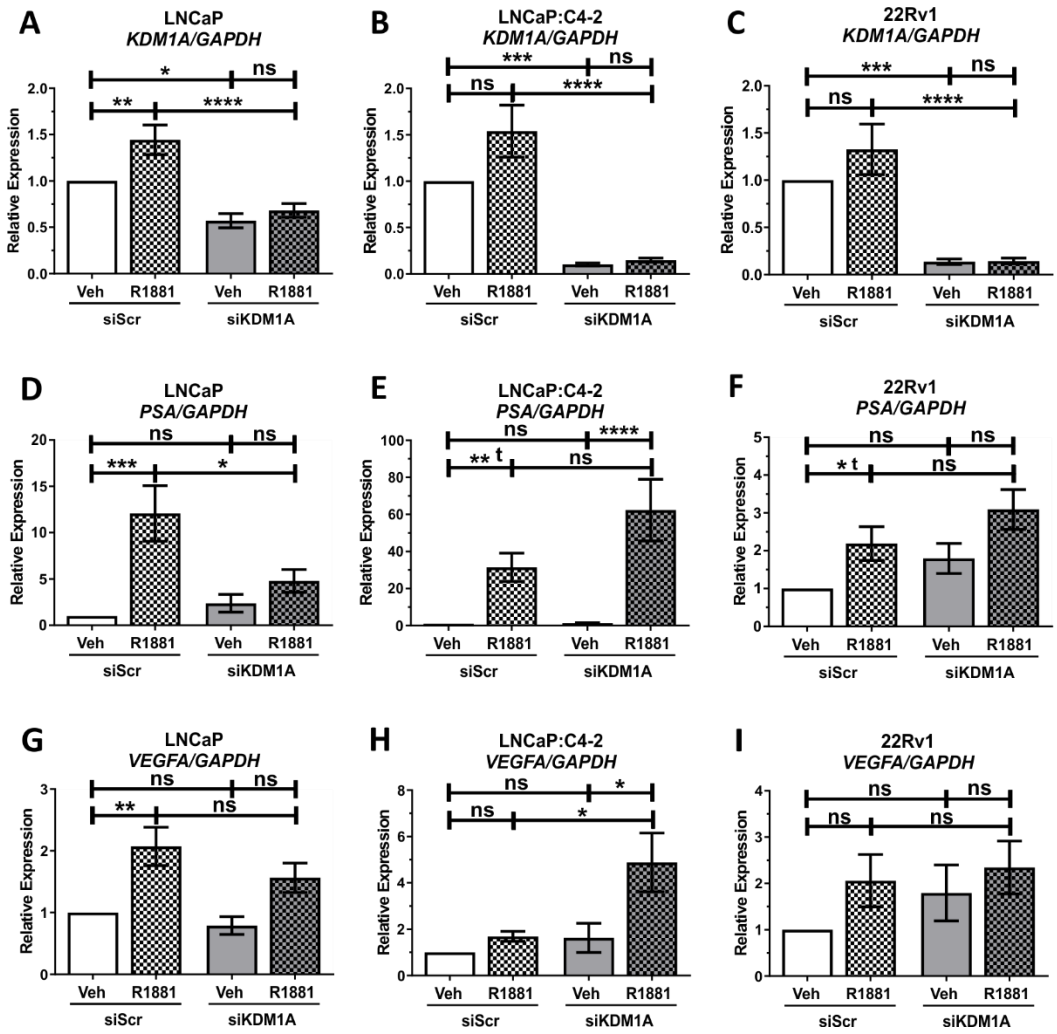

Figure 5.11: Effect of KDM1A knockdown on *PSA* and *VEGFA* expression in LNCaP, LNCaP:C4-2 and 22Rv1.

To measure *KDM1A*, *PSA* and *VEGFA* mRNA expression, qRT-PCR was used (n = min 5). In all cell lines LNCaP (**A**), LNCaP:C4-2 (**B**) and 22Rv1 (**C**), *KDM1A* was reduced upon KDM1A depletion, independent of R1881 treatment. KDM1A depletion significantly attenuated R1881-induced *PSA* expression in

LNCaP (**D**), but did not induce any significant changes in LNCaP:C42 (**E**) and 22Rv1 (**F**). In LNCaP (**G**) and 22Rv1 (**I**) siKDM5B did not have any effect on *VEGFA* expression, whereas in LNCaP:C-42 (**H**) *VEGFA* was upregulated. * = p ≤ 0.05; **p ≤ 0.005; *** = p ≤ 0.001; **** = p ≤ 0.0001 by ANOVA with Bonferroni's post hoc test and paired t-test.

5.2.6 KDM1A-selective inhibitor Namoline attenuates R1881-induced *PSA* expression

The effect of KDM1A-selective pharmaco-inhibitor Namoline (IC_{50} 51 µM) was tested on *PSA* and *VEGFA* mRNA expression in LNCaP, LNCaP:C4-2 and 22Rv1 (Willmann et al., 2012). (**Figure 5.12**). A Namoline dose curve was performed on cell proliferation to determine an appropriate inhibitor concentration (**Appendix 16**). Cells were then simultaneously treated with Namoline (50 µM) and androgen (R1881, 1 nM) for a period of three days and gene expression changes analysed by qRT-PCR. R1881-induced *PSA* mRNA expression was decreased by ~45-65% (p ≤ 0.05) in all three cell lines when treated with Namoline (**Figure 5.12, A-C**). In LNCaP cells, Namoline reduced *VEGFA* mRNA by 55% (p ≤ 0.05) (**Figure 5.12, D**), In LNCaP:C4-2, *VEGFA* mRNA was decreased by 80% (p ≤ 0.05) (**Figure 5.12, E**). In contrast, Namoline induced a ~1.7-fold (p ≤ 0.05) increase in *VEGFA* mRNA expression in 22Rv1 (**Figure 5.12, F & I**).

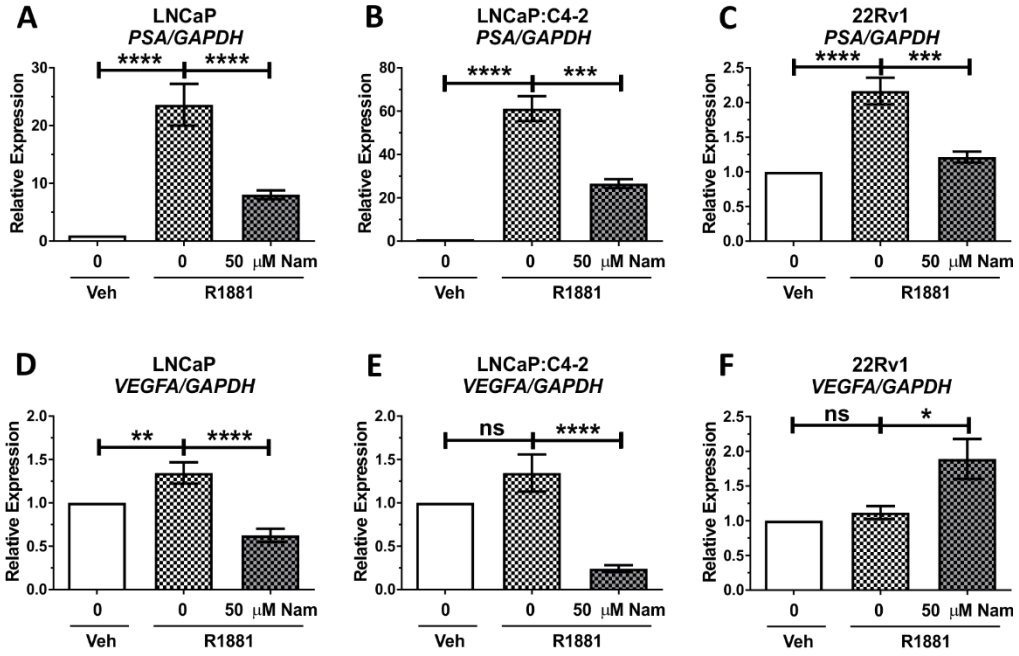

Figure 5.12: Effect of KDM1A-selective inhibitor Namoline on *PSA* and *VEGFA* expression in LNCaP, LNCaP:C4-2 and 22Rv1.

Gene expression changes were measured by qRT-PCR. In all cell lines LNCaP (n = 12) (**A**), LNCaP:C4-2 (n = 9) (**B**) and 22Rv1 (n = 6) (**C**), R1881-induced *PSA* expression was attenuated by 50 µM Namoline. *VEGFA* expression was inhibited in LNCaP (n = 12) (**D**) and LNCaP:C4-2 (n = 9) (**E**) but not in 22Rv1 (n = 6) (**F**) where *VEGFA* was increased by Namoline. * = p ≤ 0.05; **p ≤ 0.005; *** = p ≤ 0.001; **** = p ≤ 0.0001 by paired t-test.

5.2.7 KDM1A-selective inhibitor Namoline reduces proliferation of prostate cancer cells

The effect of Namoline was next tested on cell proliferation of non-malignant prostate PNT1A cells and the prostate cancer LNCaP, LNCaP:C4-2, 22Rv1, PC3 and Du134 cells using the CyQUANT™ assay (**Figure 5.13**). Cells were treated with Namoline (50 µM) and the DNA content was measured after 3 and 6 days respectively. Statistical significances were evaluated in comparison to untreated control cells. Cell proliferation of non-malignant PNT1A cells was not affected by Namoline after 6 days of treatment (**Figure 5.13, A**). Namoline had the most dramatic effect on LNCaP cells with a 70% ($p \leq 0.05$) reduction in proliferation after 6 days (**Figure 5.13, A**). In LNCaP:C4-2 and 22Rv1, Namoline inhibited proliferation by ~45-55% ($p \leq 0.05$) after 3 days, however, after 6 days only by ~30-35% ($p \leq 0.05$ in LNCaP:C4-2; not significantly in 22Rv1), indicating the ability of Namoline to diminish proliferation over time in LNCaP:C4-2 and 22Rv1 (**Figure 5.13, C-D**). PC3 cell proliferation was 40% ($p \leq 0.05$) decreased by Namoline (**Figure 5.13, E**). Surprisingly, in Du145 Namoline induced a 3.7-fold ($p \leq 0.05$) increase in cell proliferation after 6 days (**Figure 5.13, F**).

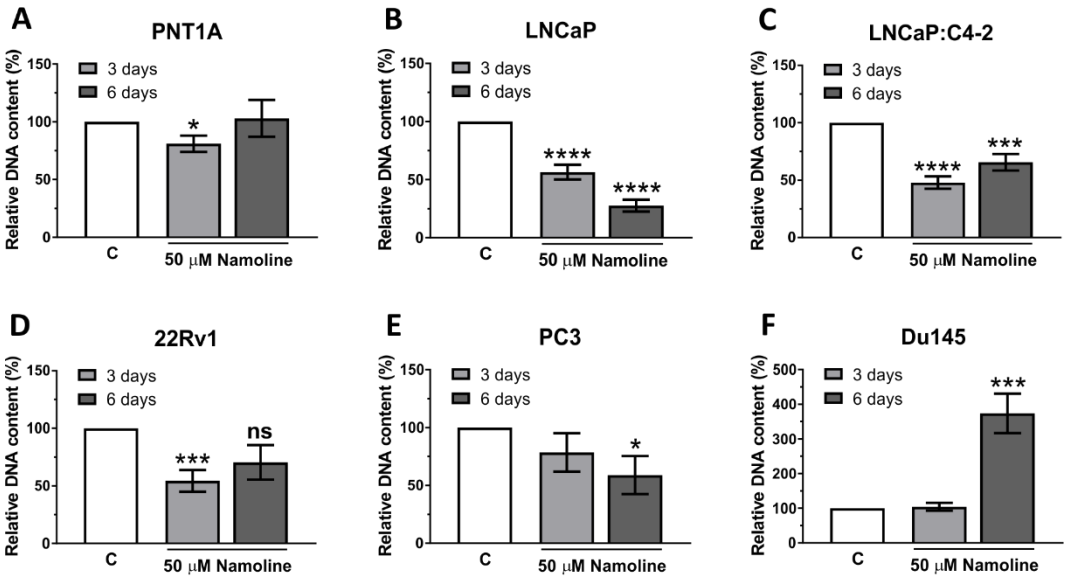

Figure 5.13: Effect of KDM1A-selective inhibitor Namoline on cell proliferation of normal prostate and PCa cell lines.
The CyQUANT™ assay was used to determine cell proliferation after 3 days and after 6 days of inhibitor treatment. Statistical significances were calculated in comparison to the untreated control cells (white column) (n = min 12). (**A**) PNT1A cell proliferation was not affected by Namoline. In LNCaP (**B**), LNCaP:C4-2 (**C**), 22Rv1 (**D**) and PC3 (**E**) cells proliferated less upon Namoline. (**F**) In contrast, Du145 cell proliferation was increased after 6 days of Namoline treatment. * = $p \leq 0.05$; **$p \leq 0.005$; *** = $p \leq 0.001$; **** = $p \leq 0.0001$ by paired t-test.

5.2.8 Combinatorial analysis of the roles of KDM1A and KDM7A in androgen signalling

5.2.8.1 Combination of siKDM1A + siKDM7A attenuates R1881-induced PSA and *VEGFA expression in LNCaP and LNCaP:C4-2 but not 22Rv1*

To investigate combinatorial functions of KDM1A and KDM7A, both proteins were simultaneously silenced by siRNAs in the androgen-sensitive cell lines LNCaP, LNCaP:C4-2 and 22Rv1 (**Figure 5.14**). As previously described, siRNA treatment and concomitant androgen treatment (R1881, 1 nM) were performed over a period of 3 days and the effects on *PSA* and *VEGFA* expression determined by qRT-PCR. When combining siKDM1A + siKDM7A, *KDM1A* mRNA was knocked down by ~70-90% ($p \leq 0.05$) in LNCaP, LNCaP:C4-2 and 22Rv1 (**Figure 5.14, A-C**). Similarly, KDM7A mRNA was 50% ($p \leq 0.05$) decreased in LNCaP in androgen treated samples, and ~70-80% ($p \leq 0.05$) reduced in LNCaP:C4-2 and 22Rv1 (**Figure 5.14, D-F**). In **Table 5.2** the knockdown efficiency of combined siRNA-mediated deletion of *KDM1A* and *KDM7A* mRNA was compared to deletion of *KDM1A* (**Figure 5.11**) and *KDM7A* (**Figure 4.11**) mRNA alone respectively. The percentages given in the table represent the knockdown with concomitant androgen-treatment (**Table 5.2**) which corresponds to the check-patterned columns in **Figure 5.14**.. In LNCaP cells, the knockdown of *KDM1A* was more efficient when combined siKDM1A and siKDM7A was applied (~71%) in comparison to siKDM1A alone (~53%), whereas *KDM7A* knockdown was less efficient in the combination treatment (53%) compared to siKDM7A alone (63%) (**Table 5.2)**. In LNCaP:C4-2 and 22Rv1, the knockdown efficiencies were similar between combined and single siRNA treatments (**Table 5.2**).

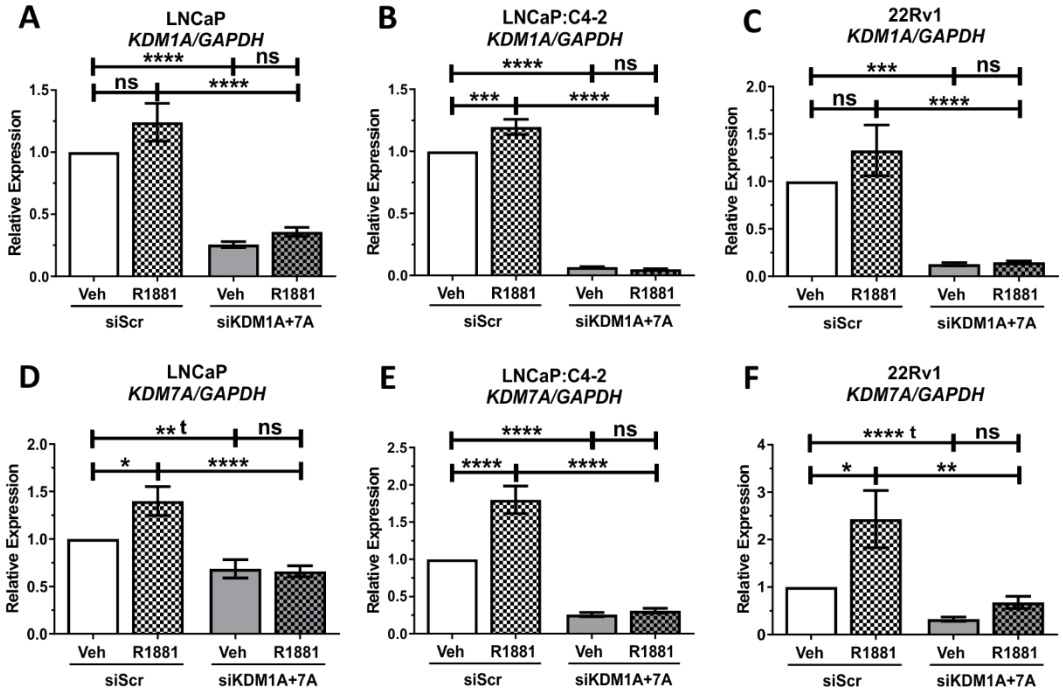

Figure 5.14: Confirmation of siRNA-mediated simultaneous knockdown of KDM1A and KDM7A in LNCaP, LNCaP:C4-2 and 22Rv1.

Knockdown of KDM1A and KDM7A and concomitant androgen (R1881, 1 nM) treatment was investigated using qRT-PCR analysis (n = min 5). *KDM1A* (A-C) and *KDM7A* (D-F) mRNA were successfully knocked down in all three cell lines, in both androgen treated and vehicle control samples. * = p ≤ 0.05; **p ≤ 0.005; *** = p ≤ 0.001; **** = p ≤ 0.0001 by ANOVA with Bonferroni's post hoc test and paired t-test.

Table 5.2: Comparison of KDM knockdown between single and combined siKDM1A and siKDM7A treatments.

The knockdown of *KDM1A* and *KDM7A* respectively after androgen (R1881, 1 nM) and siRNA treatment compared to androgen and siScramble treatment is expressed in percent. - = decrease in gene expression (down). Statistical significances are given in * = p ≤ 0.05; **p ≤ 0.005; *** = p ≤ 0.001; **** = p ≤ 0.0001.

Gene	Tretment	LNCaP	LNCaP:C4-2	22Rv1
KDM1A	siKDM1A	- 53% (down) ****	- 90% (down) ****	- 89% (down) ****
	siKDM1A+7A	**- 71% (down) ******	**- 96% (down) ******	**- 89% (down) ******
KDM7A	siKDM7A	- 63% (down) ****	- 77% (down) ****	- 76% (down) **
	siKDM1A+7A	**- 53% (down) ******	**- 83% (down) ******	**- 72% (down) **

To test if combined KDM1A + KDM7A knockdown had distinct effects on R1881-induced *PSA* expression compared to KDM1A and KDM7A knockdowns alone, qRT-PCR analysis was performed in LNCaP, LNCaP:C4-2 and 22Rv1 (Figure 5.15). The percentages of R1881-induced *PSA* attenuation or further increase after combined treatment compared to single siRNA treatments were given in Table 5.3. Combining siKDM1A + siKDM7A attenuated R1881-induced *PSA* expression by 53% (p ≤ 0.05) which was similar of as was observed by siKDM1A (~60%) and siKDM7A (~47%) alone, suggesting KDM1A and KDM7A may be functionally interdependent (Figure 5.15, A, D, G). In

contrast, there was an apparent additive effect in LNCaP:C4-2 when combined siKDM1A + siKDM7A lead to a ~54% ($p \leq 0.05$) *PSA* reduction whereas siKDM1A alone failed to impair *PSA* induction by R1881 and siKDM7A alone only reduced *PSA* by ~39% ($p \leq 0.05$) (Figure 5.15, B, E, H). In 22Rv1, siKDM1A + siKDM7A combination, similar to siKDM1A and siKDM7A respectively alone (Table 5.3), failed to attenuate R1881-induced *PSA* (Figure 5.15, C, F, I).

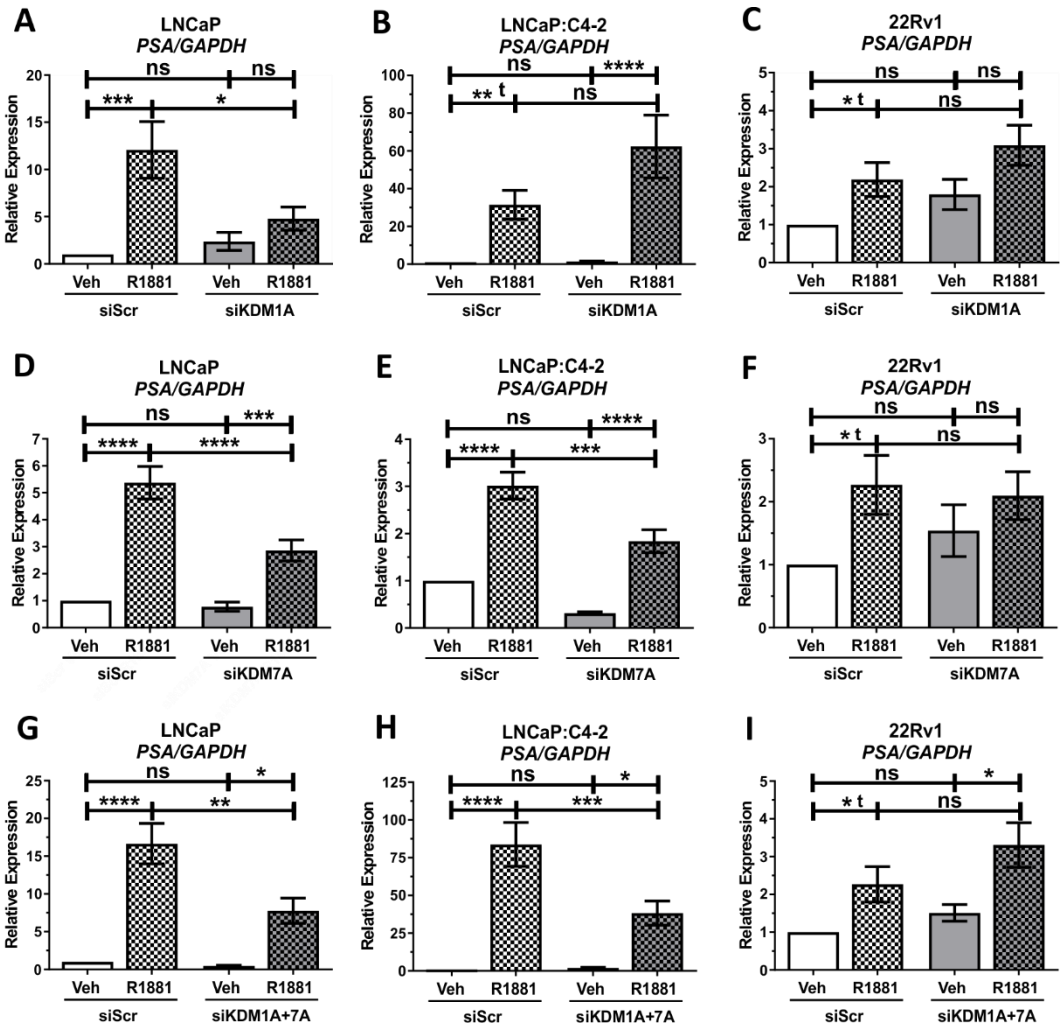

Figure 5.15: Effect of combined KDM1A and KDM7A knockdown on *PSA* expression in LNCaP, LNCaP:C4-2 and 22Rv1.

Gene expression changes after siRNA and androgen (R1881, 1 nM) treatment were investigated using qRT-PCR (n = min 5). In LNCaP, combined treatment (**G**) had the same effect on *PSA* expression as when treated with siKDM1A (**A**) and siKDM7A (**D**) individually. In LNCaP:C4-2, combining siKDM1A and siKDM7A (**H**) attenuated R1881-induced *PSA* more than in the individual siRNAs (**B**, **E**). No effect was seen on *PSA* in 22Rv1 (**C, F, I**). * = $p \leq 0.05$; **$p \leq 0.005$; *** = $p \leq 0.001$; **** = $p \leq 0.0001$ by ANOVA with Bonferroni's post hoc test and paired t-test.

Another androgen-regulated gene, *VEGFA*, was used to examine the effects of combined siKDM1A + siKDM7A application compared to single siRNA applications (Figure 5.16, Table 5.3). In LNCaP, R1881-induced *VEGFA* expression was decreased by ~56% ($p \leq 0.05$) by combined siKDM1A + siKDM7A compared to ~25-28% ($p \leq 0.05$) by single siKDM1A and

siKDM7A respectively (**Figure 5.16, A, D, G**), suggesting an additive effect. Similarly, an apparent additive effect was detected in LNCaP:C4-2, where single siRNAs either increased (**B**), or did not change (**E**), *VEGFA* expression, but combined siRNA-mediated depletion of KDM1A and KDM7A decreased *VEGFA* by ~36% ($p \leq 0.05$) (**Figure 5.16, H**). Androgen induction of *VEGFA* in 22Rv1 was unaffected by combined siRNA depletion of KDM1A and KDM7A (**I**), as well as single depletions (**Figure 5.16, C, F**).

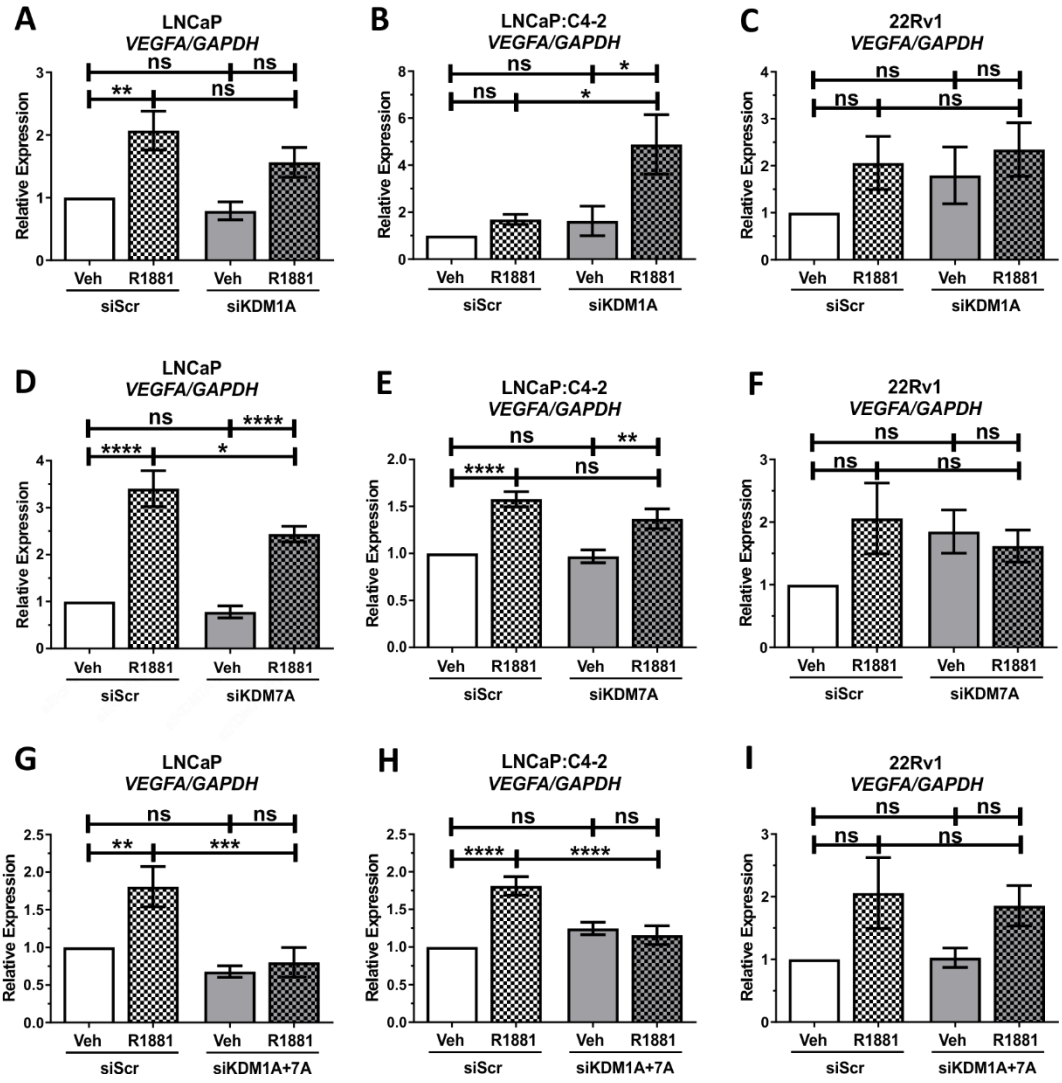

Figure 5.16: Effect of combined KDM1A and KDM7A knockdown on VEGFA expression in LNCaP, LNCaP:C4-2 and 22Rv1.

qRT-PCR was used to examine gene expression changes caused by siRNA and androgen (R1881, 1 nM) treatment (n = min 5). In both LNCaP (**G**) and LNCaP:C4-2 (**H**), combining siKDM1A and siKDM7A decreased *VEGFA* expression more than when applying single siRNAs only (**A, D** and **B, E** respectively). In 22Rv1, *VEGFA* expression was unchanged (**E, F, I**). Veh = vehicle, siScr = siScramble, * = $p \leq 0.05$, ** = $p \leq 0.005$, *** = $p \leq 0.001$, **** = $p \leq 0.0001$ by ANOVA with Bonferroni's post hoc test and paired t-test.

Table 5.3: Comparison of gene expression changes between single and combined siKDM1A and siKDM7A treatments.
Androgen (R1881, 1 nM) and siRNA treated samples were compared to androgen and siScramble control samples and the *PSA* and *VEGFA* gene expression changes are stated in percent. + = increase in gene expression (up); - = decrease in gene expression (down). Statistical significances are given in * = p ≤ 0.05; **p ≤ 0.005; *** = p ≤ 0.001; **** = p ≤ 0.0001.

Gene	Treatment	LNCaP	LNCaP:C4-2	22Rv1
PSA	siKDM1A	- 60% (down) *	+ 98% (up) ns	+ 40% (up) ns
	siKDM7A	- 47% (down) ****	- 39% (down) ***	- 8% (down) ns
	siKDM1A+7A	**- 53% (down) ****	**- 54% (down) ***	**+ 46% (up) ns**
VEGFA	siKDM1A	- 25% (down) ns	+ 188% (up) *	+ 14% (up) ns
	siKDM7A	- 28% (down) *	- 13% (down) ns	- 21% (down) ns
	siKDM1A+7A	**- 56% (down) ***	**- 36% (down) ****	**+ 10% (up) ns**

5.2.8.2 Combination of Namoline and TC-E 5002 attenuates R1881-induced PSA expression in androgen-responsive cell lines

The prostate cancer cells LNCaP, LNCaP:C4-2 and 22Rv1 were simultaneously treated with the KDM1A-selective inhibitor Namoline and the KDM7A-selective inhibitor TC-E 5002 to test if combined treatment had a different effect on *PSA* and *VEGFA* expression than single inhibitor treatments (**Figure 5.17**). The effect of combined inhibitor treatment on R1881-induced gene expression is highlighted by a red error bar in **Figure 5.17**. As before, inhibitor treatment was performed for 3 days simultaneously with androgen (R1881, 1 nM) and gene expression changes measured via qRT-PCR. The change of *PSA* expression (in percent) between R1881-treated vehicle control and inhibitor treated samples of combined and single inhibitor treatments are listed in **Table 5.4**. There was no difference in attenuation of R1881-induced *PSA* and *VEGFA* in LNCaP with Namoline and TC-E 5002, as compared with Namoline alone (**Figure 5.17, A, D**), suggesting functional interdependence. However, combined inhibition of KDM1A and KDM7A by Namoline and TC-E 5002 in LNCaP:C4-2 cells resulted in a more dramatic reduction (~82%) of R1881 induction of *PSA* as compared with Namoline (~62%) and TC-E 5002 (~2%) alone (**Figure 5.17, B**, **Table 5.4**). Similarly, in 22Rv1 Namoline + TC-E 5002 combination inhibited R1881-induced *PSA* by ~63% (p ≤ 0.05 by t-test) as compared with Namoline alone (~44%) (**Figure 5.17, C**). *VEGFA* mRNA was 30% elevated, but this was not statistically significantly, in the Namoline + TC-E 5002 combination in LNCaP:C4-2 compared to ~60% reduced *VEGFA* mRNA induced by single inhibitor treatments (**Figure 5.17, E**, and **Table 5.4**). In 22Rv1, *VEGFA* mRNA expression was increased ~2-fold (p ≤ 0.05) by combined Namoline + TC-E 5002 treatment and was at similar expression levels as *VEGFA* by individual inhibitor treatments (**Figure 5.17, F** and

Table 5.4), suggesting no additive inhibitory effect on *VEGFA* by combining Namoline with TC-E 5002.

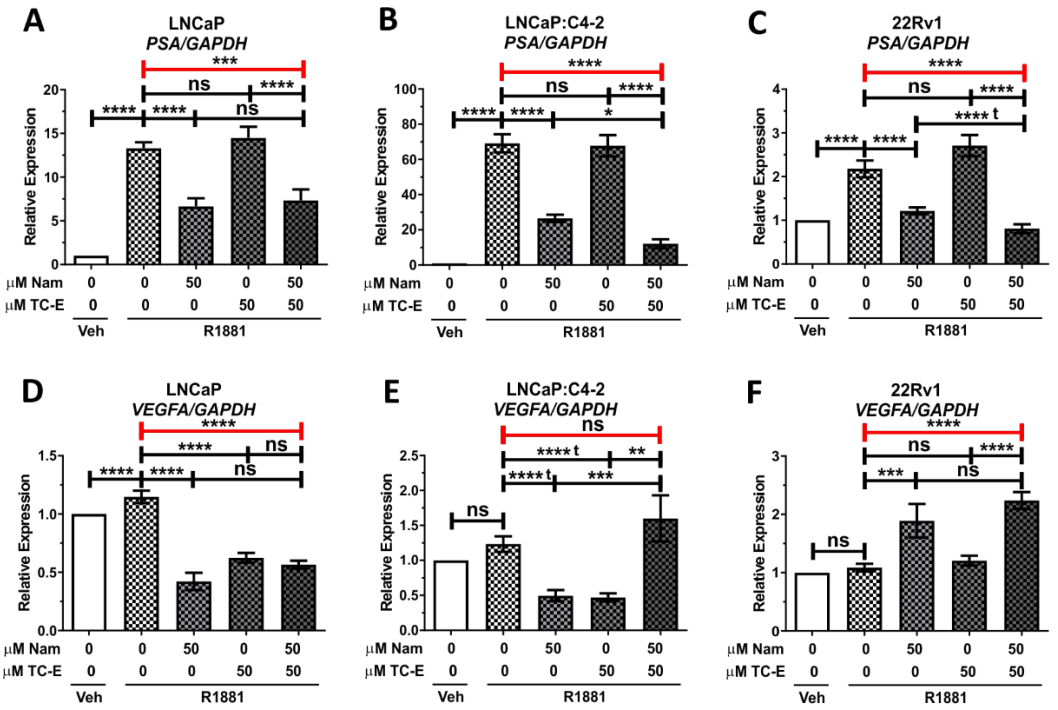

Figure 5.17: Effect of combined KDM1A- and KDM7A-selective inhibitors on *PSA* and *VEGFA* expression in LNCaP, LNCaP:C4-2 and 22Rv1.
Gene expression changes upon inhibitor and androgen (R1881, 1 nM) treatment were examined using qRT-PCR (n = min 6). Whilst in LNCaP (**A**) combining Namoline with TC-E 5002 had the same effect on R1881-induced *PSA* expression as Namoline on its own, both in LNCaP:C4-2 (**B**) and 22Rv1 (**C**) an enhanced inhibitory effect was achieved by the combination. *VEGFA* expression levels were the same between the combination and single inhibitor applications in LNCaP (**D**). In LNCaP:C4-2, Namoline and TC-E 5002 combination increased *VEGFA* (**E**). In 22Rv1, *VEGFA* mRNAwas elevated (**F**). Nam = Namoline (KDM1A-selective inhibitor), TC-E = TC-E 5002 (KDM7A-selective inhibitor), * = $p \leq 0.05$, ** = $p \leq 0.005$, *** = $p \leq 0.001$, **** = $p \leq 0.0001$ by ANOVA with Bonferroni's post hoc test and paired t-test.

Table 5.4: Comparison of gene expression changes between single and combined KDM1A and KDM7A inhibitor treatments.
Androgen (R1881, 1 nM) and inhibitor treated samples were compared to androgen and vehicle treated control samples and *PSA* gene and *VEGFA* gene and protein expression are stated in percent. + = increase in gene/protein expression; - = decrease in gene/protein expression. * = $p \leq 0.05$, ** = $p \leq 0.005$, *** = $p \leq 0.001$, **** = $p \leq 0.0001$.

Gene / protein	Treatment	LNCaP	LNCaP:C4-2	22Rv1
PSA gene	Namoline	- 50% (down) ****	- 62% (down) ****	- 44% (down) ****
	TC-E 5002	+ 9% (up) ns	- 2% (down) ns	+ 24% (up) ns
	Nam + TC-E	**- 45% (down) *****	**- 82% (down) ********	**- 63% (down) ********
VEGFA gene	Namoline	- 63% (down) ****	- 60% (down) ****	+ 74% (up) ***
	TC-E 5002	- 46% (down) ****	- 62% (down) ****	+ 11% (up) ns
	Nam + TC-E	**- 51% (down) ********	**+ 30% (up) ns**	**+ 106% (up) ********

5.2.8.3 Combination of Namoline and TC-E 5002 attenuates R1881-induced expression of androgen responsive genes

To further investigate the combinatory effects of Namoline and TC-E 5002, RNA sequencing (RNA-Seq) analysis was performed. The RNA-Seq was conducted in duplicate samples with androgen (R1881, 1 nM) and combined 50 µM Namoline + 50 µM TC-E 5002 treated samples, and androgen and DMSO treated control samples in **Figure 5.17**, for both LNCaP and LNCaP:C4-2 cells. To compare differentially expressed genes after androgen and combined inhibitor treatment between LNCaP and LNCaP:C4-2 cells, a Venn-diagram was created (**Figure 5.18**). The genes exhibiting a logFC (fold change) ≥1 and ≥-1 respectively were filtered and used for the Venn diagram. Within these criteria, 2699 genes were down-regulated and 1817 genes were up-regulated in LNCaP cells upon combined Namoline and TC-E 5002 treatment. In LNCaP:C4-2 cells, 2908 genes were down-regulated, whereas 2369 genes were up-regulated after inhibitor treatment. Interestingly, only 8.7% (449 genes) of the down-regulated genes were the same between LNCaP and LNCaP:C4-2 (**A**), whereas 22.2% (760 genes) of the up-regulated genes were common in those two cell lines (**Figure 5.18, B**).

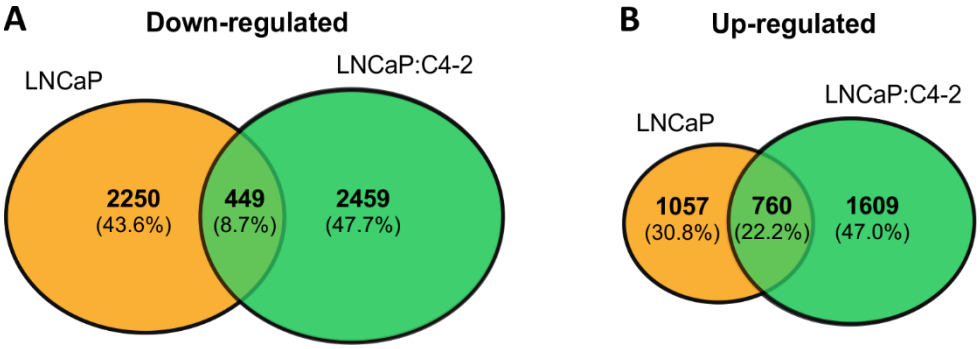

Figure 5.18: Venn diagram of differentially expressed genes between LNCaP and LNCaP:C4-2 cells. RNASeq analysis was performed to elucidate down- (**A**) and up-regulated (**B**) genes after androgen and combined Namoline + TC-E 5002 treatment. Differentially expressed genes were compared between LNCaP and LNCaP:C4-2 cells. Jennie Jeyapalan, 2019.

Heatmap analysis was performed with the RNASeq gene counts of the androgen (R1881, 1 nM) and DMSO control samples and the androgen and combined Namoline + TC-E 5002 treated samples in LNCaP (**Figure 5.19** and **Figure 5.20**) and LNCaP:C4-2 (**Figure 5.21** and **Figure 5.22**) cells. For this analysis, differentially expressed genes were investigated using a selected list of AR-regulated genes (1359 genes in total) (Sharma et al., 2013). Gene counts were expressed as log2 and hierarchical gene clustering (performed by Nigel Mongan). In both LNCaP (**Figure 5.19**) and LNCaP:C4-2 (**Figure 5.21**) cells, the combined

treatment of Namoline (50 µM) and TC-E 5002 (50 µM) reduced expression of most genes compared to DMSO control samples. In contrast, a subset of genes showed increased expression in Nam+TC-E samples than in DMSO control samples (**Figure 5.19** and **Figure 5.21**). To elucidate the genes that are in the same hierarchical cluster as *KLK3/PSA*, the *KLK/PSA* comprising cluster was analysed in more detail in both LNCaP (**Figure 5.20**) and LNCaP:C4-2 (**Figure 5.22**) cells. Interestingly, in LNCaP cells, the gene *NKX3.1* was clustered with *PSA/KLK3* (**Figure 5.20**), and in LNCaP:C4-2, *FOXA1* clustered with *PSA/KLK3* (**Figure 5.22**). Both *NKX3*.1 and *FOXA1* can function as either a tumour suppressor or oncogene (Bhatia-Gaur et al., 1999, Bowen et al., 2000, He et al., 1997, Korkmaz et al., 2000, Sahu et al., 2011, Wang et al., 2011).

To validate the RNASeq gene counts, qRT-PCR was conducted. In **Table 5.5** and **Table 5.6**, the validated genes are highlighted in grey and their RNASeq logFC and FDR are given. In addition, other *KLK3/PSA* and *VEGFA*-related genes, such as *KLK2*, *HIF1α* and *NDUFA4L2*, are shown, as well as *KDM1A*, *KDM5B* and *KDM7A* (**Table 5.5** and **Table 5.6**), however, these genes have not been validated by qRT-PCR. As already described, combined Namoline + TC-E 5002 attenuated R1881-induced *PSA* and *VEGFA* expression in LNCaP cells (**Figure 5.17, A, D** and **Table 5.4**), which is conform with the RNASeq logFC of these genes (**Table 5.5**). Similarly, in androgen treated LNCaP:C4-2 samples, Nam+TC-E induced down-regulation of *PSA* and up-regulation of *VEGFA* compared to DMSO control samples by qRT-PCR analysis (**Figure 5.17, B, E** and **Table 5.4**), which matches the RNASeq logFC results (**Table 5.6**). In addition, the gene expressions of *TMPRSS2* (**A, B**), *FOXA1* (**C, D**), *NKX3.1* (**E, F**) and *AR* (**G, H**) were downregulated in androgen and Nam+TC-E treated samples compared to androgen and DMSO treated control samples in both LNCaP and LNCaP:C4-2 cells (**Figure 5.23**, see red error bars), which was conform with the RNASeq logFC (**Table 5.5** and **Table 5.6**), thereby confirming the RNASeq gene expression results for all genes tested by qRT-PCR. Interestingly, combined Nam+TC-E treatment exhibited an additive inhibitory effect over Namoline alone only for the gene *NKX3.1* (**Figure 5.23, E**) in LNCaP cells, and for *PSA* (Figure 5.17**, B**), *NKX3.1* (**Figure 5.23, F**) and *AR* (**Figure 5.23, H**) in LNCaP:C4-2 cells. No additive inhibitory effect was seen in the other genes, suggesting the potential benefit of combined inhibition of KDM1A and KDM7A by Namoline and TC-E 5002 compared to Namoline alone is gene and cell line dependent. The gene expression changes (in percent) for *TMPRSS2, FOXA1, NKX3.1* and *AR* after single and combined KDM1A and KDM7A inhibitor treatments compared to R1881-treated vehicle control samples are summarised in **Table 5.7**.

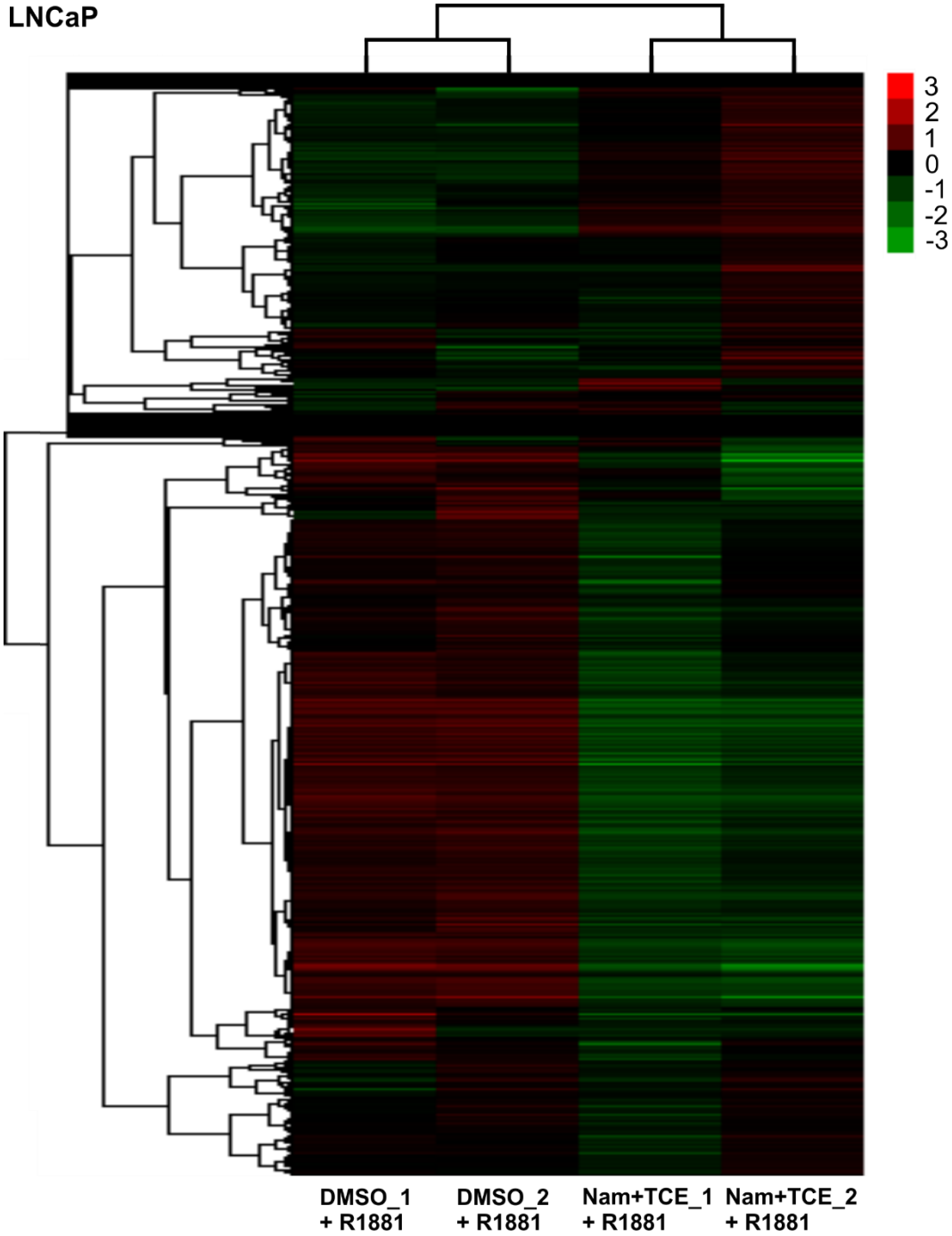

Figure 5.19: Heat map analysis of AR-regulated genes in Namoline + TC-E 5002 treated LNCaP cells. Differentially expressed genes are compared between androgen (R1881, 1 nM) and DMSO control samples and androgen and Namoline + TC-E 5002 treated samples. Gene counts were converted into log2 and highly expressed genes are depicted in red, whereas green represents genes with low expression. In LNCaP cells, most AR-regulated genes were lower expressed after CPI-455 treatment and a smaller subset of genes was upregulated.

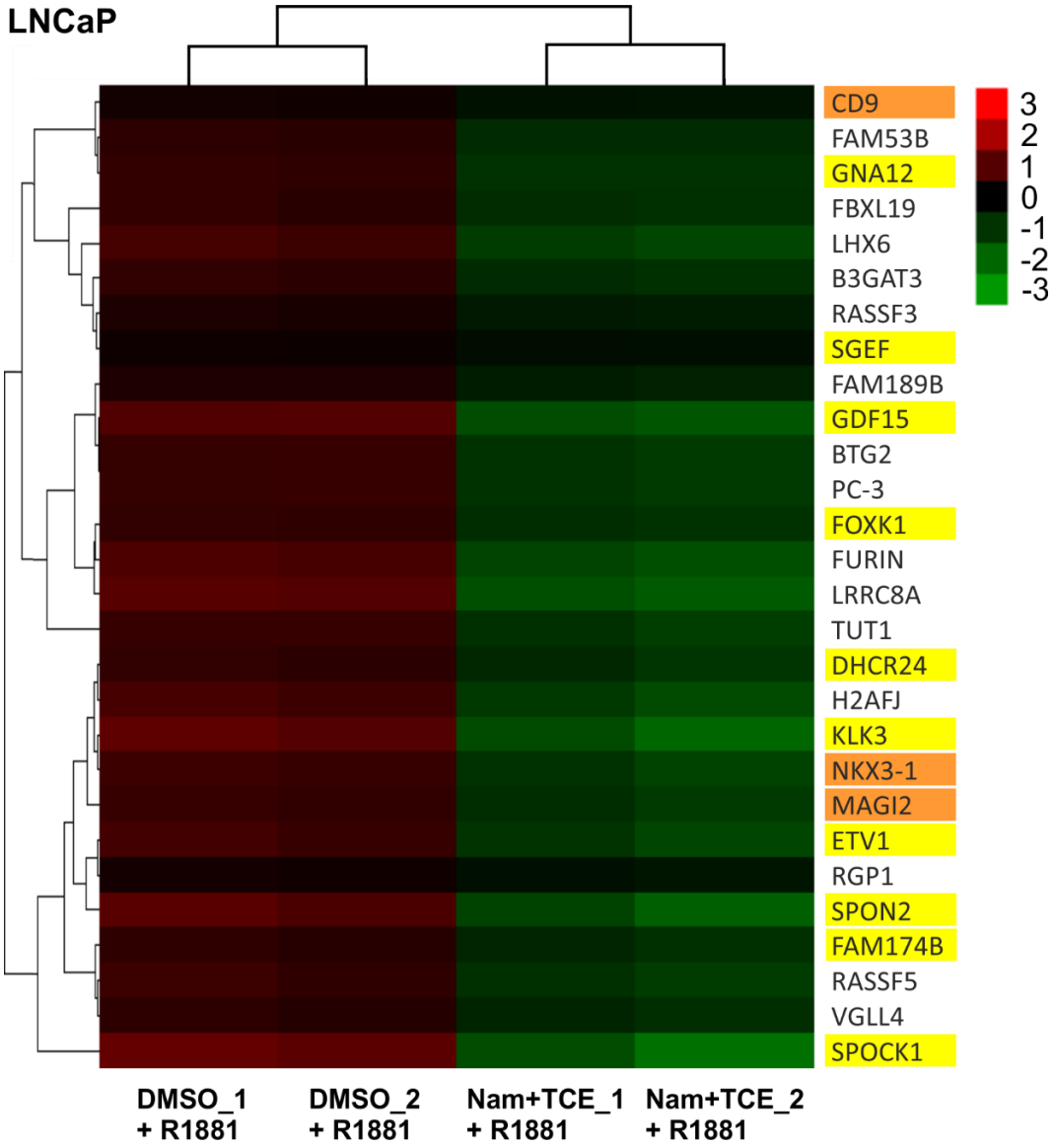

Figure 5.20: Detailed *KLK3/PSA* hierarchical cluster in LNCaP.
The gene counts were log2 converted with red being highly expressed genes and green lowly expressed genes. Known oncogenes in PCa are highlighted in yellow, and genes with both tumour suppressive and oncogenic functions are highlighted in orange.

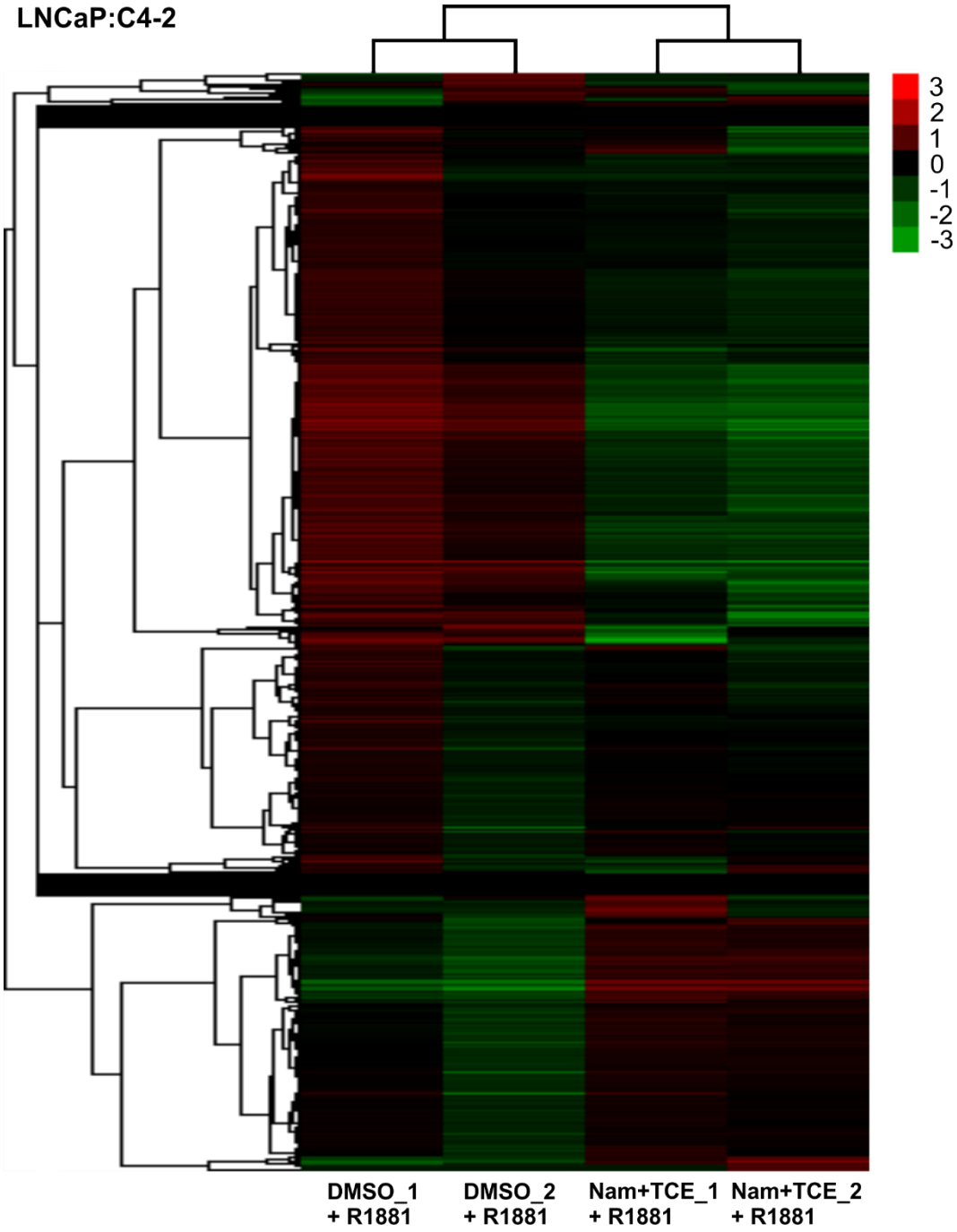

Figure 5.21: Heat map analysis of AR-regulated genes in Namoline + TC-E 5002 treated LNCaP:C4-2 cells.

Androgen (R1881, 1 nM) and Namoline + TC-E 5002 treated samples were compared with androgen (R1881, 1 nM) and DMSO control samples and the differentially expressed genes (as log2) are depicted. Red represents high gene expression, whereas green stands for low gene expression. In LNCaP:C4-2 cells, many AR-regulated genes were expressed lower in Nam+TC-E treated samples compared to DMSO samples. A smaller subset of genes was upregulated.

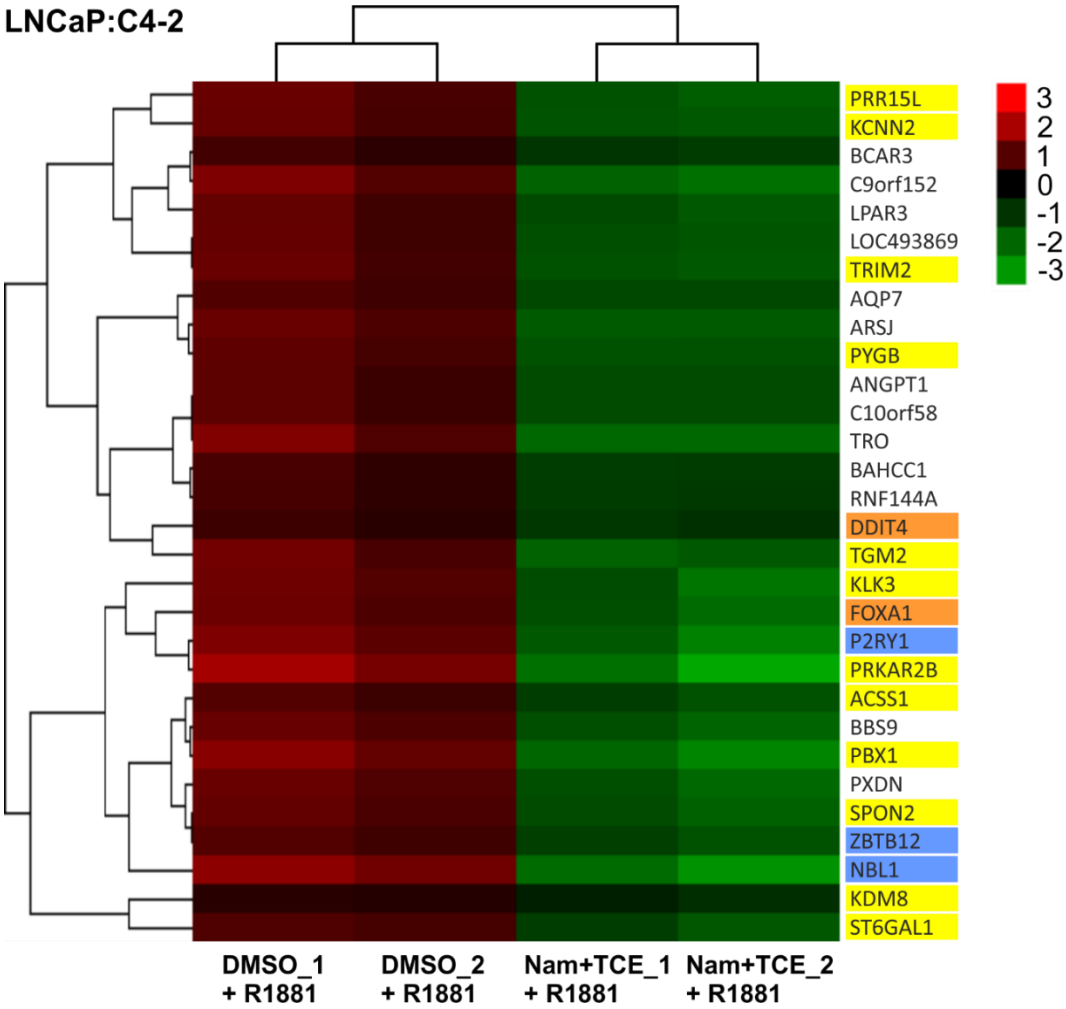

Figure 5.22: Detailed KLK3/PSA hierarchical cluster in LNCaP:C4-2.
The RNASeq gene counts are expressed as log2. Red represents high, and green depicts low gene expression. Genes with oncogenic roles in PCa are depicted yellow, tumour suppressive functions in blue, and dual functions in orange.

Table 5.5: RNASeq gene expression logFC in LNCaP cells.
The logFC was calculated by comparing androgen (R1881, 1 nM) and Namoline (50 µM) + TC-E 5002 (50 µM) treated samples with androgen and DMSO treated control samples. Negative values represent gene down-regulations, and positive values stand for up-regulations. For example, *KLK3/PSA* is down-regulated (logFC 1.769) upon Namoline+TC-E 5002 treatment compared to the DMSO control The FDR is given for each gene and coloured in red if statistically significant. The grey highlighted genes were confirmed by qPCR analysis.The FC = fold change; FDR = false discovery rate

Gene	ID	logFC	FDR
KLK3/PSA	ENSG00000142515	-1.769 (down)	≤ 0.05
KLK2	ENSG00000167751	-1.722 (down)	≤ 0.05
TMPRSS2	ENSG00000184012	-0.714 (down)	≤ 0.05
VEGFA	ENSG00000112715	-0.680 (down)	≤ 0.05
HIF1A	ENSG00000100644	0.329 (up)	0.286
NDUFA4L2	ENSG00000185633	-2.360 (down)	≤ 0.05
FOXA1	ENSG00000129514	-0.963 (down)	≤ 0.05
NKX3.1	ENSG00000167034	-1.061 (down)	≤ 0.05
AR	ENSG00000169083	-0.441 (down)	0.100
KDM1A	ENSG00000004487	0.428 (up)	0.098
KDM5B	ENSG00000117139	-1.010 (down)	≤ 0.05
KDM7A	ENSG00000006459	-0.135 (down)	0.993

Table 5.6: RNASeq gene expression logFC in LNCaP:C4-2 cells.
Androgen (R1881, 1 nM) and Namoline (50 µM) + TC-E 5002 (50 µM) treated samples were compared with androgen and DMSO treated control samples and the logFC calculated. Down-regulated genes exhibit negative values, whereas up-regulated genes are shown as positive values. For example, *KLK3/PSA* is down-regulated (logFC 2.180) through Namoline+TC-E 5002 when compared to the DMSO control. The FDR is depicted for each gene and coloured in red if statistically significant. The grey highlighted genes were confirmed by qPCR analysis. FC = fold change; FDR = false discovery rate

Gene	ID	logFC	FDR
KLK3/PSA	ENSG00000142515	-2.180 (down)	≤ 0.05
KLK2	ENSG00000167751	-1.399 (down)	≤ 0.05
TMPRSS2	ENSG00000184012	-0.853 (down)	≤ 0.05
VEGFA	ENSG00000112715	1.115 (up)	≤ 0.05
HIF1A	ENSG00000100644	1.244 (up)	≤ 0.05
NDUFA4L2	ENSG00000185633	-2.060 (down)	≤ 0.05
FOXA1	ENSG00000129514	-2.102 (down)	≤ 0.05
NKX3.1	ENSG00000167034	-0.936 (down)	≤ 0.05
AR	ENSG00000169083	-0.919 (down)	≤ 0.05
KDM1A	ENSG00000004487	-0.045 (down)	1.000
KDM5B	ENSG00000117139	0.154 (up)	0.756
KDM7A	ENSG00000006459	1.385 (up)	≤ 0.05

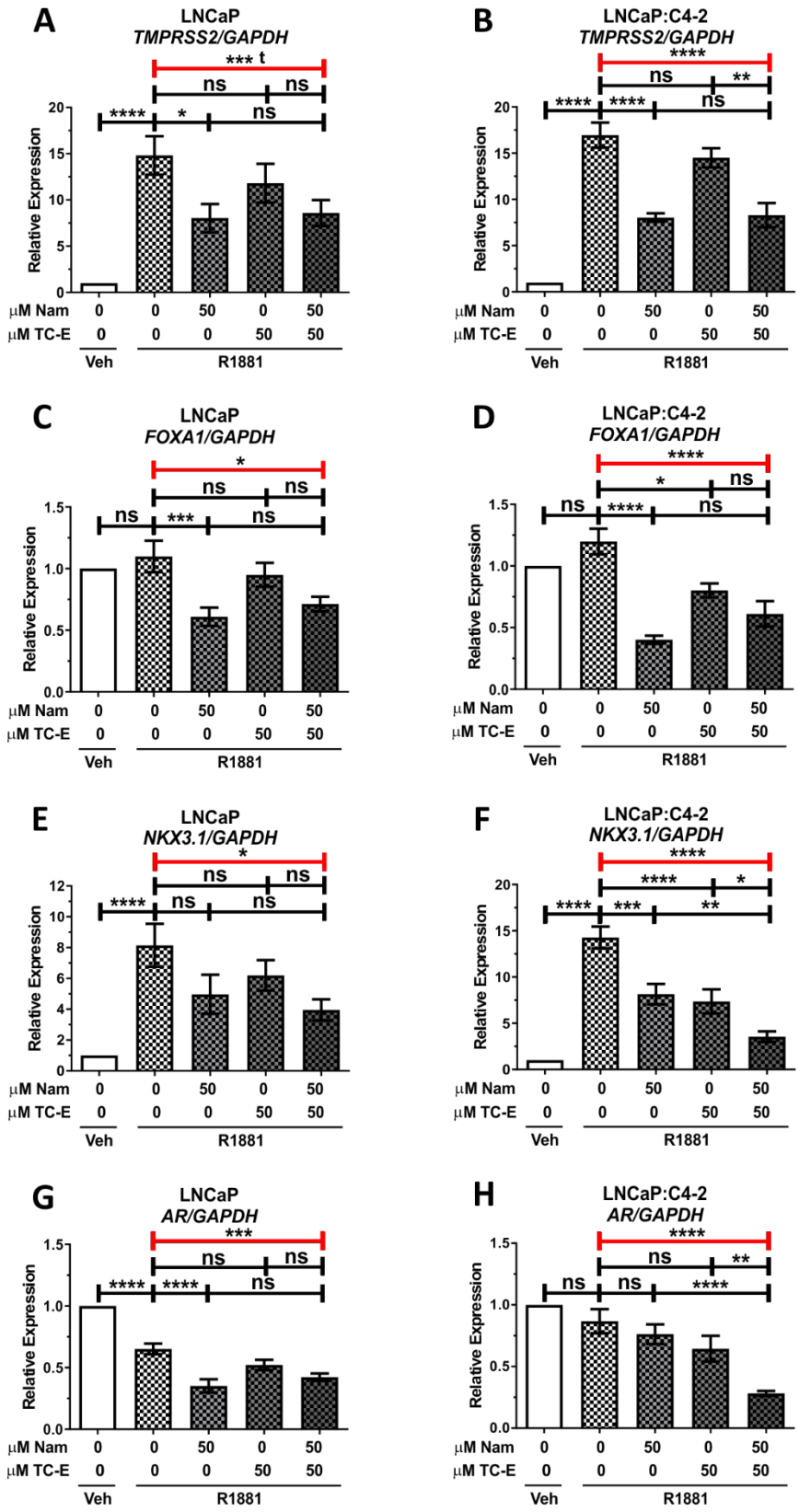

Figure 5.23: Validation of RNASeq gene counts by qPCR analysis in LNCaP and LNCaP:C4-2.
Cells were treated with androgen (R1881, 1 nM) and KDM1A- and KDM7A inhibitors respectively, combined and individually, for 3 days (n = min 6). Combined Namoline and TC-E 5002 treatment attenuated R1881-induced expression of *TMPRSS2* (**A, B**), *FOXA1* (**C, D**), *NKX3.1* (**E, F**) and decreased *AR* (**G, H**) expression in both cell lines, confirming the RNASeq gene counts. * = $p \leq 0.05$; ** $p \leq 0.005$; *** = $p \leq 0.001$; **** = $p \leq 0.0001$ by ANOVA with Bonferroni's post hoc test.

Table 5.7: Comparison of gene expression changes between single and combined KDM1A and KDM7A inhibitor treatments.
Gene expression changes of androgen (R1881, 1 nM) and inhibitor treated samples compared to androgen and vehicle control samples are given in percent. + = increase in gene expression; - = decrease in gene expression; * = p ≤ 0.05; **p ≤ 0.005; *** = p ≤ 0.001; **** = p ≤ 0.0001.

Gene	Treatment	LNCaP	LNCaP:C4-2
TMPRSS2	Namoline	- 46% (down) *	- 53% (down) ****
	TC-E 5002	- 20% (down) ns	- 14% (down) ns
	Namoline + TC-E 5002	**- 42% (down) ***t**	**- 51% (down) **** **
FOXA1	Namoline	- 44% (down) ***	- 67% (down) ****
	TC-E 5002	- 14% (down) ns	- 33% (down) *
	Namoline + TC-E 5002	**- 35% (down) ***	**- 49% (down) **** **
NKX3.1	Namoline	- 39% (down) ns	- 43% (down) ***
	TC-E 5002	- 24% (down) ns	- 48% (down) ****
	Namoline + TC-E 5002	**- 51% (down) ***	**- 75% (down) **** **
AR	Namoline	- 46% (down) ****	- 12% (down) ns
	TC-E 5002	- 20% (down) ns	- 26% (down) ns
	Namoline + TC-E 5002	**- 35% (down) ***	**- 67% (down) **** **

To further compare the effect of combined inhibition of KDM1A and KDM7A selective inhibitors on the gene regulation in cancer related pathways between LNCaP and LNCaP:C4-2, the KEGG pathway database (https://www.genome.jp/kegg/pathway.html, accessed 17.07.2019) was used (Kanehisa, 2019, Kanehisa and Goto, 2000, Kanehisa et al., 2019). Like for the Venn diagram (**Figure 5.18**), the up- and down-regulated genes from the RNASeq analysis were filtered for logFC ≥1 and ≥-1 respectively (**Figure 5.24** and **Figure 5.25**). In LNCaP cells, the treatment of combined Namoline + TC-E 5002 lead to the down-regulation of genes involved in the Notch, VEGF and HIF-1, Wnt, and PI3K-Akt signalling pathway and cytokine-cytokine interactions (**Figure 5.24, coloured green**). Very few genes were upregulated, including *p53*, and genes involved in the Ca^{2+} signalling pathway (**Figure 5.24, coloured red**). Some gene families comprised members some of which were up-, and others were down-regulated (**Figure 5.24, coloured blue**). Interestingly, in LNCaP-C4-2, the combined treatement lead to the up-regulation of more genes in cancer related pathways than in LNCaP cells, including genes involved in apoptosis, genomic stability, cell cycle (such as p21), HIF1α and VEGF signalling, and cytokine-cytokine receptor interactions (**Figure 5.25, coloured red**). In contrast, some genes involved in cytokine-cytokine receptor interactions were down-regulated, as well as genes of the Hedgehog signalling pathway and other crucial genes, such as *c-Myc*, *PI3K* and *TGF-β* (**Figure 5.25, coloured green**).

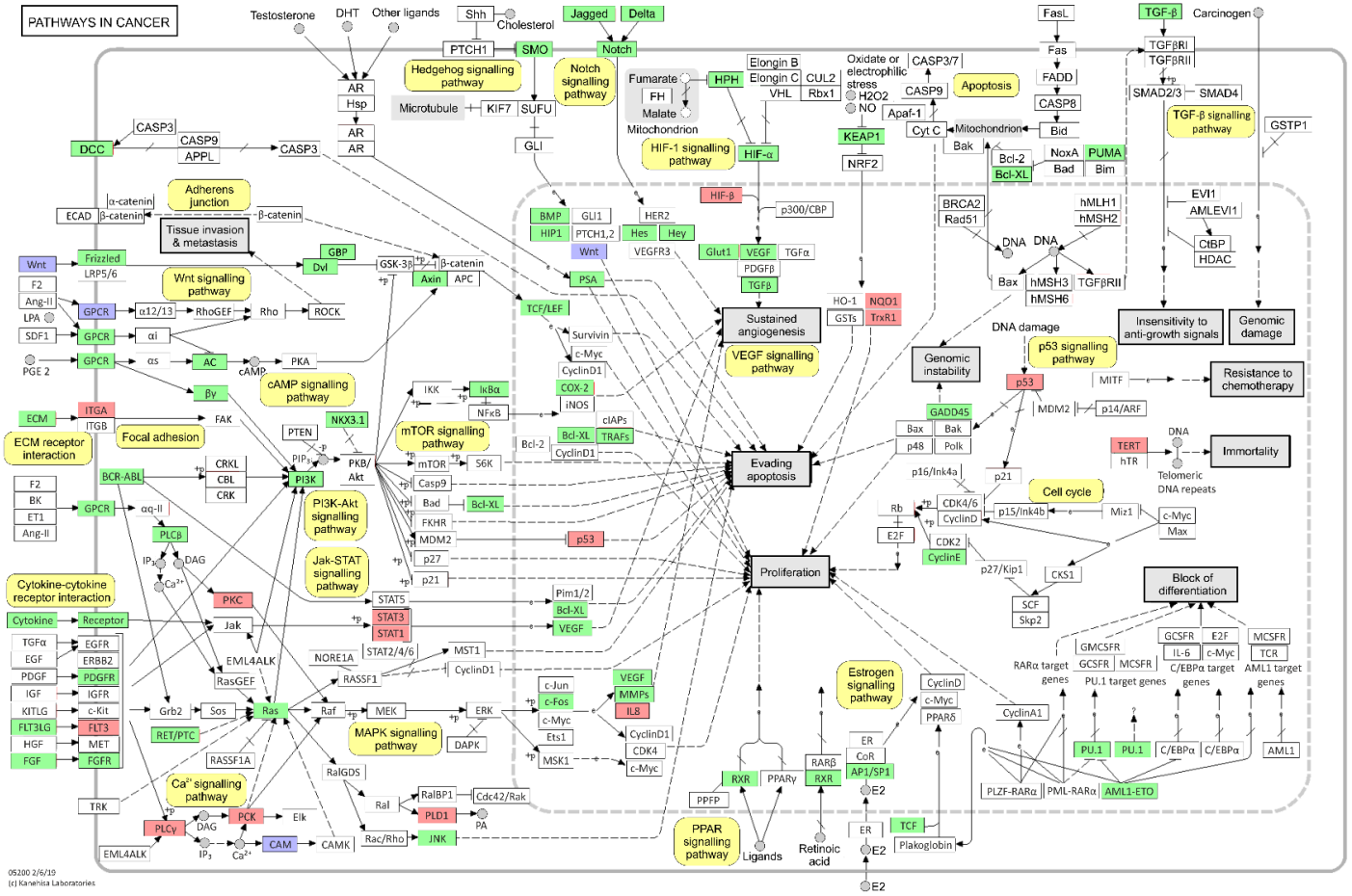

Figure 5.24: Gene regulation of cancer pathways in combined Namoline and TC-E 5002 treated LNCaP cells.
Up-regulated genes are shown in red, down-regulated genes are presented in green and blue indicates both up- and down-regulation (https://www.genome.jp/kegg/pathway.html, accessed 17.07.2019).

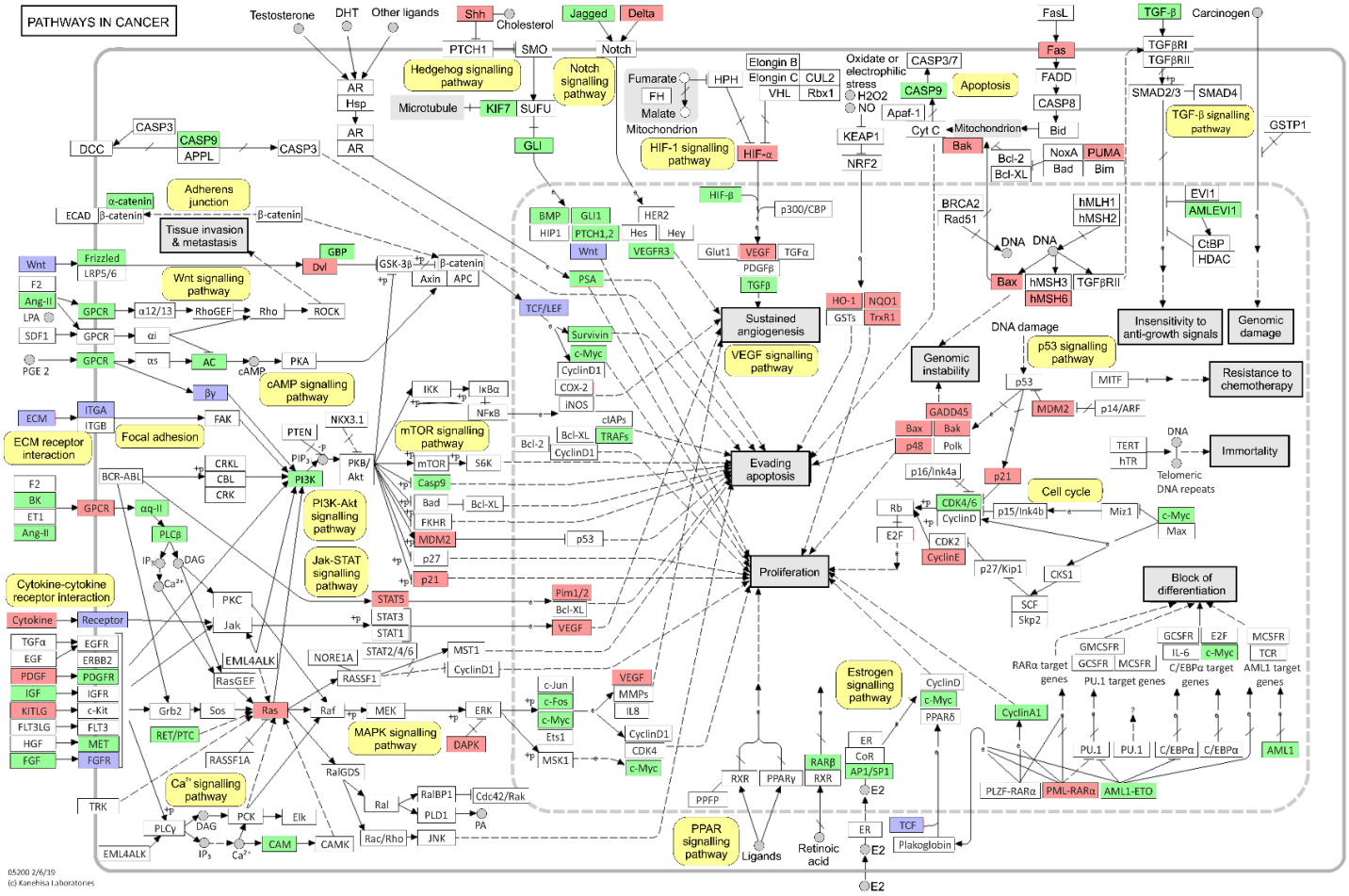

Figure 5.25: Gene regulation of cancer pathways in combined Namoline and TC-E 5002 treated LNCaP:C4-2 cells.
Genes in red are up-regulated, green represents down-regulated genes and blue describes both up- and downregulation (https://www.genome.jp/kegg/pathway.html, accessed 17.07.2019).

5.2.8.4 Combination of Namoline and TC-E 5002 impairs cell proliferation of prostate cancer cells

The effect of combined KDM1A- and KDM7A-selective inhibitors was also tested on cell proliferation of LNCaP, LNCaP:C4-2 and 22Rv1 using the CyQUANT™ assay (Figure 5.26). In all cell lines combining Namoline + TC-E 5002 lead to a greater inhibition of proliferation (G-I) than either Namoline (A-C) or TC-E 5002 (D-F) alone after both 3 and 6 days of treatment, leading to a ~85-90% reduced proliferation after 6 days compared to untreated control cells (Figure 5.26).

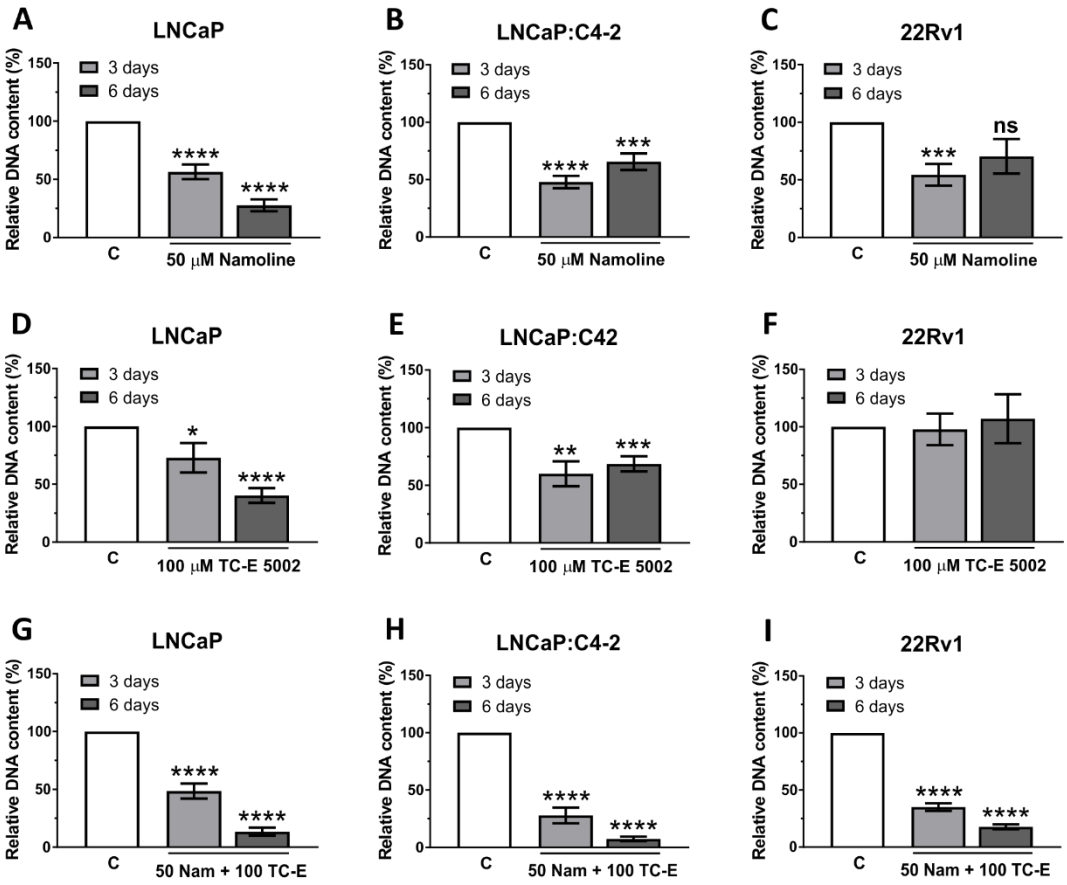

Figure 5.26: Effect of combined KDM1A- and KDM7A-selective inhibitors on cell proliferation in LNCaP, LNCaP:C4-2 and 22Rv1.

Cell proliferation was assessed using the CyQUANT™ assay (n = min 9). In all cell lines LNCaP (G), LNCaP:C4-2 (H) and 22Rv1 (I) proliferation was 80-90% reduced ($p \leq 0.05$) by combining Namoline + TC-E 5002 which was a higher inhibition than when treated with the individual inhibitor (A, D and B, E and C, F respectively) . Nam = Namoline (KDM1A-selective inhibitor), TC-E = TC-E 5002 (KDM7A-selective inhibitor), * = $p \leq 0.05$, ** = $p \leq 0.005$, *** = $p \leq 0.001$, **** = $p \leq 0.0001$ by paired t-test.

5.3 Discussion

KDM1A is the best studied KDM in PCa and various studies have described KDM1A as a promising therapeutic target (Cai et al., 2014, Ellis and Loda, 2018, Kahl et al., 2006, Kashyap et al., 2013, Ketscher et al., 2014, Metzger et al., 2005, Sehrawat et al., 2018, Wang et al., 2019d, Wissmann et al., 2007). Even though KDM1A has been shown to be a major activator of AR-regulated genes (Metzger et al., 2010, Metzger et al., 2005, Wissmann et al., 2007), it was also accredited with a suppressive function in AR signalling (Battaglia et al., 2017, Shi et al., 2004, Shi et al., 2005). Current studies suggest that the role of KDM1A changes during PCa progression and its transcriptional function seems to be dependent on the gene locus and cell type (Battaglia et al., 2017, Cai et al., 2014, Ketscher et al., 2014, Yang et al., 2015b). Therefore, it is crucial to clarify the exact roles of KDM1A in localised and advanced PCa.

Bioinformatic analysis revealed that almost 30% of PCa patients harbour an altered *KDM1A* gene with half of these patients exhibiting high mRNA levels and the other half low mRNA levels (**Figure 5.1, A, C**), reflecting the dual role of KDM1A. Interestingly, the alteration frequency of *KDM1A* is lower in metastatic adenocarcinoma, where *KDM1A* is mutated but not amplified or deleted (**Figure 5.1, B**). Interestingly, neuroendocrine patients exhibit the highest KDM1A amplification frequency (~5.26%) amongst PCa patients (**Figure 5.1, C**), suggesting a role of KDM1A in NePC. A study by Etani et al. (2019) showed that KDM1A is highly expressed in neuroendocrine-differentiated tumour specimens.

Interestingly, KDM1A is not heavily mutated, in either PCa nor in other types of cancer according to the cBioPortal for Cancer Genomics (https://www.cbioportal.org/, accessed 04.09.2019). Most of the mutations occur within the SWIRM and amino oxidase domain. In PCa, one missense mutation, Ile199Thr, was found in the SWIRM domain (**Figure 5.2**) which is most likely caused by a single point mutation (AUU→ACU, AUC→ACC, AUA→ACA). Isoleucine is an amino acid with a nonpolar, hydrophobic side chain, whereas threonine is polar and uncharged. Intriguingly, this patient harboured only few mutations overall (**Table 5.1**). A mutation in the SWIRM domain could potentially interfere with protein-protein interactions (Aravind and Iyer, 2002, Chen et al., 2006b, Stavropoulos et al., 2006). In stomach adenocarcinoma a missense mutation at the same position was found, however, it is an amino acid switch from isoleucine to methionine, which is nonpolar and

hydrophobic too (Liu et al., 2018, Network, 2014, Sanchez-Vega et al., 2018, Taylor et al., 2018).

Another KDM1A missense mutation, Pro471Ser, was found in the amino oxidase domain, more precisely the Tower domain, which is the site of interaction with CoREST and other proteins (**Figure 5.2**) (Chen et al., 2006b, Laurent and Shi, 2016). It most likely is the result of a single point mutation (CCU→UCU, CCC→UCC, CCA→UCA, CCG→UCG). Another missense mutation, Ala209Ser, in the amino oxidase domain may interfere with the coenzyme FAD binding which is responsible for the catalytic activity of KDM1A (Chen et al., 2006b, Burg et al., 2016, Ismail et al., 2018). Interestingly, this mutation was harboured by a patient with PCa metastasis and a KDM1A copy number gain (**Table 5.1**). This mutation too is most likely the result of a single point mutation (GCU→UCU, GCC→UCC, GCA→UCA, GCG→UCG).

Two other patients with metastatic PCa harboured a mutation at the same location in the amino oxidase domain. Whilst one patient had a missense mutation, Leu664Val (CUU→GUU, CUC→GUC, CUA→GUA, CUG→GUG, UUA→GUA, UUG→GUG), the other patient had an in-frame deletion, Leu664del (**Figure 5.2**). Both patients had a diploid copy number for KDM1A, however, both did not harbour many mutations overall (**Table 1.5**). These mutations likely interfere with the enzymatic activity of KDM1A, especially the in-frame deletion, which is likely to dramatically alter the protein structure of KDM1A or even lead to an unfunctional protein. Further investigations are needed to determine the effect of these mutations on KDM1A function in PCa, which can be achieved through certain softwares and mutation analysis and subsequent phenotypical characterisation (Reva et al., 2011, Shi and Moult, 2011).

Even though KDM1A has been described as an oncogene in PCa (Ellis and Loda, 2018, Kahl et al., 2006, Metzger et al., 2005, Wang et al., 2019d, Wissmann et al., 2007, Yang et al., 2015b), most PCa patients are diploid for KDM1A and about ~8% harbour a *KDM1A* deletion (**Figure 5.3**), suggesting KDM1A may exert its oncogenic role through transcriptional or translational upregulation. Indeed, KDM1A mRNA and protein was highly expressed in various PCa cell lines tested, including LNCaP, LNCaP:C4-2, 22Rv1 and Du145. PC3, a cell model representative for bone metastasis, expressed the lowest KDM1A levels which is conform with another study (Etani et al., 2019). Immunohistochemical staining of KDM1A further confirmed that KDM1A is expressed higher in tumour specimens (n = 102) compared to normal specimens (n = 45) (Figure 5.5), which has been indicated before by

several other studies (Battaglia et al., 2017, Kahl et al., 2006, Kashyap et al., 2013, Metzger et al., 2005, Wang et al., 2019d). KDM1A was reported to be expressed at even higher levels in CRPC specimens (Etani et al., 2019, Sehrawat et al., 2018) and to be correlated with Gleason (Kahl et al., 2006, Wang et al., 2019d), biochemical recurrence (Battaglia et al., 2017, Kahl et al., 2006, Kashyap et al., 2013, Wang et al., 2019d) and shorter disease-free survival (Kahl et al., 2006, Kashyap et al., 2013, Wang et al., 2019d). Similarly, a bioinformatic analysis on PCa patient cohorts confirmed that elevated KDM1A expression correlates with lower disease-free survival (Cai et al., 2014). The bioinformatic analysis in our study revealed that patients with an altered *KDM1A* gene expression have a shorter disease-free survival (**Figure 5.4**). As shown before (Kashyap et al., 2013, Metzger et al., 2005, Wang et al., 2019d), KDM1A was mainly located in the nucleus (**Figure 5.5**), however, surprisingly, the nuclear KDM1A staining in our study was not correlated with any of the clinical parameters, including Gleason and biochemical recurrence (**Appendix 14**). The reason for this may be that the cohort used in this study mainly included patients with less aggressive disease, since ~80 percent of the patients had a Gleason score of 6 or 7 (**Appendix 1**). In a study by Kashyap et al. (2013), KDM1A was not correlated with Gleason either, but correlated with biochemical recurrence, suggesting variations in the cohorts used in the different studies. However, our and other immunohistochemical and bioinformatic data strongly suggest an important role of KDM1A in PCa patients.

KDM1A has been described as an important coregulator of the AR receptor to activate or repress AR-regulated gene expression, such as *PSA*, upon ligand binding in PCa (Battaglia et al., 2017, Metzger et al., 2010, Metzger et al., 2005, Shi et al., 2004, Shi et al., 2005, Wissmann et al., 2007, Yang et al., 2015b). As expected, the depletion of *KDM1A* via RNA interference attenuated R1881-induced *PSA* expression in LNCaP cells (**Figure 5.11, D**), which has been shown before (Kashyap et al., 2013, Metzger et al., 2005, Yang et al., 2015b). Interestingly, in androgen-independent LNCaP:C4-2 and 22Rv1 cells, the siRNA-mediated depletion of KDM1A did not have any significant effect on R1881-induced *PSA* expression. This is consistent with a study in LNCaP:C4-2 (Kashyap et al., 2013) and a study in LNCaP:C4-2B cells (Sehrawat et al., 2018). In fact, Sehrawat et al. (2018) reported that siRNA-mediated depletion of KDM1A even increases a subset of AR-regulated genes, including *NKX3.1*. This is consistent with our experiments, where siRNA-mediated depletion of *KDM1A* increased *VEGFA* expression (**Figure 5.11, H**). The repressor and activator function of KDM1A has been shown to be dependent on other epigenetic modifications at histone H3 (Cai et al., 2011, Metzger et al., 2010, Metzger et al., 2008, Shi

et al., 2005). For example Metzger et al. (2010) reported that KDM1A changes its demethylation activity from H3K9 to H3K4 if threonine 6 at histone H3 (H3T6) is phosphorylated by the protein kinase C beta I, thereby acting as a co-repressor. It is therefore likely, that the function of KDM1A at AR target genes in LNCaP, LNCaP:C4-2 and 22Rv1 is controlled by the local epigenetic landscape. In addition, KDM1A has been shown to demethylate not only histone proteins, but also non-histone proteins, such as p53 (Huang et al., 2007, Wang et al., 2009a, Xie et al., 2011b). This means KDM1A may regulate effector proteins which in turn are responsible for gene regulation. According to the siRNA results, KDM1A plays an oncogenic role in LNCaP cells, but a tumour suppressive role in androgen-independent cell lines. However, the mechanisms of KDM1A activating or repressing AR target genes at different PCa stages needs further investigation. Interestingly, the treatment of androgen (R1881, 1 nM) leads to a modest decrease in *KDM1A* mRNA expression, suggesting a negative feedback mechanism, which was not found in LNCaP:C4-2 and 22Rv1 (**Figure 5.10**).

In contrast to siRNA-mediated depletion of KDM1A, enzymatic inhibition of KDM1A through the pharmaco-selective inhibitor Namoline (50 μM) attenuated R1881-induced *PSA* expression in all androgen-responsive PCa cells tested (**Figure 5.12, A-C**) (Willmann et al., 2012). Similar to the previous chapters, there seems to be a discrepancy between the two inhibition methods which may be because pharmaco-selective inhibitors seem to be more effective than siRNA-mediated depletion. The duration of inhibition may be shorter with siRNA-mediated depletion than with pharmaco-selective inhibitors, which directly bind and inhibit target proteins. Previous studies using KDM1A-selective inhibitors, such as Pargyline (Cai et al., 2014, Kashyap et al., 2013, Metzger et al., 2005), S2101 (Cai et al., 2014) and Namoline (Willmann et al., 2012), confirm that pharmaco-selective inhibition of KDM1A inhibits *PSA* expression in LNCaP cells (**Figure 5.12, A**). Importantly, the R1881-induced *PSA* expression in androgen-independent cells LNCaP:C4-2 and 22Rv1 was blocked too by Namoline (**Figure 5.12, B, C**). Kashyap et al. (2013) reported that pargyline had no effect on *VEGFA* expression in LNCaP:C4-2 cells after 48 hours, however, when treating LNCaP:C4-2 cells with androgen (R1881, 1 nM) and Namoline (50 μM) for 72 hours, Namoline attenuated *VEGFA* expression (**Figure, 5.12, E**). The duration of inhibitor treatment seems to play a significant role on whether the effect on gene expression is inhibitory, activating or absent. For example, Kashyap et al. (2013) reported divergent effects on *VEGFA* expression in PC3 when using different Pargyline concentrations and different durations of treatment. Further experiments are needed to investigate the

mechanisms behind the activating and repressing functions of KDM1A on AR target genes. KDM1A can act on cells by demethylating histone proteins and reshaping the epigenetic code at enhancers or promotors, demethylating non-histone proteins or fulfilling a protein scaffold function (Wang et al., 2019d). In future experiments it will be important to determine whether KDM1A regulates gene expression by directly binding to the DNA or indirectly through regulating other protein complexes. DNA-protein and protein-protein interactions can be investigated by using chromatin immunoprecipitation (ChIP) and pull-down assays (Jain et al., 2012, Nelson et al., 2006). In addition, it will be crucial to investigate the epigenetic modifications at KDM1A target gene loci through ChIP-Seq analysis (O'Geen et al., 2011).

As already shown by other studies, siRNA-mediated knockdown of KDM1A impairs PCa cell growth of LNCaP (Battaglia et al., 2017, Metzger et al., 2005, Sehrawat et al., 2018), LNCaP:C4-2 (Battaglia et al., 2017), PC3 and other androgen-independent cell lines (Sehrawat et al., 2018). Similarly, the pharmaco-selective inhibition of KDM1A by Namoline lead to reduced cell growth in LNCaP, LNCaP:C4-2, 22Rv1 and PC3 (**Figure, 5.13**). However, the biggest effect, which was also dose-dependent, was observed in LNCaP cells and several other studies have confirmed a negative effect on LNCaP cell growth by KDM1A inhibitors, such as Tranylcypromine (Benelkebir et al., 2011, da Mota et al., 2018, Kashyap et al., 2013), Pargyline (Kashyap et al., 2013), Namoline (Willmann et al., 2012) and GSK-2879552 (Wang et al., 2019d). A study by Chai et al. (2014) performed gene ontology analysis in siRNA treated LNCaP cells targeting KDM1A and revealed that KDM1A activates gene involved in cell cycle and lipid synthesis, whilst suppressing apopotosis-related genes. It seems therefore likely that the pharmaco-selective inhibition of KDM1A induces apoptosis in LNCaP cells. Some studies reported that pharmaco-selective inhibition of KDM1A impairs cell proliferation of androgen-independent cell lines, including LNCaP:C4-2, 22Rv1 and PC3 cells (Etani et al., 2019, Kashyap et al., 2013), which is conform with our results (**Figure 5.13, C-E**). However, the effect in PC3 appears to be modest (**Figure 5.13, E**) and the effect in LNCaP:C4-2 and 22Rv1 seems to decrease after 6 days of treatment (**Figure 5.13, C-D**). The mechanisms of inhibition need to be further investigated, however, a study by Willmann (2012) reported that Namoline impairs the expression of important cell cycle genes in PC3 cells. Etani et al. (2019) showed that the KDM1A-selective inhibitor NCL1 reduces 22Rv1 and PC3 cell numbers by apoptosis and potentially autophagy. Surprisingly, in Du145, Namoline significantly increases cell proliferation after 6 days of treatment (**Figure 5.13, F**). Importantly, Ketscher et al. (2014) showed that siRNA-mediated

depletion of KDM1A had no effect on PC3 and Du145 cell proliferation, but increased migration and invasion, suggesting KDM1A may play a tumour suppressive role in metastatic PCa. Sehrawat et al. (2018) further argued that the inhibitor SP-2509, which supposedly does not interfere with the demethylase activity of KDM1A, reduces LNCaP, LNCaP:C4-2B and PC3 cell survival, suggesting it is not the enzymatic function of KDM1A that promotes cell growth. ChiP-Seq in LNCaP revealed that KDM1A controls most of its target genes independently of H3K4 and H3K9 demethylation (Sehrawat et al., 2018).

Further experiments are needed to elucidate the mechanisms of actions of KDM1A regarding cell signalling and growth in the various PCa stages. RNASeq and pathway analysis of androgen-independent PCa cells, which have been treated with Namoline or siRNA targeting KDM1A, would give more insight into the genes and pathways regulated by KDM1A in each cell line. Our data indicate that KDM1A is a promising target to treat localised PCa, however, the effect of KDM1A inhibition in androgen-independent and CRPC needs further investigation. Even though in the recent years it has become increasingly clear, that KDM1A can also contribute to PCa progression in an AR-independent manner (Battaglia et al., 2017, Huang et al., 2007, Kashyap et al., 2013, Ketscher et al., 2014, Wang et al., 2019d), many studies report about an important role of KDM1A in androgen signalling in PCa (Cai et al., 2011, Cai et al., 2014, Kashyap et al., 2013, Metzger et al., 2010, Metzger et al., 2005, Metzger et al., 2008, Wissmann et al., 2007, Yang et al., 2015b).

Combination therapy has gained much focus in the last years in the management of cancer, especially for metastatic disease (Chou, 2006, Miles et al., 2002, Mokhtari et al., 2017, Saputra et al., 2018). In PCa management, for example, the combination of androgen deprivation therapy (ADT) with the chemotherapeutic compound docetaxel has been shown to lead to better survival in patients than ADT alone (Fizazi et al., 2015, Sweeney et al., 2015). Combining two or multiple drugs can have the advantage of being more efficient and effective than a single drug (Mokhtari et al., 2017, Xu and Qiu, 2019). In addition, it has the potential to overcome drug resistance which is a major issue of ADT in PCa (Semenas et al., 2012, Xu and Qiu, 2019). Another advantage of combination therapy is that the dose of each drug can be reduced, whilst achieving the same effect, which can have a positive impact on cytotoxicity and side effects (Mokhtari et al., 2017, Xu and Qiu, 2019). However, combination therapies can also be more toxic than single agents and it is therefore important to test the effects of combination therapies (Miles et al., 2002). It was therefore of interest to analyse the combinatorial effects of targeting both KDM1A and KDM7A

together on AR-regulated gene expression and PCa cell proliferation, compared to single KDM targeting.

Interestingly, in LNCaP and 22Rv1, the combined siRNA-mediated depletion (**Figure 5.15**) or pharmaco-selective inhibition (**Figure 5.17**) of KDM1A and KDM7A had a similar effect on *PSA* expression as targeting KDM1A alone. In contrast, in LNCaP:C4-2, combined inhibition had an additive attenuating effect on *PSA* and *VEGFA* expression compared to inhibiting single KDMs. These results indicate that it depends on the cell line, whether the combination of KDM1A and KDM7A exhibits an additive effect over KDM1A alone, reflecting the heterogeneity of PCa (Shoag and Barbieri, 2016, Yadav et al., 2018).

To further understand the effect of combinatorial inhibition of KDM1A and KDM7A on gene expression, RNASeq analysis was performed with both LNCaP and LNCaP:C4-2 cells, which have been treated with combined Namoline (50 μM) and TC-E 5002 (50 μM) and androgen (R1881, 1 nM) for three days, and compared to R1881-treated vehicle control cells. Intriguingly, LNCaP and LNCaP:C4-2 had only ~8.7% of the down-regulated genes and ~22.2% of the up-regulated gene in common after combined inhibitor treatment (**Figure 5.18**), indicating distinct roles of KDMs in different cell lines.

To further investigate AR target genes, unsupervised hierarchical clustering was conducted, using a list of AR-regulated genes identified by Sharma et al. (2013), who performed AR ChIP-seq analysis with tissue of PCa patients. Both in LNCaP (**Figure 5.19**) and LNCaP:C4-2 (**Figure 5.21**), most of the AR-regulated genes were down-regulated upon combined inhibitor treatment compared to vehicle control, however a subset of genes was up-regulated. Interestingly, KDM1A and KDM7A may be involved in *AR* gene regulation in LNCaP:C4-2 (**Table 5.6**) but not as much in LNCaP (**Table 5.5**) according to qPCR analysis (**Figure 5.23**). In both cell lines, AR-regulated genes, such as *TMPRSS2*, *FOXA1* and *NKX3.1*, were down-regulated upon combined inhibitor treatment (**Table 5.5** and **Table 5.6**), which was validated by qPCR analysis (**Figure 5.23**). However, according to qPCR analysis (**Figure 5.23**), the attenuating effect of combined inhibitor treatment on R1881-induced gene expression was the same as when cells were treated with Namoline alone, suggesting inhibiting KDM7A additionally to KDM1A may not have any benefit as Namoline alone may be sufficient. However, R1881-induced *NKX3.1* gene expression was further inhibited by combined inhibitor treatment compared to Namoline alone in LNCaP:C4-2 (**Figure 5.23, F**). Further analysis is needed to investigate the potential benefit of combined inhibition of

KDM1A and KDM7A, such as performing RNASeq analysis with Namoline alone and TC-E 5002 alone and comparing it to the combined inhibition, in both LNCaP and LNCaP:C4-2.

LNCaP and LNCaP:C4-2 also differed regarding the genes which clustered with *PSA* after combined inhibition of KDM1A and KDM7A (**Figure 5.20** and **Figure 5.22**). In LNCaP, *PSA* was clustered with the homeobox-containing transcription factor *NKX3.1* (**Figure 5.20**), whereas in LNCaP:C4-2, *PSA* was clustered with the pioneer transcription factor *FOXA1* (**Figure 5.12**). Interestingly, NKX3.1 has been shown to co-localise with AR and FOXA1 to regulate AR target genes at progressed PCa stages (Tan et al., 2012). In PCa, NKX3.1 (Bhatia-Gaur et al., 1999, Bowen et al., 2000, He et al., 1997, Korkmaz et al., 2000) and FOXA1 (Sahu et al., 2011, Wang et al., 2011) can both activate or repress gene expression. In LNCaP, however, Namoline treatment alone had the same effect as combined Namoline and TC-E 5002 treatment according to qPCR analysis (**Figure 5.23, C, E**). Interestingly, *NKX3.1* also clustered near *PSA* in CPI-455 treated LNCaP cells, which selectively inhibits KDM5B (**Figure 3.21**). KDM1A and KDM5B both are demethylases of H3K4. Thus, similar gene expression changes in Namoline (KDM1A-selective inhibitor) and CPI-455 (KDM5B-selective inhibitor) treated cells may have to do with the demethylase activity at H3K4. However, further experiments are needed to test whether *NKX3.1* gene expression is influenced by demethylase activity dependent or independent actions of KDMs. Chromatin immunoprecipitation (ChIP) experiments and western blots with antibodies targeting different histone methylation states would have to be performed to address this.

In LNCaP, the adjacent gene cluster to *PSA* included *H2AFJ* and *DHCR24* (**Figure 5.20**). *H2AFJ* is also clustered with *PSA* in CPI-455 treated LNCaP cells (**Figure 3.20**) and is a histone variant gene, which is altered in other types of cancer (Monteiro et al., 2014). These results further emphasise that *H2AFJ* may play an important role in AR signalling in PCa too. *DHCR24*, also called *seladin-1*, encodes a flavin adenine dinucleotide (FAD)-dependent oxidoreductase and has been shown to be overexpressed in PCa (Bonaccorsi et al., 2008, Dong et al., 2005). This enzyme is involved in cholesterol biosynthesis and influences the cholesterol content in membranes. (Crameri et al., 2006). Cholesterol is important for membrane proteins and signal transduction (Alonso and Millán, 2001, Simons and Sampaio, 2011), and elevated levels of cholesterol can impact on signalling pathways required for PCa progression (Bonaccorsi et al., 2008, Freeman and Solomon, 2004). However, DHCR24 has also been attributed to a tumour suppressor role by accumulating p53 upon oxidative stress and oncogenic signalling (Wu et al., 2004), and reduced levels of

DHCR24 correlate with a higher risk of metastasis (Hendriksen et al., 2006). Further studies are needed to fully elucidate the role of DHCR24 in PCa progression (Bonaccorsi et al., 2008).

Another gene, which is clustered with *PSA* in LNCaP, is *MAGI2* which encodes a membrane-associated guanylate kinase and which has been shown to bind and activate the tumour suppressor PTEN (Georgescu, 2010, Wu et al., 2000). Immunohistochemical staining of PCa specimens revealed high MAGI2 expression (Goldstein et al., 2016a, Goldstein et al., 2016b), however, decreased MAGI2 expression has been linked to PCa progression (David et al., 2018), which may be partly through the release of PTEN inhibition. *MAGI2* was also clustered with *PSA* in CPI-455 (KDM5B-selective inhibitor) treated cells (Figure 3.20). Further experiments are needed to elucidate the role of KDMs in regulating *MAGI2* expression and the impact on PCa growth and progression.

The next proximal cluster to *PSA* contained the well-studied oncogene *ETV1* (Figure 5.20). ETV1 is highly expressed in PCa and correlates with PCa recurrence, progression and PTEN loss (Baena et al., 2013, Cai et al., 2007, Shin et al., 2009). ETV1, together with ERG, which are both members of the ETS transcription factor family, have been reported to form gene fusions with TMPRSS2, which are present in the majority of PCa patients and play an important role in PCa progression (Tomlins et al., 2007, Tomlins et al., 2008). Therefore, inhibiting *ETV1* expression by combined Namoline and TC-E 5002 treatment in LNCaP cells may represent a promising way to block PCa progression. *ETV1* in turn clustered with the retrograde golgi transport protein RGP1 and with SPON2. Whereas no link between RGP1 and PCa has been reported yet, SPON2 has been shown to be overexpressed in PCa and harbours the potential to be used as a highly sensitive and specific diagnostic biomarker in PCa patient serum (Lucarelli et al., 2013, Qian et al., 2012), representing a promising alternative to the currently available and controversial PSA screening test (Ilic et al., 2018, Lin et al., 2008b, Vickers, 2017).

The next proximal cluster is composed of *FAM174B*, *RASSF5*, *VGLL4* and *SPOCK1* (Figure 5.20). FAM174B has been reported to be overexpressed in PCa (Gao et al., 2018a), but its role in PCa has not been described yet. Similarly, no link with PCa and *RASSF5* and *VGLL4* has been discovered yet, but they have been reported to be tumour suppressors in other cancer types (Deng and Fang, 2018, Volodko et al., 2014). In contrast, SPOCK1 has an oncogenic function in breast cancer and other types of cancer (Fan et al., 2016) and in PCa,

it has been reported to be overexpressed and to promote PCa progression and metastasis (Chen et al., 2016, Yang et al., 2015a). Other genes with oncogenic roles in PCa, which were closely clustered to *PSA* in LNCaP, include *FOXK1* (Chen et al., 2017), *GNA12* (Udayappan and Casey, 2017), and *GDF15* (Wang et al., 2019b). Many other genes are implicated in other cancer types but have not been attributed with a role in PCa yet, such as *TUT1* (Zhu et al., 2014), *LRRC8A* (Konishi et al., 2019), *BTG2* (Mao et al., 2015), *FAM189B* (Zhang et al., 2012, Zhang et al., 2014a), and *B3GAT3* (Zhang et al., 2019). Given these genes are downregulated by combined inhibition of KDM1A and KDM7A in LNCaP cells and closely clustered with *PSA*, it would be interesting to investigate their role in PCa further. In addition, the genes *LHX6* and *SGEF* closely clustered with *PSA* in both combined inhibitor (KDM1A- and KDM7A-selective inhibitor) treated (Figure 5.20) and CPI-455 (KDM5B-selective inhibitor) treated (Figure 3.20) LNCaP cells. Whilst SGEF has been reported to have an oncogenic function in PCa (Wang et al., 2012), LHX6 has been described as a tumour suppressor (Nathalia et al., 2018), however, to date its role in PCa is not known. Our data indicates that *SGEF* and *LHX6* expression may be regulated by several KDMs in LNCaP cells.

In contrast to LNCaP, in LNCaP:C4-2 different genes clustered with *PSA*, except for the oncogene *SPON2* which was clustered with *PSA* in both LNCaP and LNCaP:C4-2 cells (Figure 5.22). As already mentioned, *FOXA1* clustered with *PSA* in LNCaP:C4-2 and was downregulated by combined inhibition of KDM1A and KDM7A. Interestingly, FOXA1 was shown to be important to recruit KDM1A to AR regulated enhancer sites and KDM1A in turn stabilises FOXA1 and AR binding at these sites (Cai et al., 2014). KDM1A may positively regulate *FOX1A* gene expression in LNCaP:C4-2 to further enable KDM1A-regulated expression of AR target genes. However, the role of FOXA1 is complex and can act both as a transcriptional activator and repressor (Sahu et al., 2011, Wang et al., 2011). Other closely clustered genes included genes with oncogenic roles in PCa, such as *PRKAR2B* (Sha et al., 2018, Sha et al., 2017), *ACSS1* (Schug et al., 2015) and *PBX1* (Kikugawa et al., 2006, Liu et al., 2019), as well as genes with tumour suppressive functions, such as *P2RY1* (Wei et al., 2011), *NBL1* (Hayashi et al., 2013) and the well described PCa tumour suppressor *ZBTB12*, also called *PLZF*, which is a transcription factor lost in metastatic and CRPC (Cao et al., 2013, Hsieh et al., 2015, Xiao et al., 2015). Other genes, such as *BBS9* and *PXDN*, have not been attributed with a role in PCa yet. Intriguingly, the *KDM8* gene was closely clustered to PSA too (Figure 5.22). KDM8 is overexpressed in PCa and promotes PCa growth and progression to CRPC (Wang et al., 2019a). It is interesting that KDM1A and/or KDM7A

regulate the gene expression of *KDM8* which demethylates H3K36me2, adding another layer of complexity to the epigenetic landscape, and it will be important to further elucidate the mechanisms behind the regulatory actions between the different KDMs. *KDM7A* was significantly upregulated upon combined inhibition of KDM1A and KDM7A, whereas *KDM1A* was unaffected (Table 5.6), indicating in LNCaP:C4-2 cells a certain level of functional KDM7A may be crucial. In contrast, in LNCaP cells, both *KDM1A* and *KDM7A* were unchanged upon combined KDM1A and KDM7A inhibition, however, *KDM5B* expression was decreased (Figure 5.5), suggesting KDM5B regulation by other KDMs, similar to KDM8 in LNCaP:C4-2. Further experiments are needed to investigate the interdependence of the various KDM classes and their members and to examine the impact on PCa.

Two genes closely clustered with *PSA* were common in combined Namoline and TC-E 5002 treated LNCaP:C4-2 cells (Figure 5.22) and CPI-455 (KDM5B-selective inhibitor) treated LNCaP cells (Figure 3.20). Of course, if the analysis was extended to more gene clusters, more common genes between LNCaP and LNCaP:C4-2 and between the different treatments could be considered, but in this study only genes clustered in close proximity to *PSA* were described in more detail. One of these genes was *BCAR3*, which has no known role in PCa, and the other gene was *ST6GAL1*, which is an oncogene in many cancer types (Garnham et al., 2019) and also in PCa (Wei et al., 2016). Other closely clustered genes included genes with oncogenic functions in PCa, such as *PRR15L* (Jurmeister et al., 2014), *PYGB* (Wang et al., 2018), and *TGM2* (Fok and Mehta, 2008, Han et al., 2014). Two oncogenes, which are overexpressed in PCa harbouring ERG rearrangements, were closely clustered with PSA too, namely *KCNN2* (Camoes et al., 2012) and *TRIM2* (Wang et al., 2016). In addition, TRIM2 has been shown to inhibit p53 and thereby promote PCa cell growth and surival (Takayama et al., 2018). The downregulation of *TRIM2*, and the other oncogenes, through combined pharmaco-selective inhibition of KDM1A and KDM7A is therefore highly relevant in LNCaP:C4-2. Other genes closely clustered with *PSA*, such as *LPAR3* (Brusevold et al., 2014, Zuckerman et al., 2016), *AQP7* (Aikman et al., 2018), *ANGPT1* (Flores-Pérez et al., 2016, Hayes et al., 2000, Michael et al., 2017), *TRO* (Harada et al., 2007, Kim et al., 2014), and *RNF144A* have not been attributed a role in PCa yet and would therefore be interesting to study as they have been implicated in other types of (Ho and Lin, 2018, Ho et al., 2014). In contrast, the role of DDIT4 as a tumour suppressor or oncogene in PCa is controversial (Horak et al., 2010, Sahra et al., 2011, Schwarzer et al., 2005, Sinha et al., 2014, Tirado-Hurtado et al., 2018). It is a DNA damage inducible

transcript (DDIT) gene and its role is to switch off the metabolic activity in a cell during stress by inhibiting mTOR (Tirado-Hurtado et al., 2018). Another negative regulator of the PI3K/AKT/mTOR pathway is PTEN, which is important to control cell growth, proliferation and survival (Chalhoub and Baker, 2009) and a key tumour suppressor in PCa (Trotman et al., 2003).

More research is needed to investigate the genes after combined inhibition of KDM1A and KDM7A. The analysis with the Kyoto Encyclopedia of Genes and Genomes (KEGG) pathway database revealed that many of the down-regulated genes were involved in cancer-related pathways (**Figure 5.24** and **Figure 5.25**). Especially in LNCaP, many important oncogenic regulators were down-regulated and a few genes were up-regulated, including the well-known tumour suppressor p53 (Massenkeil et al., 1994, Strano et al., 2007) (**Figure 5.24**). In contrast, in LNCaP:C4-2, more genes were up-regulated in cancer-related pathways (**Figure 5.25**), compared to LNCaP cells (**Figure 5.24**), as already generally reflected in the Venn diagram analysis (**Figure 5.23**). Even though p53 expression was unchanged in LNCaP:C4-2, p21 was upregulated. P21 is activated by p53 and is known to inhibit cell cycle progression by inhibiting cyclin-dependent kinases (Elbendary et al., 1996, Macleod et al., 1995). Several genes, including *BAX* and *BAK*, which induce apoptosis, were also upregulated in LNCaP:C4-2 (Westphal et al., 2011) (**Figure 5.25**). In addition, HIF-1α is known to be activated upon hypoxia and inflammation and regulates many genes, including the angiogenesis-related *VEGF* gene (Ramakrishnan et al., 2014, Semenza, 2010). Both *HIF-1α* and *VEGF* were upregulated upon combined inhibitor treatment in LNCaP:C4-2, which could be a response to cellular stress (Pereira et al., 2014, Semenza, 2010) (**Figure 5.25**). In contrast, in LNCaP, *HIF-1α* and *VEGF* were downregulated (**Figure 5.24**). The oncogene *Ras* was downregulated in LNCaP (**Figure 5.24**), indicating KDM1A and/or KDM7A may play an important role in directly or indirectly activating *Ras*, which was shown to be crucial for PCa progression (Weber and Gioeli, 2004). On the other hand, *Ras* was upregulated in LNCaP:C4-2 cells after combined inhibition of KDM1A and KDM7A (**Figure 5.25**). This example further emphasises the differences between LNCaP and LNCaP:C4-2 and that the inhibition of KDMs can have opposing effects on tumour suppressor genes and oncogenes in distinct cell lines.

Since apoptosis- and stress-related genes were dysregulated by combined inhibition of Namoline and TC-E 5002, the effect on cell proliferation was investigated. Indeed, in all cell lines tested (LNCaP, LNCaP:C4-2 and 22Rv1), cell proliferation was inhibited to a greater

extent by combined inhibitor treatment compared to inhibiting KDM1A and KDM7A respectively alone (**Figure 5.26**). In LNCaP:C4-2, the upregulation of *p21*, *BAX* and *BAK*, inducing cell cycle arrest and apoptosis, likely explains the growth inhibition, at least in part. In addition, a study by Huang et al. (2007) showed that KDM1A keeps p53 in an inactive state by post-translationally demethylating K370me2 at p53. The inhibition of KDM1A therefore is likely to lead to active p53, resulting in cell death and growth arrest (Brooks and Gu, 2010). Apoptosis and cell cycle assays are needed to confirm the mechanisms of inhibition of cell growth (Evan and Vousden, 2001, Pietenpol and Stewart, 2002).

Overall, the RNASeq and KEGG pathway database analysis revealed that combined Namoline and TC-E 5002 treatment affected AR signalling and cancer pathways differently between LNCaP and LNCaP:C4-2 cells. This is not surprising, as the AR signalling pathway in androgen-responsive PCa differs from the one in metastatic disease where the AR signalling pathway is disrupted and many of the AR target genes are shown to be downregulated (Hendriksen et al., 2006, Henshall et al., 2003, Lapointe et al., 2004). Since PCa is a very heterogenous disease, both combinatorial and single targeting of KDMs may have their place as treatment options, depending on the PCa stage. However, more research is needed to define which KDM is best to inhibit in localised PCa vs. metastatic and CRPC.

Chapter 6: Conclusions and future perspectives

Chapter 6 Conclusions and future perspectives

Targeting epigenetic coregulators has gained much interest in the recent years and is currently a hot topic for the treatment of the aggressive and incurable castrate resistant prostate cancer (CRPC) (Graça et al., 2016, Liao and Xu, 2019, Ruggero et al., 2018). Nilsson and colleagues (2015) identified a coregulatory network of the androgen receptor (AR), which includes the extensively studied KDM1A, but also other KDMs, such as KDM5B and KDM7A. KDM1A represents a promising target for the treatment of PCa (Cai et al., 2014, Kashyap et al., 2013, Metzger et al., 2005, Wissmann et al., 2007), thus posing the question, whether KDM5B and KDM7A could also be drug targets in PCa. A potential challenge with using KDM1A as a drug target may be that KDM1A can act both as a transcriptional corepressor and coactivator by demethylating H3K4me2/me1 and H3K9me2/me1 respectively (**Figure 6.1**) (Metzger et al., 2005, Shi et al., 2004). In contrast, KDM5B demethylates H3K4me3/me2/me1 (Scibetta et al., 2007), which is a known mark for active transcription, and KDM7A demethylates H3K9me2 and H3K27me2 (Huang et al., 2010), which are considered as repressive histone marks (**Figure 6.1**) (Black et al., 2012).

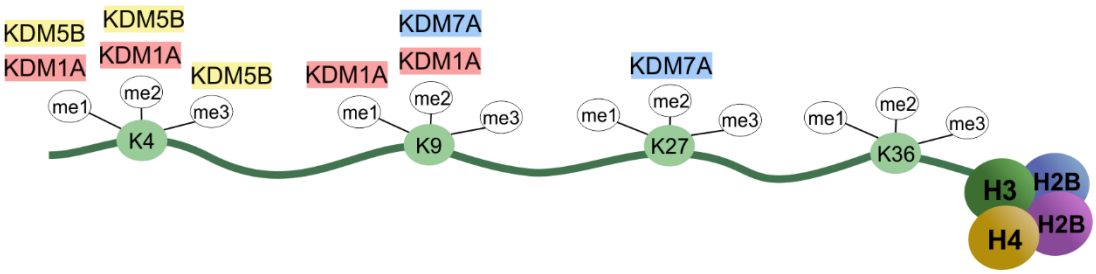

Figure 6.1: KDM1A, KDM5B and KDM7A histone marks.
The methyl-marks at H3K4me3/me2/me1 are targeted by KDM1A and KDM5B. H3K9me2/m1 can be demethylated by KDM1A and KDM7A, but not H3K9me3. KDM7A additionally demethylates H3K27me2.

To investigate the role of KDM5B and KDM7A in AR-regulated gene expression in PCa, siRNA-mediated knockdown experiments were performed. Interestingly, androgen regulated gene expression was most affected by *KDM1A, KDM5B and KDM7A* knockdown in the androgen-dependent LNCaP cell line as compared to androgen-independent cell lines tested. This is not surprising, since KDM1A, KDM5B and KDM7A are important coregulators of AR and LNCaP is androgen-dependent (Lee et al., 2018, Metzger et al., 2005, Nilsson et al., 2015, Xiang et al., 2007). However, AR signalling plays a pivotal role in CRPC too (Sharma et al., 2013), and indeed, more effective inhibition of the demethylase

activity of KDM1A, KDM5B and KDM7A respectively through pharmaco-selective drugs had an effect on AR-target gene expression in androgen-independent cell lines too. These candidate drugs inhibited both the expression of AR-regulated genes, and also PCa cell proliferation. This highlights that pharmaco-selective inhibitors, such as Namoline targeting KDM1A, CPI-455 targeting KDM5B and TC-E 5002 targeting KDM7A, could be used as drugs to treat PCa. However, in some of our experiments, KDM1A and KDM5B seemed to exhibit tumour suppressive functions in advanced PCa stages, and it will therefore be crucial to define the roles of specific KDMs at distinct PCa stages, before further clinical development of KDM inhibitors. Interestingly, the cell line 22Rv1, which harbours the ARv7 splice variant, seemed somewhat resistant to the inhibition of KDM7A, but not KDM1A and KDM5B, indicating KDM1A and KDM5B may be good targets for patients harbouring ARv7.

Our results indicate that the effect of KDM inhibition is strongly dependent on the dose and duration of treatment and varies between PCa cell lines, and may by inference, differ in different PCa stages. This will be important to consider if KDM-selective drugs were used in patients. It will be crucial to further investigate the effect of KDM-selective inhibitors on the transcriptome of PCa cells at various stages of PCa progression. Our results indicate that the inhibition of KDMs up- and down-regulates genes in distinct ways depending on the cell line. This, again, is not surprising, as the androgen signalling pathway in CRPC is disrupted and many AR-target genes are downregulated, compared to enhanced androgen signalling in androgen-dependent disease (Hendriksen et al., 2006, Henshall et al., 2003, Lapointe et al., 2004). Phenotypical analysis will be needed to further investigate the effects of KDM inhibition. It will be important to examine the mechanisms by which KDM inhibition suppresses cell growth (cell cycle arrest, apoptosis, necrosis or autophagy) and whether KDM inhibition also blocks migration and invasion, which is crucial for PCa metastasis (Hanahan and Weinberg, 2011, Seyfried and Huysentruyt, 2013).

Indeed, KDM1A has been reported to change its function during PCa progression (Battaglia et al., 2017, Cai et al., 2014, Ketscher et al., 2014, Yang et al., 2015b), indicating other KDMs, such as KDM5B and KDM7A, may change their role too. The tumour suppressive and activating role of KDM1A appears to be dependent on the context, such as cell type (Kashyap et al., 2013, Sehrawat et al., 2018), epigenetic landscape (Cai et al., 2011, Metzger et al., 2010, Metzger et al., 2008, Shi et al., 2005), and which protein partner it is bound to

(Lee et al., 2005, Metzger et al., 2005, Shi et al., 2005, Wang et al., 2009d). It will be pivotal to further examine the epigenetic landscape of KDM regulated AR-target genes in the different cell lines by using ChiP-Seq analysis. Further ChiP-Seq analysis will help answer the questions: (i) where do the KDMs bind in the genome in AR-dependent and independent cell lines; (ii) which histone modifications do KDMs induce at AR-target genes (promotor and enhancer regions); (iii) is there any functional interdependence between KDMs, and if yes, what are they and could combined inhibition of KDMs be beneficial? The latter was addressed in this study and revealed that there seems to be a functional interdependence between KDMs, which adds another layer of complexity, to their role in androgen signalling in PCa. Whether combined inhibition of KDMs was advantageous over single targeting of KDMs seemed, again, be dependent on the gene locus and cell line, and needs further investigation by ChiP-Seq.

KDMs do not only change their function during PCa progression, but also seem to have different roles in different types of PCa. For example, *KDM1A* was amplified in some NePC patient samples according to bioinformatic analysis, which is consistent with a study by Etani et al. (2019) which revealed high KDM1A expression in NePC specimens. Interestingly, *KDM5B* was amplified even more frequently than *KDM1A* in NePC patient samples, indicating *KDM5B* may have an important AR-independent role in NePC too. Even though KDMs have been shown to be crucial in androgen signalling, KDM1A, KDM5B and KDM7A seemed to be involved in regulating CRPC (PC3 and Du145) cell growth in an AR-independent manner. For future experiments, it will be important to also define the role of KDMs in aggressive PCa, which does not express AR. Interestingly, the immunohistochemical staining of KDM5B was stronger in the cytoplasm than in the nucleus, which arises the question whether this is a regulatory mechanism to keep KDM5B outside of the nucleus or whether KDM5B fufils a so far unknown, AR-independent function in the cytoplasm. KDMs can not only act by demethylating histone proteins, but also non-histone proteins, such as p53 which is a demethylation target of KDM1A (Huang et al., 2007). In addition, Sahrawat and collagues (2018) recently revealed that KDM1A contributes to PCa progression independent of its demethylase activity. It will therefore be important to further investigate, whether KDM5B and KDM7A also fulfil any demethylase independent functions in PCa, such as a scaffolding function within protein complexes. Protein-protein interaction analysis would give more insight in KDM actions and regulation. Our results indicate that in some cases the oncogenic function of the KDMs is regulated on a transcriptional and translational level.

One caveat of this study is the selectivity of the KDM inhibitors. Enzymatic studies on the inhibitors Namoline (Willmann et al., 2012), PBIT (Sayegh et al., 2013), CPI-455 (Vinogradova et al., 2016) and TC-E (Suzuki et al., 2013) have shown that these inhibitors selectively inhibit KDM1A, KDM5B and KDM7A respectively compared to other KDM family members. However, it cannot be fully excluded that the inhibitors also target other KDMs, or even other families of proteins, especially at high drug concentrations used in the cell culture experiments of this study. Drug non-selectivity and non-specificity are major drivers of side effects and represent the challenges for every drug design and application (Huggins et al., 2012, Lee et al., 2019, Mencher and Wang, 2005). It will therefore be crucial to test which other proteins the KDM inhibitors in this study potentially target, and whether the effects seen on the cellular level are caused by selective or non-selective binding. In addition, high KDM inhibitor concentrations can cause cell toxicity which in turn can lead to non-specific changes in the methylation status of the histones, which represents another challenge regarding KDM inhibitors (Hatch et al., 2017). It will be important to develop more selective and effective KDM inhibitors. One study, for example, has reported the potential use of cyclic peptide inhibitors, which are non-metal chelating and potentially more potent and selective than the currently existing KDM inhibitors (Kawamura et al., 2017). In the cell culture experiment of this study, we used siRNA-mediated gene silencing to specifically target KDMs (Yang et al., 2011). To reduce off-target effects and increase knockdown efficiency, pools of multiple siRNAs were used, which target distinct regions of the same gene (Hannus et al., 2014). Even though siRNA pools have been proven to be more effective than individual siRNAs (Parsons et al., 2009), siRNA-mediated silencing meets some challenges. Unlike pharmaceutical inhibitors, siRNA oligonucleotides require transfection reagents to be delivered into cells, which can be inefficient or toxic to the cells (Taxman et al., 2010). In this study, the pharmaceutical inhibitors had a greater effect on gene expression than the siRNA-mediated knockdown. This could be due to siRNA delivery being less efficient or nonselective inhition of other proteins by the inhibitors. In addition, siRNA-mediated silencing takes longer to show an effect than pharmaceutical drugs. An alternative for siRNAs are shRNAs which allow a more stable knockdown of the target gene (Rao et al., 2009, Taxman et al., 2010).

The cell culture experiments in this study were performed on flat, adherent cell monolayers which are also referred to as two-dimensional (2D) cell cultures (Kapałczyńska et al., 2018). 2D cultures are a common and easy method to test pharmaceutical drugs in a preclinical context and to investigate cell behaviour outside the body (Pampaloni et al., 2007).

However, 2D cultures have several limitations as they do not represent the physiological morphology and behaviour of cells *in vivo* (Baker and Chen, 2012). In fact, this discrepancy is considered to be the main cause of drugs failing clinical trials (Joseph et al., 2018, Kim, 2005). In tumours, cells interact with the surrounding microenvironment, composed of different cell types and extracellular matrix, which is vital for various cellular processes, including cell proliferation and drug metabolism (Wang et al., 2017). The size and shape of a cell have shown to influence cell signalling (Meyers et al., 2006). In addition, the artificial culture conditions of unlimited oxygen and nutrients in 2D cultures differ to physiological tumours, where events such as hypoxia and nutrient starvation can significantly influence cell behaviour and tumour progression (Hockel and Vaupel, 2001, Pampaloni et al., 2007). It will therefore be important to test the effect of the pharmacological inhibitors targeting the KDMs in 3D cell cultures, to verify comparability to results shown in 2D cultures (Mazzoleni et al., 2009). 3D cultures allow for the presence of so-called tumour niches and interaction between tumour cells and the microenvironment, and therefore more closely simulate *in vivo* conditions (Kapałczyńska et al., 2018). Eventually, the effect of targeting KDMs will have to be tested *in vivo*, which will give more insight into pharmacokinetics and toxicity (Saeidnia et al., 2015).

Overall, this study revealed that KDM5B and KDM7A represent promising targets to treat both localised and CRPC. Pharmaco-selective inhibitors of KDMs blocked AR-target gene expression and PCa cell growth, suggesting these drugs could be used to prevent PCa progression. In addition, more effective treatment may be achieved by targeting multiple KDMs. Further studies on the mechanisms of action of KDMs at different PCa stages will help define which KDMs are best to inhibit at which stage.

References

AASLAND, R., GIBSON, T. J. & STEWART, A. F. 1995. The PHD finger: implications for chromatin-mediated transcriptional regulation. *Trends in biochemical sciences,* 20**,** 56-59.

ABADILLA, K. A. & DOBS, A. S. 2012. Topical testosterone supplementation for the treatment of male hypogonadism. *Drugs,* 72**,** 1591-1603.

ABATE-SHEN, C., BANACH-PETROSKY, W. A., SUN, X., ECONOMIDES, K. D., DESAI, N., GREGG, J. P., BOROWSKY, A. D., CARDIFF, R. D. & SHEN, M. M. 2003. Nkx3. 1; Pten mutant mice develop invasive prostate adenocarcinoma and lymph node metastases. *Cancer research,* 63**,** 3886-3890.

ABDULKADIR, S. A., MAGEE, J. A., PETERS, T. J., KALEEM, Z., NAUGHTON, C. K., HUMPHREY, P. A. & MILBRANDT, J. 2002. Conditional loss of Nkx3. 1 in adult mice induces prostatic intraepithelial neoplasia. *Molecular and cellular biology,* 22**,** 1495-1503.

ABRAHAMSSON, P. A. 1999. Neuroendocrine differentiation in prostatic carcinoma. *The Prostate,* 39**,** 135-148.

ADACHI, M., TAKAYANAGI, R., TOMURA, A., IMASAKI, K., KATO, S., GOTO, K., YANASE, T., IKUYAMA, S. & NAWATA, H. 2000. Androgen-insensitivity syndrome as a possible coactivator disease. *New England Journal of Medicine,* 343**,** 856-862.

ADAMO, P. & LADOMERY, M. 2016. The oncogene ERG: a key factor in prostate cancer. *Oncogene,* 35**,** 403.

AIKMAN, B., DE ALMEIDA, A., MEIER-MENCHES, S. M. & CASINI, A. 2018. Aquaporins in cancer development: Opportunities for bioinorganic chemistry to contribute novel chemical probes and therapeutic agents. *Metallomics,* 10**,** 696-712.

AKAZA, H., HINOTSU, S., USAMI, M., ARAI, Y., KANETAKE, H., NAITO, S. & HIRAO, Y. 2009. Combined androgen blockade with bicalutamide for advanced prostate cancer: long-term follow-up of a phase 3, double-blind, randomized study for survival. *Cancer: Interdisciplinary International Journal of the American Cancer Society,* 115**,** 3437-3445.

AKAZA, H., YAMAGUCHI, A., MATSUDA, T., IGAWA, M., KUMON, H., SOEDA, A., ARAI, Y., USAMI, M., NAITO, S. & KANETAKE, H. 2004. Superior anti-tumor efficacy of bicalutamide 80 mg in combination with a luteinizing hormone-releasing hormone (LHRH) agonist versus LHRH agonist monotherapy as first-line treatment for advanced prostate cancer: interim results of a randomized study in Japanese patients. *Japanese journal of clinical oncology,* 34**,** 20-28.

ALBERT, M., SCHMITZ, S. U., KOOISTRA, S. M., MALATESTA, M., TORRES, C. M., REKLING, J. C., JOHANSEN, J. V., ABARRATEGUI, I. & HELIN, K. 2013. The histone demethylase Jarid1b ensures faithful mouse development by protecting developmental genes from aberrant H3K4me3. *PLoS genetics,* 9**,** e1003461.

ALEN, P., CLAESSENS, F., VERHOEVEN, G., ROMBAUTS, W. & PEETERS, B. 1999. The androgen receptor amino-terminal domain plays a key role in p160 coactivator-stimulated gene transcription. *Molecular and cellular biology,* 19**,** 6085-6097.

ALIMIRAH, F., CHEN, J., BASRAWALA, Z., XIN, H. & CHOUBEY, D. 2006. DU-145 and PC-3 human prostate cancer cell lines express androgen receptor: Implications for the androgen receptor functions and regulation. *FEBS letters,* 580**,** 2294-2300.

ALLFREY, V., FAULKNER, R. & MIRSKY, A. 1964. Acetylation and methylation of histones and their possible role in the regulation of RNA synthesis. *Proceedings of the National Academy of Sciences,* 51**,** 786-794.

ALLFREY, V. G. & MIRSKY, A. E. 1964. Structural modifications of histones and their possible role in the regulation of RNA synthesis. *Science,* 144**,** 559-559.

ALONSO, M. A. & MILLÁN, J. 2001. The role of lipid rafts in signalling and membrane trafficking in T lymphocytes. *Journal of cell science,* 114**,** 3957-3965.

ALTHOFF, K., BECKERS, A., ODERSKY, A., MESTDAGH, P., KÖSTER, J., BRAY, I. M., BRYAN, K., VANDESOMPELE, J., SPELEMAN, F. & STALLINGS, R. L. 2013. MiR-137 functions as a tumor suppressor in neuroblastoma by downregulating KDM1A. *International journal of cancer,* 133**,** 1064-1073.

ALTUWAIJRI, S., LEE, D. K., CHUANG, K.-H., TING, H.-J., YANG, Z., XU, Q., TSAI, M.-Y., YEH, S., HANCHETT, L. A. & CHANG, H.-C. 2004. Androgen receptor regulates expression of skeletal muscle-specific proteins and muscle cell types. *Endocrine,* 25**,** 27-32.

AMATO, A., PRIOR, T., BAROHN, R., SNYDER, P., PAPP, A. & MENDELL, J. 1993. Kennedy's disease: a clinicopathologic correlation with mutations in the androgen receptor gene. *Neurology,* 43**,** 791-791.

AMBS, S., PRUEITT, R. L., YI, M., HUDSON, R. S., HOWE, T. M., PETROCCA, F., WALLACE, T. A., LIU, C.-G., VOLINIA, S. & CALIN, G. A. 2008. Genomic profiling of microRNA and messenger RNA reveals deregulated microRNA expression in prostate cancer. *Cancer research,* 68**,** 6162-6170.

AMENTE, S., LANIA, L. & MAJELLO, B. 2013. The histone LSD1 demethylase in stemness and cancer transcription programs. *Biochimica et Biophysica Acta (BBA)-Gene Regulatory Mechanisms,* 1829**,** 981-986.

AN, W. & ROEDER, R. G. 2003. Direct association of p300 with unmodified H3 and H4 N termini modulates p300-dependent acetylation and transcription of nucleosomal templates. *Journal of Biological Chemistry,* 278**,** 1504-1510.

ANAND, R. & MARMORSTEIN, R. 2007. Structure and mechanism of lysine-specific demethylase enzymes. *Journal of Biological Chemistry,* 282**,** 35425-35429.

ANDRIOLE, G. L., CRAWFORD, E. D., GRUBB III, R. L., BUYS, S. S., CHIA, D., CHURCH, T. R., FOUAD, M. N., ISAACS, C., KVALE, P. A. & REDING, D. J. 2012. Prostate cancer screening in the randomized Prostate, Lung, Colorectal, and Ovarian Cancer Screening Trial: mortality results after 13 years of follow-up. *Journal of the National Cancer Institute,* 104**,** 125-132.

ANTONARAKIS, E., ARMSTRONG, A., DEHM, S. & LUO, J. 2016. Androgen receptor variant-driven prostate cancer: clinical implications and therapeutic targeting. *Prostate cancer and prostatic diseases,* 19**,** 231.

ANTONARAKIS, E. S., LU, C., LUBER, B., WANG, H., CHEN, Y., ZHU, Y., SILBERSTEIN, J. L., TAYLOR, M. N., MAUGHAN, B. L. & DENMEADE, S. R. 2017. Clinical significance of androgen receptor splice variant-7 mRNA detection in circulating tumor cells of men with metastatic castration-resistant prostate cancer treated with first-and second-line abiraterone and enzalutamide. *Journal of Clinical Oncology,* 35**,** 2149.

APRIKIAN, A. G., CARDON-CARDO, C., FAIR, W. R. & REUTER, V. E. 1993. Characterization of neuroendocrine differentiation in human benign prostate and prostatic adenocarcinoma. *Cancer,* 71**,** 3952-3965.

ARAVIND, L. & IYER, L. M. 2002. The SWIRM domain: a conserved module found in chromosomal proteins points to novel chromatin-modifying activities. *Genome biology,* 3**,** research0039. 1.

ARNAUDO, A. M. & GARCIA, B. A. 2013. Proteomic characterization of novel histone post-translational modifications. *Epigenetics & chromatin,* 6**,** 24.

ASANGANI, I. A., DOMMETI, V. L., WANG, X., MALIK, R., CIESLIK, M., YANG, R., ESCARA-WILKE, J., WILDER-ROMANS, K., DHANIREDDY, S. & ENGELKE, C. 2014. Therapeutic targeting of BET bromodomain proteins in castration-resistant prostate cancer. *Nature,* 510**,** 278.

ASHLEY, E. A. 2015. The precision medicine initiative: a new national effort. *Jama,* 313**,** 2119-2120.

AUDI, L., FERNÁNDEZ-CANCIO, M., CARRASCOSA, A., ANDALUZ, P., TORÁN, N., PIRÓ, C., VILARÓ, E., VICENS-CALVET, E., GUSSINYÉ, M. & ALBISU, M. 2010. Novel (60%) and recurrent (40%) androgen receptor gene mutations in a series of 59 patients with a 46, XY disorder of sex development. *The Journal of Clinical Endocrinology & Metabolism,* 95**,** 1876-1888.

BAADE, P. D., YOULDEN, D. R. & KRNJACKI, L. J. 2009. International epidemiology of prostate cancer: geographical distribution and secular trends. *Molecular nutrition & food research,* 53**,** 171-184.

BAENA, E., SHAO, Z., LINN, D. E., GLASS, K., HAMBLEN, M. J., FUJIWARA, Y., KIM, J., NGUYEN, M., ZHANG, X. & GODINHO, F. J. 2013. ETV1 directs androgen metabolism and confers aggressive prostate cancer in targeted mice and patients. *Genes & development,* 27**,** 683-698.

BAKER, B. M. & CHEN, C. S. 2012. Deconstructing the third dimension–how 3D culture microenvironments alter cellular cues. *Journal of cell science,* 125**,** 3015-3024.

BAKER, M. Albumin, steroid hormones, and the origin of vertebrates. AMERICAN ZOOLOGIST, 2001. SOC INTEGRATIVE COMPARATIVE BIOLOGY 1313 DOLLEY MADISON BLVD, NO 402, MCLEAN …, 1384-1384.

BAKIN, R. E., GIOELI, D., SIKES, R. A., BISSONETTE, E. A. & WEBER, M. J. 2003. Constitutive activation of the Ras/mitogen-activated protein kinase signaling pathway promotes androgen hypersensitivity in LNCaP prostate cancer cells. *Cancer research,* 63**,** 1981-1989.

BALAGUER, F., LINK, A., LOZANO, J. J., CUATRECASAS, M., NAGASAKA, T., BOLAND, C. R. & GOEL, A. 2010. Epigenetic silencing of miR-137 is an early event in colorectal carcinogenesis. *Cancer research,* 70**,** 6609-6618.

BALCIUNAS, D. & RONNE, H. 2000. Evidence of domain swapping within the jumonji family of transcription factors. *Trends in biochemical sciences,* 25**,** 274-276.

BALGI, A. D., FONSECA, B. D., DONOHUE, E., TSANG, T. C., LAJOIE, P., PROUD, C. G., NABI, I. R. & ROBERGE, M. 2009. Screen for chemical modulators of autophagy reveals novel therapeutic inhibitors of mTORC1 signaling. *PloS one,* 4**,** e7124.

BANERJEE, P. P., BANERJEE, S., BROWN, T. R. & ZIRKIN, B. R. 2018. Androgen action in prostate function and disease. *American journal of clinical and experimental urology,* 6**,** 62.

BANNISTER, A. J. & KOUZARIDES, T. 2011. Regulation of chromatin by histone modifications. *Cell research,* 21**,** 381.

BANNISTER, A. J., ZEGERMAN, P., PARTRIDGE, J. F., MISKA, E. A., THOMAS, J. O., ALLSHIRE, R. C. & KOUZARIDES, T. 2001. Selective recognition of methylated lysine 9 on histone H3 by the HP1 chromo domain. *Nature,* 410**,** 120.

BAO, J., ZOU, J., LI, C. & ZHENG, G. 2016. miR-194 inhibits gastric cancer cell proliferation and tumorigenesis by targeting KDM5B. *Eur Rev Med Pharmacol Sci,* 20**,** 4487-93.

BARBIERI, C. E., BACA, S. C., LAWRENCE, M. S., DEMICHELIS, F., BLATTNER, M., THEURILLAT, J.-P., WHITE, T. A., STOJANOV, P., VAN ALLEN, E. & STRANSKY, N. 2012a. Exome sequencing identifies recurrent SPOP, FOXA1 and MED12 mutations in prostate cancer. *Nature genetics,* 44**,** 685.

BARBIERI, C. E., DEMICHELIS, F. & RUBIN, M. A. 2012b. Molecular genetics of prostate cancer: emerging appreciation of genetic complexity. *Histopathology,* 60**,** 187-198.

BARRETT, A., SANTANGELO, S., TAN, K., CATCHPOLE, S., ROBERTS, K., SPENCER-DENE, B., HALL, D., SCIBETTA, A., BURCHELL, J. & VERDIN, E. 2007. Breast cancer associated transcriptional repressor PLU-1/JARID1B interacts directly with histone deacetylases. *International journal of cancer,* 121**,** 265-275.

BARSKI, A., CUDDAPAH, S., CUI, K., ROH, T.-Y., SCHONES, D. E., WANG, Z., WEI, G., CHEPELEV, I. & ZHAO, K. 2007. High-resolution profiling of histone methylations in the human genome. *Cell,* 129**,** 823-837.

BARTEL, D. P. 2004. MicroRNAs: genomics, biogenesis, mechanism, and function. *cell,* 116**,** 281-297.

BATCH, J., DAVIES, H., EVANS, B., HUGHES, I. & PATTERSON, M. 1993. Phenotypic variation and detection of carrier status in the partial androgen insensitivity syndrome. *Archives of disease in childhood,* 68**,** 453-457.

BATTAGLIA, S., KARASIK, E., GILLARD, B., WILLIAMS, J., WINCHESTER, T., MOSER, M. T., SMIRAGLIA, D. J. & FOSTER, B. A. 2017. LSD1 dual function in mediating epigenetic corruption of the vitamin D signaling in prostate cancer. *Clinical epigenetics,* 9**,** 82.

BAUBEC, T., COLOMBO, D. F., WIRBELAUER, C., SCHMIDT, J., BURGER, L., KREBS, A. R., AKALIN, A. & SCHÜBELER, D. 2015. Genomic profiling of DNA methyltransferases reveals a role for DNMT3B in genic methylation. *Nature,* 520**,** 243.

BECKER, K. L. 2001. *Principles and practice of endocrinology and metabolism*, Lippincott Williams & Wilkins.

BEDFORD, M. T. & VAN HELDEN, P. D. 1987. Hypomethylation of DNA in pathological conditions of the human prostate. *Cancer research,* 47**,** 5274-5276.

BELTRAN, H., TOMLINS, S., APARICIO, A., ARORA, V., RICKMAN, D., AYALA, G., HUANG, J., TRUE, L., GLEAVE, M. E. & SOULE, H. 2014. Aggressive variants of castration-resistant prostate cancer. *Clinical Cancer Research,* 20**,** 2846-2850.

BELTRAN, H., YELENSKY, R., FRAMPTON, G. M., PARK, K., DOWNING, S. R., MACDONALD, T. Y., JAROSZ, M., LIPSON, D., TAGAWA, S. T. & NANUS, D. M. 2013. Targeted next-generation sequencing of advanced prostate cancer identifies potential therapeutic targets and disease heterogeneity. *European urology,* 63**,** 920-926.

BENELKEBIR, H., HODGKINSON, C., DURIEZ, P. J., HAYDEN, A. L., BULLEID, R. A., CRABB, S. J., PACKHAM, G. & GANESAN, A. 2011. Enantioselective synthesis of tranylcypromine analogues as lysine demethylase (LSD1) inhibitors. *Bioorganic & medicinal chemistry,* 19**,** 3709-3716.

BENNETT, N. C., GARDINER, R. A., HOOPER, J. D., JOHNSON, D. W. & GOBE, G. C. 2010. Molecular cell biology of androgen receptor signalling. *The international journal of biochemistry & cell biology,* 42**,** 813-827.

BERGÉ-LEFRANC, J.-L., JAY, P., MASSACRIER, A., CAU, P., MATTEI, M. G., BAUER, S., MARSOLLIER, C., BERTA, P. & FONTES, M. 1996. Characterization of the human jumonji gene. *Human molecular genetics,* 5**,** 1637-1641.

BERGER, M. F., LAWRENCE, M. S., DEMICHELIS, F., DRIER, Y., CIBULSKIS, K., SIVACHENKO, A. Y., SBONER, A., ESGUEVA, R., PFLUEGER, D. & SOUGNEZ, C. 2011. The genomic complexity of primary human prostate cancer. *Nature,* 470**,** 214.

BERNSTEIN, B. E., MIKKELSEN, T. S., XIE, X., KAMAL, M., HUEBERT, D. J., CUFF, J., FRY, B., MEISSNER, A., WERNIG, M. & PLATH, K. 2006. A bivalent chromatin structure marks key developmental genes in embryonic stem cells. *Cell,* 125**,** 315-326.

BEROUKHIM, R., MERMEL, C. H., PORTER, D., WEI, G., RAYCHAUDHURI, S., DONOVAN, J., BARRETINA, J., BOEHM, J. S., DOBSON, J. & URASHIMA, M. 2010. The landscape of somatic copy-number alteration across human cancers. *Nature,* 463**,** 899.

BERRY, S. J., COFFEY, D. S., WALSH, P. C. & EWING, L. L. 1984. The development of human benign prostatic hyperplasia with age. *The Journal of urology,* 132**,** 474-479.

BERTERMANN, H. & BRIX, F. 1990. Ultrasonically guided interstitial high dose rate brachytherapy with Ir-192: technique and preliminary results in locally confined prostate cancer. *Martinez AA, Orton CG, Mould R.(szerk). Brachytherapy HDR and LDR. Remote Afterloading State of Art. Leerson, The Netherlands: Nucletron Internationa BV***,** 281-303.

BEVAN, C. L., HOARE, S., CLAESSENS, F., HEERY, D. M. & PARKER, M. G. 1999. The AF1 and AF2 domains of the androgen receptor interact with distinct regions of SRC1. *Molecular and cellular biology,* 19**,** 8383-8392.

BHATIA-GAUR, R., DONJACOUR, A. A., SCIAVOLINO, P. J., KIM, M., DESAI, N., YOUNG, P., NORTON, C. R., GRIDLEY, T., CARDIFF, R. D. & CUNHA, G. R. 1999. Roles for Nkx3. 1 in prostate development and cancer. *Genes & development,* 13**,** 966-977.

BHAVSAR, A. & VERMA, S. 2014. Anatomic imaging of the prostate. *BioMed research international,* 2014.

BIAN, Q., ANDERSON, E. C., BREJC, K. & MEYER, B. J. Dynamic control of chromosome topology and gene expression by a chromatin modification. Cold Spring Harbor symposia on quantitative biology, 2017. Cold Spring Harbor Laboratory Press, 279-291.

BIANCHINI, D., LORENTE, D., RODRIGUEZ-VIDA, A., OMLIN, A., PEZARO, C., FERRALDESCHI, R., ZIVI, A., ATTARD, G., CHOWDHURY, S. & DE BONO, J. 2014. Antitumour activity of enzalutamide (MDV3100) in patients with metastatic castration-resistant prostate cancer (CRPC) pre-treated with docetaxel and abiraterone. *European journal of cancer,* 50**,** 78-84.

BIEBERSTEIN, N. I., KOZÁKOVÁ, E., HURANOVÁ, M., THAKUR, P. K., KRCHŇÁKOVÁ, Z., KRAUSOVÁ, M., OESTERREICH, F. C. & STANĚK, D. 2016. TALE-directed local modulation of H3K9 methylation shapes exon recognition. *Scientific reports,* 6**,** 29961.

BIRD, A. P. 1986. CpG-rich islands and the function of DNA methylation. *Nature,* 321**,** 209.

BIRON, E. & BÉDARD, F. 2016. Recent progress in the development of protein–protein interaction inhibitors targeting androgen receptor–coactivator binding in prostate cancer. *The Journal of steroid biochemistry and molecular biology,* 161**,** 36-44.

BLACK, J. C., VAN RECHEM, C. & WHETSTINE, J. R. 2012. Histone lysine methylation dynamics: establishment, regulation, and biological impact. *Molecular cell,* 48**,** 491-507.

BLATTNER, M., LIU, D., ROBINSON, B. D., HUANG, D., POLIAKOV, A., GAO, D., NATARAJ, S., DEONARINE, L. D., AUGELLO, M. A. & SAILER, V. 2017. SPOP mutation drives prostate tumorigenesis in vivo through coordinate regulation of PI3K/mTOR and AR signaling. *Cancer cell,* 31**,** 436-451.

BLOCH, M., OUSINGSAWAT, J., SIMON, R., SCHRAML, P., GASSER, T., MIHATSCH, M., KUNZELMANN, K. & BUBENDORF, L. 2007. KCNMA1 gene amplification promotes tumor cell proliferation in human prostate cancer. *Oncogene,* 26**,** 2525.

BLOCH, M., SIMON, R., SCHRAML, P., GASSER, T. C., MIHATSCH, M. J. & BUBENDORF, L. 2004. Oncogenic potential of KCNMA1 in prostate cancer. AACR.

BOCK, B. J. & BOSTWICK, D. G. 1999. Does prostatic ductal adenocarcinoma exist? *The American journal of surgical pathology,* 23**,** 781.

BOEHMER, A. L., BRINKMANN, A. O., NIJMAN, R. M., VERLEUN-MOOIJMAN, M. C., DE RUITER, P., NIERMEIJER, M. F. & DROP, S. L. 2001. Phenotypic variation in a family with partial androgen insensitivity syndrome explained by differences in 5α dihydrotestosterone availability. *The Journal of Clinical Endocrinology & Metabolism,* 86**,** 1240-1246.

BOHL, C. E., GAO, W., MILLER, D. D., BELL, C. E. & DALTON, J. T. 2005. Structural basis for antagonism and resistance of bicalutamide in prostate cancer. *Proceedings of the National Academy of Sciences,* 102**,** 6201-6206.

BOLTON, E. C., SO, A. Y., CHAIVORAPOL, C., HAQQ, C. M., LI, H. & YAMAMOTO, K. R. 2007. Cell-and gene-specific regulation of primary target genes by the androgen receptor. *Genes & development,* 21**,** 2005-2017.

BONACCORSI, L., LUCIANI, P., NESI, G., MANNUCCI, E., DELEDDA, C., DICHIARA, F., PAGLIERANI, M., ROSATI, F., MASIERI, L. & SERNI, S. 2008. Androgen receptor

regulation of the seladin-1/DHCR24 gene: altered expression in prostate cancer. *Laboratory investigation,* 88**,** 1049.

BONKHOFF, H. 2001. Neuroendocrine differentiation in human prostate cancer. Morphogenesis, proliferation and androgen receptor status. *Annals of Oncology,* 12**,** S141-S144.

BONKHOFF, H. & REMBERGER, K. 1996. Differentiation pathways and histogenetic aspects of normal and abnormal prostatic growth: a stem cell model. *The Prostate,* 28**,** 98-106.

BONKHOFF, H., STEIN, U. & REMBERGER, K. 1995. Endocrine-paracrine cell types in the prostate and prostatic adenocarcinoma are postmitotic cells. *Human pathology,* 26**,** 167-170.

BONNE, C. & RAYNAUD, J.-P. 1975. Methyltrienolone, a specific ligand for cellular androgen receptors. *Steroids,* 26**,** 227-232.

BONNE, C. & RAYNAUD, J.-P. 1976. Assay of androgen binding sites by exchange with methyltrienolone (R 1881). *Steroids,* 27**,** 497-507.

BOORJIAN, S. A., EASTHAM, J. A., GRAEFEN, M., GUILLONNEAU, B., KARNES, R. J., MOUL, J. W., SCHAEFFER, E. M., STIEF, C. & ZORN, K. C. 2012. A critical analysis of the long-term impact of radical prostatectomy on cancer control and function outcomes. *European urology,* 61**,** 664-675.

BOSTWICK, D. G. & BRAWER, M. K. 1987. Prostatic intra-epithelial neoplasia and early invasion in prostate cancer. *Cancer,* 59**,** 788-794.

BOULIKAS, T., WISEMAN, J. M. & GARRARD, W. T. 1980. Points of contact between histone H1 and the histone octamer. *Proceedings of the National Academy of Sciences,* 77**,** 127-131.

BOWEN, C., BUBENDORF, L., VOELLER, H. J., SLACK, R., WILLI, N., SAUTER, G., GASSER, T. C., KOIVISTO, P., LACK, E. E. & KONONEN, J. 2000. Loss of NKX3. 1 expression in human prostate cancers correlates with tumor progression1, 2. *Cancer research,* 60**,** 6111-6115.

BOYER, L. A., LANGER, M. R., CROWLEY, K. A., TAN, S., DENU, J. M. & PETERSON, C. L. 2002. Essential role for the SANT domain in the functioning of multiple chromatin remodeling enzymes. *Molecular cell,* 10**,** 935-942.

BRADFORD, M. M. 1976. A rapid and sensitive method for the quantitation of microgram quantities of protein utilizing the principle of protein-dye binding. *Analytical biochemistry,* 72**,** 248-254.

BRAWER, M. K. 2005. Prostatic intraepithelial neoplasia: an overview. *Reviews in urology,* 7**,** S11.

BROCKERS, K. & SCHNEIDER, R. 2019. Histone H1, the forgotten histone. Future Medicine.

BROLIN, J., EKMAN, P. & SKOOG, L. 1992. Immunohistochemistry and biochemistry in detection of androgen, progesterone, and estrogen receptors in benign and malignant human prostatic tissue. *The Prostate,* 20**,** 281-295.

BROOKS, C. L. & GU, W. 2010. New insights into p53 activation. *Cell research,* 20**,** 614.

BROWN, T. R. 1995. Human androgen insensitivity syndrome. *Journal of andrology,* 16**,** 299-303.

BROWNELL, J. E., ZHOU, J., RANALLI, T., KOBAYASHI, R., EDMONDSON, D. G., ROTH, S. Y. & ALLIS, C. D. 1996. Tetrahymena histone acetyltransferase A: a homolog to yeast Gcn5p linking histone acetylation to gene activation. *Cell,* 84**,** 843-851.

BRÜCKNER, A., POLGE, C., LENTZE, N., AUERBACH, D. & SCHLATTNER, U. 2009. Yeast two-hybrid, a powerful tool for systems biology. *International journal of molecular sciences,* 10**,** 2763-2788.

BRUSEVOLD, I. J., TVETERAAS, I. H., AASRUM, M., ØDEGÅRD, J., SANDNES, D. L. & CHRISTOFFERSEN, T. 2014. Role of LPAR3, PKC and EGFR in LPA-induced cell migration in oral squamous carcinoma cells. *BMC cancer,* 14**,** 432.

BRYANT, R., PAWLOWSKI, T., CATTO, J., MARSDEN, G., VESSELLA, R., RHEES, B., KUSLICH, C., VISAKORPI, T. & HAMDY, F. 2012. Changes in circulating microRNA levels associated with prostate cancer. *British journal of cancer,* 106**,** 768.

BUNKER, C. H., PATRICK, A. L., MAHARAJ, G., KEENAN, H. A., RAMNARINE, S., BELLE, A., RICHARD, J. R. & DHIR, R. 2002. Prostate cancer risk is three-fold higher among men, aged 50-64, of African descent compared with men of Asian-Indian descent in Trinidad and Tobago. *Ethnicity and Disease,* 12**,** S3-30.

BURATOWSKI, S. & KIM, T. The role of cotranscriptional histone methylations. Cold Spring Harbor symposia on quantitative biology, 2010. Cold Spring Harbor Laboratory Press, 95-102.

BURCHARDT, T., BURCHARDT, M., CHEN, M.-W., CAO, Y., DE LA TAILLE, A., SHABSIGH, A., HAYEK, O., DORAI, T. & BUTTYAN, R. 1999. Transdifferentiation of prostate cancer cells to a neuroendocrine cell phenotype in vitro and in vivo. *The Journal of urology,* 162**,** 1800-1805.

BURG, J. M., GONZALEZ, J. J., MAKSIMCHUK, K. R. & MCCAFFERTY, D. G. 2016. Lysine-specific demethylase 1A (KDM1A/LSD1): product recognition and kinetic analysis of full-length histones. *Biochemistry,* 55**,** 1652-1662.

BURG, J. M., LINK, J. E., MORGAN, B. S., HELLER, F. J., HARGROVE, A. E. & MCCAFFERTY, D. G. 2015. KDM1 class flavin-dependent protein lysine demethylases. *Peptide Science,* 104**,** 213-246.

BURKHARDT, L., FUCHS, S., KROHN, A., MASSER, S., MADER, M., KLUTH, M., BACHMANN, F., HULAND, H., STEUBER, T. & GRAEFEN, M. 2013. CHD1 is a 5q21 tumor suppressor required for ERG rearrangement in prostate cancer. *Cancer research,* 73**,** 2795-2805.

BURNELL, S. E., SPENCER-HARTY, S., HOWARTH, S., BODGER, O., KYNASTON, H., MORGAN, C. & DOAK, S. H. 2018. STEAP2 knockdown reduces the invasive potential of prostate cancer cells. *Scientific reports,* 8**,** 6252.

BURNETT, B. 2019. Taking a Step Back: Analyzing Policy with a Changing Agenda. *Integrating Yoga Therapy into Oncology Care***,** 6.

BUSADA, J. T. & CIDLOWSKI, J. A. 2017. Mechanisms of glucocorticoid action during development. *Current topics in developmental biology.* Elsevier.

BUTLER, L. M., AGUS, D. B., SCHER, H. I., HIGGINS, B., ROSE, A., CORDON-CARDO, C., THALER, H. T., RIFKIND, R. A., MARKS, P. A. & RICHON, V. M. 2000. Suberoylanilide hydroxamic acid, an inhibitor of histone deacetylase, suppresses the growth of prostate cancer cells in vitro and in vivo. *Cancer research,* 60**,** 5165-5170.

CAI, C., HE, H. H., CHEN, S., COLEMAN, I., WANG, H., FANG, Z., CHEN, S., NELSON, P. S., LIU, X. S. & BROWN, M. 2011. Androgen receptor gene expression in prostate cancer is directly suppressed by the androgen receptor through recruitment of lysine-specific demethylase 1. *Cancer cell,* 20**,** 457-471.

CAI, C., HE, H. H., GAO, S., CHEN, S., YU, Z., GAO, Y., CHEN, S., CHEN, M. W., ZHANG, J. & AHMED, M. 2014. Lysine-specific demethylase 1 has dual functions as a major regulator of androgen receptor transcriptional activity. *Cell reports,* 9**,** 1618-1627.

CAI, C., HSIEH, C.-L., OMWANCHA, J., ZHENG, Z., CHEN, S.-Y., BAERT, J.-L. & SHEMSHEDINI, L. 2007. ETV1 is a novel androgen receptor-regulated gene that mediates prostate cancer cell invasion. *Molecular endocrinology,* 21**,** 1835-1846.

CALLEWAERT, L., CHRISTIAENS, V., HAELENS, A., VERRIJDT, G., VERHOEVEN, G. & CLAESSENS, F. 2003. Implications of a polyglutamine tract in the function of the human androgen receptor. *Biochemical and biophysical research communications,* 306**,** 46-52.

CALLEWAERT, L., VAN TILBORGH, N. & CLAESSENS, F. 2006. Interplay between two hormone-independent activation domains in the androgen receptor. *Cancer research,* 66**,** 543-553.

CAMOES, M. J., PAULO, P., RIBEIRO, F. R., BARROS-SILVA, J. D., ALMEIDA, M., COSTA, V. L., CERVEIRA, N., SKOTHEIM, R. I., LOTHE, R. A. & HENRIQUE, R. 2012. Potential downstream target genes of aberrant ETS transcription factors are differentially affected in Ewing's sarcoma and prostate carcinoma. *PloS one,* 7**,** e49819.

CAMPBELL, J. D., ALEXANDROV, A., KIM, J., WALA, J., BERGER, A. H., PEDAMALLU, C. S., SHUKLA, S. A., GUO, G., BROOKS, A. N. & MURRAY, B. A. 2016. Distinct patterns of somatic genome alterations in lung adenocarcinomas and squamous cell carcinomas. *Nature genetics,* 48**,** 607.

CAMPOS, E. & REINBERG, D. H. 2009. Annotating Chromatin. *Annu Rev Genet,* 43.

CANADA, D. Available: http://www.drugbank.ca/drugs/DB00499 [Accessed 01.08.2016].

CAO, J., ZHU, S., ZHOU, W., LI, J., LIU, C., XUAN, H., YAN, J., ZHENG, L., ZHOU, L. & YU, J. 2013. PLZF mediates the PTEN/AKT/FOXO3a signaling in suppression of prostate tumorigenesis. *PloS one,* 8**,** e77922.

CARTER, B. S., BEATY, T. H., STEINBERG, G. D., CHILDS, B. & WALSH, P. C. 1992. Mendelian inheritance of familial prostate cancer. *Proceedings of the National Academy of Sciences,* 89**,** 3367-3371.

CATO, A., SKROCH, P., WEINMANN, J., BUTKERAITIS, P. & PONTA, H. 1988. DNA sequences outside the receptor-binding sites differently modulate the responsiveness of the mouse mammary tumour virus promoter to various steroid hormones. *The EMBO journal,* 7**,** 1403-1410.

CATO, L., DE TRIBOLET-HARDY, J., LEE, I., ROTTENBERG, J. T., COLEMAN, I., MELCHERS, D., HOUTMAN, R., XIAO, T., LI, W. & UO, T. 2019. ARv7 represses Tumor-Suppressor genes in Castration-Resistant prostate cancer. *Cancer cell,* 35**,** 401-413. e6.

CERAMI, E., GAO, J., DOGRUSOZ, U., GROSS, B. E., SUMER, S. O., AKSOY, B. A., JACOBSEN, A., BYRNE, C. J., HEUER, M. L. & LARSSON, E. 2012. The cBio cancer genomics portal: an open platform for exploring multidimensional cancer genomics data. AACR.

CHAKRAVARTI, D., LAMORTE, V. J., NELSON, M. C., NAKAJIMA, T., SCHULMAN, I. G., JUGUILON, H., MONTMINY, M. & EVANS, R. M. 1996. Role of CBP/P300 in nuclear receptor signalling. *Nature,* 383**,** 99.

CHALHOUB, N. & BAKER, S. J. 2009. PTEN and the PI3-kinase pathway in cancer. *Annual Review of Pathological Mechanical Disease,* 4**,** 127-150.

CHAN, S. C., SELTH, L. A., LI, Y., NYQUIST, M. D., MIAO, L., BRADNER, J. E., RAJ, G. V., TILLEY, W. D. & DEHM, S. M. 2015. Targeting chromatin binding regulation of constitutively active AR variants to overcome prostate cancer resistance to endocrine-based therapies. *Nucleic acids research,* 43**,** 5880-5897.

CHAN, T. Y., PARTIN, A. W., WALSH, P. C. & EPSTEIN, J. I. 2000. Prognostic significance of Gleason score 3+ 4 versus Gleason score 4+ 3 tumor at radical prostatectomy. *Urology,* 56**,** 823-827.

CHANDRASEKAR, T., YANG, J. C., GAO, A. C. & EVANS, C. P. 2015. Mechanisms of resistance in castration-resistant prostate cancer (CRPC). *Translational andrology and urology,* 4**,** 365.

CHANG, C., LEE, S. O., WANG, R.-S., YEH, S. & CHANG, T.-M. 2013. Androgen receptor (AR) physiological roles in male and female reproductive systems: lessons learned from AR-knockout mice lacking AR in selective cells. *Biology of reproduction,* 89**,** 21, 1-16.

CHANG, C., SALTZMAN, A., YEH, S., YOUNG, W., KELLER, E. T., LEE, H.-J., WANG, C. & MIZOKAMI, A. 1995. Androgen receptor: an overview. *Critical Reviews™ in Eukaryotic Gene Expression,* 5.

CHATURVEDI, S. S., RAMANAN, R., WAHEED, S. O., AINSLEY, J., EVISON, M., AMES, J. M., SCHOFIELD, C. J., KARABENCHEVA-CHRISTOVA, T. G. & CHRISTOV, C. Z. 2019.

Conformational Dynamics Underlies Different Functions of Human KDM7 Histone Demethylases. *Chemistry–A European Journal,* 25**,** 5422-5426.

CHEIKHELARD, A., MOREL, Y., THIBAUD, E., LORTAT-JACOB, S., JAUBERT, F., POLAK, M. & NIHOUL-FEKETE, C. 2008. Long-term followup and comparison between genotype and phenotype in 29 cases of complete androgen insensitivity syndrome. *The Journal of urology,* 180**,** 1496-1501.

CHEN, C., GE, J., LU, Q., PING, G., YANG, C. & FANG, X. 2015. Expression of Lysine-specific demethylase 1 in human epithelial ovarian cancer. *Journal of ovarian research,* 8**,** 28.

CHEN, D., MA, H., HONG, H., KOH, S. S., HUANG, S.-M., SCHURTER, B. T., ASWAD, D. W. & STALLCUP, M. R. 1999. Regulation of transcription by a protein methyltransferase. *Science,* 284**,** 2174-2177.

CHEN, F., XIONG, W., DOU, K. & RAN, Q. 2017. Knockdown of FOXK1 suppresses proliferation, migration, and invasion in prostate cancer cells. *Oncology Research Featuring Preclinical and Clinical Cancer Therapeutics,* 25**,** 1261-1267.

CHEN, I.-H., TSAI, Y.-S. & TONG, Y.-C. 2012a. Correlations among cardiovascular risk factors, prostate blood flow, and prostate volume in patients with clinical benign prostatic hyperplasia. *Urology,* 79**,** 409-414.

CHEN, J., GUCCINI, I., DI MITRI, D., BRINA, D., REVANDKAR, A., SARTI, M., PASQUINI, E., ALAJATI, A., PINTON, S. & LOSA, M. 2018. Compartmentalized activities of the pyruvate dehydrogenase complex sustain lipogenesis in prostate cancer. *Nature genetics,* 50**,** 219.

CHEN, Q., YAO, Y.-T., XU, H., CHEN, Y.-B., GU, M., CAI, Z.-K. & WANG, Z. 2016. SPOCK1 promotes tumor growth and metastasis in human prostate cancer. *Drug design, development and therapy,* 10**,** 2311.

CHEN, S., MA, J., WU, F., XIONG, L.-J., MA, H., XU, W., LV, R., LI, X., VILLEN, J. & GYGI, S. P. 2012b. The histone H3 Lys 27 demethylase JMJD3 regulates gene expression by impacting transcriptional elongation. *Genes & development,* 26**,** 1364-1375.

CHEN, S., XU, Y., YUAN, X., BUBLEY, G. J. & BALK, S. P. 2006a. Androgen receptor phosphorylation and stabilization in prostate cancer by cyclin-dependent kinase 1. *Proceedings of the National Academy of Sciences,* 103**,** 15969-15974.

CHEN, Y., CLEGG, N. J. & SCHER, H. I. 2009. Anti-androgens and androgen-depleting therapies in prostate cancer: new agents for an established target. *The lancet oncology,* 10**,** 981-991.

CHEN, Y., SPRUNG, R., TANG, Y., BALL, H., SANGRAS, B., KIM, S. C., FALCK, J. R., PENG, J., GU, W. & ZHAO, Y. 2007. Lysine propionylation and butyrylation are novel post-translational modifications in histones. *Molecular & Cellular Proteomics,* 6**,** 812-819.

CHEN, Y., YANG, Y., WANG, F., WAN, K., YAMANE, K., ZHANG, Y. & LEI, M. 2006b. Crystal structure of human histone lysine-specific demethylase 1 (LSD1). *Proceedings of the National Academy of Sciences,* 103**,** 13956-13961.

CHEUNG, P., TANNER, K. G., CHEUNG, W. L., SASSONE-CORSI, P., DENU, J. M. & ALLIS, C. D. 2000. Synergistic coupling of histone H3 phosphorylation and acetylation in response to epidermal growth factor stimulation. *Molecular cell,* 5**,** 905-915.

CHI, K. N., AGARWAL, N., BJARTELL, A., CHUNG, B. H., PEREIRA DE SANTANA GOMES, A. J., GIVEN, R., JUÁREZ SOTO, Á., MERSEBURGER, A. S., ÖZGÜROĞLU, M. & UEMURA, H. 2019. Apalutamide for metastatic, castration-sensitive prostate cancer. *New England Journal of Medicine,* 381**,** 13-24.

CHIANG, P. K., GORDON, R. K., TAL, J., ZENG, G., DOCTOR, B., PARDHASARADHI, K. & MCCANN, P. P. 1996. S-Adenosylmethionine and methylation. *The FASEB journal,* 10**,** 471-480.

CHMELAR, R., BUCHANAN, G., NEED, E. F., TILLEY, W. & GREENBERG, N. M. 2007. Androgen receptor coregulators and their involvement in the development and progression of prostate cancer. *International Journal of cancer,* 120**,** 719-733.

CHOI, J.-Y. & JO, S. A. 2016. KDM7A histone demethylase mediates TNF-α-induced ICAM1 protein upregulation by modulating lysosomal activity. *Biochemical and biophysical research communications,* 478**,** 1355-1362.

CHOMET, P. S. 1991. Cytosine methylation in gene-silencing mechanisms. *Current opinion in cell biology,* 3**,** 438-443.

CHOONG, C. & WILSON, E. 1998. Trinucleotide repeats in the human androgen receptor: a molecular basis for disease. *Journal of molecular endocrinology,* 21**,** 235-258.

CHOONG, C. S., KEMPPAINEN, J. A., ZHOU, Z. & WILSON, E. M. 1996. Reduced androgen receptor gene expression with first exon CAG repeat expansion. *Molecular endocrinology,* 10**,** 1527-1535.

CHOU, T.-C. 2006. Theoretical basis, experimental design, and computerized simulation of synergism and antagonism in drug combination studies. *Pharmacological reviews,* 58**,** 621-681.

CHRISTOFORI, G. 2006. New signals from the invasive front. *Nature,* 441**,** 444.

CHRUN, E. S., MODOLO, F. & DANIEL, F. I. 2017. Histone modifications: A review about the presence of this epigenetic phenomenon in carcinogenesis. *Pathology-Research and Practice,* 213**,** 1329-1339.

CHULPANOVA, D. S., KITAEVA, K. V., JAMES, V., RIZVANOV, A. A. & SOLOVYEVA, V. V. 2018. Therapeutic prospects of extracellular vesicles in cancer treatment. *Frontiers in immunology,* 9.

CHURUKIAN, C. & AGARWAL, M. 1985. Human prostatic endocrine-paracrine (APUD) cells. Distributional analysis with a comparison of serotonin and neuron-specific enolase immunoreactivity and silver stains. *Archives of pathology & laboratory medicine,* 109**,** 607-612.

CIRCU, M. L., DYKES, S. S., CARROLL, J., KELLY, K., GALIANO, F., GREER, A., CARDELLI, J. & EL-OSTA, H. 2016. A novel high content imaging-based screen identifies the anti-helminthic niclosamide as an inhibitor of lysosome anterograde trafficking and prostate cancer cell invasion. *PloS one,* 11**,** e0146931.

CIVENNI, G., ZOPPI, G., VAZQUEZ, R., SHINDE, D., PAGANONI, A., KOKANOVIC, A., LEE, S. H., RUGGERI, B., CARBONE, G. M. & CATAPANO, C. V. 2018. INCB059872, a novel FAD-directed LSD1 Inhibitor, is active in prostate cancer models and impacts prostate cancer stem-like cells. AACR.

CLAESSENS, F., ALEN, P., DEVOS, A., PEETERS, B., VERHOEVEN, G. & ROMBAUTS, W. 1996. The androgen-specific probasin response element 2 interacts differentially with androgen and glucocorticoid receptors. *Journal of Biological Chemistry,* 271**,** 19013-19016.

CLAESSENS, F., DENAYER, S., VAN TILBORGH, N., KERKHOFS, S., HELSEN, C. & HAELENS, A. 2008. Diverse roles of androgen receptor (AR) domains in AR-mediated signaling. *Nuclear receptor signaling,* 6**,** nrs. 06008.

CLARK, J., MERSON, S., JHAVAR, S., FLOHR, P., EDWARDS, S., FOSTER, C., EELES, R., MARTIN, F. L., PHILLIPS, D. & CRUNDWELL, M. 2007. Diversity of TMPRSS2-ERG fusion transcripts in the human prostate. *Oncogene,* 26**,** 2667.

CLINCKEMALIE, L., VANDERSCHUEREN, D., BOONEN, S. & CLAESSENS, F. 2012. The hinge region in androgen receptor control. *Molecular and cellular endocrinology,* 358**,** 1-8.

COEN, J. J., FELDMAN, A. S., SMITH, M. R. & ZIETMAN, A. L. 2011. Watchful waiting for localized prostate cancer in the PSA era: what have been the triggers for intervention? *BJU international,* 107**,** 1582-1586.

COFFEY, D. S. & PIENTA, K. 1987. New concepts in studying the control of normal and cancer growth of the prostate. *Progress in clinical and biological research,* 239**,** 1.

COFFEY, K. & ROBSON, C. N. 2012. Regulation of the androgen receptor by post-translational modifications. *Journal of Endocrinology,* 215**,** 221-237.

COLLIN, S. M., MARTIN, R. M., METCALFE, C., GUNNELL, D., ALBERTSEN, P. C., NEAL, D., HAMDY, F., STEPHENS, P., LANE, J. A. & MOORE, R. 2008. Prostate-cancer mortality in the USA and UK in 1975–2004: an ecological study. *The lancet oncology,* 9**,** 445-452.

COOK, T. & SHERIDAN, W. P. 2000a. Development of GnRH antagonists for prostate cancer: new approaches to treatment. *The oncologist,* 5**,** 162-168.

COOK, T. & SHERIDAN, W. P. 2000b. Development of GnRH antagonists for prostate cancer: new approaches to treatment. *Oncologist,* 5**,** 162-8.

COOPER, G. & HAUSMAN, R. 2000. The cell: a molecular approach. Sinauer Associates. *Sunderland, MA*.

CORCORAN, C., RANI, S., O'BRIEN, K., O'NEILL, A., PRENCIPE, M., SHEIKH, R., WEBB, G., MCDERMOTT, R., WATSON, W. & CROWN, J. 2012. Docetaxel-resistance in prostate cancer: evaluating associated phenotypic changes and potential for resistance transfer via exosomes. *PloS one,* 7**,** e50999.

COUTINHO, I., DAY, T. K., TILLEY, W. D. & SELTH, L. A. 2016. Androgen receptor signaling in castration-resistant prostate cancer: a lesson in persistence. *Endocrine-related cancer,* 23**,** T179-T197.

CRAMERI, A., BIONDI, E., KUEHNLE, K., LÜTJOHANN, D., THELEN, K. M., PERGA, S., DOTTI, C. G., NITSCH, R. M., LEDESMA, M. D. & MOHAJERI, M. H. 2006. The role of seladin-1/DHCR24 in cholesterol biosynthesis, APP processing and Aβ generation in vivo. *The EMBO journal,* 25**,** 432-443.

CRAWFORD, E. D. & HOU, A. H. 2009. The role of LHRH antagonists in the treatment of prostate cancer. *Prostate,* 23.

CROWDER, M. K., SEACRIST, C. D. & BLIND, R. D. 2017. Phospholipid regulation of the nuclear receptor superfamily. *Advances in biological regulation,* 63**,** 6-14.

CSAPO, A. I., PULKKINEN, M. O. & WIEST, W. 1973. Effects of luteectomy and progesterone replacement therapy in early pregnant patients. *American journal of obstetrics and gynecology,* 115**,** 759-765.

CULIG, Z., KLOCKER, H., EBERLE, J., KASPAR, F., HOBISCH, A., CRONAUER, M. V. & BARTSCH, G. 1993. DNA sequence of the androgen receptor in prostatic tumor cell lines and tissue specimens assessed by means of the polymerase chain reaction. *The Prostate,* 22**,** 11-22.

CUNHA, G. R., DONJACOUR, A. A., COOKE, P. S., MEE, H., BIGSBY, R. M., HIGGINS, S. J. & SUGIMURA, Y. 1987. The endocrinology and developmental biology of the prostate. *Endocrine reviews,* 8**,** 338-362.

CUSSENOT, O., BERTHON, P., BERGER, R., MOWSZOWICZ, I., FAILLE, A., HOJMAN, F., TEILLAC, P., LE DUC, A. & CALVO, F. 1991. Immortalization of human adult normal prostatic epithelial cells by liposomes containing large T-SV40 gene. *The Journal of urology,* 146**,** 881-886.

CUTRESS, M. L., WHITAKER, H. C., MILLS, I. G., STEWART, M. & NEAL, D. E. 2008. Structural basis for the nuclear import of the human androgen receptor. *Journal of cell science,* 121**,** 957-968.

CUZICK, J., THORAT, M. A., ANDRIOLE, G., BRAWLEY, O. W., BROWN, P. H., CULIG, Z., EELES, R. A., FORD, L. G., HAMDY, F. C. & HOLMBERG, L. 2014. Prevention and early detection of prostate cancer. *The lancet oncology,* 15**,** e484-e492.

D'AMICO, A. V., WHITTINGTON, R., MALKOWICZ, S. B., SCHULTZ, D., BLANK, K., BRODERICK, G. A., TOMASZEWSKI, J. E., RENSHAW, A. A., KAPLAN, I. & BEARD, C. J. 1998. Biochemical outcome after radical prostatectomy, external beam radiation

therapy, or interstitial radiation therapy for clinically localized prostate cancer. *Jama,* 280**,** 969-974.

D'OTO, A., TIAN, Q.-W., DAVIDOFF, A. M. & YANG, J. 2016. Histone demethylases and their roles in cancer epigenetics. *Journal of medical oncology and therapeutics,* 1**,** 34.

D'HAESELEER, P., LIANG, S. & SOMOGYI, R. 2000. Genetic network inference: from co-expression clustering to reverse engineering. *Bioinformatics,* 16**,** 707-726.

DA, G., LENKART, J., ZHAO, K., SHIEKHATTAR, R., CAIRNS, B. R. & MARMORSTEIN, R. 2006. Structure and function of the SWIRM domain, a conserved protein module found in chromatin regulatory complexes. *Proceedings of the National Academy of Sciences,* 103**,** 2057-2062.

DA MOTA, S. R., BAILEY, S., STRIVENS, R. A., HAYDEN, A. L., DOUGLAS, L. R., DURIEZ, P. J., BORRELLO, M. T., BENELKEBIR, H., GANESAN, A. & PACKHAM, G. 2018. LSD1 inhibition attenuates androgen receptor V7 splice variant activation in castration resistant prostate cancer models. *Cancer cell international,* 18**,** 71.

DANG, Q., LI, L., XIE, H., HE, D., CHEN, J., SONG, W., CHANG, L. S., CHANG, H.-C., YEH, S. & CHANG, C. 2015. Anti-androgen enzalutamide enhances prostate cancer neuroendocrine (NE) differentiation via altering the infiltrated mast cells→ androgen receptor (AR)→ miRNA32 signals. *Molecular oncology,* 9**,** 1241-1251.

DANIELS, G., PEI, Z., LOGAN, S. K. & LEE, P. 2013. Mini-review: androgen receptor phosphorylation in prostate cancer. *American journal of clinical and experimental urology,* 1**,** 25.

DARIMONT, B. D., WAGNER, R. L., APRILETTI, J. W., STALLCUP, M. R., KUSHNER, P. J., BAXTER, J. D., FLETTERICK, R. J. & YAMAMOTO, K. R. 1998. Structure and specificity of nuclear receptor–coactivator interactions. *Genes & development,* 12**,** 3343-3356.

DAVID, S. N., ARNOLD EGLOFF, S. A., GOYAL, R., CLARK, P. E., PHILLIPS, S., GELLERT, L. L., HAMEED, O. & GIANNICO, G. A. 2018. MAGI2 is an independent predictor of biochemical recurrence in prostate cancer. *The Prostate,* 78**,** 616-622.

DE BROT, S., NTEKIM, A., CARDENAS, R., JAMES, V., ALLEGRUCCI, C., HEERY, D. M., BATES, D. O., ØDUM, N., PERSSON, J. L. & MONGAN, N. P. 2015. Regulation of vascular endothelial growth factor in prostate cancer. *Endocrine-related cancer,* 22**,** R107-R123.

DE MARZO, A. M., MARCHI, V. L., EPSTEIN, J. I. & NELSON, W. G. 1999. Proliferative inflammatory atrophy of the prostate: implications for prostatic carcinogenesis. *The American journal of pathology,* 155**,** 1985-1992.

DEBES, J. D., CULIG, Z. & TINDALL, D. J. 2005. The Coactivators CBP and p300 in Androgen Independent Prostate Cancer. *Hormonal Carcinogenesis IV.* Springer.

DEBES, J. D., SCHMIDT, L. J., HUANG, H. & TINDALL, D. J. 2002. p300 mediates androgen-independent transactivation of the androgen receptor by interleukin 6. *Cancer research,* 62**,** 5632-5636.

DEGEORGES, A., HOFFSCHIR, F., CUSSENOT, O., GAUVILLE, C., LE DUC, A., DUTRILLAUX, B. & CALVO, F. 1995. Recurrent cytogenetic alterations of prostate carcinoma and amplification of c-myc or epidermal growth factor receptor in subclones of immortalized PNT1 human prostate epithelial cell line. *International journal of cancer,* 62**,** 724-731.

DEHM, S. M., SCHMIDT, L. J., HEEMERS, H. V., VESSELLA, R. L. & TINDALL, D. J. 2008. Splicing of a novel androgen receptor exon generates a constitutively active androgen receptor that mediates prostate cancer therapy resistance. *Cancer research,* 68**,** 5469-5477.

DEL RÍO, I. B., YOUNG, L. C., SARI, S., JONES, G. G., RINGHAM-TERRY, B., HARTIG, N., REJNOWICZ, E., LEI, W., BHAMRA, A. & SURINOVA, S. 2019. SHOC2 complex-driven

RAF dimerization selectively contributes to ERK pathway dynamics. *Proceedings of the National Academy of Sciences*, 201902658.

DENAYER, S., HELSEN, C., THORREZ, L., HAELENS, A. & CLAESSENS, F. 2010. The rules of DNA recognition by the androgen receptor. *Molecular endocrinology,* 24**,** 898-913.

DENG, X. & FANG, L. 2018. VGLL4 is a transcriptional cofactor acting as a novel tumor suppressor via interacting with TEADs. *American journal of cancer research,* 8**,** 932.

DENMEADE, S. R. & ISAACS, J. T. 2002. A history of prostate cancer treatment. *Nature Reviews Cancer,* 2**,** 389.

DEVAIAH, B. N., GEGONNE, A. & SINGER, D. S. 2016. Bromodomain 4: a cellular Swiss army knife. *Journal of leukocyte biology,* 100**,** 679-686.

DEY, A., ELLENBERG, J., FARINA, A., COLEMAN, A. E., MARUYAMA, T., SCIORTINO, S., LIPPINCOTT-SCHWARTZ, J. & OZATO, K. 2000. A bromodomain protein, MCAP, associates with mitotic chromosomes and affects G2-to-M transition. *Molecular and cellular biology,* 20**,** 6537-6549.

DHALLUIN, C., CARLSON, J. E., ZENG, L., HE, C., AGGARWAL, A. K. & ZHOU, M.-M. 1999. Structure and ligand of a histone acetyltransferase bromodomain. *Nature,* 399**,** 491.

DI LORENZO, A. & BEDFORD, M. T. 2011. Histone arginine methylation. *FEBS letters,* 585**,** 2024-2031.

DI MEO, A., BARTLETT, J., CHENG, Y., PASIC, M. D. & YOUSEF, G. M. 2017. Liquid biopsy: a step forward towards precision medicine in urologic malignancies. *Molecular cancer,* 16**,** 80.

DIEUDONNE, M., PECQUERY, R., BOUMEDIENE, A., LENEVEU, M. & GIUDICELLI, Y. 1998. Androgen receptors in human preadipocytes and adipocytes: regional specificities and regulation by sex steroids. *American Journal of Physiology-Cell Physiology,* 274**,** C1645-C1652.

DILLON, S. C., ZHANG, X., TRIEVEL, R. C. & CHENG, X. 2005. The SET-domain protein superfamily: protein lysine methyltransferases. *Genome biology,* 6**,** 227.

DING, J., ZHANG, Z., XIA, Y., LIAO, G., PAN, Y., LIU, S., ZHANG, Y. & YAN, Z. 2013. LSD1-mediated epigenetic modification contributes to proliferation and metastasis of colon cancer. *British journal of cancer,* 109**,** 994.

DOEHNERT, U., BERTELLONI, S., WERNER, R., DATI, E. & HIORT, O. 2015. Characteristic features of reproductive hormone profiles in late adolescent and adult females with complete androgen insensitivity syndrome. *Sexual Development,* 9**,** 69-74.

DONG, Y., ZHANG, H., GAO, A. C., MARSHALL, J. R. & IP, C. 2005. Androgen receptor signaling intensity is a key factor in determining the sensitivity of prostate cancer cells to selenium inhibition of growth and cancer-specific biomarkers. *Molecular cancer therapeutics,* 4**,** 1047-1055.

DOROSZ, J., KRISTENSEN, L. H., ADURI, N. G., MIRZA, O., LOUSEN, R., BUCCIARELLI, S., MEHTA, V., SELLÉS-BAIGET, S., SOLBAK, S. M. Ø. & BACH, A. 2019. Molecular architecture of the Jumonji C family histone demethylase KDM5B. *Scientific reports,* 9**,** 4019.

DOYU, M., SOBUE, G., MUKAI, E., KACHI, T., YASUDA, T., MITSUMA, T. & TAKAHASHI, A. 1992. Severity of X-linked recessive bulbospinal neuronopathy correlates with size of the tandem CAG repeat in androgen receptor gene. *Annals of neurology,* 32**,** 707-710.

DRAGOMIR, M., CHEN, B. & CALIN, G. A. 2018. Exosomal lncRNAs as new players in cell-to-cell communication. *Translational cancer research,* 7**,** S243.

DRUART, X. & DE GRAAF, S. 2018. Seminal plasma proteomes and sperm fertility. *Animal reproduction science,* 194**,** 33-40.

DUFF, J. & MCEWAN, I. J. 2005. Mutation of histidine 874 in the androgen receptor ligand-binding domain leads to promiscuous ligand activation and altered p160 coactivator interactions. *Molecular endocrinology,* 19**,** 2943-2954.

DUTNALL, R. N. & RAMAKRISHNAN, V. 1997. Twists and turns of the nucleosome: tails without ends. *Structure,* 5**,** 1255-1259.

EBERHARTER, A. & BECKER, P. B. 2002. Histone acetylation: a switch between repressive and permissive chromatin. *EMBO reports,* 3**,** 224-229.

EDELSTEIN, R. A., CARR, M. C., CAESAR, R., YOUNG, M., ATALA, A. & FREEMAN, M. R. 1994. Detection of human androgen receptor mRNA expression abnormalities by competitive PCR. *DNA and cell biology,* 13**,** 265-273.

EDWARDS, J. & BARTLETT, J. M. 2005. The androgen receptor and signal-transduction pathways in hormone-refractory prostate cancer. Part 1: Modifications to the androgen receptor. *BJU international,* 95**,** 1320-1326.

EDWARDS, J., KRISHNA, N. S., WITTON, C. J. & BARTLETT, J. M. 2003. Gene amplifications associated with the development of hormone-resistant prostate cancer. *Clinical cancer research,* 9**,** 5271-5281.

EISERMANN, K., BRODERICK, C. J., BAZAROV, A., MOAZAM, M. M. & FRAIZER, G. C. 2013. Androgen up-regulates vascular endothelial growth factor expression in prostate cancer cells via an Sp1 binding site. *Molecular cancer,* 12**,** 7.

EISERMANN, K. & FRAIZER, G. 2017. The androgen receptor and VEGF: mechanisms of androgen-regulated angiogenesis in prostate cancer. *Cancers,* 9**,** 32.

EL-ALFY, M., PELLETIER, G., HERMO, L. S. & LABRIE, F. 2000. Unique features of the basal cells of human prostate epithelium. *Microscopy research and technique,* 51**,** 436-446.

ELLINGER, J., KAHL, P., VON DER GATHEN, J., ROGENHOFER, S., HEUKAMP, L. C., GÜTGEMANN, I., WALTER, B., HOFSTÄDTER, F., BÜTTNER, R. & MÜLLER, S. C. 2010. Global levels of histone modifications predict prostate cancer recurrence. *The Prostate,* 70**,** 61-69.

ELLIS, L. & LODA, M. 2018. LSD1: A single target to combat lineage plasticity in lethal prostate cancer. *Proceedings of the National Academy of Sciences,* 115**,** 4530-4531.

EMERSON, R. E., KOCH, M. O., DAGGY, J. K. & CHENG, L. 2005. Closest distance between tumor and resection margin in radical prostatectomy specimens: lack of prognostic significance. *The American journal of surgical pathology,* 29**,** 225-229.

ERNST, J. & KELLIS, M. 2010. Discovery and characterization of chromatin states for systematic annotation of the human genome. *Nature biotechnology,* 28**,** 817.

ESTÉBANEZ-PERPIÑÁ, E., MOORE, J. M., MAR, E., DELGADO-RODRIGUES, E., NGUYEN, P., BAXTER, J. D., BUEHRER, B. M., WEBB, P., FLETTERICK, R. J. & GUY, R. K. 2005. The molecular mechanisms of coactivator utilization in ligand-dependent transactivation by the androgen receptor. *Journal of Biological Chemistry,* 280**,** 8060-8068.

ESTRADA, M., UHLEN, P. & EHRLICH, B. E. 2006. Ca2+ oscillations induced by testosterone enhance neurite outgrowth. *Journal of cell science,* 119**,** 733-743.

ETANI, T., NAIKI, T., NAIKI-ITO, A., SUZUKI, T., IIDA, K., NOZAKI, S., KATO, H., NAGAYASU, Y., SUZUKI, S. & KAWAI, N. 2019. NCL1, A highly selective lysine-specific demethylase 1 inhibitor, suppresses castration-resistant prostate cancer growth via regulation of apoptosis and autophagy. *Journal of clinical medicine,* 8**,** 442.

ETANI, T., SUZUKI, T., NAIKI, T., NAIKI-ITO, A., ANDO, R., IIDA, K., KAWAI, N., TOZAWA, K., MIYATA, N. & KOHRI, K. 2015. NCL1, a highly selective lysine-specific demethylase 1 inhibitor, suppresses prostate cancer without adverse effect. *Oncotarget,* 6**,** 2865.

ETZIONI, R., TSODIKOV, A., MARIOTTO, A., SZABO, A., FALCON, S., WEGELIN, J., KARNOFSKI, K., GULATI, R., PENSON, D. F. & FEUER, E. 2008. Quantifying the role of PSA screening in the US prostate cancer mortality decline. *Cancer Causes & Control,* 19**,** 175-181.

EVAN, G. I. & VOUSDEN, K. H. 2001. Proliferation, cell cycle and apoptosis in cancer. *nature,* 411**,** 342.

EVANS, A. J., HENRY, P. C., VAN DER KWAST, T. H., TKACHUK, D. C., WATSON, K., LOCKWOOD, G. A., FLESHNER, N. E., CHEUNG, C., BELANGER, E. C. & AMIN, M. B. 2008. Interobserver variability between expert urologic pathologists for extraprostatic extension and surgical margin status in radical prostatectomy specimens. *The American journal of surgical pathology,* 32**,** 1503-1512.

EVANS, B. A. J., HUGHES, I., BEVAN, C., PATTERSON, M. & GREGORY, J. W. 1997. Phenotypic diversity in siblings with partial androgen insensitivity syndrome. *Archives of disease in childhood,* 76**,** 529-531.

FAN, L.-C., JENG, Y.-M., LU, Y.-T. & LIEN, H.-C. 2016. SPOCK1 Is a Novel Transforming Growth Factor-β–Induced Myoepithelial Marker That Enhances Invasion and Correlates with Poor Prognosis in Breast Cancer. *PloS one,* 11**,** e0162933.

FAN, W., YANASE, T., NOMURA, M., OKABE, T., GOTO, K., SATO, T., KAWANO, H., KATO, S. & NAWATA, H. 2005. Androgen receptor null male mice develop late-onset obesity caused by decreased energy expenditure and lipolytic activity but show normal insulin sensitivity with high adiponectin secretion. *Diabetes,* 54**,** 1000-1008.

FANG, Z. & CUI, X. 2011. Design and validation issues in RNA-seq experiments. *Briefings in bioinformatics,* 12**,** 280-287.

FAUZEE, N. J. S., DONG, Z. & WANG, Y.-L. 2011. Taxanes: promising anti-cancer drugs. *Asian Pac J Cancer Prev,* 12**,** 837-51.

FELDMAN, B. J. & FELDMAN, D. 2001. The development of androgen-independent prostate cancer. *Nature Reviews Cancer,* 1**,** 34.

FENG, Y., PAN, T.-C., PANT, D. K., CHAKRABARTI, K. R., ALVAREZ, J. V., RUTH, J. R. & CHODOSH, L. A. 2014. SPSB1 promotes breast cancer recurrence by potentiating c-MET signaling. *Cancer discovery,* 4**,** 790-803.

FERLAY, J., SHIN, H., BRAY, F., FORMAN, D., MATHERS, C. & PARKIN, D. 2010. GLOBOCAN 2008, cancer incidence and mortality worldwide: IARC cancerbase no. 10. Lyon, France: International Agency for Research on Cancer; 2010. *Disponible en: URL: http://globocan. iarc. fr*.

FERLAY, J., SOERJOMATARAM, I., DIKSHIT, R., ESER, S., MATHERS, C., REBELO, M., PARKIN, D. M., FORMAN, D. & BRAY, F. 2015. Cancer incidence and mortality worldwide: sources, methods and major patterns in GLOBOCAN 2012. *International journal of cancer,* 136**,** E359-E386.

FERLAY, J., STELIAROVA-FOUCHER, E., LORTET-TIEULENT, J., ROSSO, S., COEBERGH, J. W., COMBER, H., FORMAN, D. & BRAY, F. 2013. Cancer incidence and mortality patterns in Europe: estimates for 40 countries in 2012. *Eur J Cancer,* 49**,** 1374-403.

FERRALDESCHI, R., WELTI, J., LUO, J., ATTARD, G. & DE BONO, J. 2015. Targeting the androgen receptor pathway in castration-resistant prostate cancer: progresses and prospects. *Oncogene,* 34**,** 1745.

FERRARI, P. & BONNY, O. 2003. Forms of mineralocorticoid hypertension. *Vitamins and hormones,* 66**,** 114-157.

FINGERMAN, I. M., DU, H.-N. & BRIGGS, S. D. 2008. Controlling histone methylation via trans-histone pathways. Taylor & Francis.

FISCHLE, W., TSENG, B. S., DORMANN, H. L., UEBERHEIDE, B. M., GARCIA, B. A., SHABANOWITZ, J., HUNT, D. F., FUNABIKI, H. & ALLIS, C. D. 2005. Regulation of HP1–chromatin binding by histone H3 methylation and phosphorylation. *Nature,* 438**,** 1116.

FIZAZI, K., FAIVRE, L., LESAUNIER, F., DELVA, R., GRAVIS, G., ROLLAND, F., PRIOU, F., FERRERO, J.-M., HOUEDE, N. & MOUREY, L. 2015. Androgen deprivation therapy plus docetaxel and estramustine versus androgen deprivation therapy alone for high-risk localised prostate cancer (GETUG 12): a phase 3 randomised controlled trial. *The Lancet Oncology,* 16**,** 787-794.

FIZAZI, K., SCHER, H. I., MOLINA, A., LOGOTHETIS, C. J., CHI, K. N., JONES, R. J., STAFFURTH, J. N., NORTH, S., VOGELZANG, N. J. & SAAD, F. 2012. Abiraterone acetate for treatment of metastatic castration-resistant prostate cancer: final overall survival analysis of the COU-AA-301 randomised, double-blind, placebo-controlled phase 3 study. *The lancet oncology,* 13**,** 983-992.

FIZAZI, K., SHORE, N., TAMMELA, T. L., ULYS, A., VJATERS, E., POLYAKOV, S., JIEVALTAS, M., LUZ, M., ALEKSEEV, B. & KUSS, I. 2019. Darolutamide in nonmetastatic, castration-resistant prostate cancer. *New England Journal of Medicine,* 380**,** 1235-1246.

FLORES-PÉREZ, A., MARCHAT, L. A., RODRÍGUEZ-CUEVAS, S., BAUTISTA-PIÑA, V., HIDALGO-MIRANDA, A., OCAMPO, E. A., MARTÍNEZ, M. S., PALMA-FLORES, C., FONSECA-SÁNCHEZ, M. A. & ASTUDILLO-DE LA VEGA, H. 2016. Dual targeting of ANGPT1 and TGFBR2 genes by miR-204 controls angiogenesis in breast cancer. *Scientific reports,* 6**,** 34504.

FOK, J. & MEHTA, K. 2008. Significance of increased tissue transglutaminase expression in androgen-refractory prostate carcinoma. AACR.

FOLEY, C. & MITSIADES, N. 2016. Moving beyond the androgen receptor (AR): targeting AR-interacting proteins to treat prostate cancer. *Hormones and Cancer,* 7**,** 84-103.

FORNERIS, F., BINDA, C., VANONI, M. A., BATTAGLIOLI, E. & MATTEVI, A. 2005. Human histone demethylase LSD1 reads the histone code. *Journal of Biological Chemistry,* 280**,** 41360-41365.

FRANKLIN, S. G. & ZWEIDLER, A. 1977. Non-allelic variants of histones 2a, 2b and 3 in mammals. *Nature,* 266**,** 273.

FREEDMAN, L. P. 1998. *Molecular biology of steroid and nuclear hormone receptors*, Springer Science & Business Media.

FREEMAN, M. R. & SOLOMON, K. R. 2004. Cholesterol and prostate cancer. *Journal of cellular biochemistry,* 91**,** 54-69.

FRESCAS, D., GUARDAVACCARO, D., KUCHAY, S. M., KATO, H., POLESHKO, A., BASRUR, V., ELENITOBA-JOHNSON, K. S., KATZ, R. A. & PAGANO, M. 2008. KDM2A represses transcription of centromeric satellite repeats and maintains the heterochromatic state. *Cell cycle,* 7**,** 3539-3547.

FUEYO, R., GARCÍA, M. A. & MARTÍNEZ-BALBÁS, M. A. 2015. Jumonji family histone demethylases in neural development. *Cell and tissue research,* 359**,** 87-98.

GAN, Y., SHI, C., INGE, L., HIBNER, M., BALDUCCI, J. & HUANG, Y. 2010. Differential roles of ERK and Akt pathways in regulation of EGFR-mediated signaling and motility in prostate cancer cells. *Oncogene,* 29**,** 4947.

GAO, L., ZHANG, L.-J., LI, S.-H., WEI, L.-L., LUO, B., HE, R.-Q. & XIA, S. 2018a. Role of miR-452-5p in the tumorigenesis of prostate cancer: A study based on the Cancer Genome Atl (TCGA), Gene Expression Omnibus (GEO), and bioinformatics analysis. *Pathology-Research and Practice,* 214**,** 732-749.

GAO, N., ZHANG, J., RAO, M. A., CASE, T. C., MIROSEVICH, J., WANG, Y., JIN, R., GUPTA, A., RENNIE, P. S. & MATUSIK, R. J. 2003. The role of hepatocyte nuclear factor-3α (Forkhead Box A1) and androgen receptor in transcriptional regulation of prostatic genes. *Molecular endocrinology,* 17**,** 1484-1507.

GAO, Q., LIANG, W.-W., FOLTZ, S. M., MUTHARASU, G., JAYASINGHE, R. G., CAO, S., LIAO, W.-W., REYNOLDS, S. M., WYCZALKOWSKI, M. A. & YAO, L. 2018b. Driver fusions and their implications in the development and treatment of human cancers. *Cell reports,* 23**,** 227-238. e3.

GAO, W., BOHL, C. E. & DALTON, J. T. 2005. Chemistry and structural biology of androgen receptor. *Chemical reviews,* 105**,** 3352-3370.

GARNHAM, R., SCOTT, E., LIVERMORE, K. E. & MUNKLEY, J. 2019. ST6GAL1: A key player in cancer. *Oncology Letters*.

GEHANI, S. S., AGRAWAL-SINGH, S., DIETRICH, N., CHRISTOPHERSEN, N. S., HELIN, K. & HANSEN, K. 2010. Polycomb group protein displacement and gene activation through MSK-dependent H3K27me3S28 phosphorylation. *Molecular cell,* 39**,** 886-900.

GENG, C., RAJAPAKSHE, K., SHAH, S. S., SHOU, J., EEDUNURI, V. K., FOLEY, C., FISKUS, W., RAJENDRAN, M., CHEW, S. A. & ZIMMERMANN, M. 2014. Androgen receptor is the key transcriptional mediator of the tumor suppressor SPOP in prostate cancer. *Cancer research,* 74**,** 5631-5643.

GEORGESCU, M.-M. 2010. PTEN tumor suppressor network in PI3K-Akt pathway control. *Genes & cancer,* 1**,** 1170-1177.

GERKEN, P. A., WOLSTENHULME, J. R., TUMBER, A., HATCH, S. B., ZHANG, Y., MÜLLER, S., CHANDLER, S. A., MAIR, B., LI, F. & NIJMAN, S. M. 2017. Discovery of a Highly Selective Cell-Active Inhibitor of the Histone Lysine Demethylases KDM2/7. *Angewandte Chemie International Edition,* 56**,** 15555-15559.

GHADIRIAN, P., HOWE, G., HISLOP, T. & MAISONNEUVE, P. 1997. Family history of prostate cancer: A multi-center case-control study in Canada. *International journal of cancer,* 70**,** 679-681.

GHOSH, R., LIPSON, K. L., SARGENT, K. E., MERCURIO, A. M., HUNT, J. S., RON, D. & URANO, F. 2010. Transcriptional regulation of VEGF-A by the unfolded protein response pathway. *PloS one,* 5**,** e9575.

GILLATT, D. 2006. Antiandrogen treatments in locally advanced prostate cancer: are they all the same? *Journal of cancer research and clinical oncology,* 132**,** 17-26.

GILLOTEAUX, J., EZE, N., JAMISON, J. M., MCGUIRE, K. & SUMMERS, J. L. 2013. A rare, human prostate oncocyte cell originates from the prostatic carcinoma (DU145) cell line. *Ultrastructural pathology,* 37**,** 440-448.

GIOELI, D., BLACK, B. E., GORDON, V., SPENCER, A., KESLER, C. T., EBLEN, S. T., PASCHAL, B. M. & WEBER, M. J. 2006. Stress kinase signaling regulates androgen receptor phosphorylation, transcription, and localization. *Molecular endocrinology,* 20**,** 503-515.

GIOELI, D., MANDELL, J. W., PETRONI, G. R., FRIERSON, H. F. & WEBER, M. J. 1999. Activation of mitogen-activated protein kinase associated with prostate cancer progression. *Cancer research,* 59**,** 279-284.

GIOELI, D. & PASCHAL, B. M. 2012. Post-translational modification of the androgen receptor. *Molecular and cellular endocrinology,* 352**,** 70-78.

GIUSIANO, S., GARCIA, S., ANDRIEU, C., DUSETTI, N. J., BASTIDE, C., GLEAVE, M., TARANGER-CHARPIN, C., IOVANNA, J. L. & ROCCHI, P. 2012. TP53INP1 overexpression in prostate cancer correlates with poor prognostic factors and is predictive of biological cancer relapse. *The Prostate,* 72**,** 117-128.

GLEASON, D. F. & MELLINGER, G. T. 1974. Prediction of prognosis for prostatic adenocarcinoma by combined histological grading and clinical staging. *The Journal of urology,* 111**,** 58-64.

GLEAVE, M., HSIEH, J.-T., GAO, C., VON ESCHENBACH, A. C. & CHUNG, L. W. 1991. Acceleration of human prostate cancer growth in vivo by factors produced by prostate and bone fibroblasts. *Cancer research,* 51**,** 3753-3761.

GOLDSTEIN, J., BOROWSKY, A. D., GOYAL, R., ROLAND, J. T., ARNOLD, S. A., GELLERT, L. L., CLARK, P. E., HAMEED, O. & GIANNICO, G. A. 2016a. MAGI-2 in prostate cancer: an immunohistochemical study. *Human pathology,* 52**,** 83-91.

GOLDSTEIN, J., GOYAL, R., ROLAND, J. T., GELLERT, L. L., CLARK, P. E., HAMEED, O. & GIANNICO, G. A. 2016b. MAGI-2 is a sensitive and specific marker of prostatic adenocarcinoma: a comparison with AMACR. *American journal of clinical pathology,* 146**,** 294-302.

GOMELLA, L. G. 2009. Effective testosterone suppression for prostate cancer: is there a best castration therapy? *Reviews in urology,* 11**,** 52.

GOTTLIEB, B., BEITEL, L. K., NADARAJAH, A., PALIOURAS, M. & TRIFIRO, M. 2012. The androgen receptor gene mutations database: 2012 update. *Human mutation,* 33**,** 887-894.

GOULD, V., WIEDENMANN, B., LEE, I., SCHWECHHEIMER, K., DOCKHORN-DWORNICZAK, B., RADOSEVICH, J., MOLL, R. & FRANKE, W. W. 1987. Synaptophysin expression in neuroendocrine neoplasms as determined by immunocytochemistry. *The American journal of pathology,* 126**,** 243.

GOULDING, H., PINDER, S., CANNON, P., PEARSON, D., NICHOLSON, R., SNEAD, D., BELL, J., ELSTON, C., ROBERTSON, J. & BLAMEY, R. 1995. A new immunohistochemical antibody for the assessment of estrogen receptor status on routine formalin-fixed tissue samples. *Human pathology,* 26**,** 291-294.

GRAÇA, I., PEREIRA-SILVA, E., HENRIQUE, R., PACKHAM, G., CRABB, S. J. & JERÓNIMO, C. 2016. Epigenetic modulators as therapeutic targets in prostate cancer. *Clinical epigenetics,* 8**,** 98.

GRASSO, C. S., WU, Y.-M., ROBINSON, D. R., CAO, X., DHANASEKARAN, S. M., KHAN, A. P., QUIST, M. J., JING, X., LONIGRO, R. J. & BRENNER, J. C. 2012. The mutational landscape of lethal castrate resistant prostate cancer. *Nature,* 487**,** 239.

GREENBAUM, D., COLANGELO, C., WILLIAMS, K. & GERSTEIN, M. 2003. Comparing protein abundance and mRNA expression levels on a genomic scale. *Genome biology,* 4**,** 117.

GREER, E. L. & SHI, Y. 2012. Histone methylation: a dynamic mark in health, disease and inheritance. *Nature Reviews Genetics,* 13**,** 343.

GREWAL, S. I. & MOAZED, D. 2003. Heterochromatin and epigenetic control of gene expression. *science,* 301**,** 798-802.

GRIFFITH, J. S. & MAHLER, H. R. 1969. DNA ticketing theory of memory. *Nature*.

GRINO, P. B., GRIFFIN, J. E. & WILSON, J. D. 1990. Testosterone at high concentrations interacts with the human androgen receptor similarly to dihydrotestosterone. *Endocrinology,* 126**,** 1165-1172.

GRÖNBERG, H., DAMBER, L. & DAMBER, J.-E. 1994. Studies of genetic factors in prostate cancer in a twin population. *The Journal of urology,* 152**,** 1484-1487.

GUO, T., CHUNG, J. H., WANG, T., MCDONALD-MCGINN, D. M., KATES, W. R., HAWUŁA, W., COLEMAN, K., ZACKAI, E., EMANUEL, B. S. & MORROW, B. E. 2015. Histone modifier genes alter conotruncal heart phenotypes in 22q11. 2 deletion syndrome. *The American Journal of Human Genetics,* 97**,** 869-877.

GUO, Z., YANG, X., SUN, F., JIANG, R., LINN, D. E., CHEN, H., CHEN, H., KONG, X., MELAMED, J. & TEPPER, C. G. 2009. A novel androgen receptor splice variant is up-regulated during prostate cancer progression and promotes androgen depletion–resistant growth. *Cancer research,* 69**,** 2305-2313.

GUPTA, S., WESTON, A., BEARRS, J., THODE, T., NEISS, A., SOLDI, R. & SHARMA, S. 2016. Reversible lysine-specific demethylase 1 antagonist HCI-2509 inhibits growth and decreases c-MYC in castration-and docetaxel-resistant prostate cancer cells. *Prostate cancer and prostatic diseases,* 19**,** 349.

HAELENS, A., TANNER, T., DENAYER, S., CALLEWAERT, L. & CLAESSENS, F. 2007. The hinge region regulates DNA binding, nuclear translocation, and transactivation of the androgen receptor. *Cancer research,* 67**,** 4514-4523.

HAKIMI, M.-A., BOCHAR, D. A., CHENOWETH, J., LANE, W. S., MANDEL, G. & SHIEKHATTAR, R. 2002. A core–BRAF35 complex containing histone deacetylase mediates repression of neuronal-specific genes. *Proceedings of the National Academy of Sciences,* 99**,** 7420-7425.

HALKIDOU, K., GAUGHAN, L., COOK, S., LEUNG, H. Y., NEAL, D. E. & ROBSON, C. N. 2004. Upregulation and nuclear recruitment of HDAC1 in hormone refractory prostate cancer. *The Prostate,* 59**,** 177-189.

HALKIDOU, K., GNANAPRAGASAM, V. J., MEHTA, P. B., LOGAN, I. R., BRADY, M. E., COOK, S., LEUNG, H. Y., NEAL, D. E. & ROBSON, C. N. 2003. Expression of Tip60, an androgen receptor coactivator, and its role in prostate cancer development. *Oncogene,* 22**,** 2466.

HAM, J., THOMSON, A., NEEDHAM, M., WEBB, P. & PARKER, M. 1988. Characterization of response elements for androgens, glucocorticoids and progestins in mouse mammary tumour virus. *Nucleic Acids Research,* 16**,** 5263-5276.

HAN, A. L., KUMAR, S., FOK, J. Y., TYAGI, A. K. & MEHTA, K. 2014. Tissue transglutaminase expression promotes castration-resistant phenotype and transcriptional repression of androgen receptor. *European journal of cancer,* 50**,** 1685-1696.

HAN, M., XU, W., CHENG, P., JIN, H. & WANG, X. 2017. Histone demethylase lysine demethylase 5B in development and cancer. *Oncotarget,* 8**,** 8980.

HAN, W., GAO, S., BARRETT, D., AHMED, M., HAN, D., MACOSKA, J. A., HE, H. H. & CAI, C. 2018. Reactivation of androgen receptor-regulated lipid biosynthesis drives the progression of castration-resistant prostate cancer. *Oncogene,* 37**,** 710.

HANAHAN, D. & WEINBERG, R. A. 2011. Hallmarks of cancer: the next generation. *cell,* 144**,** 646-674.

HANDA, R. J. & WEISER, M. J. 2014. Gonadal steroid hormones and the hypothalamo–pituitary–adrenal axis. *Frontiers in neuroendocrinology,* 35**,** 197-220.

HANNUS, M., BEITZINGER, M., ENGELMANN, J. C., WEICKERT, M.-T., SPANG, R., HANNUS, S. & MEISTER, G. 2014. siPools: highly complex but accurately defined siRNA pools eliminate off-target effects. *Nucleic acids research,* 42**,** 8049-8061.

HARADA, O., SUGA, T., SUZUKI, T., NAKAMOTO, K., KOBAYASHI, M., NOMIYAMA, T., NADANO, D., OHYAMA, C., FUKUDA, M. N. & NAKAYAMA, J. 2007. The role of trophinin, an adhesion molecule unique to human trophoblasts, in progression of colorectal cancer. *International journal of cancer,* 121**,** 1072-1078.

HARISCHANDRA, D. S., GHAISAS, S., ROKAD, D. & KANTHASAMY, A. G. 2017. Exosomes in toxicology: Relevance to chemical exposure and pathogenesis of environmentally linked diseases. *Toxicological Sciences,* 158**,** 3-13.

HASSAN, A. H., PROCHASSON, P., NEELY, K. E., GALASINSKI, S. C., CHANDY, M., CARROZZA, M. J. & WORKMAN, J. L. 2002. Function and selectivity of bromodomains in anchoring chromatin-modifying complexes to promoter nucleosomes. *Cell,* 111**,** 369-379.

HATCH, S. B., YAPP, C., MONTENEGRO, R. C., SAVITSKY, P., GAMBLE, V., TUMBER, A., RUDA, G. F., BAVETSIAS, V., FEDOROV, O. & ATRASH, B. 2017. Assessing histone demethylase inhibitors in cells: lessons learned. *Epigenetics & chromatin,* 10**,** 9.

HAYASHI, T., SENTANI, K., OUE, N., OHARA, S., TEISHIMA, J., ANAMI, K., SAKAMOTO, N., MATSUBARA, A. & YASUI, W. 2013. The search for secreted proteins in prostate cancer by the Escherichia coli ampicillin secretion trap: expression of NBL1 is highly restricted to the prostate and is related to cancer progression. *Pathobiology,* 80**,** 60-69.

HAYES, A., HUANG, W., YU, J., MAISONPIERRE, P., LIU, A., KERN, F., LIPPMAN, M. E., MCLESKEY, S. & LI, L. 2000. Expression and function of angiopoietin-1 in breast cancer. *British journal of cancer,* 83**,** 1154.

HAYWARD, D. & COLE, P. 2016. LSD1 histone demethylase assays and inhibition. *Methods in enzymology.* Elsevier.

HE, B., GAMPE JR, R. T., KOLE, A. J., HNAT, A. T., STANLEY, T. B., AN, G., STEWART, E. L., KALMAN, R. I., MINGES, J. T. & WILSON, E. M. 2004. Structural basis for androgen receptor interdomain and coactivator interactions suggests a transition in nuclear receptor activation function dominance. *Molecular cell,* 16**,** 425-438.

HE, B., KEMPPAINEN, J. A., VOEGEL, J. J., GRONEMEYER, H. & WILSON, E. M. 1999. Activation function 2 in the human androgen receptor ligand binding domain mediates interdomain communication with the NH2-terminal domain. *Journal of Biological Chemistry,* 274**,** 37219-37225.

HE, B., KEMPPAINEN, J. A. & WILSON, E. M. 2000. FXXLF and WXXLF sequences mediate the NH2-terminal interaction with the ligand binding domain of the androgen receptor. *Journal of Biological Chemistry,* 275**,** 22986-22994.

HE, W. W., SCIAVOLINO, P. J., WING, J., AUGUSTUS, M., HUDSON, P., MEISSNER, P. S., CURTIS, R. T., SHELL, B. K., BOSTWICK, D. G. & TINDALL, D. J. 1997. A novel human prostate-specific, androgen-regulated homeobox gene (NKX3. 1) that maps to 8p21, a region frequently deleted in prostate cancer. *Genomics,* 43**,** 69-77.

HECK, M. M., GSCHWEND, J. E. & RETZ, M. 2013. Enzalutamide (formerly MDV3100) prolongs survival in docetaxel-pretreated castration-resistant prostate cancer patients. *Translational andrology and urology,* 2**,** 92.

HEEMERS, H. V., DEBES, J. D. & TINDALL, D. J. 2008. The role of the transcriptional coactivator p300 in prostate cancer progression. *Hormonal Carcinogenesis V.* Springer.

HEEMERS, H. V., SCHMIDT, L. J., KIDD, E., RACLAW, K. A., REGAN, K. M. & TINDALL, D. J. 2010. Differential regulation of steroid nuclear receptor coregulator expression between normal and neoplastic prostate epithelial cells. *The Prostate,* 70**,** 959-970.

HEEMERS, H. V. & TINDALL, D. J. 2005. Androgen receptor coregulatory proteins as potential therapeutic targets in the treatment of prostate cancer. *Current cancer therapy reviews,* 1**,** 175-186.

HEERY, D. M., KALKHOVEN, E., HOARE, S. & PARKER, M. G. 1997. A signature motif in transcriptional co-activators mediates binding to nuclear receptors. *Nature,* 387**,** 733.

HEIDELBAUGH, J. 2016. Endocrinology Update: Testicular Hypogonadism. *FP essentials,* 451**,** 31-41.

HEIDENREICH, A., BASTIAN, P. J., BELLMUNT, J., BOLLA, M., JONIAU, S., VAN DER KWAST, T., MASON, M., MATVEEV, V., WIEGEL, T. & ZATTONI, F. 2014a. EAU guidelines on prostate cancer. Part II: treatment of advanced, relapsing, and castration-resistant prostate cancer. *European urology,* 65**,** 467-479.

HEIDENREICH, A., BASTIAN, P. J., BELLMUNT, J., BOLLA, M., JONIAU, S., VAN DER KWAST, T., MASON, M., MATVEEV, V., WIEGEL, T., ZATTONI, F., MOTTET, N. & EUROPEAN ASSOCIATION OF, U. 2014b. EAU guidelines on prostate cancer. part 1: screening, diagnosis, and local treatment with curative intent-update 2013. *Eur Urol,* 65**,** 124-37.

HEINLEIN, C. A. & CHANG, C. 2002. Androgen receptor (AR) coregulators: an overview. *Endocrine reviews,* 23**,** 175-200.

HEINLEIN, C. A. & CHANG, C. 2004. Androgen receptor in prostate cancer. *Endocrine reviews,* 25**,** 276-308.

HELPAP, B. & KÖLLERMANN, J. 1999. Undifferentiated carcinoma of the prostate with small cell features: immunohistochemical subtyping and reflections on histogenesis. *Virchows Archiv,* 434**,** 385-391.

HELPAP, B., KÖLLERMANN, J. & OEHLER, U. 1999. Neuroendocrine differentiation in prostatic carcinomas: histogenesis, biology, clinical relevance, and future therapeutical perspectives. *Urologia internationalis,* 62**,** 133-138.

HENDRIKSEN, P. J., DITS, N. F., KOKAME, K., VELDHOVEN, A., VAN WEERDEN, W. M., BANGMA, C. H., TRAPMAN, J. & JENSTER, G. 2006. Evolution of the androgen receptor pathway during progression of prostate cancer. *Cancer research,* 66**,** 5012-5020.

HENRIQUE, R. & JERÓNIMO, C. 2004. Molecular detection of prostate cancer: a role for GSTP1 hypermethylation. *European urology,* 46**,** 660-669.

HENSHALL, S. M., AFAR, D. E., HILLER, J., HORVATH, L. G., QUINN, D. I., RASIAH, K. K., GISH, K., WILLHITE, D., KENCH, J. G. & GARDINER-GARDEN, M. 2003. Survival analysis of genome-wide gene expression profiles of prostate cancers identifies new prognostic targets of disease relapse. *Cancer research,* 63**,** 4196-4203.

HENZLER, C., LI, Y., YANG, R., MCBRIDE, T., HO, Y., SPRENGER, C., LIU, G., COLEMAN, I., LAKELY, B. & LI, R. 2016. Truncation and constitutive activation of the androgen receptor by diverse genomic rearrangements in prostate cancer. *Nature communications,* 7**,** 13668.

HERMAN, J. G. & MEADOWS, G. G. 2007. Increased class 3 semaphorin expression modulates the invasive and adhesive properties of prostate cancer cells. *International journal of oncology,* 30**,** 1231-1238.

HERRSCHER, R. F., KAPLAN, M. H., LELSZ, D. L., DAS, C., SCHEUERMANN, R. & TUCKER, P. W. 1995. The immunoglobulin heavy-chain matrix-associating regions are bound by Bright: a B cell-specific trans-activator that describes a new DNA-binding protein family. *Genes & development,* 9**,** 3067-3082.

HESSVIK, N. P. & LLORENTE, A. 2018. Current knowledge on exosome biogenesis and release. *Cellular and Molecular Life Sciences,* 75**,** 193-208.

HIORT, O. 2013. Clinical and molecular aspects of androgen insensitivity. *Hormone Resistance and Hypersensitivity.* Karger Publishers.

HIROTA, T., LIPP, J. J., TOH, B.-H. & PETERS, J.-M. 2005. Histone H3 serine 10 phosphorylation by Aurora B causes HP1 dissociation from heterochromatin. *Nature,* 438**,** 1176.

HO, C. K. & HABIB, F. K. 2011. Estrogen and androgen signaling in the pathogenesis of BPH. *Nature Reviews Urology,* 8**,** 29.

HO, S.-R. & LIN, W.-C. 2018. RNF144A sustains EGFR signaling to promote EGF-dependent cell proliferation. *Journal of Biological Chemistry,* 293**,** 16307-16323.

HO, S.-R., MAHANIC, C. S., LEE, Y.-J. & LIN, W.-C. 2014. RNF144A, an E3 ubiquitin ligase for DNA-PKcs, promotes apoptosis during DNA damage. *Proceedings of the National Academy of Sciences,* 111**,** E2646-E2655.

HOADLEY, K. A., YAU, C., HINOUE, T., WOLF, D. M., LAZAR, A. J., DRILL, E., SHEN, R., TAYLOR, A. M., CHERNIACK, A. D. & THORSSON, V. 2018. Cell-of-origin patterns dominate the molecular classification of 10,000 tumors from 33 types of cancer. *Cell,* 173**,** 291-304. e6.

HOCKEL, M. & VAUPEL, P. 2001. Tumor hypoxia: definitions and current clinical, biologic, and molecular aspects. *Journal of the National Cancer Institute,* 93**,** 266-276.

HODGSON, M. C., SHEN, H. C., HOLLENBERG, A. N. & BALK, S. P. 2008. Structural basis for nuclear receptor corepressor recruitment by antagonist-liganded androgen receptor. *Molecular cancer therapeutics,* 7**,** 3187-3194.

HOFFMANN, I., ROATSCH, M., SCHMITT, M. L., CARLINO, L., PIPPEL, M., SIPPL, W. & JUNG, M. 2012. The role of histone demethylases in cancer therapy. *Molecular oncology,* 6**,** 683-703.

HOLLAND, A. M., ROBERTS, M. D., MUMFORD, P. W., MOBLEY, C. B., KEPHART, W. C., CONOVER, C. F., BEGGS, L. A., BALAEZ, A., OTZEL, D. M. & YARROW, J. F. 2016.

Testosterone inhibits expression of lipogenic genes in visceral fat by an estrogen-dependent mechanism. *Journal of Applied Physiology,* 121**,** 792-805.

HOLST, J. P., SOLDIN, O. P., GUO, T. & SOLDIN, S. J. 2004. Steroid hormones: relevance and measurement in the clinical laboratory. *Clinics in laboratory medicine,* 24**,** 105.

HORAK, P., CRAWFORD, A. R., VADYSIRISACK, D. D., NASH, Z. M., DEYOUNG, M. P., SGROI, D. & ELLISEN, L. W. 2010. Negative feedback control of HIF-1 through REDD1-regulated ROS suppresses tumorigenesis. *Proceedings of the National Academy of Sciences,* 107**,** 4675-4680.

HÖRNBERG, E., YLITALO, E. B., CRNALIC, S., ANTTI, H., STATTIN, P., WIDMARK, A., BERGH, A. & WIKSTRÖM, P. 2011. Expression of androgen receptor splice variants in prostate cancer bone metastases is associated with castration-resistance and short survival. *PloS one,* 6**,** e19059.

HORTON, J. R., ENGSTROM, A., ZOELLER, E. L., LIU, X., SHANKS, J. R., ZHANG, X., JOHNS, M. A., VERTINO, P. M., FU, H. & CHENG, X. 2016. Characterization of a linked Jumonji domain of the KDM5/JARID1 family of histone H3 lysine 4 demethylases. *Journal of Biological Chemistry,* 291**,** 2631-2646.

HORTON, J. R., UPADHYAY, A. K., QI, H. H., ZHANG, X., SHI, Y. & CHENG, X. 2010. Enzymatic and structural insights for substrate specificity of a family of jumonji histone lysine demethylases. *Nature structural & molecular biology,* 17**,** 38.

HOTCHKISS, R. D. 1948. The quantitative separation of purines, pyrimidines, and nucleosides by paper chromatography. *Journal of Biological Chemistry,* 175**,** 315-332.

HOU, H. & YU, H. 2010. Structural insights into histone lysine demethylation. *Current opinion in structural biology,* 20**,** 739-748.

HSIEH, C.-L., BOTTA, G., GAO, S., LI, T., VAN ALLEN, E. M., TREACY, D. J., CAI, C., HE, H. H., SWEENEY, C. J. & BROWN, M. 2015. PLZF, a tumor suppressor genetically lost in metastatic castration-resistant prostate cancer, is a mediator of resistance to androgen deprivation therapy. *Cancer research,* 75**,** 1944-1948.

HSING, A. W., GAO, Y.-T., WU, G., WANG, X., DENG, J., CHEN, Y.-L., SESTERHENN, I. A., MOSTOFI, F. K., BENICHOU, J. & CHANG, C. 2000. Polymorphic CAG and GGN repeat lengths in the androgen receptor gene and prostate cancer risk: a population-based case-control study in China. *Cancer research,* 60**,** 5111-5116.

HSU, C.-C. & HU, C.-D. 2013. Transcriptional activity of c-Jun is critical for the suppression of AR function. *Molecular and cellular endocrinology,* 372**,** 12-22.

HU, R., DENMEADE, S. R. & LUO, J. 2010. Molecular processes leading to aberrant androgen receptor signaling and castration resistance in prostate cancer. *Expert review of endocrinology & metabolism,* 5**,** 753-764.

HU, W. Y., XU, L., CHEN, B., OU, S., MUZZARELLI, K. M., HU, D. P., LI, Y., YANG, Z., VANDER GRIEND, D. J. & PRINS, G. S. 2019. Targeting prostate cancer cells with enzalutamide-HDAC inhibitor hybrid drug 2-75. *The Prostate*.

HU, Y., IPPOLITO, J. E., GARABEDIAN, E. M., HUMPHREY, P. A. & GORDON, J. I. 2002. Molecular characterization of a metastatic neuroendocrine cell cancer arising in the prostates of transgenic mice. *Journal of Biological Chemistry,* 277**,** 44462-44474.

HUANG, C.-K., TSAI, M.-Y., LUO, J., KANG, H.-Y., LEE, S. O. & CHANG, C. 2013. Suppression of androgen receptor enhances the self-renewal of mesenchymal stem cells through elevated expression of EGFR. *Biochimica et Biophysica Acta (BBA)-Molecular Cell Research,* 1833**,** 1222-1234.

HUANG, C., XIANG, Y., WANG, Y., LI, X., XU, L., ZHU, Z., ZHANG, T., ZHU, Q., ZHANG, K. & JING, N. 2010. Dual-specificity histone demethylase KIAA1718 (KDM7A) regulates neural differentiation through FGF4. *Cell research,* 20**,** 154.

HUANG, C. & ZHU, B. 2018. Roles of H3K36-specific histone methyltransferases in transcription: antagonizing silencing and safeguarding transcription fidelity. *Biophysics reports,* 4**,** 170-177.

HUANG, F. W., MOSQUERA, J. M., GAROFALO, A., OH, C., BACO, M., AMIN-MANSOUR, A., RABASHA, B., BAHL, S., MULLANE, S. A. & ROBINSON, B. D. 2017. Exome sequencing of African-American prostate cancer reveals loss-of-function ERF mutations. *Cancer discovery,* 7**,** 973-983.

HUANG, J., SENGUPTA, R., ESPEJO, A. B., LEE, M. G., DORSEY, J. A., RICHTER, M., OPRAVIL, S., SHIEKHATTAR, R., BEDFORD, M. T. & JENUWEIN, T. 2007. p53 is regulated by the lysine demethylase LSD1. *Nature,* 449**,** 105.

HUANG, J., ZHANG, H., WANG, X., DOBBS, K. B., YAO, J., QIN, G., WHITWORTH, K., WALTERS, E. M., PRATHER, R. S. & ZHAO, J. 2015. Impairment of preimplantation porcine embryo development by histone demethylase KDM5B knockdown through disturbance of bivalent H3K4me3-H3K27me3 modifications. *Biology of reproduction,* 92.

HUGGINS, C. & HODGES, C. V. 1972. Studies on prostatic cancer: I. The effect of castration, of estrogen and of androgen injection on serum phosphatases in metastatic carcinoma of the prostate. *CA: a cancer journal for clinicians,* 22**,** 232-240.

HUGGINS, C. & NEAL, W. 1942. Coagulation and liquefaction of semen: proteolytic enzymes and citrate in prostatic fluid. *Journal of Experimental Medicine,* 76**,** 527-541.

HUGGINS, C., SCOTT, W. W. & HODGES, C. V. 1941. Studies on prostatic cancer. III. The effects of fever, of desoxycorticosterone and of estrogen on clinical patients with metastatic carcinoma of the prostate. *The Journal of Urology,* 46**,** 997-1006.

HUGGINS, D. J., SHERMAN, W. & TIDOR, B. 2012. Rational approaches to improving selectivity in drug design. *Journal of medicinal chemistry,* 55**,** 1424-1444.

HUGHES, I. A., WERNER, R., BUNCH, T. & HIORT, O. Androgen insensitivity syndrome. Seminars in reproductive medicine, 2012. Thieme Medical Publishers, 432-442.

HUMPHREY, P. A. 2004. Gleason grading and prognostic factors in carcinoma of the prostate. *Modern pathology,* 17**,** 292.

HUMPHREY, P. A. 2012. Histological variants of prostatic carcinoma and their significance. *Histopathology,* 60**,** 59-74.

HUR, E., PFAFF, S. J., PAYNE, E. S., GRØN, H., BUEHRER, B. M. & FLETTERICK, R. J. 2004. Recognition and accommodation at the androgen receptor coactivator binding interface. *PLoS biology,* 2**,** e274.

HYUN, K., JEON, J., PARK, K. & KIM, J. 2017. Writing, erasing and reading histone lysine methylations. *Experimental & molecular medicine,* 49**,** e324.

IGARASHI, S., TANNO, Y., ONODERA, O., YAMAZAKI, M., SATO, S., ISHIKAWA, A., MIYATANI, N., NAGASHIMA, M., ISHIKAWA, Y. & SAHASHI, K. 1992. Strong correlation between the number of CAG repeats in androgen receptor genes and the clinical onset of features of spinal and bulbar muscular atrophy. *Neurology,* 42**,** 2300-2300.

IIZUKA, M. & SMITH, M. M. 2003. Functional consequences of histone modifications. *Current opinion in genetics & development,* 13**,** 154-160.

IKEDA, Y., AIHARA, K.-I., SATO, T., AKAIKE, M., YOSHIZUMI, M., SUZAKI, Y., IZAWA, Y., FUJIMURA, M., HASHIZUME, S. & KATO, M. 2005. Androgen receptor gene knockout male mice exhibit impaired cardiac growth and exacerbation of angiotensin II-induced cardiac fibrosis. *Journal of Biological Chemistry,* 280**,** 29661-29666.

ILIC, D., DJULBEGOVIC, M., JUNG, J. H., HWANG, E. C., ZHOU, Q., CLEVES, A., AGORITSAS, T. & DAHM, P. 2018a. Prostate cancer screening with prostate-specific antigen (PSA) test: a systematic review and meta-analysis. *bmj,* 362**,** k3519.

ILIC, D., EVANS, S. M., ALLAN, C. A., JUNG, J. H., MURPHY, D. & FRYDENBERG, M. 2018b. Laparoscopic and robot-assisted vs open radical prostatectomy for the treatment

of localized prostate cancer: a Cochrane systematic review. *BJU international,* 121**,** 845-853.

IMASAKI, K., HASEGAWA, T., OKABE, T., SAKAI, Y., HAJI, M., TAKAYANAGI, R. & NAWATA, H. 1994. Single amino acid substitution (840Arg→ His) in the hormone-binding domain of the androgen receptor leads to incomplete androgen insensitivity syndrome associated with a thermolabile androgen receptor. *European journal of endocrinology,* 130**,** 569-574.

IRVINE, R. F. 2003. Nuclear lipid signalling. *Nature Reviews Molecular Cell Biology,* 4**,** 349.

ISBARN, H., BOCCON-GIBOD, L., CARROLL, P. R., MONTORSI, F., SCHULMAN, C., SMITH, M. R., STERNBERG, C. N. & STUDER, U. E. 2009. Androgen deprivation therapy for the treatment of prostate cancer: consider both benefits and risks. *European urology,* 55**,** 62-75.

ISMAIL, T., LEE, H.-K., KIM, C., KWON, T., PARK, T. J. & LEE, H.-S. 2018. KDM1A microenvironment, its oncogenic potential, and therapeutic significance. *Epigenetics & chromatin,* 11**,** 33.

IVERSEN, P., TYRRELL, C. J., KAISARY, A. V., ANDERSON, J. B., VAN POPPEL, H., TAMMELA, T. L., CHAMBERLAIN, M., CARROLL, K. & MELEZINEK, I. 2000. Bicalutamide monotherapy compared with castration in patients with nonmetastatic locally advanced prostate cancer: 6.3 years of followup. *The Journal of urology,* 164**,** 1579-1582.

IWASE, S., LAN, F., BAYLISS, P., DE LA TORRE-UBIETA, L., HUARTE, M., QI, H. H., WHETSTINE, J. R., BONNI, A., ROBERTS, T. M. & SHI, Y. 2007. The X-linked mental retardation gene SMCX/JARID1C defines a family of histone H3 lysine 4 demethylases. *Cell,* 128**,** 1077-1088.

IYER, L. M., KOONIN, E. V. & ARAVIND, L. 2002. Extensive domain shuffling in transcription regulators of DNA viruses and implications for the origin of fungal APSES transcription factors. *Genome biology,* 3**,** research0012. 1.

JÄÄSKELÄINEN, J. 2012. Molecular biology of androgen insensitivity. *Molecular and cellular endocrinology,* 352**,** 4-12.

JAIN, A., LIU, R., XIANG, Y. K. & HA, T. 2012. Single-molecule pull-down for studying protein interactions. *Nature protocols,* 7**,** 445.

JAMESON, J. L. & LONGO, D. L. 2015. Precision medicine—personalized, problematic, and promising. *Obstetrical & gynecological survey,* 70**,** 612-614.

JANKNEGT, R., ABBOU, C., BARTOLETTI, R., BERNSTEIN-HAHN, L., BRACKEN, B., BRISSET, J., DA SILVA, F. C., CHISHOLM, G., CRAWFORD, E. & DEBRUYNE, F. 1993. Orchiectomy and nilutamide or placebo as treatment of metastatic prostatic cancer in a multinational double-blind randomized trial. *The Journal of urology,* 149**,** 77-82.

JASON, S. & CUI, W. 2016. Proliferation, survival and metabolism: the role of PI3K/AKT/mTOR signalling in pluripotency and cell fate determination. *Development,* 143**,** 3050-3060.

JEMAL, A., CENTER, M. M., DESANTIS, C. & WARD, E. M. 2010. Global patterns of cancer incidence and mortality rates and trends. *Cancer Epidemiology and Prevention Biomarkers,* 19**,** 1893-1907.

JEMAL, A., SIEGEL, R., WARD, E., MURRAY, T., XU, J., SMIGAL, C. & THUN, M. J. 2006a. Cancer statistics, 2006. *CA Cancer J Clin,* 56**,** 106-30.

JEMAL, A., SIEGEL, R., WARD, E., MURRAY, T., XU, J., SMIGAL, C. & THUN, M. J. 2006b. Cancer statistics, 2006. *CA: a cancer journal for clinicians,* 56**,** 106-130.

JENSTER, G., VAN DER KORPUT, H. A., VAN VROONHOVEN, C., VAN DER KWAST, T. H., TRAPMAN, J. & BRINKMANN, A. O. 1991. Domains of the human androgen receptor involved in steroid binding, transcriptional activation, and subcellular localization. *Molecular endocrinology,* 5**,** 1396-1404.

JENUWEIN, T. & ALLIS, C. D. 2001. Translating the histone code. *Science,* 293**,** 1074-1080.

JETER, C. R., BADEAUX, M., CHOY, G., CHANDRA, D., PATRAWALA, L., LIU, C., CALHOUN-DAVIS, T., ZAEHRES, H., DALEY, G. Q. & TANG, D. G. 2009. Functional evidence that the self-renewal gene NANOG regulates human tumor development. *Stem cells,* 27**,** 993-1005.

JETER, C. R., LIU, B., LIU, X., CHEN, X., LIU, C., CALHOUN-DAVIS, T., REPASS, J., ZAEHRES, H., SHEN, J. & TANG, D. G. 2011. NANOG promotes cancer stem cell characteristics and prostate cancer resistance to androgen deprivation. *Oncogene,* 30**,** 3833.

JI, R., SANCHEZ, C., CHOU, C., CHEN, X., WOODWARD, D. & REGAN, J. W. 2012. Prostanoid EP1 receptors mediate up-regulation of the orphan nuclear receptor Nurr1 by cAMP-independent activation of protein kinase A, CREB and NF-κB. *British journal of pharmacology,* 166**,** 1033-1046.

JIANG, T., ZHOU, X., TAGHIZADEH, K., DONG, M. & DEDON, P. C. 2007. N-formylation of lysine in histone proteins as a secondary modification arising from oxidative DNA damage. *Proceedings of the National Academy of Sciences,* 104**,** 60-65.

JIN, H.-J., ZHAO, J. C., OGDEN, I., BERGAN, R. C. & YU, J. 2013. Androgen receptor-independent function of FoxA1 in prostate cancer metastasis. *Cancer research,* 73**,** 3725-3736.

JIN, L., GARCIA, J., CHAN, E., DE LA CRUZ, C., SEGAL, E., MERCHANT, M., KHARBANDA, S., RAISNER, R., HAVERTY, P. M. & MODRUSAN, Z. 2017. Therapeutic targeting of the CBP/p300 bromodomain blocks the growth of castration-resistant prostate cancer. *Cancer research,* 77**,** 5564-5575.

JOHN, J. S., POWELL, K., CONLEY-LACOMB, M. K. & CHINNI, S. R. 2012. TMPRSS2-ERG fusion gene expression in prostate tumor cells and its clinical and biological significance in prostate cancer progression. *Journal of cancer science & therapy,* 4**,** 94.

JONES, G. G., DEL RÍO, I. B., SARI, S., SEKERIM, A., YOUNG, L. C., HARTIG, N., ZUBIAUR, I. A., EL-BAHRAWY, M. A., HYNDS, R. E. & LEI, W. 2019. SHOC2 phosphatase-dependent RAF dimerization mediates resistance to MEK inhibition in RAS-mutant cancers. *Nature communications,* 10**,** 2532.

JONES, P. A. 2012. Functions of DNA methylation: islands, start sites, gene bodies and beyond. *Nature Reviews Genetics,* 13**,** 484.

JOSEPH, J. S., MALINDISA, S. T. & NTWASA, M. 2018. Two-dimensional (2D) and three-dimensional (3D) cell culturing in drug discovery. *Cell Culture,* 2**,** 1-22.

JOSSO, N., REY, R. A. & PICARD, J.-Y. 2013. Anti-Müllerian hormone: a valuable addition to the toolbox of the pediatric endocrinologist. *International journal of endocrinology,* 2013.

JURMEISTER, S., RAMOS-MONTOYA, A., NEAL, D. E. & FRYER, L. G. 2014. Transcriptomic analysis reveals inhibition of androgen receptor activity by AMPK in prostate cancer cells. *Oncotarget,* 5**,** 3785.

JUSTUS, C. R., LEFFLER, N., RUIZ-ECHEVARRIA, M. & YANG, L. V. 2014. In vitro cell migration and invasion assays. *JoVE (Journal of Visualized Experiments)***,** e51046.

KAHL, P., GULLOTTI, L., HEUKAMP, L. C., WOLF, S., FRIEDRICHS, N., VORREUTHER, R., SOLLEDER, G., BASTIAN, P. J., ELLINGER, J. & METZGER, E. 2006. Androgen receptor coactivators lysine-specific histone demethylase 1 and four and a half LIM domain protein 2 predict risk of prostate cancer recurrence. *Cancer research,* 66**,** 11341-11347.

KAIGHN, M., NARAYAN, K. S., OHNUKI, Y., LECHNER, J. F. & JONES, L. 1979. Establishment and characterization of a human prostatic carcinoma cell line (PC-3). *Investigative urology,* 17**,** 16-23.

KAMAKAKA, R. T. 2003. Heterochromatin: proteins in flux lead to stable repression. *Current Biology,* 13**,** R317-R319.

KAMAKAKA, R. T. & BIGGINS, S. 2005. Histone variants: deviants? *Genes & development,* 19**,** 295-316.

KANEHISA, M. 2019. Toward understanding the origin and evolution of cellular organisms. *Protein Science,* 28**,** 1947-1951.

KANEHISA, M. & GOTO, S. 2000. KEGG: kyoto encyclopedia of genes and genomes. *Nucleic acids research,* 28**,** 27-30.

KANEHISA, M., SATO, Y., FURUMICHI, M., MORISHIMA, K. & TANABE, M. 2019. New approach for understanding genome variations in KEGG. *Nucleic acids research,* 47**,** D590-D595.

KANO, Y., KONNO, M., OHTA, K., HARAGUCHI, N., NISHIKAWA, S., KAGAWA, Y., HAMABE, A., HASEGAWA, S., OGAWA, H. & FUKUSUMI, T. 2013. Jumonji/Arid1b (Jarid1b) protein modulates human esophageal cancer cell growth. *Molecular and clinical oncology,* 1**,** 753-757.

KAPAŁCZYŃSKA, M., KOLENDA, T., PRZYBYŁA, W., ZAJĄCZKOWSKA, M., TERESIAK, A., FILAS, V., IBBS, M., BLIŹNIAK, R., ŁUCZEWSKI, Ł. & LAMPERSKA, K. 2018. 2D and 3D cell cultures–a comparison of different types of cancer cell cultures. *Archives of medical science: AMS,* 14**,** 910.

KARNES, R. J., BERGSTRALH, E. J., DAVICIONI, E., GHADESSI, M., BUERKI, C., MITRA, A. P., CRISAN, A., ERHO, N., VERGARA, I. A. & LAM, L. L. 2013. Validation of a genomic classifier that predicts metastasis following radical prostatectomy in an at risk patient population. *The Journal of urology,* 190**,** 2047-2053.

KARYTINOS, A., FORNERIS, F., PROFUMO, A., CIOSSANI, G., BATTAGLIOLI, E., BINDA, C. & MATTEVI, A. 2009. A novel mammalian flavin-dependent histone demethylase. *Journal of Biological Chemistry,* 284**,** 17775-17782.

KASHYAP, V., AHMAD, S., NILSSON, E. M., HELCZYNSKI, L., KENNA, S., PERSSON, J. L., GUDAS, L. J. & MONGAN, N. P. 2013. The lysine specific demethylase-1 (LSD1/KDM1A) regulates VEGF-A expression in prostate cancer. *Molecular oncology,* 7**,** 555-566.

KAWAMURA, A., MÜNZEL, M., KOJIMA, T., YAPP, C., BHUSHAN, B., GOTO, Y., TUMBER, A., KATOH, T., KING, O. N. & PASSIOURA, T. 2017. Highly selective inhibition of histone demethylases by de novo macrocyclic peptides. *Nature communications,* 8**,** 14773.

KAWANO, H., SATO, T., YAMADA, T., MATSUMOTO, T., SEKINE, K., WATANABE, T., NAKAMURA, T., FUKUDA, T., YOSHIMURA, K. & YOSHIZAWA, T. 2003. Suppressive function of androgen receptor in bone resorption. *Proceedings of the National Academy of Sciences,* 100**,** 9416-9421.

KE, X.-S., QU, Y., ROSTAD, K., LI, W.-C., LIN, B., HALVORSEN, O. J., HAUKAAS, S. A., JONASSEN, I., PETERSEN, K. & GOLDFINGER, N. 2009. Genome-wide profiling of histone h3 lysine 4 and lysine 27 trimethylation reveals an epigenetic signature in prostate carcinogenesis. *PloS one,* 4**,** e4687.

KEBEDE, A. F., SCHNEIDER, R. & DAUJAT, S. 2015. Novel types and sites of histone modifications emerge as players in the transcriptional regulation contest. *The FEBS journal,* 282**,** 1658-1674.

KELLER, E. T., ERSHLER, W. B. & CHANG, C. 1996. The androgen receptor: a mediator of diverse responses. *Front Biosci,* 1**,** d59-71.

KELLY, R. S., SINNOTT, J. A., RIDER, J. R., EBOT, E. M., GERKE, T., BOWDEN, M., PETTERSSON, A., LODA, M., SESSO, H. D. & KANTOFF, P. W. 2016. The role of tumor metabolism as a driver of prostate cancer progression and lethal disease: results from a nested case-control study. *Cancer & metabolism,* 4**,** 22.

KETSCHER, A., JILG, C., WILLMANN, D., HUMMEL, B., IMHOF, A., RÜSSELER, V., HÖLZ, S., METZGER, E., MÜLLER, J. & SCHÜLE, R. 2014. LSD1 controls metastasis of androgen-independent prostate cancer cells through PXN and LPAR6. *Oncogenesis,* 3**,** e120.

KHANI, F., MOSQUERA, J. M., PARK, K., BLATTNER, M., O'REILLY, C., MACDONALD, T. Y., CHEN, Z., SRIVASTAVA, A., TEWARI, A. K. & BARBIERI, C. E. 2014. Evidence for

molecular differences in prostate cancer between African American and Caucasian men. *Clinical Cancer Research,* 20**,** 4925-4934.

KIKUGAWA, T., KINUGASA, Y., SHIRAISHI, K., NANBA, D., NAKASHIRO, K. I., TANJI, N., YOKOYAMA, M. & HIGASHIYAMA, S. 2006. PLZF regulates Pbx1 transcription and Pbx1–HoxC8 complex leads to androgen-independent prostate cancer proliferation. *The Prostate,* 66**,** 1092-1099.

KIM, E. H., LARSON, J. A. & ANDRIOLE, G. L. 2016. Management of benign prostatic hyperplasia. *Annual Review of Medicine,* 67**,** 137-151.

KIM, J. B. Three-dimensional tissue culture models in cancer biology. Seminars in cancer biology, 2005. Elsevier, 365-377.

KIM, M. J., BHATIA-GAUR, R., BANACH-PETROSKY, W. A., DESAI, N., WANG, Y., HAYWARD, S. W., CUNHA, G. R., CARDIFF, R. D., SHEN, M. M. & ABATE-SHEN, C. 2002. Nkx3. 1 mutant mice recapitulate early stages of prostate carcinogenesis. *Cancer research,* 62**,** 2999-3004.

KIM, S. W., YANG, H. G., KANG, M. C., LEE, S., NAMKOONG, H., LEE, S.-W. & SUNG, Y. C. 2014. KIAA1114, a full-length protein encoded by the trophinin gene, is a novel surface marker for isolating tumor-initiating cells of multiple hepatocellular carcinoma subtypes. *Oncotarget,* 5**,** 1226.

KIMURA, H. 2013. Histone modifications for human epigenome analysis. *Journal of human genetics,* 58**,** 439.

KIVINUMMI, K., URBANUCCI, A., LEINONEN, K., TAMMELA, T. L., ANNALA, M., ISAACS, W. B., BOVA, G. S., NYKTER, M. & VISAKORPI, T. 2017. The expression of AURKA is androgen regulated in castration-resistant prostate cancer. *Scientific reports,* 7**,** 17978.

KLEIN, B. J., PIAO, L., XI, Y., RINCON-ARANO, H., ROTHBART, S. B., PENG, D., WEN, H., LARSON, C., ZHANG, X. & ZHENG, X. 2014. The histone-H3K4-specific demethylase KDM5B binds to its substrate and product through distinct PHD fingers. *Cell reports,* 6**,** 325-335.

KLEIN, S., ROMIJN, J., REED, P., KRONENBERG, H., MELMED, S. & POLONSKY, K. 2011. Williams textbook of endocrinology. Elsevier Saunders.

KLOSE, R. J., KALLIN, E. M. & ZHANG, Y. 2006. JmjC-domain-containing proteins and histone demethylation. *Nature reviews genetics,* 7**,** 715.

KLOTZ, L. 2010. Active surveillance for prostate cancer: a review. *Current urology reports,* 11**,** 165-171.

KOHLI, R. M. & ZHANG, Y. 2013. TET enzymes, TDG and the dynamics of DNA demethylation. *Nature,* 502**,** 472.

KOLESINSKA, Z., AHMED, S. F., NIEDZIELA, M., BRYCE, J., MOLINSKA-GLURA, M., RODIE, M., JIANG, J., SINNOTT, R. O., HUGHES, I. A. & DARENDELILER, F. 2014. Changes over time in sex assignment for disorders of sex development. *Pediatrics,* 134**,** e710-e715.

KONDO, A., NONAKA, A., SHIMAMURA, T., YAMAMOTO, S., YOSHIDA, T., KODAMA, T., ABURATANI, H. & OSAWA, T. 2017. Long noncoding RNA JHDM1D-AS1 promotes tumor growth by regulating angiogenesis in response to nutrient starvation. *Molecular and cellular biology,* 37**,** e00125-17.

KONISHI, T., SHIOZAKI, A., KOSUGA, T., KUDOU, M., SHODA, K., ARITA, T., KONISHI, H., KOMATSU, S., KUBOTA, T. & FUJIWARA, H. 2019. LRRC8A Expression Influences Growth of Esophageal Squamous Cell Carcinoma. *The American journal of pathology*.

KORKMAZ, K. S., KORKMAZ, C. G., RAGNHILDSTVEIT, E., KIZILDAG, S., PRETLOW, T. G. & SAATCIOGLU, F. 2000. Full-length cDNA sequence and genomic organization of human NKX3A—alternative forms and regulation by both androgens and estrogens. *Gene,* 260**,** 25-36.

KORNBERG, R. D. 1974. Chromatin structure: a repeating unit of histones and DNA. *Science,* 184**,** 868-871.

KORPAL, M., KORN, J. M., GAO, X., RAKIEC, D. P., RUDDY, D. A., DOSHI, S., YUAN, J., KOVATS, S. G., KIM, S. & COOKE, V. G. 2013. An F876L mutation in androgen receptor confers genetic and phenotypic resistance to MDV3100 (enzalutamide). *Cancer discovery,* 3**,** 1030-1043.

KOULIBALY, M., KABBA, I. S., CISSÉ, A., DIALLO, S. B., DIALLO, M. B., KEITA, N., CAMARA, N. D., DIALLO, M. S., SYLLA, B. S. & PARKIN, D. 1997. Cancer incidence in Conakry, Guinea: first results from the Cancer Registry 1992–1995. *International Journal of Cancer,* 70**,** 39-45.

KOUZARIDES, T. 2007. Chromatin modifications and their function. *Cell,* 128**,** 693-705.

KOVACS, M. & SCHALLY, A. V. 2001. Comparison of mechanisms of action of luteinizing hormone-releasing hormone (LHRH) antagonist cetrorelix and LHRH agonist triptorelin on the gene expression of pituitary LHRH receptors in rats. *Proceedings of the National Academy of Sciences,* 98**,** 12197-12202.

KRAUSCH, M., RAFFEL, A., ANLAUF, M., SCHOTT, M., WILLENBERG, H., LEHWALD, N., HAFNER, D., CUPISTI, K., EISENBERGER, C. & KNOEFEL, W. 2011. Loss of PTEN expression in neuroendocrine pancreatic tumors. *Hormone and metabolic research,* 43**,** 865-871.

KUIPER, G., DE RUITER, P., TRAPMAN, J., BOERSMA, W., GROOTEGOED, J. & BRINKMANN, A. 1993. Localization and hormonal stimulation of phosphorylation sites in the LNCaP-cell androgen receptor. *Biochemical Journal,* 291**,** 95-101.

KUMAR, S., CHENG, X., KLIMASAUSKAS, S., MI, S., POSFAI, J., ROBERTS, R. J. & WILSON, G. G. 1994. The DNA (cytosine-5) methyltransferases. *Nucleic acids research,* 22**,** 1.

KUMARI, S., SENAPATI, D. & HEEMERS, H. V. 2017. Rationale for the development of alternative forms of androgen deprivation therapy. *Endocrine-related cancer,* 24**,** R275-R295.

LABBÉ, R. M., HOLOWATYJ, A. & YANG, Z.-Q. 2014. Histone lysine demethylase (KDM) subfamily 4: structures, functions and therapeutic potential. *American journal of translational research,* 6**,** 1.

LABRIE, F., BELANGER, A., DUPONT, A., SIMARD, J. & LABRIE, C. 1993. Science behind total androgen blockade: from gene to combination therapy. *Clinical and investigative medicine. Medecine clinique et experimentale,* 16**,** 475-492.

LABRIE, F., DUPONT, A., BELANGER, A., GIGUERE, M., LACOURSIERE, Y., EMOND, J., MONFETTE, G. & BERGERON, V. 1985. Combination therapy with flutamide and castration (LHRH agonist or orchiectomy) in advanced prostate cancer: a marked improvement in response and survival. *Journal of steroid biochemistry,* 23**,** 833-841.

LACHNER, M., O'CARROLL, D., REA, S., MECHTLER, K. & JENUWEIN, T. 2001. Methylation of histone H3 lysine 9 creates a binding site for HP1 proteins. *Nature,* 410**,** 116.

LAGARDE, W. H., BLACKWELDER, A. J., MINGES, J. T., HNAT, A. T., FRENCH, F. S. & WILSON, E. M. 2012. Androgen receptor exon 1 mutation causes androgen insensitivity by creating phosphorylation site and inhibiting melanoma antigen-A11 activation of NH2-and carboxyl-terminal interaction-dependent transactivation. *Journal of Biological Chemistry,* 287**,** 10905-10915.

LAI, J.-J., LAI, K.-P., ZENG, W., CHUANG, K.-H., ALTUWAIJRI, S. & CHANG, C. 2012. Androgen receptor influences on body defense system via modulation of innate and adaptive immune systems: lessons from conditional AR knockout mice. *The American journal of pathology,* 181**,** 1504-1512.

LAITY, J. H., LEE, B. M. & WRIGHT, P. E. 2001. Zinc finger proteins: new insights into structural and functional diversity. *Current opinion in structural biology,* 11**,** 39-46.

LALA, D. S. & HEYMAN, R. A. 2000. Orphan nuclear receptors. *Principles of Molecular Regulation.* Springer.

LALLOUS, N., DALAL, K., CHERKASOV, A. & RENNIE, P. 2013. Targeting alternative sites on the androgen receptor to treat castration-resistant prostate cancer. *International journal of molecular sciences,* 14**,** 12496-12519.

LAMONT, K. R. & TINDALL, D. J. 2011. Minireview: Alternative activation pathways for the androgen receptor in prostate cancer. *Molecular Endocrinology,* 25**,** 897-907.

LAPOINTE, J., LI, C., HIGGINS, J. P., VAN DE RIJN, M., BAIR, E., MONTGOMERY, K., FERRARI, M., EGEVAD, L., RAYFORD, W. & BERGERHEIM, U. 2004. Gene expression profiling identifies clinically relevant subtypes of prostate cancer. *Proceedings of the National Academy of Sciences,* 101**,** 811-816.

LAU, P. N. I. & CHEUNG, P. 2011. Histone code pathway involving H3 S28 phosphorylation and K27 acetylation activates transcription and antagonizes polycomb silencing. *Proceedings of the National Academy of Sciences,* 108**,** 2801-2806.

LAURENT, B. & SHI, Y. 2016. Expression, purification, and biochemical analysis of the LSD1/KDM1A histone demethylase. *Methods in enzymology.* Elsevier.

LECOUVET, F. E., GEUKENS, D., STAINIER, A., JAMAR, F., JAMART, J., D'OTHÉE, B. J., THERASSE, P., BERG, B. V. & TOMBAL, B. 2007. Magnetic resonance imaging of the axial skeleton for detecting bone metastases in patients with high-risk prostate cancer: diagnostic and cost-effectiveness and comparison with current detection strategies. *Journal of Clinical Oncology,* 25**,** 3281-3287.

LEE, A. C.-L., HARRIS, J. L., KHANNA, K. K. & HONG, J.-H. 2019. A comprehensive review on current advances in peptide drug development and design. *International journal of molecular sciences,* 20**,** 2383.

LEE, K., PARK, J.-W., SUNG, H., CHOI, Y., KIM, W. H., LEE, H., CHUNG, H., SHIN, H., CHO, C.-H. & KIM, T. 2015. PHF2 histone demethylase acts as a tumor suppressor in association with p53 in cancer. *Oncogene,* 34**,** 2897.

LEE, K. H., HONG, S., KANG, M., JEONG, C. W., KU, J. H., KIM, H. H. & KWAK, C. 2018. Histone demethylase KDM7A controls androgen receptor activity and tumor growth in prostate cancer. *International journal of cancer,* 143**,** 2849-2861.

LEE, M. G., WYNDER, C., COOCH, N. & SHIEKHATTAR, R. 2005. An essential role for CoREST in nucleosomal histone 3 lysine 4 demethylation. *Nature,* 437**,** 432.

LEE, Y.-F., SHYR, C.-R., THIN, T. H., LIN, W.-J. & CHANG, C. 1999. Convergence of two repressors through heterodimer formation of androgen receptor and testicular orphan receptor-4: a unique signaling pathway in the steroid receptor superfamily. *Proceedings of the National Academy of Sciences,* 96**,** 14724-14729.

LI, H., ILIN, S., WANG, W., DUNCAN, E. M., WYSOCKA, J., ALLIS, C. D. & PATEL, D. J. 2006. Molecular basis for site-specific read-out of histone H3K4me3 by the BPTF PHD finger of NURF. *Nature,* 442**,** 91.

LI, J., WAN, X., QIANG, W., LI, T., HUANG, W., HUANG, S., WU, D. & LI, Y. 2015a. MiR-29a suppresses prostate cell proliferation and induces apoptosis via KDM5B protein regulation. *International journal of clinical and experimental medicine,* 8**,** 5329.

LI, K., CHEN, M., LI, L., LU, M., SHAO, C., SU, Z., HE, D., PANG, J. & GAO, X. 2013. The predictive value of semaphorins 3 expression in biopsies for biochemical recurrence of patients with low-and intermediate-risk prostate cancer. *Neoplasma,* 60**,** 683-689.

LI, M., MIWA, S., KOBAYASHI, Y., MERRY, D. E., YAMAMOTO, M., TANAKA, F., DOYU, M., HASHIZUM, Y., FISCHBECK, K. H. & SOBUE, G. 1998. Nuclear inclusions of the androgen receptor protein in spinal and bulbar muscular atrophy. *Annals of Neurology: Official Journal of the American Neurological Association and the Child Neurology Society,* 44**,** 249-254.

LI, Q., SHI, L., GUI, B., YU, W., WANG, J., ZHANG, D., HAN, X., YAO, Z. & SHANG, Y. 2011. Binding of the JmjC demethylase JARID1B to LSD1/NuRD suppresses angiogenesis and metastasis in breast cancer cells by repressing chemokine CCL14. *Cancer research,* 71**,** 6899-6908.

LI, W., CAVASOTTO, C. N., CARDOZO, T., HA, S., DANG, T., TANEJA, S. S., LOGAN, S. K. & GARABEDIAN, M. J. 2005. Androgen receptor mutations identified in prostate cancer and androgen insensitivity syndrome display aberrant ART-27 coactivator function. *Molecular Endocrinology,* 19**,** 2273-2282.

LI, Y. F., JI, H. H., ZHANG, Z. L., ZHANG, T. T., GAN, W. & ZHANG, S. F. 2017. Targeting MRP4 expression by anti-androgen treatment reverses MRP4-mediated docetaxel resistance in castration-resistant prostate cancer. *Oncology letters,* 14**,** 1748-1756.

LI, Z., SUN, Y., CHEN, X., SQUIRES, J., NOWROOZIZADEH, B., LIANG, C. & HUANG, J. 2015b. p53 mutation directs AURKA overexpression via miR-25 and FBXW7 in prostatic small cell neuroendocrine carcinoma. *Molecular Cancer Research,* 13**,** 584-591.

LIAO, S., LIANG, T., FANG, S., CASTAÑEDA, E. & SHAO, T.-C. 1973. Steroid structure and androgenic activity specificities involved in the receptor binding and nuclear retention of various androgens. *Journal of Biological Chemistry,* 248**,** 6154-6162.

LIAO, Y., SMYTH, G. K. & SHI, W. 2013. featureCounts: an efficient general purpose program for assigning sequence reads to genomic features. *Bioinformatics,* 30**,** 923-930.

LIAO, Y. & XU, K. 2019. Epigenetic regulation of prostate cancer: the theories and the clinical implications. *Asian journal of andrology,* 21**,** 279.

LICHTENSTEIN, P., HOLM, N. V., VERKASALO, P. K., ILIADOU, A., KAPRIO, J., KOSKENVUO, M., PUKKALA, E., SKYTTHE, A. & HEMMINKI, K. 2000. Environmental and heritable factors in the causation of cancer—analyses of cohorts of twins from Sweden, Denmark, and Finland. *New England journal of medicine,* 343**,** 78-85.

LIEBERHERR, M. & GROSSE, B. 1994. Androgens increase intracellular calcium concentration and inositol 1, 4, 5-trisphosphate and diacylglycerol formation via a pertussis toxin-sensitive G-protein. *Journal of Biological Chemistry,* 269**,** 7217-7223.

LIM, H. N., HAWKINS, J. R. & HUGHES, I. A. 2001. Genetic evidence to exclude the androgen receptor co-factor, ARA70 (NCOA4) as a candidate gene for the causation of undermasculinised genitalia. *Clinical genetics,* 59**,** 284-286.

LIN, H., WANG, Y., WANG, Y., TIAN, F., PU, P., YU, Y., MAO, H., YANG, Y., WANG, P. & HU, L. 2010. Coordinated regulation of active and repressive histone methylations by a dual-specificity histone demethylase ceKDM7A from Caenorhabditis elegans. *Cell research,* 20**,** 899.

LIN, J. H., WALTER, P. & YEN, T. B. 2008a. Endoplasmic reticulum stress in disease pathogenesis. *Annu. Rev. pathmechdis. Mech. Dis.,* 3**,** 399-425.

LIN, K., LIPSITZ, R., MILLER, T. & JANAKIRAMAN, S. 2008b. Benefits and harms of prostate-specific antigen screening for prostate cancer: an evidence update for the US Preventive Services Task Force. *Annals of internal medicine,* 149**,** 192-199.

LIU, C., LOU, W., ZHU, Y., NADIMINTY, N., SCHWARTZ, C. T., EVANS, C. P. & GAO, A. C. 2014. Niclosamide inhibits androgen receptor variants expression and overcomes enzalutamide resistance in castration-resistant prostate cancer. *Clinical cancer research,* 20**,** 3198-3210.

LIU, J., LICHTENBERG, T., HOADLEY, K. A., POISSON, L. M., LAZAR, A. J., CHERNIACK, A. D., KOVATICH, A. J., BENZ, C. C., LEVINE, D. A. & LEE, A. V. 2018. An integrated TCGA pan-cancer clinical data resource to drive high-quality survival outcome analytics. *Cell,* 173**,** 400-416. e11.

LIU, L., ZHAO, Y., WANG, Y., LI, Q., WANG, Z., WANG, L. & QIAO, Z. 2005. Testosterone Induced Ca 2 Influx in Bone Marrow-Derived Macrophages via Surface Binding Sites. *Methods Find Exp Clin Pharmacol,* 27**,** 623-628.

LIU, Y., BEYER, A. & AEBERSOLD, R. 2016. On the dependency of cellular protein levels on mRNA abundance. *Cell,* 165**,** 535-550.

LIU, Y., WANG, Y., CHEN, C., ZHANG, J., QIAN, W., DONG, Y., LIU, Z., ZHANG, X., WANG, X. & ZHANG, Z. 2017. LSD1 binds to HPV16 E7 and promotes the epithelial-mesenchymal transition in cervical cancer by demethylating histones at the Vimentin promoter. *Oncotarget,* 8**,** 11329.

LIU, Y., XU, X., LIN, P., HE, Y., ZHANG, Y., CAO, B., ZHANG, Z., SETHI, G., LIU, J. & ZHOU, X. 2019. Inhibition of the deubiquitinase USP9x induces pre-B cell homeobox 1 (PBX1) degradation and thereby stimulates prostate cancer cell apoptosis. *Journal of Biological Chemistry,* 294**,** 4572-4582.

LO, W.-S., TRIEVEL, R. C., ROJAS, J. R., DUGGAN, L., HSU, J.-Y., ALLIS, C. D., MARMORSTEIN, R. & BERGER, S. L. 2000. Phosphorylation of serine 10 in histone H3 is functionally linked in vitro and in vivo to Gcn5-mediated acetylation at lysine 14. *Molecular cell,* 5**,** 917-926.

LOTAN, T. L., GUPTA, N. S., WANG, W., TOUBAJI, A., HAFFNER, M. C., CHAUX, A., HICKS, J. L., MEEKER, A. K., BIEBERICH, C. J. & DE MARZO, A. M. 2011. ERG gene rearrangements are common in prostatic small cell carcinomas. *Modern pathology,* 24**,** 820.

LOVE, H. D., BOOTON, S. E., BOONE, B. E., BREYER, J. P., KOYAMA, T., REVELO, M. P., SHAPPELL, S. B., SMITH, J. R. & HAYWARD, S. W. 2009. Androgen regulated genes in human prostate xenografts in mice: relation to BPH and prostate cancer. *PLoS One,* 4**,** e8384.

LU, L., SINGHAL, U., SKOLARUS, T. A., PALAPATTU, G. S., MONTGOMERY, J. S., WEIZER, A. Z., HOLLENBECK, B. K., MILLER, D. C., MCNAMARA, A. & MEHRA, R. 2015a. Prognostic significance of perineural invasion in localized prostate cancer. American Society of Clinical Oncology.

LU, P. J., SUNDQUIST, K., BAECKSTROM, D., POULSOM, R., HANBY, A., MEIER-EWERT, S., JONES, T., MITCHELL, M., PITHA-ROWE, P. & FREEMONT, P. 1999. A novel gene (PLU-1) containing highly conserved putative DNA/chromatin binding motifs is specifically up-regulated in breast cancer. *Journal of Biological Chemistry,* 274**,** 15633-15645.

LU, W., LIU, S., LI, B., XIE, Y., ADHIAMBO, C., YANG, Q., BALLARD, B. R., NAKAYAMA, K. I., MATUSIK, R. J. & CHEN, Z. 2015b. SKP2 inactivation suppresses prostate tumorigenesis by mediating JARID1B ubiquitination. *Oncotarget,* 6**,** 771.

LUCARELLI, G., RUTIGLIANO, M., BETTOCCHI, C., PALAZZO, S., VAVALLO, A., GALLEGGIANTE, V., TRABUCCO, S., DI CLEMENTE, D., SELVAGGI, F. P. & BATTAGLIA, M. 2013. Spondin-2, a secreted extracellular matrix protein, is a novel diagnostic biomarker for prostate cancer. *The Journal of urology,* 190**,** 2271-2277.

LUCAS-HERALD, A. K., ALVES-LOPES, R., MONTEZANO, A. C., AHMED, S. F. & TOUYZ, R. M. 2017. Genomic and non-genomic effects of androgens in the cardiovascular system: clinical implications. *Clinical Science,* 131**,** 1405-1418.

LUGER, K., MÄDER, A. W., RICHMOND, R. K., SARGENT, D. F. & RICHMOND, T. J. 1997. Crystal structure of the nucleosome core particle at 2.8 Å resolution. *Nature,* 389**,** 251.

LUISI, B. F. & SIGLER, P. 1991. Crystallographic analysis of the interaction of the glucocorticoid receptor with DNA. *Nature,* 352**,** 497.

LUISI, B. F., XU, W., OTWINOWSKI, Z., FREEDMAN, L., YAMAMOTO, K. & SIGLER, P. 1991. Crystallographic analysis of the interaction of the glucocorticoid receptor with DNA. *Nature,* 352**,** 497.

LUPIEN, M., EECKHOUTE, J., MEYER, C. A., WANG, Q., ZHANG, Y., LI, W., CARROLL, J. S., LIU, X. S. & BROWN, M. 2008. FoxA1 translates epigenetic signatures into enhancer-driven lineage-specific transcription. *Cell,* 132**,** 958-970.

LV, T., YUAN, D., MIAO, X., LV, Y., ZHAN, P., SHEN, X. & SONG, Y. 2012. Over-expression of LSD1 promotes proliferation, migration and invasion in non-small cell lung cancer. *PloS one,* 7**,** e35065.

MA, J., CHANG, K., PENG, J., SHI, Q., GAN, H., GAO, K., FENG, K., XU, F., ZHANG, H. & DAI, B. 2018. SPOP promotes ATF2 ubiquitination and degradation to suppress prostate cancer progression. *Journal of Experimental & Clinical Cancer Research,* 37**,** 145.

MA, Q., CHEN, Z., JIA, G., LU, X., XIE, X. & JIN, W. 2015. The histone demethylase PHF8 promotes prostate cancer cell growth by activating the oncomiR miR-125b. *OncoTargets and therapy,* 8**,** 1979.

MACDONALD, N., WELBURN, J. P., NOBLE, M. E., NGUYEN, A., YAFFE, M. B., CLYNES, D., MOGGS, J. G., ORPHANIDES, G., THOMSON, S. & EDMUNDS, J. W. 2005. Molecular basis for the recognition of phosphorylated and phosphoacetylated histone h3 by 14-3-3. *Molecular cell,* 20**,** 199-211.

MACLEAN, H. E., CHIU, W. M., NOTINI, A. J., AXELL, A.-M., DAVEY, R. A., MCMANUS, J. F., MA, C., PLANT, D. R., LYNCH, G. S. & ZAJAC, J. D. 2008. Impaired skeletal muscle development and function in male, but not female, genomic androgen receptor knockout mice. *The FASEB Journal,* 22**,** 2676-2689.

MADSEN, B., TARSOUNAS, M., BURCHELL, J. M., HALL, D., POULSOM, R. & TAYLOR-PAPADIMITRIOU, J. 2003. PLU-1, a transcriptional repressor and putative testis-cancer antigen, has a specific expression and localisation pattern during meiosis. *Chromosoma,* 112**,** 124-132.

MAGLIULO, D., BERNARDI, R. & MESSINA, S. 2018. Lysine-specific demethylase 1A as a promising target in acute myeloid leukemia. *Frontiers in oncology,* 8.

MAIA, J., CAJA, S., STRANO MORAES, M. C., COUTO, N. & COSTA-SILVA, B. 2018. Exosome-based cell-cell communication in the tumor microenvironment. *Frontiers in cell and developmental biology,* 6**,** 18.

MAIER, T., GÜELL, M. & SERRANO, L. 2009. Correlation of mRNA and protein in complex biological samples. *FEBS letters,* 583**,** 3966-3973.

MAKAREVIĆ, J., RUTZ, J., JUENGEL, E., MAXEINER, S., MANI, J., VALLO, S., TSAUR, I., ROOS, F., CHUN, F. & BLAHETA, R. 2018. HDAC inhibition counteracts metastatic re-activation of prostate cancer cells induced by chronic mTOR suppression. *Cells,* 7**,** 129.

MALIK, H. S. & HENIKOFF, S. 2003. Phylogenomics of the nucleosome. *Nature structural & molecular biology,* 10**,** 882.

MALIK, S. N., BRATTAIN, M., GHOSH, P. M., TROYER, D. A., PRIHODA, T., BEDOLLA, R. & KREISBERG, J. I. 2002. Immunohistochemical demonstration of phospho-Akt in high Gleason grade prostate cancer. *Clinical cancer research,* 8**,** 1168-1171.

MALLA, B., AEBERSOLD, D. M. & DAL PRA, A. 2018. Protocol for serum exosomal miRNAs analysis in prostate cancer patients treated with radiotherapy. *Journal of translational medicine,* 16**,** 223.

MANGELSDORF, D. J., THUMMEL, C., BEATO, M., HERRLICH, P., SCHÜTZ, G., UMESONO, K., BLUMBERG, B., KASTNER, P., MARK, M. & CHAMBON, P. 1995. The nuclear receptor superfamily: the second decade. *Cell,* 83**,** 835.

MAO, B., ZHANG, Z. & WANG, G. 2015. BTG2: a rising star of tumor suppressors. *International journal of oncology,* 46**,** 459-464.

MARCIAS, G., ERDMANN, E., LAPOUGE, G., SIEBERT, C., BARTHÉLÉMY, P., DUCLOS, B., BERGERAT, J. P., CÉRALINE, J. & KURTZ, J. E. 2010. Identification of novel truncated androgen receptor (AR) mutants including unreported pre-mRNA splicing variants in the 22Rv1 hormone-refractory prostate cancer (PCa) cell line. *Human mutation,* 31**,** 74-80.

MARMORSTEIN, R. & ZHOU, M.-M. 2014. Writers and readers of histone acetylation: structure, mechanism, and inhibition. *Cold Spring Harbor perspectives in biology,* 6**,** a018762.

MARSH, J. D., LEHMANN, M. H., RITCHIE, R. H., GWATHMEY, J. K., GREEN, G. E. & SCHIEBINGER, R. J. 1998. Androgen receptors mediate hypertrophy in cardiac myocytes. *Circulation,* 98**,** 256-261.

MARSHALL, J. R. 2012. Diet and prostate cancer prevention. *World journal of urology,* 30**,** 157-165.

MARWICK, C. 1998. ACS sets blueprint for action against prostate cancer in African Americans. *JAMA,* 279**,** 418-419.

MASSENKEIL, G., OBERHUBER, H., HAILEMARIAM, S., SULSER, T., DIENER, P., BANNWART, F., SCHÄFER, R. & SCHWARTE-WALDHOFF, I. 1994. P53 mutations and loss of heterozygosity on chromosomes 8p, 16q, 17p, and 18q are confined to advanced prostate cancer. *Anticancer research,* 14**,** 2785-2790.

MATSUMOTO, T., SAKARI, M., OKADA, M., YOKOYAMA, A., TAKAHASHI, S., KOUZMENKO, A. & KATO, S. 2013. The androgen receptor in health and disease. *Annual review of physiology,* 75**,** 201-224.

MAZZOLENI, G., DI LORENZO, D. & STEIMBERG, N. 2009. Modelling tissues in 3D: the next future of pharmaco-toxicology and food research? *Genes & nutrition,* 4**,** 13.

MCCALL, P., GEMMELL, L., MUKHERJEE, R., BARTLETT, J. & EDWARDS, J. 2008. Phosphorylation of the androgen receptor is associated with reduced survival in hormone-refractory prostate cancer patients. *British journal of cancer,* 98**,** 1094.

MCCREA, E. M., LEE, D. K., SISSUNG, T. M. & FIGG, W. D. 2018. Precision medicine applications in prostate cancer. *Therapeutic advances in medical oncology,* 10**,** 1758835918776920.

MCINERNEY, E. M., ROSE, D. W., FLYNN, S. E., WESTIN, S., MULLEN, T.-M., KRONES, A., INOSTROZA, J., TORCHIA, J., NOLTE, R. T. & ASSA-MUNT, N. 1998. Determinants of coactivator LXXLL motif specificity in nuclear receptor transcriptional activation. *Genes & development,* 12**,** 3357-3368.

MCKAY, A. C. & SHARMA, S. 2019. Anatomy, Abdomen and Pelvis, Seminal Vesicle. *StatPearls [Internet].* StatPearls Publishing.

MCKENNA, N. J., LANZ, R. B. & O'MALLEY, B. W. 1999. Nuclear receptor coregulators: cellular and molecular biology. *Endocrine reviews,* 20**,** 321-344.

MCNEAL, J. E. 1988. Normal histology of the prostate. *The American journal of surgical pathology,* 12**,** 619-633.

MCNEAL, J. E. & BOSTWICK, D. G. 1986. Intraductal dysplasia: a premalignant lesion of the prostate. *Human pathology,* 17**,** 64-71.

MELO, K. F., MENDONCA, B. B., BILLERBECK, A. E. C., COSTA, E. M., INACIO, M., SILVA, F. A., LEAL, A. M., LATRONICO, A. C. & ARNHOLD, I. J. 2003. Clinical, hormonal, behavioral, and genetic characteristics of androgen insensitivity syndrome in a Brazilian cohort: five novel mutations in the androgen receptor gene. *The Journal of Clinical Endocrinology & Metabolism,* 88**,** 3241-3250.

MENCHER, S. K. & WANG, L. G. 2005. Promiscuous drugs compared to selective drugs (promiscuity can be a virtue). *BMC clinical pharmacology,* 5**,** 3.

MENG, Z., LIU, Y., WANG, J., FAN, H., FANG, H., LI, S., YUAN, L., LIU, C., PENG, Y. & ZHAO, W. 2019. Histone demethylase KDM7A is required for stem cell maintenance and apoptosis inhibition in breast cancer. *Journal of Cellular Physiology*.

MERMEL, C. H., SCHUMACHER, S. E., HILL, B., MEYERSON, M. L., BEROUKHIM, R. & GETZ, G. 2011. GISTIC2. 0 facilitates sensitive and confident localization of the targets of focal somatic copy-number alteration in human cancers. *Genome biology,* 12**,** R41.

MERSFELDER, E. L. & PARTHUN, M. R. 2006. The tale beyond the tail: histone core domain modifications and the regulation of chromatin structure. *Nucleic acids research,* 34**,** 2653-2662.

METZGER, E., IMHOF, A., PATEL, D., KAHL, P., HOFFMEYER, K., FRIEDRICHS, N., MÜLLER, J. M., GRESCHIK, H., KIRFEL, J. & JI, S. 2010. Phosphorylation of histone H3T6 by PKCβ I controls demethylation at histone H3K4. *Nature,* 464**,** 792.

METZGER, E., WILLMANN, D., MCMILLAN, J., FORNE, I., METZGER, P., GERHARDT, S., PETROLL, K., VON MAESSENHAUSEN, A., URBAN, S. & SCHOTT, A.-K. 2016. Assembly of methylated KDM1A and CHD1 drives androgen receptor–dependent transcription and translocation. *Nature structural & molecular biology,* 23**,** 132.

METZGER, E., WISSMANN, M., YIN, N., MÜLLER, J. M., SCHNEIDER, R., PETERS, A. H., GÜNTHER, T., BUETTNER, R. & SCHÜLE, R. 2005. LSD1 demethylates repressive histone marks to promote androgen-receptor-dependent transcription. *Nature,* 437**,** 436.

METZGER, E., YIN, N., WISSMANN, M., KUNOWSKA, N., FISCHER, K., FRIEDRICHS, N., PATNAIK, D., HIGGINS, J. M., POTIER, N. & SCHEIDTMANN, K.-H. 2008. Phosphorylation of histone H3 at threonine 11 establishes a novel chromatin mark for transcriptional regulation. *nature cell biology,* 10**,** 53.

MEYERS, J., CRAIG, J. & ODDE, D. J. 2006. Potential for control of signaling pathways via cell size and shape. *Current biology,* 16**,** 1685-1693.

MICHAEL, I. P., OREBRAND, M., LIMA, M., PEREIRA, B., VOLPERT, O., QUAGGIN, S. E. & JEANSSON, M. 2017. Angiopoietin-1 deficiency increases tumor metastasis in mice. *BMC cancer,* 17**,** 539.

MIGEON, B. R., BROWN, T. R., AXELMAN, J. & MIGEON, C. J. 1981. Studies of the locus for androgen receptor: localization on the human X chromosome and evidence for homology with the Tfm locus in the mouse. *Proceedings of the National Academy of Sciences,* 78**,** 6339-6343.

MILES, D., VON MINCKWITZ, G. & SEIDMAN, A. D. 2002. Combination versus sequential single-agent therapy in metastatic breast cancer. *The oncologist,* 7**,** 13-19.

MILLER, V. L., MILLER, V. M. & HAY, M. 2004. *Principles of sex-based differences in physiology*, Gulf Professional Publishing.

MILNE, T. A., ZHAO, K. & HESS, J. L. 2009. Chromatin immunoprecipitation (ChIP) for analysis of histone modifications and chromatin-associated proteins. *Leukemia.* Springer.

MINTON, D. R., FU, L., MONGAN, N. P., SHEVCHUK, M. M., NANUS, D. M. & GUDAS, L. J. 2016. Role of NADH dehydrogenase (ubiquinone) 1 alpha subcomplex 4-like 2 in clear cell renal cell carcinoma. *Clinical Cancer Research,* 22**,** 2791-2801.

MIYAGI, H., KANEMOTO, S., SAITO, A., ASADA, R., IWAMOTO, H., IZUMI, S., KIDO, M., GOMI, F., NISHIDA, K. & KIUCHI, Y. 2013. Transcriptional regulation of VEGFA by the endoplasmic reticulum stress transducer OASIS in ARPE-19 cells. *PloS one,* 8**,** e55155.

MIYAMOTO, H., YEH, S., WILDING, G. & CHANG, C. 1998. Promotion of agonist activity of antiandrogens by the androgen receptor coactivator, ARA70, in human prostate cancer DU145 cells. *Proceedings of the National Academy of Sciences,* 95**,** 7379-7384.

MOKHTARI, R. B., HOMAYOUNI, T. S., BALUCH, N., MORGATSKAYA, E., KUMAR, S., DAS, B. & YEGER, H. 2017. Combination therapy in combating cancer. *Oncotarget,* 8**,** 38022.

MONGAN, N., LIM, H. & HUGHES, I. 2001. Genetic evidence to exclude the androgen receptor-polyglutamine associated coactivator, ARA-24, as a cause of male undermasculinisation. *European journal of endocrinology,* 145**,** 809-811.

MONGAN, N. P., JAASKELAINEN, J., BHATTACHARYYA, S., LEU, R. M. & HUGHES, I. A. 2003. Steroid receptor coactivator-3 glutamine repeat polymorphism and the androgen insensitivity syndrome. *European journal of endocrinology,* 148**,** 277-279.

MONGAN, N. P., TADOKORO-CUCCARO, R., BUNCH, T. & HUGHES, I. A. 2015. Androgen insensitivity syndrome. *Best practice & research Clinical endocrinology & metabolism,* 29**,** 569-580.

MONTANI, M., HERRMANNS, T., MÜNTENER, M., WILD, P., SULSER, T. & KRISTIANSEN, G. 2013. Multidrug resistance protein 4 (MRP4) expression in prostate cancer is associated with androgen signaling and decreases with tumor progression. *Virchows Archiv,* 462**,** 437-443.

MONTEIRO, F. L., BAPTISTA, T., AMADO, F., VITORINO, R., JERÓNIMO, C. & HELGUERO, L. A. 2014. Expression and functionality of histone H2A variants in cancer. *Oncotarget,* 5**,** 3428.

MONTIE, J. E. & PIENTA, K. J. 1994. Review of the role of androgenic hormones in the epidemiology of benign prostatc hyperplasia and prostate cancer. *Urology,* 43**,** 892-899.

MONTIRONI, R., NAVARRETE, R. V., LOPEZ-BELTRAN, A., MAZZUCCHELLI, R., MIKUZ, G. & BONO, A. V. 2006. Histopathology reporting of prostate needle biopsies. 2005 update. *Virchows Archiv,* 449**,** 1-13.

MONTIRONI, R., VAN DER KWAST, T., BOCCON-GIBOD, L., BONO, A. V. & BOCCON-GIBOD, L. 2003. Handling and pathology reporting of radical prostatectomy specimens. *European urology,* 44**,** 626-636.

MORRIS, J. M. 1953. The syndrome of testicular feminization in male pseudohermaphrodites. *American Journal of Obstetrics & Gynecology,* 65**,** 1192-1211.

MORSELLI, M., PASTOR, W. A., MONTANINI, B., NEE, K., FERRARI, R., FU, K., BONORA, G., RUBBI, L., CLARK, A. T. & OTTONELLO, S. 2015. In vivo targeting of de novo DNA methylation by histone modifications in yeast and mouse. *Elife,* 4**,** e06205.

MOSQUERA, J. M., BELTRAN, H., PARK, K., MACDONALD, T. Y., ROBINSON, B. D., TAGAWA, S. T., PERNER, S., BISMAR, T. A., ERBERSDOBLER, A. & DHIR, R. 2013. Concurrent AURKA and MYCN gene amplifications are harbingers of lethal treatment-related neuroendocrine prostate cancer. *Neoplasia (New York, NY),* 15**,** 1.

MOSTAGHEL, E. A. 2014. Abiraterone in the treatment of metastatic castration-resistant prostate cancer. *Cancer management and research,* 6**,** 39.

MUCCI, N. R., AKDAS, G., MANELY, S. & RUBIN, M. A. 2000. Neuroendocrine expression in metastaticprostate cancer: Evaluation of high throughput tissue microarrays to detect heterogeneous protein expression. *Human pathology,* 31**,** 406-414.

MURRAY, K. 1964. The occurrence of iε-N-methyl lysine in histones. *Biochemistry,* 3**,** 10-15.

MUSSELMAN, C. A., KHORASANIZADEH, S. & KUTATELADZE, T. G. 2014. Towards understanding methyllysine readout. *Biochimica et Biophysica Acta (BBA)-Gene Regulatory Mechanisms,* 1839**,** 686-693.

NAGAI, Y., KOJIMA, T., MURO, Y., HACHIYA, T., NISHIZAWA, Y., WAKABAYASHI, T. & HAGIWARA, M. 1997. Identification of a novel nuclear speckle-type protein, SPOP. *FEBS letters,* 418**,** 23-26.

NAGORNY, P. & CICHOWICZ, N. 2016. New strategy based on sequential Michael/Aldol reactions for the asymmetric synthesis of cardenolides. *Strategies and Tactics in Organic Synthesis.* Elsevier.

NAKABAYASHI, M., REGAN, M. M., LIFSEY, D., KANTOFF, P. W., TAPLIN, M. E., SARTOR, O. & OH, W. K. 2005. Efficacy of nilutamide as secondary hormonal therapy in androgen-independent prostate cancer. *BJU international,* 96**,** 783-786.

NASR, N. J., KAMINSKI JR, M. V. & SRIRAM, K. 1982. Childhood versus adult onset obesity in a comprehensive, multidisciplinary weight reduction program. *Journal of the American College of Nutrition,* 1**,** 187-192.

NATHALIA, E., THEARDY, M. S., ELVIRA, S., ROSELLINNY, G., LIYANTO, A. S., UTAMA, M. P. & SUMARPO, A. 2018. Downregulation of tumor-suppressor gene LHX6 in cancer: a systematic review. *Romanian Journal of Internal Medicine,* 56**,** 135-142.

NAWROCKI, M., STRUGAŁA, A., PIOTROWSKI, P., WUDARSKI, M., OLESIŃSKA, M. & JAGODZIŃSKI, P. 2015. JHDM1D and HDAC1–3 mRNA expression levels in peripheral blood mononuclear cells of patients with systemic lupus erythematosus. *Zeitschrift für Rheumatologie,* 74**,** 902-910.

NAZARETH, L. V., STENOIEN, D. L., BINGMAN III, W. E., JAMES, A. J., WU, C., ZHANG, Y., EDWARDS, D. P., MANCINI, M., MARCELLI, M. & LAMB, D. J. 1999. A C619Y mutation in the human androgen receptor causes inactivation and mislocalization of the receptor with concomitant sequestration of SRC-1 (steroid receptor coactivator 1). *Molecular endocrinology,* 13**,** 2065-2075.

NELSON, J. D., DENISENKO, O. & BOMSZTYK, K. 2006. Protocol for the fast chromatin immunoprecipitation (ChIP) method. *Nature protocols,* 1**,** 179.

NELSON, P. S., CLEGG, N., ARNOLD, H., FERGUSON, C., BONHAM, M., WHITE, J., HOOD, L. & LIN, B. 2002. The program of androgen-responsive genes in neoplastic prostate epithelium. *Proceedings of the National Academy of Sciences,* 99**,** 11890-11895.

NELSON, W. G. & YEGNASUBRAMANIAN, S. 2013. Resistance emerges to second-generation antiandrogens in prostate cancer. *Cancer discovery,* 3**,** 971-974.

NEMOTO, T., OHARA-NEMOTO, Y. & OTA, M. 1992. Association of the 90-kDa heat shock protein does not affect the ligand-binding ability of androgen receptor. *The Journal of steroid biochemistry and molecular biology,* 42**,** 803-812.

NETWORK, C. G. A. R. 2014. Comprehensive molecular characterization of gastric adenocarcinoma. *Nature,* 513**,** 202.

NETWORK, C. G. A. R. 2017. Integrated genomic characterization of oesophageal carcinoma. *Nature,* 541**,** 169.

NI, L., LLEWELLYN, R., KESLER, C. T., KELLEY, J. B., SPENCER, A., SNOW, C. J., SHANK, L. & PASCHAL, B. M. 2013. Androgen induces a switch from cytoplasmic retention to nuclear import of the androgen receptor. *Molecular and cellular biology,* 33**,** 4766-4778.

NICHOLSON, T. B. & CHEN, T. 2009. LSD1 demethylates histone and non-histone proteins. *Epigenetics,* 4**,** 129-132.

NILSSON, E. M., LAURSEN, K. B., WHITCHURCH, J., MCWILLIAM, A., ØDUM, N., PERSSON, J. L., HEERY, D. M., GUDAS, L. J. & MONGAN, N. P. 2015. MiR137 is an androgen regulated repressor of an extended network of transcriptional coregulators. *Oncotarget,* 6**,** 35710.

NIMURA, K., URA, K. & KANEDA, Y. 2010. Histone methyltransferases: regulation of transcription and contribution to human disease. *Journal of molecular medicine,* 88**,** 1213-1220.

NIWA, H. & UMEHARA, T. 2017. Structural insight into inhibitors of flavin adenine dinucleotide-dependent lysine demethylases. *Epigenetics,* 12**,** 340-352.

NOTINI, A. J., DAVEY, R. A., MCMANUS, J., BATE, K. & ZAJAC, J. 2005. Genomic actions of the androgen receptor are required for normal male sexual differentiation in a mouse model. *Journal of molecular endocrinology,* 35**,** 547-555.

NUSSEY, S. S. & WHITEHEAD, S. A. 2013. *Endocrinology: an integrated approach*, CRC Press.

O'GEEN, H., ECHIPARE, L. & FARNHAM, P. J. 2011. Using ChIP-seq technology to generate high-resolution profiles of histone modifications. *Epigenetics Protocols.* Springer.

OKI, M., AIHARA, H. & ITO, T. 2007. Role of histone phosphorylation in chromatin dynamics and its implications in diseases. *Chromatin and Disease.* Springer.

OLINS, A. L. & OLINS, D. E. 1974. Spheroid chromatin units (ν bodies). *Science,* 183**,** 330-332.

OLINS, D. E. & OLINS, A. L. 2003. Chromatin history: our view from the bridge. *Nature reviews Molecular cell biology,* 4**,** 809.

OPHOFF, J., VAN PROEYEN, K., CALLEWAERT, F., DE GENDT, K., DE BOCK, K., VANDEN BOSCH, A., VERHOEVEN, G., HESPEL, P. & VANDERSCHUEREN, D. 2009. Androgen signaling in myocytes contributes to the maintenance of muscle mass and fiber type regulation but not to muscle strength or fatigue. *Endocrinology,* 150**,** 3558-3566.

ORAFIDIYA, F. A. & MCEWAN, I. J. 2015. Trinucleotide repeats and protein folding and disease: the perspective from studies with the androgen receptor. *Future science OA,* 1.

ORIHUELA, E. & GREEN, J. M. Ductal prostate cancer: contemporary management and outcomes. Urologic Oncology: Seminars and Original Investigations, 2008. Elsevier, 368-371.

ORTLUND, E., LACOUNT, M. W. & LEBIODA, L. 2003. Crystal structures of human prostatic acid phosphatase in complex with a phosphate ion and α-benzylaminobenzylphosphonic acid update the mechanistic picture and offer new insights into inhibitor design. *Biochemistry,* 42**,** 383-389.

OSAWA, T., MURAMATSU, M., WANG, F., TSUCHIDA, R., KODAMA, T., MINAMI, T. & SHIBUYA, M. 2011. Increased expression of histone demethylase JHDM1D under nutrient starvation suppresses tumor growth via down-regulating angiogenesis. *Proceedings of the National Academy of Sciences,* 108**,** 20725-20729.

OUYANG, X., JESSEN, W. J., AL-AHMADIE, H., SERIO, A. M., LIN, Y., SHIH, W.-J., REUTER, V. E., SCARDINO, P. T., SHEN, M. M. & ARONOW, B. J. 2008. Activator protein-1 transcription factors are associated with progression and recurrence of prostate cancer. *Cancer research,* 68**,** 2132-2144.

PAJTLER, K. W., WEINGARTEN, C., THOR, T., KÜNKELE, A., HEUKAMP, L. C., BÜTTNER, R., SUZUKI, T., MIYATA, N., GROTZER, M. & RIEB, A. 2013. The KDM1A histone demethylase is a promising new target for the epigenetic therapy of medulloblastoma. *Acta neuropathologica communications,* 1**,** 19.

PAMPALONI, F., REYNAUD, E. G. & STELZER, E. H. 2007. The third dimension bridges the gap between cell culture and live tissue. *Nature reviews Molecular cell biology,* 8**,** 839-845.

PAN, M.-R., HSU, M.-C., CHEN, L.-T. & HUNG, W.-C. 2015. G9a orchestrates PCL3 and KDM7A to promote histone H3K27 methylation. *Scientific reports,* 5**,** 18709.

PANET-RAYMOND, V., GOTTLIEB, B., BEITEL, L. K., PINSKY, L. & TRIFIRO, M. A. 2000. Interactions between androgen and estrogen receptors and the effects on their transactivational properties. *Molecular and cellular endocrinology,* 167**,** 139-150.

PARK, K., DALTON, J. T., NARAYANAN, R., BARBIERI, C. E., HANCOCK, M. L., BOSTWICK, D. G., STEINER, M. S. & RUBIN, M. A. 2014. TMPRSS2: ERG gene fusion predicts subsequent detection of prostate cancer in patients with high-grade prostatic intraepithelial neoplasia. *Journal of Clinical Oncology,* 32**,** 206.

PARKER, M. G. & WHITE, R. 1996. Nuclear receptors spring into action. *Nature structural biology,* 3**,** 113.

PARSONS, B. D., SCHINDLER, A., EVANS, D. H. & FOLEY, E. 2009. A direct phenotypic comparison of siRNA pools and multiple individual duplexes in a functional assay. *PLoS One,* 4.

PARTHUN, M. R., WIDOM, J. & GOTTSCHLING, D. E. 1996. The major cytoplasmic histone acetyltransferase in yeast: links to chromatin replication and histone metabolism. *Cell,* 87**,** 85-94.

PARTIN, A. W., VAN NESTE, L., KLEIN, E. A., MARKS, L. S., GEE, J. R., TROYER, D. A., RIEGER-CHRIST, K., JONES, J. S., MAGI-GALLUZZI, C. & MANGOLD, L. A. 2014. Clinical validation of an epigenetic assay to predict negative histopathological results in repeat prostate biopsies. *The Journal of urology,* 192**,** 1081-1087.

PATRA, S. K., PATRA, A. & DAHIYA, R. 2001. Histone deacetylase and DNA methyltransferase in human prostate cancer. *Biochemical and biophysical research communications,* 287**,** 705-713.

PAUL, R., BREUL, J. & HARTUNG, R. 1995. Prostate-specific antigen density and age-specific prostate-specific antigen values: the solution of prostate cancer screening? *European urology,* 27**,** 286-291.

PAUL, S. M. & PURDY, R. 1992. Neuroactive steroids. *The FASEB Journal,* 6**,** 2311-2322.

PAZ, J. C., PARK, S., PHILLIPS, N., MATSUMURA, S., TSAI, W.-W., KASPER, L., BRINDLE, P. K., ZHANG, G., ZHOU, M.-M. & WRIGHT, P. E. 2014. Combinatorial regulation of a signal-dependent activator by phosphorylation and acetylation. *Proceedings of the National Academy of Sciences,* 111**,** 17116-17121.

PEACOCK, J. W., TAKEUCHI, A., HAYASHI, N., LIU, L., TAM, K. J., AL NAKOUZI, N., KHAZAMIPOUR, N., TOMBE, T., DEJIMA, T. & LEE, K. C. 2018. SEMA3C drives cancer growth by transactivating multiple receptor tyrosine kinases via Plexin B1. *EMBO molecular medicine,* 10**,** 219-238.

PEER, A., GOTTFRIED, M., SINIBALDI, V., CARDUCCI, M. A., EISENBERGER, M. A., SELLA, A., LEIBOWITZ-AMIT, R., BERGER, R. & KEIZMAN, D. 2014. Comparison of abiraterone acetate versus ketoconazole in patients with metastatic castration resistant prostate cancer refractory to docetaxel. *The Prostate,* 74**,** 433-440.

PENNINGTON, J. W., PRENTISS, R. J. & HOWE, G. 1967. Radical prostatectomy for cancer: significance of perineural lymphatic invasion. *The Journal of urology,* 97**,** 1075-1077.

PENSON, D. F., ARMSTRONG, A. J., CONCEPCION, R., AGARWAL, N., OLSSON, C., KARSH, L., DUNSHEE, C., WANG, F., WU, K. & KRIVOSHIK, A. 2016. Enzalutamide versus bicalutamide in castration-resistant prostate cancer: the STRIVE trial. *Journal of Clinical Oncology,* 34**,** 2098-2106.

PEREIRA, E. R., FRUDD, K., AWAD, W. & HENDERSHOT, L. M. 2013. ER stress and hypoxia response pathways interact to potentiate HIF-1 transcriptional activity on targets like VEGF. *Journal of Biological Chemistry***,** jbc. M113. 507194.

PEREIRA, E. R., FRUDD, K., AWAD, W. & HENDERSHOT, L. M. 2014. Endoplasmic reticulum (ER) stress and hypoxia response pathways interact to potentiate hypoxia-inducible factor 1 (HIF-1) transcriptional activity on targets like vascular endothelial growth factor (VEGF). *Journal of Biological Chemistry,* 289**,** 3352-3364.

PETERSON, C. L. & LANIEL, M.-A. 2004. Histones and histone modifications. *Current Biology,* 14**,** R546-R551.

PETROVICS, G., LIU, A., SHAHEDUZZAMAN, S., FURASATO, B., SUN, C., CHEN, Y., NAU, M., RAVINDRANATH, L., CHEN, Y. & DOBI, A. 2005. Frequent overexpression of ETS-related gene-1 (ERG1) in prostate cancer transcriptome. *Oncogene,* 24**,** 3847.

PETRYLAK, D. P., TANGEN, C. M., HUSSAIN, M. H., LARA JR, P. N., JONES, J. A., TAPLIN, M. E., BURCH, P. A., BERRY, D., MOINPOUR, C. & KOHLI, M. 2004. Docetaxel and estramustine compared with mitoxantrone and prednisone for advanced refractory prostate cancer. *New England Journal of Medicine,* 351**,** 1513-1520.

PFAFFL, M. W. 2001. A new mathematical model for relative quantification in real-time RT–PCR. *Nucleic acids research,* 29**,** e45-e45.

PIENTA, K. J. & ESPER, P. S. 1993. Risk factors for prostate cancer. *Annals of internal medicine,* 118**,** 793-803.

PIETENPOL, J. & STEWART, Z. 2002. Cell cycle checkpoint signaling:: Cell cycle arrest versus apoptosis. *Toxicology,* 181**,** 475-481.

PINSKAYA, M. & MORILLON, A. 2009. Histone H3 lysine 4 di-methylation: a novel mark for transcriptional fidelity? *Epigenetics,* 4**,** 302-306.

PONTING, C. P., OLIVER, P. L. & REIK, W. 2009. Evolution and functions of long noncoding RNAs. *Cell,* 136**,** 629-641.

POWELL, I. J., BANERJEE, M., SAKR, W., GRIGNON, D., WOOD JR, D. P., NOVALLO, M. & PONTES, E. 1999. Should African-American men be tested for prostate carcinoma at an earlier age than white men? *Cancer: Interdisciplinary International Journal of the American Cancer Society,* 85**,** 472-477.

PRATT, W. B. & TOFT, D. O. 1997. Steroid receptor interactions with heat shock protein and immunophilin chaperones. *Endocrine reviews,* 18**,** 306-360.

PROBERT, C., DOTTORINI, T., SPEAKMAN, A., HUNT, S., NAFEE, T., FAZELI, A., WOOD, S., BROWN, J. & JAMES, V. 2019. Communication of prostate cancer cells with bone cells via extracellular vesicle RNA; a potential mechanism of metastasis. *Oncogene,* 38**,** 1751.

QIAN, X., LI, C., PANG, B., XUE, M., WANG, J. & ZHOU, J. 2012. Spondin-2 (SPON2), a more prostate-cancer-specific diagnostic biomarker. *PloS one,* 7**,** e37225.

QU, Y., DAI, B., YE, D., KONG, Y., CHANG, K., JIA, Z., YANG, X., ZHANG, H., ZHU, Y. & SHI, G. 2015. Constitutively active AR-V7 plays an essential role in the development and progression of castration-resistant prostate cancer. *Scientific reports,* 5**,** 7654.

QUIGLEY, C. A., DE BELLIS, A., MARSCHKE, K. B., EL-AWADY, M. K., WILSON, E. M. & FRENCH, F. S. 1995. Androgen receptor defects: historical, clinical, and molecular perspectives. *Endocrine reviews,* 16**,** 271-321.

QUIGLEY, C. A., TAN, J.-A., HE, B., ZHOU, Z.-X., MEBARKI, F., MOREL, Y., FOREST, M. G., CHATELAIN, P., RITZÉN, E. M. & FRENCH, F. S. 2004. Partial androgen insensitivity with phenotypic variation caused by androgen receptor mutations that disrupt activation function 2 and the NH2-and carboxyl-terminal interaction. *Mechanisms of ageing and development,* 125**,** 683-695.

RAAIJMAKERS, R., WILDHAGEN, M. F., ITO, K., PÀEZ, A., DE VRIES, S. H., ROOBOL, M. J. & SCHRÖDER, F. H. 2004. Prostate-specific antigen change in the European Randomized Study of Screening for Prostate Cancer, section Rotterdam. *Urology,* 63**,** 316-320.

RAISNER, R., KHARBANDA, S., JIN, L., JENG, E., CHAN, E., MERCHANT, M., HAVERTY, P. M., BAINER, R., CHEUNG, T. & ARNOTT, D. 2018. Enhancer activity requires CBP/P300 bromodomain-dependent histone H3K27 acetylation. *Cell reports,* 24**,** 1722-1729.

RAMAEKERS, B. L., RIEMSMA, R., TOMINI, F., VAN ASSELT, T., DESHPANDE, S., DUFFY, S., ARMSTRONG, N., SEVERENS, J. L., KLEIJNEN, J. & JOORE, M. A. 2017. Abiraterone acetate for the treatment of chemotherapy-naïve metastatic castration-resistant prostate cancer: an evidence review group perspective of an NICE single technology appraisal. *Pharmacoeconomics,* 35**,** 191-202.

RAMAKRISHNAN, S., ANAND, V. & ROY, S. 2014. Vascular endothelial growth factor signaling in hypoxia and inflammation. *Journal of Neuroimmune Pharmacology,* 9**,** 142-160.

RAMSAY, G., STANTON, L., SCHWAB, M. & BISHOP, J. M. 1986. Human proto-oncogene N-myc encodes nuclear proteins that bind DNA. *Molecular and cellular biology,* 6**,** 4450-4457.

RAMTEKE, A., TING, H., AGARWAL, C., MATEEN, S., SOMASAGARA, R., HUSSAIN, A., GRANER, M., FREDERICK, B., AGARWAL, R. & DEEP, G. 2015. Exosomes secreted under hypoxia enhance invasiveness and stemness of prostate cancer cells by targeting adherens junction molecules. *Molecular carcinogenesis,* 54**,** 554-565.

RANA, K., DAVEY, R. A. & ZAJAC, J. D. 2014. Human androgen deficiency: insights gained from androgen receptor knockout mouse models. *Asian journal of andrology,* 16**,** 169.

RANA, K., FAM, B. C., CLARKE, M. V., PANG, T. P., ZAJAC, J. D. & MACLEAN, H. E. 2011. Increased adiposity in DNA binding-dependent androgen receptor knockout male mice associated with decreased voluntary activity and not insulin resistance. *American Journal of Physiology-Endocrinology and Metabolism,* 301**,** E767-E778.

RANDALL, V. A. 1994. 9 Role of 5α-reductase in health and disease. *Bailliere's clinical endocrinology and metabolism,* 8**,** 405-431.

RAO, D. D., VORHIES, J. S., SENZER, N. & NEMUNAITIS, J. 2009. siRNA vs. shRNA: similarities and differences. *Advanced drug delivery reviews,* 61**,** 746-759.

RASTINEJAD, F. 2001. Retinoid X receptor and its partners in the nuclear receptor family. *Current opinion in structural biology,* 11**,** 33-38.

RATHKOPF, D. & SCHER, H. I. 2013. Androgen receptor antagonists in castration-resistant prostate cancer. *Cancer journal (Sudbury, Mass.),* 19**,** 43.

REA, S., EISENHABER, F., O'CARROLL, D., STRAHL, B. D., SUN, Z.-W., SCHMID, M., OPRAVIL, S., MECHTLER, K., PONTING, C. P. & ALLIS, C. D. 2000. Regulation of chromatin structure by site-specific histone H3 methyltransferases. *Nature,* 406**,** 593.

REVA, B., ANTIPIN, Y. & SANDER, C. 2011. Predicting the functional impact of protein mutations: application to cancer genomics. *Nucleic acids research,* 39**,** e118-e118.

RHODES, D. R., YU, J., SHANKER, K., DESHPANDE, N., VARAMBALLY, R., GHOSH, D., BARRETTE, T., PANDER, A. & CHINNAIYAN, A. M. 2004. ONCOMINE: a cancer microarray database and integrated data-mining platform. *Neoplasia,* 6**,** 1-6.

RISSI, V. B., GLANZNER, W. G., DE MACEDO, M. P., GUTIERREZ, K., BALDASSARRE, H., GONÇALVES, P. B. D. & BORDIGNON, V. 2019. The histone lysine demethylase KDM7A is required for normal development and first cell lineage specification in porcine embryos. *Epigenetics*.

ROBERTSON, K. D. 2005. DNA methylation and human disease. *Nature Reviews Genetics,* 6**,** 597.

ROBINSON, D., VAN ALLEN, E. M., WU, Y.-M., SCHULTZ, N., LONIGRO, R. J., MOSQUERA, J.-M., MONTGOMERY, B., TAPLIN, M.-E., PRITCHARD, C. C. & ATTARD, G. 2015. Integrative clinical genomics of advanced prostate cancer. *Cell,* 161**,** 1215-1228.

ROBINSON, J. L., HICKEY, T. E., WARREN, A. Y., VOWLER, S. L., CARROLL, T., LAMB, A. D., PAPOUTSOGLOU, N., NEAL, D. E., TILLEY, W. D. & CARROLL, J. S. 2014. Elevated levels of FOXA1 facilitate androgen receptor chromatin binding resulting in a CRPC-like phenotype. *Oncogene,* 33**,** 5666.

ROBINSON, M. D., MCCARTHY, D. J. & SMYTH, G. K. 2010. edgeR: a Bioconductor package for differential expression analysis of digital gene expression data. *Bioinformatics,* 26**,** 139-140.

RODRÍGUEZ-BERRIGUETE, G., FRAILE, B., MARTÍNEZ-ONSURBE, P., OLMEDILLA, G., PANIAGUA, R. & ROYUELA, M. 2012. MAP kinases and prostate cancer. *Journal of signal transduction,* 2012.

ROOS, G. & ROOS, C. 2014. *Organic chemistry concepts: An EFL approach*, Academic Press.

ROSE, K. A., STAPLETON, G., DOTT, K., KIENY, M. P., BEST, R., SCHWARZ, M., RUSSELL, D. W., BJÖRKHEM, I., SECKL, J. & LATHE, R. 1997. Cyp7b, a novel brain cytochrome P450, catalyzes the synthesis of neurosteroids 7α-hydroxy dehydroepiandrosterone and 7α-hydroxy pregnenolone. *Proceedings of the National Academy of Sciences,* 94**,** 4925-4930.

ROSE, N. R., WOON, E. C., TUMBER, A., WALPORT, L. J., CHOWDHURY, R., LI, X. S., KING, O. N., LEJEUNE, C., NG, S. S. & KROJER, T. 2012. Plant growth regulator daminozide is a selective inhibitor of human KDM2/7 histone demethylases. *Journal of medicinal chemistry,* 55**,** 6639-6643.

ROSNER, W., HRYB, D. J., KHAN, M. S., NAKHLA, A. M. & ROMAS, N. A. 1991. Sex hormone-binding globulin: anatomy and physiology of a new regulatory system. *The Journal of steroid biochemistry and molecular biology,* 40**,** 813-820.

ROTHBART, S. B. & STRAHL, B. D. 2014. Interpreting the language of histone and DNA modifications. *Biochimica et Biophysica Acta (BBA)-Gene Regulatory Mechanisms,* 1839**,** 627-643.

ROWLANDS, M. G., BARRIE, S. E., CHAN, F., HOUGHTON, J., JARMAN, M., MCCAGUE, R. & POTTER, G. A. 1995. Esters of 3-pyridylacetic acid that combine potent inhibition of 17. alpha.-hydroxylase/C17, 20-lyase (cytochrome P45017. alpha.) with resistance to esterase hydrolysis. *Journal of medicinal chemistry,* 38**,** 4191-4197.

ROY, S., PACKMAN, K., JEFFREY, R. & TENNISWOOD, M. 2005. Histone deacetylase inhibitors differentially stabilize acetylated p53 and induce cell cycle arrest or apoptosis in prostate cancer cells. *Cell death and differentiation,* 12**,** 482.

RUBICZ, R., ZHAO, S., WRIGHT, J. L., COLEMAN, I., GRASSO, C., GEYBELS, M. S., LEONARDSON, A., KOLB, S., APRIL, C. & BIBIKOVA, M. 2017. Gene expression panel predicts metastatic-lethal prostate cancer outcomes in men diagnosed with clinically localized prostate cancer. *Molecular oncology,* 11**,** 140-150.

RUGGERO, K., FARRAN-MATAS, S., MARTINEZ-TEBAR, A. & AYTES, A. 2018. Epigenetic regulation in prostate cancer progression. *Current molecular biology reports,* 4**,** 101-115.

RUJIRABANJERD, S., NELSON, J., TARPEY, P. S., HACKETT, A., EDKINS, S., RAYMOND, F. L., SCHWARTZ, C. E., TURNER, G., IWASE, S. & SHI, Y. 2010. Identification and characterization of two novel JARID1C mutations: suggestion of an emerging genotype–phenotype correlation. *European journal of human genetics,* 18**,** 330.

RUNDLETT, S. E., WU, X.-P. & MIESFELD, R. L. 1990. Functional characterizations of the androgen receptor confirm that the molecular basis of androgen action is transcriptional regulation. *Molecular Endocrinology,* 4**,** 708-714.

RYAN, C. J., SMITH, M. R., DE BONO, J. S., MOLINA, A., LOGOTHETIS, C. J., DE SOUZA, P., FIZAZI, K., MAINWARING, P., PIULATS, J. M. & NG, S. 2013. Abiraterone in metastatic prostate cancer without previous chemotherapy. *New England Journal of Medicine,* 368**,** 138-148.

SAEIDNIA, S., MANAYI, A. & ABDOLLAHI, M. 2015. From in vitro experiments to in vivo and clinical studies; pros and cons. *Current drug discovery technologies,* 12**,** 218-224.

SAHRA, I. B., REGAZZETTI, C., ROBERT, G., LAURENT, K., LE MARCHAND-BRUSTEL, Y., AUBERGER, P., TANTI, J.-F., GIORGETTI-PERALDI, S. & BOST, F. 2011. Metformin, independent of AMPK, induces mTOR inhibition and cell-cycle arrest through REDD1. *Cancer research,* 71**,** 4366-4372.

SAHU, B., LAAKSO, M., OVASKA, K., MIRTTI, T., LUNDIN, J., RANNIKKO, A., SANKILA, A., TURUNEN, J. P., LUNDIN, M. & KONSTI, J. 2011. Dual role of FoxA1 in androgen receptor binding to chromatin, androgen signalling and prostate cancer. *The EMBO journal,* 30**,** 3962-3976.

SAMANTA, S., RAJASINGH, S., DROSOS, N., ZHOU, Z., DAWN, B. & RAJASINGH, J. 2018. Exosomes: new molecular targets of diseases. *Acta Pharmacologica Sinica,* 39**,** 501.

SANCHEZ-VEGA, F., MINA, M., ARMENIA, J., CHATILA, W. K., LUNA, A., LA, K. C., DIMITRIADOY, S., LIU, D. L., KANTHETI, H. S. & SAGHAFINIA, S. 2018. Oncogenic signaling pathways in the cancer genome atlas. *Cell,* 173**,** 321-337. e10.

SANCHEZ, R. & ZHOU, M.-M. 2011. The PHD finger: a versatile epigenome reader. *Trends in biochemical sciences,* 36**,** 364-372.

SANG, H., LI, T., LI, H. & LIU, J. 2013. Down-regulation of Gab1 inhibits cell proliferation and migration in hilar cholangiocarcinoma. *PLoS One,* 8**,** e81347.

SANTOURLIDIS, S., FLORL, A., ACKERMANN, R., WIRTZ, H. C. & SCHULZ, W. A. 1999. High frequency of alterations in DNA methylation in adenocarcinoma of the prostate. *The Prostate,* 39**,** 166-174.

SAPORITA, A. J., ZHANG, Q., NAVAI, N., DINCER, Z., HAHN, J., CAI, X. & WANG, Z. 2003. Identification and characterization of a ligand-regulated nuclear export signal in androgen receptor. *Journal of Biological Chemistry,* 278**,** 41998-42005.

SAPUTRA, E. C., HUANG, L., CHEN, Y. & TUCKER-KELLOGG, L. 2018. Combination therapy and the evolution of resistance: the theoretical merits of synergism and antagonism in cancer. *Cancer research,* 78**,** 2419-2431.

SASAKI, M., KANEUCHI, M., SAKURAGI, N., FUJIMOTO, S., CARROLL, P. R. & DAHIYA, R. 2003. The polyglycine and polyglutamine repeats in the androgen receptor gene in Japanese and Caucasian populations. *Biochemical and biophysical research communications,* 312**,** 1244-1247.

SATO, T., MATSUMOTO, T., KAWANO, H., WATANABE, T., UEMATSU, Y., SEKINE, K., FUKUDA, T., AIHARA, K.-I., KRUST, A. & YAMADA, T. 2004. Brain masculinization requires androgen receptor function. *Proceedings of the National Academy of Sciences,* 101**,** 1673-1678.

SAWICKA, A. & SEISER, C. 2014. Sensing core histone phosphorylation—A matter of perfect timing. *Biochimica et Biophysica Acta (BBA)-Gene Regulatory Mechanisms,* 1839**,** 711-718.

SAYEGH, J., CAO, J., ZOU, M. R., MORALES, A., BLAIR, L. P., NORCIA, M., HOYER, D., TACKETT, A. J., MERKEL, J. S. & YAN, Q. 2013. Identification of small molecule inhibitors of Jumonji AT-rich interactive domain 1B (JARID1B) histone demethylase by a sensitive high throughput screen. *Journal of Biological Chemistry,* 288**,** 9408-9417.

SCHER, H. I. & KELLY, W. K. 1993. Flutamide withdrawal syndrome: its impact on clinical trials in hormone-refractory prostate cancer. *Journal of Clinical Oncology,* 11**,** 1566-1572.

SCHER, H. I., LU, D., SCHREIBER, N. A., LOUW, J., GRAF, R. P., VARGAS, H. A., JOHNSON, A., JENDRISAK, A., BAMBURY, R. & DANILA, D. 2016. Association of AR-V7 on circulating tumor cells as a treatment-specific biomarker with outcomes and survival in castration-resistant prostate cancer. *JAMA oncology,* 2**,** 1441-1449.

SCHERER, P. E., WILLIAMS, S., FOGLIANO, M., BALDINI, G. & LODISH, H. F. 1995. A novel serum protein similar to C1q, produced exclusively in adipocytes. *Journal of Biological chemistry,* 270**,** 26746-26749.

SCHILLING, K. & LIAO, S. 1984. The use of radioactive 7α, 17α-dimethyl-19-nortestosterone (mibolerone) in the assay of androgen receptors. *The Prostate,* 5**,** 581-588.

SCHLEUTKER, J. 2012. Polymorphisms in androgen signaling pathway predisposing to prostate cancer. *Molecular and cellular endocrinology,* 360**,** 25-37.

SCHMITZ, S. U., ALBERT, M., MALATESTA, M., MOREY, L., JOHANSEN, J. V., BAK, M., TOMMERUP, N., ABARRATEGUI, I. & HELIN, K. 2011. Jarid1b targets genes regulating development and is involved in neural differentiation. *The EMBO journal,* 30**,** 4586-4600.

SCHRÖDER, F. H., HUGOSSON, J., CARLSSON, S., TAMMELA, T., MÄÄTTÄNEN, L., AUVINEN, A., KWIATKOWSKI, M., RECKER, F. & ROOBOL, M. J. 2012. Screening for prostate cancer decreases the risk of developing metastatic disease: findings from the European Randomized Study of Screening for Prostate Cancer (ERSPC). *European urology,* 62**,** 745-752.

SCHUG, Z. T., PECK, B., JONES, D. T., ZHANG, Q., GROSSKURTH, S., ALAM, I. S., GOODWIN, L. M., SMETHURST, E., MASON, S. & BLYTH, K. 2015. Acetyl-CoA synthetase 2 promotes acetate utilization and maintains cancer cell growth under metabolic stress. *Cancer cell,* 27**,** 57-71.

SCHULZ, W. A., ELO, J. P., FLORL, A. R., PENNANEN, S., SANTOURLIDIS, S., ENGERS, R., BUCHARDT, M., SEIFERT, H. H. & VISAKORPI, T. 2002. Genomewide DNA hypomethylation is associated with alterations on chromosome 8 in prostate carcinoma. *Genes, Chromosomes and Cancer,* 35**,** 58-65.

SCHULZ, W. A., INGENWERTH, M., DJUIDJE, C. E., HADER, C., RAHNENFÜHRER, J. & ENGERS, R. 2010. Changes in cortical cytoskeletal and extracellular matrix gene expression in prostate cancer are related to oncogenic ERG deregulation. *BMC cancer,* 10**,** 505.

SCHWARZER, R., TONDERA, D., ARNOLD, W., GIESE, K., KLIPPEL, A. & KAUFMANN, J. 2005. REDD1 integrates hypoxia-mediated survival signaling downstream of phosphatidylinositol 3-kinase. *Oncogene,* 24**,** 1138.

SCHWEIZER, M. & PLYMATE, S. 2016. Targeting constitutively active androgen receptor splice variants in castration resistant prostate cancer. Taylor & Francis.

SCIBETTA, A. G., SANTANGELO, S., COLEMAN, J., HALL, D., CHAPLIN, T., COPIER, J., CATCHPOLE, S., BURCHELL, J. & TAYLOR-PAPADIMITRIOU, J. 2007. Functional analysis of the transcription repressor PLU-1/JARID1B. *Molecular and cellular biology,* 27**,** 7220-7235.

SEHRAWAT, A., GAO, L., WANG, Y., BANKHEAD, A., MCWEENEY, S. K., KING, C. J., SCHWARTZMAN, J., URRUTIA, J., BISSON, W. H. & COLEMAN, D. J. 2018. LSD1 activates a lethal prostate cancer gene network independently of its demethylase function. *Proceedings of the National Academy of Sciences,* 115**,** E4179-E4188.

SEKIYA, T., MUTHURAJAN, U. M., LUGER, K., TULIN, A. V. & ZARET, K. S. 2009. Nucleosome-binding affinity as a primary determinant of the nuclear mobility of the pioneer transcription factor FoxA. *Genes & development,* 23**,** 804-809.

SELIGSON, D. B., HORVATH, S., SHI, T., YU, H., TZE, S., GRUNSTEIN, M. & KURDISTANI, S. K. 2005. Global histone modification patterns predict risk of prostate cancer recurrence. *Nature,* 435**,** 1262.

SEMENAS, J., ALLEGRUCCI, C., A BOORJIAN, S., P MONGAN, N. & LIAO PERSSON, J. 2012. Overcoming drug resistance and treating advanced prostate cancer. *Current drug targets,* 13**,** 1308-1323.

SEMENAS, J., DIZEYI, N. & PERSSON, J. L. 2013. Enzalutamide as a second generation antiandrogen for treatment of advanced prostate cancer. *Drug design, development and therapy,* 7**,** 875.

SEMENZA, G. L. 2003. Targeting HIF-1 for cancer therapy. *Nature reviews cancer,* 3**,** 721.

SEMENZA, G. L. 2010. Vascular responses to hypoxia and ischemia. *Arteriosclerosis, thrombosis, and vascular biology,* 30**,** 648-652.

SERUGA, B., OCANA, A. & TANNOCK, I. F. 2011. Drug resistance in metastatic castration-resistant prostate cancer. *Nature reviews Clinical oncology,* 8**,** 12.

SETO, E. & YOSHIDA, M. 2014. Erasers of histone acetylation: the histone deacetylase enzymes. *Cold Spring Harbor perspectives in biology,* 6**,** a018713.

SEYFRIED, T. N. & HUYSENTRUYT, L. C. 2013. On the origin of cancer metastasis. *Critical reviews in oncogenesis,* 18**,** 43.

SHA, J., HAN, Q., CHI, C., ZHU, Y., PAN, J., DONG, B., HUANG, Y., XIA, W. & XUE, W. 2018. PRKAR2B promotes prostate cancer metastasis by activating Wnt/β-catenin and inducing epithelial-mesenchymal transition. *Journal of cellular biochemistry,* 119**,** 7319-7327.

SHA, J., XUE, W., DONG, B., PAN, J., WU, X., LI, D., LIU, D. & HUANG, Y. 2017. PRKAR2B plays an oncogenic role in the castration-resistant prostate cancer. *Oncotarget,* 8**,** 6114.

SHAFFER, P. L., JIVAN, A., DOLLINS, D. E., CLAESSENS, F. & GEWIRTH, D. T. 2004. Structural basis of androgen receptor binding to selective androgen response elements. *Proceedings of the National Academy of Sciences,* 101**,** 4758-4763.

SHARIFI, N., GULLEY, J. L. & DAHUT, W. L. 2005. Androgen deprivation therapy for prostate cancer. *Jama,* 294**,** 238-244.

SHARMA, N. L., MASSIE, C. E., RAMOS-MONTOYA, A., ZECCHINI, V., SCOTT, H. E., LAMB, A. D., MACARTHUR, S., STARK, R., WARREN, A. Y. & MILLS, I. G. 2013. The androgen

receptor induces a distinct transcriptional program in castration-resistant prostate cancer in man. *Cancer cell,* 23**,** 35-47.

SHEN, M. M. & ABATE-SHEN, C. 2010. Molecular genetics of prostate cancer: new prospects for old challenges. *Genes & development,* 24**,** 1967-2000.

SHEN, X., ZHUANG, Z., ZHANG, Y., CHEN, Z., SHEN, L., PU, W., CHEN, L. & XU, Z. 2015. JARID1B modulates lung cancer cell proliferation and invasion by regulating p53 expression. *Tumor Biology,* 36**,** 7133-7142.

SHI, Y.-J., MATSON, C., LAN, F., IWASE, S., BABA, T. & SHI, Y. 2005. Regulation of LSD1 histone demethylase activity by its associated factors. *Molecular cell,* 19**,** 857-864.

SHI, Y., LAN, F., MATSON, C., MULLIGAN, P., WHETSTINE, J. R., COLE, P. A., CASERO, R. A. & SHI, Y. 2004. Histone demethylation mediated by the nuclear amine oxidase homolog LSD1. *Cell,* 119**,** 941-953.

SHI, Z. & MOULT, J. 2011. Structural and functional impact of cancer-related missense somatic mutations. *Journal of molecular biology,* 413**,** 495-512.

SHIN, S.-H., LEE, G. Y., LEE, M., KANG, J., SHIN, H.-W., CHUN, Y.-S. & PARK, J.-W. 2018. Aberrant expression of CITED2 promotes prostate cancer metastasis by activating the nucleolin-AKT pathway. *Nature communications,* 9**,** 4113.

SHIN, S., KIM, T.-D., JIN, F., VAN DEURSEN, J. M., DEHM, S. M., TINDALL, D. J., GRANDE, J. P., MUNZ, J.-M., VASMATZIS, G. & JANKNECHT, R. 2009. Induction of prostatic intraepithelial neoplasia and modulation of androgen receptor by ETS variant 1/ETS-related protein 81. *Cancer research,* 69**,** 8102-8110.

SHIOTA, M., FUJIMOTO, N., KASHIWAGI, E. & ETO, M. 2019. The Role of Nuclear Receptors in Prostate Cancer. *Cells,* 8**,** 602.

SHMAKOVA, A., BATIE, M., DRUKER, J. & ROCHA, S. 2014. Chromatin and oxygen sensing in the context of JmjC histone demethylases. *Biochemical Journal,* 462**,** 385-395.

SHOAG, J. & BARBIERI, C. E. 2016. Clinical variability and molecular heterogeneity in prostate cancer. *Asian journal of andrology,* 18**,** 543.

SHUKLA, G., PLAGA, A., SHANKAR, E. & GUPTA, S. 2016. Androgen receptor-related diseases: what do we know? *Andrology,* 4**,** 366-381.

SIEGEL, R. L., MILLER, K. D. & JEMAL, A. 2019. Cancer statistics, 2019. *CA: a cancer journal for clinicians,* 69**,** 7-34.

SIMENTAL, J., SAR, M., LANE, M., FRENCH, F. & WILSON, E. 1991. Transcriptional activation and nuclear targeting signals of the human androgen receptor. *Journal of Biological Chemistry,* 266**,** 510-518.

SIMONS, K. & SAMPAIO, J. L. 2011. Membrane organization and lipid rafts. *Cold Spring Harbor perspectives in biology,* 3**,** a004697.

SINHA, I., ALLEN, J. E., PINTO, J. T. & SINHA, R. 2014. Methylseleninic acid elevates REDD1 and inhibits prostate cancer cell growth despite AKT activation and mTOR dysregulation in hypoxia. *Cancer medicine,* 3**,** 252-264.

SMITH, M. R., RATHKOPF, D. E., MULDERS, P. F., CARLES, J., VAN POPPEL, H., LI, J., KHEOH, T., GRIFFIN, T. W., MOLINA, A. & RYAN, C. J. 2015. Efficacy and safety of abiraterone acetate in elderly (75 years or older) chemotherapy naive patients with metastatic castration resistant prostate cancer. *The Journal of urology,* 194**,** 1277-1284.

SMITH, S. M. & VALE, W. W. 2006. The role of the hypothalamic-pituitary-adrenal axis in neuroendocrine responses to stress. *Dialogues in clinical neuroscience,* 8**,** 383.

SOARES, L. M., HE, P. C., CHUN, Y., SUH, H., KIM, T. & BURATOWSKI, S. 2017. Determinants of histone H3K4 methylation patterns. *Molecular cell,* 68**,** 773-785. e6.

SOBIN, L. 2009. International Union Against Cancer (UICC) TNM classification of malignant tumours. *Oesophagus including Oesophagogastric Junction***,** 66-72.

SOBIN, L. H., GOSPODAROWICZ, M. K. & WITTEKIND, C. 2011. *TNM classification of malignant tumours*, John Wiley & Sons.

SOKALINGAM, S., RAGHUNATHAN, G., SOUNDRARAJAN, N. & LEE, S.-G. 2012. A study on the effect of surface lysine to arginine mutagenesis on protein stability and structure using green fluorescent protein. *PloS one,* 7**,** e40410.

SOLLER, M. J., ISAKSSON, M., ELFVING, P., SOLLER, W., LUNDGREN, R. & PANAGOPOULOS, I. 2006. Confirmation of the high frequency of the TMPRSS2/ERG fusion gene in prostate cancer. *Genes, Chromosomes and Cancer,* 45**,** 717-719.

SOLOWAY, M. S., HARDEMAN, S. W., HICKEY, D., TODD, B., SOLOWAY, S., RAYMOND, J. & MOINUDDIN, M. 1988. Stratification of patients with metastatic prostate cancer based on extent of disease on initial bone scan. *Cancer,* 61**,** 195-202.

SON, M. J., KIM, W. K., OH, K.-J., PARK, A., LEE, D. S., HAN, B. S., LEE, S. C. & BAE, K.-H. 2016. Methyltransferase and demethylase profiling studies during brown adipocyte differentiation. *BMB reports,* 49**,** 388.

SONN, G. A., ARONSON, W. & LITWIN, M. 2005. Impact of diet on prostate cancer: a review. *Prostate Cancer and Prostatic Diseases,* 8**,** 304.

SØRENSEN, M. B., STOLTENBERG, M., DANSCHER, G. & ERNST, E. 1999. Chelation of intracellular zinc ions affects human sperm cell motility. *Molecular human reproduction,* 5**,** 338-341.

SRAMKOSKI, R. M., PRETLOW, T. G., GIACONIA, J. M., PRETLOW, T. P., SCHWARTZ, S., SY, M.-S., MARENGO, S. R., RHIM, J. S., ZHANG, D. & JACOBBERGER, J. W. 1999. A new human prostate carcinoma cell line, 22Rv1. *In Vitro Cellular & Developmental Biology-Animal,* 35**,** 403-409.

STARK, J. R., PERNER, S., STAMPFER, M. J., SINNOTT, J. A., FINN, S., EISENSTEIN, A. S., MA, J., FIORENTINO, M., KURTH, T. & LODA, M. 2009. Gleason score and lethal prostate cancer: does 3+ 4= 4+ 3? *Journal of Clinical Oncology,* 27**,** 3459.

STAVROPOULOS, P., BLOBEL, G. & HOELZ, A. 2006. Crystal structure and mechanism of human lysine-specific demethylase-1. *Nature structural & molecular biology,* 13**,** 626.

STEEG, P. S. & THEODORESCU, D. 2008. Metastasis: a therapeutic target for cancer. *Nature Reviews Clinical Oncology,* 5**,** 206.

STEIN, J., MAJORES, M., ROHDE, M., LIM, S., SCHNEIDER, S., KRAPPE, E., ELLINGER, J., DIETEL, M., STEPHAN, C. & JUNG, K. 2014. KDM5C is overexpressed in prostate cancer and is a prognostic marker for prostate-specific antigen-relapse following radical prostatectomy. *The American journal of pathology,* 184**,** 2430-2437.

STEWART, G. D., VAN NESTE, L., DELVENNE, P., DELRÉE, P., DELGA, A., MCNEILL, S. A., O'DONNELL, M., CLARK, J., VAN CRIEKINGE, W. & BIGLEY, J. 2013. Clinical utility of an epigenetic assay to detect occult prostate cancer in histopathologically negative biopsies: results of the MATLOC study. *The Journal of urology,* 189**,** 1110-1116.

STILLWELL, W. 2016. *An introduction to biological membranes: composition, structure and function*, Elsevier.

STONE, K. R., MICKEY, D. D., WUNDERLI, H., MICKEY, G. H. & PAULSON, D. F. 1978. Isolation of a human prostate carcinoma cell line (DU 145). *International journal of cancer,* 21**,** 274-281.

STRAHL, B. D. & ALLIS, C. D. 2000. The language of covalent histone modifications. *Nature,* 403**,** 41.

STRANO, S., DELL'ORSO, S., DI AGOSTINO, S., FONTEMAGGI, G., SACCHI, A. & BLANDINO, G. 2007. Mutant p53: an oncogenic transcription factor. *Oncogene,* 26**,** 2212.

STRICKER, H. J. 2001. Luteinizing hormone-releasing hormone antagonists in prostate cancer. *Urology,* 58**,** 24-7.

STURGE, J., CALEY, M. P. & WAXMAN, J. 2011. Bone metastasis in prostate cancer: emerging therapeutic strategies. *Nature reviews Clinical oncology,* 8**,** 357.

SUGANUMA, T. & WORKMAN, J. L. 2008. Crosstalk among histone modifications. *Cell,* 135**,** 604-607.

SUN, S., SPRENGER, C. C., VESSELLA, R. L., HAUGK, K., SORIANO, K., MOSTAGHEL, E. A., PAGE, S. T., COLEMAN, I. M., NGUYEN, H. M. & SUN, H. 2010. Castration resistance in human prostate cancer is conferred by a frequently occurring androgen receptor splice variant. *The Journal of clinical investigation,* 120**,** 2715-2730.

SURAWEERA, A., O'BYRNE, K. J. & RICHARD, D. J. 2018. Combination therapy with histone deacetylase inhibitors (HDACi) for the treatment of cancer: achieving the full therapeutic potential of HDACi. *Frontiers in oncology,* 8**,** 92.

SURVEILLANCE RESEARCH PROGRAM, N. C. I. 2016. Fast stats: An interactive tool for access to SEER cancer statistics.

SUZUKI, T., OZASA, H., ITOH, Y., ZHAN, P., SAWADA, H., MINO, K., WALPORT, L., OHKUBO, R., KAWAMURA, A. & YONEZAWA, M. 2013. Identification of the KDM2/7 histone lysine demethylase subfamily inhibitor and its antiproliferative activity. *Journal of medicinal chemistry,* 56**,** 7222-7231.

SWEENEY, C. J., CHEN, Y.-H., CARDUCCI, M., LIU, G., JARRARD, D. F., EISENBERGER, M., WONG, Y.-N., HAHN, N., KOHLI, M. & COONEY, M. M. 2015. Chemohormonal therapy in metastatic hormone-sensitive prostate cancer. *New England Journal of Medicine,* 373**,** 737-746.

SZPIECH, Z. A., STRAULI, N. B., WHITE, K. A., RUIZ, D. G., JACOBSON, M. P., BARBER, D. L. & HERNANDEZ, R. D. 2017. Prominent features of the amino acid mutation landscape in cancer. *PloS one,* 12**,** e0183273.

TAKAYAMA, K.-I., SUZUKI, T., TANAKA, T., FUJIMURA, T., TAKAHASHI, S., URANO, T., IKEDA, K. & INOUE, S. 2018. TRIM25 enhances cell growth and cell survival by modulating p53 signals via interaction with G3BP2 in prostate cancer. *Oncogene,* 37**,** 2165.

TAKAYAMA, K. I. & INOUE, S. 2013. Transcriptional network of androgen receptor in prostate cancer progression. *International Journal of Urology,* 20**,** 756-768.

TAKEUCHI, T., YAMAZAKI, Y., KATOH-FUKUI, Y., TSUCHIYA, R., KONDO, S., MOTOYAMA, J. & HIGASHINAKAGAWA, T. 1995. Gene trap capture of a novel mouse gene, jumonji, required for neural tube formation. *Genes & development,* 9**,** 1211-1222.

TAM, K. J., HUI, D. H., LEE, W. W., DONG, M., TOMBE, T., JIAO, I. Z., KHOSRAVI, S., TAKEUCHI, A., PEACOCK, J. W. & IVANOVA, L. 2017. Semaphorin 3 C drives epithelial-to-mesenchymal transition, invasiveness, and stem-like characteristics in prostate cells. *Scientific reports,* 7**,** 11501.

TAN, H.-L., SOOD, A., RAHIMI, H. A., WANG, W., GUPTA, N., HICKS, J., MOSIER, S., GOCKE, C. D., EPSTEIN, J. I. & NETTO, G. J. 2014. Rb loss is characteristic of prostatic small cell neuroendocrine carcinoma. *Clinical cancer research,* 20**,** 890-903.

TAN, K., SHAW, A. L., MADSEN, B., JENSEN, K., TAYLOR-PAPADIMITRIOU, J. & FREEMONT, P. S. 2003. Human PLU-1 Has transcriptional repression properties and interacts with the developmental transcription factors BF-1 and PAX9. *Journal of Biological Chemistry,* 278**,** 20507-20513.

TAN, M., LUO, H., LEE, S., JIN, F., YANG, J. S., MONTELLIER, E., BUCHOU, T., CHENG, Z., ROUSSEAUX, S. & RAJAGOPAL, N. 2011. Identification of 67 histone marks and histone lysine crotonylation as a new type of histone modification. *Cell,* 146**,** 1016-1028.

TAN, M. E., LI, J., XU, H. E., MELCHER, K. & YONG, E.-L. 2015. Androgen receptor: structure, role in prostate cancer and drug discovery. *Acta Pharmacologica Sinica,* 36**,** 3.

TAN, P. Y., CHANG, C. W., CHNG, K. R., WANSA, K. S. A., SUNG, W.-K. & CHEUNG, E. 2012. Integration of regulatory networks by NKX3-1 promotes androgen-dependent prostate cancer survival. *Molecular and cellular biology,* 32**,** 399-414.

TANAKA, Y., NAKAYAMADA, S. & OKADA, Y. 2005. Osteoblasts and osteoclasts in bone remodeling and inflammation. *Current Drug Targets-Inflammation & Allergy,* 4**,** 325-328.

TANG, L., NOGALES, E. & CIFERRI, C. 2010. Structure and function of SWI/SNF chromatin remodeling complexes and mechanistic implications for transcription. *Progress in biophysics and molecular biology,* 102**,** 122-128.

TANG, Y., CHEN, Z.-Y., HONG, Y.-Z., WU, Q., LIN, H.-Q., CHEN, C. D. & YANG, H.-T. 2014. Expression profiles of histone lysine demethylases during cardiomyocyte differentiation of mouse embryonic stem cells. *Acta Pharmacologica Sinica,* 35**,** 899.

TAPLIN, M.-E., BUBLEY, G. J., KO, Y.-J., SMALL, E. J., UPTON, M., RAJESHKUMAR, B. & BALK, S. P. 1999. Selection for androgen receptor mutations in prostate cancers treated with androgen antagonist. *Cancer research,* 59**,** 2511-2515.

TASLIM, C., CHEN, Z., HUANG, K., HUANG, T. H.-M., WANG, Q. & LIN, S. 2012. Integrated analysis identifies a class of androgen-responsive genes regulated by short combinatorial long-range mechanism facilitated by CTCF. *Nucleic acids research,* 40**,** 4754-4764.

TAXMAN, D. J., MOORE, C. B., GUTHRIE, E. H. & HUANG, M. T.-H. 2010. Short hairpin RNA (shRNA): design, delivery, and assessment of gene knockdown. *RNA therapeutics.* Springer.

TAYLOR, A. M., SHIH, J., HA, G., GAO, G. F., ZHANG, X., BERGER, A. C., SCHUMACHER, S. E., WANG, C., HU, H. & LIU, J. 2018. Genomic and functional approaches to understanding cancer aneuploidy. *Cancer cell,* 33**,** 676-689. e3.

TAYLOR, B. S., SCHULTZ, N., HIERONYMUS, H., GOPALAN, A., XIAO, Y., CARVER, B. S., ARORA, V. K., KAUSHIK, P., CERAMI, E. & REVA, B. 2010. Integrative genomic profiling of human prostate cancer. *Cancer cell,* 18**,** 11-22.

TAYLOR, L. G., CANFIELD, S. E. & DU, X. L. 2009. Review of major adverse effects of androgen-deprivation therapy in men with prostate cancer. *Cancer,* 115**,** 2388-2399.

TELLO, D., BALSA, E., ACOSTA-IBORRA, B., FUERTES-YEBRA, E., ELORZA, A., ORDÓÑEZ, Á., CORRAL-ESCARIZ, M., SORO, I., LÓPEZ-BERNARDO, E. & PERALES-CLEMENTE, E. 2011. Induction of the mitochondrial NDUFA4L2 protein by HIF-1α decreases oxygen consumption by inhibiting Complex I activity. *Cell metabolism,* 14**,** 768-779.

TEPPER, C. G. & TSUBOTA, T. 2013. Molecular targeting of prostate cancer during androgen ablation: inhibition of CHES1/FOXN3. CALIFORNIA UNIV DAVIS.

TESSARZ, P. & KOUZARIDES, T. 2014. Histone core modifications regulating nucleosome structure and dynamics. *Nature reviews Molecular cell biology,* 15**,** 703.

THALMANN, G. N., ANEZINIS, P. E., CHANG, S.-M., ZHAU, H. E., KIM, E. E., HOPWOOD, V. L., PATHAK, S., VON ESCHENBACH, A. C. & CHUNG, L. W. 1994. Androgen-independent cancer progression and bone metastasis in the LNCaP model of human prostate cancer. *Cancer research,* 54**,** 2577-2581.

THOMPSON, I. M. 2001. Flare associated with LHRH-agonist therapy. *Reviews in urology,* 3**,** S10.

THOMPSON, I. M., TANGEN, C. M., TOLCHER, A., CRAWFORD, E. D., EISENBERGER, M. & MOINPOUR, C. M. 2001. Association of African-American ethnic background with survival in men with metastatic prostate cancer. *Journal of the National Cancer Institute,* 93**,** 219-225.

TILLEY, W. D., BUCHANAN, G., HICKEY, T. E. & BENTEL, J. M. 1996. Mutations in the androgen receptor gene are associated with progression of human prostate cancer to androgen independence. *Clinical Cancer Research,* 2**,** 277-285.

TIRADO-HURTADO, I., FAJARDO, W. & PINTO, J. A. 2018. DNA damage inducible transcript 4 gene: the switch of the metabolism as potential target in cancer. *Frontiers in oncology,* 8**,** 106.

TOIVANEN, R. & SHEN, M. M. 2017. Prostate organogenesis: tissue induction, hormonal regulation and cell type specification. *Development,* 144**,** 1382-1398.

TOMLINS, S. A., LAXMAN, B., DHANASEKARAN, S. M., HELGESON, B. E., CAO, X., MORRIS, D. S., MENON, A., JING, X., CAO, Q. & HAN, B. 2007. Distinct classes of chromosomal rearrangements create oncogenic ETS gene fusions in prostate cancer. *Nature,* 448**,** 595.

TOMLINS, S. A., LAXMAN, B., VARAMBALLY, S., CAO, X., YU, J., HELGESON, B. E., CAO, Q., PRENSNER, J. R., RUBIN, M. A. & SHAH, R. B. 2008. Role of the TMPRSS2-ERG gene fusion in prostate cancer. *Neoplasia (New York, NY),* 10**,** 177.

TOMLINS, S. A., RHODES, D. R., PERNER, S., DHANASEKARAN, S. M., MEHRA, R., SUN, X.-W., VARAMBALLY, S., CAO, X., TCHINDA, J. & KUEFER, R. 2005. Recurrent fusion of TMPRSS2 and ETS transcription factor genes in prostate cancer. *science,* 310**,** 644-648.

TRAN, C., OUK, S., CLEGG, N. J., CHEN, Y., WATSON, P. A., ARORA, V., WONGVIPAT, J., SMITH-JONES, P. M., YOO, D. & KWON, A. 2009. Development of a second-generation antiandrogen for treatment of advanced prostate cancer. *Science,* 324**,** 787-790.

TROTMAN, L. C., NIKI, M., DOTAN, Z. A., KOUTCHER, J. A., DI CRISTOFANO, A., XIAO, A., KHOO, A. S., ROY-BURMAN, P., GREENBERG, N. M. & VAN DYKE, T. 2003. Pten dose dictates cancer progression in the prostate. *PLoS biology,* 1**,** e59.

TRUMP, D. L. Antiandrogen withdrawal alone or in combination with ketoconazole in androgen-independent prostate cancer patients: A phase III trial (CALGB 9583). Small EJ, Halabi S, Dawson NA, Stadler WM, Rini BI, Picus J, Gable P, Torti FM, Kaplan E, Vogelzang NJ, UCSF Comprehensive Cancer Center, University of California San Francisco, San Francisco, CA.: J Clin Oncol 2004; 22: 1025–33. Urologic Oncology: Seminars and Original Investigations, 2004. Elsevier, 433.

TSUKADA, Y.-I. 2012. Hydroxylation mediates chromatin demethylation. *The Journal of Biochemistry,* 151**,** 229-246.

TSUKADA, Y.-I., FANG, J., ERDJUMENT-BROMAGE, H., WARREN, M. E., BORCHERS, C. H., TEMPST, P. & ZHANG, Y. 2006. Histone demethylation by a family of JmjC domain-containing proteins. *Nature,* 439**,** 811.

TU, S., TENG, Y.-C., YUAN, C., WU, Y.-T., CHAN, M.-Y., CHENG, A.-N., LIN, P.-H., JUAN, L.-J. & TSAI, M.-D. 2008. The ARID domain of the H3K4 demethylase RBP2 binds to a DNA CCGCCC motif. *Nature structural & molecular biology,* 15**,** 419.

TUEM, K. B. & ATEY, T. M. 2017. Neuroactive steroids: receptor interactions and responses. *Frontiers in neurology,* 8**,** 442.

TURCU, A., SMITH, J. M., AUCHUS, R. & RAINEY, W. E. 2011. Adrenal androgens and androgen precursors—definition, synthesis, regulation and physiologic actions. *Comprehensive Physiology,* 4**,** 1369-1381.

UDAYAPPAN, U. & CASEY, P. 2017. c-Jun contributes to transcriptional control of GNA12 expression in prostate cancer cells. *Molecules,* 22**,** 612.

UEDA, T., BRUCHOVSKY, N. & SADAR, M. D. 2002a. Activation of the androgen receptor N-terminal domain by interleukin-6 via MAPK and STAT3 signal transduction pathways. *Journal of Biological Chemistry,* 277**,** 7076-7085.

UEDA, T., MAWJI, N. R., BRUCHOVSKY, N. & SADAR, M. D. 2002b. Ligand-independent activation of the androgen receptor by interleukin-6 and the role of steroid receptor coactivator-1 in prostate cancer cells. *Journal of Biological Chemistry,* 277**,** 38087-38094.

UMAR, A., BERREVOETS, C. A., VAN, N. M., VAN LEEUWEN, M., VERBIEST, M., KLEIJER, W. J., DOOIJES, D., GROOTEGOED, J. A., DROP, S. L. & BRINKMANN, A. O. 2005. Functional analysis of a novel androgen receptor mutation, Q902K, in an individual with partial androgen insensitivity. *The Journal of Clinical Endocrinology & Metabolism,* 90**,** 507-515.

UPADHYAY, A. K., ROTILI, D., HAN, J. W., HU, R., CHANG, Y., LABELLA, D., ZHANG, X., YOON, Y.-S., MAI, A. & CHENG, X. 2012. An analog of BIX-01294 selectively inhibits a family of histone H3 lysine 9 Jumonji demethylases. *Journal of molecular biology,* 416**,** 319-327.

VAN CRIEKINGE, W. & BEYAERT, R. 1999. Yeast two-hybrid: state of the art. *Biological procedures online,* 2**,** 1.

VAN LAAR, J., BOLT-DE VRIES, J., ZEGERS, N., TRAPMAN, J. & BRINKMANN, A. 1990. Androgen receptor heterogeneity and phosphorylation in human LNCaP cells. *Biochemical and biophysical research communications,* 166**,** 193-200.

VAN NESTE, L., GROSKOPF, J., GRIZZLE, W. E., ADAMS, G. W., DEGUENTHER, M. S., KOLETTIS, P. N., BRYANT, J. E., KEARNEY, G. P., KEARNEY, M. C. & VAN CRIEKINGE, W. 2017. Epigenetic risk score improves prostate cancer risk assessment. *The Prostate,* 77**,** 1259-1264.

VANDEL, L. & TROUCHE, D. 2001. Physical association between the histone acetyl transferase CBP and a histone methyl transferase. *EMBO reports,* 2**,** 21-26.

VEERAMANI, S., YUAN, T.-C., CHEN, S.-J., LIN, F.-F., PETERSEN, J. E., SHAHEDUZZAMAN, S., SRIVASTAVA, S., MACDONALD, R. G. & LIN, M.-F. 2005. Cellular prostatic acid phosphatase: a protein tyrosine phosphatase involved in androgen-independent proliferation of prostate cancer. *Endocrine-Related Cancer,* 12**,** 805-822.

VEGAS, A. J., FULLER, J. H. & KOEHLER, A. N. 2008. Small-molecule microarrays as tools in ligand discovery. *Chemical Society Reviews,* 37**,** 1385-1394.

VELDSCHOLTE, J., BERREVOETS, C., RIS-STALPERS, C., KUIPER, G., JENSTER, G., TRAPMAN, J., BRINKMANN, A. & MULDER, E. 1992a. The androgen receptor in LNCaP cells contains a mutation in the ligand binding domain which affects steroid binding characteristics and response to antiandrogens. *The Journal of steroid biochemistry and molecular biology,* 41**,** 665-669.

VELDSCHOLTE, J., BERREVOETS, C. A., ZEGERS, N. D., VAN DER KWAST, T. H., GROOTEGOED, J. A. & MULDER, E. 1992b. Hormone-induced dissociation of the androgen receptor-heat-shock protein complex: use of a new monoclonal antibody to distinguish transformed from nontransformed receptors. *Biochemistry,* 31**,** 7422-7430.

VENKEN, K., DE GENDT, K., BOONEN, S., OPHOFF, J., BOUILLON, R., SWINNEN, J. V., VERHOEVEN, G. & VANDERSCHUEREN, D. 2006. Relative impact of androgen and estrogen receptor activation in the effects of androgens on trabecular and cortical bone in growing male mice: a study in the androgen receptor knockout mouse model. *Journal of Bone and Mineral Research,* 21**,** 576-585.

VERHAGEN, A. P., RAMAEKERS, F. C., AALDERS, T. W., SCHAAFSMA, H. E., DEBRUYNE, F. M. & SCHALKEN, J. A. 1992. Colocalization of basal and luminal cell-type cytokeratins in human prostate cancer. *Cancer research,* 52**,** 6182-6187.

VERHAMME, K., DIELEMAN, J., BLEUMINK, G., VAN DER LEI, J., STURKENBOOM, M. & PANEL, T. P. E. E. 2002. Incidence and prevalence of lower urinary tract symptoms suggestive of benign prostatic hyperplasia in primary care—the Triumph project. *European urology,* 42**,** 323-328.

VICKERS, A. J. 2017. Prostate cancer screening: time to question how to optimize the ratio of benefits and harms. *Annals of internal medicine,* 167**,** 509-510.

VIGNALI, M., HASSAN, A. H., NEELY, K. E. & WORKMAN, J. L. 2000. ATP-dependent chromatin-remodeling complexes. *Molecular and cellular biology,* 20**,** 1899-1910.

VILENCHIK, L. Z., SHETH, P. R., CHUANG, C.-C. & LE, H. V. 2011. Affinity characterization–mass spectrometry methodology for quantitative analyses of small molecule protein binding in solution. *Analytical biochemistry,* 418**,** 10-18.

VINOGRADOVA, M., GEHLING, V. S., GUSTAFSON, A., ARORA, S., TINDELL, C. A., WILSON, C., WILLIAMSON, K. E., GULER, G. D., GANGURDE, P. & MANIERI, W. 2016. An

inhibitor of KDM5 demethylases reduces survival of drug-tolerant cancer cells. *Nature chemical biology,* 12**,** 531.

VOLODKO, N., GORDON, M., SALLA, M., GHAZALEH, H. A. & BAKSH, S. 2014. RASSF tumor suppressor gene family: biological functions and regulation. *FEBS letters,* 588**,** 2671-2684.

WADDINGTON, C. H. 1940. Organisers and genes. *Organisers and genes.*

WADDINGTON, C. H. 2011. The epigenotype. *International journal of epidemiology,* 41**,** 10-13.

WAHID, F., SHEHZAD, A., KHAN, T. & KIM, Y. Y. 2010. MicroRNAs: synthesis, mechanism, function, and recent clinical trials. *Biochimica et Biophysica Acta (BBA)-Molecular Cell Research,* 1803**,** 1231-1243.

WALLER, D. G. & SAMPSON, T. 2017. *Medical pharmacology and therapeutics E-Book*, Elsevier Health Sciences.

WALTER, W., CLYNES, D., TANG, Y., MARMORSTEIN, R., MELLOR, J. & BERGER, S. L. 2008. 14-3-3 interaction with histone H3 involves a dual modification pattern of phosphoacetylation. *Molecular and cellular biology,* 28**,** 2840-2849.

WANG, D., GARCIA-BASSETS, I., BENNER, C., LI, W., SU, X., ZHOU, Y., QIU, J., LIU, W., KAIKKONEN, M. U. & OHGI, K. A. 2011. Reprogramming transcription by distinct classes of enhancers functionally defined by eRNA. *Nature,* 474**,** 390.

WANG, D. & WANG, J. 2018. Neurophysiological effects of seminal vesicles. *Zhonghua nan ke xue= National journal of andrology,* 24**,** 360-363.

WANG, H.-J., POCHAMPALLI, M., WANG, L.-Y., ZOU, J. X., LI, P.-S., HSU, S.-C., WANG, B.-J., HUANG, S.-H., YANG, P. & YANG, J. C. 2019a. KDM8/JMJD5 as a dual coactivator of AR and PKM2 integrates AR/EZH2 network and tumor metabolism in CRPC. *Oncogene,* 38**,** 17.

WANG, H., WU, R., YU, L., WU, F., LI, S., ZHAO, Y., LI, H., LUO, G., WANG, J. & ZHOU, J. 2012. SGEF is overexpressed in prostate cancer and contributes to prostate cancer progression. *Oncology reports,* 28**,** 1468-1474.

WANG, J., HEVI, S., KURASH, J. K., LEI, H., GAY, F., BAJKO, J., SU, H., SUN, W., CHANG, H. & XU, G. 2009a. The lysine demethylase LSD1 (KDM1) is required for maintenance of global DNA methylation. *Nature genetics,* 41**,** 125.

WANG, J., SCULLY, K., ZHU, X., CAI, L., ZHANG, J., PREFONTAINE, G. G., KRONES, A., OHGI, K. A., ZHU, P. & GARCIA-BASSETS, I. 2007. Opposing LSD1 complexes function in developmental gene activation and repression programmes. *Nature,* 446**,** 882.

WANG, M., LIU, X., GUO, J., WENG, X., JIANG, G., WANG, Z. & HE, L. 2015. Inhibition of LSD1 by Pargyline inhibited process of EMT and delayed progression of prostate cancer in vivo. *Biochemical and biophysical research communications,* 467**,** 310-315.

WANG, M., ZHAO, J., ZHANG, L., WEI, F., LIAN, Y., WU, Y., GONG, Z., ZHANG, S., ZHOU, J. & CAO, K. 2017. Role of tumor microenvironment in tumorigenesis. *Journal of Cancer,* 8**,** 761.

WANG, R.-S., YEH, S., TZENG, C.-R. & CHANG, C. 2009b. Androgen receptor roles in spermatogenesis and fertility: lessons from testicular cell-specific androgen receptor knockout mice. *Endocrine reviews,* 30**,** 119-132.

WANG, S., KOLLIPARA, R. K., HUMPHRIES, C. G., MA, S.-H., HUTCHINSON, R., LI, R., SIDDIQUI, J., TOMLINS, S. A., RAJ, G. V. & KITTLER, R. 2016. The ubiquitin ligase TRIM25 targets ERG for degradation in prostate cancer. *Oncotarget,* 7**,** 64921.

WANG, W., YANG, X., DAI, J., LU, Y., ZHANG, J. & KELLER, E. T. 2019b. Prostate cancer promotes a vicious cycle of bone metastasis progression through inducing osteocytes to secrete GDF15 that stimulates prostate cancer growth and invasion. *Oncogene,* 38**,** 4540.

WANG, X., KRUITHOF-DE JULIO, M., ECONOMIDES, K. D., WALKER, D., YU, H., HALILI, M. V., HU, Y.-P., PRICE, S. M., ABATE-SHEN, C. & SHEN, M. M. 2009c. A luminal epithelial stem cell that is a cell of origin for prostate cancer. *Nature,* 461**,** 495.

WANG, X., PENG, J., YANG, Z., ZHOU, P.-J., AN, N., WEI, L., ZHU, H. H., LU, J., FANG, Y.-X. & GAO, W.-Q. 2019c. Elevated expression of Gab1 promotes breast cancer metastasis by dissociating the PAR complex. *Journal of Experimental & Clinical Cancer Research,* 38**,** 27.

WANG, Y., HAYWARD, S. W., CAO, M., THAYER, K. A. & CUNHA, G. R. 2001. Cell differentiation lineage in the prostate. *Differentiation,* 68**,** 270-279.

WANG, Y., ZHANG, H., CHEN, Y., SUN, Y., YANG, F., YU, W., LIANG, J., SUN, L., YANG, X. & SHI, L. 2009d. LSD1 is a subunit of the NuRD complex and targets the metastasis programs in breast cancer. *Cell,* 138**,** 660-672.

WANG, Z., GAO, S., HAN, D., HAN, W., LI, M. & CAI, C. 2019d. LSD1 activates PI3K/AKT signaling through regulating p85 expression in prostate cancer cells. *Frontiers in oncology,* 9**,** 721.

WANG, Z., HAN, G., LIU, Q., ZHANG, W. & WANG, J. 2018. Silencing of PYGB suppresses growth and promotes the apoptosis of prostate cancer cells via the NF-κB/Nrf2 signaling pathway. *Molecular medicine reports,* 18**,** 3800-3808.

WANG, Z. A., MITROFANOVA, A., BERGREN, S. K., ABATE-SHEN, C., CARDIFF, R. D., CALIFANO, A. & SHEN, M. M. 2013. Lineage analysis of basal epithelial cells reveals their unexpected plasticity and supports a cell-of-origin model for prostate cancer heterogeneity. *Nature cell biology,* 15**,** 274.

WANG, Z. A., TOIVANEN, R., BERGREN, S. K., CHAMBON, P. & SHEN, M. M. 2014. Luminal cells are favored as the cell of origin for prostate cancer. *Cell reports,* 8**,** 1339-1346.

WARD, R. D. & WEIGEL, N. L. 2009. Steroid receptor phosphorylation: Assigning function to site-specific phosphorylation. *Biofactors,* 35**,** 528-536.

WEBB, B. A., CHIMENTI, M., JACOBSON, M. P. & BARBER, D. L. 2011. Dysregulated pH: a perfect storm for cancer progression. *Nature Reviews Cancer,* 11**,** 671.

WEBER, M. J. & GIOELI, D. 2004. Ras signaling in prostate cancer progression. *Journal of cellular biochemistry,* 91**,** 13-25.

WEI, A., FAN, B., ZHAO, Y., ZHANG, H., WANG, L., YU, X., YUAN, Q., YANG, D. & WANG, S. 2016. ST6Gal-I overexpression facilitates prostate cancer progression via the PI3K/Akt/GSK-3β/β-catenin signaling pathway. *Oncotarget,* 7**,** 65374.

WEI, Q., COSTANZI, S., LIU, Q.-Z., GAO, Z.-G. & JACOBSON, K. A. 2011. Activation of the P2Y1 receptor induces apoptosis and inhibits proliferation of prostate cancer cells. *Biochemical pharmacology,* 82**,** 418-425.

WEICHERT, W., RÖSKE, A., GEKELER, V., BECKERS, T., STEPHAN, C., JUNG, K., FRITZSCHE, F., NIESPOREK, S., DENKERT, C. & DIETEL, M. 2008. Histone deacetylases 1, 2 and 3 are highly expressed in prostate cancer and HDAC2 expression is associated with shorter PSA relapse time after radical prostatectomy. *British journal of cancer,* 98**,** 604.

WEIKUM, E. R., LIU, X. & ORTLUND, E. A. 2018. The nuclear receptor superfamily: A structural perspective. *Protein Science,* 27**,** 1876-1892.

WELTI, J., RODRIGUES, D. N., SHARP, A., SUN, S., LORENTE, D., RIISNAES, R., FIGUEIREDO, I., ZAFEIRIOU, Z., RESCIGNO, P. & DE BONO, J. S. 2016. Analytical validation and clinical qualification of a new immunohistochemical assay for androgen receptor splice variant-7 protein expression in metastatic castration-resistant prostate cancer. *European urology,* 70**,** 599-608.

WESTPHAL, D., DEWSON, G., CZABOTAR, P. E. & KLUCK, R. M. 2011. Molecular biology of Bax and Bak activation and action. *Biochimica et Biophysica Acta (BBA)-Molecular Cell Research,* 1813**,** 521-531.

WHIRLEDGE, S. & CIDLOWSKI, J. A. 2019. Steroid Hormone Action. *Yen and Jaffe's Reproductive Endocrinology.* Elsevier.

WHITE, K. A., GRILLO-HILL, B. K. & BARBER, D. L. 2017. Cancer cell behaviors mediated by dysregulated pH dynamics at a glance. *J Cell Sci,* 130**,** 663-669.

WHITELAND, H., SPENCER-HARTY, S., MORGAN, C., KYNASTON, H., THOMAS, D. H., BOSE, P., FENN, N., LEWIS, P., JENKINS, S. & DOAK, S. H. 2014. A role for STEAP2 in prostate cancer progression. *Clinical & experimental metastasis,* 31**,** 909-920.

WILES, E. T. & SELKER, E. U. 2017. H3K27 methylation: a promiscuous repressive chromatin mark. *Current opinion in genetics & development,* 43**,** 31-37.

WILLEMS, E., DEDOBBELEER, M., DIGREGORIO, M., LOMBARD, A., LUMAPAT, P. N. & ROGISTER, B. 2018. The functional diversity of Aurora kinases: a comprehensive review. *Cell Division,* 13**,** 7.

WILLMANN, D., LIM, S., WETZEL, S., METZGER, E., JANDAUSCH, A., WILK, W., JUNG, M., FORNE, I., IMHOF, A. & JANZER, A. 2012. Impairment of prostate cancer cell growth by a selective and reversible lysine-specific demethylase 1 inhibitor. *International journal of cancer,* 131**,** 2704-2709.

WILSON, J. D. 2011. The critical role of androgens in prostate development. *Endocrinology and Metabolism Clinics,* 40**,** 577-590.

WILSON, J. D., HARROD, M. J., GOLDSTEIN, J. L., HEMSELL, D. L. & MACDONALD, P. C. 1974. Familial incomplete male pseudohermaphroditism, type 1: evidence for androgen resistance and variable clinical manifestations in a family with the Reifenstein syndrome. *New England Journal of Medicine,* 290**,** 1097-1103.

WINTER, S., SIMBOECK, E., FISCHLE, W., ZUPKOVITZ, G., DOHNAL, I., MECHTLER, K., AMMERER, G. & SEISER, C. 2008. 14-3-3 proteins recognize a histone code at histone H3 and are required for transcriptional activation. *The EMBO journal,* 27**,** 88-99.

WISE, S. C., BURMEISTER, L. A., ZHOU, X.-F., BUBULYA, A., OBERFIELD, J. L., BIRRER, M. J. & SHEMSHEDINI, L. 1998. Identification of domains of c-Jun mediating androgen receptor transactivation. *Oncogene,* 16**,** 2001.

WIŚNIEWSKI, J. R., ZOUGMAN, A. & MANN, M. 2007. N ε-formylation of lysine is a widespread post-translational modification of nuclear proteins occurring at residues involved in regulation of chromatin function. *Nucleic acids research,* 36**,** 570-577.

WISSMANN, M., YIN, N., MÜLLER, J. M., GRESCHIK, H., FODOR, B. D., JENUWEIN, T., VOGLER, C., SCHNEIDER, R., GÜNTHER, T. & BUETTNER, R. 2007. Cooperative demethylation by JMJD2C and LSD1 promotes androgen receptor-dependent gene expression. *Nature cell biology,* 9**,** 347.

WOODCOCK, C. Ultrastructure of inactive chromatin. Journal of Cell Biology, 1973. ROCKEFELLER UNIV PRESS 1114 FIRST AVE, 4TH FL, NEW YORK, NY 10021, A368-A368.

WU, C., MILOSLAVSKAYA, I., DEMONTIS, S., MAESTRO, R. & GALAKTIONOV, K. 2004. Regulation of cellular response to oncogenic and oxidative stress by Seladin-1. *Nature,* 432**,** 640.

WU, F. C., TAJAR, A., PYE, S. R., SILMAN, A. J., FINN, J. D., O'NEILL, T. W., BARTFAI, G., CASANUEVA, F., FORTI, G. & GIWERCMAN, A. 2008. Hypothalamic-pituitary-testicular axis disruptions in older men are differentially linked to age and modifiable risk factors: the European Male Aging Study. *The Journal of Clinical Endocrinology & Metabolism,* 93**,** 2737-2745.

WU, X., HEPNER, K., CASTELINO-PRABHU, S., DO, D., KAYE, M. B., YUAN, X.-J., WOOD, J., ROSS, C., SAWYERS, C. L. & WHANG, Y. E. 2000. Evidence for regulation of the PTEN tumor suppressor by a membrane-localized multi-PDZ domain containing scaffold protein MAGI-2. *Proceedings of the National Academy of Sciences,* 97**,** 4233-4238.

WUNDERLICH, F., BENTEN, W. P. M., LIEBERHERR, M., GUO, Z., STAMM, O., WREHLKE, C., SEKERIS, C. E. & MOSSMANN, H. 2002. Testosterone signaling in T cells and macrophages. *Steroids,* 67**,** 535-538.

XIANG, Y., ZHU, Z., HAN, G., YE, X., XU, B., PENG, Z., MA, Y., YU, Y., LIN, H. & CHEN, A. P. 2007. JARID1B is a histone H3 lysine 4 demethylase up-regulated in prostate cancer. *Proceedings of the National Academy of Sciences,* 104**,** 19226-19231.

XIAO, G.-Q., UNGER, P., YANG, Q., KINOSHITA, Y., SINGH, K., MCMAHON, L., NASTIUK, K., SHA, K., KROLEWSKI, J. & BURSTEIN, D. 2015. Loss of PLZF expression in prostate cancer by immunohistochemistry correlates with tumor aggressiveness and metastasis. *PloS one,* 10**,** e0121318.

XIE, G., LIU, X., ZHANG, Y., LI, W., LIU, S., CHEN, Z., XU, B., YANG, J., HE, L. & ZHANG, Z. 2017. UTX promotes hormonally responsive breast carcinogenesis through feed-forward transcription regulation with estrogen receptor. *Oncogene,* 36**,** 5497.

XIE, L., PELZ, C., WANG, W., BASHAR, A., VARLAMOVA, O., SHADLE, S. & IMPEY, S. 2011a. KDM5B regulates embryonic stem cell self-renewal and represses cryptic intragenic transcription. *The EMBO journal,* 30**,** 1473-1484.

XIE, Q., BAI, Y., WU, J., SUN, Y., WANG, Y., ZHANG, Y., MEI, P. & YUAN, Z. 2011b. Methylation-mediated regulation of E2F1 in DNA damage-induced cell death. *Journal of Receptors and Signal Transduction,* 31**,** 139-146.

XIE, Z., DAI, J., DAI, L., TAN, M., CHENG, Z., WU, Y., BOEKE, J. D. & ZHAO, Y. 2012. Lysine succinylation and lysine malonylation in histones. *Molecular & Cellular Proteomics,* 11**,** 100-107.

XU, J. & QIU, Y. 2019. Current opinion and mechanistic interpretation of combination therapy for castration-resistant prostate cancer. *Asian journal of andrology,* 21**,** 270.

XU, S., YUE, Y., ZHANG, S., ZHOU, C., CHENG, X., XIE, X., WANG, X. & LU, W. 2018. STON2 negatively modulates stem-like properties in ovarian cancer cells via DNMT1/MUC1 pathway. *Journal of Experimental & Clinical Cancer Research,* 37**,** 305.

XUE, Y., SMEDTS, F., DEBRUYNE, F. M., DE LA ROSETTE, J. J. & SCHALKEN, J. A. 1998. Identification of intermediate cell types by keratin expression in the developing human prostate. *The Prostate,* 34**,** 292-301.

YADAV, S. S., STOCKERT, J. A., HACKERT, V., YADAV, K. K. & TEWARI, A. K. Intratumor heterogeneity in prostate cancer. Urologic Oncology: Seminars and Original Investigations, 2018. Elsevier, 349-360.

YAM, L. T. 1974. Clinical significance of the human acid phosphatases: a review. *The American journal of medicine,* 56**,** 604-616.

YAMANE, K., TATEISHI, K., KLOSE, R. J., FANG, J., FABRIZIO, L. A., ERDJUMENT-BROMAGE, H., TAYLOR-PAPADIMITRIOU, J., TEMPST, P. & ZHANG, Y. 2007. PLU-1 is an H3K4 demethylase involved in transcriptional repression and breast cancer cell proliferation. *Molecular cell,* 25**,** 801-812.

YAN, M., QI, H., LI, J., YE, G., SHAO, Y., LI, T., LIU, J., PIAO, H.-L. & XU, G. 2017. Identification of SPOP related metabolic pathways in prostate cancer. *Oncotarget,* 8**,** 103032.

YANG, C., FISCHER-KEŠO, R., SCHLECHTER, T., STRÖBEL, P., MARX, A. & HOFMANN, I. 2015a. Plakophilin 1-deficient cells upregulate SPOCK1: implications for prostate cancer progression. *Tumor Biology,* 36**,** 9567-9577.

YANG, C., QIU, L. & XU, Z. 2011. Specific gene silencing using RNAi in cell culture. *Neurodegeneration.* Springer.

YANG, G.-J., LEI, P.-M., WONG, S.-Y., MA, D.-L. & LEUNG, C.-H. 2018. Pharmacological inhibition of LSD1 for cancer treatment. *Molecules,* 23**,** 3194.

YANG, L., XIE, S., JAMALUDDIN, M. S., ALTUWAIJRI, S., NI, J., KIM, E., CHEN, Y.-T., HU, Y.-C., WANG, L. & CHUANG, K.-H. 2005. Induction of androgen receptor expression by

phosphatidylinositol 3-kinase/Akt downstream substrate, FOXO3a, and their roles in apoptosis of LNCaP prostate cancer cells. *Journal of Biological Chemistry,* 280**,** 33558-33565.

YANG, S., ZHANG, J., ZHANG, Y., WAN, X., ZHANG, C., HUANG, X., HUANG, W., PU, H., PEI, C. & WU, H. 2015b. KDM1A triggers androgen-induced miRNA transcription via H3K4me2 demethylation and DNA oxidation. *The Prostate,* 75**,** 936-946.

YANG, X., WANG, G., WANG, Y., ZHOU, J., YUAN, H., LI, X., LIU, Y. & WANG, B. 2019. Histone demethylase KDM7A reciprocally regulates adipogenic and osteogenic differentiation via regulation of C/EBPα and canonical Wnt signalling. *Journal of cellular and molecular medicine,* 23**,** 2149-2162.

YANG, Y., HU, L., WANG, P., HOU, H., LIN, Y., LIU, Y., LI, Z., GONG, R., FENG, X. & ZHOU, L. 2010. Structural insights into a dual-specificity histone demethylase ceKDM7A from Caenorhabditis elegans. *Cell research,* 20**,** 886.

YE, W., QIN, F., ZHANG, J., LUO, R. & CHEN, H.-F. 2012. Atomistic mechanism of microRNA translation upregulation via molecular dynamics simulations. *PloS one,* 7**,** e43788.

YEH, S., LIN, H.-K., KANG, H.-Y., THIN, T. H., LIN, M.-F. & CHANG, C. 1999. From HER2/Neu signal cascade to androgen receptor and its coactivators: a novel pathway by induction of androgen target genes through MAP kinase in prostate cancer cells. *Proceedings of the National Academy of Sciences,* 96**,** 5458-5463.

YEH, S., TSAI, M.-Y., XU, Q., MU, X.-M., LARDY, H., HUANG, K.-E., LIN, H., YEH, S.-D., ALTUWAIJRI, S. & ZHOU, X. 2002. Generation and characterization of androgen receptor knockout (ARKO) mice: an in vivo model for the study of androgen functions in selective tissues. *Proceedings of the National Academy of Sciences,* 99**,** 13498-13503.

YOKOTA, K., SATOU, K. & OHKI, S.-Y. 2006. Comparative analysis of protein thermostability: Differences in amino acid content and substitution at the surfaces and in the core regions of thermophilic and mesophilic proteins. *Science and Technology of Advanced Materials,* 7**,** 255.

YOKOYAMA, A., OKUNO, Y., CHIKANISHI, T., HASHIBA, W., SEKINE, H., FUJIKI, R. & KATO, S. 2010. KIAA1718 is a histone demethylase that erases repressive histone methyl marks. *Genes to Cells,* 15**,** 867-873.

YOSHIDA, K., KAWANO, N., YOSHIIKE, M., YOSHIDA, M., IWAMOTO, T. & MORISAWA, M. 2008. Physiological roles of semenogelin I and zinc in sperm motility and semen coagulation on ejaculation in humans. *MHR: Basic science of reproductive medicine,* 14**,** 151-156.

YOU, A., TONG, J. K., GROZINGER, C. M. & SCHREIBER, S. L. 2001. CoREST is an integral component of the CoREST-human histone deacetylase complex. *Proceedings of the National Academy of Sciences,* 98**,** 1454-1458.

YU, Z., CAI, C., GAO, S., SIMON, N. I., SHEN, H. C. & BALK, S. P. 2014. Galeterone prevents androgen receptor binding to chromatin and enhances degradation of mutant androgen receptor. *Clinical Cancer Research,* 20**,** 4075-4085.

YUAN, C., LI, Z., QI, B., ZHANG, W., CHENG, J. & WANG, Y. 2015. High expression of the histone demethylase LSD 1 associates with cancer cell proliferation and unfavorable prognosis in tongue cancer. *Journal of Oral Pathology & Medicine,* 44**,** 159-165.

YUAN, T.-C., VEERAMANI, S. & LIN, M.-F. 2007. Neuroendocrine-like prostate cancer cells: neuroendocrine transdifferentiation of prostate adenocarcinoma cells. *Endocrine-related cancer,* 14**,** 531-547.

YUAN, X., CAI, C., CHEN, S., YU, Z. & BALK, S. 2014. Androgen receptor functions in castration-resistant prostate cancer and mechanisms of resistance to new agents targeting the androgen axis. *Oncogene,* 33**,** 2815.

ZARATIEGUI, M., IRVINE, D. V. & MARTIENSSEN, R. A. 2007. Noncoding RNAs and gene silencing. *Cell,* 128**,** 763-776.

ZHANG, D., ZHAO, S., LI, X., KIRK, J. S. & TANG, D. G. 2018a. Prostate luminal progenitor cells in development and cancer. *Trends in cancer*.

ZHANG, H., DONG, Y., ZHAO, H., BROOKS, J. D., HAWTHORN, L., NOWAK, N., MARSHALL, J. R., GAO, A. C. & IP, C. 2005. Microarray data mining for potential selenium targets in chemoprevention of prostate cancer. *Cancer Genomics-Proteomics,* 2**,** 97-113.

ZHANG, H., HUANG, C.-J., TIAN, Y., WANG, Y.-P., HAN, Z.-G. & LI, X.-C. 2012. Ectopic overexpression of COTE1 promotes cellular invasion of hepatocellular carcinoma. *Asian Pacific Journal of Cancer Prevention,* 13**,** 5799-5804.

ZHANG, H., TIAN, Y., SHEN, J., WANG, Y., XU, Y., WANG, Y., HAN, Z. & LI, X. 2014a. Upregulation of the putative oncogene COTE1 contributes to human hepatocarcinogenesis through modulation of WWOX signaling. *International journal of oncology,* 45**,** 719-731.

ZHANG, L., HUI, T.-L., WEI, Y.-X., CAO, Z.-M., FENG, F., REN, G.-S. & LI, F. 2018b. The expression and biological function of the PHF2 gene in breast cancer. *RSC advances,* 8**,** 39520-39528.

ZHANG, W. & LIU, H. T. 2002. MAPK signal pathways in the regulation of cell proliferation in mammalian cells. *Cell research,* 12**,** 9.

ZHANG, Y.-L., DING, C. & SUN, L. 2019. High expression B3GAT3 is related with poor prognosis of liver cancer. *Open Medicine,* 14**,** 251-258.

ZHANG, Y., LIANG, J. & LI, Q. 2014b. Coordinated regulation of retinoic acid signaling pathway by KDM5B and polycomb repressive complex 2. *Journal of cellular biochemistry,* 115**,** 1528-1538.

ZHANG, Y., YANG, H., GUO, X., RONG, N., SONG, Y., XU, Y., LAN, W., ZHANG, X., LIU, M. & XU, Y. 2014c. The PHD1 finger of KDM5B recognizes unmodified H3K4 during the demethylation of histone H3K4me2/3 by KDM5B. *Protein & cell,* 5**,** 837-850.

ZHAO, L. & LIU, H. 2015. Immunohistochemical detection and clinicopathological significance of JARID1B/KDM5B and P16 expression in invasive ductal carcinoma of the breast. *Genet Mol Res,* 14**,** 5417.

ZHAO, X.-Y., MALLOY, P. J., KRISHNAN, A. V., SWAMI, S., NAVONE, N. M., PEEHL, D. M. & FELDMAN, D. 2000. Glucocorticoids can promote androgen-independent growth of prostate cancer cells through a mutated androgen receptor. *Nature medicine,* 6**,** 703.

ZHAO, Y. & GARCIA, B. A. 2015. Comprehensive catalog of currently documented histone modifications. *Cold Spring Harbor perspectives in biology,* 7**,** a025064.

ZHAO, Z.-K., YU, H.-F., WANG, D.-R., DONG, P., CHEN, L., WU, W.-G., DING, W.-J. & LIU, Y.-B. 2012. Overexpression of lysine specific demethylase 1 predicts worse prognosis in primary hepatocellular carcinoma patients. *World Journal of Gastroenterology: WJG,* 18**,** 6651.

ZHOU, X. 2010. Roles of androgen receptor in male and female reproduction: lessons from global and cell-specific androgen receptor knockout (ARKO) mice. *Journal of andrology,* 31**,** 235-243.

ZHOU, Z., KEMPPAINEN, J. A. & WILSON, E. M. 1995. Identification of three proline-directed phosphorylation sites in the human androgen receptor. *Molecular Endocrinology,* 9**,** 605-615.

ZHOU, Z., SAR, M., SIMENTAL, J. A., LANE, M. V. & WILSON, E. M. 1994. A ligand-dependent bipartite nuclear targeting signal in the human androgen receptor. Requirement for the DNA-binding domain and modulation by NH2-terminal and carboxyl-terminal sequences. *Journal of Biological Chemistry,* 269**,** 13115-13123.

ZHU, D.-Q., LOU, Y.-F., HE, Z.-G. & JI, M. 2014. Nucleotidyl transferase TUT1 inhibits lipogenesis in osteosarcoma cells through regulation of microRNA-24 and microRNA-29a. *Tumor Biology,* 35**,** 11829-11835.

ZONG, Y. & GOLDSTEIN, A. S. 2013. Adaptation or selection—mechanisms of castration-resistant prostate cancer. *Nature Reviews Urology,* 10**,** 90.

ZOU, M. R., CAO, J., LIU, Z., HUH, S. J., POLYAK, K. & YAN, Q. 2014. Histone demethylase jumonji AT-rich interactive domain 1B (JARID1B) controls mammary gland development by regulating key developmental and lineage specification genes. *Journal of Biological Chemistry,* 289**,** 17620-17633.

ZUCCARELLO, D., FERLIN, A., VINANZI, C., PRANA, E., GAROLLA, A., CALLEWAERT, L., CLAESSENS, F., BRINKMANN, A. & FORESTA, C. 2008. Detailed functional studies on androgen receptor mild mutations demonstrate their association with male infertility. *Clinical endocrinology,* 68**,** 580-588.

ZUCKERMAN, V., SOKOLOV, E., SWET, J. H., AHRENS, W. A., SHOWLATER, V., IANNITTI, D. A. & MCKILLOP, I. H. 2016. Expression and function of lysophosphatidic acid receptors (LPARs) 1 and 3 in human hepatic cancer progenitor cells. *Oncotarget,* 7**,** 2951.

Appendix 1 – TMA patient database

Table i: Clinical parameters of PCa TMA.
The TMA patient database included 104 patients. The number of patients in each group within the parameters is given. PSA = prostate specific antigen; PIN = prostate intraepithelial neoplasia; TNM = tumour, node, metastasis; NTF = never tumour free.

Parameters	Number of patients				
Age (years)	<60	≥60			
	44	60			
Ethnicity	White	Mixed/Black Carribean	Any other	N/A	
	94	2	2	6	
Pre-OP PSA (ng/mL)	≤10	>10	N/A		
	55	46	3		
High grade PIN	No	Yes			
	32	72			
Perineural invasion	No	Yes			
	32	72			
Gleason	3+3	3+4	4+3	8 or 9	N/A
	12	46	22	23	1
Positive surgical margin	No	Yes	N/A		
	55	47	2		
Extraprostatic extension	No	Yes	N/A		
	66	36	2		
TNM	T1, T2	T3	N/A		
	66	33	5		
Lymph nodes examined	No	Yes			
	76	28			
Lymph nodes with disease	No	Yes			
	27	1			
Biochemical recurrence (BCR)	No	Yes	NTF		
	59	33	12		
Time for BCR to occur (years)	≤2	>2			
	15	18			
Alive/dead status	Alive	dead			
	92	12			

Appendix 2 – TMA maps

Table ii: TMA map for coring.

The TMA map contained 166 cores, including 2x three cores at the top (liver) and at the bottom (tonsil) of the block as orientation cores. The orange highlighted fields represented cores for tumour tissue (104 cores) and the green highlighted ones were cores for normal tissue (56 cores).

	X1	X2	X3	X4	X5	X6	X7	X8	X9	X10
Y1	Liver	Liver	Liver							
Y2	001	002	003	004	005	006	007	008	009	011
Y3	012	013	014	015	016	017	018	019	020	021
Y4	023	024	025	026	027	028	029	030	031	032
Y5	033	034	035	036	037	038	039	040	041	043
Y6	045	046	047	048	049	050	052	053	054	056
Y7	057	059	061	062	063	064	065	066	067	068
Y8										
Y9	069	070	071	072	073	074	075	077	078	079
Y10	080	081	082	083	084	085	086	087	088	090
Y11	091	092	093	094	095	096	097	098	099	100
Y12	101	102	104	105	106	107	108	109	110	111
Y13	112	113	114	115	001N	007N	008N	009N	011N	013N
Y14										
Y15	017N	018N	019N	020N	023N	024N	025N	029N	031N	033N
Y16	035N	036N	037N	038N	039N	040N	043N	047N	050N	052N
Y17	054N	057N	062N	064N	066N	068N	072N	073N	074N	075N
Y18	077N	078N	079N	082N	083N	084N	085N	092N	094N	096N
Y19	097N	098N	099N	101N	104N	105N	107N	108N	112N	113N
Y20	Tonsil	Tonsil	Tonsil							

Table iii: TMA map VM1.

The first TMA contained 90 tumour cores, 50 normal cores, 13 missing cores and 7 stroma cores. T = tumour tissue, N = normal tissue, M = missing core, S = stroma tissue only.

VM1	X1	X2	X3	X4	X5	X6	X7	X8	X9	X10
Y1	Liver	Liver	Liver							
Y2	T	T	T	T	T	T	T	N	M	M
Y3	T	M	N	S	T	T	T	T	T	T
Y4	T	T	T	T	T	T	T	T	T	T
Y5	T	T	T	S	T	T	T	T	T	T
Y6	T	T	N	T	T	T	T	T	T	T
Y7	T	T	T	T	T	T	T	T	T	T
Y8										
Y9	T	T	T	T	T	T	T	T	T	T
Y10	T	T	T	N	T	M	T	N	T	T
Y11	T	T	T	N	T	T	T	T	N	S
Y12	T	T	T	T	T	T	T	T	T	S
Y13	T	T	T	T	N	N	N	N	N	N
Y14										
Y15	N	N	M	M	N	N	N	M	S	T
Y16	N	N	N	N	S	N	M	N	N	N
Y17	N	N	M	N	N	N	N	M	M	S
Y18	N	N	N	N	N	N	N	N	N	N
Y19	N	M	N	N	N	N	N	N	N	M
Y20	Tonsil	Tonsil	Tonsil							

Table iv: TMA map VM2.

The second TMA included 86 tumour cores, 58 normal cores, 14 missing cores and 2 stroma cores. N = normal tissue, M = missing core, S = stroma tissue only.

VM2	X1	X2	X3	X4	X5	X6	X7	X8	X9	X10
Y1	Liver	Liver	Liver							
Y2	T	T	T	N	T	T	T	N	M	T
Y3	M	M	M	M	T	T	M	T	T	T
Y4	M	M	M	T	N	T	T	T	T	T
Y5	M	M	T	T	M	T	T	T	T	T
Y6	T	T	T	T	T	T	T	T	T	T
Y7	T	T	T	T	T	T	T	T	T	T
Y8										
Y9	T	T	T	T	T	S	T	T	T	T
Y10	T	T	T	T	T	M	T	N	T	T
Y11	T	T	T	T	T	T	T	T	T	S
Y12	T	T	T	T	T	T	T	T	T	T
Y13	T	T	T	T	N	N	N	N	N	N
Y14										
Y15	N	N	N	N	N	N	N	N	N	T
Y16	N	N	N	N	N	N	N	N	N	N
Y17	N	N	N	N	N	N	N	N	N	M
Y18	N	N	N	N	N	N	N	N	N	N
Y19	N	N	N	N	N	N	N	N	N	N
Y20	Tonsil	Tonsil	Tonsil							

Table v: TMA map VM3.

The third TMA included 93 tumour cores, 50 normal cores and 17 missing cores. N = normal tissue, M = missing core.

VM3	X1	X2	X3	X4	X5	X6	X7	X8	X9	X10
Y1	Liver	Liver	Liver							
Y2	T	M	T	T	T	T	T	M	M	T
Y3	M	M	N	T	M	T	T	T	T	T
Y4	T	T	T	T	N	T	T	T	T	T
Y5	T	T	T	T	T	T	T	T	T	T
Y6	T	T	N	T	T	T	T	T	T	T
Y7	T	T	T	T	T	T	T	T	T	T
Y8										
Y9	T	T	T	T	T	T	T	T	T	T
Y10	T	T	T	N	T	M	T	N	T	T
Y11	T	T	T	T	T	T	T	T	T	T
Y12	T	T	T	T	T	T	T	T	T	T
Y13	T	T	T	T	N	M	N	N	N	N
Y14										
Y15	N	M	N	N	N	N	N	T	N	N
Y16	N	N	M	N	N	N	N	N	N	N
Y17	N	N	N	M	N	N	M	M	N	N
Y18	N	N	N	N	N	T	N	N	N	N
Y19	N	N	N	M	M	N	M	N	N	M
Y20	Tonsil	Tonsil	Tonsil							

Table vi: TMA map VM4.

The fourth TMA included 97 tumour cores, 51 normal cores, 6 missing cores and 6 stroma cores. N = normal tissue, M = missing core, S = stroma core.

VM4	X1	X2	X3	X4	X5	X6	X7	X8	X9	X10
Y1	Liver	Liver	Liver							
Y2	T	T	T	M	T	T	T	T	T	T
Y3	T	T	T	N	T	T	T	T	T	T
Y4	T	T	T	T	N	T	T	T	T	T
Y5	T	T	T	T	T	T	T	T	T	T
Y6	T	T	T	T	N	T	T	T	T	T
Y7	T	T	T	T	T	T	T	T	T	T
Y8										
Y9	T	T	T	T	T	T	T	T	T	T
Y10	T	T	T	N	T	T	T	N	T	T
Y11	T	T	T	N	S	N	T	T	T	S
Y12	T	T	T	T	T	T	T	T	T	T
Y13	T	T	T	T	N	N	N	N	N	N
Y14										
Y15	N	N	T	T	N	N	N	N	N	S
Y16	N	N	S	N	T	N	N	N	M	N
Y17	N	N	N	N	N	N	N	M	N	S
Y18	N	N	N	N	N	N	N	N	N	N
Y19	N	N	M	N	S	N	N	N	M	M
Y20	Tonsil	Tonsil	Tonsil							

Appendix 3 – Protein ladders for western blots

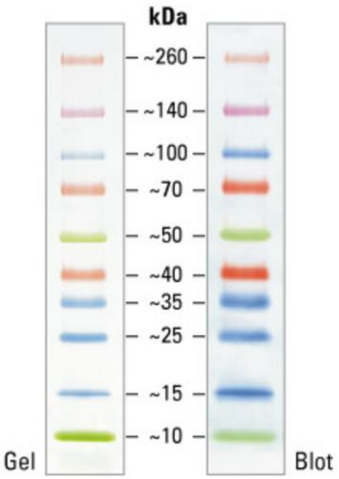

Figure i: Protein ladder used for western blot analysis in human cells.
Thermo Scientific Spectra Multicolor Broad Range Protein Ladder, #26624, Thermo Fisher Scientific.

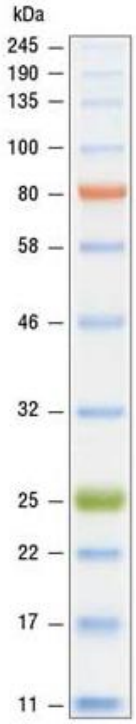

Figure ii: Protein ladder used for western blot analysis in yeast cells.
Color Protein Standard Broad Range, #87712S, New England Biolabs® Inc.

Appendix 4 – Validation of TMA patient database

Table vii: Validation of TMA patient database by correlating clinical data.
Clinical relevant patient parameters were correlated with each other to validate the tissue microarray (TMA) patient database. The parameters included Age, Gleason Score, Pathologic TNM (tumour, node, metastasis) stage, High grade prostate intraepithelial neoplasia (PIN), Extraprostatic extension, Perineural invasion, Pre-OP PSA and Biochemical recurrence (BCR). Gleason 4 groups, 1 = Gleason 3+3, 2 = Gleason 3+4, 3 = Gleason 4+3, 4 = Gleason 8 & 9; Gleason 2 groups, 1 = Gleason 3+3 & 3+4, 2 = Gleason 4+3 & 8 & 9. Statistical p-values were evaluated by χ^2-test and $p \leq 0.05$ were highlighted in grey in table.

	Age	Path. TNM	High grade PIN	Extra-prostatic ext.	Peri-neural inv.	Pre-OP PSA	BCR
Age		0.062	0.113	0.080	0.530	0.148	0.316
Gleason 4 groups	0.197	**0.001**	0.793	**0.001**	**0.001**	0.188	0.108
Gleason 2 groups	**0.036**	**0.000**	0.506	**0.000**	**0.010**	0.083	**0.023**
Pathologic TNM	0.062		0.669	**0.000**	**0.000**	**0.020**	**0.003**
High grad PIN	0.113	0.669		0.522	0.222	0.064	0.120
Extraprostatic ext.	0.080	**0.000**	0.522		**0.000**	0.115	**0.000**
Perineural invasion	0.530	**0.000**	0.222	**0.000**		0.559	0.240
Pre-OP PSA	0.148	**0.020**	0.064	0.115	0.559		0.969
BCR	0.316	**0.003**	0.120	**0.000**	0.240	0.969	

Appendix 5 – Distribution curve of KDM5B staining

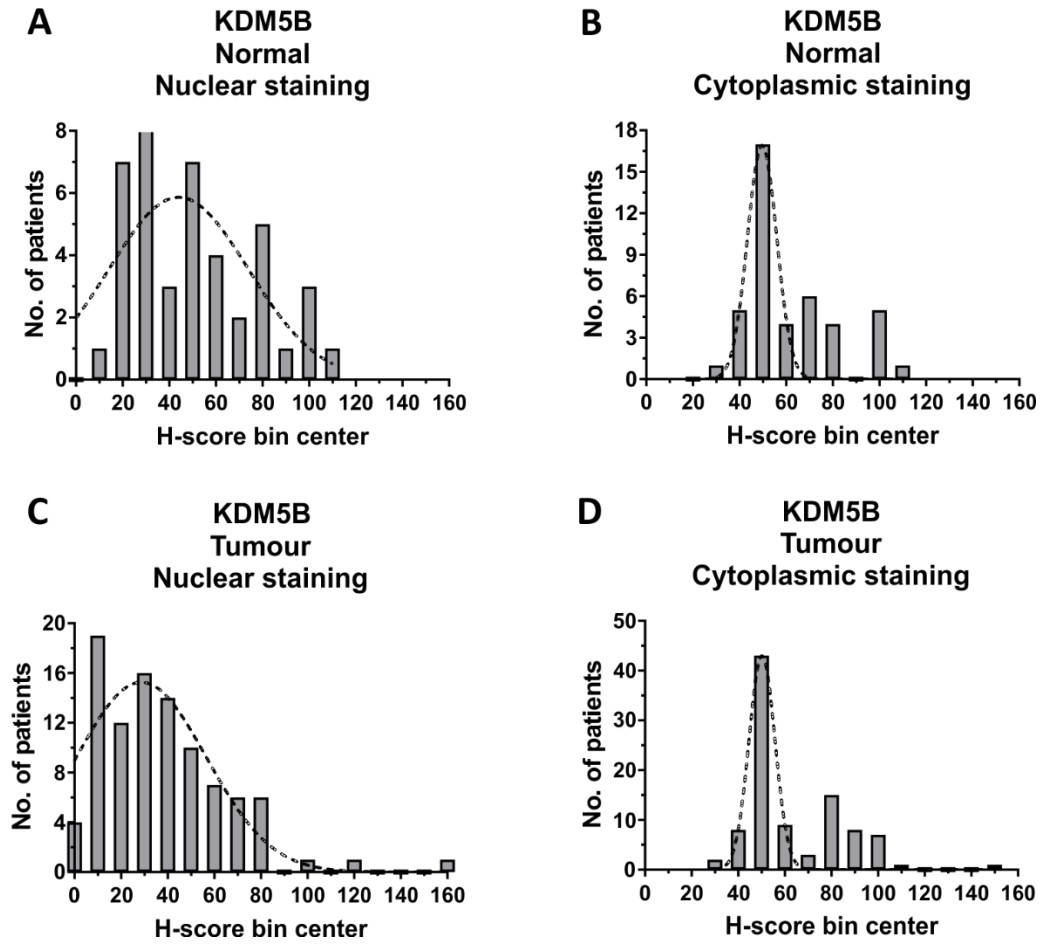

Figure iii: Distribution curve of KDM5B staining.
KDM5B nuclear (A, C) and cytoplasmic (B, D) staining in normal (A, B) and tumour (C, D) tissue. The distribution of KDM5B staining is expressed in H-score bin centers and the number of patients in each bin center given.

Appendix 6 – Correlating KDM5B staining with clinical data

Table viii: Correlation of KDM5B staining with clinical data.
Both KDM5B nuclear and cytoplasmic staining was correlated with clinical relevant patient parameters. Gleason 4 groups, 1 = Gleason 3+3, 2 = Gleason 3+4, 3 = Gleason 4+3, 4 = Gleason 8 & 9; Gleason 3 groups, 1 = Gleason 6, 2 = Gleason 7, 3 = Gleason 8 & 9; Gleason 2 groups, 1 = Gleason 3+3 & 3+4, 2 = Gleason 4+3 & 8 & 9; TNM = tumour, node, metastasis; PIN = prostate intraepithelial neoplasia; PSA = prostate specific antigen; BCR = biochemical recurrence. Statistical p-values were determined by χ^2-test and $p \leq 0.05$ was highlighted grey in table.

	Nuclear staining			Cytoplasmic staining		
	4 groups	3 groups	2 groups	4 groups	3 groups	2 groups
Age	0.516	0.293	0.280	0.672	0.496	0.374
Gleason 4 groups	0.319	0.257	0.750	0.722	0.657	0.287
Gleason 3 groups	0.535	0.123	0.706	0.795	0.573	0.275
Gleason 2 groups	0.241	0.317	0.946	0.662	0.592	0.306
TNM	0.024	0.018	1.000	0.779	0.780	0.745
High grade PIN	0.129	0.609	0.112	0.592	0.914	0.868
Extraprostatic extension	0.034	0.018	0.805	0.771	0.851	0.736
Perineural invasion	0.954	0.556	0.500	0.654	0.494	0.478
Pre-OP PSA	0.287	0.795	0.423	0.981	0.948	0.887
BCR	0.770	0.895	0.431	0.452	0.410	0.346
Time for BCR to occur	0.847	0.486	0.713	0.522	1.000	1.000
Cytopl. staining 4 groups	0.337	0.614	0.135			
Cytopl. staining 3 groups	0.265	0.622	0.160			
Cytopl. staining 2 groups	0.182	0.416	0.056			

Appendix 7 – Confirmation of KDM5B knockdown

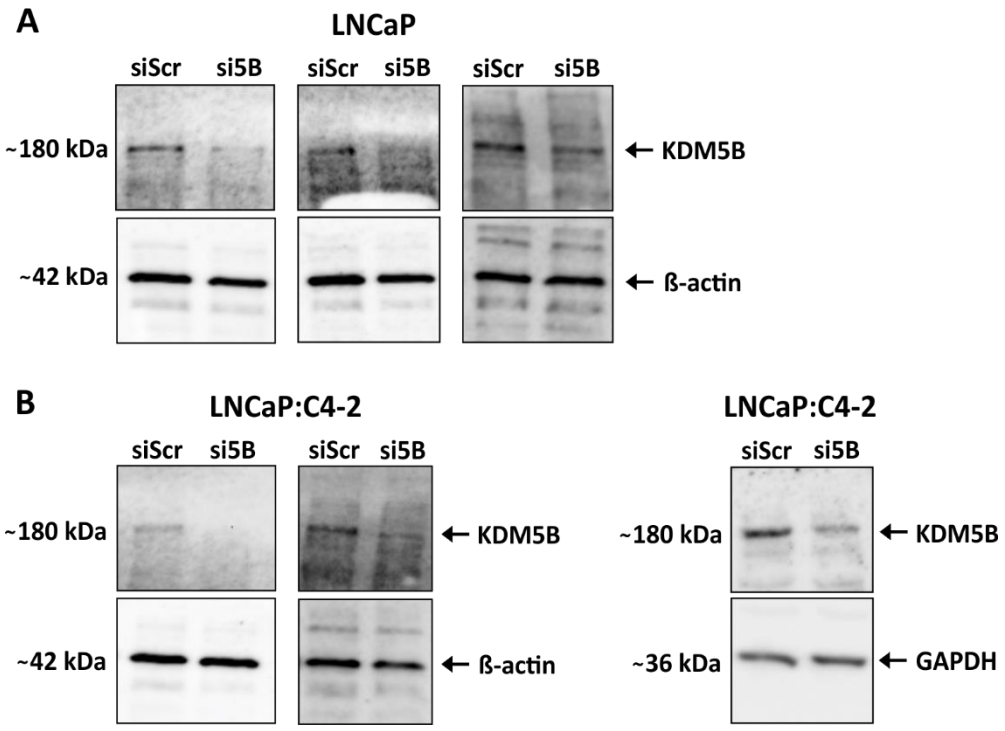

Figure iv: Confirmation of siRNA-mediated knockdown of KDM5B in LNCaP and LNCaP:C4-2.
Western blot analysis was performed with n = 3. Both in LNCaP (**A**) and LNCaP:C4-2 (**B**) the band was weaker in the siKDM5B lane compared to the siScramble control lane.

Appendix 8 – Distribution curve of KDM7A staining

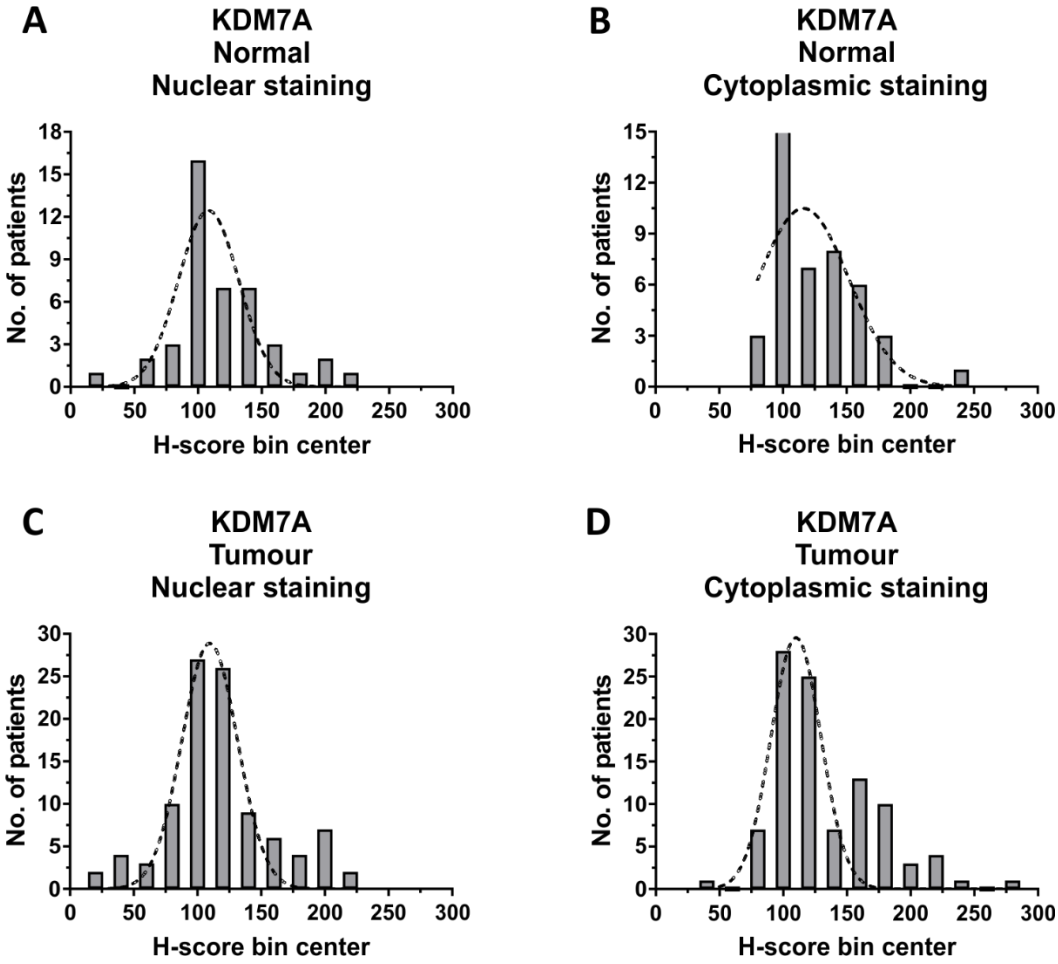

Figure v: Distribution curve of KDM7A staining.

KDM7A nuclear (A, C) and cytoplasmic (B, D) staining in normal (A, B) and tumour (C, D) tissue. The distribution of KDM7A staining is expressed as H-score bin centers and the number of patients in each bin center is depicted.

Appendix 9 – Correlating KDM7A staining with clinical data

Table ix: Correlation of KDM7A staining with clinical data.
KDM7A nuclear and cytoplasmic staining was correlated with clinical patient parameters. Gleason 4 groups, 1 = Gleason 3+3, 2 = Gleason 3+4, 3 = Gleason 4+3, 4 = Gleason 8 & 9; Gleason 3 groups, 1 = Gleason 6, 2 = Gleason 7, 3 = Gleason 8 & 9; Gleason 2 groups, 1 = Gleason 3+3 & 3+4, 2 = Gleason 4+3 & 8 & 9; TNM = tumour, node, metastasis; PIN = prostate intraepithelial neoplasia; PSA = prostate specific antigen; BCR = biochemical recurrence. Statistical p-values were calculated by χ^2-test and $p \leq 0.05$ was highlighted grey in table.

	Nuclear staining			Cytoplasmic staining		
	4 groups	3 groups	2 groups	4 groups	3 groups	2 groups
Age	0.225	0.153	0.177	0.197	0.873	1.000
Gleason 4 groups	0.236	0.608	0.876	0.113	0.107	0.172
Gleason 3 groups	0.209	0.410	0.924	0.702	0.814	0.767
Gleason 2 groups	0.045	0.494	0.616	0.107	0.058	0.044
TNM	0.529	0.344	0.859	0.577	0.261	0.568
High grade PIN	0.564	0.757	0.477	0.099	0.236	0.687
Extraprostatic extension	0.622	0.463	0.644	0.488	0.283	0.675
Perineural invasion	0.772	0.574	0.748	0.935	0.438	0.517
Pre-OP PSA	0.882	0.887	0.810	0.647	0.842	0.606
BCR	0.437	0.643	0.407	0.857	0.549	0.803
Time for BCR to occur	0.251	0.373	0.169	0.268	0.901	0.265
Cytoplasmic staining 4 groups	0.000	0.000	0.000			
Cytoplasmic staining 3 groups	0.000	0.000	0.000			
Cytoplasmic staining 2 groups	0.000	0.000	0.000			

Appendix 10 – Confirmation of KDM7A knockdown

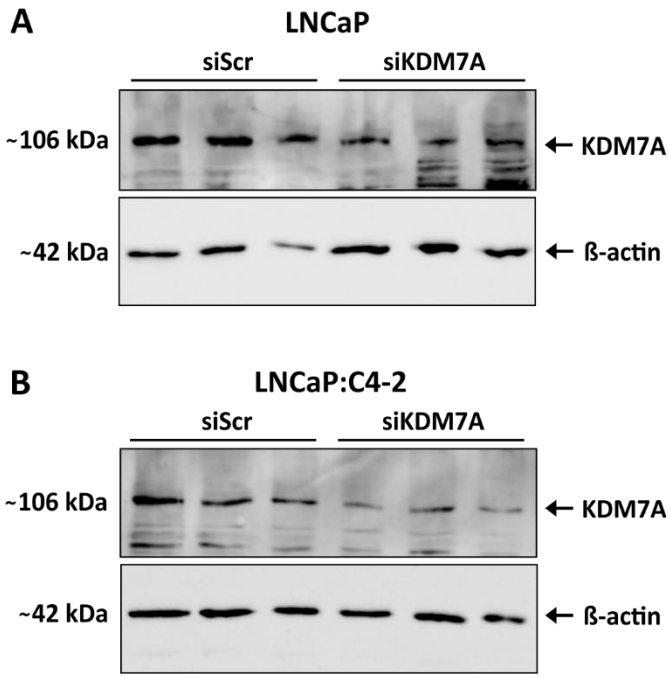

Figure vi: Confirmation of siRNA-mediated knockdown of KDM7A in LNCaP and LNCaP:C4-2.
Western blot analysis was performed with n = 3. Both in LNCaP (**A**) and LNCaP:C4-2 (**B**) the bands were weaker in the siKDM5B lanes compared to the siScramble control lanes.

Appendix 11 – Daminozide dose curve

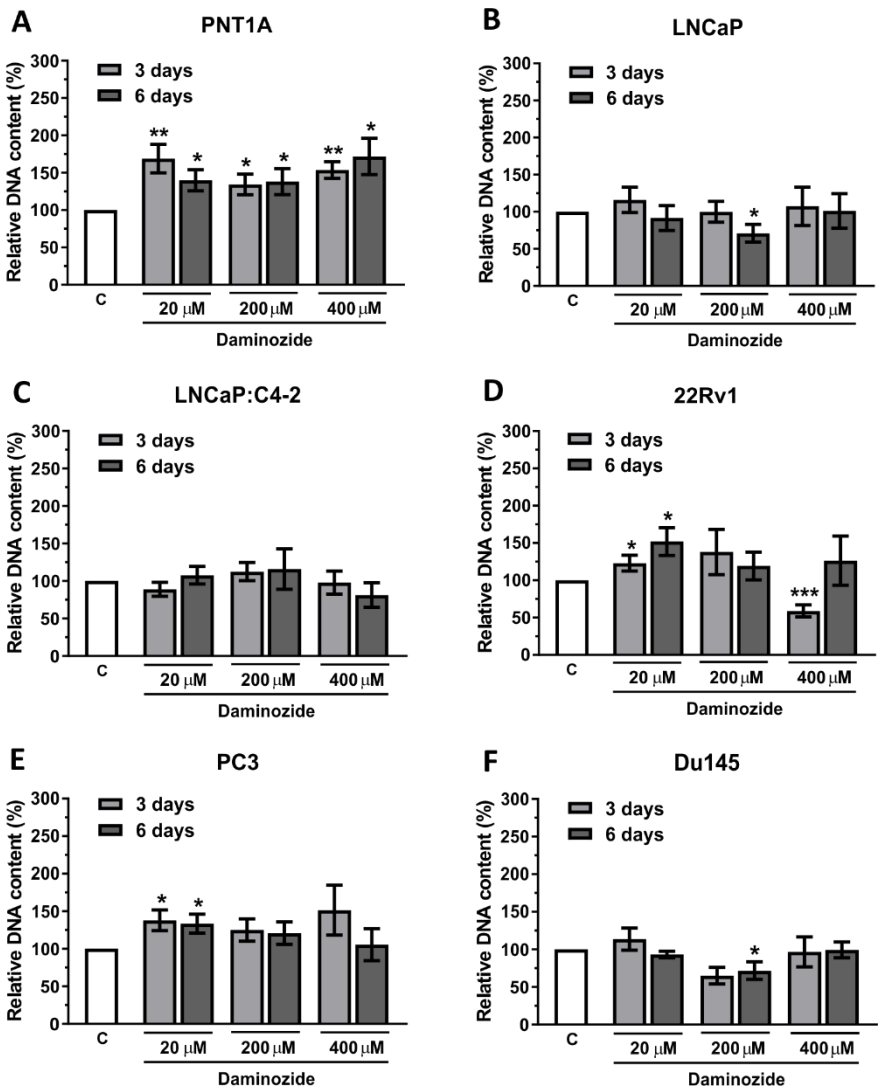

Figure vii: Dose curve of Daminozide on normal prostate and PCa cell proliferation.
Cell proliferation was assessed using the CyQUANT™ assay. (**A**) Daminozide increased cell proliferation in PNT1A at any concentration after 3 and 6 days. (**B**) Proliferation in LNCaP cells was not affected by Daminozide except at 200 µM after 6 days. (**C**) LNCaP:C4-2 cell proliferation did not change upon Daminozide treatment. (**D**) 22Rv1 proliferated more at 20 µM Daminozide, but less at 400 µM after 3 days compared to control cells. (**E**) PC3 cell proliferation was increased by 20 µM Daminozide but at higher Daminozide concentrations no effect was detected. (**F**) In Du145, Daminozide inhibited proliferation at 200 µM after 6 days but not at 400 µM. * = $p \leq 0.05$, ** = $p \leq 0.005$, *** = $p \leq 0.001$, **** = $p \leq 0.0001$ by paired t-test.

Appendix 12 – TC-E 5002 dose curve

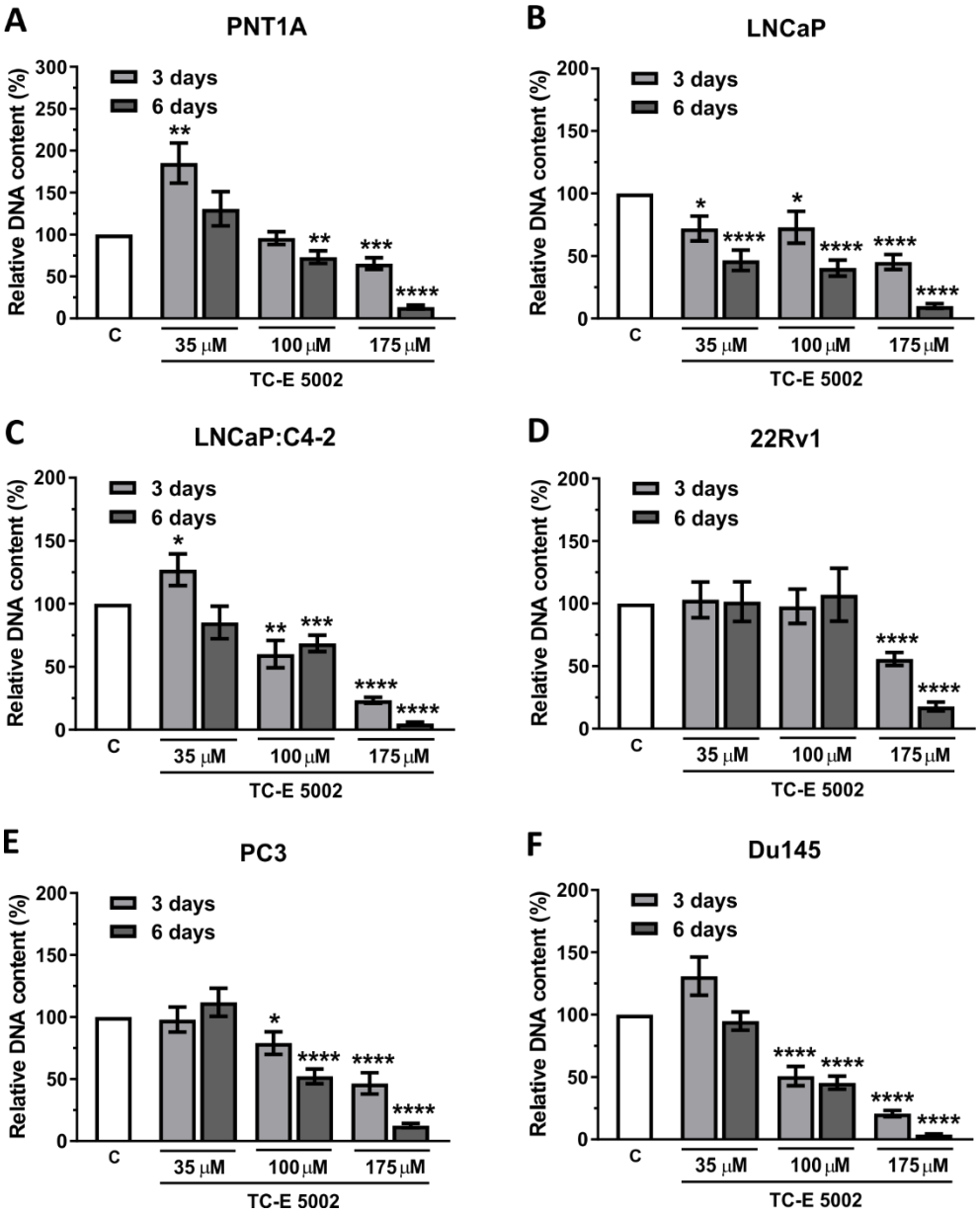

Figure viii: Dose curve of TC-E 5002 on normal prostate and PCa cell proliferation.

The CyQUANT™ assay was used to examine cell proliferation. (**A**) In PNT1A, cell proliferation was increased by 35 μM TC-E 5002 but decreased at higher concentrations. (**B**) LNCaP cell proliferation was reduced by any TC-E 5002 concentration with the strongest effect at 175 μM after 6 days. (**C**) TC-E 5002 did not inhibit LNCaP:C4-2 cell proliferation at 35 μM but did so at 100 μM and 175 μM (**D**) 22Rv1 exhibited the strongest resistance to TC-E 5002 with no effect on proliferation at 35 μM and 100 μM but reduced proliferation at 175 μM. Both PC3 (**E**) and Du145 (**F**) showed the same trend as PNT1A and LNCaP:C4-2 with no reduction in proliferation at 35 μM but inhibited proliferation at higher concentrations. * = $p \leq 0.05$, ** = $p \leq 0.005$, *** = $p \leq 0.001$, **** = $p \leq 0.0001$ by paired t-test.

Appendix 13 – Distribution curve of KDM1A staining

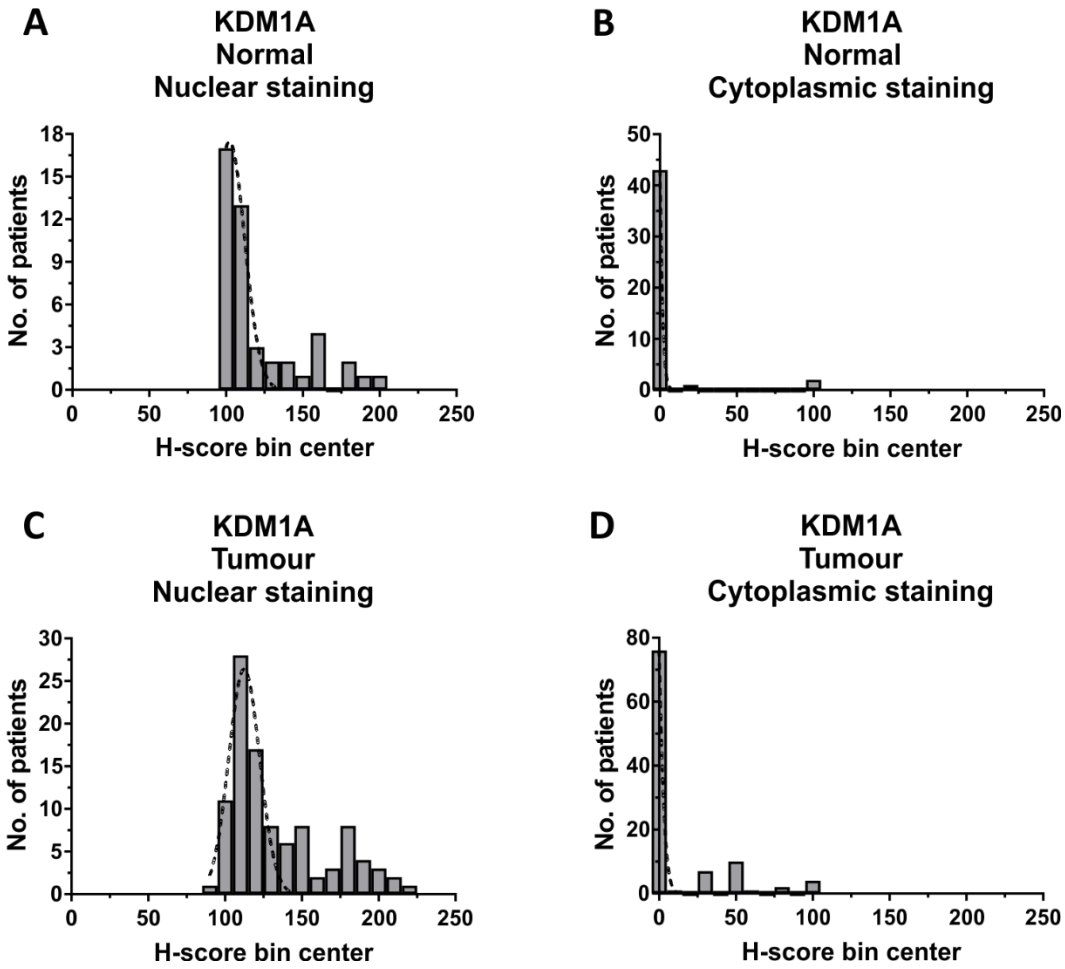

Figure ix: Distribution curve of KDM1A staining.
KDM1A nuclear (A, C) and cytoplasmic (B, D) staining in normal (A, B) and tumour (C, D) tissue. The distribution of KDM1A staining is expressed as H-score bin centers and the number of patients in each bin center is given.

Appendix 14 – Correlating KDM1A staining with clinical data

Table x: Correlation of KDM1A staining with clinical data.
Both KDM1A nuclear and cytoplasmic staining was correlated with clinical patient parameters. Gleason 4 groups, 1 = Gleason 3+3, 2 = Gleason 3+4, 3 = Gleason 4+3, 4 = Gleason 8 & 9; Gleason 3 groups, 1 = Gleason 6, 2 = Gleason 7, 3 = Gleason 8 & 9; Gleason 2 groups, 1 = Gleason 3+3 & 3+4, 2 = Gleason 4+3 & 8 & 9; TNM = tumour, node, metastasis; PIN = prostate intraepithelial neoplasia; PSA = prostate specific antigen; BCR = biochemical recurrence. Statistical p-values were evaluated by χ^2-test and $p \leq 0.05$ was highlighted grey in table.

	Nuclear staining			Cytoplasmic staining	
	4 groups	3 groups	2 groups	3 groups	2 groups
Age	0.860	0.588	0.678	0.133	0.218
Gleason 4 groups	0.176	0.418	0.571	0.092	0.979
Gleason 3 groups	0.135	0.210	0.405	0.035	9.984
Gleason 2 groups	0.638	0.232	0.252	0.099	0.689
TNM	0.314	0.568	0.677	0.001	0.007
High grade PIN	0.208	0.437	0.523	0.742	0.606
Extraprostatic extension	0.405	0.348	0.440	0.009	0.013
Perineural invasion	0.427	0.212	0.705	0.286	0.341
Pre-OP PSA	0.248	0.897	0.411	0.456	0.221
BCR	0.547	0.339	0.382	0.404	0.191
Time for BCR to occur	0.091	0.657	0.982	0.272	0.457
Cytoplasmic staining 3 groups	0.097	0.522	0.226		
Cytoplasmic staining 2 groups	0.087	0.623	0.960		

Appendix 15 – Correlating KDM stainings

Table xi: Correlation of KDM1A staining with KDM5B and KDM7A staining.
KDM1A nuclear and cytoplasmic staining was correlated with nuclear and cytoplasmic staining of KDM5B and KDM7A respectively. Statistical p-values were determined by χ^2-test and $p \leq 0.05$ was highlighted grey in table.

	KDM1A nuclear staining			KDM1A cytoplasmic staining	
	4 groups	3 groups	2 groups	3 groups	2 groups
KDM5B nuclear staining 4 groups	0.000	0.000	0.000	0.901	0.704
KDM5B nuclear staining 3 groups	0.000	0.000	0.000	0.968	0.932
KDM5B nuclear staining 2 groups	0.000	0.000	0.000	0.355	0.238
KDM5B cytopl. staining 4 groups	0.190	0.300	0.641	0.231	0.100
KDM5B cytopl. staining 3 groups	0.313	0.542	0.674	0.203	0.119
KDM5B cytopl. staining 2 groups	0.276	0.303	0.516	0.077	0.058
KDM7A nuclear staining 4 groups	0.004	0.024	0.004	0.082	0.240
KDM7A nuclear staining 3 groups	0.001	0.001	0.001	0.198	0.957
KDM7A nuclear staining 2 groups	0.001	0.008	0.002	0.958	0.775
KDM7A cytopl. staining 4 groups	0.002	0.012	0.014	0.152	0.058
KDM7A cytopl. staining 3 groups	0.000	0.000	0.005	0.100	0.046
KDM7A cytopl. staining 2 groups	0.000	0.002	0.003	0.055	0.032

Table xii: Correlation of KDM5B staining with KDM7A staining.
KDM5B nuclear and cytoplasmic staining was correlated with KDM7A nuclear and cytoplasmic staining. Statistical p-values were calculated by χ^2-test and $p \leq 0.05$ was highlighted grey in table.

	KDM5B nuclear staining			KDM5B cytoplasmic staining		
	4 groups	3 groups	2 groups	4 groups	3 groups	2 groups
KDM7A nuclear staining 4 groups	0.000	0.000	0.000	0.592	0.531	0.260
KDM7A nuclear staining 3 groups	0.000	0.000	0.000	0.535	0.403	0.209
KDM7A nuclear staining 2 groups	0.001	0.000	0.013	0.223	0.162	0.077
KDM7A cytopl. staining 4 groups	0.002	0.003	0.052	0.065	0.289	0.601
KDM7A cytopl. staining 3 groups	0.001	0.000	0.002	0.124	0.293	0.614
KDM7A cytopl. staining 2 groups	0.002	0.001	0.014	0.116	0.108	0.538

Appendix 16 – Namoline dose curve

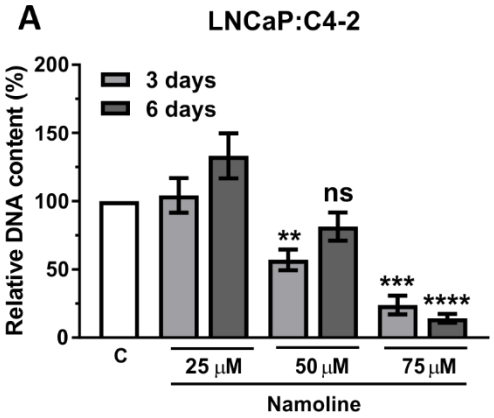

Figure x: Dose curve of Namoline on LNCaP:C4-2 cell proliferation.

Cell proliferation was assessed using the CyQUANT™ assay. (**A**) Namoline had no effect on LNCaP:C4-2 cell proliferation at 25 µM. Increasing the Namoline concentration to 50 µM significantly inhibited proliferation by ~40% at 3 days of treatment. The strongest effect was measured at 75 µM where proliferation was reduced more than 80% by Namoline. * = $p \leq 0.05$, ** = $p \leq 0.005$, *** = $p \leq 0.001$, **** = $p \leq 0.0001$ by paired t-test.

Appendix 17 – Publication 1

Placenta 56 (2017) 79–85

Contents lists available at ScienceDirect

Placenta

journal homepage: www.elsevier.com/locate/placenta

Androgen dependent mechanisms of pro-angiogenic networks in placental and tumor development

Veronika M. Metzler [a], Simone de Brot [a], Robert S. Robinson [a], Jennie N. Jeyapalan [a], Emad Rakha [b], Thomas Walton [c], David S. Gardner [a], Emma F. Lund [a], Jonathan Whitchurch [d], Daisy Haigh [a], Jack M. Lochray [a], Brian D. Robinson [e], Cinzia Allegrucci [a], Rupert G. Fray [f], Jenny L. Persson [g, h], Niels Ødum [i], Regina R. Miftakhova [h, j], Albert A. Rizvanov [j], Ieuan A. Hughes [k], Rieko Tadokoro-Cuccaro [k], David M. Heery [d], Catrin S. Rutland [a, **], Nigel P. Mongan [a, l, *]

[a] Faculty of Medicine and Health Sciences, School of Veterinary Medicine and Health Sciences, University of Nottingham, LE12 5RD, UK
[b] School of Medicine and Sciences, University of Nottingham, Nottingham City Hospital, NG5 1PB, UK
[c] Department of Urology, Nottingham University Hospitals NHS Trust, NG5 1PB, UK
[d] School of Pharmacy, University of Nottingham, NG7 2TQ, UK
[e] Department of Pathology, Weill Cornell Medicine, New York 10065, USA
[f] School of Biosciences, University of Nottingham, LE12 5RD, UK
[g] Department of Translational Medicine, Lund University, Malmö, Sweden
[h] Department of Molecular Biology, Umeå University, Sweden
[i] Department of Immunology and Microbiology, University of Copenhagen, Denmark
[j] Kazan Federal University, Kazan, Republic of Tatarstan 420008, Russian Federation
[k] Department of Paediatrics, University of Cambridge, Hills Rd, Cambridge CB2 0QQ, UK
[l] Department of Pharmacology, Weill Cornell Medicine, New York 10065, USA

ARTICLE INFO

Article history:
Received 14 November 2016
Received in revised form
14 February 2017
Accepted 15 February 2017

Keywords:
Nuclear receptor
Epigenetics
Angiogenesis
VEGF

ABSTRACT

The placenta and tumors share important characteristics, including a requirement to establish effective angiogenesis. In the case of the placenta, optimal angiogenesis is required to sustain the blood flow required to maintain a successful pregnancy, whereas in tumors establishing new blood supplies is considered a key step in supporting metastases. Therefore the development of novel angiogenesis inhibitors has been an area of active research in oncology. A subset of the molecular processes regulating angiogenesis are well understood in the context of both early placentation and tumorigenesis. In this review we focus on the well-established role of androgen regulation of angiogenesis in cancer and relate these mechanisms to placental angiogenesis. The physiological actions of androgens are mediated by the androgen receptor (AR), a ligand dependent transcription factor. Androgens and the AR are essential for normal male embryonic development, puberty and lifelong health. Defects in androgen signalling are associated with a diverse range of clinical disorders in men and women including disorders of sex development (DSD), polycystic ovary syndrome in women and many cancers. We summarize the diverse molecular mechanisms of androgen regulation of angiogenesis and infer the potential significance of these pathways to normal and pathogenic placental function. Finally, we offer potential research applications of androgen-targeting molecules developed to treat cancer as investigative tools to help further delineate the role of androgen signalling in placental function and maternal and offspring health in animal models.

1. Introduction

It has long been recognized that the placenta and tumors share important characteristics. These include mechanisms related to

* Corresponding author. Faculty of Medicine and Health Sciences, School of Veterinary Medicine and Health Sciences, University of Nottingham, LE12 5RD, UK.
** Corresponding author.
E-mail addresses: Catrin.rutland@nottingham.ac.uk (C.S. Rutland), Nigel.mongan@nottingham.ac.uk (N.P. Mongan).

http://dx.doi.org/10.1016/j.placenta.2017.02.018
0143-4004/

immune privilege and most notably in the context of this review, a requirement to establish effective neovascularization and angiogenesis. Placental angiogenesis is a tightly regulated process involving complex interactions of pro- and anti-angiogenic factors, which if dysregulated can lead to different pregnancy complications including preeclampsia [1]. Examples of important pro-angiogenic factors in the placenta include vascular endothelial growth factor (VEGF), placental growth factor (PlGF) and fibroblast growth factor (FGF) [2], whereas soluble fms-like tyrosine kinase 1 (sFlt-1) is noted as a key anti-angiogenic factor [3]. A better understanding of placental angiogenesis would be beneficial in understanding pathological conditions such as preeclampsia and intrauterine growth restriction. This review will provide a summary of current understanding of the role of angiogenesis in cancer and placental physiology, with an emphasis on androgen regulation of pro-angiogenesis pathways.

Androgens have long been known to play essential roles in male embryonic development and pubertal maturation [4] and are now recognized as having a role in angiogenesis [reviewed in Ref. [5]]. The most abundant physiological androgens in men are testosterone and its more potent derivative 5α-dihydrotestosterone (DHT) which is produced by steroid-5α-reductase enzymes [6]. Testosterone can also be converted to the primary estrogen (β-estradiol) by aromatase [7], therefore it is often essential to consider the relative roles of androgen and estrogen signalling. Androgen production is regulated in the hypothalamus, where gonadotrophin hormone-releasing hormone (GnRH) triggers the release of luteinizing hormone (LH) from the pituitary gland [8]. LH in turn acts on the testes where the majority of the testosterone is synthesized. Testosterone is transported to target tissues primarily bound to the sex hormone-binding globulin or to albumin [9,10]. Secondary androgens, such as androstenedione (AED) and Dehydroepiandrosterone (DHEA) are produced primarily by the adrenal glands [8]. As we will discuss in detail later, there is also evidence of androgen synthesis [11] and androgen receptor (AR) expression in the placenta and endometrium [12–14].

1.1. Androgen receptor signalling

The actions of androgens are mediated primarily by the AR, also referred to as NR3C4 [15]. The AR is a member of the ligand dependent superfamily of nuclear receptor transcription factors which, in the presence of androgens, regulates the transcription of target genes [15]. Nuclear receptors consist of three major domains: the *N*-terminal region, the DNA-binding domain (DBD) and the *C*-terminal ligand-binding domain (LBD) [16]. The *N*-terminal region is variable in both sequence and size and in the AR harbors an agonist independent transcriptional activation function (AF-1) [17]. The highly conserved DBD is situated in the centre of the polypeptide and selectively and preferentially binds to androgen response elements in the regulatory regions of androgen target genes. The DBD and LBD are separated through a variable hinge region that contains DNA minor-groove binding residues [18]. The LBD is the site where both ligands and coregulators bind and where the second transcriptional activation function (AF-2) region is situated. In contrast to AF-1, AF-2 is ligand-dependent and full transcriptional activity can only be accomplished when AF-1 and AF-2 act together [19]. The AR regulates gene expression by recruiting multiple epigenetic coregulators, often through a conserved LxxLL motif, which control transcription via covalent histone modifications (Fig. 1) [20]. The role of coregulators in gene activation and how these relate to the modulation of histone lysine acetylation and methylation is an area of active research. Nuclear receptor-coregulator complexes, and by inference the AR-coregulator complex, are believed to be dynamic [21] and involve the recruitment of diverse enzymes which covalently modify the *N*-terminal tail of histones such as lysine acetyltransferases (KATs), deacetylases (HDACs), lysine methyltransferases (KMTs) and lysine demethylases (KDMs), kinases/phosphatases, poly(ADP)ribosylases and ubiquitin ligases [22]. KATs and HDACs have been intensively studied and the general paradigm is that KAT activity increases DNA accessibility, thus activating gene transcription, whereas HDACs are associated with transcriptional repression [23,24]. It is important to note that certain coregulators, including KDM1A which is also expressed in the placenta [25], can exhibit transcriptional activation and repression properties in a cellular and epigenomic context-dependent manner [26].

1.2. Androgens and fetal development

During normal embryonic development and sex determination, the 46XY fetus instructs the primitive bipotential gonad to develop into testes [4]. Testicular androgen production and the ability to respond to these androgenic hormones are both then required to enable the XY fetus to complete male sex differentiation [4 and references therein]. Yet, it is estimated that between 1 in 20,400 and 1 in 99,100 infants are unable to respond to androgens and present with complete 46 XY sex reversal, termed complete androgen insensitivity [4]. Complete androgen insensitivity syndrome (CAIS) results in 46XY sex reversal and typically presents with pubertal amenorrhea or inguinal swelling in infants [27]. About 90–95% of all CAIS cases show mutations in the AR causing hormone resistance [28]. Partial androgen insensitivity syndrome (PAIS) is more common and the PAIS phenotype is much more complex and diverse [4]. We [29–32] and others [33] have identified and functionally characterized numerous loss of function and intronic mutations in the *AR* locus in individuals with complete and partial AIS. As we will explore in more detail later, the inability of the CAIS fetus and the fetal placenta component to respond to androgens suggests that pregnancy is sufficiently sustained by the ability of the maternal placental component to respond to androgens.

1.3. Androgens, angiogenesis and cancer

Much of our understanding of androgen regulation of angiogenesis has been obtained in cancer studies. Androgens and androgen signalling are implicated in many human cancer types, including prostate [34,35], testicular germ cell [36] and bladder [37] cancers. Androgens are also known to have complex roles in breast tumors [38–40]. AR coregulators, including the lysine demethylase KDM1A/LSD1 [37,41,42] and p160 coactivators [43–45] have also been implicated in cancer, most notably prostate cancer (PCa). PCa is the most common non-cutaneous cancer affecting men [46]. The treatment options for PCa are often dependent upon the age and general health of the patient, as well as the stage and grade of the cancer. Watchful waiting, active surveillance, radical prostatectomy and radiotherapy remain the most effective initial therapies of localized PCa, however these can be associated with negative impacts on quality of life [47,48] and post-treatment recurrence remains common [49]. In the case of PCa, treatments which block androgen biosynthesis or signalling, so called androgen deprivation therapies (ADT) are important treatments for advanced PCa (Fig. 2). Existing ADTs target AR function by blocking androgen biosynthesis (GnRH analogues), acting as AR selective antagonists (bicalutamide, enzalutamide) or blocking intra-tumoral androgen biosynthesis (abiraterone) [50,51]. Unfortunately, ADTs are ineffective in the long term for many patients, as incurable hormone refractory PCa tumors which are resistant to ADTs, commonly emerge within ~18 months at which point only

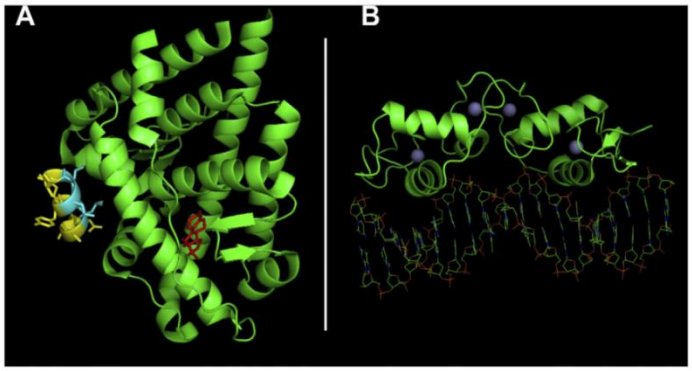

Fig. 1. (A) Crystal structure (PDB: 2AO6) of the AR ligand binding domain in complex with agonist R1881 and the LXXLL motif derived from SRC2/TIF2/NCOA2 [93]. The LBD is represented in cartoon format (green) and shows the three layer antiparallel alpha-helical sandwich conformation typical of NRs. The SRC2/TIF2/NCOA2 coactivator peptide is shown in yellow and adopts an alpha helical conformation. Conserved leucine residues are shown in cyan and contact the cofactor binding cleft on the LBD surface. The ligand R1881 is shown in red with the ligand binding pocket. (B) Crystal structure (PDB: 1R4I) of the rat AR DNA binding domain (DBD) bound to the direct repeat of the hexamer AGAACA as a direct repeat, separated by thee nucleotides (DR3) [94]. The double stranded DNA duplex is shown in wireframe. The DBD dimer is represented in cartoon format (green) and zinc atoms are portrayed as grey spheres. The DBD monomers adopt alpha-helical conformations of which one these, the DNA recognition helix, contacts specific bases and sugar-phosphate backbone of the 'response element'. Interactions between the DBD monomers stabilise the dimer.

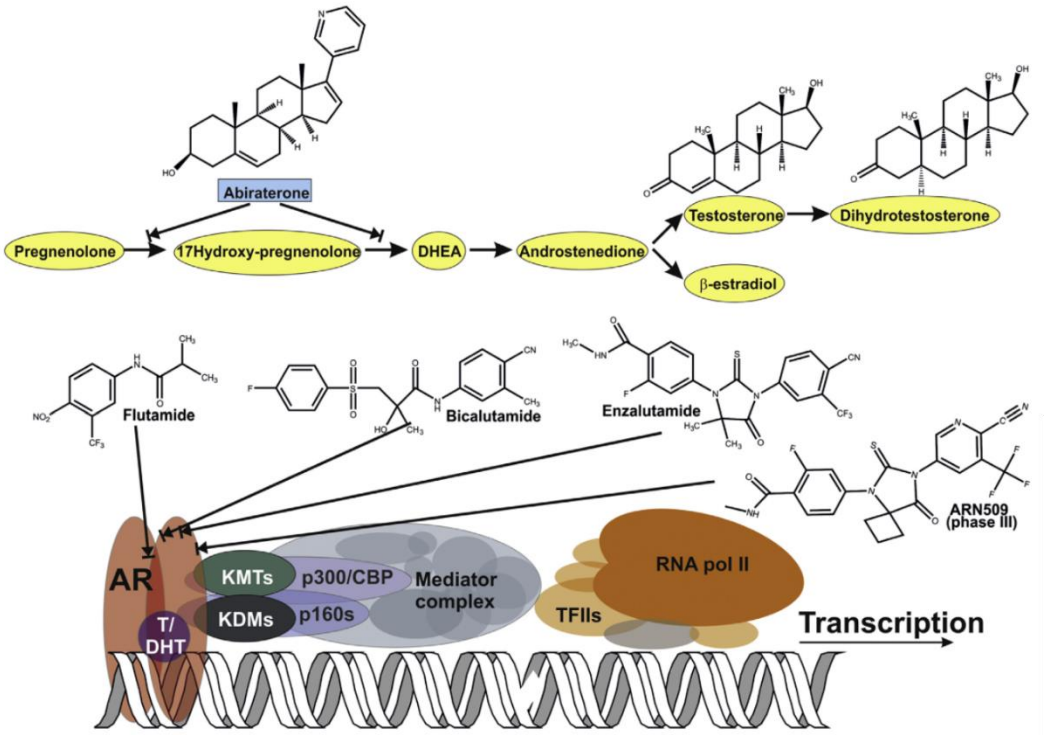

Fig. 2. Androgen deprivation therapies are important treatment approaches for advanced prostate cancer. Abiraterone blocks adrenal and gonadal androgen biosynthesis by inhibiting the Cyp17/17-a-hydroxylase/C17,20 lyase enzyme. Flutamide, bicalutamide and enzalutamide block androgen signalling by acting as AR antagonists. ARN-509, also termed JNJ-56021927 is in clinical phase III trials for advanced PCa (clinicaltrials.gov accessions: NCT02772588, NCT02489318, NCT02123758, NCT02578797, NCT01946204, NCT01790126, NCT01792687, NCT02106507, accessed November 10, 2016).

palliative treatments are available. For this reason, great effort was invested to develop novel therapies targeting tumor angiogenesis. Indeed >20 years ago, Marshall and Narayan suggested a role for androgens in PCa angiogenesis [52]. Subsequent studies in mouse PCa xenograft models indicated castration decreased angiogenesis with a concomitant decrease in levels of vascular endothelial growth factor A (VEGFA) [53]. More recently, we and others found that androgens and AR-coregulators regulate VEGFA levels (Fig. 3) [35,54,55]. Consistent with this there is clinical [54] and genetic [56] evidence suggesting a link between VEGFA expression and poorer outcomes in PCa patients. Androgen depletion has been found to significantly induce apoptosis of tumor associated endothelial cells, suggesting a direct effect on angiogenesis, independent of the effect of androgen withdrawal on PCa cell proliferation and/or viability [53]. For these reasons there was much hope for treatments targeting pro-angiogenesis mediators such as VEGFA. However, clinical trials of angiogenesis inhibitors have been disappointing with only modest anti-tumor activity achieved in patients [57], though the use of *anti*-VEGFA therapy in combination with other agents shows more promise [58,59].

1.4. Androgens and angiogenesis in endometrial and placental function

There is robust AR expression in the endometrium [13,60] and both the AR and dihydrotestosterone are implicated in endometrial cancer. There is also evidence of endometrial and placental androgen biosynthesis [11,12]. However the expression of AR in the placenta is controversial [14,60–62]. In normal pregnancy, circulating androgen levels generally increase, compared with non-pregnant female hormone levels. Testosterone has been shown to increase by day 15 after the luteinizing hormone surge with reports of ~1.55–1.7 fold average increase from day 15 through to week 33 in comparison to non-pregnant women, changes were not observed prior to day 13 [63,64]. Androstenedioine levels rise from day 14 and increase on average by 1.3 fold from week 5–40 in comparison to non-pregnant women [63,64]. Additionally, testosterone decreased uterine blood flow to the placenta [65]. It is interesting to note that the free androgen index fell rapidly from weeks 5–21, plateauing at week 21 and rising marginally at 40 weeks [63]. Interestingly, aberrant placental function has not been described in the pregnancies of CAIS fetuses, suggesting that maternal androgen signalling may be sufficient to mediate any required androgen-regulated angiogenesis during placental development. Excess testosterone during pregnancy can negatively impact placental angiogenesis [66,67]. For example, androgen levels are higher in pregnant women with polycystic ovary syndrome (PCOS) as compared with normal pregnancy [68]. Free androgen index, testosterone, androstenedione, and dehydroepiandrosterone (DHEA) levels were all increased in PCOS pregnancies compared with normal pregnancies during weeks 22–28, but not earlier in pregnancy (weeks 10–16) [68]. Despite differing circulating levels of androgens during pregnancy, fetal virilisation was not observed. However this was likely due to fetal virilisation occurring between weeks 8 and 13 of gestation, whilst the increased levels of androgens were observed at week 16 [63,64,68]. The placenta also expresses aromatase which rapidly converts androgens to estrogen [68,69]. This could explain why the fetus is not affected by virilisation in normal pregnancy. No associations have been observed between concentrations of testosterone and the sex of the baby in pregnant vs non-pregnant women [63]. Levels of DHEA, androstenedione or testosterone in normal pregnant women vs pregnant PCOS women were also not dependent on the sex of the baby [68].

Increased first trimester total testosterone levels in women was also shown to be an independent predictor of gestational diabetes mellitus (GDM) [70]. Increased androgen sensitivity in the human GDM placenta compared to healthy placentas has also been reported [69] as have increased AR mRNA and protein levels of in GDM placentae. In contrast aromatase protein expression was decreased in GDM placentas compared with healthy placentas, which was suggested to lead to reduced conversion of testosterone to estrogen [69]. Placentas from women with GDM also showed decreased human placental mRNA and protein expression of *VEGFR2* and *VEGFA* compared to control placentas. Qualitative analysis of immunohistochemical localization reported that although mRNA and protein levels were lower, and immunestaining was weaker, VEGFR2 and VEGFA were expressed in the same cells and localities within the GDM and control placentas [67].

There is evidence that suggests the mechanisms of angiogenesis are similar in the placenta and prostate cancer. Evidence from early studies on first generation angiogenesis inhibitors such as TNP-470, implicated impaired angiogenesis as a contributing factor in intrauterine growth restriction of the fetus [71]. TNP-470 was shown to have an effect on human PCa cells and a number of tumors in patients [72,73]. Similarly, the endogenous angiogenesis inhibitor, angiostatin4.5, has also shown activity in tumors [74]. Like TNP-470, angiostatin4.5 also reduces murine placental angiogenesis and with the offspring showing skeletal growth delays [75]. Maliqueo and colleagues have recently provided a comprehensive review of the diverse roles of the sex steroids in the regulation of the uterine-placental vasculature [76]. Yet current understanding of the role of androgen signalling in placental development and particularly its potential role in regulating angiogenesis in the placenta, is incomplete. Androgens are known to stimulate proliferation of human umbilical vein endothelial cells (HUVECs) [77], indicating a role for androgens during pregnancy. Interestingly, this androgen effect on HUVEC function was not sex dependent. There is also evidence from rat models that excess androgen reduces uterine blood flow and increases maternal and adult offspring blood

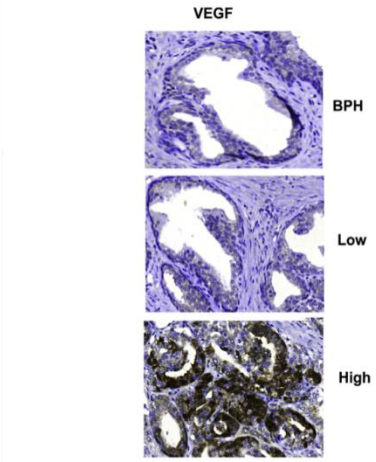

Fig. 3. Evaluation of the expression of vascular endothelial growth factor (VEGF-A) in prostate cancer specimens as previously reported (Wegiel et al., 2008). Representative staining examples are provided for benign prostate hyperplasia (BPH), low and high grade malignant prostate tissue. Reproduced with permission from Kashyap et al. [54] in Molecular Oncology, 2013 Jun; 7 (3):555–66. http://dx.doi.org/10.1016/j.molonc.2013.01.003; Elsevier.

pressure, by a convergence of mechanisms involving angiotensin II, reduced eNOS activity, a consequent reduction in NO production and AR activation of protein kinase C (PKCδ) [78–81]. Furthermore, increased testosterone results in elevated expression of hypoxia related genes including hypoxia inducible factor 1 α (HIF1α) [80], an established positive regulator of VEGFA [82]. VEGFA is believed to play important roles in the earliest stages of embryonic implantation [83]. Yet the potential role of androgens in regulating VEGFAand angiogenesis in the placenta remains poorly defined. But in a recent ovine study examining the effects of testosterone on the placenta, *VEGFA* expression was observed to be androgen responsive. Indeed AR and the KDM1A coregulator are recruited to an androgen response element (ARE) in the ovine *VEGFA* locus [25]. On gestational day 90, placental *VEGFA* mRNA, placental VEGFA and AR protein levels increased in testosterone-treated ewes compared with control placentas [25].

Beyond androgen regulation of VEGFAin angiogenesis [35,54], there is also evidence for a role for androgens in regulation of the Slt/Robo pathway [84]. The slits (1–3) are secreted glycoproteins act as ligands for the Robos (1–4) transmembrane receptors. In one recent study, expression of Slit and Robo mRNA was compared in normal and preeclamptic (characterised by impaired angiogenesis and hypoxia) human placental tissue specimens [1]. *Robo1* and *Robo4* were shown to have significantly higher expression in preeclamptic as compared to healthy tissue [85]. Additionally, hypoxia was shown to increase expression of Slit 2 in BeWo choriocarcinoma cells and Robo1 and 4 and Slit 3 in human umbilical vein endothelial cells (HUVEC) cells. Robo4 is a vascular specific and its activation by Slit2 has been shown in vitro to inhibit mouse lung endothelial cell migration, tube formation and permeability induced by vascular endothelial growth factor (VEGF)-165 [85]. Conversely, human malignant melanoma cells found to be expressing Slit2 were shown to induce angiogenesis in a xenograft animal model [86]. This effect was reversed, and tumour growth impeded, by Robo1 blocking antibodies or soluble Robo1 receptor. Slit/Robo signalling is implicated in multiple, often contradictory, ways in several cancers relating to invasion, migration and apoptosis as well as angiogenesis (Gara et al., 2015). In most cases the Slits and Robos are under expressed due to promoter hypermethylation. Indeed there is evidence that androgen excess during pregnancy can reduce Robo1 expression [84]. One consequence of this would be to impact angiogenesis.

Human trophoblast cells isolated at late stage pregnancy have been shown to express the angiogenesis inhibitor, pigment epithelium-derived factor (PEDF), at higher levels than those from early pregnancy [87]. Additionally, only late stage pregnancy derived cells were capable of reducing angiogenesis of human placental endothelial cells. This anti-angiogenic effect could be reduced with the addition of a PEDF blocking antibody. Recombinant PEDF was also shown to induce an anti-angiogenic effect through inhibiting VEGFAsignalling. This suggests PDGF acts in a paracrine manner to slow angiogenesis in the latter stages of pregnancy. Expression of PEDF has also been shown to be reduced in PCa as compared to healthy control [88]. However, there is evidence that androgen can both activate [89] and reduce [88] PEDF expression in testicular peritubular cells and PCa respectively. Whether androgens regulate PEDF in the placenta remains unknown.

It is also worth noting that whilst the placenta is undergoing angiogenesis and remodelling, so is the maternal endometrium. The imbalance of pro- and anti-angiogenic factors has also been shown to play a major role in disorders such as preeclampsia, where vascular disruption is evident in both the placenta and maternal endothelium during this essential vascular remodelling period [90,91]. A number of studies have indicated that a key component of circulating angiogenesis inhibitors is whether or not the vascular endothelial cells are quiescent or activated and therefore expressing Fas at higher levels [92].

2. Conclusion

In this review we have discussed the current understanding of androgen signalling and how this relates to angiogenesis in placental and cancer contexts. Previous studies have reported changes in androgen levels during pregnancy and in pathogenic processes including PCOS and GDM which are associated with concomitant changes in placental angiogenesis. However, further work is required to elucidate the complex role of androgens and their metabolites in placental angiogenesis and development. The extensive repertoire of pharmacological inhibitors of androgen signalling developed for PCa represent excellent tools to interrogate the androgen signalling pathway in placental development. The availability of potent pharmacological agents which can inhibit androgen synthesis (abiraterone) and conversion to estrogen (aromatase inhibitors), coupled with AR-antagonists such as bicalutamide and enzalutamide (Fig. 2), afford the potential to further delineate the complex roles of androgens in placental angiogenesis in animal models. Such approaches will also help advance understanding of the life-long consequences of deregulated androgen signalling *in utero*.

Acknowledgements

The authors gratefully acknowledge the support of the University of Nottingham, Prostate Cancer UK (NPM, DMH, SdB) and the BBSRC University of Nottingham Doctoral Training Programme BB/J014508/1 and the School of Veterinary Medicine and Science, University of Nottingham (NPM, CSR, DMH, VM, JW, DH, JL, EL). RRM and AAR were supported by Program of Competitive Growth of Kazan Federal University, Russian Federation.

References

[1] W.X. Liao, L.C. Laurent, S. Agent, J. Hodges, D.B. Chen, Human placental expression of SLIT/ROBO signaling cues: effects of preeclampsia and hypoxia, Biol. Reprod. 86 (4) (2012) 111.
[2] R.J. Levine, S.E. Maynard, C. Qian, K.H. Lim, L.J. England, K.F. Yu, E.F. Schisterman, R. Thadhani, B.P. Sachs, F.H. Epstein, B.M. Sibai, V.P. Sukhatme, S.A. Karumanchi, Circulating angiogenic factors and the risk of preeclampsia, N. Engl. J. Med. 350 (7) (2004) 672–683.
[3] D.P. Sundrani, U.S. Reddy, P.M. Chavan-Gautam, S.S. Mehendale, G.R. Chandak, S.R. Joshi, Altered methylation and expression patterns of genes regulating placental angiogenesis in preterm pregnancy, Reprod. Sci. 21 (12) (2014) 1508–1517.
[4] I.A. Hughes, J.D. Davies, T.I. Bunch, V. Pasterski, K. Mastroyannopoulou, J. MacDougall, Androgen insensitivity syndrome, Lancet 380 (9851) (2012) 1419–1428.
[5] S. de Brot, A. Ntekim, R. Cardenas, V. James, C. Allegrucci, D.M. Heery, D.O. Bates, N. Odum, J.L. Persson, N.P. Mongan, Regulation of vascular endothelial growth factor in prostate cancer, Endocrine-related cancer 22 (3) (2015) R107–R123.
[6] V.A. Randall, Role of 5 alpha-reductase in health and disease, Bailliere's Clin. Endocrinol. Metabolism 8 (2) (1994) 405–431.
[7] F.L. Bellino, S.S. Gilani, S.S. Eng, Y. Osawa, W.L. Duax, Active-site-directed inactivation of aromatase from human placental microsomes by brominated androgen derivatives, Biochemistry 15 (21) (1976) 4730–4736.
[8] S.S. Nussey, S.A. Whitehead, Endocrinology: an Integrated Approach, CRC Press, 2013.
[9] M.E. Baker, Albumin, steroid hormones and the origin of vertebrates, J. Endocrinol. 175 (1) (2002) 121–127.
[10] W. Rosner, D.J. Hryb, M.S. Khan, A.M. Nakhla, N.A. Romas, Sex hormone-binding globulin: anatomy and physiology of a new regulatory system, J. Steroid Biochem. Mol. Biol. 40 (4–6) (1991) 813–820.
[11] J.C. Escobar, S.S. Patel, V.E. Beshay, T. Suzuki, B.R. Carr, The human placenta expresses CYP17 and generates androgens de novo, J. Clin. Endocrinol. Metabolism 96 (5) (2011) 1385–1392.
[12] K. Ito, T. Suzuki, J. Akahira, T. Moriya, C. Kaneko, H. Utsunomiya, N. Yaegashi, K. Okamura, H. Sasano, Expression of androgen receptor and 5alpha-

reductases in the human normal endometrium and its disorders, Int. J. Cancer J. Int. Du Cancer 99 (5) (2002) 652–657.
[13] B. Cloke, K. Huhtinen, L. Fusi, T. Kajihara, M. Yliheikkila, K.K. Ho, G. Teklenburg, S. Lavery, M.C. Jones, G. Trew, J.J. Kim, E.W. Lam, J.E. Cartwright, M. Poutanen, J.J. Brosens, The androgen and progesterone receptors regulate distinct gene networks and cellular functions in decidualizing endometrium, Endocrinology 149 (9) (2008) 4462–4474.
[14] K. Horie, K. Takakura, K. Imai, S. Liao, T. Mori, Immunohistochemical localization of androgen receptor in the human endometrium, decidua, placenta and pathological conditions of the endometrium, Hum. Reprod. 7 (10) (1992) 1461–1466.
[15] P. Germain, B. Staels, C. Dacquet, M. Spedding, V. Laudet, Overview of nomenclature of nuclear receptors, Pharmacol. Rev. 58 (4) (2006) 685–704.
[16] J.A. Simental, M. Sar, M.V. Lane, F.S. French, E.M. Wilson, Transcriptional activation and nuclear targeting signals of the human androgen receptor, J. Biol. Chem. 266 (1) (1991) 510–518.
[17] P. Huang, V. Chandra, F. Rastinejad, Structural overview of the nuclear receptor superfamily: insights into physiology and therapeutics, Annu. Rev. Physiology 72 (2010) 247.
[18] F. Rastinejad, Retinoid X receptor and its partners in the nuclear receptor family, Curr. Opin. Struct. Biol. 11 (1) (2001) 33–38.
[19] A. Wärnmark, E. Treuter, A.P. Wright, J.-A. Gustafsson, Activation functions 1 and 2 of nuclear receptors: molecular strategies for transcriptional activation, Mol. Endocrinol. 17 (10) (2003) 1901–1909.
[20] B.W. O'Malley, A. Malovannaya, J. Qin, Minireview: nuclear receptor and coregulator proteomics–2012 and beyond, Mol. Endocrinol. 26 (10) (2012) 1646–1650.
[21] R. Metivier, G. Penot, M.R. Hubner, G. Reid, H. Brand, M. Kos, F. Gannon, Estrogen receptor-alpha directs ordered, cyclical, and combinatorial recruitment of cofactors on a natural target promoter, Cell 115 (6) (2003) 751–763.
[22] M.G. Rosenfeld, V.V. Lunyak, C.K. Glass, Sensors and signals: a coactivator/corepressor/epigenetic code for integrating signal-dependent programs of transcriptional response, Genes & Dev. 20 (11) (2006) 1405–1428.
[23] A. Eberharter, P.B. Becker, Histone acetylation: a switch between repressive and permissive chromatin, EMBO Rep. 3 (3) (2002) 224–229.
[24] G. Legube, D. Trouche, Regulating histone acetyltransferases and deacetylases, EMBO Rep. 4 (10) (2003) 944–947.
[25] E.R. Cleys, J.L. Halleran, V.A. Enriquez, J.C. da Silveira, R.C. West, Q.A. Winger, R.V. Anthony, J.E. Bruemmer, C.M. Clay, G.J. Bouma, Androgen receptor and histone lysine demethylases in ovine placenta, PLoS One (2) (2015) 10 e0117472.
[26] C. Cai, H.H. He, S. Chen, I. Coleman, H. Wang, Z. Fang, S. Chen, P.S. Nelson, X.S. Liu, M. Brown, Androgen receptor gene expression in prostate cancer is directly suppressed by the androgen receptor through recruitment of lysine-specific demethylase 1, Cancer Cell 20 (4) (2011) 457–471.
[27] A. Berglund, T.H. Johannsen, K. Stochholm, M.H. Viuff, J. Fedder, K.M. Main, C.H. Gravholt, Incidence, prevalence, diagnostic delay, and clinical presentation of female 46,XY disorders of sex development, J. Clin. Endocrinol. Metab. 101 (12) (2016 Dec) 4532–4540. Epub 2016 Sep 7.
[28] O. Hiort, Clinical and Molecular Aspects of Androgen Insensitivity, Karger Publishers, 2013, pp. 33–40.
[29] R. Tadokoro-Cuccaro, J. Davies, N.P. Mongan, T. Bunch, R.S. Brown, L. Audi, K. Watt, I.J. McEwan, I.A. Hughes, Promoter-dependent activity on androgen receptor N-terminal domain mutations in androgen insensitivity syndrome, Sex. Dev. Genet. Mol. Biol. Evol. Endocrinol. Embryology, Pathology Sex Determ. Differ. 8 (6) (2014) 339–349.
[30] J. Jaaskelainen, N.P. Mongan, S. Harland, I.A. Hughes, Five novel androgen receptor gene mutations associated with complete androgen insensitivity syndrome, Hum. Mutat. 27 (3) (2006) 291.
[31] S. Rosa, A. Biason-Lauber, N.P. Mongan, F. Navratil, E.J. Schoenle, Complete androgen insensitivity syndrome caused by a novel mutation in the ligand-binding domain of the androgen receptor: functional characterization, J. Clin. Endocrinol. metabolism 87 (9) (2002) 4378–4382.
[32] N.P. Mongan, J. Jaaskelainen, K. Green, J.W. Schwabe, N. Shimura, M. Dattani, I.A. Hughes, Two de novo mutations in the AR gene cause the complete androgen insensitivity syndrome in a pair of monozygotic twins, J. Clin. Endocrinol. Metabolism 87 (3) (2002) 1057–1061.
[33] B. Gottlieb, L.K. Beitel, A. Nadarajah, M. Paliouras, M. Trifiro, The androgen receptor gene mutations database: 2012 update, Hum. Mutat. 33 (5) (2012) 887–894.
[34] M. Sarwar, J. Semenas, R. Miftakhova, A. Simoulis, B. Robinson, A. Gjorloff Wingren, N.P. Mongan, D.M. Heery, H. Johnsson, P.A. Abrahamsson, N. Dizeyi, J. Luo, J.L. Persson, Targeted suppression of AR-V7 using PIP5K1alpha inhibitor overcomes enzalutamide resistance in prostate cancer cells, Oncotarget 7 (39) (2016) 63065–63081.
[35] E.M. Nilsson, K.B. Laursen, J. Whitchurch, A. McWilliam, N. Odum, J.L. Persson, D.M. Heery, L.J. Gudas, N.P. Mongan, MiR137 is an androgen regulated repressor of an extended network of transcriptional coregulators, Oncotarget 6 (34) (2015) 35710–35725.
[36] W. Jiang, J. Zhang, Q. Zhou, S. Liu, M. Ni, P. Zhu, Q. Wu, W. Li, M. Zhang, X. Xia, Predictive value of GGN and CAG repeat polymorphisms of androgen receptors in testicular cancer: a meta-analysis, Oncotarget 7 (12) (2016) 13754–13764.
[37] E.C. Kauffman, B.D. Robinson, M.J. Downes, L.G. Powell, M.M. Lee, D.S. Scherr, L.J. Gudas, N.P. Mongan, Role of androgen receptor and associated lysine-demethylase coregulators, LSD1 and JMJD2A, in localized and advanced human bladder cancer, Mol. Carcinog. 50 (12) (2011) 931–944.
[38] G.A. Tarulli, L.M. Butler, W.D. Tilley, T.E. Hickey, Bringing androgens up a NOTCH in breast cancer, Endocrine-related Cancer 21 (4) (2014) T183–T202.
[39] K. Elebro, S. Borgquist, M. Simonsson, A. Markkula, K. Jirstrom, C. Ingvar, C. Rose, H. Jernstrom, Combined androgen and estrogen receptor status in breast cancer: treatment prediction and prognosis in a population-based prospective cohort, Clin. Cancer Res. Official J. Am. Assoc. Cancer Res. 21 (16) (2015) 3640–3650.
[40] M.A. Aleskandarany, R. Abduljabbar, I. Ashankyty, A. Elmouna, D. Jerjees, S. Ali, L. Buluwela, M. Diez-Rodriguez, C. Caldas, A.R. Green, I.O. Ellis, E.A. Rakha, Prognostic significance of androgen receptor expression in invasive breast cancer: transcriptomic and protein expression analysis, Breast Cancer Res. Treat. 159 (2) (2016) 215–227.
[41] P. Kahl, L. Gullotti, L.C. Heukamp, S. Wolf, N. Friedrichs, R. Vorreuther, G. Solleder, P.J. Bastian, J. Ellinger, E. Metzger, R. Schule, R. Buettner, Androgen receptor coactivators lysine-specific histone demethylase 1 and four and a half LIM domain protein 2 predict risk of prostate cancer recurrence, Cancer Res. 66 (23) (2006) 11341–11347.
[42] C. Cai, H.H. He, S. Chen, I. Coleman, H. Wang, Z. Fang, P.S. Nelson, X.S. Liu, M. Brown, S.P. Balk, Androgen receptor gene expression in prostate cancer is directly suppressed by the androgen receptor through recruitment of lysine-specific demethylase 1, Cancer Cell 20 (4) (2011) 457–471.
[43] X.B. Shi, L. Xue, J.X. Zou, R. Gandour-Edwards, H. Chen, R.W. deVere White, Prolonged androgen receptor loading onto chromatin and the efficient recruitment of p160 coactivators contribute to androgen-independent growth of prostate cancer cells, Prostate 68 (16) (2008) 1816–1826.
[44] J.X. Zou, Z. Zhong, X.B. Shi, C.G. Tepper, R.W. deVere White, H.J. Kung, H. Chen, ACTR/AIB1/SRC-3 and androgen receptor control prostate cancer cell proliferation and tumor growth through direct control of cell cycle genes, Prostate 66 (14) (2006) 1474–1486.
[45] X.E. Zhou, K.M. Suino-Powell, J. Li, Y. He, J.P. Mackeigan, K. Melcher, E.L. Yong, H.E. Xu, Identification of SRC3/AIB1 as a preferred coactivator for hormone-activated androgen receptor, J. Biol. Chem. 285 (12) (2010) 9161–9171.
[46] R.L. Siegel, K.D. Miller, A. Jemal, Cancer statistics, 2016, CA Cancer J. Clin. 66 (1) (2016) 7–30.
[47] L. Bourke, S.A. Boorjian, A. Briganti, L. Klotz, L. Mucci, M.J. Resnick, D.J. Rosario, T.A. Skolarus, D.F. Penson, Survivorship and improving quality of life in men with prostate cancer, Eur. Urol. 68 (3) (2015) 374–383.
[48] V. Muralidhar, P.L. Nguyen, Maximizing resources in the local treatment of prostate cancer: a summary of cost-effectiveness studies, Urol. Oncol. (2016).
[49] S.A. Boorjian, J.A. Eastham, M. Graefen, B. Guillonneau, R.J. Karnes, J.W. Moul, E.M. Schaeffer, C. Stief, K.C. Zorn, A critical analysis of the long-term impact of radical prostatectomy on cancer control and function outcomes, Eur. Urol. 61 (4) (2012) 664–675.
[50] A. Heidenreich, P.J. Bastian, J. Bellmunt, M. Bolla, S. Joniau, T. van der Kwast, M. Mason, V. Matveev, T. Wiegel, F. Zattoni, N. Mottet, EAU guidelines on prostate cancer. Part II: treatment of advanced, relapsing, and castration-resistant prostate cancer, Eur. Urol. 65 (2) (2014) 467–479.
[51] J.S. de Bono, C.J. Logothetis, A. Molina, K. Fizazi, S. North, L. Chu, K.N. Chi, R.J. Jones, O.B. Goodman Jr., F. Saad, J.N. Staffurth, P. Mainwaring, S. Harland, T.W. Flaig, T.E. Hutson, T. Cheng, H. Patterson, J.D. Hainsworth, C.J. Ryan, C.N. Sternberg, S.L. Ellard, A. Flechon, M. Saleh, M. Scholz, E. Efstathiou, A. Zivi, D. Bianchini, Y. Loriot, N. Chieffo, T. Kheoh, C.M. Haqq, H.I. Scher, Abiraterone and increased survival in metastatic prostate cancer, N. Engl. J. Med. 364 (21) (2011) 1995–2005.
[52] S. Marshall, P. Narayan, Treatment of prostatic bleeding: suppression of angiogenesis by androgen deprivation, J. Urology 149 (6) (1993) 1553–1554.
[53] R.K. Jain, N. Safabakhsh, A. Sckell, Y. Chen, P. Jiang, L. Benjamin, F. Yuan, E. Keshet, Endothelial cell death, angiogenesis, and microvascular function after castration in an androgen-dependent tumor: role of vascular endothelial growth factor, Proc. Natl. Acad. Sci. U. S. A. 95 (18) (1998) 10820–10825.
[54] V. Kashyap, S. Ahmad, E.M. Nilsson, L. Helczynski, S. Kenna, J.L. Persson, L.J. Gudas, N.P. Mongan, The lysine specific demethylase-1 (LSD1/KDM1A) regulates VEGF-A expression in prostate cancer, Mol. Oncol. 7 (3) (2013) 555–566.
[55] K. Eisermann, C.J. Broderick, A. Bazarov, M.M. Moazam, G.C. Fraizer, Androgen up-regulates vascular endothelial growth factor expression in prostate cancer cells via an Sp1 binding site, Mol. Cancer 12 (2013) 7.
[56] P. Orlandi, A. Fontana, A. Fioravanti, T. Di Desidero, L. Galli, L. Derosa, B. Canu, R. Marconcini, E. Biasco, A. Solini, G. Francia, R. Danesi, A. Falcone, G. Bocci, VEGF-A polymorphisms predict progression-free survival among advanced castration-resistant prostate cancer patients treated with metronomic cyclophosphamide, Br. J. cancer 109 (4) (2013) 957–964.
[57] W.K. Kelly, S. Halabi, M. Carducci, D. George, J.F. Mahoney, W.M. Stadler, M. Morris, P. Kantoff, J.P. Monk, E. Kaplan, N.J. Vogelzang, Small EJ. Randomized, Double-blind, placebo-controlled phase III trial comparing docetaxel and prednisone with or without bevacizumab in men with metastatic castration-resistant prostate cancer: CALGB 90401, J. Clin. Oncol. Official J. Am. Soc. Clin. Oncol. (2012).
[58] R.R. McKay, A.J. Zurita, L. Werner, J.Y. Bruce, M.A. Carducci, M.N. Stein, E.I. Heath, A. Hussain, H.T. Tran, C.J. Sweeney, R.W. Ross, P.W. Kantoff, S.F. Slovin, M.E. Taplin, A randomized phase II trial of short-course androgen deprivation therapy with or without bevacizumab for patients with recurrent prostate cancer after definitive local therapy, J. Clin. Oncol. Official J. Am. Soc.

Clin. Oncol. 34 (16) (2016) 1913–1920.
[59] R.R. McKay, K.P. Gray, J.H. Hayes, G.J. Bubley, J.E. Rosenberg, A. Hussain, P.W. Kantoff, M.E. Taplin, Docetaxel, bevacizumab, and androgen deprivation therapy for biochemical disease recurrence after definitive local therapy for prostate cancer, Cancer 121 (15) (2015) 2603–2611.
[60] M. Uhlen, L. Fagerberg, B.M. Hallstrom, C. Lindskog, P. Oksvold, A. Mardinoglu, A. Sivertsson, C. Kampf, E. Sjostedt, A. Asplund, I. Olsson, K. Edlund, E. Lundberg, S. Navani, C.A. Szigyarto, J. Odeberg, D. Djureinovic, J.O. Takanen, S. Hober, T. Alm, P.H. Edqvist, H. Berling, H. Tegel, J. Mulder, J. Rockberg, P. Nilsson, J.M. Schwenk, M. Hamsten, K. von Feilitzen, M. Forsberg, L. Persson, F. Johansson, M. Zwahlen, G. von Heijne, J. Nielsen, Ponten F. Proteomics, Tissue-based map of the human proteome, Science 347 (6220) (2015), 1260419.
[61] J.O. Macaulay, G.L. Warne, Z.S. Krozowski, Human placenta contains a high affinity R1881 binding site that is not the androgen receptor, J. Steroid Biochem. 29 (5) (1988) 497–503.
[62] P.D. McCormick, A.J. Razel, T.C. Spelsberg, C.B. Coulam, Evidence for an androgen receptor in the human placenta, Am. J. Obstetrics Gynecol. 140 (1) (1981) 8–13.
[63] P. O'Leary, P. Boyne, P. Flett, J. Beilby, I. James, Longitudinal assessment of changes in reproductive hormones during normal pregnancy, Clin. Chem. 37 (5) (1991) 667–672.
[64] V.D. Castracane, D.R. Stewart, T. Gimpel, J.W. Overstreet, B.L. Lasley, Maternal serum androgens in human pregnancy: early increases within the cycle of conception, Hum. Reprod. 13 (2) (1998) 460–464.
[65] A. Abbas, S. Gupta, The role of histone deacetylases in prostate cancer, Epigenetics 3 (6) (2008) 300–309.
[66] R. Fornes, M. Hu, M. Maliqueo, M. Kokosar, A. Benrick, D. Carr, H. Billig, T. Jansson, L. Manni, E. Stener-Victorin, Maternal testosterone and placental function: effect of electroacupuncture on placental expression of angiogenic markers and fetal growth, Mol. Cell. Endocrinol. 433 (2016) 1–11.
[67] Q. Meng, L. Shao, X. Luo, Y. Mu, W. Xu, L. Gao, H. Xu, Y. Cui, Expressions of VEGF-A and VEGFR-2 in placentae from GDM pregnancies, Reprod. Biol. Endocrin 14 (1) (2016) 61.
[68] T. Sir-Petermann, M. Maliqueo, B. Angel, H. Lara, F. Perez-Bravo, S. Recabarren, Maternal serum androgens in pregnant women with polycystic ovarian syndrome: possible implications in prenatal androgenization, Hum. Reprod. 17 (10) (2002) 2573–2579.
[69] P. Uzelac, X. Li, J. Lin, L. Neese, L. Lin, S. Nakajima, H. Bohler, Z. Lei, Dysregulation of leptin and testosterone production and their receptor expression in the human placenta with gestational diabetes mellitus, Placenta 31 (7) (2010) 581–588.
[70] Y.M. Gözükara, H. Aytan, D. Ertunc, E.C. Tok, F. Demirtürk, Ş. Şahin, P. Aytan, Role of first trimester total testosterone in prediction of subsequent gestational diabetes mellitus, J. Obstetrics Gynaecol. Res. 41 (2) (2015) 193–198.
[71] C.S. Rutland, M. Mukhopadhyay, S. Underwood, N. Clyde, T.M. Mayhew, C.A. Mitchell, Induction of intrauterine growth restriction by reducing placental vascular growth with the angioinhibin TNP-470, Biol. Reprod. 73 (6) (2005) 1164–1173.
[72] V. Castronovo, D. Belotti, TNP-470 (AGM-1470): mechanisms of action and early clinical development, Eur. J. Cancer 32A (14) (1996) 2520–2527.
[73] J. Horti, S.C. Dixon, C.J. Logothetis, Y. Guo, E. Reed, W.D. Figg, Increased transcriptional activity of prostate-specific antigen in the presence of TNP-470, an angiogenesis inhibitor, Br. J. Cancer 79 (9–10) (1999) 1588–1593.
[74] G.A. Soff, H. Wang, D.L. Cundiff, K. Jiang, B. Martone, A.W. Rademaker, J.A. Doll, T.M. Kuzel, In vivo generation of angiostatin isoforms by administration of a plasminogen activator and a free sulfhydryl donor: a phase I study of an angiostatic cocktail of tissue plasminogen activator and mesna, Clin. Cancer Res. 11 (17) (2005) 6218–6225.
[75] C.S. Rutland, S.D. Atkinson, M. Mukhopadhyay, K. Jiang, G.A. Soff, T.M. Mayhew, C.A. Mitchell, Thrombophilic-type placental pathologies and skeletal growth delay following maternal administration of angiostatin4.5 in mice, Biol. Reprod. 84 (3) (2011) 505–513.
[76] M. Maliqueo, B. Echiburu, N. Crisosto, Sex steroids modulate uterine-placental vasculature: implications for obstetrics and neonatal outcomes, Front. Physiology 7 (2016) 152.
[77] V. Torres-Estay, D.V. Carreno, P. Fuenzalida, A. Watts, I.F. San Francisco, V.P. Montecinos, P.C. Sotomayor, J. Ebos, G.J. Smith, A.S. Godoy, Androgens modulate male-derived endothelial cell homeostasis using androgen receptor-dependent and receptor-independent mechanisms, Angiogenesis (2016).
[78] V. Chinnathambi, M. Balakrishnan, J. Ramadoss, C. Yallampalli, K. Sathishkumar, Testosterone alters maternal vascular adaptations: role of the endothelial NO system, Hypertension 61 (3) (2013) 647–654.
[79] C.S. Blesson, V. Chinnathambi, G.D. Hankins, C. Yallampalli, K. Sathishkumar, Prenatal testosterone exposure induces hypertension in adult females via androgen receptor-dependent protein kinase Cdelta-mediated mechanism, Hypertension 65 (3) (2015) 683–690.
[80] V. Chinnathambi, C.S. Blesson, K.L. Vincent, G.R. Saade, G.D. Hankins, C. Yallampalli, K. Sathishkumar, Elevated testosterone levels during rat pregnancy cause hypersensitivity to angiotensin II and attenuation of endothelium-dependent vasodilation in uterine arteries, Hypertension 64 (2) (2014) 405–414.
[81] K. Gopalakrishnan, J.S. Mishra, V. Chinnathambi, K.L. Vincent, I. Patrikeev, M. Motamedi, G.R. Saade, G.D. Hankins, K. Sathishkumar, Elevated testosterone reduces uterine blood flow, spiral artery elongation, and placental oxygenation in pregnant rats, Hypertension 67 (3) (2016) 630–639.
[82] L.J. Gudas, L. Fu, D.R. Minton, N.P. Mongan, D.M. Nanus, The role of HIF1alpha in renal cell carcinoma tumorigenesis, J. Mol. Med. Berl. 92 (8) (2014) 825–836.
[83] N.J. Hannan, P. Paiva, K.L. Meehan, L.J. Rombauts, D.K. Gardner, L.A. Salamonsen, Analysis of fertility-related soluble mediators in human uterine fluid identifies VEGFAas a key regulator of embryo implantation, Endocrinology 152 (12) (2011) 4948–4956.
[84] K. Hogg, A.S. McNeilly, W.C. Duncan, Prenatal androgen exposure leads to alterations in gene and protein expression in the ovine fetal ovary, Endocrinology 152 (5) (2011) 2048–2059.
[85] C.A. Jones, N.R. London, H. Chen, K.W. Park, D. Sauvaget, R.A. Stockton, J.D. Wythe, W. Suh, F. Larrieu-Lahargue, Y.S. Mukouyama, P. Lindblom, P. Seth, A. Frias, N. Nishiya, M.H. Ginsberg, H. Gerhardt, K. Zhang, D.Y. Li, Robo4 stabilizes the vascular network by inhibiting pathologic angiogenesis and endothelial hyperpermeability, Nat. Med. 14 (4) (2008) 448–453.
[86] B. Wang, Y. Xiao, B.B. Ding, N. Zhang, X. Yuan, L. Gui, K.X. Qian, S. Duan, Z. Chen, Y. Rao, J.G. Geng, Induction of tumor angiogenesis by Slit-Robo signaling and inhibition of cancer growth by blocking Robo activity, Cancer Cell 4 (1) (2003) 19–29.
[87] J. Loegl, E. Nussbaumer, U. Hiden, A. Majali-Martinez, N. Ghaffari-Tabrizi-Wizy, S. Cvitic, I. Lang, G. Desoye, B. Huppertz, Pigment epithelium-derived factor (PEDF): a novel trophoblast-derived factor limiting feto-placental angiogenesis in late pregnancy, Angiogenesis 19 (3) (2016) 373–388.
[88] J.A. Doll, V.M. Stellmach, N.P. Bouck, A.R. Bergh, C. Lee, L.P. Abramson, M.L. Cornwell, M.R. Pins, J. Borensztajn, S.E. Crawford, Pigment epithelium-derived factor regulates the vasculature and mass of the prostate and pancreas, Nat. Med. 9 (6) (2003) 774–780.
[89] S. Windschuttl, C. Kampfer, C. Mayer, F. Flenkenthaler, T. Frohlich, J.U. Schwarzer, F.M. Kohn, H. Urbanski, G.J. Arnold, A. Mayerhofer, Human testicular peritubular cells secrete pigment epithelium-derived factor (PEDF), which may be responsible for the avascularity of the seminiferous tubules, Sci. Rep. 5 (2015) 12820.
[90] L.O. Kurlak, H.D. Mistry, T. Cindrova-Davies, G.J. Burton, F. Broughton Pipkin, Human placental renin-angiotensin system in normotensive and pre-eclamptic pregnancies at high altitude and after acute hypoxia-reoxygenation insult, J. Physiol. 594 (5) (2016) 1327–1340.
[91] C.E. Powe, R.J. Levine, S.A. Karumanchi, Preeclampsia, a disease of the maternal endothelium: the role of antiangiogenic factors and implications for later cardiovascular disease, Circulation 123 (24) (2011) 2856–2869.
[92] M. Tiwari, Apoptosis, angiogenesis and cancer therapies, J. Cancer Ther. Res. (1) (2012) 1.
[93] B. He, R.T. Gampe Jr., A.J. Kole, A.T. Hnat, T.B. Stanley, G. An, E.L. Stewart, R.I. Kalman, Minges JT and Wilson EM. Structural basis for androgen receptor interdomain and coactivator interactions suggests a transition in nuclear receptor activation function dominance, Mol. Cell 16 (3) (2004) 425–438.
[94] P.L. Shaffer, A. Jivan, D.E. Dollins, F. Claessens, D.T. Gewirth, Structural basis of androgen receptor binding to selective androgen response elements, Proc. Natl. Acad. Sci. U. S. A. 101 (14) (2004) 4758–4763.

Appendix 18 – Publication 2

Copyright Clearance Center RightsLink®

Home | Create Account | Help | LIVE CHAT

Title: Expression of NAD(P)H quinone dehydrogenase 1 (NQO1) is increased in the endometrium of women with endometrial cancer and women with polycystic ovary syndrome

Author: Nigel P. Mongan, Emma J. Crosbie, David M. Heery, et al

Publication: Clinical Endocrinology

Publisher: John Wiley and Sons

Date: Aug 18, 2017

LOGIN

If you're a copyright.com user, you can login to RightsLink using your copyright.com credentials.

Already a RightsLink user or want to learn more?

Welcome to RightsLink

This article is available under the terms of the Creative Commons Attribution License (CC BY) (which may be updated from time to time) and permits use, distribution and reproduction in any medium, provided that the Contribution is properly cited.

For an understanding of what is meant by the terms of the Creative Commons License, please refer to Wiley's Open Access Terms and Conditions.

Permission is not required for this type of reuse.

Wiley offers a professional reprint service for high quality reproduction of articles from over 1400 scientific and medical journals. Wiley's reprint service offers:

- Peer reviewed research or reviews
- Tailored collections of articles
- A professional high quality finish
- Glossy journal style color covers
- Company or brand customisation
- Language translations
- Prompt turnaround times and delivery directly to your office, warehouse or congress.

Please contact our Reprints department for a quotation. Email corporatesaleseurope@wiley.com or corporatesalesusa@wiley.com or corporatesalesDE@wiley.com .

CLOSE WINDOW

Received: 9 January 2017 | Revised: 11 May 2017 | Accepted: 24 July 2017

DOI: 10.1111/cen.13436

ORIGINAL ARTICLE

WILEY

Expression of NAD(P)H quinone dehydrogenase 1 (NQO1) is increased in the endometrium of women with endometrial cancer and women with polycystic ovary syndrome

William Atiomo[1] | Mohamad Nasir Shafiee[1,2] | Caroline Chapman[1] | Veronika M. Metzler[3] | Jad Abouzeid[3] | Ayşe Latif[4] | Amy Chadwick[5] | Sarah Kitson[5,6,7] | Vanitha N. Sivalingam[5,6,7] | Ian J. Stratford[4] | Catrin S. Rutland[3] | Jenny L. Persson[8,9] | Niels Ødum[10] | Pablo Fuentes-Utrilla[11] | Jennie N. Jeyapalan[3] | David M. Heery[12] | Emma J. Crosbie[5,6,7] | Nigel P. Mongan[3,13]

[1]Faculty of Medicine and Health Sciences, Division of Obstetrics and Gynaecology and Child Health, School of Medicine, Queen's Medical Centre, Nottingham University Hospital, Nottingham, UK

[2]Faculty of Medicine, Department Obstetrics and Gynaecology, UKM Medical Centre, Cheras, Kuala Lumpur, Malaysia

[3]Faculty of Medicine and Health Sciences, School of Veterinary Medicine and Science, University of Nottingham, Nottingham, UK

[4]Faculty of Biology, Medicine and Health, Division of Pharmacy and Optometry, School of Health Sciences, University of Manchester, Manchester, UK

[5]Faculty of Biology, Division of Molecular & Clinical Cancer Sciences, Medicine and Health, University of Manchester, Manchester, UK

[6]Department of Obstetrics and Gynaecology, Central Manchester University Hospitals NHS Foundation Trust, Manchester Academic Health Science Centre, Manchester, UK

[7]Manchester School of Pharmacy, University of Manchester, Manchester, UK

[8]Clinical Research Center, Lund University, Malmö, Sweden

[9]Department of Molecular Bology, Umeå University, Umeå, Sweden

[10]Department of Immunology and Microbiology, University of Copenhagen, Kobenhavn, Denmark

[11]Edinburgh Genomics, University of Edinburgh, Edinburgh, UK

[12]School of Pharmacy, University of Nottingham, Nottingham, UK

[13]Department of Pharmacology, Weill Cornell Medicine, New York, NY, USA

Correspondence
Nigel P. Mongan, Faculty of Medicine and Health Sciences, School of Veterinary Medicine and Science, University of Nottingham, Nottingham, UK.
Email: nigel.mongan@nottingham.ac.uk

Funding information
Biotechnology and Biological Sciences Research Council [grant number BB/1024291/1]; University of Nottingham; Prostate Cancer UK; Wellcome Trust/Wellbeing of Women Research Training Fellowship; National Institute for Health Research (NIHR) Clinician Scientist Fellowship, Grant/Award Number: NIHR-CS-012-009; Greater Manchester Local Clinical Research Network

[Correction added on 25 October 2017 after first online publication: The surname "Fuentes-Utrillia" was changed to "Fuentes-Utrilla".]

Summary

Objective: Women with a prior history of polycystic ovary syndrome (PCOS) have an increased risk of endometrial cancer (EC).

Aim: To investigate whether the endometrium of women with PCOS possesses gene expression changes similar to those found in EC.

Design and Methods: Patients with EC, PCOS and control women unaffected by either PCOS or EC were recruited into a cross-sectional study at the Nottingham University Hospital, UK. For RNA sequencing, representative individual endometrial biopsies were obtained from women with EC, PCOS and a woman unaffected by PCOS or EC. Expression of a subset of differentially expressed genes identified by RNA sequencing, including NAD(P)H quinone dehydrogenase 1 (*NQO1*), was validated by quantitative reverse transcriptase PCR validation (n = 76) and in the cancer genome atlas UCEC (uterine corpus endometrioid carcinoma) RNA sequencing data set

(n = 381). The expression of NQO1 was validated by immunohistochemistry in EC samples from a separate cohort (n = 91) comprised of consecutive patients who underwent hysterectomy at St Mary's Hospital, Manchester, between 2011 and 2013. A further 6 postmenopausal women with histologically normal endometrium who underwent hysterectomy for genital prolapse were also included. Informed consent and local ethics approval were obtained for the study.

Results: We show for the first that *NQO1* expression is significantly increased in the endometrium of women with PCOS and EC. Immunohistochemistry confirms significantly increased NQO1 protein expression in EC relative to nonmalignant endometrial tissue ($P < .0001$).

Conclusions: The results obtained here support a previously unrecognized molecular link between PCOS and EC involving NQO1.

KEYWORDS
endometrial cancer, endometrium, NQO1, polycystic ovary syndrome

1 | INTRODUCTION

Endometrial cancer (EC) is the most common gynaecological cancer affecting women in the United States, with an estimated 60 050 new cases in 2016.[1] The incidence of EC has increased by over 65% since the late 1970s correlating with rising incidence of obesity and increased longevity.[2,3] EC is usually treated by hysterectomy, but surgery carries increased risk in obese women and renders premenopausal women infertile. In addition to its negative impact on quality of life, EC poses a significant economic burden on health services.

Polycystic ovary syndrome (PCOS) is the commonest female endocrinopathy affecting 3%-20% of women of reproductive age.[4,5] Women with PCOS experience obesity, infrequent menstrual periods, infertility, excess systemic androgens, insulin resistance and hirsutism, and have enlarged ovaries with multiple small follicles on ultrasound imaging.[6] Women with PCOS have an increased risk of type 2 diabetes in later life and a threefold to fourfold increased risk of EC.[7,8]

The exact mechanisms that predispose PCOS women to EC remain unknown. Current hypotheses include a link between obesity and elevated oestrogen levels, inflammation, type 2 diabetes and hyperinsulinaemia.[9] In recently published studies, we found altered expression of genes involved in insulin signalling (IGF-1, IGFBP1 and PTEN) and lipogenic gene regulation in the endometrium and serum of women with PCOS and EC compared with controls.[10,11] Genes related to immunoregulation/inflammation,[12] antioxidants[9] and impaired progesterone-mediated decidualization[13] have also been suggested as possible mechanisms linking PCOS and EC.

This complexity highlights the need to characterize the transcriptome of the endometrium of women with PCOS to advance understanding of mechanisms linking PCOS and EC. To our knowledge, comparative transcriptomic, proteomic or metabolomic studies of patients with PCOS and EC are as yet unavailable. The aim of this proof of principle study was to perform comparative RNA sequencing profiling of endometrial biopsies from women with PCOS and EC and validate these findings in a large cohort of patients with EC.

2 | METHODS

2.1 | Study design, patient recruitment, sample acquisition and processing

Details of the methods used in patient recruitment for the Nottingham cohort have been previously described in detail elsewhere.[10,11] Briefly, patients (N = 76) were recruited into to a cross-sectional study conducted within the division of Obstetrics and Gynaecology and Child Health, at Nottingham University Hospital in the United Kingdom. Participants were prospectively recruited from July 2013 to February 2014. Research ethics approval was obtained from the National Research Ethics Service, East Midlands-Northampton committee (13/EM/0119) prior to commencement of recruitment. The project was also reviewed and approved by the relevant local ethics committees at the University of Nottingham. The Helsinki Declaration was strictly observed. Informed consent was obtained from all participants. For RNAseq, representative endometrial biopsies were obtained from individual women from each arm, specifically with EC (age 43, BMI = 35.9), polycystic ovary syndrome (age = 41, BMI = 35.9) and an age- and BMI-matched women unaffected by PCOS or EC (age = 42, BMI 32.01) and stored immediately in RNAlater (Sigma-Aldrich, Gillingham, UK). For qRT-PCR validation, participants were recruited in three arms: PCOS (n = 26), EC (n = 25) and control (n = 25). The participants were between 19 and 84 years of age and not on any hormonal treatment. Pregnancy was excluded prior to the recruitment using standard urine pregnancy tests. The EC group consisted of women with histopathologically proven endometrioid (type 1) adenocarcinoma of the endometrium undergoing total hysterectomy (by laparotomy or laparoscopically) who had not received previous neo-adjuvant chemo- or radiotherapy. Women were excluded from the study for prior history of papillary serous

TABLE 1 Participants' characteristic, biochemical and hormonal data of the Nottingham cohort. One-way ANOVA test was used to determine the difference between the groups

	Control (n = 25)	PCOS (n = 26)	Endometrial cancer (n = 25)	*P* value
Age (years);Mean (SD)	45.96 (13.34)	31.88 (5.975)	62.64 (11.10)	<.0001*
BMI (Kg/m^2);Mean (SD)	29.27 (2.467)	29.60 (3.116)	33.12 (5.959)	.0021*
WHC ratio; Mean (SD)	88.56 (3.241)	88.5 (3.992)	96.86 (12.99)	.0003*
Systolic BP(mm Hg);Mean (SD)	135.9 (8.729)	134.1 (7.591)	148.2 (11.42)	<.0001*
Diastolic BP (mm Hg);Mean (SD)	81.88 (7.563)	83.35 (7.746)	84.80 (7.455)	.4012
Fasting insulin; Mean (SD)	13.47 (6.002)	20.04 (31.79)	18.3 (16.26)	.5199
Fasting glucose; Mean (SD)	4.844 (0.4788)	5.142 (0.8363)	6.4 (1.649)	<.0001*
HOMA-IR; Mean (SD)	0.1809 (0.1065)	0.2617 (0.4405)	0.3139 (0.3766)	.3871
LDL; Mean (SD)	2.820 (0.8539)	2.738 (0.8174)	2.632 (0.9919)	.7561
HDL; Mean (SD)	1.5 (0.3136)	1.415 (0.2664)	1.648 (0.3754)	.0381*
TG; Mean (SD)	1.344 (0.6752)	1.373 (0.4609)	1.54 (0.5694)	.4305
Total cholesterol; Mean (SD)	5.004 (0.9654)	1.373 (0.4609)	1.54 (0.5694)	.5293
FSH; Mean (SD)	17.88 (24.81)	5.008 (2.788)	49.01 (20.83)	<.0001*
LH; Mean (SD)	12.95 (12.04)	12.31 (11.08)	28.64 (13.08)	<.0001*
Testosterone; Mean (SD)	1.516 (0.6309)	2.846 (0.7089)	1.492 (0.8684)	<.0001*
Oestradiol; Mean (SD)	414.5 (655.8)	331.9 (261.3)	96.72 (55.39)	.0204*
Progesterone; Mean (SD)	6.448 (15.37)	11.2 (14.54)	1.28 (0.5292)	.0192*
SHBG; Mean (SD)	55.36 (38.65)	34.46 (14.03)	50.6 (17.01)	.0120*

*P value <.5 is significant are indicated.

adenocarcinoma or metachronous cancers of the ovary, endometrium or cervix. The PCOS cohort was defined using the Rotterdam European Society for Human Reproduction and Embryology (ESHRE) and the American Society of Reproductive Medicine (ASRM) criteria. Baseline demographic details, blood pressure, weight and body mass index were calculated (kg/m^2), the Ferriman Gallwey hirsuitism score was recorded, and hip-waist circumference was recorded (cm) with participants wearing indoor clothing. The control group comprised of healthy women without EC or PCOS, not on any hormonal therapy, undergoing pelvic surgery for benign indications. The following clinical parameters were measured in participants using standard UK National Health Service services: fasting blood glucose, low-density lipoprotein, high-density lipoprotein, triglycerides, sex hormone bind globulin, testosterone, follicle stimulating hormone, luteinizing hormone, prolactin, 17-hydroxy-progesterone and thyroid function. A Pipelle® endometrial catheter was used to biopsy endometrial tissue, and samples were snap frozen at −80 C for subsequent processing. Patient characteristics and the results of endocrine and metabolic assays were as previously reported (Table 1).

2.2 | RNA sequencing (RNAseq) and quantitative reverse transcriptase PCR (qRT-PCR) analysis of patient endometrial samples

Total RNA was isolated using an RNeasy extraction kit, with on-column DNAse digestion (Qiagen, Manchester, UK). RNA quality (RIN > 7) was confirmed using an Agilent bioanalyser. Samples were submitted to Edinburgh Genomics for library preparation and analysed using an Illumina HiSeq platform using standard protocols. For quantitative reverse transcriptase PCR validation of RNAseq results, the samples were a subset (Table 1) of the patients described previously.[10] The expression of identified differentially expressed genes was examined in the cancer genome atlas UCEC (uterine corpus endometrioid carcinoma) RNA sequencing data set.[14]

Paired end raw reads (fastq format) were quality- and adapter-filtered using the Trim-galore wrapper for FastQC and cutadapt (http://www.bioinformatics.babraham.ac.uk/projects/trim_galore/). The retained paired reads were aligned to the Ensembl annotated HG19 human Illumina iGenome build using Tophat2, and differential gene expression was calculated for PCOS and EC specimens relative to the control specimen using Cuffdiff[15] on the basis of fold changes >1.5 and *P*-value <.05. Statistically significantly enriched gene ontologies and pathways for differentially expressed genes were obtained using WebGestalt and the Cytoscape Genemania plugin.[16] Next-generation RNAseq and associated clinical information was obtained from the cancer genome atlas endometrium cancer (UCEC) data set.[14] Normalized RSEM expression counts scaled to library size from each patient were compiled and correlated with specific clinical features including tumour and nontumour endometrial tissue and grade were analysed using EdgeR[17] or the Wilcoxon test with Benjamini-Hochberg false discovery rate correction for multiple testing.

We used qRT-PCR to validate differential endometrial gene expression identified by RNAseq in a subset of Nottingham cohort of PCOS, EC and control patients for whom mRNA and cDNA were available as previously described.[10] The hydrolysis probe PCR reagents employed

were as follows: β-*actin*: Hs01060665_g1; *NQO1*: Hs02512143_s1. Each sample was analysed in triplicate using the Plaffl method. For qPCR experiments, unpaired *t* tests were used to compare expression between control, PCOS and EC specimens.

2.3 | Immunohistochemistry

Samples from a separate cohort at the University of Manchester investigating prognostic biomarkers in EC using immunohistochemistry provided an opportunity to further investigate and validate the role of differentially expressed genes in EC. The Manchester cohort consisted of consecutive patients (n = 91) who underwent hysterectomy for EC at St Mary's Hospital in Manchester between 2011 and 2013, and who provided written, informed consent for their tumour samples to be stored in the BRC Biobank and used for future research. A further 6 postmenopausal women with histologically normal endometrium who underwent hysterectomy for genital prolapse were also included. The study received ethical approval from NRES Committee London - Fulham (REC reference 12/LO/0364) and R&D approval (R01960) from Central Manchester University Hospitals NHS Foundation Trust. The EC cohort comprised different histological subtypes, grades and stages of EC that were fully annotated with respect to patient demographics and clinical follow-up data. The average follow-up for the Manchester cohort was 34 months (range 1-64), during which time there were 19 recurrences and 23 deaths, of which 13 were EC-specific.

Formalin-fixed, paraffin-embedded tissue samples were cut into 4-μm sections for IHC analysis. This was performed using a fully automated IHC platform, Leica BOND-MAX together with Bond™ Polymer Refine Detection kit (DS9800) and on-board retrieval system. The sections were labelled with NQO1 (Sigma, 1:75 dilution) primary antibody according to standard validated Protocol *F* written by Leica. The detection kit was a biotin-free, polymeric horseradish peroxidase (HRP)-linker antibody conjugate system that detects tissue-bound IgG primary antibodies using the chromogen 3,3′-diaminobenzidine tetrahydrochloride hydrate (DAB) via a brown precipitate. Tissue sections were then counterstained with haematoxylin. Immunohistochemical evaluation was performed blindly by two independent observers (AL and AC) and discordant cases settled by review. NQO-1 staining was scored using the product of the area score (proportion of positively staining tumour cells) and the intensity of staining (0-3, 0 = zero staining, 3 = high-intensity staining). The score range was 0-300, and tumours were then dichotomised into low expression (score < 200) and high expression (score > 200).

2.4 | Statistical analysis

NQO1 protein expression in normal and malignant endometrium was compared using the Mann-Whitney *U* test. The association between NQO1 protein expression and clinical-pathological variables in women with endometrial cancer was tested using the Mann-Whitney *U* test for nonparametric variables and Spearman rank correlation for continuous and ordinal variables. Kaplan-Meier curves were constructed to estimate the effect of NQO1 expression on overall, cancer-specific and recurrence-free survival, with curves compared using the log-rank test. Overall survival was defined as the time between date of surgery and death from any cause, while cancer-specific survival referred to the time interval between surgery and death from endometrial cancer. Recurrence-free survival was defined as the time between date of surgery and first documented local or distant recurrence. Data without events were censored at date of last clinical follow-up visit. A Cox proportional hazard regression model was used in a univariate analysis of cancer-specific and recurrence-free survival, after confirming that the data were complied with the proportional hazards assumption using log-log curves. All clinical-pathological variables with known prognostic value in endometrial cancer were included in the univariate analysis alongside NQO1.

3 | RESULTS

3.1 | Patient demographics for samples used for the RNA sequencing and PCR validation study

Samples from three women were submitted for RNA sequencing. One patient with EC (BMI = 35.9, age 43), one PCOS patient without EC (BMI = 35.9, age 41) and an unaffected control woman (BMI = 32, age 42) were used for the RNA sequencing experiments. RNAseq identified differentially expressed genes (using standard criteria of fold changes [FC] >1.5, *P*-value <.05) in PCOS (700 genes) and EC (776 genes) endometrial specimens relative to control nonmalignant endometrium (Figure 1A-D, Tables S1, S2). We found that the global transcriptional profile of endometrial tissue from the woman with PCOS was most similar to the control obese woman (Figure 1). Of these genes, 94 genes were differentially expressed in both EC and PCOS relative to control endometrium (Table S1). Specifically, 12 genes were higher and 82 were lower in PCOS and EC specimens relative to control endometrium (Table S1, S2).

In the qRT-PCR validation cohort, the BMIs of women with EC (33.12 ± 5.959 kg/m^2), PCOS (31.88 ± 5.975 kg/m^2) and controls (29.27 ± 2.467 kg/m^2) were not significantly different. PCOS women were however younger (31.88 ± 5.975 years) than women with EC (62.64 ± 11.10 years) and controls (45.96 ± 13.34 years). Women with PCOS were recruited during their proliferative menstrual phase (based on their menstrual histories). We next used qRT-PCR to validate the expression of a subset of these genes in our patient cohorts (Figure 1E, Figure S1B). We confirmed expression of *NQO1* (Figure 1E), the NQO1 target *p53* and another exemplar gene identified by RNAseq, *GJB2*, (Figure S1) was significantly increased ($P < .05$) in endometrial specimens from women with PCOS (n = 25) and EC (n = 25) as compared to control, unaffected women (n = 25). We next examined expression of these 94 genes in patients with EC using the cancer genome atlas.[17] Of these 94 genes, 14 genes (*NQO1, SLPI, GJB2, DNAJC15, S100A8, PLEKHS1, ESPN, RSPH1, KRT5, FOXJ1, IFI27, IFI6, LGR5 and MUC16*) were significantly altered in tumour as compared to nontumour endometrial specimens (Figure S1). Expression of *NQO1* and its target *p53* mRNA are all significantly higher in primary endometrial tumour (n = 370) than nontumour (n = 11) specimens (Figure S1) as reported in the cancer genome atlas UCEC data set. The Genemania Cytoscape plugin was used

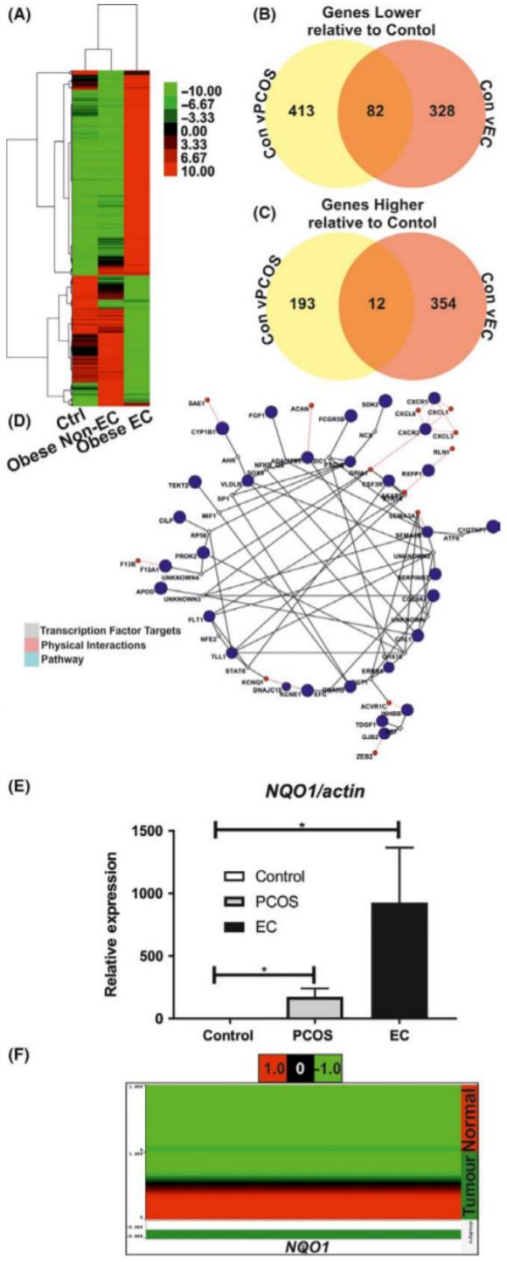

FIGURE 1 Next-generation RNA sequencing was used to compare the transcriptome of endometrial samples from unaffected, PCOS and EC patients. Unsupervised hierarchical clustering indicates nonmalignant endometrial specimens from unaffected control and PCOS patients are most similar. Elevated gene expression is indicated in red, and lower gene expression is indicated in green (A). A subset of 94 genes comprised of 82 down-regulated genes and 12 upregulated (B, C) are commonly dysregulated in PCOS and malignant endometrium. The Genemania cytoscape plugin was used to identify common pathways and infer potential transcriptional regulators of the gene network (D). We used qRT-PCR (E) and the cancer genome atlas (F) to compare expression of *NQO1* normalized to actin in endometrial biopsies from PCOS (n = 25) and EC (n = 25) women relative to unaffected women (n = 25). **** = $P < .005$ by Kruskal-Wallis nonparametric analysis of variance with Dunn's post hoc multiple comparisons test. We also analysed expression of *NQO1*, and it downstream target *p53* in the cancer genome atlas UCEC data set (N = 370 EC, N = 11 nonmalignant endometrium). Expression of *NQO1* is significantly elevated in tumour, relative to nonmalignant endometrial tissue as determined by Wilcoxon test with Benjamini-Hochberg false discovery rate correction for multiple testing. [Colour figure can be viewed at wileyonlinelibrary.com]

to identify pathways and infer potential transcriptional regulators of the genes identified common to PCOS and EC (Figure 1D). Enriched gene ontologies defined by these differential genes were identified (Table S2). Interestingly, the significantly enriched gene ontologies included gene networks involved in microtubule motor activity and cilia function.

3.2 | Immunohistochemistry validating the role of NQO1 in EC

The Manchester EC patient demographics and clinicopathological features are shown (Table 2). The control women were postmenopausal with histologically normal endometrium and underwent hysterectomy for genital prolapse. Histologically normal postmenopausal endometrium did not express NQO1 (Figure 2). In EC, there was a statistically significant association between high NQO1 expression and advancing age (Table S3). There was no statistically significant correlation between NQO1 expression and standard clinicopathological features with established prognostic value, including histological subtype, grade or stage of disease, deep myometrial invasion or LVSI (Table S3). Both type 1 (endometrioid) and type 2 (nonendometrioid) EC expressed NQO1, and there was a trend towards poorer outcomes with higher NQO1 staining; however, NQO1 expression was not associated with recurrence-free, EC-specific or overall survival in the Manchester cohort (Table S3, Figure S2). This may reflect the good overall prognosis of EC and an insufficient number of events to demonstrate significance.

4 | DISCUSSION

Known risk factors for EC include increasing age, polycystic ovary syndrome (PCOS), obesity and type 2 diabetes.[18-21] We and others have identified altered SREBP1,[11] and insulin signalling in endometrial specimens from women with PCOS or EC.[10,22] Anovulatory menstrual cycles, commonly found in PCOS women, have also been linked with EC.[23] The mechanisms are thought to involve a state of progesterone deficiency. Progesterone protects the endometrium from the mitogenic effects of oestrogen and withdrawal of progesterone triggers endometrial sloughing (menstruation), which allows

TABLE 2 Relationship between known prognostic variables and NQO1 expression in the Manchester cohort

Characteristic	NQO1 All n = 91	NQO1 score <200 n = 53	NQO1 score ≥200 n = 38	*P* value
Median age at diagnosis years (IQR)	68 (58-74)	67 (56-72)	72.5 (63.3-77.8)	.007**
Median BMI at diagnosis kg/m^2 (IQR)	30.1 (26.1-37.1)	30.1 (26.0-39.1)	29.6 (26.3-35.2)	.622
Diabetic, n (%)				
No	71 (78.0)	43 (81.1)	28 (73.7)	.629
Yes	20 (22.0)	10 (18.9)	10 (26.3)	
Histological grade, n (%)				
1	23 (25.3)	15 (28.3)	8 (21.1)	.164
2	20 (22.0)	12 (22.6)	8 (21.1)	
3	48 (52.7)	26 (49.1)	22 (57.9)	
FIGO (2009) stage, n (%)				
1	59 (64.8)	34 (64.2)	25 (65.8)	.115
2	12 (13.2)	9 (17.0)	3 (7.9)	
3	18 (19.8)	9 (17.0)	9 (23.7)	
4	2 (2.2)	1 (1.9)	1 (2.6)	
Histological type, n (%)				
Endometrioid	48 (52.7)	31 (58.4)	17 (44.7)	.100
Nonendometrioid	43 (47.3)	22 (41.5)	21 (55.3)	
Lymphovascular space invasion, n (%)				
Absent	50 (53.8)	32 (60.4)	18 (47.4)	.356
Present	38 (41.8)	18 (34.0)	20 (52.6)	
Missing data	3 (3.3)	3 (5.7)	0 (0)	
Depth of myometrial invasion, n (%)				
<50%	51 (56.0)	31 (58.5)	20 (52.6)	.412
≥ 50%	40 (44.0)	22 (41.5)	18 (47.4)	
Any adjuvant treatment, n (%)				
No	37 (40.7)	23 (43.4)	14 (36.8)	.366
Yes	54 (59.3)	30 (56.6)	24 (63.2)	

**indicates *p* values <0.01.

the natural shedding of abnormal endometrial cells. A common systemic pathway such as an aberrant insulin signalling pathway may cause oligo/amenorrhoea as well as endometrial hyperplasia and EC independent of body mass index (BMI). In such a scenario, aberrant systemic signalling programs pro-oncogenic transcriptional networks in the endometrium of women with PCOS that may predispose to EC. Indeed, while previous gene expression studies have investigated PCOS[24] and EC,[25] the exact mechanisms that predispose obese women to EC are unclear. Thus, while the epidemiological evidence supporting an association between PCOS and an increased risk of endometrial carcinogenesis is robust,[10,19-21] a definitive mechanistic link between the conditions has yet to be identified. For this reason, the goal of this study was to compare endometrial gene expression profiles from women with endometrial cancer and PCOS. The current study is the first to compare global gene expression in endometrial specimens from women with PCOS and EC. Our findings have identified 94 genes, including *NQO1*, commonly altered in endometrial specimens from women with PCOS and EC, suggesting a potential common mechanism in the disorders.

NQO1 has an established role in the endometrium.[26] *NQO1* encodes NAD(P)H:quinone oxidoreductase 1 in detoxification pathways[27-29] and has been reported to activate specific quinone-derived pharmaceuticals including mitomycin C and apaziquone.[30,31] NQO1 also acts to protect the p53 tumour suppressor protein, and many other proteins involved in proliferation from proteasomal degradation.[32] Interestingly, missense variants in *NQO1* are implicated in many cancer types[33-35] and more recently, increased NQO1 expression is associated with poor prognosis in ovarian[36] and lung[37] cancers. There is also considerable interest in NQO1 as a cancer therapeutic target. Its ability to activate cytotoxic therapies

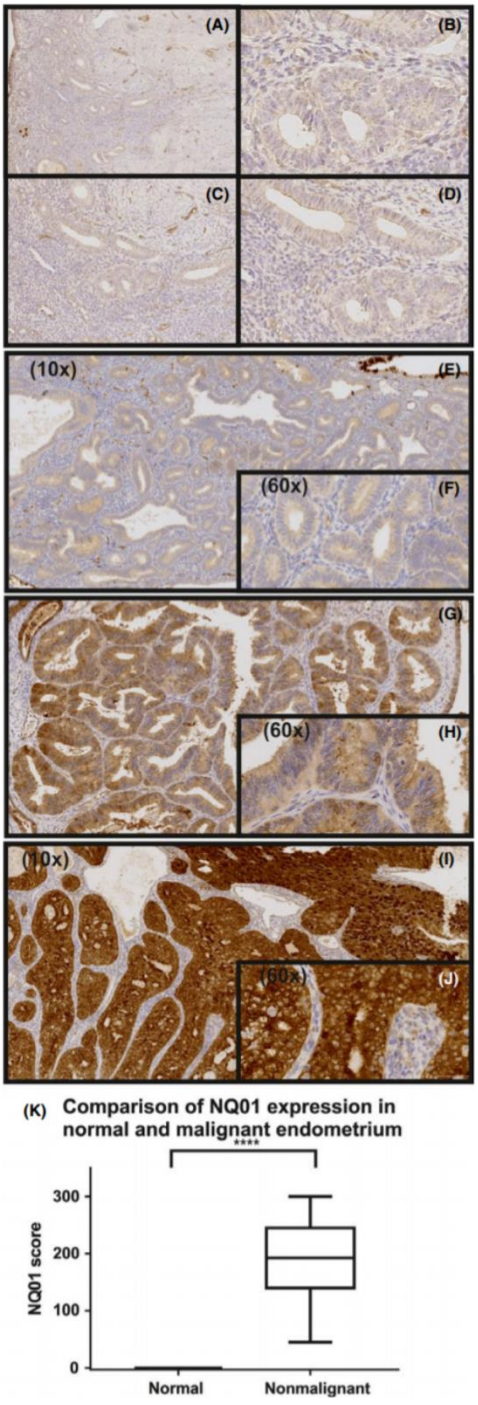

FIGURE 2 Immunohistochemistry was used to evaluate expression of NQO1 protein in nontumour (A-D) and endometrial cancer specimens (E-J). Representative NQO1 staining of endometrial cancer specimens with intensity scores of 1 (E, F), 2 (G, H) and 3 (I, J) at 10× and 60× magnification is shown. (F) Comparison of NQ01 expression in normal and malignant endometrium as determined by immunohistochemistry. NQ01 was expressed solely in endometrial cancers and not demonstrated in normal endometrium from control patients ($P < .0001$). [Colour figure can be viewed at wileyonlinelibrary.com]

selectively within malignant tissue may be an attractive therapeutic approach.[38] Consistent with this NQO1 null mice are more sensitive to chemical induced carcinogenesis[32] and NQO1 plays an essential role in oncogene-induced senescence. However, the association of overexpression of NQO1 with poorer outcomes in certain cancer types[36,37] suggests that tumours can bypass the antiproliferative actions of NQO1, potentially through the activation of procarcinogenic compounds.[39]

In this current study, expression of *NQO1* was significantly higher in tumour as compared to matched nontumour specimens (Figures 1, 2). NQO1 expression is regulated by the oestrogen receptor-α (ERα/NR3A1) and oestrogen receptor-β (ERβ/NR3A2)[40] and by progesterone.[41] As outlined above, aberrant oestrogen and progesterone signalling contributes to EC risk. Related to this, the antibreast cancer selective oestrogen receptor modulator, tamoxifen, is known to increase EC risk by inducing oestrogen-regulated gene expression[42] and altering oestrogen metabolism in endometrial cells.[43] NQO1 may therefore play a key role in the oestrogen-related links between EC and PCOS.

In conclusion, we have used a preliminary RNAseq analysis to identify aberrant gene expression in EC and endometrium from women with PCOS. One limitation to our study was that only individual patient samples were sequenced. However, we confirmed expression of a key gene identified by RNAseq, *NQO1*, in larger cohorts of patients with PCOS and EC at the mRNA and protein levels. In this study, increased NQO1 expression was not associated with standard prognostic clinicopathological features including tumour type, grade, stage and myometrial invasion lymphovascular space invasion (LVSI). Indeed, NQO1 was expressed ubiquitously in most tumours and was not associated with recurrence-free, endometrial cancer-specific or overall survival. However, *NQO1* expression, like that of 93 other transcripts, was deregulated in both PCOS and EC. This supports the hypothesis that PCOS can induce gene expression changes in the endometrium that resembles EC. It is possible such changes in gene expression contribute to the increased risk of EC in women with PCOS. NQO1 represents a potential therapeutic target in EC. NQO1 is inhibited by dicoumarol, and more specific next-generation NQO1-inhibitors are now available (Figure 3).[44] Therefore, the preclinical testing of such compounds for the treatment of EC and prevention of future EC in PCOS is warranted. Finally, further studies are now warranted to examine NQO1 protein expression in endometrial biopsies from women with PCOS in a prospective study to determine whether NQO1 may be useful to distinguish women at increased risk of developing EC.

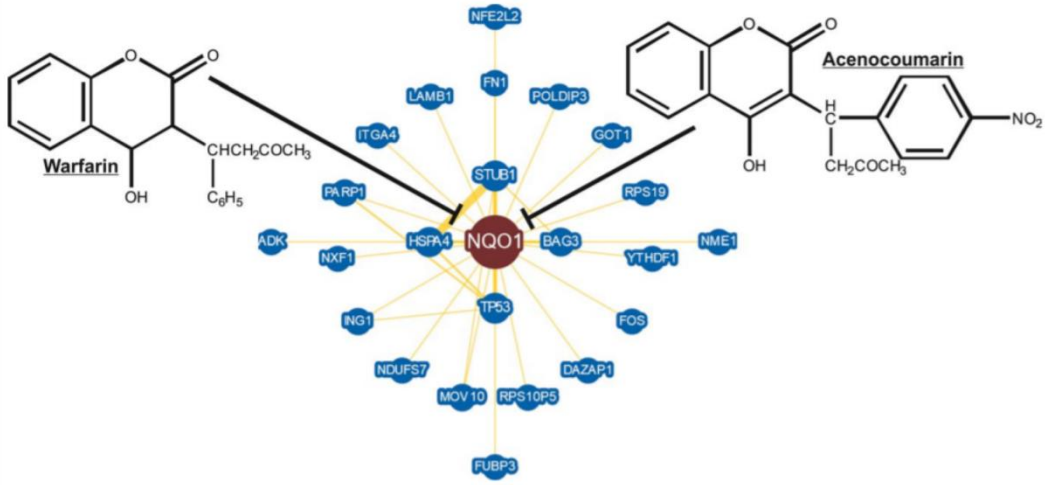

FIGURE 3 The BioGRID database[45] reports NQO1 functionally interacts with key regulators of cell proliferation including TP53. Furthermore, the enzymatic activity of NQO1 can be inhibited by the anticoagulants, warfarin and acenocoumarin and more specific next-generation NQO1-inhibitors are now available. This may point to potential chemo-preventative approaches to pharmacologically target elevated expression of NQO1 function in women with PCOS. [Colour figure can be viewed at wileyonlinelibrary.com]

ACKNOWLEDGEMENTS

We gratefully acknowledge the financial support of the University of Nottingham, the BBSRC-Doctoral training program (BB/I024291/1: VM, CSR, DMH, NPM) and Prostate Cancer UK (JJ, DMH, NPM). Assistance with slide preparation and optimization of the immunohistochemistry staining protocol was provided by Hannah Gregson and the Histology Department at the Cancer Research UK Manchester Institute. We would like to thank Dr Rhona McVey and Dr James Bolton for expert histopathological review of the Manchester tissue samples. VS is funded through a Wellcome Trust/Wellbeing of Women Research Training Fellowship. EC and SK are funded through a National Institute for Health Research (NIHR) Clinician Scientist Fellowship (award reference NIHR-CS-012-009). This article presents independent research partly funded by the NIHR and facilitated by the Greater Manchester Local Clinical Research Network. The views expressed are those of the authors and not necessarily those of the NHS, the NIHR or the Department of Health. This work was supported by the Biotechnology and Biological Sciences Research Council (grant number BB/I024291/1).

CONFLICT OF INTERESTS

The authors confirm no conflict of interests related to this study.

AUTHOR CONTRIBUTIONS

WA, EJC, MNS and NPM involved in study design, patient recruitment and project management. MNS, CC, VMM, JA, AL, AC, SK, VS, IS, CSR, JLP, NO, PF-U, DMH, CSR, NPM, EJC and WA conducted the experiments and data analysis. WA, EJC, JA, VNS, AL, NO, JLP, JJ, CSR, IJS, DMH and NPM wrote the manuscript.

REFERENCES

1. Siegel RL, Miller KD, Jemal A. Cancer statistics, 2016. *CA Cancer J Clin*. 2016;66:7-30.
2. Crosbie EJ, Zwahlen M, Kitchener HC, Egger M, Renehan AG. Body mass index, hormone replacement therapy, and endometrial cancer risk: a meta-analysis. *Cancer Epidemiol Biomarkers Prev*. 2010;19:3119-3130.
3. Crosbie E, Morrison J. The emerging epidemic of endometrial cancer: time to take action. *Cochrane Database Syst Rev* 2014;12:ED000095. https://doi.org/10.1002/14651858.ED000095
4. Hickey M, Doherty DA, Atkinson H, et al. Clinical, ultrasound and biochemical features of polycystic ovary syndrome in adolescents: implications for diagnosis. *Hum Reprod*. 2011;26:1469-1477.
5. Yildiz BO, Bozdag G, Yapici Z, Esinler I, Yarali H. Prevalence, phenotype and cardiometabolic risk of polycystic ovary syndrome under different diagnostic criteria. *Hum Reprod*. 2012;27:3067-3073.
6. Peigne M, Dewailly D. Long term complications of polycystic ovary syndrome (PCOS). *Ann Endocrinol (Paris)*. 2014;75:194-199.
7. Haoula Z, Salman M, Atiomo W. Evaluating the association between endometrial cancer and polycystic ovary syndrome. *Hum Reprod*. 2012;27:1327-1331.
8. Barry JA, Azizia MM, Hardiman PJ. Risk of endometrial, ovarian and breast cancer in women with polycystic ovary syndrome: a systematic review and meta-analysis. *Hum Reprod Update*. 2014;20:748-758.
9. Shafiee MN, Chapman C, Barrett D, Abu J, Atiomo W. Reviewing the molecular mechanisms which increase endometrial cancer (EC) risk in women with polycystic ovarian syndrome (PCOS): time for paradigm shift? *Gynecol Oncol*. 2013;131:489-492.
10. Shafiee MN, Seedhouse C, Mongan N, et al. Up-regulation of genes involved in the insulin signalling pathway (IGF1, PTEN and IGFBP1) in

the endometrium may link polycystic ovarian syndrome and endometrial cancer. *Mol Cell Endocrinol*. 2016;424:94-101.
11. Shafiee MN, Mongan N, Seedhouse C, et al. Sterol regulatory element binding protein-1 (SREBP1) gene expression is similarly increased in polycystic ovary syndrome and endometrial cancer. *Acta Obstet Gynecol Scand*. 2017;96:556-562.
12. Galazis N, Pang YL, Galazi M, Haoula Z, Layfield R, Atiomo W. Proteomic biomarkers of endometrial cancer risk in women with polycystic ovary syndrome: a systematic review and biomarker database integration. *Gynecol Endocrinol*. 2013;29:638-644.
13. Piltonen TT, Chen JC, Khatun M, et al. Endometrial stromal fibroblasts from women with polycystic ovary syndrome have impaired progesterone-mediated decidualization, aberrant cytokine profiles and promote enhanced immune cell migration in vitro. *Hum Reprod*. 2015;30:1203-1215.
14. Kandoth C, Schultz N, Cherniack AD, et al. Integrated genomic characterization of endometrial carcinoma. *Nature*. 2013;497:67-73.
15. Trapnell C, Roberts A, Goff L, et al. Differential gene and transcript expression analysis of RNA-seq experiments with TopHat and Cufflinks. *Nat Protoc*. 2012;7:562-578.
16. Montojo J, Zuberi K, Rodriguez H, Bader GD, Morris Q. GeneMANIA: fast gene network construction and function prediction for Cytoscape. *F1000Res* 2014;3:153.
17. Robinson MD, McCarthy DJ, Smyth GK. edgeR: a Bioconductor package for differential expression analysis of digital gene expression data. *Bioinformatics*. 2010;26:139-140.
18. Schmandt RE, Iglesias DA, Co NN, Lu KH. Understanding obesity and endometrial cancer risk: opportunities for prevention. *Am J Obstet Gynecol*. 2011;205:518-525.
19. Husing A, Dossus L, Ferrari P, et al. An epidemiological model for prediction of endometrial cancer risk in Europe. *Eur J Epidemiol*. 2016;31:51-60.
20. Wild S, Pierpoint T, Jacobs H, McKeigue P. Long-term consequences of polycystic ovary syndrome: results of a 31 year follow-up study. *Hum Fertil (Camb)*. 2000;3:101-105.
21. Fearnley EJ, Marquart L, Spurdle AB, Weinstein P, Webb PM, Australian Ovarian Cancer Study, G, Australian National Endometrial Cancer Study, G. Polycystic ovary syndrome increases the risk of endometrial cancer in women aged less than 50 years: an Australian case-control study. *Cancer Causes Control*. 2010;21:2303-2308.
22. Shafiee MN, Khan G, Ariffin R, et al. Preventing endometrial cancer risk in polycystic ovarian syndrome (PCOS) women: could metformin help? *Gynecol Oncol*. 2014;132:248-253.
23. Schindler AE. Progestogen deficiency and endometrial cancer risk. *Maturitas*. 2009;62:334-337.
24. Jansen E, Laven JS, Dommerholt HB, et al. Abnormal gene expression profiles in human ovaries from polycystic ovary syndrome patients. *Mol Endocrinol*. 2004;18:3050-3063.
25. Zorn KK, Bonome T, Gangi L, et al. Gene expression profiles of serous, endometrioid, and clear cell subtypes of ovarian and endometrial cancer. *Clin Cancer Res*. 2005;11:6422-6430.
26. Hevir N, Ribic-Pucelj M, Lanisnik Rizner T. Disturbed balance between phase I and II metabolizing enzymes in ovarian endometriosis: a source of excessive hydroxy-estrogens and ROS? *Mol Cell Endocrinol*. 2013;367:74-84.
27. Asher G, Lotem J, Kama R, Sachs L, Shaul Y. NQO1 stabilizes p53 through a distinct pathway. *Proc Natl Acad Sci U S A*. 2002;99:3099-3104.
28. Ross D, Siegel D. NAD(P)H:quinone oxidoreductase 1 (NQO1, DT-diaphorase), functions and pharmacogenetics. *Methods Enzymol*. 2004;382:115-144.
29. Talalay P, Dinkova-Kostova AT. Role of nicotinamide quinone oxidoreductase 1 (NQO1) in protection against toxicity of electrophiles and reactive oxygen intermediates. *Methods Enzymol*. 2004;382:355-364.
30. Phillips RM, Hendriks HR, Peters GJ, Pharmacology E, Molecular Mechanism G. EO9 (Apaziquone): from the clinic to the laboratory and back again. *Br J Pharmacol*. 2013;168:11-18.
31. Siegel D, Beall H, Kasai M, Arai H, Gibson NW, Ross D. pH-dependent inactivation of DT-diaphorase by mitomycin C and porfiromycin. *Mol Pharmacol*. 1993;44:1128-1134.
32. Iskander K, Gaikwad A, Paquet M, et al. Lower induction of p53 and decreased apoptosis in NQO1-null mice lead to increased sensitivity to chemical-induced skin carcinogenesis. *Cancer Res*. 2005;65:2054-2058.
33. Lajin B, Alachkar A. The NQO1 polymorphism C609T (Pro187Ser) and cancer susceptibility: a comprehensive meta-analysis. *Br J Cancer*. 2013;109:1325-1337.
34. Fagerholm R, Hofstetter B, Tommiska J, et al. NAD(P)H:quinone oxidoreductase 1 NQO1*2 genotype (P187S) is a strong prognostic and predictive factor in breast cancer. *Nat Genet*. 2008;40:844-853.
35. Jamshidi M, Bartkova J, Greco D, et al. NQO1 expression correlates inversely with NFkappaB activation in human breast cancer. *Breast Cancer Res Treat*. 2012;132:955-968.
36. Cui X, Li L, Yan G, et al. High expression of NQO1 is associated with poor prognosis in serous ovarian carcinoma. *BMC Cancer*. 2015;15:244.
37. Li Z, Zhang Y, Jin T, et al. NQO1 protein expression predicts poor prognosis of non-small cell lung cancers. *BMC Cancer*. 2015;15:207.
38. Bey EA, Bentle MS, Reinicke KE, et al. An NQO1- and PARP-1-mediated cell death pathway induced in non-small-cell lung cancer cells by beta-lapachone. *Proc Natl Acad Sci U S A*. 2007;104:11832-11837.
39. Martin FL, Patel II, Sozeri O, et al. Constitutive expression of bioactivating enzymes in normal human prostate suggests a capability to activate pro-carcinogens to DNA-damaging metabolites. *Prostate*. 2010;70:1586-1599.
40. Montano MM, Jaiswal AK, Katzenellenbogen BS. Transcriptional regulation of the human quinone reductase gene by antiestrogen-liganded estrogen receptor-alpha and estrogen receptor-beta. *J Biol Chem*. 1998;273:25443-25449.
41. Morrissy S, Strom J, Purdom-Dickinson S, Chen QM. NAD(P)H:quinone oxidoreductase 1 is induced by progesterone in cardiomyocytes. *Cardiovasc Toxicol*. 2012;12:108-114.
42. Shang Y, Brown M. Molecular determinants for the tissue specificity of SERMs. *Science*. 2002;295:2465-2468.
43. Williams-Brown MY, Salih SM, Xu X, et al. The effect of tamoxifen and raloxifene on estrogen metabolism and endometrial cancer risk. *J Steroid Biochem Mol Biol*. 2011;126:78-86.
44. Scott KA, Barnes J, Whitehead RC, Stratford IJ, Nolan KA. Inhibitors of NQO1: identification of compounds more potent than dicoumarol without associated off-target effects. *Biochem Pharmacol*. 2011;81:355-363.
45. Chatr-Aryamontri A, Breitkreutz BJ, Oughtred R, et al. The BioGRID interaction database: 2015 update. *Nucleic Acids Res*. 2015;43:D470-D478.

SUPPORTING INFORMATION

Additional Supporting Information may be found online in the supporting information tab for this article.

How to cite this article: Atiomo W, Shafiee MN, Chapman C, et al. Expression of NAD(P)H quinone dehydrogenase 1 (NQO1) is increased in the endometrium of women with endometrial cancer and women with polycystic ovary syndrome. *Clin Endocrinol (Oxf)*. 2017;87:557–565. https://doi.org/10.1111/cen.13436

Appendix 19 – Publication 3

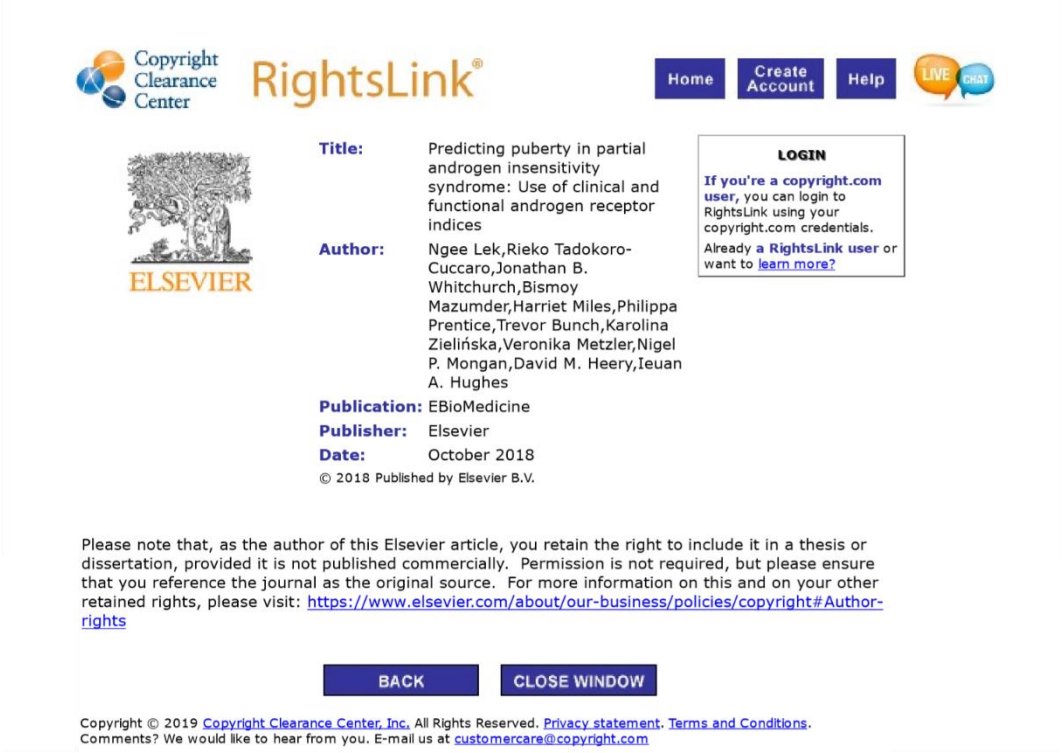

Copyright Clearance Center RightsLink®

Home | Create Account | Help | LIVE CHAT

ELSEVIER

Title: Predicting puberty in partial androgen insensitivity syndrome: Use of clinical and functional androgen receptor indices

Author: Ngee Lek,Rieko Tadokoro-Cuccaro,Jonathan B. Whitchurch,Bismoy Mazumder,Harriet Miles,Philippa Prentice,Trevor Bunch,Karolina Zielińska,Veronika Metzler,Nigel P. Mongan,David M. Heery,Ieuan A. Hughes

Publication: EBioMedicine

Publisher: Elsevier

Date: October 2018

© 2018 Published by Elsevier B.V.

LOGIN

If you're a copyright.com user, you can login to RightsLink using your copyright.com credentials.

Already **a RightsLink user** or want to learn more?

Please note that, as the author of this Elsevier article, you retain the right to include it in a thesis or dissertation, provided it is not published commercially. Permission is not required, but please ensure that you reference the journal as the original source. For more information on this and on your other retained rights, please visit: https://www.elsevier.com/about/our-business/policies/copyright#Author-rights

BACK CLOSE WINDOW

Copyright © 2019 Copyright Clearance Center, Inc. All Rights Reserved. Privacy statement. Terms and Conditions.
Comments? We would like to hear from you. E-mail us at customercare@copyright.com

EBioMedicine 36 (2018) 401–409

Contents lists available at ScienceDirect

EBioMedicine

journal homepage: www.ebiomedicine.com

EBioMedicine
Published by THE LANCET

Research paper

Predicting puberty in partial androgen insensitivity syndrome: Use of clinical and functional androgen receptor indices

Ngee Lek [a,b,c,1], Rieko Tadokoro-Cuccaro [a,1], Jonathan B. Whitchurch [d], Bismoy Mazumder [d], Harriet Miles [a], Philippa Prentice [a], Trevor Bunch [a], Karolina Zielińska [a], Veronika Metzler [e], Nigel P. Mongan [e], David M. Heery [d], Ieuan A. Hughes [a,*]

[a] University of Cambridge, Department of Paediatrics, Cambridge, United Kingdom
[b] KK Women's and Children's Hospital, Department of Paediatrics, Singapore
[c] Duke-NUS Medical School, National University of Singapore, Singapore
[d] School of Pharmacy, University of Nottingham, United Kingdom
[e] School of Veterinary Medicine and Science, University of Nottingham, United Kingdom

ARTICLE INFO

Article history:
Received 10 August 2018
Received in revised form 17 September 2018
Accepted 26 September 2018
Available online 11 October 2018

Keywords:
Androgen insensitivity
External masculinisation score
Puberty outcome
Sex assignment
Gynaecomastia
Androgen receptor
Mutation
Reporter assays
in silico modelling

ABSTRACT

Background: PAIS exhibits a complex spectrum of phenotypes and pubertal outcomes. The paucity of reliable prognostic indicators can confound management decisions including sex-of-rearing. We assessed whether external masculinisation score (EMS) at birth or functional assays correlates with pubertal outcome in PAIS patients and whether the EMS is helpful in sex assignment.

Methods: We collected pubertal outcome data for 27 male-assigned PAIS patients, all with confirmed androgen receptor (*AR*) mutations, including two previously uncharacterized variants (I899F; Y916C). Patients were grouped as follows; EMS at birth <5 and ≥ 5 (EMS in normal males is 12; median EMS in PAIS is 4·7) and pubertal outcomes compared.

Findings: Only 6/9 patients (67%) with EMS <5 underwent spontaneous onset of puberty, *versus* all 18 patients with EMS ≥5 ($p = .03$). Only 1/6 patients (17%) with EMS <5 developed adult genitalia reaching Tanner stage 4 or 5, *versus* 11/13 (85%) with EMS ≥5 ($p = 0{\cdot}01$). There was no significant difference between the two groups of patients in being prescribed androgen replacement, who reached adult testicular volume ≥ 15 ml, pubic hair Tanner stage 4 or 5, above average adult height, had gynaecomastia, and mastectomy. No correlation was observed between EMS and *in vitro* AR function.

Interpretation: In PAIS with *AR* mutation, birth EMS is a simple predictor of spontaneous pubertal onset and satisfactory adult genitalia. This provides useful information when discussing the likely options for management at puberty.

Fund: European Commission Framework 7 Programme, NIHR Cambridge Biomedical Research Centre, BBSRC DTP.

1. Introduction

Androgen insensitivity syndrome (AIS) is the most common cause of undermasculinisation in XY males with a disorder of sex development (DSD) when characterised by a phenotype consistent with androgen resistance [3–5]. The complete form (CAIS) is characterised by a female phenotype, while the partial form (PAIS) is expressed as a variable male phenotype. This includes hypospadias, micropenis, bifid scrotum and undescended testes at birth, or in later life, gynaecomastia and infertility as a result of oligospermia or azoospermia in a male with otherwise normal genitalia.

CAIS is invariably caused by a mutation in the androgen receptor (*AR*) gene, whereas a pathogenic *AR* mutation is found in only 22% of patients with a PAIS-like phenotype [6]. Consequently, it is important to exclude other conditions which can present with a similar XY DSD phenotype when undertaking studies in PAIS. Demonstrating an *AR* mutation which was confirmed to be pathogenic as a cause of the PAIS phenotype was a requirement for inclusion of cases for this present

Abbreviations: DSD, disorder of sex development; PAIS, partial androgen insensitivity syndrome; EMS, external masculinisation score; AR, androgen receptor; SDS, standard deviation score; DHT, dihydrotestosterone; NID, nuclear receptor interaction domain; LBD, ligand-binding domain; DBD, DNA-binding domain; WT, wild-type.

* Corresponding author at: Department of Paediatrics, University of Cambridge, Level 8, Box 116, Addenbrooke's Hospital, Hills Road, Cambridge CB2 0QQ, United Kingdom.
E-mail address: iah1000@cam.ac.uk (I.A. Hughes).

[1] Contributed equally.

https://doi.org/10.1016/j.ebiom.2018.09.047

Research in context

Evidence before this study

There are limited data on pubertal outcome in patients with partial androgen insensitivity syndrome (PAIS) assigned male at birth. We searched PubMed using the search term "('androgen insensitivity' AND (partial NOT complete)) AND ('long term' OR 'follow up' OR pubert* OR outcome)" (last searched in June 2018). After review, we could only identify two relevant articles [1,2]. One study reported pubertal outcome in 14 PAIS patients, all of whom had an external masculinisation score (EMS) of 5 or more, thus excluding information on the more severely undermasculinised infants at birth [1]. A more recent study reported pubertal outcome in a larger group of 29 males with a proven *AR* mutation and a range of EMS at birth [2]. A specific feature of this study was the universal finding of pubertal gynaecomastia.

Added value of this study

The paucity of outcome data at puberty makes it difficult to predict what will happen at puberty in boys with PAIS particularly when there is severe undermasculinisation of the external genitalia at birth. This study analysed prospectively collected data on EMS at birth and function of *AR* mutations in 27 PAIS patients to determine whether useful predictors of puberty outcome could be identified. The cohort included two patients with *AR* mutations (I899F and Y916C) for which functional studies had not previously been undertaken. All 18 patients who had EMS ≥5 at birth had spontaneous onset of puberty, whereas three of nine patients whose EMS <5 at birth failed to start puberty spontaneously. In contrast to the clinical findings, there was no clear predictor of puberty outcome from the functional analysis of *AR* variants.

Implications of all the available evidence

Our study indicates that in PAIS patients with a confirmed *AR* mutation, the EMS at birth is a simple predictor of spontaneous pubertal onset and adult genital development. Consistent with recent reports of gynaecomastia prevalence in PAIS [1,2], the majority of patients in this study developed the problem at puberty and irrespective of their EMS at birth. Consideration should be given to selectively starting an anti-estrogen or aromatase inhibitor in early puberty. Functional analysis of *AR* mutations *in vitro* provided detailed information to explain the PAIS phenotype but was not as predictive as clinical findings for puberty outcome. However, these assays together with *in silico* modelling of AR structure may prove beneficial in guiding optimal treatment in those patients requiring high dose androgen treatment.

study and knowledge of *AR* mutation status is important to guide management of PAIS in the longer term [2].

Sex assignment at birth for an infant with DSD is a central component of management undertaken jointly by health professionals and the family. In PAIS characterised by severe undermasculinisation, a key question raised is whether masculinisation is likely to occur at puberty. Data on such outcomes are limited [1,2]. Consistent findings appear to be a variable degree of spontaneous masculinisation at puberty, the need for androgen supplements to induce puberty in nearly half the cases, and the frequent occurrence of gynaecomastia.

There is a trend in recent decades towards male sex-of-rearing for all causes of XY DSD, including PAIS infants who are severely undermasculinised [7]. This poses a challenge of formulating predictive factors which inform puberty and subsequent development in early adulthood in males. We hypothesised that the degree of masculinisation at birth as assessed by a validated external masculinisation score (EMS) [8] and functional analysis of the cognate mutant *AR* would be clinically informative. Thus, clinical follow-up data and the results of *in vitro* functional studies for 19 unique *AR* mutations within the study cohort were analysed, including two previously uncharacterised *AR* mutants (I899F and Y916C) for which preliminary structure/function analysis is presented.

2. Patients and methods

2.1. Patients

The Cambridge DSD Database contains detailed information on each case based on a questionnaire completed by the referring clinician at the time of notification. Using this resource, 27 PAIS patients were identified with known *AR* mutations characterised functionally who were assigned male and were of pubertal or post-pubertal age at the last known clinical assessment.

2.2. Clinical data

Information on the external genitalia at birth was verified and further information on the status of pubertal development was obtained *via* a second questionnaire distributed to their current clinician following written informed consent from the patient and/or parents. The questionnaire was completed opportunistically during a routine clinic visit. The pubertal data were collected in binary format (yes/no): spontaneous onset of puberty; whether androgen replacement was given; testicular volume ≥ 15 ml (as assessed using Prader Orchidometer); Tanner stage 4 or 5 for pubic hair and genitalia (penile length was not measured consistently, with 'satisfactory penile development' often recorded); final adult height standard deviation score (SDS) ≥ 0 (*i.e.* taller than the average adult male in the UK using 1990 UK population reference); presence of gynaecomastia and whether mastectomy was performed. Data on testosterone and gonadotrophin concentrations were available in only 10 subjects, thereby an insufficient number for analysis in this study. The degree of virilisation at birth was quantified by the EMS [8]. The composite EMS ranges from a minimum of 0 (indicating complete lack of masculinisation) to a maximum of 12 (normal masculinisation).

The median EMS among all PAIS patients raised male in the Cambridge DSD Database ($n = 41$) is 4·7. The 27 patients in this study cohort were sub-divided into 2 groups based on an EMS at birth <5 (below median) and ≥ 5 (at or above median). The clinical data collated at puberty and beyond were compared between the two groups and analysed using Fisher's exact test for categorical variables as being the appropriate test for the relatively small sample size; statistical significance was taken to be $p < 0{\cdot}05$.

2.3. PAIS-associated AR mutations

Genomic DNA was isolated from peripheral leukocytes or genital skin fibroblasts using standard techniques. The coding exons and exon/intron boundaries of the *AR* gene were analysed by direct sequencing. Amino acid numbering for the human AR (1—920) is based on NM_000044.2 (NCBI). A total of 19 unique *AR* mutations were identified in the study cohort, which were assessed for their impact on AR-dependent reporter activation. Two previously uncharacterised variants were also assessed for dimerization and coactivator binding in yeast two-hybrid assays [9].

2.4. Mammalian expression plasmids

Wild-type (WT) human *AR* cDNA expression vector pSVAR0 was used to generate *AR* mutant expression vectors by QuikChange Site-Directed Mutagenesis Kit (Agilent Technologies) [10]. All *AR* constructs were verified by sequencing. The luciferase reporter construct pGRE2-TATA-Luc has been described previously [11]. Renilla luciferase constructs pGL4-TK and phRG-TK (Promega) or pCH110 (β-galactosidase) were used as transfection controls.

2.5. Transient transfection and reporter assays

For AR transactivation studies, COS-1 or HeLa cells were seeded into 12-well tissue culture plates in Dulbecco's modified essential medium (DMEM) containing 2 mM glutamine and 10% charcoal-stripped serum. Cells were transfected with 250 ng pGRE2-TATA-Luc, 25 ng pSVAR0 and a control reporter 25 ng phRG-TK (Renilla Luciferase) or pCH110 (β-galactosidase) as indicated using standard transfection procedures. After 16 h incubation the cells were exposed to fresh medium containing 0–10 nmol dihydrotestosterone (DHT; Sigma) or the synthetic androgen mibolerone (Steraloids Inc) for a further 24 h. The cells were then lysed in 500 μl passive lysis buffer (Promega) and the ratio of firefly to renilla was determined using Nanolight technology Alternatively, Dual-light System (Applied Biosystems) was used to measure Luciferase and β-galactosidase activities. Reporter assays were quantified using a Microplate Luminometer LB 960 (Berthold).

2.6. Yeast two-hybrid assays

Yeast two-hybrid interaction studies were performed as described previously using the *S. cerevisiae* L40 reporter strain transformed with expression vectors for LexA-SRC1 NID 431–761 (nuclear receptor interaction domain) in combination with VP16-AR LBD (627–920) [9]. VP16-AR LBD mutants I899F and Y916C were generated by site-directed PCR mutagenesis, and constructs were validated by sequencing. For AR-LBD dimerization assays, LexA-AR-LBD was co-transformed with VP16-*AR* expression plasmids. Construct expression levels were determined by western blotting using antibodies specific for the LexA (06–719; Millipore) and VP16 (sc-7546; Santa Cruz) epitopes. Co-transformants were purified and grown in selective medium in the presence of 1 μM Mibolerone or vehicle. Reporter β-galactosidase activities are presented as the mean of three independent clones with error bars to indicate standard deviations.

2.7. Ethical approval

Ethical approval for this study was obtained from the local research ethics committee (09/H0308/158), and institutional approval was obtained from the Research and Development Committee at the Cambridge University Hospitals NHS Foundation Trust, Cambridge, UK.

2.8. Role of the funding source

The funders had no role in study design, collection, analysis or interpretation of the data, writing the report, or the decision to submit the report for publication.

3. Results

3.1. EMS at birth and age of last clinical assessment

Table 1A, 1B shows EMS at birth and pubertal status at the last assessment for each of the 27 study participants in relation to their *AR* mutation type. The age range at last assessment was 14–44 years. Two of the participants (2-E and 2-O) were aged 14 years and both had entered puberty spontaneously but were not contactable at the time of the analysis. The remaining 25 participants had either recently completed puberty or were in young adulthood.

3.2. EMS and AR mutation type

Fig. 1 illustrates the distribution of mutations in the *AR* gene in this PAIS cohort. All were missense mutations and located in the DNA-binding (DBD) or ligand-binding (LBD) domains. There was no association between EMS at birth and the nature of the missense mutation. Indeed, some participants harbouring identical mutations displayed a widely variable EMS. For example, four participants (1-D, 1-E, 2-F and 2-G) with the same *AR* mutation (R841C) had an EMS of 1, 4, 5, and 9, respectively (see Table 1A, 1B).

Table 1A
Clinical pubertal data for the 9 patients with PAIS Group 1 (EMS at birth <5).

Study participant		1-A	1-B	1-C	1-D	1-E	1-F	1-G	1-H	1-I
AR mutation		R630W	S704G	F755 L	R841C	R841C	I899F #	R856H	A897E	A897E
Codon change		2247C > T	2469 A > G	2624C > G	2880C > T	2880C > T	3057 A > T	3016 G > A	3049C > A	3049C > A
Clinical features at birth										
EMS at birth (0—12)		3	2	1	1	4	1	3	3	3
	Scrotal fusion (0; 3)	0	0	0	0	0	0	0	0	0
	Microphallus (0; 3)	0	0	0	0	0	0	0	0	0
	Urethral meatus (0; 1; 2; 3)	0	0	0	0	1	0	0	0	0
	Right gonad (0; 0.5; 1.0; 1.5)	1.5	1	0.5	0.5	1.5	0.5	1.5	1.5	1.5
	Left gonad (0; 0.5; 1.0; 1.5)	1.5	1	0.5	0.5	1.5	0.5	1.5	1.5	1.5
Last known clinical features										
Age (years) at the last assessment		26	31	18	38	18	16	21	15	18
Spontaneous onset of puberty		Yes	No	No	Yes	No	Yes	Yes	Yes	Yes
Androgen replacement given		Yes	Yes	Yes	No	Yes	No	Yes	No	No
Adult testes ≥ 15 ml		No	No	Yes	–	Yes	Yes	No	–	Yes
Adult pubic hair PH4-PH5		Yes	No	Yes	No	Yes	Yes	Yes	Yes	Yes
Adult genitalia G4-G5		No	–	Yes	No	No	No	No	–	–
Adult height SDS > 0		No	No	Yes	No	Yes	Yes	No	Yes	Yes
Presence of gynaecomastia		Yes	Yes	Yes	Yes	Yes	Yes	Yes	No	No
Mastectomy done		Yes	Yes	Yes	Yes	Yes	Yes	No	No	No

Table 1B
Clinical pubertal data for the 18 patients with PAIS Group 2 (EMS at birth ≥ 5).

Study participant	2-A	2-B	2-C	2-D	2-E	2-F	2-G	2-H	2-I	2-J	2-K	2-L	2-M	2-N	2-O	2-P	2-Q	2-R
AR mutation	I665T	F674C	D691E	F755S	Y764C	R841C	R841C	R841H	I870M	I870M	A871V	M625 L	Y916C #	A597T	A871V	L713F &	L713F &	L713F &
Codon change	2353 T > C	2380 T > G	2432C > A	2623 T > C	2650 A > G	2880C > T	2880C > T	2881 G > A	2969 T > G	2969 T > G	2971C > T	2232 A > T	3106 A > G	2148 G > A	2971C > T	2496C > T	2496C > T	2496C > T
Clinical features at birth																		
EMS at birth (0–12)	6	6	5	8	8	5	9	5	6	6	10	7	5	6	6	8	8.5	9
scrotal fusion (0; 3)	3	0	0	3	3	0	3	0	0	0	3	0	0	0	0	0	3	3
microphallus (0; 3)	0	3	0	0	3	3	3	0	3	3	3	3	0	3	3	3	0	0
urethral meatus (0; 1; 2; 3)	0	0	2	2	1	1	1	2	0	0	1	1	2	0	0	3	3	3
right gonad (0; 0.5; 1.0; 1.5)	1.5	1.5	1.5	1.5	0.5	0.5	1	1.5	1.5	1.5	1.5	1.5	1.5	1.5	1.5	1	1	1.5
left gonad (0; 0.5; 1.0; 1.5)	1.5	1.5	1.5	1.5	0.5	0.5	1	1.5	1.5	1.5	1.5	1.5	1.5	1.5	1.5	1	1.5	1.5
Last known clinical features																		
Age (years) at the last assessment	18	18	31	17	14	17	27	20	18	18	44	21	30	16	14	19	17	16
Spontaneous onset of puberty	Yes	Yes	Yes	Yes	Yes	Yes	Yes	Yes	Yes	Yes	Yes	Yes	Yes	Yes	Yes	Yes	Yes	Yes
Androgen replacement given	–	Yes	Yes	Yes	–	No	–	Yes	–	–	No	No	Yes	No	–	Yes	Yes	Yes
Adult testes ≥ 15 ml	Yes	Yes	Yes	No	–	Yes	No	Yes	Yes	Yes	Yes	No	Yes	Yes	–	No	No	–
Adult pubic hair PH4-PH5	Yes	Yes	–	–	–	Yes	Yes	Yes	Yes	Yes	–	Yes	–	Yes	–	Yes	Yes	Yes
Adult genitalia G4-G5	Yes	Yes	No	–	–	Yes	No	Yes	Yes	Yes	–	Yes	–	Yes	–	Yes	Yes	Yes
Adult height SDS > 0	–	Yes	No	Yes	–	No	Yes	Yes	No	Yes	–	No	Yes	–	–	Yes	Yes	–
Presence of gynaecomastia	Yes	Yes	Yes	Yes	–	–	Yes	Yes	Yes	–	Yes	Yes	Yes	Yes	–	Yes	Yes	Yes
Mastectomy done	–	–	Yes	Yes	–	–	Yes	Yes	Yes	–	–	No	No	–	–	Yes	Yes	Yes

In this cohort of 27 patients with PAIS, a total of 19 different mutations in the *AR* were found.
All the mutations except I899F and Y916C (the ones marked with #) have accompanying data from functional studies for comparison with the clinical pubertal data.
Three siblings with *AR* mutation L713F (the ones marked with &) were included in the study by Lucas-Herald et al. See reference 2.

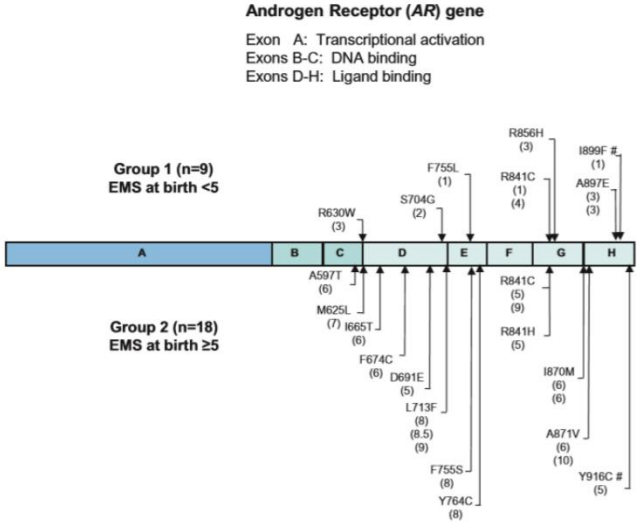

Fig. 1. Scheme of androgen receptor gene. Androgen receptor mutations and patients' EMS at birth (in parentheses) were illustrated. Upper; Group 1 (EMS < 5) and below; Group 2 (EMS ≥5). Mutations I899F and Y916C (marked with #) were characterised in Fig. 3.

3.3. EMS and pubertal outcome

Table 2 shows a quantitative summary of the study cohort (where data were available). For comparison of pubertal outcomes, the participants were sub-divided according to the EMS: Group 1, EMS <5 at birth ($n = 9$) and Group 2, EMS ≥5 at birth ($n = 18$). This cohort of 27 PAIS patients had a higher median (interquartile range) EMS of 6·0 (3·0 to 7·5), compared to an EMS of 4·8 (3·0 to 6·0) recorded in a previously published cohort of 36 male-assigned PAIS patients [6] and a median EMS of 4·7 in all 41 male-assigned PAIS patients recorded in the Cambridge DSD Database. In this study, there was no statistically significant difference between Groups 1 and 2 for age at last assessment. There was a trend towards less data on pubertal outcome in Group 2, and particularly on whether mastectomy had occurred ($p = 0·03$). Overall differences in data availability between the two groups did not reach statistical significance.

3.4. Spontaneous onset of puberty

24 of the total cohort of 27 participants (89%) entered puberty spontaneously, based primarily on evidence of an increase in testicular volume. There was a statistically significant difference in spontaneous *versus* non-spontaneous pubertal onset according to the EMS: 6/9

Table 2
Results of statistical analyses on the clinical pubertal data for the 27 patients with PAIS in the study cohort.

Study cohort [median (IQR)]	Group 1 (EMS at birth < 5), n = 9				Group 2 (EMS at birth ≥ 5), n = 18				p-value *	(Group 1 + Group 2), $n = 27$	
EMS at birth (0–12)	3.0 (1.0 to 3.0)				6.0 (6.0 to 8.0)				<0.001	6.0 (3.0 to 7.5)	
Age (years) at last assessment	18.0 (18.0 to 26.0)				18.0 (17.0 to 20.8)				0.53	18.0 (17.0 to 23.5)	
	Group 1 (EMS at birth < 5), $n = 9$				Group 2 (EMS at birth ≥ 5), n = 18					(Group 1 + Group 2), n = 27	
Pubertal outcomes [binary]	Yes	No	Total data, n [%] ^		Yes	No	Total data, n [%] ^		p-value **	Total available data, n [%] ^	
Spontaneous onset of puberty	6	3	9	[100]	18	0	18	[100]	0.03	27	[100]
Androgen replacement given	5	4	9	[100]	8	4	12	[67]	0.67	21	[78]
Adult Testes ≥ 15 ml	4	3	7	[78]	10	5	15	[83]	1.00	22	[81]
Adult Pubic Hair PH4-PH5	7	2	9	[100]	12	0	12	[67]	0.17	21	[78]
Adult Genitalia G4-G5	1	5	6	[67]	11	2	13	[72]	0.01	19	[70]
Adult Height SDS > 0	5	4	9	[100]	8	4	12	[67]	0.67	21	[78]
Presence of gynaecomastia	7	2	9	[100]	14	0	14	[78]	0.14	23	[79]
Mastectomy done	6	3	9	[100]	8	2	10	[56]	0.63	19	[70]

Statistical analyses
There was no statistically significant difference in the age at last clinical assessment between patients in the two groups.
All the 18 patients with EMS at birth ≥ 5 (Group 2) had spontaneous onset of pubertal development, compared to 6 of 9 patients with EMS at birth <5 (Group 1).
Only 1 of 6 patients with EMS at birth <5 (Group 1) attained Genitalia Tanner Stage G4 or G5 in adulthood, compared to 11 of 13 patients with EMS at birth ≥ 5 (Group 2).
^ Data availability:
In this cohort of 27 patients with PAIS, information on evidence of spermatogenesis was available in six patients (22%).
There was fewer availability of pubertal outcome data in Group 2 (EMS ≥ 5) for whether mastectomy was done (Fisher's exact test; $p = .03$).
There was a trend towards fewer availability of pubertal outcome data in Group 2 (EMS ≥ 5) for whether androgen replacement was given,
Whether Pubic Hair Tanner Stage PH4 or PH5 in adulthood was attained, and whether Height SDS >0 in adulthood was attained (Fisher's exact test; all $p = .07$).
Differences in data availability between the two groups for the other pubertal outcomes did not reach statistical significance (Fisher's exact test; all $p > .10$).
* Mann-Whitney *U* test was used to test for differences in EMS at birth and age at last clinical assessment of puberty between patients in the two groups.
** Fisher's exact test was used to test for differences in pubertal outcome (binary) parameters between patients in the two groups.

participants (67%) with EMS < 5 had spontaneous onset of puberty, compared to all 18 participants with EMS ≥5 ($p = 0{\cdot}03$).

3.5. Tanner stage 4 or 5 in adult genitalia

Data on this outcome parameter were available in 19/27 participants (70%). Only 1/6 participants (17%) with EMS <5 had adult genitalia reaching Tanner stage 4 or 5, compared to 11/13 participants (85%) with EMS ≥5 ($p = 0{\cdot}01$).

For all the other pubertal outcomes, there was no statistically significant difference between Groups 1 and 2 for androgen replacement ($n = 21$; $p = 0{\cdot}67$), achieving adult testicular volume ≥ 15 ml ($n = 22$; $p = 1{\cdot}00$), pubic hair Tanner stage 4 or 5 (n = 21; p = 0·17), above average adult male height (n = 21; p = 0·67), development of gynaecomastia ($n = 23$; p = 0·14), or mastectomy surgery ($n = 19$; p = 0·63). Importantly, among the participants in whom data were available (n = 23), 21 (91%) developed gynaecomastia irrespective of the EMS at birth or the type of *AR* mutation. Two siblings (1-H and 1-I) with *AR* mutation A897E showed no gynaecomastia with EMS at birth of 3 in both.

3.6. EMS and functional analysis of AR mutants

PAIS–associated mutations in *AR* may potentially impact on different AR functions including expression of the *AR* gene, stability of the mRNA or AR protein, or protein functions such as DNA or ligand binding, dimerization and cofactor binding, nuclear localisation, and transcriptional activity. As *AR* transcriptional activity is a readout for most of these functions, we assessed androgen-dependent reporter gene activation by wild-type and mutant AR proteins in well-established reporter assays using transiently transfected cells. Fig. 2 depicts reporter gene activation by wild-type and mutant AR proteins in response to increasing DHT/mibolerone concentrations. Transcriptional activity of mutant *AR*s was significantly impaired except for R630W, A597T (Fig. 2A), and for A897E (Fig. 2B). Although these three mutant *AR*s show a normal transcriptional response, the associated EMS in the cognate participants were reduced to 3 (1-A, 1-H and 1-I) and 6 (2-N). Furthermore, the phenotype at birth as defined by the EMS was extremely variable (including the four participants with the R841C mutation) and did not correlate with the results of *in vitro* transcriptional activation studies. The poor correlation between the specific pathologic mutation in the *AR* sequence and the clinical presentation at birth suggests other factors impact on phenotype.

3.7. Mutant AR activity and spontaneous onset of puberty

The activity of 17 different mutant *AR*s as based on transactivation assays *in vitro* was analysed in relation to whether puberty occurred spontaneously or not. The data are summarised in Fig. 2 and Table 1A, 1B. Increasing concentrations of DHT or mibolerone were used in the assay and the transcriptional response of a reporter gene was compared with the wild-type *AR*. There was no consistent relationship between the degree of transcriptional *AR* deficit and puberty outcome. Mutants R841H and F674C in participants 2-H and 2-B, respectively, had low

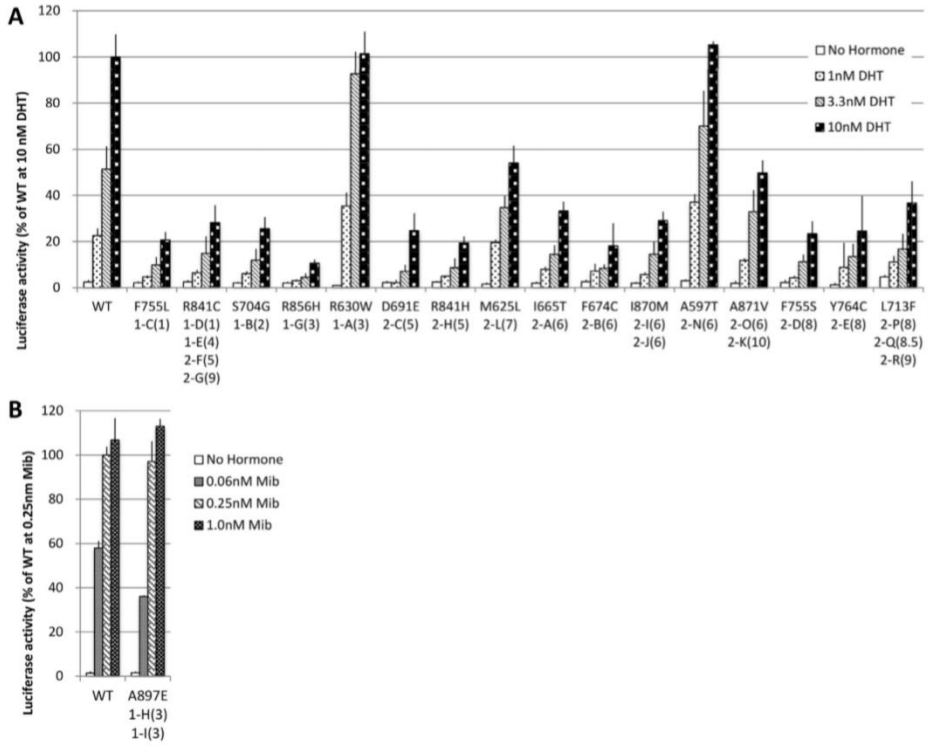

Fig. 2. A: Reporter assays using extracts of transiently transfected COS-1 cells showing dose-dependent activation of an androgen-responsive luciferase reporter gene by wild-type (WT) or variant AR proteins in response to dihydrotestosterone (DHT). B: Reporter assay for A897E was performed separately using COS-1 cells and mibolerone (Mib).

transcriptional activity relative to wild-type *AR* and yet in both cases, puberty occurred spontaneously. In contrast, mutant S704G identified in participant 1-B was similarly transcriptionally inactive and in this instance, puberty did not occur spontaneously and response to androgen treatment was not satisfactory. Nevertheless, although *AR* transcriptional activity in reporter assays was invariably reduced in most of the cohort, only three boys did not enter puberty spontaneously. Mutant R841C characterised by low transcriptional activity was identified in four separate participants of whom three entered puberty spontaneously and one did not. The widespread inconsistency between this phenotypic marker and the results of *AR* function assessed *in vitro* indicates that the *AR* functional assays employed here may not be a reliable predictor of pubertal outcome.

3.8. Structure and function analysis of I899F and Y916C AR variants

Two *AR* mutations were identified during our molecular investigation of this cohort of patients with PAIS who were raised male, namely I899F (identified in participant 1-G, Group 1) and Y916C (identified in participant 2-M, Group 2) where the variants were previously uncharacterised. A preliminary analysis of structure and function was undertaken as part of this study.

Examination of the crystal structures of agonist-bound AR LBD monomers (PDB: 3L3X, 4OEY) or the AR LBD homodimer (PDB: 5JJM) in complex with cofactor peptides revealed that the I899 sidechain forms part of the cofactor binding site whereas the Y916 side chain lies exposed on an outer surface of the AR LBD, distant from ligand binding, dimerisation or cofactor binding sites (Supplementary Figs. S1 and S2). Consistent with this, both *AR* mutants (I899F and Y916C) displayed reduced ability to activate the reporter, compared to wild-type *AR*, especially at the low concentration (0·1 nM) of exogenous androgen tested (Fig. 3A). This effect on activity was more pronounced with *AR* mutant I899F. To assess whether these mutations impact on the function of the AR LBD, we performed yeast two-hybrid studies as described previously [12]. As shown in Fig. 3B, wild-type AR LBD showed a strong ligand–dependent interaction with the nuclear receptor interaction domain (NID) of the Steroid Receptor coactivator (SRC1), a known cofactor for AR containing three LXXLL motifs. This interaction was significantly compromised by the I899F substitution (Fig. 3B and C) consistent with the proximity of the residue to the surface required for both cofactor binding and N/C domain interactions (Supplementary Fig. S2). In contrast the I899F mutation had no significant impact on the ability of the AR LBD to form homodimers in these assays in response to ligand (Fig. 3D), indicating that other major LBD functions were not affected.

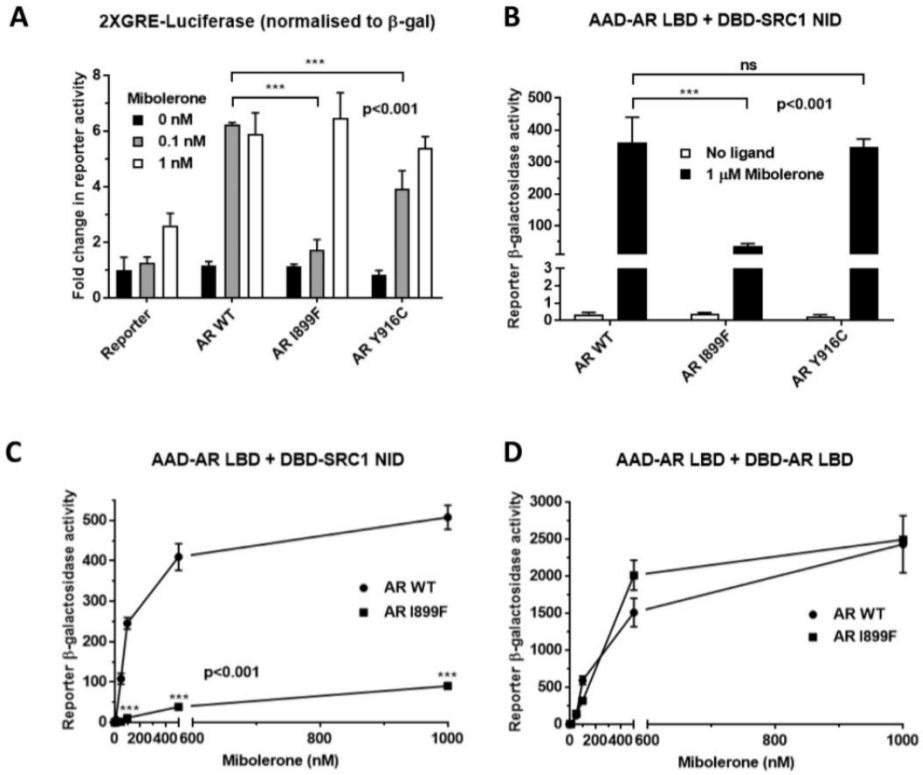

Fig. 3. A: Reporter assays using extracts of transiently transfected HeLa cells showing dose-dependent activation of an androgen-responsive luciferase reporter gene by wild-type (WT) or variant AR proteins in response to mibolerone. B: Yeast two-hybrid assays to assess cofactor binding by AR proteins. Shown is reporter activity due to interaction of AAD-AR LBD WT, I899F or Y916C constructs with the nuclear receptor interaction domain (NID) of steroid receptor coactivator 1 protein (DBD-SRC1 NID) in the presence of vehicle or mibolerone (1 μM) as indicated. C: Dose response curve in yeast two-hybrid assay comparing interaction of AAD-AR LBD WT and I899F proteins with DBD-SRC1 NID. D: Yeast two-hybrid assay assessing homo-dimerization capabilities of AR LBD WT or AR-LBD I899F constructs. The data shown represent the mean of triplicates and the error bars indicate standard deviations. *** = $p <$ .001 by 2-way ANOVA.

Western blots confirmed similar expression levels of the wild-type and mutant AR and SRC1 two-hybrid proteins (Supplementary Fig. S3),

4. Discussion

We report the largest cohort of PAIS patients to date whose puberty has been systematically characterised and quantitatively analysed in relation to the nature of their *AR* mutation. All 18 patients with median-or-higher EMS at birth achieved spontaneous onset of puberty, whereas three of the nine patients with lower-than-median EMS needed androgen treatment to induce puberty. This confirms the utility of assessing the degree of virilisation at birth to predict likely spontaneous pubertal development. The finding has practical importance in assisting health professionals and families when discussing the likely options for management at puberty, particularly in light of the recent trend for male assignment in PAIS [7].

Indicators of final pubertal progression were also informative. There was failure to reach Tanner stage 4 or 5 in more of the PAIS patients with low EMS. There were no significant differences between the two groups of PAIS patients with high or low EMS in terms of adult testicular volume, Tanner staging of pubic hair, adult height and incidence of gynaecomastia. Sperm analysis had been undertaken in 5 patients all of whom had oligo/azoospermia (1-A, 1-D, 2-C, 2-G, 2-L). A further patient was reported to have two children but no additional details were available (2-K). Overall, the results of this study suggest that the higher the EMS is at birth the more likely that puberty will occur spontaneously with satisfactory genital development.

A previous study from Denmark reported gynaecomastia in 13 of 14 PAIS patients in their cohort [1]. The study group was unusual since eight patients had a normal EMS at birth and first presented in puberty with gynaecomastia as a sign of PAIS. The authors estimated that their small cohort accounted for 74% of PAIS patients in Denmark, suggesting the more severely undermasculinised patients presenting at birth were not included. A larger study of boys with PAIS through the International Disorders of Sex Development Registry reported universal development of gynaecomastia at puberty [2]. This also seemed to be the case in our study apart from two siblings who showed no gynaecomastia. Both had an EMS of 3 at birth and entered puberty spontaneously. That pubertal gynaecomastia is generally common in PAIS raises the possibility of prevention with the use of anti-estrogens and aromatase inhibitors to avoid surgical reduction mammoplasty [13].

A specific aspect of the current study was inclusion of patients in whom not only was the diagnosis confirmed by sequencing the *AR* gene, but the pathogenicity of the mutation was also assessed. The results show that all mutations located in the AR LBD displayed reduced transcriptional activity as measured in a reporter gene activation assay. However, this *in vitro* profile was not sufficiently specific in relation to clinical parameters such as the EMS and whether puberty started spontaneously. Two mutations, A597T and R630W, were located outside the LBD and both demonstrated wild-type activity *in vitro*. A597T occurs in the DNA-binding domain and was originally reported in two families with Reifenstein syndrome, a previously used eponymous term to describe the severe form of PAIS [14]. Subsequent studies showed this mutation disrupts AR dimerization and hence DNA binding [14,15]. The R630 residue lies at the DBD-hinge domain boundary and its role is poorly understood. A mutation in this residue (R629Q using the former numbering system) was identified in a prostate cancer patient with hormone refractory/androgen independent disease and was revealed to enhance *AR* transcriptional activation [16]. This suggests that the substitution of arginine by glutamine, an amino acid of similar volume, promotes AR function whereas the presence of a bulkier aromatic tryptophan side chain cannot be accommodated and thereby disrupts androgen signalling.

A combination of reporter assays, yeast two-hybrid assays and *in silico* modelling was used for functional characterisation of Y916C and I899F, two novel *AR* mutations identified during the course of this study. The results show that I899F compromises the recruitment of the coactivator, SRC1 and consequently is likely to impair AR-regulated transcription [17]. Structural data for the LBD in complex with LXXLL or FXXLF motifs support this conclusion. I899 makes important stabilising contacts with the first conserved leucine or phenylalanine in these motifs that would be sterically disrupted by a phenylalanine side chain, consistent with the yeast two-hybrid data (Figs. 3B–3D).

The Y916 residue does not participate in the cofactor binding site, nor at the recently characterised AR dimerization interface [18]. However, it may be involved in interactions with other proteins due to its exposed location on the AR LBD surface in both the monomeric and dimeric structures (Supplementary Fig. S1). A previous study has shown that Y916 is phosphorylated by Src kinase and that this event is important for recruitment of AR to chromatin [19]. Disruption of such function is unlikely to be detected in a reporter gene assay. Future studies should address the developmental regulation of AR phosphorylation as its physiological significance may have relevance to the timing of pubertal onset and subsequent progression [20].

Since the phenotype associated with PAIS is so variable and pleiotropic in its causation, it is generally accepted that a diagnosis of PAIS should be confirmed by identifying a mutation in the *AR* gene [3]. Furthermore, additional studies of the mutant receptor are needed, particularly when the mutation is novel. While the additional use of yeast two-hybrid assays provides mechanistic insights into the nature of the functional defect in AR signalling, it is evident that the use of *in vitro* assays of androgen action used in this study is not sufficiently informative to predict how puberty will develop in PAIS associated with a particular *AR* mutation. This may be due to variable responses according to different promoters used in reporter gene assays under the conditions employed [21,22]. The complexity of nuclear receptor coregulator dynamics is now well established, where the activity of the receptor itself is influenced by the DNA elements bound, together with coregulator expression and recruitment. Current *in vitro* methods are likely to be sensitive enough only to detect the most extreme of functional defects. There are also examples of mosaic expression of *AR* mutations in PAIS which can explain variable phenotypes [23–25]. The question of mosaicism was not systematically examined in this study. It is likely to be infrequent as in most cases, genital skin fibroblast lines had been established for androgen binding assays and furthermore, many of the cases were familial.

The strength of the present study is a relatively large cohort of patients with PAIS demonstrating a range of EMS values which reliably indicated the likelihood of spontaneous onset of puberty. The outcome parameters of puberty were generally complete, apart from systematic evidence of spermatogenesis. Furthermore, the clinical dataset was coupled with detailed information about the *AR* mutation identified in each patient, including the use of *in silico* modelling. The propensity for infants with PAIS now to be more likely assigned male at birth requires a management policy that addresses the clinical challenges which may be faced at puberty and beyond. The majority of patients with PAIS assigned male appear to enter puberty spontaneously. Thereafter, androgen supplementation may be required for which it may be possible to utilise data on AR structure and function as a guide for the type and dose of androgen preparation.

Contributors

NL, RTC, PP, HM, and IAH designed the study, collected, analysed, and interpreted the data and wrote the report. TB, KZ, and JW performed reporter assays. DMH designed the Y2H experiments, analysed data and co-wrote the manuscript. JW and BM generated Y2H constructs and performed Y2H reporter assays, and western blots. NPM, VM analysed data and edited the manuscript.

Declaration of interests

We declare no competing interests.

Acknowledgements

NL was funded by Singapore National Medical Research Council (NMRC) Transition Award (NMRC/TA/0037/2015). RTC was supported by the National Institute for Health Research Cambridge Biomedical Research Centre. JW and VM were supported by the University of Nottingham BBSRC Doctoral Training program (BB/M008770/1). BM was supported by a University of Nottingham Vice Chancellors scholarship.

We thank the multidisciplinary members of the DSD team who have contributed to the care of these children with complex needs. We are extremely grateful to the following clinicians for notifying cases and for contributing to the data analysed in this study: Prof D Powell, Drs C Costigan and S O'Connell (Our Lady's Children Hospital, Dublin), Drs C S Smith and J Blair (Alder Hey Children's Hospital, Liverpool), Prof J Wass, Drs F Ryan and C W Burke (The Oxford University Hospitals), Dr. R Stanhope (University College Hospital, London), Dr. J A Hulse (St Thomas's Hospital, London), Prof P Hindmarsh and Dr. R Amin (Great Ormond Street Hospital for Children, London), Dr. S Hannema (Leiden University), Dr. J Kirk (Birmingham Children's Hospital, Birmingham), Prof M Savage, and Drs VK A Kumar and V Lawrence (St. Bartholomew's and The London Hospital, London), Dr. L Bath (Royal Hospital for Sick Children, Edinburgh), Dr. J Davies (Southampton University Hospital, Southampton), Prof J Gregory and Dr. J Warner (University Hospital of Wales, Cardiff), Dr. E Crowne (Bristol Children's Hospital, Bristol), Drs T Cheetham and S G Ball (Royal Victoria Infirmary, Newcastle), Dr. E Cheyne (Stoke Mandeville Hospital), Prof R Semple (Queens Medical Research Institute, Edinburgh), Prof O Hiort (University of Lübeck).

Appendix A. Supplementary data

Supplementary data to this article can be found online at https://doi.org/10.1016/j.ebiom.2018.09.047.

References

[1] Hellmann P, Christiansen P, Johannsen TH, Main KM, Duno M, Juul A. Male patients with partial androgen insensitivity syndrome: a longitudinal follow-up of growth, reproductive hormones and the development of gynaecomastia. Arch Dis Child 2012;97(5):403–9.
[2] Lucas-Herald A, Bertelloni S, Juul A, et al. The Long-Term Outcome of Boys with Partial Androgen Insensitivity Syndrome and a Mutation in the Androgen Receptor Gene. J Clin Endocrinol Metab 2016;101(11):3959–67.
[3] Hughes IA, Davies JD, Bunch TI, Pasterski V, Mastroyannopoulou K, MacDougall J. Androgen insensitivity syndrome. Lancet 2012;380(9851):1419–28.
[4] Mongan NP, Tadokoro-Cuccaro R, Bunch T, Hughes IA. Androgen insensitivity syndrome. Best Pract Res Clin Endocrinol Metab 2015;29(4):569–80.
[5] Tadokoro-Cuccaro R, Hughes IA. Androgen insensitivity syndrome. Curr Opin Endocrinol Diabetes Obes 2014;21(6):499–503.
[6] Lek N, Miles H, Bunch T, et al. Low frequency of androgen receptor gene mutations in 46 XY DSD, and fetal growth restriction. Arch Dis Child 2014;99(4):358–61.
[7] Kolesinska Z, Ahmed SF, Niedziela M, et al. Changes over time in sex assignment for disorders of sex development. Pediatrics 2014;134(3):e710–5.
[8] Ahmed SF, Khwaja O, Hughes IA. The role of a clinical score in the assessment of ambiguous genitalia. BJU Int 2000;85(1):120–4.
[9] Chan CM, Fulton J, Montiel-Duarte C, et al. A signature motif mediating selective interactions of BCL11A with the NR2E/F subfamily of orphan nuclear receptors. Nucleic Acids Res 2013;41(21):9663–79.
[10] Brinkmann AO, Faber PW, van Rooij HC, et al. The human androgen receptor: domain structure, genomic organization and regulation of expression. J Steroid Biochem 1989;34(1–6):307–10.
[11] Knoke I, Allera A, Wieacker P. Significance of the CAG repeat length in the androgen receptor gene (AR) for the transactivation function of an M780I mutant AR. Hum Genet 1999;104(3):257–61.
[12] Chen CV, Brummet JL, Lonstein JS, Jordan CL, Breedlove SM. New knockout model confirms a role for androgen receptors in regulating anxiety-like behaviors and HPA response in mice. Horm Behav 2014;65(3):211–8.
[13] Soliman AT, De Sanctis V, Yassin M. Management of Adolescent Gynecomastia: an Update. Acta Biomed 2017;88(2):204–13.
[14] Klocker H, Kaspar F, Eberle J, Uberreiter S, Radmayr C, Bartsch G. Point mutation in the DNA binding domain of the androgen receptor in two families with Reifenstein syndrome. Am J Hum Genet 1992;50(6):1318–27.
[15] Gast A, Neuschmid-Kaspar F, Klocker H, Cato AC. A single amino acid exchange abolishes dimerization of the androgen receptor and causes Reifenstein syndrome. Mol Cell Endocrinol 1995; 111(1): 93–8.
[16] Haelens A, Tanner T, Denayer S, Callewaert L, Claessens F. The hinge region regulates DNA binding, nuclear translocation, and transactivation of the androgen receptor. Cancer Res 2007;67(9):4514–23.
[17] Stashi E, York B, O'Malley BW. Steroid receptor coactivators: servants and masters for control of systems metabolism. Trends Endocrinol Metab 2014;25(7):337–47.
[18] Nadal M, Prekovic S, Gallastegui N, et al. Structure of the homodimeric androgen receptor ligand-binding domain. Nat Commun 2017;8:14388.
[19] Guo Z, Dai B, Jiang T, et al. Regulation of androgen receptor activity by tyrosine phosphorylation. Cancer Cell 2006;10(4):309–19.
[20] Zakharov MN, Pillai BK, Bhasin S, et al. Dynamics of coregulator-induced conformational perturbations in androgen receptor ligand binding domain. Mol Cell Endocrinol 2011;341(1–2):1–8.
[21] Simon S, Mueller SO. Human reporter gene assays: transcriptional activity of the androgen receptor is modulated by the cellular environment and promoter context. Toxicology 2006;220(2–3):90–103.
[22] Tadokoro-Cuccaro R, Davies J, Mongan NP, et al. Promoter-dependent activity on androgen receptor N-terminal domain mutations in androgen insensitivity syndrome. Sex Dev 2014;8(6):339–49.
[23] Batista RL, Rodrigues AS, Machado AZ, et al. Partial androgen insensitivity syndrome due to somatic mosaicism of the androgen receptor. J Pediatr Endocrinol Met 2018; 31(2):223–8.
[24] Gottlieb B, Beitel LK, Trifiro MA. Variable expressivity and mutation databases: the androgen receptor gene mutations database. Hum Mutat 2001;17(5):382–8.
[25] Holterhus PM, Wiebel J, Sinnecker GH, et al. Clinical and molecular spectrum of somatic mosaicism in androgen insensitivity syndrome. Pediatr Res 1999;46(6): 684–90.

Appendix 20 – PIPS reflective statement

Note to examiners:

This statement is included as an appendix to the thesis in order that the thesis accurately captures the PhD training experienced by the candidate as a BBSRC Doctoral Training Partnership student.

The Professional Internship for PhD Students is a compulsory 3-month placement which must be undertaken by DTP students. It is usually centred on a specific project and must not be related to the PhD project. This reflective statement is designed to capture the skills development which has taken place during the student's placement and the impact on their career plans it has had.

PIPS Reflective Statement

I did my PIP at the Cancer Council NSW as a Communication and event manager in Byron Bay, Australia. Every year, the Cancer Council runs the "Pink campaign" to fundraise money to help people affected with breast cancer. As part of this campaign, the "Health Project" was introduced, which aimed to involve gyms, yoga centres and health centres as fundraisers of the Pink campaign and raise awareness for breast cancer. The Health Project was run for the first time at the Cancer Council and I was given the lead for this project. This enabeled me to learn more about project management (incl. conception, planning, execution & poject closing). First, I defined the project. Here it was important to think about what is feasible to do and to set achievable goals within the budget. After the planning, the project was initiated and launched. What brought me out of my comfort most, was the countless phone calls I had to make and ask gym/yoga/health centre managers whether they would like to invest their vabluable time in running a fundraing event for the Cancer Council. Through this task, I improved my communication, and probably also my negotiation skills. I then supported the fundraisers with organising their events and providing them with merchandise, posters, advertisement, etc. At the end of the project, I wrote a report on that the targets were successfully met and made suggestions on how to improve the Health Project for next year. Being the lead of this project was a very fulfilling task. I greatly enjoyed the contact with people who want to help their community and it was great to see so many funds being raised which will help people affected with cancer. This PIP helped me gain insight into charity work and project management, and after my PhD I aspire to be involved in a similar role.